HIGH RESOLUTION PALYNOLOGICAL RECORDS FROM ATLANTIC CANADA: REGIONAL HOLOCENE PALEOCEANOGRAPHIC AND PALEOCLIMATIC HISTORY

by

Elisabeth Levac

Submitted in partial fulfillment of the requirements
for the degree of Ph.D. in Earth Sciences

at

Dalhousie University
Halifax, Nova Scotia
May 2002

0-612-79417-2

DALHOUSIE UNIVERSITY

FACULTY OF GRADUATE STUDIES

The undersigned hereby certify that they have read and recommend to the Faculty of Graduate Studies for acceptance a thesis entitled "High Resolution Palynological Records From Atlantic Canada and Newfoundland: Regional Paleoceanographic and Paleoclimatic History", by Elisabeth Levac, in partial fulfillment of the requirements for the degree of Doctor of Philosophy.

Dated: July 12, 2002

External Examiner:

Research Supervisor:

Examining Committee:

[redacted]

DALHOUSIE UNIVERSITY

DATE: August 1st 2002

AUTHOR: Elisabeth Levac

TITLE: High resolution palynological records from Atlantic Canada: regional Holocene paleoceanographic and paleoclimatic history

DEPARTMENT OR SCHOOL:

DEGREE: PhD CONVOCATION: Oct 19 YEAR: 2002

Permission is herewith granted to Dalhousie University to circulate and to have copied for non-commercial purposes, at its discretion, the above title upon the request of individuals or institutions.

[redacted]

Signature of Author

The author reserves other publication rights, and neither the thesis nor extensive extracts from it may be printed or otherwise reproduced without the author's written permission.

The author attests that permission has been obtained for the use of any copyrighted material appearing in the thesis (other than the brief excerpts requiring only proper acknowledgement in scholarly writing), and that all such use is clearly acknowledged.

This thesis is dedicated to Bin Tang,
who accompanied me everywhere, in good or uncertain times:
in 2 countries foreign to him,
during 3 happily married years,
4 of which at Dalhousie,
at 5 hilarious Christmas where he "drank like a man" with my dad,
through 6 years of cultural exchange,
...and 7 apartments.

But mainly, if it was not for him, I would never come to Dalhousie, I would never work with these two great supervisors.

The only constant in life is change,
the only certainty is uncertainty.
Laozi

TABLE OF CONTENTS

LIST OF FIGURES

LIST OF TABLES

ABSTRACT

During the Holocene, the interaction of various forcings (shrinking ice sheet, meltwater, insolation) along the Eastern Canadian Margin caused changes in atmospheric circulation and climate which are reflected in the pollen records from Nova Scotia lakes. In contrast, earlier paleoceanographic studies based on low resolution records, did not show major changes in the past 8000 years.

A high resolution palynological study was undertaken to establish the Holocene history of paleoceanographic changes in the region. Cores from La Have and St. Anne's Basins (Scotian Shelf) and Bay of Islands (western Newfoundland) provided dinoflagellate cyst data that was used to reconstruct sea surface conditions (temperature, salinity and sea ice cover duration), using transfer functions. Ocean-atmosphere interactions are determined by onshore-offshore correlation of pollen records from Nova Scotia and Newfoundland.

In the early Holocene, the three cores record sea surface temperature (SST) 3 to 5 °C warmer than today's average and higher salinity, followed by cooler SST than present. The last 7000 years are characterized by frequent oscillations of SST and salinity around the present day average.

Comparison with other sites from the Labrador Shelf and Northern Baffin Bay show that paleoceanographic events are progressively younger toward the north and suggests that difference in paleoceanography are most likely due to the location relative to Laurentide ice sheet and meltwater sources. Overall, these records reveal a complex Holocene paleoceanography and illustrate the importance of obtaining high resolution records as SST can change by a few degrees (as much as 4-5 °C) in less than 100 years.

Timing of paleoclimatic events relative to paleoceanographic events is variable. The mid-Holocene warm climatic event (hypsithermal) is apparently delayed relative to optimum SST. While forest migration delay cannot be totally excluded, other factors might be involved (competition). The late Holocene Neoglacial cooling trend started earlier on land at the southern location (Scotian Shelf and Bay of Islands) but earlier in the sea surface at the northern sites (Labrador Shelf and Baffin Bay). Paleoclimatic reconstructions independent from pollen are necessary to determine which of the land or the ocean leads the changes.

MOST COMMONLY USED ABBREVIATIONS

AP/NAP: arborescent/non arborescent pollen
CAA: Canadian Arctic Archipelago
CS: Cartwright Saddle
Dinocyst: Abbreviation of dinoflagellate cysts

NAD: North Atlantic Drift
NWP: North Water Polynya
psu: practical salinity units (now used instead of ‰)

TPD: Transpolar Drift
SST: Sea surface temperature

Acknowledgments

I am very grateful to so many people for helping me during my doctoral study. I always feel so lucky to be the student of two great supervisors, Dr. Mudie and Dr. Scott. Dr. Mudie's passion for palynology has always been the inspiration and driving force of my research. I am very thankful for the numerous learning opportunities that she provided me with (cruise, meetings). She helped to plan to project and insure it would run quickly and smoothly. Our discussions have been frank, challenging, wonderful and lead to many great ideas. I appreciate her rigorous reviews of my papers.

Dr. Scott has been very supportive in all aspects of my study and was always enthusiastic about reading a new paper or chapter. I especially enjoyed the discussions we had and his frankness when we could not agree on something.

Special thanks to Dr. de Vernal for introducing me to palynology years ago and for giving me the chance to participate in this project funded by the CHSD (Climate History System Dynamics). Free use of her laboratory for processing my samples was essential to my work.

I owe big thanks to André Rochon at BIO for his help with transfer functions, with preparing my defense, and for his friendship.

Many persons in the department of Earth Sciences also need to be thanked: Peter Reynolds and Jane Barrett for help with administrative issues, Darlene and Norma for help in the office, Franco Medioli for providing me with the most important tool: a microscope, Chloe Younger for the curation of my samples, Martin Gibling and Marcos Zentilli for their constructive comments about my department talk. I also thank Jane for her moral support and kindness.

David Piper deserves a special thanks for giving me the chance to go on the Hudson, for providing me with additional box core samples. I learned a lot about seismics and the world of oil industry. Dr. David Mosher also kindly provided me with box core samples.

The acquisition of new surface samples relied on Iris Hardy at BIO. Her advice and company on the *Hudson* were most appreciated. I will keep a good souvenir of the time spent with on the CCGS *Hudson* and RV *Marion Dufresne* with crew and technicians. Bob Fitzgerald kindly let me use his laboratory on a few occasions to prepare slides.

Francine McCarthy, at Brock University, kindly had some of my samples processed in her lab and gave me lots of useful advice.

In Montreal, Maryse Henry and Virginie Loucheur were essential to my work in the lab. I wish to thank Sophie and Annie who played with HF to process some of my samples. Odile Peyron helped with transfer functions.

John Cullen (Dalhousie University) is also acknowledged for helpful comments on chapter 3 and for serving on my committee. Lucy Edwards (US Geological Survey) and an anonymous reviewer are acknowledged for their review of the paper on La Have Basin (chapter 3) and useful comments. Lucy Edwards also kindly agreed to be the external examiner for this thesis on very short notice.

At Memorial University, Ali Aksu and Rick Hiscott generously allowed me to sample the Bay of Islands core and provided the ^{14}C ages. Helen Gillepsie, Michelle Miskell and Steve assisted in the subsampling operation. Doreen and her boyfriend gave me a taste of Newfoundland hospitality by welcoming me in their home when I was in St. John's.

The chapter on Bay of Islands greatly benefited from discussion with Martin Batterson, Geological Survey of Newfoundland and John Shaw, BIO. John Smith from BIO shared his knowledge of mixing rates and bioturbation with me.

Teaching with my colleagues in the Earth Science department at St. Francis Xavier University was most enjoyable. Brendan Murphy, Hugo Beltrami, Lisa Kellman, Allan Anderson, provided precious advice about their profession.

Cindy Murphy kept me alive with our badminton games.

Pauline MacIntosh offered her moral support during difficult periods.

And I am not forgetting my colleagues at Dalhousie. Mark Deptuck, Duncan, Charu, Sarah, Trecia, Eugene, Heidi.

Finally, Bin should be rewarded for being the perfect husband, cooking for me, fixing the computer... what more can I say?

CHAPTER 1 Introduction

1.1 History of marine palynology off Eastern Canada

This thesis builds on previous palynological studies off Eastern Canada and further explores the use of marine palynology to answer questions regarding the paleoceanography of the Scotian Shelf, and as a mean to relate the terrestrial and oceanic environments.

25 years ago, marine palynology was starting to emerge as a useful tool to study paleoceanography and paleoclimates (for example Wall et al. 1977; Balsam and Heusser 1976; Mudie 1980). Wall et al. (1977) investigated the relation between dinocysts and water masses in difference parts of the North Atlantic (along east coast of United States, equatorial Atlantic, Bermudas etc.). Balsam and Heusser (1976) studied the pollen content of 2 continental slope cores off eastern United States.

In Eastern Canada, Mudie (1980) contributed to the establishment of marine palynology as a useful paleoceanographic tool and to the integration of pollen and dinocyst records, which allow correlations with onshore pollen stratigraphies and comparisons of ocean-atmosphere interactions. Mudie (1980) determined which extraction method were safe for the palynomorphs and also undertook the necessary pioneering work by studying the modern distribution of marine (see also Mudie and Short 1985; Mudie 1992; Mudie and Harland 1996) and terrestrial palynomorphs in continental shelf sediments off Eastern Canada, and be assessing transport mechanicms for pollen and spores transport (Mudie 1980, 1982; Mudie and McCarthy 1994). Finally, Mudie (1980) applied the result of these findings to the paleoecology of the later Quaternary in shelf cores (results were later published in: Vilks and Mudie 1978; 1983; Scott et al. 1984; Mudie and Aksu 1984; Mudie and Short 1985).

Application of palynology to cores from Baffin Bay and the Labrador Sea further demonstrated the sensitivity of dinoflagellate cysts to environmental changes in subarctic regions, and their ability to document changes in paleoceanography (Aksu and Mudie 1985; Aksu et al. 1989; de Vernal and Mudie 1989; 1992).

Efforts to improve the knowledge about dinoflagellate cysts distribution and their relation with sea surface conditions and water masses led to several more studies, among these, the distribution of dinoflagellate cysts and pollen in the Estuary and Gulf of St. Lawrence (de Vernal and Giroux 1991) and the distribution of palynomorphs in Labrador Sea (Rochon and de Vernal 1994). Edwards (1992) proposed a semi-quantitative method to estimate paleotemperatures based on the known ecological ranges of dinoflagellate cysts. Mudie (1992) demonstrated onshore-offshore trends in dinocyst assemblages in transects from Nova Scotia to Baffin Bay, and used multivariate statistical analysis to delimit geographical assemblages and correlate cyst distribution with SST and sea surface salinity. Principal component analysis also showed a positive correlation of cyst assemblages with SST and sea surface salinity (de Vernal et al. 1994; Rochon et al. 1999).

Eventually, the use of transfer functions, to quantitatively reconstruct sea surface conditions from dinocyst data was introduced by Mudie (1992) who applied the Imbrie and Kipp method, already widely used for foraminifera, to cores from the North Atlantic.

After testing various transfer function methods (canonical regressions, best analogues, etc.) using a larger surface sample database from the North Atlantic and adjacent basins, de Vernal et al. (1994) proposed an adaptation of the best analogue method of Guiot (1990). The fact that ubiquitous species often dominate dinocyst assemblages probably explains the non-linear relation between assemblages and environmental data and the relatively poor results of the regressions method (de Vernal et al. 1994).

Work on the best analogues method and the expansion of the database has been has been pursued by Rochon et al. (1999). Over the last few years, lots of efforts were directed further expanding the modern North Atlantic surface database and filling the gap in coverage in some areas (de Vernal et al. 2001), including the Scotian Shelf (see appendices 2 and 3).

Recently, Mudie et al. (2001) summarized the advantages of dinoflagellate cysts for biostratigraphic and paleoceanographic studies and explained why they are better proxies than foraminifera for quantitative reconstructions in the Arctic and high-latitudes environments.

1.2 Problem

The Holocene in Eastern Canada was a time of important changes with decreasing summer insolation following the maximum at 9 ka (Kutzbach and Webb 1993; Bradley 1999), the northward retreat and gradual disappearance of the Laurentide Ice Sheet (Dyke and Prest 1987), its declining impact on the climate (Kutzbach and Webb 1993; Vettoretti et al. 1998; Webb et al. 1993), and the reorganization of atmospheric patterns (COHMAP 1988; Kutzbach and Webb 1993; Mudie and McCarthy 1994; Bourgeois et al. 2000). Due to these variables, climate had a complex history during the Holocene (see section 6.6.4 about climatic models).

When it comes to paleoceanography, it seems that many scientists make it a duty not to mention the Holocene (for example Lowe and Walker 1997), perhaps because it is considered event-less when compared to more spectacular nature of changes during the late glacial, and many books about the Quaternary end with the Younger Dryas, or the 8.2 ka episode (see Alley et al. 1999), although recent work has focussed on land-sea comparison of the 6 ka hypsithermal event (Sawada et al. 1999; Gajewski et al. 2000) and the role of ocean in the mid-Holocene warming, especially in the Arctic (Vettoretti et al. 1998; Kerwin et al. 1999).

This underemphasis of the Holocene probably arises from the following: 1- Deep sea records have been used extensively because they are more likely to provide continuous sedimentary records, despite their low resolution which might obscure many paleoceanographic events, especially after deglaciation when sedimentation rates are much lower in Holocene pelagic environments; 2- The amplitude of events is believed to be much smaller during the Holocene (see Ruddiman 2001).

Recently, there has been suggestions that the Holocene ocean was far from being "static" with recurrent ice rafting events (Bond et al. 1997; 1999) and evidence for episodic southward incursions of surface Arctic waters into the temperate Norwegian Sea, coincident with a weakening of the North Atlantic Drift current system (Bischof 2000).

The Holocene around the southeastern Canadian Margin provides an example of this apparent contrast between variable climate and static ocean. While the southeastern Canadian margin was submitted to the changing influence of various forcings during the Holocene (changes in insolation, effect of remaining ice sheet on climate, meltwater, changes in main surface currents; as stated above), which were reflected in the climatic records (Livingstone 1968; McCarthy et al. 1995), similar trends in the sea surface paleoceanographic records from the Scotian Shelf (Vilks and Rashid 1976; Mudie 1980; Scott et al. 1984) are sometimes absent, due to low resolution, low numbers of planktonic foraminifera, lack of quantitative data, or are not dated precisely.

1.3 Objectives

The objectives of this thesis are as follows:

1. To provide quantitative data for paleoceanographic conditions and changes in the southeastern Canadian continental margin region during the Holocene interglacial interval.
2. to improve the sampling and time resolution of shelf core studies.
3. To compare ocean-atmosphere interactions using quantitative estimates sea surface and lake temperatures at critical time intervals, including the earliest Holocene, the mid-Holocene climate optimum and the Neoglacial cooling event.
4. to compare the paleoceanographic signals of planktonic dinoflagellates and benthic bottom foraminifera in selected shelf basins.

The use of palynological proxies for such a study has many advantages. It offers an alternative to dissolution-prone calcareous microfossils. It also eliminates the uncertainties about whether or not planktonic foraminifera record the sea surface conditions or live below the surface. Palynology provides a means to directly correlate paleoceanographic and climatic records, since dinoflagellate cysts and pollen are from the same sample and counted simultaneously.

1.4 Selection of study area

The southeastern Canadian Margin was a good location for this study for a variety of reasons, the first and most important being its present location near the confluence of polar and subpolar air masses (Anderson 1987), and near the transition between major surface currents (Smith and Schwing 1991). This is important because the boundaries of vegetation zones are closely related with the position of main air masses (Davis and Webb 1975), and therefore the pollen records should reflect changes in climate, while the dinoflagellate cyst data should reflect changes in sea surface conditions (Rochon et. al 1999).

Another advantage of the eastern Canadian Margin is the existence of basins where sedimentation rates are high, which can provide expanded Holocene records and high resolution. In addition, the close proximity of these basins to land areas (or pollen sources) allows a good correlation between the marine and the terrestrial (lake) pollen records (Mudie 1982; Rochon and de Vernal 1994), and therefore, a way to compare the evolution of marine and terrestrial environments. Finally, the previous micropaleontological studies from the southeastern Canadian Margin basins can be used to compare paleoceanographic signals from the sea surface and from the sea bottom.

Based on the following additional criteria, 3 core locations were selected (see figure 2.1).

1) La Have Basin on the central Scotian shelf was selected because of its high sedimentation rate, thus allowing high resolution studies that can be can be compared with previous palynological and foraminiferal studies from the Scotian Shelf (Emerald and Canso Basins; Mudie et al. 1980; Scott et al. 1984). It is an open shelf environment where changes in the main surface circulation should be recorded, but its relatively close

location to the shore allows correlation with Nova Scotia lake pollen assemblages (Livingstone 1968; McCarthy et al. 1995).

2) Bay of Islands is a good location to study the influence of the retreating Laurentide Ice Sheet on the Holocene climate because of its closer proximity, and it is also a good location to detect the discharge of meltwater through the St. Lawrence River system (see Moore et al. 2000 about discharge episodes). A core from Bay of Islands provides a better record compared to cores from the Gulf of St. Lawrence by being an enclosed bay, thus the pollen records reflect vegetation of Newfoundland more accurately. The Holocene section from Core MD99-2225 is represented by 18 m of sediments compared to 2-5 m in the Gulf of St. Lawrence, which should enable to detect short duration events.

3) St. Anne's Basin is an intermediate location between La Have Basin and Bay of Islands and was used to examine the timing of paleoceanographic and climatic events on the eastern Scotian Shelf and in Cape Breton, and to determine whether the timing of the hypsithermal or warm sea surface temperatures depended on the distance relative to the Laurentide ice sheet.

1.5 Organization of the thesis

After a brief description of the palynological processing methods used in this study, and data collection procedures, chapter 2 puts the emphasis on the description of the transfer functions applied to the dinoflagellate cyst data to reconstruct sea surface conditions.

As most of this thesis was written in the form of papers, all details specific to the cores (environmental setting, method, stratigraphy, results, discussion and references) are presented in a separate chapter for each core.

Chapter 3 presents the results from La Have Basin and addresses the problems identified in the introduction for that paper. Chapter 4 presents the results from Bay of Islands and compare these with results from La Have Basin. Chapter 5 includes the results from St. Anne's Basin and also a synthesis of paleoceanographic studies from the southeastern Canadian Margin (Scotian Shelf, Gulf of St. Lawrence, Grand Banks, northwest North Atlantic), including La Have Basin and Bay of Islands.

Chapter 6 is a broader synthesis which expands outside the study area to include northern shelf areas. It reviews palynological studies from the Labrador Shelf and Baffin Bay. It compares the paleoceanography of different regions along the eastern Canadian Margin. Sources of meltwater and their potential impact on sea surface conditions in the three basins (La Have, St. Anne's and Bay of Islands) are examined. Also examined are the changes in sea surface conditions/circulation as inferred from various proxies, and based on deep-sea records from the Labrador Sea, Baffin Bay, Canadian Arctic, and the Greenland shelves. Comparison of reconstructed sea surface conditions with pollen records from adjacent lands addresses the question of the leads and lag between climate and sea surface conditions.

Chapter 3 was already published by Levac (2001) in Marine Micropaleontology and references are generally made to that publication. Chapter 4 is being reviewed in Palynology and is referred to as Levac 2002a. Chapters 5 and 6 will be submitted shortly and are referred to as Levac 2002b and Levac et al. 2002.

All the ages in this thesis are radiocarbon ages corrected for marine reservoir effect.

CHAPTER 2 Methods

2.1 Location of coring sites

Three cores were analyzed for this study. Two of the coring sites are located on the Scotian Shelf, in La Have and St. Anne's Basin, and one along the west coast of Newfoundland, Bay of Islands. Figure 2.1 shows the locations of the three sites.

Table 2.1 Locations of coring sites

Basin	**Core number**	**Location**	**Water depth**	**August SST**	**August salinity**	**Duration ice cover > 50% of surface**	**Chapter**
La Have Basin	95-030-24	43°46'N 63°43'W	256	17	31.5	0	3
St. Anne's Basin	84-011-12	45°47'N; 58°39'W	270	16	30	40 days	4
Bay of Islands	MD99-2225	49°N; 58°05'W	104	17	30.7	60 days	5

2.2 Sample processing

In general, the sample volume was 5 cm^3 of sediment. They were first sieved at 10 micrometer mesh size, then digested in 10% HCl and concentrated HF to remove carbonates and silicates, respectively. The addition of *Lycopodium* tablets (with a known number of spores) allowed the determination of the concentration of palynomorphs per unit volume of sediment (cm^3). The residue was mounted on slides in glycerine gel.

Details concerning each core (core stratigraphy, sampling interval, ^{14}C dating) are found in chapters 3, 4 and 5.

2.3 Analysis

Slides were examined using a Zeiss Ultraphot light microscope. Whenever possible, 300 dinocysts were counted. A few samples provided lesser counts but cyst numbers always exceeded 200. The same procedure was followed for pollen. Also counted were spores, organic lining of foraminifera and reworked palynomorphs.

The nomenclature conforms to the 1998 Lentin and Williams index of fossil dinoflagellates (Williams et al. 1998). The classification of the main dinoflagellate cyst species mentioned in this thesis can be found in appendix 1. The author referred to de Vernal et al. (1992b) and Rochon et al. (1999) for the identification of dinoflagellate cysts. The species previously called *Algidasphaeridium*? *minutum* has recently been assigned to the new genus *Islandinium* by Head et al. (2001). Pollen and spores identification are based on Andrews et al. (1973) and on Bassett et al. (1978).

Data from La Have Basin core 95-030-24 (raw counts and percentages) can be found in appendices 10 to 12, those for Bay of Islands core MD99-2225 in appendices 13 to 17, and those from St. Anne's Basin core 84-011-12 in appendices 18 to 22.

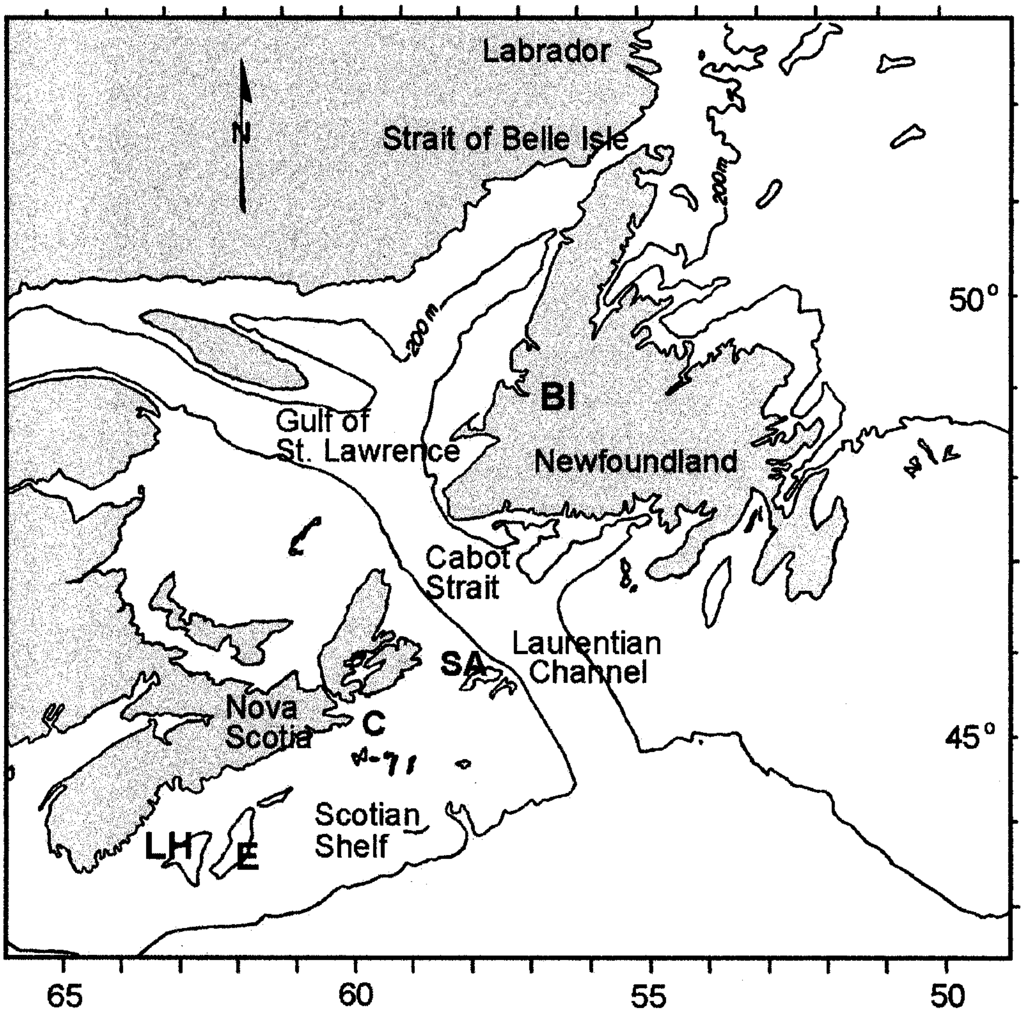

Figure 2.1: Location map. LH: La Have Basin, E: Emerald Basin, C: Canso Basin, SA: St. Anne's Basin, BI: Bay of Islands

2.4 Transfer functions

2.4.1 The best analogue method

The method used for this thesis is the best analogue technique of Guiot (1990) initially adapted to dinocyst data by de Vernal et al. (1993; 1994) and later by Rochon et al. (1999) and de Vernal et al. (2001). In this method, the hydrographic parameters of modern analogues are used to reconstruct sea surface conditions.

The procedure is as follows. Raw dinoflagellate cyst counts are transformed into per mil. Each assemblage is then equivalent to a vector of relative abundance of the dinocyst taxa considered. At this point, a principal component analysis can be used to determine the weight of each taxon, but tests have yielded better results with neutral weighting of taxa (de Vernal et al. 1994).

Each fossil assemblage is compared with all the modern spectra in the reference database and the 10 most similar analyses are selected. The degree of similarity is ranked based on log transfermed Euclidian distance (LED) between the fossil and the modern analogues, which is calculated with the following formula (Guiot 1990):

$$\mathrm{LED}^2 = \sum_{k=1}^{m} [\ \ln (10\ S_{ik} +1) - \ln (10\ S_{tk} +1)\ ]^2$$

where k = taxa,

S_{ik} = frequency of taxa k in modern analogue i,

S_{tk} = frequency of taxa k in fossil analogue t.

Logarithmic transformation of data before the search of analogues helps to emphasize the importance of species present in low percentages. These species are often characterized by more restrictive environmental requirements than the dominant ones.

Reconstructions are then based on the hydrographic data of the 10 best analogues and their inverse distance (Guiot 1990) and the best estimate (${}^{o}R_t$) is given by:

$${}^{o}R_t = \left(\sum_{i=1}^{S} C_i / d_{ti}^{2}\right) / \left(\sum_{i=1}^{S} d_{ti}^{2}\right)$$

where C_i = hydrographic parameter for modern analogue i, and

d_{ti} = distance between fossil and modern assemblages.

The upper and lower limits of the confidence interval (1 σ, 68%) are:

$${}^{-}R_t = {}^{o}R_t - \left[\left(\sum_{i=1}^{S-} C_k^{2} / d_{tk}^{2}\right) / \left(\sum_{i=1}^{S-} d_{tk}^{2}\right) - {}^{o}R_t^{2} \right]^{1/2}$$

$${}^{+}R_t = {}^{o}R_t + \left[\left(\sum_{i=1}^{S+} C_k^{2} / d_{tk}^{2}\right) / \left(\sum_{i=1}^{S+} d_{tk}^{2}\right) - {}^{o}R_t^{2} \right]^{1/2}$$

S^{-} = the set of modern analogues whose modern hydrographic data C_k is greater than ${}^{o}R_t$

S^{+} = the set of modern analogues whose modern hydrographic data C_k is smaller than ${}^{o}R_t$

2.4.2 New surface samples

The reconstructions are based on the GEOTOP database of surface sediment dinoflagellate cyst assemblages. Reconstructions in this thesis were based on a version of the database containing 540 samples[1] from sites in the North Atlantic Ocean and adjacent basins (Gulf of St. Lawrence, Gulf of Maine, Hudson Bay, Labrador Sea, Norwegian Sea) and the Arctic Ocean. In addition to these 540 samples, new surface sediment samples were added along the eastern Canadian Margin, especially the Scotian Shelf where the coverage was sparse. In total, 58 new sites were added (appendices 2 to 9). This database was called DIN598 (appendix 25).

Samples for the database are preferentially selected from box cores or gravity cores. The top 1 cm of sediment is taken. The list of 58 new core tops used for this thesis is found in appendix 2, and a location map in appendix 3. Total palynomorph counts, raw dinoflagellate cyst counts and percentages are found in appendices 5 to 7. Hydrographic data for these new surface sites are in appendix 4. They include the mean duration of the seasonal sea ice cover (i.e. the number of months with sea ice concentration greater than 50% of the sea surface), the sea surface (0 m depth) temperature and salinity. The

---

[1] The last updated version of the GEOTOP database was recently published as the "n=677" database (de Vernal et al. 2001). The dinocyst counts and percentages for the 30 taxa selected in this database are available on the GEOTOP website http://www.geotop.uqam.ca/.

hydrographic data were compiled from the National Ocean Data Center (NODC 1994; see also de Vernal et al. 2001).

The reconstructions for La Have Basin and Bay of Islands were performed with a database of 576 sites, as the last 22 sites were obtained in the latest stages of this study. However, a suybsequent run with the whole database (598 sites) showed similar results. Reconstructions for St. Anne's Basin are based on the DIN598 database. Various files related to the reconstructions (modern analogues and reconstructed data) are included in appendices 28 to 33.

Reasonably good results were obtained when reconstructing the modern environmental parameters using the database (appendices 26 and 27). Linear regression between the measurements and the reconstruced values show coefficients ranging from R= 0.91 for salinity to R= 0.96 for SST. For the seasonal ice cover duration, the coefficient of correlation is 0.94.

The accuracy of the method, defined by the differences between the measured and reconstructed values is respectively ± 1.06 °C and ± 1.35 °C for February and August SST. For salinity, the accuracy is ± 2 psu and for the seasonal duration of the ice cover, ± 1.28 months/year.

The accuracy is determined by running the database on itself, i.e., by reconstructing the sea surface conditions of each reference site (which are already known) using the transfer functions. The program is set to prevent each modern reference site to use itself as an analogue. The difference between the measured (instrumental) and the reconstructed sea surface conditions are used to define the accuracy (see appendices 26 and 27).

CHAPTER 3 High resolution Holocene palynological record from the Scotian Shelf

Abstract

Because of their location at the confluence of polar and subtropical airmasses and near a transition zone between the cold Labrador Current and the Gulf Stream, the Atlantic Provinces experience some of the most dynamic climate conditions in Canada. Major climate changes occurred during the Holocene, as shown by pollen records from lakes, but previous paleoceanographic studies based on low resolution proxy-data records do not show major changes during the past 8000 yrs. Therefore, the Holocene history of Canada's Atlantic region was examined using a high resolution palynological record from the Scotian Shelf (La Have Basin). Sea surface conditions were reconstructed using proxy-data from dinoflagellate cysts and paleobioclimatic transfer functions. Pollen was used for onshore-offshore correlation between core 24 and pollen records from Nova Scotia lakes. This allows to compare the evolution of the marine and terrestrial environments.

Results show a succession of major paleoceanographic events. Sea surface temperatures (February and August) up to 5°C higher than today's average and a slightly higher salinity are reconstructed between 10,000 and 8500 BP. The last pulse of meltwater from the residual ice sheet affected the shelf waters between 8500 and 6500 BP by lowering the sea surface temperature (in February) and the salinity. Most previous studies failed to record this event. Since 6500 BP, August temperature generally

remained around today's value, while February temperature was generally 2°C above it, except for recurring colder and lower salinity intervals. These cold intervals have a recurrence of about 1000 years. A slight cooling of summer SST is recorded in the last 500 years.

Comparison with climatic reconstructions from Nova Scotia pollen records shows a difference in timing between ocean and atmosphere climate signals. The onset of the climatic optimum (hypsithermal) in Nova Scotia lags by about 2000 years (until 8000 BP) relative to the ocean but it lasted longer. The Neoglacial cooling in Atlantic Canada however, started earlier (2000 BP) than the late Holocene ocean cooling.

La Have Basin's Holocene paleoceanography presents some differences from most other studies from the region: 1- the SST optimum started earlier than the hypsithermal; 2- the last pulse of meltwater is recorded; 3- the last 6500 years are punctuated by colder intervals.

Increased productivity and blooms of toxic algae in the early Holocene are probably due to a combination of factors: increased nutrients and a greater stability of the water column because of meltwaters, higher sea surface temperature and increased upwelling or storm activity.

3.1 Introduction

3.1.1 Choice of the study area

During the Holocene, the interaction of various forcings (shrinking ice sheet, meltwater, insolation) caused changes in the atmospheric circulation over North America and the ocean circulation on the Eastern Canadian margin, which in turn affected the climate (COHMAP 1988; Kutzbach and Webb 1993). Because of its location at the confluence of the polar and subpolar air masses (Anderson 1987), and near the zone of transition between the Labrador Current and the North Atlantic Drift (Smith and Schwing 1991), the Scotian Shelf is a strategic region to study Holocene paleoclimate and paleoceanography.

The vegetation zones in northeastern North America are determined by the average position of the major air masses (i.e. polar and subpolar; Davis and Webb 1975). Pollen sequences from the Scotian Shelf sediments therefore provide a proxy for changing air masses and climatic conditions. Pollen stratigraphies for sediments from Nova Scotian bays and the Scotian Shelf (fig. 3.1) also show a close correlation between onshore and offshore pollen sequences and major climatic events are clearly evident in regional marine deposits (Mudie 1980, Piper et al. 1990; Scott et al. 1984; Mudie and McCarthy 1994). Dinoflagellate cysts (dinocysts), whose distribution is related to sea surface conditions, provide a proxy for sea surface temperature, salinity and ice cover (Edwards and Andrle 1992; Mudie 1992; Rochon et al. 1999).

3.1.2 Previous studies and problems

Pollen records from lakes in Nova Scotia and New Brunswick (eg. Livingstone 1968; Anderson 1985; McCarthy et al. 1995) show that the climate of the Atlantic provinces underwent major climatic changes during the Holocene. In particular, quantitative reconstruction of August temperature for Penhorn Lake in southern Nova Scotia (McCarthy et al. 1995) shows that early Holocene cool conditions were followed by a middle Holocene warm interval (hypsithermal) and a late Holocene cooling (also referred to as the "Neoglacial").

In contrast, previous paleoceanographic studies of dinoflagellates (Mudie 1980; Piper et al. 1990; Scott et al. 1984) from the Scotian Shelf do not reveal a clear response of shelf surface water conditions to these climate changes. Mudie (1980; see also Piper et al. 1990) used dinoflagellate cysts as proxies of surface water conditions and showed that the boundaries of 3 dinocyst assemblage zones appear to lead climate warming in the late glacial and climate cooling in the late Holocene. However, these low resolution, non-quantitative data show no clear evidence of a hypsithermal interval.

Foraminiferal and isotopic studies conducted on cores from the Scotian Shelf (Scott et al. 1984, 1989a) have shown a mid-Holocene warm interval and a late Holocene cooling trend in bottom water from Emerald and Canso Basins. In a synthesis of benthic data, Gajewski et al. (2000) indicate for the Scotian Shelf a mid-Holocene influx of warmer water and a late Holocene cooling starting at about 2.5 ka. However, detailed shelf foraminiferal studies are only available for the benthic fauna because sea surface salinity on the Scotian Shelf is not favorable to planktonic foraminifera and these are present in reduced numbers and diversity in the water column (Scott et al. 1984). The micropaleontological data therefore provide information about bottom water conditions only.

Most other paleoceanographic studies in the southeastern Canadian and adjacent northwest Atlantic regions were based on low resolution proxy-data records and do not show major changes during the Holocene after the establishment of modern oceanographic conditions, except for the late Holocene cooling (Vilks and Rashid 1976; Balsam and Heusser 1976; Keigwin and Jones 1995) and a hypsithermal temperature increase of ~1°C south of the Grand Banks (Mudie 1992).

The difference between the variable land record and the apparently relatively stable ocean record may be partly due to poor preservation of foraminifera in bathyal slope sediments. For example, greater dissolution of planktonic foraminifera in more distal cores on the continental slope off Chesapeake Bay may have resulted in faulty reconstructions (Balsam and Heusser 1976; Balsam 1981). Many of the early studies were also weakened by the lack of a well constrained chronology: few radiocarbon ages were obtained and most of these ages were from total organic carbon samples which often results in overestimates of ages because of contamination by older carbon (Mudie and Gilbault 1983).

To solve these problems, a high resolution palynological study using pollen and organic-walled dinoflagellate cysts was carried out on a radiocarbon-dated high sedimentation core 95-030-24 from La Have Basin on the Scotian Shelf. The deepest parts of the shelf basins, such as La Have Basin (256 m), are the site of fine sediment accumulation (Piper 1991) and provide expanded Holocene records. Pollen and dinocysts are resistant to dissolution and are useful for high latitude studies of land-sea correlation and reconstruction of sea surface changes (Mudie 1982; 1992).

The purpose of this study was to obtain a century-scale record of Holocene changes in vegetation and climate as recorded by marine pollen assemblages and to compare this with the dinocyst proxy-record of changes in surface water conditions. The quantitative links between the distribution of dinoflagellate cysts in the North Atlantic and sea surface conditions have already been demonstrated by several studies (Edwards and Andrle 1992; Mudie 1992; Rochon et al. 1999). In this paper, paleobioclimatic transfer functions based on these dinocyst data were used to reconstruct quantitative estimates of sea surface temperature (SST), salinity and duration of the sea-ice cover, using the method described by Rochon et al. (1999). Six AMS radiocarbon ages provided a good age control for core 95-030-24; correlation of pollen zones from the core with the onshore zonation is also used to confirm the validity of the radiocarbon ages and to refine the stratigraphy. Correlation between the decadal-scale record of changes in abundance of dinocysts that cause red tides (harmful algal blooms) was also be examined in relation to the sedimentology of the core and the proxy-data for climate change.

Figure 3.1: Location map and bathymetry (meters). The location of core 95-030-24 is indicated by a star. Other cores cited in the text are indicated by numbers. Some numbers correspond to more than one core in places where sites are located too close together.

Terrestrial sites:
1- Silver Lake (Livingstone 1968) and Penhorn Lake (McCarthy et al. 1995);

Bays:
1- Bedford Basin (Miller et al. 1982);
2- St Margaret's Bay (Mudie 1980);

Marine sites:
☆ LaHave Basin 95-030-24 (This paper);
3- Emerald Basin (Mudie 1980; Scott et al. 1984; 1989a; Vilks and Rashid 1976);
4- Canso Basin (Scott et al. 1984; 1989a);
5- Cabot Strait (de Vernal et al. 1993; Simard and de Vernal. 1998);
6- Laurentian Channel (Keigwin and Jones 1995);
7- Laurentian Channel (Simard and de Vernal 1998);
8- SW Grand Banks Rise (Simard and de Vernal 1998);
9- Laurentian Fan (Keigwin and Jones 1995);
10- Fogo Seamount (Mudie 1992).

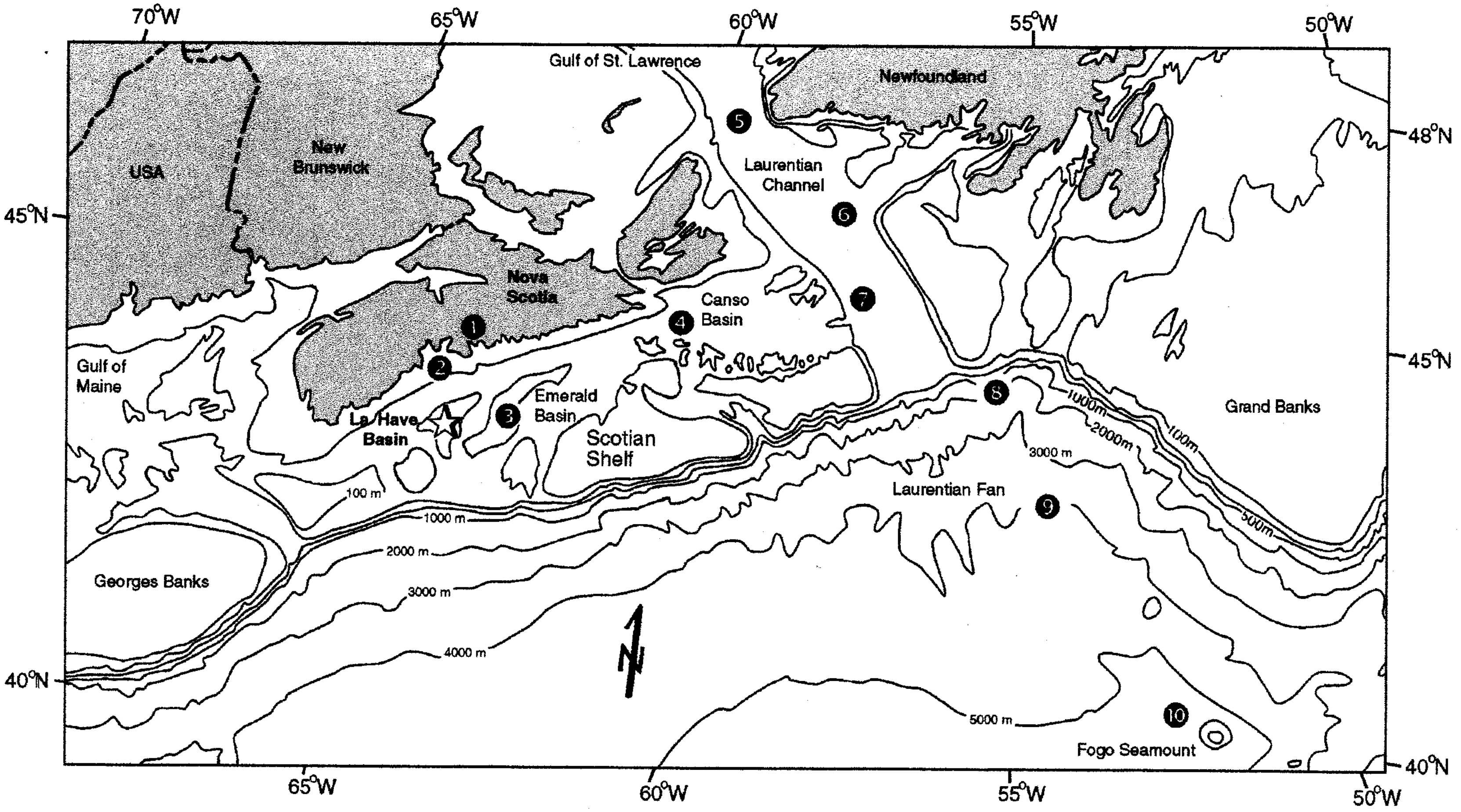

Figure 3.1 Location map and bathymetry of the Scotian Shelf

3.2 Environmental setting

The Scotian shelf is a fairly shallow and broad (~50-250 depth, 100-200 km wide) continental margin. Middle shelf basins, such as La Have Basin, are the site of fine sediment deposition (Amos and Judge 1991; Piper 1991). Preservation of organic matter is better in shelf basins than other shelf areas (e.g. banks), because of reducing conditions and more rapid sedimentation rate (Buckley 1991) and their sediments contain greater concentrations of organic matter (Pocklington et al. 1991). The youngest formation (Holocene) in the shelf basins is a bioturbated olive-grey silty clay, the La Have Clay (King and Fader 1986).

3.2.1 Surface circulation

The main surface circulation on the Scotian Shelf flows toward the southwest and is dominated by waters from the Gulf of St. Lawrence and the Newfoundland Shelf (fig. 3.2). Waters from the Gulf of St. Lawrence, characterized by lower temperature and salinity, flow out of Cabot Strait onto the inner Scotian Shelf to form the Nova Scotian Current (Loder et al. 1997). The flow of the Nova Scotia Current is parallel to the coast in the eastern half of the shelf. Near Halifax, part of this current branches and sweeps through the northern edge of Emerald Basin and then through La Have Basin (Loder et al. 1997; Shore et al. 2000). Part of the waters from the Southern Newfoundland Shelf (from >200 m depth) move across the Laurentian Channel and along the outer shelf (Loder et al. 1997). Waters above the

Scotian Slope and Rise are periodically under the influence of eddies from the North Atlantic Drift (Smith and Schwing 1991) which flows offshore toward the northeast.

Coastal upwellings can occur when strong winds blow from the southwest to the northeast. Upwelling-favorable winds are more common during the summer months but this phenomenon can also take place during the winter. These upwellings are thought to be an important source of nutrients for the shelf basins (Petrie et al. 1987).

3.2.2 Sea surface temperature, salinity, ice cover

The surface waters of the Scotian Shelf are cold in winter. The average sea surface temperatures above La Have Basin are 1.8°C and 17°C in February and August, respectively. The sea surface temperature increases toward the Gulf Stream. The surface salinity is higher in February (32 psu) than in summer (31.5 psu) (Petrie et al. 1996a). Ice is present over the inner Scotian Shelf around Cape Breton for an average of 20 to 40 days a year (Drinkwater et al. 1999).

3.2.3 Climate

The weather over Nova Scotia and the Scotian Shelf, with its frequent frontal storms and rare tropical storms, is the result of interactions between polar and subtropical air masses (Anderson 1987). The climate of Nova Scotia is also greatly influenced by the ocean: the cold water of the inner shelf is responsible for cooler temperatures in the coastal regions and frequent fog (Hare 1997). The mean daily air temperature is -5°C in February and 17.5°C in August, except for Cape Sable on the southwestern tip of Nova Scotia where it is 15°C in August. The dominant winds in summer are from the south and southwest (Environment Canada 1984).

3.2.4 Vegetation

Most of Nova Scotia, with the exception of the coastal areas and Cape Breton, belong to the Atlantic Uplands and Central Lowlands subdivisions of the Acadian forest region of Rowe (1972). The forest of Atlantic Uplands sub-region is composed mainly of *Picea rubens*, with *Tsuga canadensis*, *Picea mariana*, *Betula papyrifera*, *Acer rubrum*, *Abies balsamea*, and *Pinus strobus*. In addition to these species, the vegetation of the central lowlands also include *Betula*, *A. saccharum* and *Fagus grandifolia*. Dense low stands of *Abies balsamea*, *Picea mariana* and *P. glauca* are found along the coast in the Eastern Atlantic shore sub-region (Rowe 1972) and *Sphagnum* bogs occupy areas with poor drainage (Rowe 1972; Environment Canada 1989).

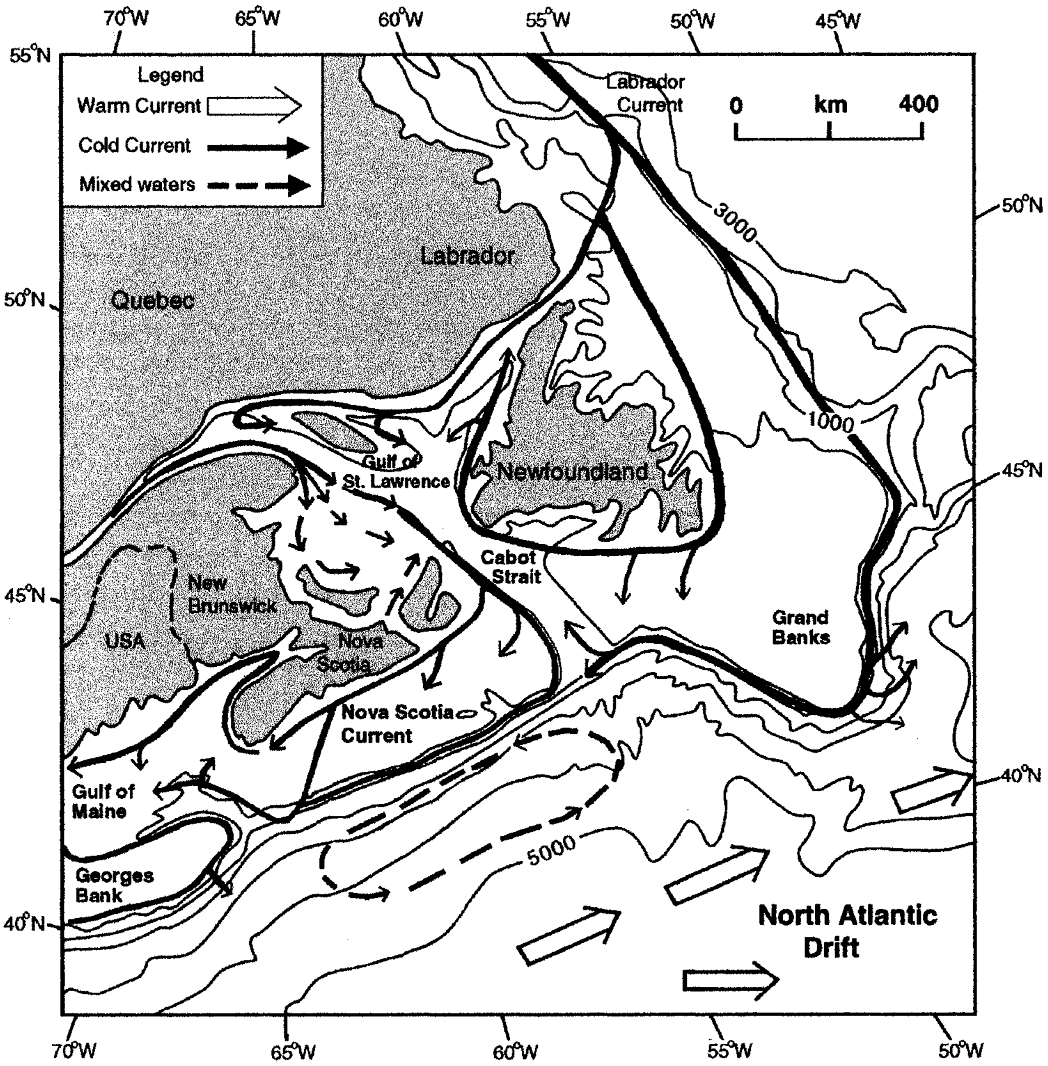

Figure 3.2: Sea surface circulation over the southeastern Canadian Margin (based on Piper et al. 1990; Han et al. 1999; Shore et al. 2000).

3.3 Methods

3.3.1 Stratigraphy, sampling and laboratory procedure

Core 95-030-24 was taken at 43°46'N 63°43'W, in a water depth of 256 m. The trigger weight and piston cores are 180 cm and 800 cm long, respectively. The pollen records indicate that there is an overlap of 80 cm between the trigger weight and piston cores (fig. 3.3). The total composite core is 900 cm long. The whole sedimentary sequence consists of olive grey La Have Clay.

The age control is provided by six radiocarbon ages from shells (table 3.1). They were corrected for marine reservoir effect. Correlation of the pollen record with regional pollen zonations (Nova Scotia) was also used to verify the validity of the radiocarbon ages. Comparison of pollen zones from the piston core with the regional pollen zonation and with the trigger weight core showed that about 1000 years is missing from the top of the piston core. Piston corers occasionally fail to recover the softer surficial sediments because of a late triggering due to imprecise setting of trigger core slack, or in high wave conditions. Comparison of the pollen assemblages with modern assemblages from Nova Scotia also suggest that the last hundred years are missing from the top of the trigger weight core.

Table 3.1 Radiocarbon ages

Core	Depth (cm)	Description	Lab number	Age (yrs BP)	Cal BP
95-030-24 TWC	143	Dentalina scaphopod	TO-5842	1830 ± 50	1283 (1325-1250)
95-030-24 Piston	100	Dentalina scaphopod	TO-5850	2900 ± 60	2560 (2693-2435)
95-030-24 Piston	308	Clam shell valve	TO-5849	6030 ± 60	6336 (6406-6281)
95-030-24 Piston	393	Clam shell valve	TO-5839	6960 ± 60	7401 (7427-7316)
95-030-24 Piston	403-410	Clam shell valve	TO-5853	7210 ± 60	7583 (7648-7551)
95-030-24 Piston	560	Dentalina scaphopod	TO-5851	8530 ± 70	8929 (8985-8866)

The age model used to plot figures 3.5, 3.6 and 3.7 is a linear interpolation between the radiocarbon ages (see figure 3.3 for the sedimentation rate estimates used). For this study, the base of the core is assumed not to be older than 10,000 years because there is no evidence of the Younger Dryas. The would translate into a sedimentation rate of 177 cm/1000 years for sediments below the level dated at 8.5 ka.

Palynology samples were taken every 10 cm in the trigger weight core and upper metre of the piston core. In the rest of the core, samples were taken at 20 cm intervals. This provides a resolution of 130 to 300 years, depending on the sampling interval and on the sedimentation rates, which vary between 117 cm/1000 years and 35 cm/1000 years (fig. 3.3). The cores are bioturbated throughout and ^{210}Pb measurements (J.N. Smith, pers. comm., 2000) suggest that mixing occurs to a depth of 7 cm, thereby limiting the time resolution.

Samples of 5 cm^3 volume were sieved at 10 micrometer mesh size, then digested in HCl and HF to remove carbonates and silicates, respectively. *Lycopodium* tablets (containing a known number of spores) were added to each sample to determine the concentration of palynomorphs per volume of sediment (cm^3). Because they are dyed red, the marker *Lycopodium* spores are easily distinguished from in situ *Lycopodium* spores. The residue was mounted on slides in glycerine gel and examined using a Zeiss Ultraphot light microscope.

To ensure that the data are statistically significant, 300 dinocysts were counted in most samples. A few samples provided lesser counts but the number of cysts always exceeded 200. The same procedure was followed for pollen. Spores, organic linings of foraminifera and reworked palynomorphs were also counted.

3.3.1 Quantitative reconstructions

The Best Analogue method of Guiot (1990), adapted for dinocyst assemblages by Rochon et al. (1999), was used to reconstruct summer and winter temperature and salinity, and the duration of an ice cover equal to or greater than 50% of the sea surface. The reconstructions are based on the GEOTOP database of 540 reference sites throughout the North Atlantic and adjacent basins. Because the Scotian Shelf was poorly represented in the database, the author added 26 new sites from the Scotian Shelf and the northwest Atlantic (appendices 2 to 9). This addition to the dataset provides better coverage of sea surface conditions and modern dinoflagellate cysts assemblages in the study area.

Percentage abundances of 30 selected taxa (see Rochon et al. 1999) were logarithmically transformed; then, using the same weight (same importance) for each taxa, the 10 closest modern analogues were selected within the reference database. This set of analogues provides the paleoenvironmental data. The most probable estimate for each sea surface parameter is calculated on the weighted average of these environmental data. The minimum and maximum environmental values in the set of analogues are used to define the confidence interval.

With the present database, temperature reconstructions are accurate to ± 1.15°C for February and ± 1.44°C for August. Salinity reconstructions are accurate to ± 2.00 psu for February and August. For the duration of the sea ice cover, the accuracy of reconstructions is ± 1.4 month per year (Rochon et al. 1999).

Despite their close geographic proximity, the sites from the Estuary and Gulf of St. Lawrence were not selected as analogs because their dinoflagellate assemblages present significant differences with those of the Scotian Shelf. Cysts of the genus *Impagidinium* are absent, and proportions of *Ataxiodinium choanum* are much lower, while the proportions of *Selenopemphix quanta* are much higher. These differences are due to the environment. The Estuary and Gulf of St. Lawrence are enclosed water masses with important fresh water inputs, where the seasonal ice cover has a duration of 2 to 3 months per year. The Scotian Shelf is an open marine environment with limited fresh water inputs and ice is present only in the northwest sector of the Scotian Shelf around Cape Breton and for at most 20-40 days per year (Drinkwater et al. 1999).

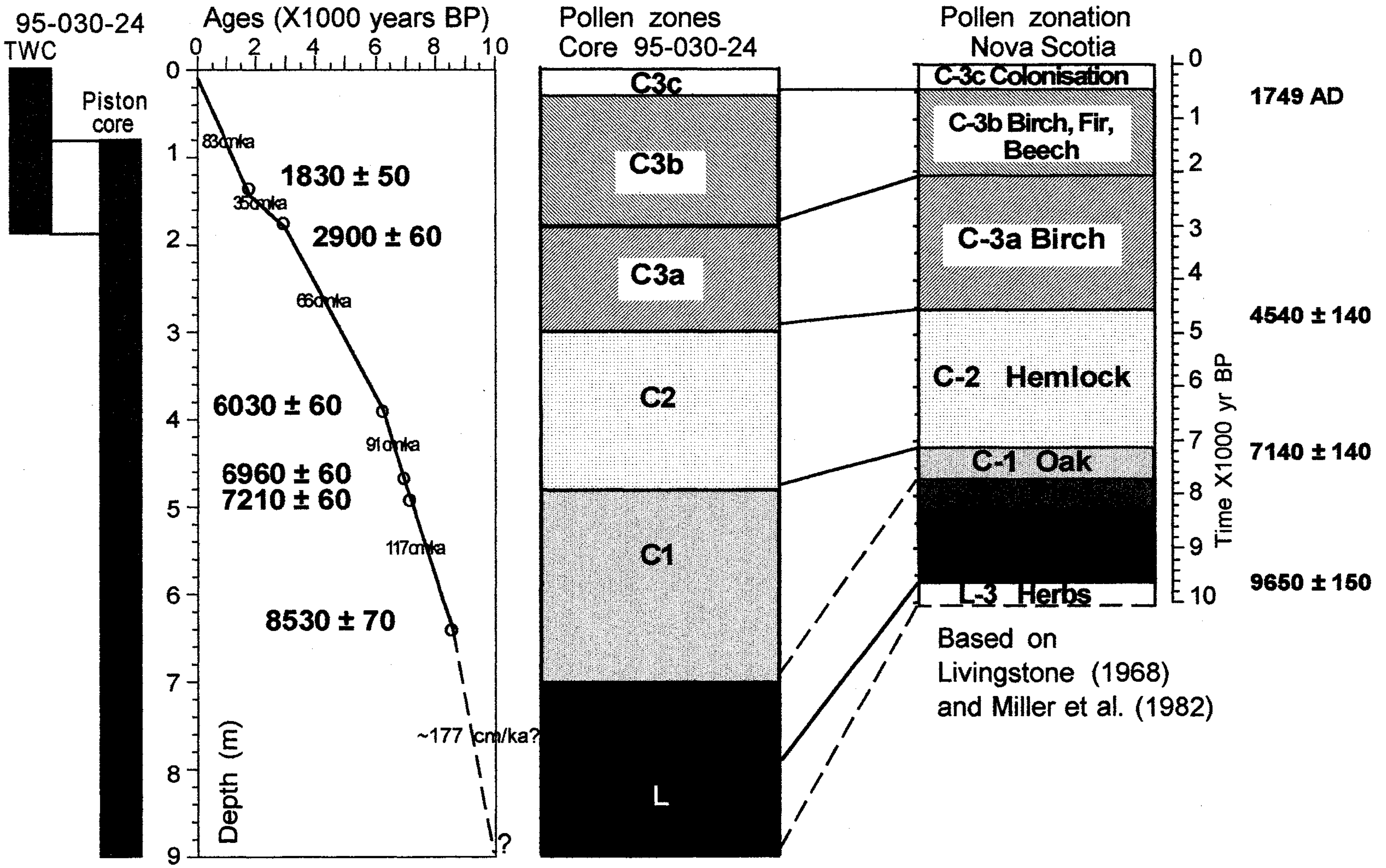

Figure 3.3: Correlation between the trigger and piston cores. The overlap is 80 cm. Marine pollen zonation is correlated with the pollen zonation from Nova Scotia lakes (Livingstone 1968; Miller et al. 1982). Maximum age of core assumed not to be older than 10,000 years BP.

3.4 Results

3.4.1 Palynomorph concentrations

Dinoflagellate cysts and pollen grains are the most abundant palynomorphs in core 95-030-24, with concentrations higher than 10,000 cysts or pollen grains per cm^3 of sediment in most samples (fig. 3.4). Fern and moss spores are far less abundant, with concentrations generally around $1000/cm^3$ of sediment. Organic linings of foraminifera reach 10,000 $linings/cm^3$, presumably reflecting changes in benthic productivity (de Vernal et al., 1992a). Concentrations of benthic and planktonic foraminifera reach maximum of 2000 and 300 tests/cm3, respectively (fig. 3.4). Reworked palynomorphs (mainly trilete spores) are present in all samples, with concentrations varying from 100 to 600 $grains/cm^3$ throughout the sequence.

Dinoflagellate cyst concentrations (fig. 3.4) are the greatest in the lowest half of the core below 520 cm, suggesting greater phytoplankton productivity before 7500 BP. This peak of concentration occurs in the interval where the sedimentation rate is the highest. We can therefore assume that this acme is significant and would have been even more important without the dilution by the sediment. Concentrations of planktonic foraminifers follow a different trend, being close to zero between 580 and 720 cm and being the highest between 460 and 580 cm (fig. 3.4), above the peak in dinoflagellate cysts. Benthic proxies are in better agreement: the increased concentrations of organic linings between 520-560 cm coincide with peak concentrations of benthic foraminifers.

Fern and club moss spore concentrations are the highest at the base of the core, while pollen concentrations are relatively low, consistent with a postglacial vegetation where forests are not established yet. Also, because Polypodiaceae and *Lycopodium* are carried to the ocean mainly by fluvial transport (Mudie 1982), their greater proportions could suggest increased runoff.

In the upper 2 meters of the core, the concentration curves of dinocysts, pollen, spores and organic linings all exhibit the same trends. This is possibly correlative with sedimentation rate (intervals of greater/lesser winnowing of fine particles). However, the fact that the curve of reworked palynomorphs is totally different from the others argues against this.

3.4.2 Pollen assemblages

The pollen diagram (fig. 3.5) can be subdivided into 5 zones, based on the dominance of certain taxa, following Piper et al. (1990) who have summarized the late Quaternary pollen stratigraphy from Nova Scotia lakes. The pollen zones from La Have Basin were compared and correlated with the radiocarbon-dated pollen zones of Silver Lake (Livingstone 1968) and Bedford Basin (Miller et al. 1982; fig. 3.3).

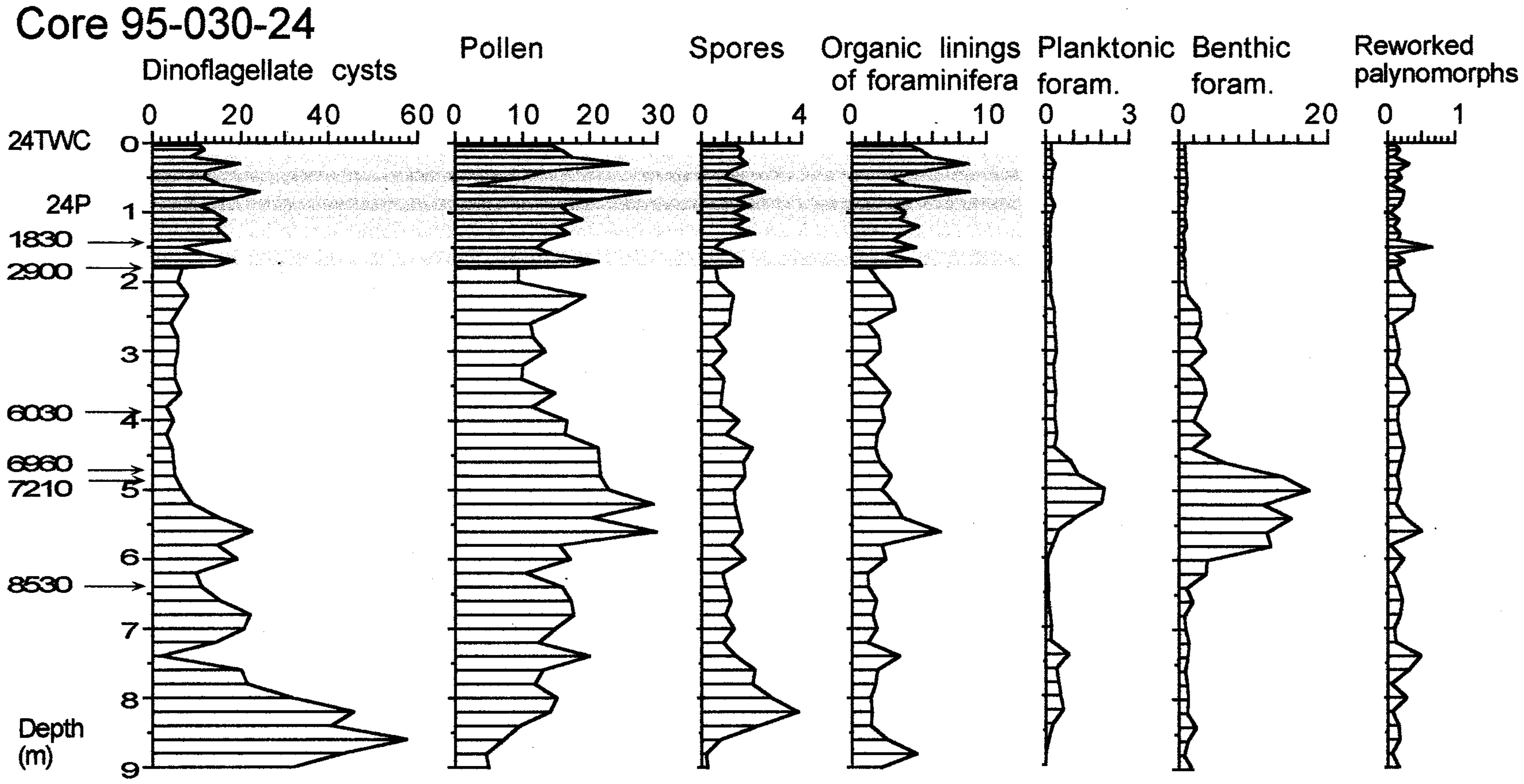

Figure 3.4: Concentrations of palynomorphs per gram of sediments (X10^3) in core 95-030-24. The vertical axis is the combined depth of the trigger weight and the piston cores (refer to fig. 3.3). Spores include mainly the Polypodiaceae and *Lycopodium* (*L. clavatum* and *L. lucidulum*) and *Sphagnum*. Radiocarbon ages are indicated on the left. Total foraminiferal concentrations (per 10 cm^3 sediments) are from Paul Mandell (unpublished data). The grey shading indicates intervals where similar trends are seen: light grey for increasing, darker grey for decreasing concentrations.

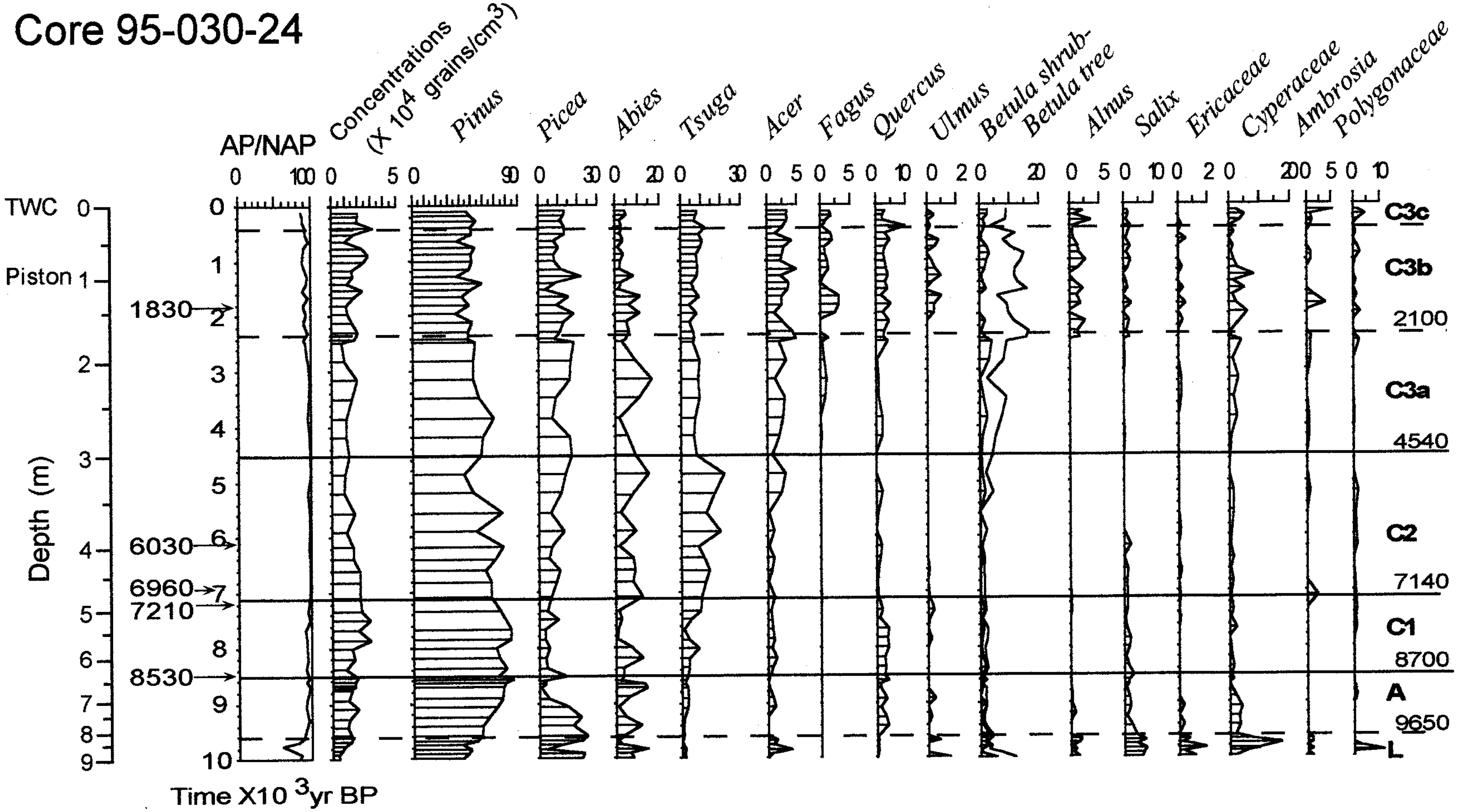

Figure 3.5: Pollen diagram of core 95-030-24 (trigger weight and piston). Pollen percentages were calculated on the pollen sum, which excludes spores. AP/NAP are the proportions of tree and non-tree pollen. Vertical axis is the corrected radiocarbon age. Scale on left indicates depth in core.

The marine pollen sequence shows a succession of assemblage zones very similar to that of Silver Lake. The main difference in composition between onshore and offshore assemblages is the smaller proportion of *Betula*, *Alnus* and *Tsuga* pollen at the marine site, as expected from the surface distribution studies of Mudie (1982) and Mudie and McCarthy (1994) which show that the proportion of these taxa decreases rapidly across the Scotian Shelf.

At the base of the sequence, the pollen assemblage L (probably L-3) is dominated by Cyperaceae, Polygonaceae and *Salix*, with minor amounts of *Betula*. The proportion of non-tree pollen is the highest in this zone. It probably corresponds to a tundra vegetation (the presence of *Picea*, *Tsuga* and *Acer* represents long distance transport). *Picea*, *Abies* and *Pinus* characterize pollen zone A between ~ 9500 and 8700 BP.

In the classical North American zones of Deevey (see Anderson 1985), zone A is followed by an interval characterized by a peak abundance of *Pinus,* zone B, and then an interval defined on a *Quercus* maximum, zone C1. In core 95-30-24, no zone B was defined because the peak abundance of *Pinus* does not clearly stand out and it occurs at the same time as the peak of *Quercus*. The same thing is observed at Silver and Bluff Lakes (Livingstone 1968).

Zone C1 (defined by the *Quercus* maximum) existed from ~8700 to 7100 BP. The pollen assemblages of this zone indicate the existence of a forest similar to present day forests around Halifax but the higher proportion of *Pinus*, *Tsuga*, *Fraxinus* suggests a warmer climate than today (Livingstone 1968).

The interval with the maximum abundance of *Tsuga* between 7100 and 4500 BP is assigned to zone C2. The *Tsuga* maximum is not as marked as at Silver Lake, probably because the proportion of *Tsuga* decline rapidly offshore as shown by modern pollen distribution (Mudie 1982). The abundance of *Tsuga* suggests a climate warmer than today.

Zone C3 is characterized by *Betula* (arboreal) and temperate hardwood pollen, but the proportion of these is lower in equivalent zones at Silver Lake and Bedford Basin. The midshelf location of the core site explains the poor representation of the temperate hardwood pollen (Mudie 1982; Mudie and McCarthy 1994).

The C3 zone has been subdivided into three subzones. Sub-zone C3a records an increase in percentages of *Betula* and the first occurrence of *Fagus*. In subzone C3b, the proportions of *Betula* (arboreal) and *Fagus* pollen reach their maximum, those of *Quercus* increase and *Ulmus*, *Alnus* and *Salix* are present again in the assemblages. The expansion of *Fagus* indicates a moister climate.

The base of subzone C3c corresponds to the European settlement of Nova Scotia (1750 AD) and the beginning of land clearance. In Emerald Basin the land clearance is indicated by an increase in non-arboreal pollen such as Gramineae, Compositae, *Ambrosia*, and *Rumex* (Mudie 1980). In La Have Basin, a slight increase in the representation of *Ambrosia* and Polygonaceae (including *Rumex*) in the upper 30-40 cm represents the base of zone C3c. However, the core failed to record the subsequent increase in grass pollen (Gramineae) and Compositeae, suggesting that the last 100 years are probably missing from that record.

3.4.3 Dinoflagellate cysts assemblages

Four dinocyst assemblage zones are recognized based on the dominance of the main taxa (fig. 3.6).

Before 9.5 ka, (zone 1) cyst concentrations reach their maximum and there is a major abundance peak of cf. *Alexandrium tamarense*. Other dominant species are *Pentapharsodinium dalii* and *Operculodinium centrocarpum*. *Brigantedinium* spp., *Bitectatodinium tepikiense* and *Spiniferites elongatus* are also present. A similar assemblage was found in Emerald Basin in the early Holocene (Scott et al. 1984).

Several of the dinocyst species dominating the assemblages of this zone are known to produce harmful algal blooms (cf. *Alexandrium tamarense*[1], *O. centrocarpum*, *Spiniferites* spp.). Influxes for these taxa range from 50 to 1800 cysts per cm^2 per year (Mudie et al. 2002) and suggest that large red tide blooms occurred at this time. For comparison, Mudie et al. (2002) calculated that a concentration of at least 500 cysts/cm^3 of sediment corresponds to more than 1000 cells/ml of water and a level of toxicity at which shellfish harvest must be closed.

At the base of zone 2, between 9.5 and 7.3 ka, *P. dalii*, *O. centrocarpum* and *B. tepikiense* are the dominant taxa. Higher in zone 2 (after 8.5 ka), *Islandinium minutum* also becomes one of the dominant species with *O. centrocarpum* and *P. dalii*. Proportion of *P. dalii* and total concentrations gradually decreased in this zone.

---

[1] Similar cysts were called *A. excavatum* by Simard 1996. Rochon et al. 1999 call them *A. tamarense*

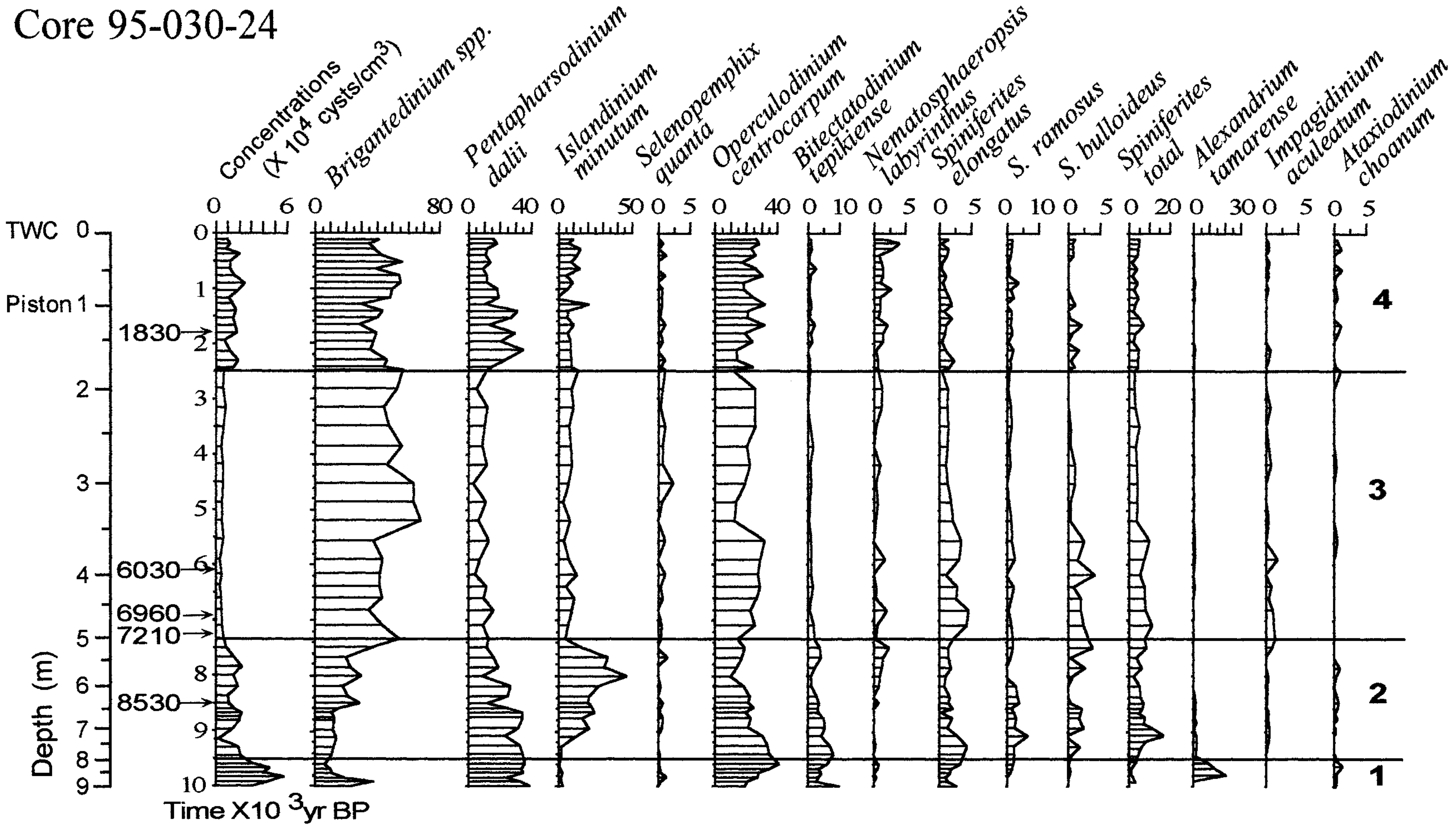

Figure 3.6: Dinoflagellate cyst diagram of core 95-030-24 (trigger weight and piston). *Brigantedinium* spp. includes *B. cariacoense* and *B. simplex*. *Spiniferites* total includes mainly *S. elongatus, S. ramosus, S. bulloides*. Vertical scale is the corrected radiocarbon age. Small scale on left is downcore depth.

In zone 2, cysts that ressemble those of cf. *A. tamarense* (Rochon et al. 1999) are sporadically present and always in very small proportions but other (non-toxic bloom-causing) species are still abundant. Influx of *O. centrocarpum*, *S. elongatus*, *S. ramosus*, *S. bulloideus* were high at the beginning of zone 2 but gradually declined while the proportions of *I. minutum*, a cold water taxon, increased to a maximum (40-45%) at ~8 ka. This suggests that conditions initially favourable to blooms and high productivity, gradually deteriorated.

Brigantedinium spp. and *O. centrocarpum* become the dominant species in zone 3 (7.3 to 2.5 ka). Taxa that were dominant in the previous zone, such as *I. minutum*, *P. dalii*, and *B. tepikiense*, are still present but their proportions are much reduced. The assemblages of zone 3 differ from the modern ones by their lower percentages of *P. dalii* and higher percentages of *Impagidinium aculeatum* between 7.5 and 5.5 ka. Today, the distribution of *I. aculeatum* appears to follow more or less the path of the Gulf Stream (Mudie 1992). It is found on the southwest Scotian Shelf but not on the northeastern sector of the shelf where waters are colder. This assemblage indicates that sea surface conditions were fairly similar to the present day, but possibly with a stronger influence of Gulf Stream water.

In zone 4, (2.5 ka to present) assemblages are similar to zone 3, with *Brigantedinium* spp., *O. centrocarpum* as the dominant species but with greater proportion of *P. dalii.* Concentrations increase slightly and influx of some non-toxic bloom causing species (especially *O. centrocarpum*) increase slightly.

3.4.4 Chronological problems of Emerald Basin core 77-002-20

The definition of a time frame for Emerald Basin core 77-002-20 is difficult to achieve due to disagreement over the validity of the ^{14}C ages used to date that core. Efforts are being invested right now at Dalhousie University, to obtain sufficient amounts of foraminifera for AMS dating. New ^{14}C ages should be available in the coming months (fall 2002-winter 2003) and solve the mystery. In the meantime, caution must be exerted.

Three radiocarbon dates were available for core 77-002-20: 10,100 ± 300 years, 11,500 ± 300 years, and 12,100 ± 360 years at 3-3.25 m; 4-4.25m and 6.75-6.95m. They were based on molluscs. If these radiocarbon ages are correct, the upper 3m of core 77-002-20 would represent the Holocene.

According to David B. Scott (Dalhousie University, personal communication 2002), these radiocarbon ages are incorrect. The very low percentages of *Elphidium excavatum*, a species typical of ice margin sediments (Scott et al. 1984) preclude an age older than Holocene for the lower part of the core (below 4 m). If so, the whole core is believed to be Holocene, with *Cassidulina laevigata* defining the mid-Holocene warm interval from 4.5 m (approximately 8 ka) to 2 m (approximately 2.5 ka) on the ground that *C. laevigata* is not abundant north of Cape Cod today (Scott et al. 1984).

In contrast, Peta J. Mudie (Geological Survey of Canada, Atlantic, personal communication 2002) strongly believes that these ages, included in the pollen and dinocyst diagram of Scott et al. (1984), are indeed valid. The dominance of *Brigantedinium* spp. and *A. minutum* in dinocyst assemblages from the lower half of the core with are very similar to those of Baffin Bay (Mudie and Short 1985), and the North Water Polynya (northern Baffin Bay; Levac et al. 2001). Pollen assemblages also compare well with the established onshore palynostratigraphy (Livingstone 1968; Livingstone and Livingstone 1958; Davis and Webb 1975; Anderson 1985; Piper et al. 1990). Pollen assemblages from the L-Zone are mainly composed of pioneer species that are hardy and do not like shade (*Betula, Alnus, Salix*, Ericaceae). Relatively high amounts of *Quercus* probably represent hardy variety of oak able to grow on sandy and nutrient poor soils, possibly exposed banks (Mudie 1980).

Comparison of dinoflagellate cyst assemblages also support the idea that the Holocene starts at 3 m in core 20. In La Have Basin core 95-030-24, a small peak in *I. minutum* between 8.5 and 7 ka is followed by an increase in the percentages of *Brigantedinium* spp. (Levac 2001). A similar succession is seen in Emerald Basin core 20 above 2.5 m. This supports the idea that only the upper 3 m of core 20 represents the Holocene.

In view of these various arguments, one should be cautious. In the meantime, the age chronology proposed by David B Scott will be used for Emerald Basin.

3.5 Transfer functions and sea surface reconstructions

Sea surface temperature (February and August) was periodically higher than present between the base of the core, until 8.5 ka (fig. 3.7). After 8 ka, August temperature generally remained around today's value, except around 6 ka where it was slightly cooler (by about 3°

C). It decreased slightly in the last 500 years of the record. Temperature in February was slightly lower than today between 8.5 and 6.5 ka, but then it was generally warmer (on average 2° C) than present since 6.5 ka, except for recurrent colder episodes, at intervals of 1000 years.

Throughout the sequence, salinity for February and August both show trends that are similar to the February temperature. Sea surface salinities were 1 to 2 psu higher before 8.5 ka. Between 8.5 and 6.5, they were below today's values (1 to 1.5 psu lower). After 6.5 ka, salinities oscillated around today's values. Short episodes with an ice duration of 1 month per year were reconstructed around 9, 5, 2.5 and 1.5 ka but given the precision of the method (± 1 month), they are insignificant.

3.5.1 Comparison with terrestrial records

In La Have Basin, sea surface temperature up to 5°C warmer than present are reconstructed before 8 ka (fig. 3.7). This is consistent with an early Holocene summer insolation maximum (Kutzbach and Webb 1993). The hypsithermal lasted at least 2500 years at La Have Basin. Onshore, the hypsithermal (characterized by air temperature 0.5°C warmer than today), is delayed relative to the marine environment. Summer temperatures of 16-17°C are reconstructed from pollen data (McCarthy et al. 1995) before 9 ka. This is close to the present day average of 17.5°C. The interval between 9 and 8 ka was a rapid transition toward the hypsithermal, with an increase in July temperatures from 17 of 20°C. The hypsithermal lasted longer onshore, with July temperature remaining almost 3°C higher than today from 8 to ~2 ka. Gajewski et al. (2000) also reconstructed summer temperatures 0.5 to 2.5°C higher than today in Nova Scotia during the hypsithermal (6 ka).

The reconstructed sea surface temperature and salinity are 1 °C and 1 psu lower between 8 and 6.5 ka. From 6.5 until the present, the reconstructed sea surface temperatures and salinities are characterized by frequent oscillations around the present day average (fig. 3.7). No such cooling or temperature fluctuations are recorded by lake pollen records.

Terrestrial records indicate a cooling in the last 2000 years (McCarthy et al. 1995; Livingstone 1968). There is no clear indication of a similar cooling of the sea surface in the La Have Basin (fig. 3.7) core although the evidence is clear in Canso Basin on the eastern Scotian Shelf and in Emerald Basin with stable oxygen isotopes (Scott et al. 1984) .

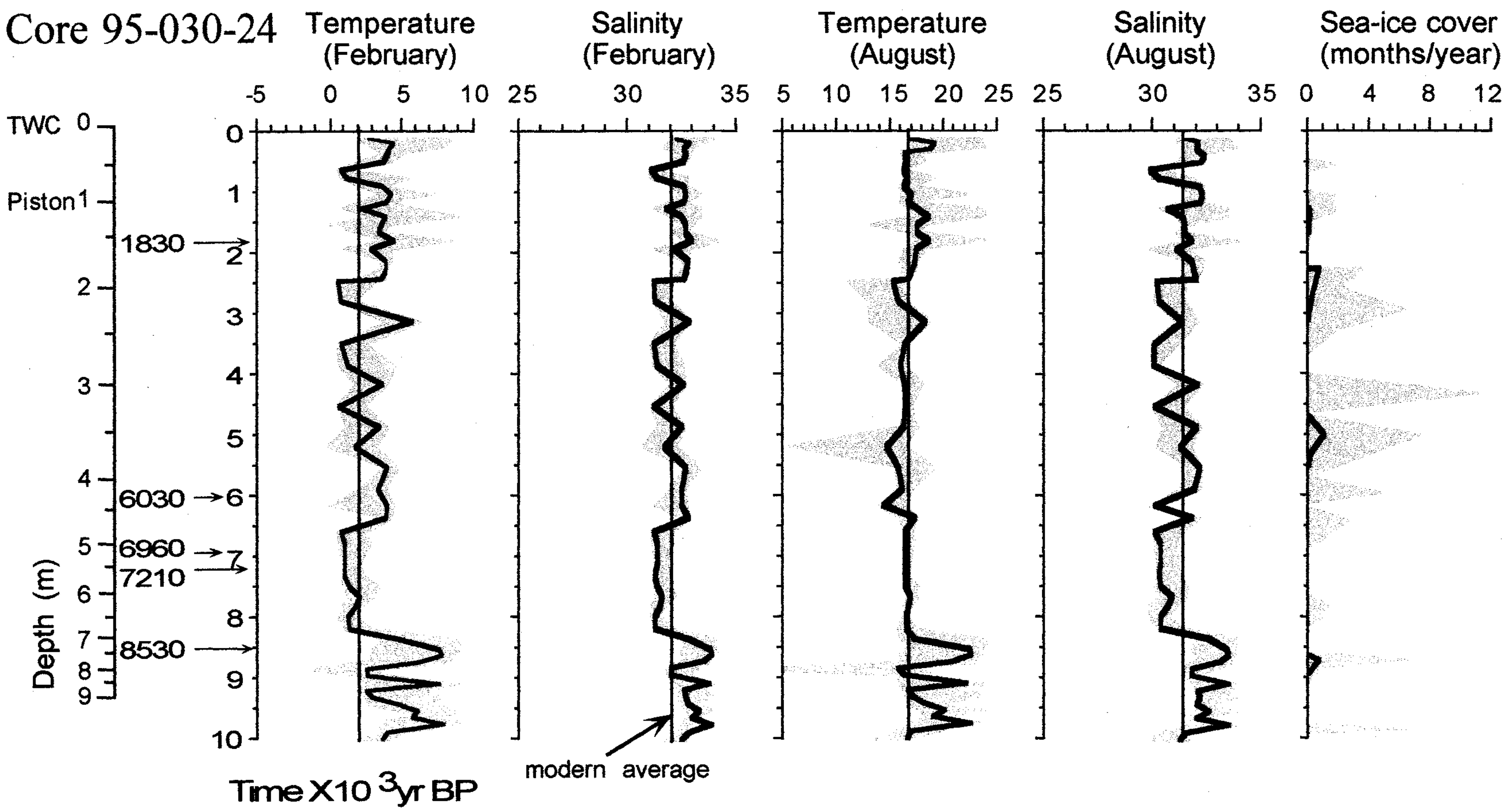

Figure 3.7: Reconstructions of sea surface conditions from core 95-030-24. The solid line represents the best estimate while the grey area corresponds to the confidence interval. The vertical line across each curve indicates modern values. The duration of time for which at least 50% of the sea surface is covered by ice. Vertical scale is radiocarbon age, small scale on the left is downcore depth.

3.6 Discussion

3.6.1 Hypsithermal

In La Have Basin, the hypsithermal occurred early (10-8ka) and lasted ~2500 years. Regionally, the hypsithermal is apparently also recorded in Bedford Basin (Miller et al. 1984), Emerald Basin (Mudie 1980; Scott et al. 1984; 1989a) in Cabot Strait (de Vernal et al. 1993; Keigwin and Jones 1995), Laurentian Fan (Keigwin and Jones 1995) and Fogo Seamounts (Mudie 1992). On the Laurentian Channel and Fan, the hypsithermal is recorded between 10-6 ka. (Keigwin and Jones 1995) but their resolution is very low.

Many authors have suggested a northward shift in the position of the Gulf Stream or a decreased influence of the Labrador Current to explain the warmer sea surface conditions along the Eastern margin of North America during the late glacial-early Holocene (Fillon 1976; Vilks and Rashid 1976; Balsam 1981). Rahman and de Vernal (1994) suggested that the Labrador current was not flowing into the southeastern Labrador Sea before 9 ka and that it intensified after 8.4 ka. Another possibility is the offshore diversion of the Labrador Current because of shallower banks around Newfoundland and on the Scotian Shelf. The sea level was 35-40 meters lower than today (Stea et al. 1994; Edgecombe et al. 1999) and the rugged topography of the Scotian Shelf, with its deep basins and shallow banks, has a great influence on the structure and variability of the circulation (Smith and Schwing 1991).

A decreased influence of the Labrador Current might also explain the higher sea surface temperatures in winter at a time where the winter insolation was lower than today (COHMAP 1988).

The hypsithermal ended sooner (~8 ka) in Cabot Strait, La Have and Canso Basins, than in Emerald Basin and Fogo seamounts (~2 ka). Today, one branch of the Nova Scotia Current flows over La Have Basin and the influence of the Labrador Current, even if it is indirect, is greater in La Have Basin than in Emerald Basin. This could explain the different timing between these two basins. Similarly, the Fogo Seamount is located further offshore and is under the influence of the Gulf Stream.

The start of the hypsithermal was delayed on land but it lasted longer (McCarthy et al. 1995). Delays caused by the migration of the temperate forest vegetation may partly explain this time lag. However, the aforestation in Nova Scotia was rapid, probably in response to the establishment of conditions favourable to forest development and expansion (Green 1985). The presence of cold air south of the remaining Laurentide ice sheet is most likely responsible for this delay. Despite its much reduced size and height and the fact that the remaining ice sheet was located on Quebec-Labrador at that time, climatic models show that it still had an influence on the climate of northeastern North America (COHMAP 1988; Vettoretti 1998).

3.6.2 Mid-Holocene cooling

The reconstructed sea surface temperature and salinity are slightly lower in winter between 8 and 7 ka. This corresponds with the maximum abundance of the cold water species *I. minutum*. Regionally, this peak of *I. minutum* is recorded at about the same time in Emerald Basin (Scott et al. 1984), Cabot Strait and the Gulf of St. Lawrence (de Vernal et al. 1993), and at Cartwright Saddle on the Labrador Shelf (Levac and de Vernal 1997). Keigwin and Jones (1995) mention a short-lived cool interval around 7.1 ka in the Laurentian Channel and the Laurentian Fan (based on ^{18}O measurements of planktonic foraminifers) that they interpret as the last meltwater pulse from the residual ice sheet. These meltwaters probably transited through the Labrador Current because sea surface temperature reconstructions from Cabot Strait do not show a cold interval at that time (de Vernal et al. 1993). Furthermore, the relatively stable ^{13}C profile measured on benthic foraminifera from Canso Basin (NE Scotian Shelf), indicative of constant salinities, argues against greater water influx from the Gulf of St. Lawrence at any time during the Holocene (Scott et al. 1989a).

Other shorter episodes of lower temperature and salinity in La Have Basin occur after 7 ka. They have a duration between 50 and 300 years and a recurrence of 1000 years. They might also represent episodic pulses of increased ice melting. Scott and Collins (1996) suggested, based on evidence from sea level records, that melting in the Arctic was enhanced by the hypsithermal, with a certain lag, and continued later than previously believed, until ~4 ka. Bond et al. (1997) identified numerous ice rafting debris events, accompanied by increased proportions of cold water foraminifera (*G. quinqueloba* or *N. pachyderma*, depending on the location) throughout the Holocene, in cores from the North Atlantic. To explain these events, they proposed a periodic increase in export of ice from the Labrador sea.

3.6.3 Late Holocene cooling

The Late Holocene cooling has been observed in most marine records from the area (Mudie 1980; Scott et al. 1984; 1989a; Mudie 1992; Keigwin and Jones 1995) in the last few thousand years. To explain this cooling, Balsam and Heusser (1976) proposed a southward and offshore migration of the Gulf Stream after 4 ka while Fillon (1976) believed that the inner Labrador Shelf Current became stronger since 3.5 ka. Petrie and Drinkwater (1993) have indeed demonstrated that changes in the westward flow of the Labrador Current contributed to temperature and salinity (throughout the water column) on the Scotian Shelf between 1945-1990 AD.

When we consider the last few thousand years of core 95-030-24, a cooling of sea surface temperatures is not obvious (and only ~100 years are missing from the record). But if the late Holocene cooling along the Eastern Canadian margin is really due to changes in the surface currents, then the colder, lower salinity intervals that punctuated the last 7000 years in La Have Basin might be an indication of the influence of Labrador Current-derived waters as early as 7 ka. This might be equivalent to the late Holocene cooling observed elsewhere. The shelf would have been affected first by the cooling effect of the inner Labrador Current. Then, as the inner Labrador Current continued to intensify, the Gulf Stream would be deflected southward and the cooling effect would progress seaward, affecting the Laurentian Fan by 5 ka (Keigwin and Jones 1995) and finally the Fogo Seamounts at 2 ka (Mudie 1992).

The onshore climate was affected later by the late Holocene cooling (1-2 ka) as shown by lake pollen records (McCarthy et al. 1995; Livingstone 1968).

3.6.4 Paleoproductivity

High dinoflagellate cyst abundance and high percentages of bloom-causing species (especially cf. *Alexandrium tamarense*-type cyst) appear to have been a widespread phenomenon in the early Holocene. In La Have Basin, very high influx of cf. *A. tamarense* occurs between 9.5-10 ka, and a high influx of non-toxic bloom-causing species occurs between 10-8 ka. Locally, high influxes of cf. *A. tamarense* are reported in Emerald Basin in the early Holocene (Mudie 1980; Scott et al. 1984) and in Bedford Basin at ~7.7 and ~6 ka (Miller et al. 1982). High influxes are also recorded in the Gulf of St. Lawrence, Cabot Strait and the Laurentian Channel between 10 and about 8 ka (Simard and de Vernal 1998).

It is tempting to equate the high abundance of dinoflagellate cysts with a high primary productivity. The biologists' definition of productivity is very inclusive but in this study, with only one indicator, it is impossible to tell whether the "general" productivity was greater or if conditions were favorable to only one group of organisms, the dinoflagellates.

However, on a regional scale, high abundance was not restricted to dinoflagellate cysts which lends support to the interpretation of high abundance as being the result of high productivity. In a core from Cabot Strait, the maximum concentration of diatoms occurs in the early Holocene (Lapointe 2000). An abundance of fecal pellets around 9.3 ka in cores from the slope and rise east of Newfoundland probably denotes an increased zooplankton productivity (Schafer et al. 1985) on the continental slope.

The situation was different for foraminifera. In La Have Basin, concentrations of foraminifera (benthic, planktonic and organic linings) remained low until the concentrations of dinoflagellate cysts started to decrease around 8 ka (this paper; Dave Scott, comm. pers. 2000). In Emerald Basin, concentrations of foraminifera (benthic, planktonic) also increased after ~8 ka (Scott et al. 1984).

3.6.5 Causes of high dinoflagellate cyst abundance/ blooms

In the normal succession of phytoplankton dominance, diatoms dominate after winter-spring mixing, when water is replete in nutrients, but as the water column becomes stratified, nutrients are depleted and dinoflagellates replace diatoms as the dominant phytoplankton. Dinoflagellate blooms/red tides result from the unusual combination of high nutrients and low water turbulence (Margalef 1978). Depletion of nutrients is inevitable after the turbulent phase/diatom bloom of the spring, unless a larger amount of nutrient is available (Reynolds and Smayda 1998).

Therefore, an increased availability of nutrients is the most likely cause for the blooms in the early Holocene. Nutrients and organic matter were abundant in the suspended sediment from glacial meltwater, and exposed parts of the Grand Banks were probably another important source (Schafer et al. 1985). Peaks of terrestrial spore concentrations at that time also suggest increased runoff and support this hypothesis. One might argue that the turbidity caused by suspended sediment would reduce the availability of light and the productivity. MacIntyre and Cullen (1996) showed that rates of photosynthesis in the turbid waters of San Antonio Bay are comparable to the rates in clearer waters and furthermore, turbidity and mixing protect algae from photoinhibition.

The enhancement of water stratification in summer because of the warmer sea surface temperature provided the kind of low turbulence environment necessary for dinoflagellate blooms. Low turbulence and strong stratification appear to favor the development of blooms because they allow the cells to form aggregates (Carreto et al. 1986; Parkhill and Cembella 1999). *Alexandrium* has also a great competitive advantage: it has large daily migrational capability and can modify its behavior to adapt to changes in the distribution of nutrients (MacIntyre et al. 1997).

Greater storm or upwelling activity in the early Holocene might also have contributed to the dinoflagellate blooms by preventing a nutrient depletion resulting from the strong stratification and high productivity (Margalef 1978), and by allowing the resuspension of cysts into the photic zone, which is necessary to maintain the blooms (Therriault and Levasseur 1985; Carreto et al. 1986). Sandy laminae were more frequent in adjacent Emerald Basin (Campbell 1999) which suggests a higher storm frequency on the

Scotian Shelf. The ice sheet, even with its reduced size at that time, caused a southward deflection of the Jet Stream (COHMAP 1988) and stormtracks tended to move along it (Kutzbach and Webb 1993). Before 9 ka, the westerly flows were also stronger (COHMAP 1988) and such winds are favourable to the formation of upwellings (Petrie et al. 1987).

When comparing the occurrence of similar early Holocene dinoflagellate blooms in records from the Scotian Shelf and the Pacific, Mudie et al. (2002) identified warmer summer SST as the only common factor. Indeed, where the peak of *Alexandrium* coincides with the hypsithermal (La Have, Emerald, Laurentian Channel), the concentrations of *Alexandrium* are much higher (10^4 cysts/cm^3 of sediments). In Cabot Strait and the Gulf of St. Lawrence, the peak of *Alexandrium* occurs before the hypsithermal and its concentrations are one or two orders of magnitude lower (10^2 to 10^3 cysts/cm^3 of sediments). This suggests that warmer SST are probably not the cause of the blooms but have an influence on their magnitude.

3.7 Conclusions

On the Scotian Shelf, sea surface conditions seem to lead climate warming in the early Holocene and perhaps climate cooling in the late Holocene. They also reflect important changes in the surface circulation.

The marine hypsithermal, characterised by sea surface temperature up to 5°C higher than present, started around 10 ka and lasted about 2500 years. The onset of the hypsithermal onshore lasted longer, but was delayed by about 2000 years, probably due to cold air south of the remaining Laurentide ice sheet. Summer temperatures remained 3°C higher than today from 8 ka until 2 ka (McCarthy et al. 1995). The marine hypsithermal was followed by an interval of lower sea surface temperature and salinity between 8.5 and 7 ka, probably resulting from inputs of meltwater probably via the Labrador Current.

Frequent sea surface temperature and salinity oscillations are reconstructed after 7 ka. They have a recurrence of ~1000 years. It can be proposed that the intensification of the cold Inner Labrador Current occurred earlier than previously believed (Fillon 1976) and affected La Have Basin (at least indirectly) as early as 7 ka. Pollen records show a cooling in the last 1000-2000 years (Livingstone 1968; McCarthy et al. 1995).

The higher productivity and blooms of dinoflagellates in the early Holocene was probably the result of higher nutrient concentration from meltwater inputs, and stronger water column stratification during the summer. Cyst resuspension caused by increased upwelling and/or storm activity may also have contributed to the blooms. While they are probably not the cause of the blooms, warmer summer SST appears to have an influence on the magnitude of the bloom sizes.

CHAPTER 4 Palynological records from Bay of Islands, Newfoundland: direct correlation of Holocene paleoceanographic and climatic changes

Abstract

Recent studies around the southeastern Canadian Margin suggest a complex Holocene paleoceanographic history and difference in timing between events in the sea surface and changes in onshore climates. A high resolution palynological record from Bay of Islands (western Newfoundland) was used in an attempt to explain the occurrence of a cold interval following the thermal optimum in the sea surface, the apparent cyclicity of periodic cold SST intervals, and the lag in the start of the hypsithermal onshore. A record of changes in sea surface conditions was obtained with dinocyst proxy-data and paleobioclimatic transfer functions. Correlation of onshore-offshore pollen records was used to compare the evolution of marine and terrestrial environments.

At 9.5 ka, a dramatic decrease in concentrations of pollen and cysts was probably caused by a greater dilution by sediments during the drainage of a glacial lake. At the same time, dinocyst assemblages dominated by *Brigantedinium* indicate a colder environment and reconstructions show lower sea surface temperature and salinity until 8.6 ka. After 9.2 ka, pollen assemblages suggest the retreat of spruce and a return to a shrub-tundra vegetation. These suggest that both the marine and the terrestrial environments were affected by colder conditions, which may be the result of a large influx of glacial meltwater. The effect on the vegetation was delayed by about 300 years.

The end of the meltwater event was followed by the marine hypsithermal with SST up to 5 °C warmer than today until 6.8 ka. This corresponds to greater amounts of solar insolation in summer (which were still 7% higher than today at 9ka; Kutzbach and Webb 1993). During this interval, the expansion of boreal forest trees from Cape Breton, then from SW Newfoundland was probably made possible by an amelioration of the climate over Newfoundland. The expansion of more temperate tree species (*Fraxinus*, *Ulmus*, *Acer spicatum*) beyond the northern limit of their modern distribution suggests a warmer climate than today and the start of the hypsithermal onshore around 6 ka. The onshore hypsithermal may have been delayed by the lingering effect of the remaining Laurentide ice sheet on the regional climate. At that time however, SST in summer were cooler than today. The sea surface waters may have been affected by influx of meltwater from the Arctic until ~ 4 ka.

Increased proportions of spruce and sedge after 3.3 ka suggest a regional cooling trend, which was recorded later in the surface waters of the Bay (800 years ago) and was preceded by a interval of SST warmer than today between 4.1 and 1 ka. Numerous short-lived intervals of cooler SST could correspond with the 1-2 kyr ice rafting events identified in the North Atlantic.

These results suggest that sea surface conditions in the bay are controlled, at least indirectly by the position of the major currents and influx of meltwater, while Newfoundland climate remained under the influence of the Laurentide ice sheet until 6 ka, after which it is probably controlled by the position of air masses rather than by the conditions in the adjacent sea surface.

4.1 Introduction

The climate over North America and the sea surface conditions on the southeastern Canadian Margin were greatly affected during the Holocene by changes in the atmospheric and ocean circulation, and interaction of various forcings, including shrinking of the Laurentide ice sheet, meltwater discharge and solar insolation (COHMAP 1988).

The pollen records from lakes in Nova Scotia and in Newfoundland show major climatic changes during the Holocene (Livingstone 1968; Macpherson 1981, Anderson 1985; McCarthy et al. 1995). However, comparisons of these climatic changes with the paleoceanographic history is difficult due to a variety of problems: lack of quantitative reconstructions and lack of well constrained chronology, low resolution sampling and dissolution of planktonic foraminifera (Vilks and Rashid 1976; Scott et al. 1984; 1989a; Mudie 1992; de Vernal et al. 1993; Keigwin and Jones 1995). A recent palynological study of a core from La Have Basin, on the Scotian Shelf (Levac 2001), provided quantitative reconstructions of sea surface conditions, a higher resolution and better time constraint of paleoceanographic events. Results suggest that the surface water paleoceanography was more complex than previously believed and that the timing of major changes differed from the onshore climatic record.

Figure 4.1: Location map. Numbers indicate other cores cited in the text. Some numbers correspond to more than one core in places where sites are located too close together. Detailed bathymetry for Bay of Islands (inset) is shown on figure 2.

Marine sites:
1- Bay of Islands MD99-2225 (this study);
2- La Have Basin (Levac 2001);
3- Emerald Basin (Mudie 1980; Scott et al. 1984; 1989a; Vilks and Rashid 1976);
4- Canso Basin (Scott et al. 1984; 1989a);
5- NW Laurentian Channel (Simard and de Vernal 1998);
6- Anticosti Channel core 16 (de Vernal et al. 1993);
7- Anticosti Channel core 21 (de Vernal et al. 1993);
8- Esquimans Channel (de Vernal et al. 1993);
9- Notre Dame Channel (Scott et al. 1984);
10- Cabot Strait (de Vernal et al. 1993; Simard and de Vernal. 1998);
11- Laurentian Channel (Keigwin and Jones 1995);
12- Laurentian Channel (Simard and de Vernal 1998);
13- SW Grand Banks Rise (Simard and de Vernal 1998);
14- Laurentian Fan (Keigwin and Jones 1995);
15- Fogo Seamount (Mudie 1992).

Bays sites:
A- Mahone Bay (Mudie 1980);
B- Chezzetcook Inlet (Mudie 1980);
G- Port au Port Bay (Brookes et al. 1985; Forbes et al. 1993);
H- St. Georges Bay, Newfoundland (Brookes et al. 1985; Forbes et al. 1993);
17- St. Georges Bay, Nova Scotia (Schafer and Mudie 1980).

Terrestrial sites:
C- Compass Pond (Dyer 1986);
D- Southwest Brook Lake (Anderson and Lewis 1992);
E- Robinsons Pond and Joe's Pond (McCarthy et al. 1995);
F- Sugarloaf Pond (Macpherson 1995);
J- Deer Lake Basin (Vanderveer and Sparkes 1982);
K- Cow Head (Brookes and Stevens 1985);
N- Northwest Gander Lake (Vardy 1991).

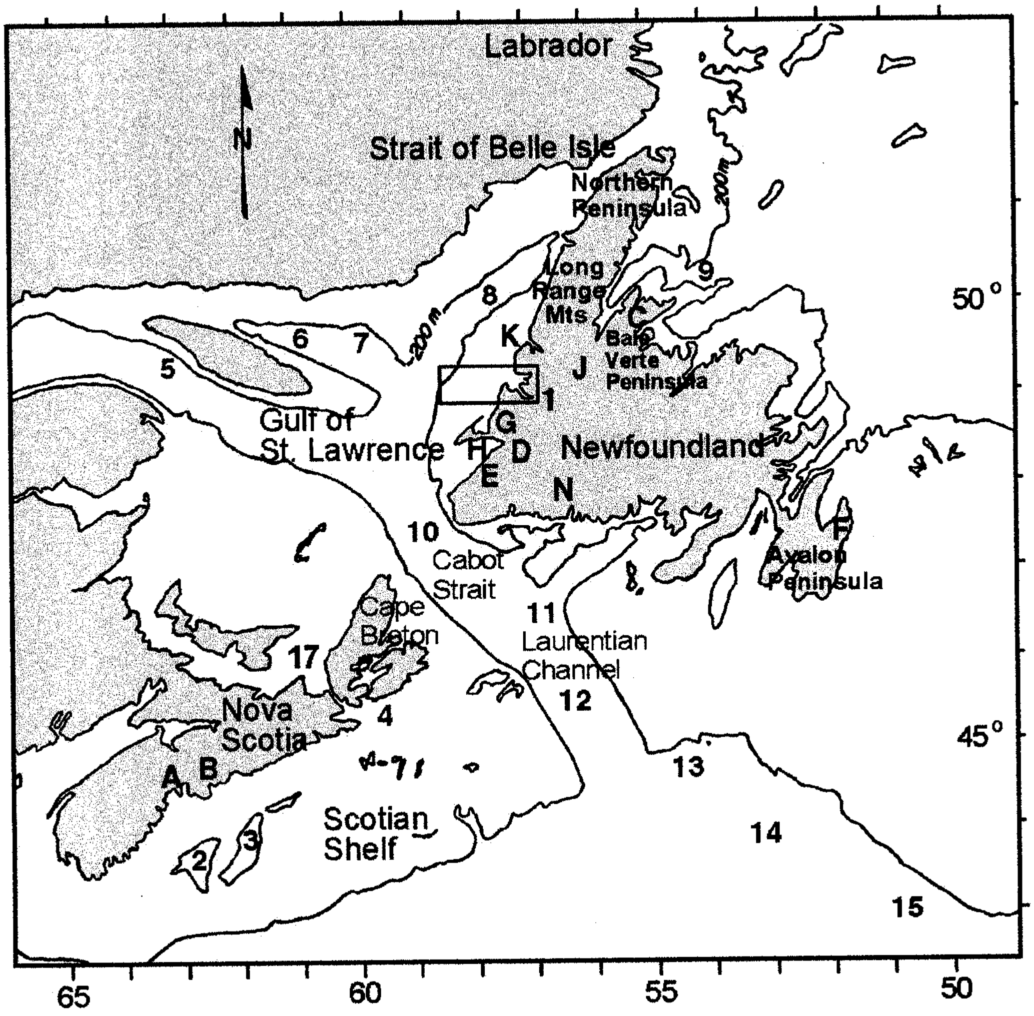

Figure 4.1: location map (caption on previous page)

A high resolution palynological study of radiocarbon-dated core MD99-2225 from Bay of Islands (Fig. 4.1 and 4.2), western Newfoundland, was undertaken in order to further investigate the Holocene paleoceanography and answer some of the questions about the difference of timing between paleoceanographic events and climatic changes. The goal was to obtain a century-scale record of changes in surface water conditions, provided by dinocyst proxy-data and to compare this with a record of changes in vegetation and climate recorded in the pollen assemblages.

The quantitative link between the distribution of dinoflagellate cysts and sea surface conditions in the North Atlantic (Edwards and Andrle 1992; Mudie 1992; Rochon et al. 1999) allows the use of transfer functions for the reconstruction of changes in sea surface temperature (SST), salinity and duration of the sea-ice cover. The method used in this paper is the paleobioclimatic transfer functions method described by Rochon et al. (1999). The position of air masses controls the distribution of vegetation zones in northeastern North America (Davis and Webb 1975) and pollen assemblages provide a record of changes in the vegetation and climate. Previous studies (Scott et al. 1984; Piper et al. 1990; Mudie and McCarthy 1994) have shown close correlation between onshore and offshore pollen sequences and evidence of the major climatic changes in regional marine deposits.

Comparison of the quantitative reconstructions from La Have Basin with previous studies in the area outlined three differences (Levac 2001) that will be addressed (investigated) in this paper: 1-A difference between the timing of the hypsithermal and the Neoglacial events in the ocean and on land; 2-The occurrence of colder SST than today right after the marine temperature optimum; 3-The occurrence of intervals with lower SST and salinity than today during the last 6500 years.

1- The comparison of SST with onshore climatic reconstructions from Nova Scotia (McCarthy et al. 1995) indicate a 2000 years lag between the occurrence of warm sea surface and the start of the hypsithermal in Nova Scotia (Levac 2001), as already suggested by Mudie (1980). The reverse scenario is seen for the Neoglacial, with an earlier onset in the climate (McCarthy et al. 1995; Livingstone 1968) than in the sea surface (Levac 2001). Levac (2001) proposed that this delay was due to the persistence of cold air south of the remaining Laurentide ice sheet rather than tree migration delays. Because it is located closer to the Laurentide Ice Sheet, Bay of Islands probably remained longer under the influence of the ice sheet and the delay might also be greater there. As for the Neoglacial, there are no explanations at this time.

2- It has been suggested that the cold SST interval that followed the marine hypsithermal in La Have Basin (8.5-6.5 ka) could be the result of meltwater discharge from the Laurentide ice sheet (Levac 2001) but the source is not known. Moore et al. (2000) mention a meltwater discharge (the Late Stanley event) through the Great Lakes-St. Lawrence River system between 8.5 and 7.5 ka. This event is absent in records from the Gulf of St. Lawrence and Cabot Strait (de Vernal et al. 1993), probably because of low resolution but it might be detected in core MD99-2225.

3- The occurrence of intervals with SST and salinity slightly lower than today during the last 6500 years cannot be explained by meltwater discharge from the ice sheet and could be equivalent to the millennial cycles of Bond et al. (1997; 1999). Variations of

SST and salinity in La Have and St. Anne's Basins are small however. In core MD99-2225 the Holocene section is represented by 18 m of sediment (compared to 10 m in La Have Basin) which should provide better reconstruction of the size and frequency of these variations.

4.2 Environmental setting

4.2.1 Location and surface circulation in adjacent Gulf of St. Lawrence

Bay of Islands is a located on the west coast of Newfoundland, north of Port au Port Bay (fig. 4.1). It is a large bay of about 300 km^2,with maximum water depths of 200 m (fig. 4.2). The regional topography has elevation ranging from 0 to 800 meters asl.

Core MD99-2225 was taken in the Humber Arm, in the east side of the bay (48° 59.88'N; 58° 05.08'W), in a water depth of 104 m, about14 km from the Humber River and 11 km from Corner Brook (fig. 4.2). Most of the bay is deeper than the adjacent shelf. The sill depth at the entrance of the bay is less than 100 m deep on the southern side, and less than 40 m deep on the northern side. There is also a sill (<100 m) at the entrance of the Humber Arm.

The Gulf of St. Lawrence is a highly stratified, semi-enclosed sea which receives 600 km^3 of freshwater annually, most of it (84 %) from the St. Lawrence River system (Koutitonsky and Bugden 1991). It is connected with the North Atlantic Ocean through the Cabot Strait and Belle Isle Strait. The general circulation in the Gulf is cyclonic.

Labrador coastal water enters on the north side of the Strait of Belle Isle (fig. 4.3), branches around Anticosti Island, then joins the outflow from the St. Lawrence River to form the Gaspe Current (El-Sabh 1976). Within the Gulf, one branch flows out along the southern side of the Laurentian Channel and a smaller one flows over the Magdalen Shallows (Han et al. 1999). The outflow is along the western side of Cabot Strait. On the east side of Cabot Strait, there is a weak inflow from the Atlantic Ocean, with one branch moving northeastward along western Newfoundland toward the Strait of Belle Isle (El-Sabh 1976). Bay of Islands is therefore influenced primarily by the inflow of Inner Labrador Current through Cabot Strait and by the sea surface conditions in the eastern sector of the Gulf of St. Lawrence.

4.2.2 Sea surface conditions

During the winter, the temperature is below 0 °C all over the Gulf. Sea surface temperatures are more variable in summer (Han et al. 1999), ranging from 12 to 16 °C (Petrie et al. 1996b). Seasonal changes in surface temperature are large (10 to 15 °C) (Han et al. 1999). In Bay of Islands, the average SST in February is -0.4 °C and in August, it reaches 16.96 °C (NOAA 1994).

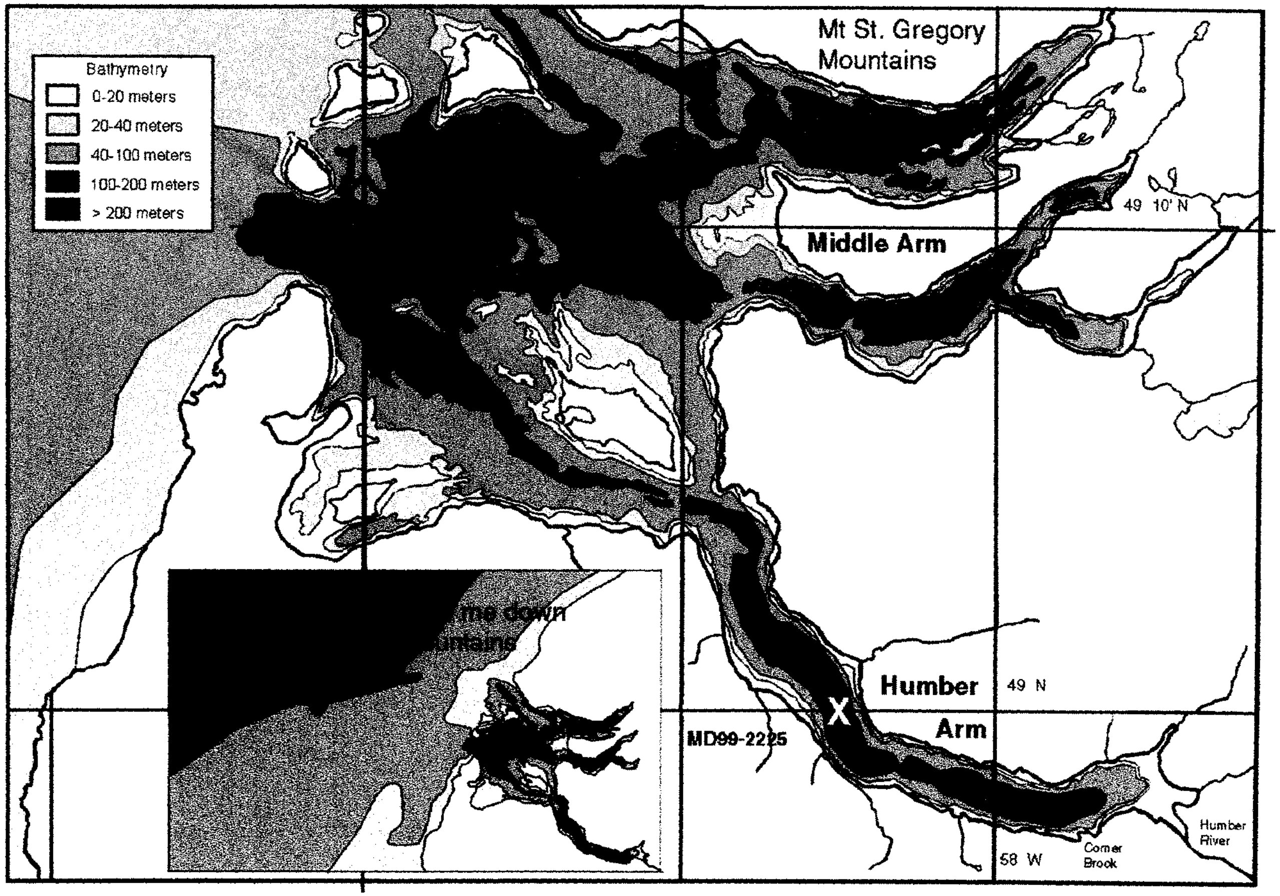

Figure 4.2: Bathymetric map of Bay of Islands. Water depth is in meters. The location of the coring site is indicated by an X (modified from Geological Survey of Canada, 1958).

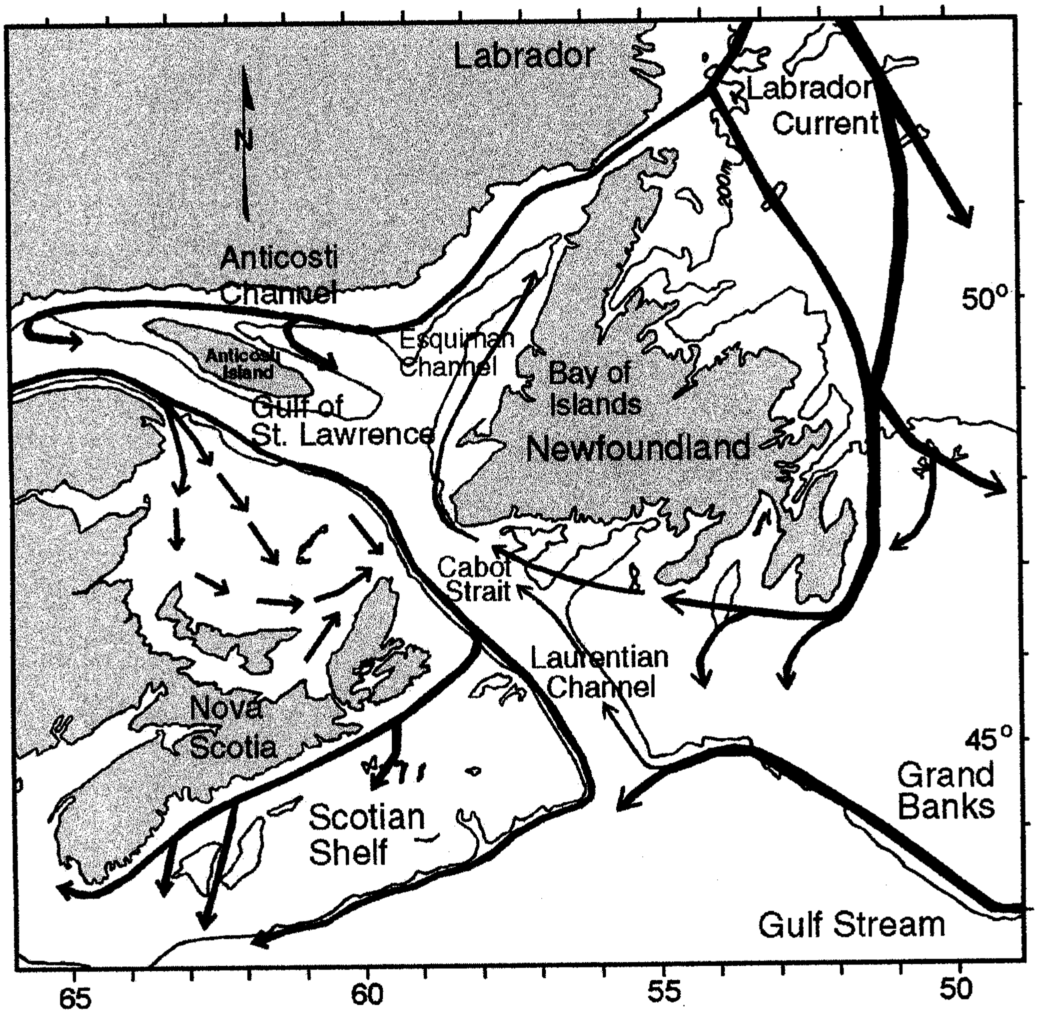

Figure 4.3: Surface circulation in the Gulf of St. Lawrence, around Newfoundland and on the Scotian Shelf (based on Greenberg and Petrie 1988; Han et al. 1999; Shore et al. 2000). bathymetric contour is 200 m.

Sea surface salinity ranges from 30 to 32 psu in winter and from 28 to 30 psu in summer (Petrie et al. 1996b). The peak of freshwater discharge occurs in the spring (Han et al. 1999), from April to June (Koutitonski and Bugden 1991) and highest salinity is found in the Strait of Belle Isle, away from the St. Lawrence river influence (Petrie et al. 1988). Salinity in Bay of Islands is the same as in the Gulf: the averages are 32 in February and 30.65 in August (NOAA 1994; Petrie et al. 1996b).

On the shelf along the west coast of Newfoundland, including Bay of Islands, sea ice is present for 2 months per year, on average. The ice first appears at the end of January and disappears at the end of March (Drinkwater et al. 1999). In the west part of Newfoundland, most rivers are frozen around mid-December and clear of ice around mid-April (Banfield 1983).

4.2.3 Climate

The climate of Newfoundland is greatly influenced by the cold Labrador Current. The Gulf of St. Lawrence also influences the heat and moisture properties of air masses coming from the west (Banfield 1983). Most of the year, the climate of Newfoundland is controlled by the mean core of the Jet Stream. In winter, the dominant wind is from the northwest while in summer, it comes from the southwest. In April and May, cold winds and low sea surface temperatures may delay the spring season.

The west coast of Newfoundland around Bay of Islands, experiences a better climate because the Long Range Mountains provide a protection against the cold winds from the north and east. The Humber Arm is a sheltered embayment where calm or low velocity winds are more frequent, and fog is rare (Banfield 1983). The Humber Arm is also characterized by higher mean daily temperature maxima than other parts of western Newfoundland (Banfield 1983) and a higher mean annual temperature (5 °C around Bay of Islands compared to 4 °C for the rest of western Newfoundland; Ullah 1992). The mean air temperature in Bay of Islands in February is -7.5 °C, in August, 15 °C (Environment Canada 1984). Total annual precipitation ranges from 1150 mm per year in the Humber Arm area, to 1300 mm per year along the northern coast of the bay. The region also receives the greatest amount of snow along the west coast with a mean annual total of 400 cm per year (Ullah 1992).

4.2.4 Regional vegetation

The Bay of Islands is in the western Newfoundland ecoregion of Damman (1983). This ecoregion is characterized by the most favorable climate in the island for plant growth and more fertile soils. Because of high precipitation, forest fires are rare (Damman 1983).

In general, the region is heavily forested, with *Abies balsamea* as the dominant tree. Other conifers present are *Picea glauca*, *P. mariana* and *Pinus strobus*. (Damman 1983). Small stands of deciduous trees (*Betula* spp. and *Populus tremuloides*) can be found locally (Rowe 1972; Damman 1983). Some tree species reach their northern limit of distribution in this ecoregion: *Pinus strobus*, *Acer rubrum*, *Populus tremuloides*. This is the only Newfoundland ecoregion where *Fraxinus nigra*, which requires a long and warm vegetative season, is present, and where *Acer spicatum* is sufficiently vigorous to compete with other trees. *Acer spicatum* and *Alnus rugosa* thickets are common, while *Salix* thickets are sporadic (Damman 1983).

4.3 Core stratigraphy

Core MD99-2225 is 37.5 m long in total but only the first 18 m were analyzed for this Holocene study. The upper part of the core (0 to 14.7 m, with a void between 865-985 cm) is composed of dark grey to black clayey silt, and sandier in the upper 4 meters (fig. 4.4). Bioturbation is locally important. The clayey silt unit between 14.7 and 16.6 m shows grey and reddish brown banding and local lamination. Graded sequences are also common. Between 16.6 and 18 m, a lenticular silty clay with burrows shows similarities with the upper unit (Turon et al. 1999).

The clayey silt unit (14.7-16.6 m) has the appearance of an outburst event (Rick Hiscott pers. comm 2001), and could be the result of the rapid drainage of a late-glacial lake in central Newfoundland through the Humber River. According to Shaw (pers. comm 2001), the red clay could come from erosion and re-suspension of red proglacial muds from the Deer Lake Basin. Proglacial lakes formed in the Deer Lake Basin area during the deglaciation, when the deposition of recessional moraines blocked the flow of rivers (Vandeveer and Sparkes 1982). The red mudstone and siltstones of the Deer Lake

Group (Mississipian) are probably the source of the red clay (see Vandeveer and Sparkes 1982).

A similar reddish brown clay unit is encountered in core 94138-104 from Humber Arm, very near the location of core MD99-2225 (Shaw et al. 1995). However, this unit is much younger, with a ^{14}C age of 5770 years on a shell. Evidence of slumping is present on the fjord sidewalls (Shaw et al. 1995) and it is also possible that this process was involved in the formation of the red clay unit.

Three radiocarbon ages were obtained for core MD99-2225 (table 1). An age of 3310 ± 60 ^{14}C years BP was measured for tree bark at 341 cm. The other ages were measured on bivalves: 9120 ± 90 ^{14}C years BP at 1440 cm (just above the upper red/laminated interval) and 10980 ± 80 ^{14}C years BP at 2166 cm. A marine reservoir correction was applied to ages measured on bivalves. These ages were calibrated using the program CALIB 4.3 (Stuiver and Reimer 1993; Stuiver et al. 1998) and results are shown also in table 4.1.

Table 4.1

Depth	Lab number	type of sample	^{14}C age	cal. yr. BP
341 cm,	TO8459	tree bark	3310 ± 60 BP	3500 (3587-3470)
1440 cm,	TO8460	bivalve	9120 ± 90 BP	9725 (10400-10206)
2166 cm,	TO8461	bivalve	10980 ± 80 BP	12334 (13134-12924)

A linear interpolation was used to determine the ages between the radiocarbon dates. The sedimentation rates estimates used for the interpolation are higher at the base of the core and decrease toward the top. Between 12 and 10 ka cal BP, it is 280 cm/ 1000 yrs, between 10 and 3.5ka cal BP, it is 180 cm/1000 yrs and in the last 3500 cal years BP, it was only 100 cm/1000 yrs. According the these calculations, the age at the base of the studied section of the core (18m) is ~11,000 cal BP. The sampling interval was 20 to 30 cm in the first two meters of the core, and 50 cm between 2 and 18 meters. This corresponds to a resolution of 200 to 300 years throughout the core.

The author chose to refer to the radiocarbon ages throughout the paper, as numerous studies mentioned in this paper use non-calibrated. Also, one has to be aware that dissolved bicarbonate from the limestone bedrock around the Bay and freshwater inputs from rivers might affect the ^{14}C ages in Bay of Islands.

4.4 Methods

4.4.1 Laboratory procedure

Samples (5cm^3) were washed with distilled water through 120 and 10 micron sieves. This sieving removes the coarser fraction and part of the fine silt and clay. The sediment fraction between 10 and 120 microns was kept and underwent chemical processing. A tablet of *Lycopodium* spores was added to the sediment before processing in a Micro-digest 3.6, an automated focused microwave digestion system. The procedure followed was tested by Loucheur (1999) to ensure that the palynomorphs were not affected by the digestion. The sediment was first heated at 27% power, first with 10 % HCl for 15 minutes, then with concentrated HF for 20 minutes and finally, with $AlCl_3$ for

20 minutes. HCl and HF were used to remove carbonate and silicate. The $AlCl_3$ was used to neutralize HF. The chemical processing was followed by another wash with distilled water in a 10 microns sieve, to remove the residues from the digestion. Slides were mounted with glycerine jelly.

Counts reached a minimum of 300 dinocysts and a minimum of 300 pollen grain in most samples. This ensures the statistical significance of the data. Lesser counts were reached in only a few samples, in the lowest 4 meters of the studied section. Spores, organic lining of foraminifera, *Halodinium*, *Pediastrum* and reworked palynomorphs were also counted. *Lycopodium* spore markers were stained red, therefore they were easily distinguished from in situ *Lycopodium* spores. *Betula* pollen grains can represent either shrub or tree species and discrimination is based on size. Grains smaller than 20 microns represent shrub species and those with a diameter greater than 20 microns are assumed to represent tree species (Dyer 1986).

4.4.2 Transfer functions

The transfer functions used in this study is the Best Analogues method of Guiot (1990) adapted for dinocyst assemblages by Rochon et al. (1999). It was used to reconstruct summer and winter temperature and salinity, and the duration of a sea ice cover on more than 50% of the sea surface. The GEOTOP database of 540 reference sites throughout the North Atlantic and adjacent basins, to which 36 new sites from the

Scotian Shelf and northwest Atlantic were added (Appendices 2 to 9), was the basis of the reconstructions.

The first step was a logarithmic transformation of percentage abundance (see Rochon et al. 1999). Then, the 10 closest modern analogues were selected within the reference database, using the same weight for each taxa. The set of analogues provides the paleoenvironmental data, which are used to calculate the most probable estimate for each sea surface parameter. Each estimate is calculated on the weighted average of these environmental data, the weight being determined by the Euclidian distance (degree of similarity) between the fossil assemblage and each modern analogue selected. The minimum and maximum environmental values in the set of analogues are used to define the confidence interval. The temperature reconstructions are accurate to ± 1.15°C for February and ± 1.44°C for August. For salinity, the accuracy of the reconstructions is ± 2.07 psu and ± 1.98 psu for February and August respectively. The reconstructed duration of the sea ice cover, is accurate to ± 1.3 month per year. The wide range of salinity values and its great variability in Arctic sites probably contribute to the relatively poor accuracy of salinity reconstructions but the lack of accurate instrumental data is probably the main cause for the poor accuracy of salinity estimates (see de Vernal et al. 2001).

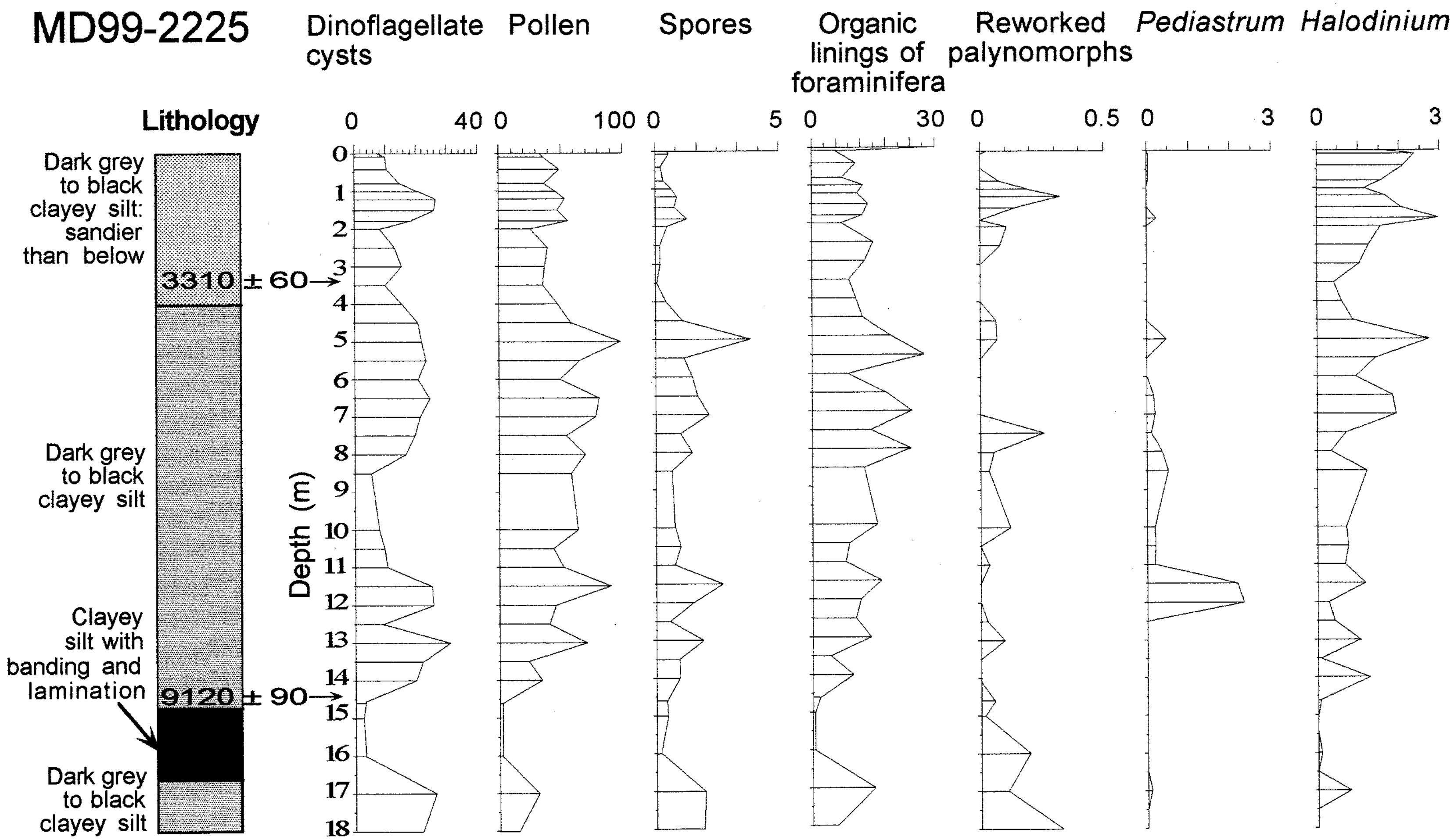

Figure 4.4: Concentrations of various palynomorphs per gram of sediments (x10^4). Spores include mainly Filicales (Osmundaceae and Polypodiaceae), *Sphagnum* and *Lycopodium* (*L. annotinum, L. clavatum* and *L. lucidulum*). Two radiocarbon dates are shown.

4.5 Results

4.5.1 Palynomorph concentrations

Most palynomorphs are fairly abundant in sediments of core MD99-2225, except for the interval between between 14 and 17 metres (fig. 4.4). Lower concentrations from 5 to 2.5 meters affect all palynomorphs and is probably the result of higher sedimentation rates.

Marine palynomorph concentrations are comparable to those found in sediments from the western sector of the Gulf of St. Lawrence, the Scotian Shelf and the northeast Newfoundland shelf (see Scott et al. 1984; Rochon et al. 1999; Levac 2001). Concentrations of dinoflagellate cysts (Fig. 4.4) are between 10,000 and 30,000 cysts/cm^3. Concentrations of organic linings of foraminifera, which indicate benthic foraminifera productivity, are between 5000 to 30,000 linings/cm^3. Concentrations of both marine microfossil groups drop to much lower values between 14 and 17 m, where sedimentation rates are much higher.

Palynomorphs of terrestrial origin (pollen and spores) are abundant and their concentrations are comparable to those of lacustrine environments (20,000 to 100,000 pollen grains/cm^3; 2000 to 5000 spores/cm^3).

Low concentrations of *Pediastrum* are found in most samples (below 500 coenobia/cm^3), except for a peak between 11 and 12 m (7.8-7.3 ka cal BP). As most extant species of *Pediastrum* live in freshwater environments (Batten 1996), it was probably transported by streams from a nearby lakes or ponds into the Humber Arm. The peak could be an indication of increased freshwater inputs. It could also be caused by nutrient input from sediment slumping, as *Pediastrum* likes nutrient-rich waters (Batten 1996).

Halodinium, an acritarch with unknown biological affinities is present in concentrations between 1000 and 3000 individuals/cm^3, becoming more abundant in the later half of the Holocene. *Halodinium* appears to have more affinity with low salinity marine environments: its concentrations in the sediments increase from the lower St. Lawrence Estuary toward the Gulf, while it is absent from the upper Estuary (Giroux 1990). *Halodinium* is more abundant near the Mackenzie Delta plume, in the Beaufort Sea, and near glacier meltwater plumes in the Baffin Bay (Mudie 1992).

Reworked Tertiary palynomorphs are present in very small concentrations (<500 palynomorphs/cm^3), throughout the core. They include mainly trilete spores, a few dinocysts (including *Hystrichokolpoma*) and pollen of gymnosperms (and one fenestrate Compositae).

4.5.2 Pollen assemblages

Zone 1: 18-14.6 m depth, 10,050 to 9200 BP (11,000 to 9850 cal yrs BP)

The pollen assemblages (fig. 4.5) at the base of the studied section (zone 1a) are dominated by shrub and conifer pollen, with herb pollen. Shrubs include *Betula* and

Alnus, with *Salix* and Cyperaceae. Herb pollen of *Artemisia* and *Ambrosia* and Polygonaceae is present. The vegetation around Bay of Islands at that time was probably a shrub tundra.

In subzone 1b, percentages of *Picea* and herbs increase and those of *Betula* decrease. At other sites from southwestern Newfoundland, the increase in *Picea* is interpreted as the establishment of a spruce forest in the region (Anderson and Lewis 1992; Macpherson 1995). If *Picea* really arrived in southwestern Newfoundland around 10 ka (Anderson and Lewis 1992; Macpherson 1995), probably migrating from Cape Breton (see Green 1987), it is reasonable to believe it reached Bay of Islands by 9.5 ka. The drop in pollen concentrations between 9.5 and 9.2 ka is probably the result of higher sedimentation rates (see discussion).

Similar peaks of *Betula*, followed by a peak of *Picea* percentages, as in subzones 1a and 1b are seen in the other pollen diagrams from southwestern Newfoundland. At Joe's Pond, this correspond to subzones 1a and 1b, dated 10.5-9.7 ka and 9.7 to 9.5 ka (McCarthy et al. 1995). At Southwest Brook Lake, the corresponding zones are numbered 4 and 5 (dated 10.2-9.7 ka and 9.7-9.5 ka), and at Woody Hill Brook Pond, they are numbered 2 and 1 (Anderson and Macpherson 1994). The same trends are seen at Romaine River (Anderson and Lewis 1992) but the pollen diagram has not been divided into zones.

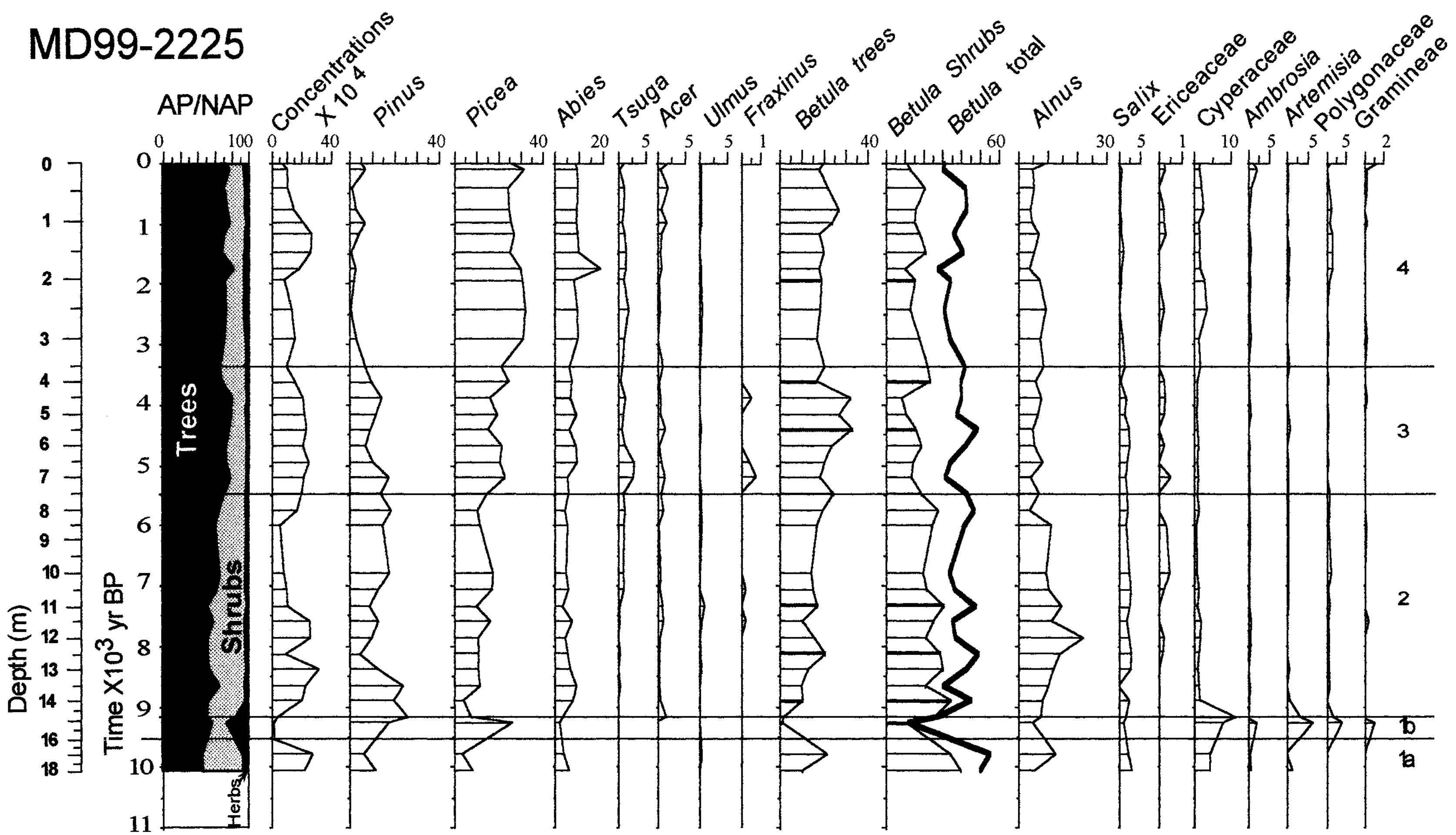

Figure 4.5: Pollen diagram of core MD99-2225. Pollen percentages were calculated on the pollen sum, excluding spores. Proportion of tree, shrub and herb pollen is shown on the left. *Betula* pollen smaller than 2 microns are assumed to represent shrub variety. The solid line, right of the shrub-*Betula* curve is the total *Betula* pollen, i.e. shrub and tree. The vertical axis represents radiocarbon ages.

Zone 2: 14.6 to 7.5 m, 9200 to 5500 BP (9850 to 5850 cal yrs BP)

In zone 2, pollen assemblages are dominated by *Betula* (mainly shrub), conifers (*Pinus*, *Picea*, *Abies*) and *Alnus*. Herbs and Cyperaceae are less important compared to the previous zone. Zone 2 is also characterized by the presence of small percentages of *Tsuga*, *Acer*, and the sporadic occurrence of *Ulmus* and *Fraxinus*. Ericaceae appear in the assemblages. Pollen concentrations increase at the lower half of the zone and decrease again after 7.5 ka, but are never as low as in subzone 1b.

Overall, zone 2 probably represents the development of the boreal forest. As previously mentioned, *Picea* probably arrived in the area ~9.5 ka. According to Macpherson (1995) *Abies* followed *Picea* within a few centuries. The increased percentages of *Pinus* pollen between 9.2 and 8.6 ka could represent the arrival of this species. There is evidence for the presence of *Pinus* at Southwest Brook Lake, located 70 km south of Bay of Islands, around 8.5 ka (Macpherson 1995). The Humber Valley is more sheltered, and possibly became warm enough to allow an earlier establishment of *Pinus*.

After 8000 BP, the main components of the present day forests in the western Newfoundland ecoregion are represented in the pollen assemblages. However, the relative proportions of the more thermophilous trees (*Acer*, *Ulmus*, *Fraxinus*, tree *Betula*) remain low. The increased proportion of *Alnus* pollen could represent the expansion of shrubs on the hills around the Bay.

The drop in *Picea* percentages and the coincident increase of shrub *Betula* at the beginning of zone 2 (9.2 to 8.6 ka) are also seen in the other pollen records from western Newfoundland (Joe's Pond, Romaine River, Southwest Brook Lake and Woody Hill Brook Pond; McCarthy et al. 1995; Anderson and Lewis 1992; Anderson and Macpherson 1994), immediately following the *Picea* peak of the previous zone. There are two possible interpretations for this interval, one of which is the return of the shrub tundra because of a climatic deterioration (Anderson and Lewis 1992), the other being the expansion of shrub birch heath on higher or more exposed areas (Macpherson 1995). These two hypothesis will be examined further in the discussion.

Zone 3: 7.5 to 3.5 m, 5500 to 3300 BP (5850 to 3500 cal yrs BP)

Zone 3 is characterized by increased proportions of total tree pollen and higher percentages of thermophilous trees *Acer rubrum*, *A. spicatum* and *Fraxinus nigra*. Percentages of *Picea* also increase, while those of *Alnus* decrease. The proportions of tree *Betula* are greater than those of shrub *Betula*.

The increase of *Acer*, *Fraxinus* and tree *Betula*, and the decline of shrub birch, suggest expansion of hardwood forest, probably reflecting warmer summers and a longer growing season than today. The decrease of *Alnus* pollen and the increase of *Picea* could indicate the expansion of *Picea* on the slopes, where it replaced *Alnus*.

These assemblages present many differences with those of time equivalent assemblages at Joe's Pond and Southwest Brook Lake and are difficult to correlate. This probably indicates difference in the composition of the vegetation around the lakes and the bay (see section 4.7.5).

Zone 4: upper 3.5 m, last 3300 years BP (3500 cal yrs BP)

Zone 4 is characterized by a decrease in *Pinus* and tree *Betula* pollen, and an increase in *Picea*, sedge, and shrub pollen. *Fraxinus* is absent. These changes suggest colder, moister climate. A small increase of *Ambrosia* and Gramineae pollen in the last 400 years could represent the recent settlement of the area by Europeans.

Similar changes are also seen in other pollen diagrams from the area, but they occur earlier, around 5ka. A decrease in *Pinus* and an increase in Cyperaceae occur in zone 3 of Joe's and Robinson's Ponds (McCarthy et al. 1995). At Southwest Brook Lake, there are increased proportions of *Picea* (Macpherson 1995).

4.5.3 Modern dinoflagellate cyst assemblages

The dinoflagellate cyst assemblage at the top of the Bay of Island core is different from most assemblages in the adjacent Gulf of St. Lawrence, St. Georges Bay being the exception. The assemblage is dominated by *Brigantedinium* spp. (38%) and *Operculodinium centrocarpum* (30%) with *Pentapharsodinium dalii* (8%) and *S. ramosus* (11%). In surface samples from St. Georges Bay, total *Peridinium* make up to 31% of the assemblages, *O. centrocarpum* 10 to 20%, *P. dalii* 3 to 7% and *S. ramosus* 8 to 21%

(Mudie 1980, 1992; Schafer and Mudie 1980). In surface samples from eastern Cabot Strait, assemblages are dominated by *P. dalii* (40%) and *O. centrocarpum* (30-33%), with *Brigantedinium* spp. (11-15%) and much smaller proportions of *S. ramosus* (1%) (Giroux 1990; de Vernal and Giroux 1991).

The assemblage from Bay of Islands also differ from those from bays along the southern coast of Nova Scotia by their lesser percentages of *B. tepikiense*. In the inner part of shallow (<15 m) silled bays such as Mahone Bay, assemblages are dominated by *B. tepikiense*, present in proportions of more than 60%. In bays where the oceanic influences are stronger (greater sill depth or deeper basins), *O. centrocarpum* and Peridiniales are the dominant species and the proportions of *B. tepikiense* are comparable to those of Bay of Islands. (Mudie 1980; 1992; Mudie and Harland 1996).

Minor taxa that are occasionally represented by 1-2 cysts in surface samples from Nova Scotia bays reach larger proportions (>1-2%) in Bay of Islands and are usually present throughout the core. These include *P. dalii*, *N. labyrinthus* and *Ataxiodinium choanum*. *Islandinium minutum* is absent from the Nova Scotia bay assemblages.

4.5.4 Dinoflagellate cyst assemblages

Two taxa are dominant throughout the Holocene: *Brigantedinium* spp. and *Operculodinium centrocarpum.* The assemblages have been divided into 4 zones, based on the proportions of the accompanying species.

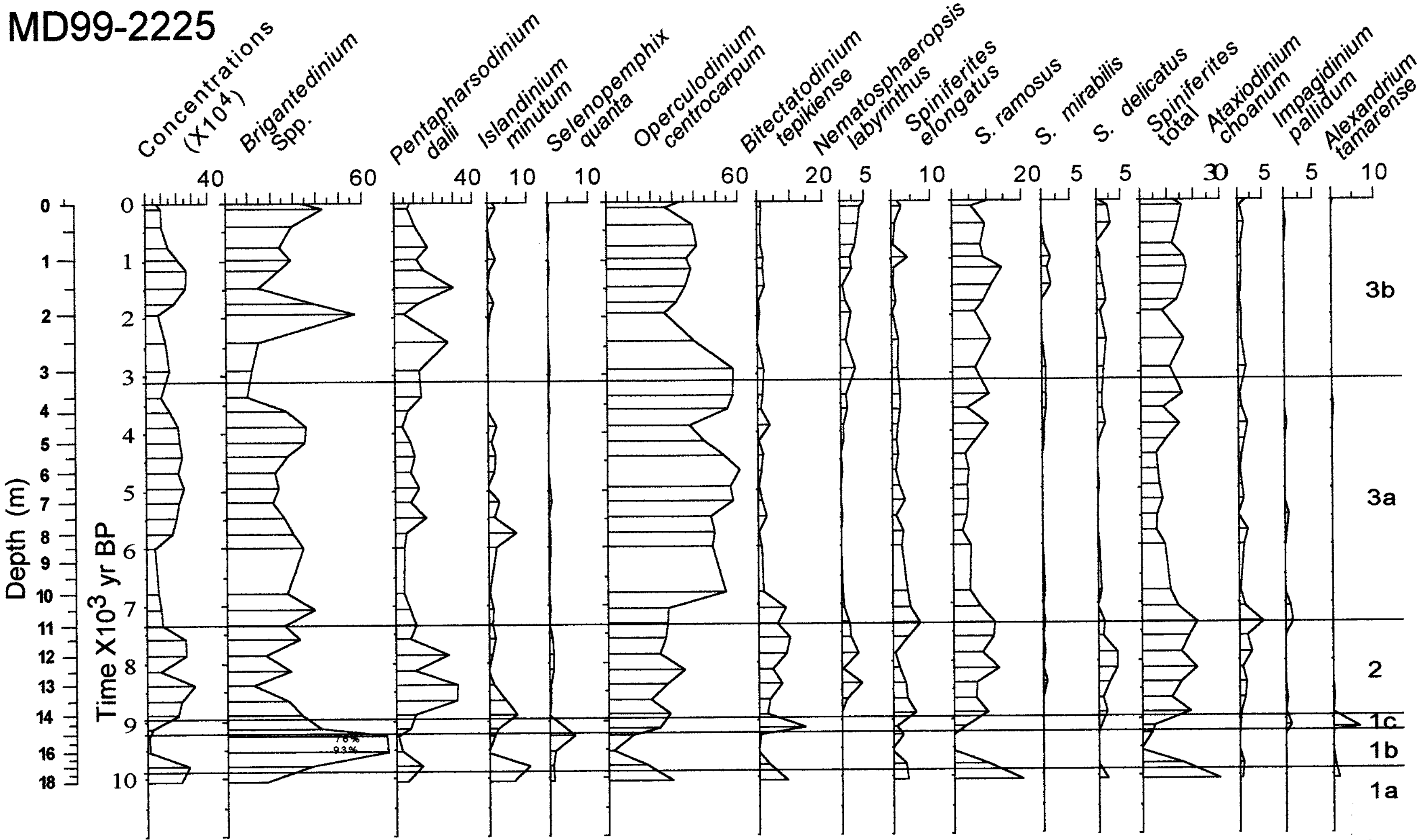

Figure 4.6: Dinoflagellate cyst diagram for core MD99-2225. *Brigantedinium* spp. includes *B. cariacoense* and *B. simplex*. *Spiniferites* total includes *S. bulloides*, *S. delicatus*, *S. elongatus*, *S. frigidus*, *S. mirabilis*, *S. ramosus*. The vertical axis represents radiocarbon ages.

Zone 1: 18 to 13.5 meters, 10,050 to 8600 BP (11,000 to 9300 cal yrs BP)

Zone 1 assemblages are dominated by *Brigantedinium* spp., with *Operculodinium centrocarpum* and *Spiniferites ramosus.* The other taxa, *Pentapharsodinium dalii, I. minutum, Selenopemphix quanta, Bitectatodinium tepikiense* and *Spiniferites elongatus* are also present in significant proportions. It is the only zone in which cysts similar to *Alexandrium tamaranse*[1] (Rochon et al. 1999), a species known for causing red tides, is important. Zone 1 has been divided into three subzones, based on the proportion of *Brigantedinium.*

The assemblages of subzone 1a resemble those from the Gulf of St. Lawrence or the Scotian Shelf. In subzone 1b, the assemblages are almost monospecific with up to 93% of *Brigantedinium*, and suggest harsher conditions and lower sea surface temperature (Mudie and Short 1985; Mudie and Rochon 2002). Concentrations also drop sharply due to higher sedimentation rates. In subzone 1c, assemblages and concentrations similar to those of subzone 1a suggest the end of the harsh sea surface conditions and increased concentrations indicate reduced rates of sedimentation.

Zone 2: 13.5 to 10.5 m, 8600 to 7000 BP (9300 to 7600 cal yrs BP)

Assemblages of zone 2 have great species diversity. Four taxa, *Brigantedinium* spp., *O. centrocarpum*, *P. dalii* and *Spiniferites ramosus* dominate the assemblages. Also,

---

[1] Similar cysts called A. excavatum by Simard 1996

the proportions of some of the accompanying taxa (*B. tepikiense*, *Ataxiodinium choanum*, *S. delicatus*) are the highest in this zone.

Zone 2 is also characterized by the first occurrence of *Spiniferites mirabilis* and *Nematosphaeropsis labyrinthus*. *N. labyrinthus* appeared around 7800 BP in core 111 from Cabot Strait and almost simultaneously in cores from the Gulf of St. Lawrence (de Vernal et al. 1993).

The reduced percentages of *I. minutum* and the greater proportion of *S. mirabilis*, *B. tepikiense*, and *A. choanum* in this interval, suggests warmer sea surface conditions. *S. mirabilis* is more abundant when SST in August are greater than 15 °C, while *A. choanum* is more abundant in temperatures between ~10 and 17 °C (de Vernal et al. 1998). For *B. tepikiense*, August SST greater than 12 °C corresponds with higher percentages (Rochon et al. 1999).

The greater percentages of *B. tepikiense*, which is more abundant in shallow silled bays (Mudie 1980) could be interpreted as the result of a lower relative sea level causing an isolation of the Bay (shallower sill depth). However, while *B. tepikiense* is dominant (>60%) in some restricted Nova Scotia Bays (Mudie 1992), percentages of this species in zone 2 are comparable to those of La Have estuary (8-10%) where oceanic influences are strong (Mudie 1992), or to those of the Laurentian Fan (Rochon et al. 1999).

The relatively high proportions of *A. choanum*, also suggest that the bay remained open to the Gulf of St. Lawrence during this interval. This species rarely makes up more than 1% of modern assemblages (Rochon et al. 1999; this study), but assemblages from

St. Georges Bay, in the southwest Gulf of St. Lawrence seem to be the exception with up to 3% of *A. choanum* (Mudie 1980).

Zone 3: 10.5 to 3 meters, 7000 to 2900 BP (7600 to 3000 cal yrs BP)

This zone is dominated by *O. centrocarpum* and *Brigantedinium* spp. Most accompanying taxa are still present but their proportions are much lower. The resurgence of *I. minutum* (6 to 4 ka) could indicate a colder conditions.

The relative sea level (RSL) is believed to have reached its lowstand ~ 6.5 ka (Shaw and Forbes 1995), which is at the beginning of this time interval. As previously mentioned (see also section 4.7.2), the lowstand was probably only a few meters below the present day level. The dominance of *O. centrocarpum* and *Brigantedinium*, typical of bays with strong oceanic influences (Mudie 1980; 1992) supports this hypothesis.

Zone 4: Upper 3 meters, last 2900 years (3000 cal yrs BP)

The youngest zone is dominated by *Brigantedinium* spp., *O. centrocarpum* and *P. dalii*. Just as in zone 3, the accompanying taxa are only a minor component of the assemblages, but the proportions of *N. labyrinthus*, *S. ramosus*, *S. bulloideus*, *S. delicatus* and *S. mirabilis* increase slightly relative to zone 3. The base of this zone probably marks the establishment of modern sea surface conditions for Bay of Islands.

4.6 Reconstructions of sea surface conditions

Reconstructions of past sea surface conditions are shown on figure 4.7. SST and sea ice cover exhibit large changes throughout the Holocene, but salinity only shows large differences before 8500 BP (9300 cal yrs BP).

In the early Holocene (between 10,050 and 8600 BP; 11,000-9300 cal yrs BP), sea surface temperatures and salinities were lower than today. Temperatures were lower by ~1 °C in February and 3 to 7 °C in August, while surface salinities were between 3 to 5 psu lower than the present day average. Ice cover had a duration of 3 months per year, which is slightly longer than today.

In the interval between 8600 and 6800 BP (9300-7300 cal yrs BP), temperature was significantly warmer than today (by 2 to 5 °C) in February, and slightly warmer in August (~ 1 °C). Salinity was 1 to 2 psu higher than today. The seasonal duration of the ice cover was reduced.

Sea surface conditions were similar to the present day's conditions in the mid Holocene (6800-4100 BP; 7300-4400 cal yrs BP), except for August temperature, which was lower than today by about 3 °C.

Between 4100 and 1000 BP (4400-1000 cal yrs BP), sea surface temperatures and salinities were periodically much higher than today's average. Temperatures were up to 5 °C higher in February and salinities were about 2 psu higher. Around 4100 and 1400 yrs BP, there was no ice cover. SST cooled 800 years ago and August SST shows an increase of 2 °C in the past~ 200 years.

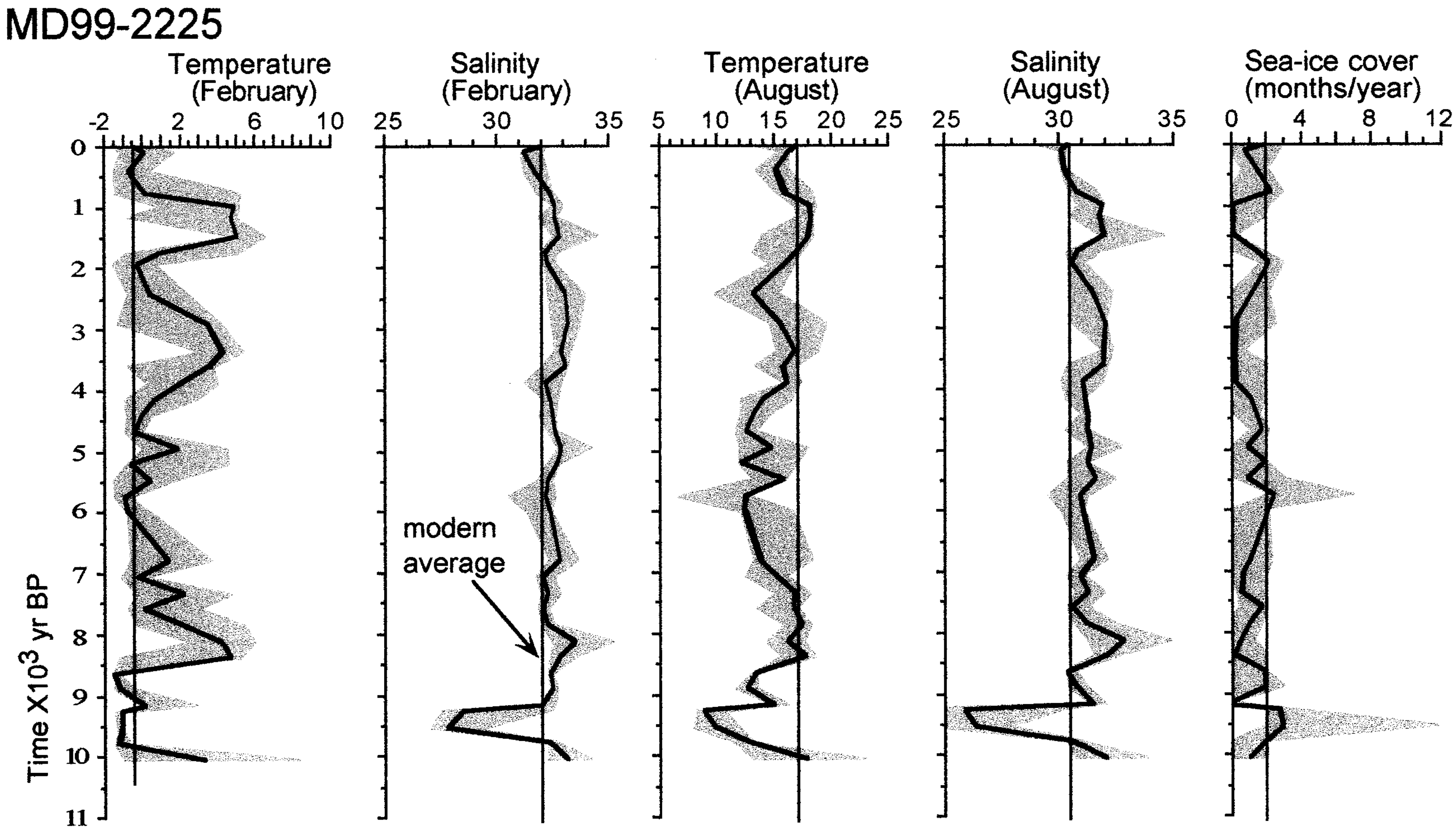

Figure 4.7: Reconstructions of sea surface conditions from core MD99-2225. Solid line represents the best estimate while the grey area corresponds to the confidence interval. The vertical line across each curve indicates modern values. The duration of the ice cover is the period of time for which at least 50% of the sea surface is covered by ice. The vertical axis represent radiocarbon ages.

4.7 Discussion

4.7.1 Deglaciation of the Island of Newfoundland

The age of the final deglaciation of Newfoundland is not known with certainty. Based on Dyke and Prest (1987), it occurred between 10 and 9 ka. Their maps of the deglaciation show a withdrawal of ice from the coasts by 13 ka, followed by melting in the interior part of the island. Basal dates from Baie Verte Peninsula lakes indicate that deglaciation occurred just before 12,000 BP (Dyer 1986). At 11 ka, the western coastal regions were deglaciated. The Newfoundland Ice Cap was much divided and diminished, with ice remaining on the Long Range Mountains and central Newfoundland (Dyke and Prest 1987). Some ages are available for the deglaciation of some central Newfoundland sites: 10,464 BP at Northwest Gander River Pond, 10,248 BP at Moose Pond (Vardy 1991). At 10 ka, only small ice caps remained. One of those covered the northern part of Deer Lake and the upstream of Humber River. The Dyke and Prest (1987) map for the 9ka time slice shows that no ice remained over Newfoundland.

It is also possible that the retreat of upland ice-caps was delayed until around 8 ka by an unnamed post-Younger Dryas cold interval, as suggested by the delayed onset of organic deposition at some high-elevation sites in western Newfoundland, and moraine deposits (Anderson and Lewis 1992; Anderson and Macpherson 1994; Macpherson 1995; Shaw et al. 2000).

4.7.2 Postglacial changes in relative sea level

Postglacial relative sea-level curves for western Newfoundland show a rapid emergence from an initial highstand, followed by a slow submergence from the lowstand to the present RSL. This corresponds to RSL type B of Quinlan and Beaumont (1981). Overall, it is in the early Holocene that the RSL fell below the present sea level (Shaw and Forbes 1995) but the age and depth below present of the postglacial lowstand vary from site to site.

There is unfortunately no RSL curve specifically for Bay of Islands, as most detailed studies from western Newfoundland focus mainly either on the Port au Port Bay or the Northern Peninsula, respectively south and north of Bay of Islands. In Port au Port Bay, Brookes et al. (1985) located the postglacial lowstand at 11 to 14m below the present level and placed it around 5800 ka, while Forbes et al. (1993) believed the lowstand was as low as ~25 m below the present level and occurred as early as 9500 BP. At Cow Head, north of Bay of Islands, the RSL minimum was reached ~ 6500 BP and was only a few meters below the present level (Brookes and Stevens, 1985; Shaw and Forbes 1995).

In a compilation of RSL data for the whole island Shaw and Forbes (1995) illustrated the diachronous nature of the postglacial RSL lowstand, as it occurred later (and was also shallower) in region closer to the former centre of ice loading than offshore. Their map indicates a lowstand 6 m below the present sea level in the Humber Arm, and they estimate it occurred around 6500 BP.

The increase in concentrations of *Halodinium* after 5500 BP (fig. 4.4), could be an indication of greater oceanic influences (or influences from the Gulf) as this palynomorph is more abundant in the Gulf of St. Lawrence than in the Estuary (Giroux 1990). This would be consistent with a gradual sea level rise towards the present level.

4.7.3 Evolution of sea surface conditions and climate

Early Holocene

Around 10,000 BP (11,000 cal yrs BP), the dinoflagellate cyst assemblage was similar to modern assemblages from the Gulf of St. Lawrence or the Scotian Shelf and reconstructions suggest that sea surface conditions might have been warmer than today. However, this is based on a single sample and validation of this assumption would require more study. Pollen assemblages probably represented a shrub-tundra vegetation, indicative of colder climatic conditions than today can be inferred. Reconstructions based on pollen indicate that mean July air temperatures were still 5 °C colder than today (McCarthy et al. 1995).

The interval between 9500 and 9200 BP is the most difficult to intepret with changes in lithology (suggesting turbidites), an important drop in the concentrations of all the palynomorphs (including pollen and dinoflagellate cysts) and major changes in the composition of dinoflagellate cysts assemblages. Reconstructions show colder SST and lower salinity (table 4.2).

TABLE 4.2 Proportions of main palynomorphs in the early Holocene disturbed section

Depth	**Age**	**Dinoflagellate cysts**	**Pollen**	**Concentrations**
14.6 m	9170	45% *Brigantedinium*	drop *Picea*, increase *Betula*	higher conc.
15 m	9275	76% *Brigantedinium*	peak of *Picea*	low conc.
16 m	9530	93% *Brigantedinium*	no data	low conc.
17 m	9700	30% *Brigantedinium*	Shrub *Betula*	higher conc.

Among the possible explanations for the change in lithology there are glacial lake discharge and sediment slumping from the walls of the valley into the fjord (see stratigraphy section). In either case, one might argue that the composition of dinoflagellate cysts and pollen assemblages for this interval could be solely the result of reworking and could represent late-glacial conditions, not the conditions at the time of deposition. In that case, the reconstructions of sea surface conditions would be meaningless.

However, a few elements argue against the reworking hypothesis. The first element is the composition of the pollen assemblages. In the interval where the pollen concentrations are the lowest, the pollen diagram shows exactly the same trends as the other pollen diagrams from western Newfoundland: Romaine River (Anderson and Lewis 1992) Southwest Brook Lake and Woody Hill Brook Pond (Anderson and Macpherson 1994) Joe's Pond (McCarthy et al. 1995). We see the same peak in *Picea* and the coincident drop in total *Betula* percentages, followed by the simultaneous drop in the percentages of *Picea* and the increase in total *Betula* (table 4.2 and fig. 4.5). These trends are too similar for the assemblages to be composed of reworked pollen. Therefore, it would seem reasonable to assume the same thing about the dinoflagellate cysts assemblages.

A second element could argue against the idea of reworked dinocysts: the assemblages are composed almost entirely of *Brigantedinium* spp and this genus is one of the least resistant to high amount of oxygen in the sediments (Zonneveld et al. 1997). The stirring causing the sediment re-suspension of the clays from the pro-glacial lake certainly caused the lake and the water draining from it to be well oxygenated. Of all the species of dinoflagellate cysts, *Brigantedinium* would be the first to disappear because of oxidation.

According to Anderson and Lewis (1992), the eastward discharge of meltwater from glacial Lake Agassiz, starting around 9600 BP, was the cause of a climatic deterioration which affected the vegetation along the drainage path, from Lake Superior to the Gulf of St. Lawrence. It ended around 8400 BP when the meltwater drainage changed to Hudson Bay. Pollen succession show evidence of this temporary return to colder conditions, while sites located far from this meltwater drainage show normal pollen successions, indicative of continuous climatic amelioration (Anderson and Lewis1992).

In southwest Newfoundland, Anderson and Lewis (1992) believed that by 9700 BP, spruce forest had replaced the shrub tundra almost everywhere but that colder climatic conditions between 9500 and 8500 BP caused the return of a birch-dominated shrub tundra vegetation. They believe *Picea* reinvaded the region after 8500 BP. This interpretation is challenged by Macpherson (1995), who interprets the increase in shrub

Betula as the expansion of shrubs birch heath on higher or more exposed areas. The evidence for cold sea surface conditions in Bay of Islands during this interval lend support to the first interpretation.

Many sites from southwest Newfoundland record this climatic deterioration, as shown by anomalies in their pollen succession. At nearby Joe's Pond, spruce dominated the pollen assemblages (60%) after 10 ka, but was replaced by shrub-birch (70%) around 9400 BP (McCarthy et al. 1995). The same thing was observed at Romaine River, Woody Hill Brook Pond, and Southwest Brook Lake (Anderson and Lewis 1992; Anderson and Macpherson 1994). At the later site, the size of *Betula* pollen shows a dominance of shrubs during the meltwater event. The return of spruce is dated around 8500 BP at Southwest Brook Lake, and larger *Betula* pollen indicates that the birch trees became abundant after 8500 BP (Anderson and Lewis 1992). A pollen diagram from Compass Pond, in the Baie Verte Peninsula (Dyer 1986), shows no apparent effects of this meltwater event, probably because of its location on the northeast coast, away from the meltwater discharge.

It is important to note that in southwest Newfoundland, this cold period is not characterized by lithological changes in lake sediments (Anderson and Macpherson 1994). And finally, while the changes in dinoflagellate cyst assemblages and the reconstructed cold and lower salinity interval started at 9500 BP in Bay of Islands, changes in the pollen assemblages from that core occurred only around 9200 BP. If reworking was solely responsible for the changes in the composition of assemblages, they should occur at the same time for both the pollen and the dinoflagellate cysts. This also implies that the vegetation reversal started 300 years later around Bay of Islands than at the other southwest Newfoundland sites previously mentioned.

Recently, Moore et al. (2000) estimated meltwater flows into the North Atlantic during the deglaciation. A meltwater episode, dated 10,500-10,300 cal BP, the Middle Stanley Phase, would correspond to our interval of low palynomorph concentrations and lowest salinity. Around the great lakes, this phase was followed by the Main Mattawa climatic phase, characterized by a cooler climate than previous phases. This would correspond with the low SST interval (9500-8500 BP).

Transfer function data from dinoflagellate cysts in Gulf of St. Lawrence cores (see de Vernal et al. 1993) show a slight cooling in Anticosti Channel, and a slightly cooler interval around 9000-8000 BP (not dated precisely) in Cabot Strait core 111. However, there is no indication of the meltwater event in most of the Gulf of St. Lawrence, the Laurentian Channel and Eastern Scotian Shelf (Scott et al. 1989a; Keigwin and Jones 1995). Further downstream, in La Have Basin, the marine hypsithermal event occurs at that time (Levac 2001). This suggests that the effects of the meltwater drainage event were not felt beyond the Gulf of St. Lawrence.

Marine hypsithermal in Bay of Islands

In Bay of Islands, the hypsithermal started as soon as the meltwater drainage event was over around 8600 and lasted until 6800 BP. The presence of *S. mirabilis*, which is found in the Gulf of Maine and southwest Scotian Shelf today, increased percentages of *B.*

tepikiense, and relatively more important percentages of *A. choanum*, are indications of warmer sea surface conditions.

Other sites also recorded an early Holocene marine hypsithermal: La Have Basin (10,000-8000 BP; Levac 2001), the Laurentian Channel and Fan (10,000-6000 BP; Keigwin and Jones 1995). In Notre Dame Channel, the presence of *Spiniferites* spp. in the early Holocene, in assemblages otherwise dominated by *I. minutum* and *Brigantedinium* spp. (which reflect the influence of the Labrador Current) suggests slightly warmer SST than today (Scott et al. 1984). Based on correlation with well dated pollen diagrams from the northcentral Newfoundland (Macpherson 1988), this interval appears to stretch from ~11.5 000 ka until ~7000 BP.

In the Gulf of St. Lawrence, the start of the hypsithermal is later: in core 111 from Cabot Strait, and in core 16 from Anticosti Channel, it is recorded between ~8000 and 6000 BP. The hypsithermal is also recorded for 70000-5000 BP in Bedford Basin (Miller et al. 1982), and in the mid-Holocene for Emerald and Canso Basins (Scott et al. 1984; 1989a) but these sites are not well dated. In the Esquiman Channel, there is no evidence of a hyspithermal event (see de Vernal et al. 1993).

When the various sites are compared, it appears that the hypsithermal started earlier on the outer continental margin (in the early Holocene), than inshore sites affected by the 9500-8500 BP meltwater episode, i.e. in the Gulf of St. Lawrence and Bay of Islands.

To explain the presence of warmer sea surface temperature along the Eastern Margin of North America during the early Holocene, two scenarios were proposed: a northward shift in the position of the Gulf Stream (Balsam 1981) and a decreased influence of the

Labrador Current (Fillon 1976). The main path of the Gulf Stream is located too far to the south and offshore to realistically expect a direct influence from its warm waters, even with a northward shift in its position. Fillon (1976) suggested that a deflection of the Labrador Current along the seaward edge of the Grand Banks allowed penetration of warmer water along the Eastern Canadian Margin as far north as Newfoundland. This could have an influence on surface waters south of Newfoundland and possibly on the waters entering the Gulf of St. Lawrence through Cabot Strait.

The insolation also played a role in the occurrence of the marine hypsithermal in the early Holocene. Between 15 and 9 ka, the summer insolation increased as a result of an increase in axial tilt and change in the precession of the earth resulting in a decrease in the earth-sun distance in summer. The maximum summer insolation occurred between 12 and 9 ka, but its effects on climate were more important around 9 ka than 12 ka. This is due primarily to a reduced influence of the Laurentide ice sheet between 12 and 9 ka and to the fact that the perihelion occurred in July at 9 ka, while it occurred in April at 12 ka (COHMAP 1988; Bradley 1999). At 9 ka, the northern hemisphere received 7 % more radiation than today in July (Bradley 1999).

While the summer insolation was greater, the winter insolation was proportionally lower (COHMAP 1988), and the warmer winter SST at 9 ka might seem an anomaly. However, the ocean has a large heat capacity and the reduction of sea ice thickness and the prolongation of the ice free season, probably helped to maintain warmer conditions over the high latitude oceans, even throughout the winter months (Bradley 1999).

During the marine hypsithermal (8600-6800 BP), the vegetation around Bay of Islands does show an amelioration of the climate with the arrival of trees in the area, including more temperate species like *Fraxinus* and *Acer*, and a reduction in the proportion of grass pollen. The disappearance of the last small ice caps on Newfoundland, whether by 9000 or 8000 BP , certainly contributed to this climatic amelioration. Macpherson (1995) believes that summer temperatures in Newfoundland were at least as warm as today by 8500 BP. Reconstructions of summer temperature based on pollen show a rapid warming at Joe's Pond between 8000 and 7000 BP (see McCarthy et al. 1995) but warmer temperatures than today were not reached until after 7000 BP.

Terrestrial Hypsithermal

The hypsithermal appears to have started at about the same time all over Newfoundland. Around Bay of Islands, the hypsithermal is assigned to the interval 6000 to 3500 BP, based on the maximum percentages of tree-*Betula*, *Fraxinus* and total tree pollen. Reconstructions based on pollen indicate that summer temperatures were 1°C warmer than today at Joe's Pond between 6500 and 4500 BP (McCarthy et al. 1995). Higher percentages of *Abies* after 6000 BP at Southwest Brook Lake also suggest higher winter temperatures (Macpherson 1995).

At Compass Pond, the hypsithermal is defined by the presence or expansion of temperate forest species such as *Fraxinus*, *Ulmus* and *Acer spicatum* in the area between

6700 and 3200 BP. Compass Pond is located northward from the modern distribution range of most of these species and this suggests a longer growing season (Dyer 1986). On the Avalon peninsula (Sugarloaf Pond), a decrease in the proportion of shrub-birch and an increase in that of tree pollen, indicate warmer temperatures from around 6000 to 4500 BP (Macpherson 1995). On the coast, the hypsithermal is either absent or has a very short duration. At Robinson's Pond for example, the reconstructions show a very short interval of warmer July temperature around 4 ka (McCarthy et al. 1995). This is most likely due to the wind exposure.

A few authors have suggested that the hypsithermal on land was a response to warmer sea surface temperature (Dyer 1986; Macpherson 1995). The reconstructions, both in La Have Basin (Levac 2001) and Bay of Islands, show that this is not the case, since SST were actually lower than today's average during the terrestrial hypsithermal.

Evidence for the local establishment of some temperate tree species in western Newfoundland before the hypsithermal argue against migration delays as an explanation for the later start of the hypsithermal on land relative to the ocean. For example, *Fraxinus* pollen was present as early as 7600 BP in the Bay of Islands core, but peaked only between 6000 and 3500 BP. Because *Fraxinus nigra* is a very poor pollen producer, even very small percentages in the pollen assemblages could correspond with its presence in the vegetation around the bay at 7500 BP. Tree birch was also present since 8600 BP but peaked only after 6000 BP. At Joe's Pond, the hypsithermal is characterized by a peak in pine pollen, which occurred only after 7000 BP, despite its presence in the area as early as 8500 BP (Macpherson 1995). The climate could have been warm enough to allow these more temperate trees to migrate fairly early into western Newfoundland but not warm enough to allow their expansion until ~6000 or 7000 BP. The cooling effect of the remaining Laurentide ice sheet on the regional climate might be responsible for this. Paleoclimatic models show the presence of an anticyclonic system over the ice sheet, responsible for cold northeasterly winds over Newfoundland and Nova Scotia (COHMAP 1988). Alternatively, some ecological factors, such as competition from already established tree species might be involved (Delcourt and Delcourt 1987). In that case, the hypsithermal could have started earlier but its effect would not be reflected immediately by the vegetation.

Mid/Late Holocene cool summer SST

During the terrestrial hypsithermal, the August SST were lower than today (6800 to 4100 BP; 7300-4400 cal BP) and there was a resurgence of the cold water species *I. minutum*.

In La Have Basin, a similar episode of cooler SST and lower salinities is reconstructed after the marine hypsithermal, but it occurs earlier (8500-7000 BP; Levac 2001). Timewise, the cold interval in La Have Basin coincides with a meltwater discharge from the Great Lakes through the Gulf of St. Lawrence from 8500 to 7500 BP (the Late Stanley phase of Moore et al. 2000). In contrast, this is the time of the marine hypsithermal in Bay of Islands. This event is also apparently absent in records from the Gulf of St. Lawrence and Cabot Strait (de Vernal et al. 1993).

Keigwin and Jones (1995) mention a short-lived cool interval in the Laurentian Channel and Laurentian Fan around 7000 (based on O^{18} measurements of planktonic foraminifers) that they interpreted as the final meltwater pulse. But the duration of this event is too short to explain the prolonged episode of cool summer SST.

Scott and Collins (1996) suggested, based on evidence from sea-level records, that melting in the Arctic could have been enhanced by the hypsithermal and possibly continued until ~ 4000 BP. This last scenario would explain the occurrence of prolonged cool SST, but not the short cool summer SST intervals around 2.5 ka and 800 years ago.

The numerous summer SST drops could be the result of cyclic climatic oscillations. Bond et al. (1997) observed cyclic increases of ice rafting debris during the Holocene in the North Atlantic. They correspond to colder temperature and lower salinity in the sea surface, caused by increased rates of iceberg discharge and more southern advection. These episodes have a recurrence of about 1 to 2 kyrs. Bond et al. (1999) identified 8 such climatic shifts within the Holocene and relates them with the Dansgaard/Oeschger oscillations. Despite the blurring effect of bioturbation, the episodes of lower summer SST in Bay of Islands appear to correlate with events 2 to 7 of Bond et al. (1999). In general, the SST oscillation have a greater amplitude (± 5 °C) than those of La Have Basin, and variations in salinity are similar.

Late Holocene warm SST interval (4000-1000 BP)

An interval of winter SST warmer than today started in Bay of Islands at the same time as the regional Late Holocene cooling trend. One might question the validity of the reconstructions for this interval since it was not observed elsewhere. However, the presence of *Spiniferites mirabilis*, a species indicative of warmer sea surface conditions, lends support to the reconstruction of warmer than present SST. Today, this species is not found north of the Gulf of Maine and southwest Scotian Shelf (Rochon et al. 1999), except for George's Bay in the southwest sector of the Gulf of St. Lawrence (Mudie 1980; Schafer and Mudie 1980). Its presence into the Bay of Islands is a clear indication of warmer SST.

So far, the cause of this warm interval is unknown but solar insolation could partly explain the occurrence of warmer sea surface temperatures in the Late Holocene. While the summer insolation decreased after 9ka, the winter insolation increased gradually toward the present day value (COHMAP 1988). It can be inferred from the GISP2 ice core that winter temperatures were warmer than today between 4 and 2 ka, and atmospheric general circulation models support the idea of a wintertime warming since the middle Holocene (Alley et al. 1999).

Late Holocene cooling

Effects of the Late Holocene cooling become apparent earlier in the vegetation than in the marine environment. In the Bay of Islands pollen diagram, it started at 3300 BP, while the reconstructions show decreasing SST only in the last 800 years, after the 4000-1000 BP warm interval.

At many sites in western Newfoundland (Joe's Pond, Compass Pond) the cooling trend on land started at 4500 BP. At Joe's Pond, it is marked by a reduction in *Pinus* and increased proportions of *Alnus* (McCarthy et al. 1995). At Compass Pond, a cooling is inferred from the resurgence of black spruce, the increase in shrub-birch, and the disappearance of *Fraxinus* (Dyer 1986). The last 3000 years are missing from the Southwest Brook Lake record but there seems to be a decrease in the proportion of *Pinus* in the last samples (Macpherson 1995). Because the cooling started earlier at coastal sites (Joe's Pond) than inland (Southwest Brook Lake), Macpherson (1995) suggested that it was led by a change in ocean surface temperature. The warm SST in Bay of Islands at that time would argue against that.

The interval of lower summer SST which started about 800 years ago could correspond to the Little Ice Age and represent the most recent cold phase of the 1-2 kyr cycles of Bond et al. (1999). This cooling occurs much later than the late Holocene cooling trend that characterized many cores from the Eastern Canadian Margin.

In most marine cores, a Late Holocene cooling is recorded during the last few millenia. It started 5000 years ago over the Laurentian Fan (Keigwin and Jones 1995) and

2000 years ago at the Fogo Seamounts (Mudie 1992). Scott at al. (1984; 1989a) placed the start of the late Holocene cooling at 2.5 ka in Notre Dame Channel, Emerald and Canso Basins. The Late Holocene cooling is not apparent in the cores from the Gulf of St. Lawrence (de Vernal et al. 1993), possibly because of the low resolution of the record. It is believed that a southward and offshore migration of the Gulf Stream after 4000 BP (Balsam and Heusser 1976) and a greater strength of the inner Labrador Current after 3500 BP (Fillon 1976) were responsible for the Late Holocene cooling trend.

To explain the absence of an obvious Late Holocene cooling trend in La Have Basin, Levac (2001) suggested that the colder, lower salinity intervals that punctuated the record from La Have Basin could be an indication of increased influence of the Labrador Current as early as 7000 years ago, equivalent to the Late Holocene in other records. This would imply that the Late Holocene cooling was not a continuous trend that started 3000 to 5000 years ago, but was instead a series of episodic sea surface cooling events. The results from Bay of Islands, do not support this hypothesis.

4.7.4 Early Holocene cf. *Alexandrium tamarense* event

Important influx of cysts similar to cf. *Alexandrium tamarense,* a species known to cause red tides, is reported in numerous cores from the Scotian Shelf, Laurentian Channel and Gulf of St. Lawrence in the early Holocene (see de Vernal et al. 1993; Simard and de Vernal 1998; Mudie et al. 2002; Levac 2001). They most likely represent episodes of high plankton productivity (blooms).

While the occurrence of cf. *Alexandrium tamarense* in Bay of Islands between 8500 and 10,000 BP coincided with occurrences in the Gulf of St. Lawrence, Cabot Strait and Laurentian Channel (de Vernal et al. 1993; Simard and de Vernal, 1998), concentrations in the bay were minimal in comparison with the other sites. Regionally, concentrations of cf. *A. tamarense* range from 10^2 to 10^3 in the Gulf and Cabot Strait (de Vernal et al. 1993; Simard and de Vernal 1998) to 10^4 in the Laurentian Channel, La Have and Emerald Basin (Mudie et al. 2002; Levac 2001) and Laurentian Channel (Simard and de Vernal 1998). In Bay of Islands, concentrations of cf. *A. tamarense* do not exceed 300 cysts/cm^3, which corresponds to influx of 60 cysts/cm$^2\cdot$yr.

In a comparison of Holocene red tide histories on the Pacific and the Atlantic coasts of Canada, Mudie et al. (2002) identified warmer SST as a common denominator and most likely the cause of the blooms. They also suggested that sediment disturbance may have played a role in "seeding" and sustaining blooms. On the Scotian Shelf, Levac (2001) suggested that early Holocene blooms of cf. *A. tamarense* (and other non-toxic, bloom-causing species) were caused by the higher nutrient concentrations of the meltwater, and a stronger water column stratification during the summer, while warmer SST appeared to influence the magnitude of the blooms. She also pointed out that the magnitude of cf. *A. tamarense* influx was much higher when it coincided with warm SST.

The very small influx of cf. *A. tamarense* could be the result of high sedimentation rates in Bay of Islands during the early Holocene. However, percentages of *A. tamarense* also remained low (1-6%). So, it is proposed here that cf. *A. tamarense* was introduced in the Bay by the same mechanisms that distributed it throughout the region (from the Scotian Shelf to Gulf of St. Lawrence; see Simard and de Vernal 1998), but that the conditions in the Bay at that time were not favorable to this species. The SST were probably too cold to allow the development of major blooms. Water turbulence and/or the absence of strong water column stratification, might also have been detrimental to cf. *A. tamarense*.

4.7.5 Pollen zones differences

Differences between the pollen diagrams from Bay of Islands, Joe's Pond and Southwest Brook Lake indicating differences in the composition of the vegetation and overall, could suggest that Bay of Islands benefited from a warmer climate than other regions throughout most of the Holocene. *Abies*, for example, is represented in all the analysed samples from the Bay of Island core, suggesting its local presence very early in the Holocene. *Abies* appears in the diagrams from Joe's Pond and Southwest Brook Lake after 9500 BP. *Pinus* percentages remain below 10% at Joe's Pond until 7500 BP and at Southwest Brook Lake until 5 ka, while they reach 25 % at Bay of Islands between 9000-8000 BP and decrease after 3500 BP. It could be suggested that relatively important *Pinus* populations developed earlier around Bay of Islands. At Joe's Pond, conditions probably became more favourable to *Pinus* during the hypsithermal and it peaks between 7500 and 4500 BP. Finally, the proportion of temperate trees (*Acer*, *Fraxinus*, *Ulmus*) is greater in pollen assemblages from Bay of Islands, suggesting they always grew in greater number there.

4.8 Conclusions

1- The sea surface conditions in Bay of Islands, as well as the vegetation surrounding the bay, were greatly affected by a major meltwater event between 9500 and 8600 BP.

2- The marine hypsithermal occurred between 8600 and 6800 BP and was characterized by SST up to 5°C warmer than today. At that time, summer solar insolation amounts were still greater than today. The terrestrial environment is characterized by a climatic amelioration at that time and the rapid development of the boreal forest.

3- The hypsithermal occurred later in western Newfoundland (6000 to 3500 BP). The cold influence of the remaining Laurentide ice sheet could account for this lag between the land and the sea, since migration delays are unlikely.

4- The terrestrial hypsithermal coincides with an interval of slightly cooler summer SST that followed the marine hypsithermal (6800-4100 BP).

5- Changes in the composition of the vegetation are indicative of a climatic deterioration after 3300 BP, which is about a thousand years later than other sites in western Newfoundland. In the sea surface, the late Holocene cooling was preceded by an interval of warmer winter SST than today (from 4100 to 1000 BP). The reconstructions could be questioned due to the absence of explanation for this event, but the presence in this interval of *S. mirabilis*, which require warmer conditions, lend support to the reconstructions.

6- The late Holocene cooling of summer SST started 800 years ago, much later than the late Holocene cooling trend that characterized many marine cores from the Eastern Canadian Margin.

7- The numerous drops in summer SST that punctuated the Bay of Islands record could correspond with the 1-2 kyr climatic events identified by Bond et al. (1997; 1999).

8- These results show that the oceanic and terrestrial environments were controlled by different forcings. The sea surface temperature and salinity in Bay of Islands appear to depend indirectly on the position of the major surface currents (Gulf Stream and Labrador Current) and perhaps on influx of meltwater (variations in iceberg advection could also play a role). Newfoundland Holocene climate was initially under the influence of the Laurentide ice sheet (until ~ 6000 BP), after which it was probably controlled by the position of air masses, since the conditions in the adjacent sea surface do not appear to have affected it: relatively cool SST are reconstructed during the terrestrial hypsithermal, while much warmer SST than today are reconstructed during the late Holocene climatic cooling. The early Holocene meltwater event would be the only exception.

9- There is no evidence of a high productivity event in the early Holocene in Bay of Islands. cf. *Alexandrium tamarense* was present in Bay of Islands between 8500 and 10,000 BP, which coincides with its occurrence in the Gulf of St. Lawrence (de Vernal et al. 1993; Simard and de Vernal 1998), but cold SST, water turbulence and/or the absence of water column stratification at that time probably prevented the development of major blooms.

CHAPTER 5 Holocene paleoceanography of St. Anne's Basin, Scotian Shelf: palynological records

Abstract

A high resolution palynological record from St. Anne's Basin was studied to investigate the apparent time transgressive nature of the early Holocene sea surface temperature (SST) maximum over the Scotian Shelf and the subsequent cool SST interval.

Reconstructions of sea surface conditions are based on paleobioclimatic transfer functions using dinoflagellate cyst data from core 84-011-12, St. Anne's Basin (northeastern Scotian Shelf), an area influenced by waters derived from the Labrador Current and lower salinity inputs from the Gulf of St. Lawrence. Comparison of onshore-offshore palynological records was used to determine ocean-atmosphere interactions. Results show a series of alternating warm and cold episodes, as well as frequent oscillations of SST and salinity.

Before 8500 BP, SST and salinity were higher than the present day average by 3-4 °C and by 1.5-2psu. An interval of SST cooler than modern time precedes the early Holocene optimum (7500-6000 BP) when SST was higher by up to 4 °C in August and up to 1.5 °C in February. From 6000 to 4000 BP, SST is 2 to 4 °C below modern average and a second warm interval occurs between 4000 and 2500 BP. At this time, February SST is 2 to 4 °C higher, while August SST remains around the present day average.

Between 2500 and 1500 BP, a drop in SST affected mainly the August SST. In the last 1500 years, most sea surface parameters were close to the present.

The early Holocene SST optimum and post-optimum cool intervals are common features of eastern Canadian Margin records, but the late Holocene warm interval is only present in St. Anne's Basin and Bay of Islands. The late Holocene cooling trend is either absent or proceeded as a series of episodic cooling events.

Correlations with lake pollen records from Cape Breton indicate that the hypsithermal onshore followed the early SST optimum. Vegetation changes around 3000 BP indicate cooler climatic conditions preceding an episode of cooler August SST between 2500 and 1500 BP.

5.1 Introduction

Previous paleoceanographic studies on the southeastern Canadian Margin established the following sequence of events: an early Holocene interval of cool sea surface conditions (or conditions similar to the present day), a mid-Holocene warm interval, and a late Holocene cooling trend (Vilks and Rashid 1976; Mudie 1980; Scott et al. 1984; 1989a).

Results of a high resolution quantitative study from La Have Basin (Levac 2001) differ from the conclusions of previous studies by the earlier occurrence of warm SST (10,000-8500 BP), the subsequent cool interval (8500-6000 BP), and the presence of frequent oscillations of SST in the last 7000 years. Correlation of pollen zones with pollen records from Nova Scotia Lakes (Livingstone 1968; McCarthy et al. 1995) indicate a lag of the terrestrial hypsithermal relative to the SST optimum. A core from Bay of Islands, western Newfoundland, showed that the early Holocene warm interval (8600-6800 BP) was delayed by a meltwater event (9500-8600 BP). At this site, there is also an unexplained late Holocene warm interval (4000-1000 BP), as well as frequent oscillations of SST and salinity, as yet unexplained just as in La Have Basin (Levac 2002a).

The results of the La Have Basin and Newfoundland cores suggest that the Holocene marine hypsithermal event was time transgressive from the southwest to the northeast. Therefore a core (84-011-12) was studied from St. Anne's Basin in an intermediate location near the Laurentian Channel on the eastern Scotian Shelf, to investigate the timing of the early Holocene SST optimum. In addition, the St. Anne's Basin core was used to investigate the subsequent cool interval (observed in both La Have Basin and Bay of Islands cores) and to determine if it was a regional phenomenon. Another objective was to verify the presence of a late Holocene warm interval similar to that reconstructed in Bay of Islands between 4000 and 1000 BP, and the presence of recurrent oscillations in SST and salinity.

Figure 5.1: Location map. Numbers indicate other cores cited in the text. Some numbers correspond to more than one core in places where sites are located too close together. Detailed bathymetry for St. Anne's Basin is shown on figure 5.2.

Marine sites:
1- St. Anne's Basin core 84-011-12 (this study);
2- La Have Basin (Levac 2001);
3- Emerald Basin (Mudie 1980; Scott et al. 1984; 1989a; Vilks and Rashid 1976);
4- Canso Basin (Scott et al. 1984; 1989a);
5- NW Laurentian Channel (Simard and de Vernal, 1998);
6- Anticosti Channel core 16 (de Vernal et al. 1993);
7- Anticosti Channel core 21 (de Vernal et al. 1993);
8- Esquimans Channel (de Vernal et al. 1993);
9- Notre Dame Channel (Scott et al. 1984);
10- Cabot Strait (de Vernal et al. 1993; Simard and de Vernal. 1998);
11- Laurentian Channel (Keigwin and Jones 1995);
12- Laurentian Channel (Simard and de Vernal 1998);
13- SW Grand Banks Rise (Simard and de Vernal 1998);
14- Laurentian Fan (Keigwin and Jones 1995);
15- Fogo Seamount (Mudie 1992).

Bays sites:
A- Mahone Bay (Mudie 1980);
B- Chezzetcook Inlet (Mudie 1980);
16- Bay of Islands MD99-2225 (Levac 2002a);
17- St. Georges Bay, Nova Scotia (Schafer and Mudie 1980)

Terrestrial sites:
E- Robinsons Pond and Joe's Pond (McCarthy et al. 1995);
F- Sugarloaf Pond (Macpherson 1995);
H- Wreck Cove (Livingstone and Estes 1967);
M- Gillis Lake (Livingstone and Livingstone 1958); Salmon River (Livingstone 1968);
N- Upper Gillies Lake and McDougal Lake (Livingstone 1968).

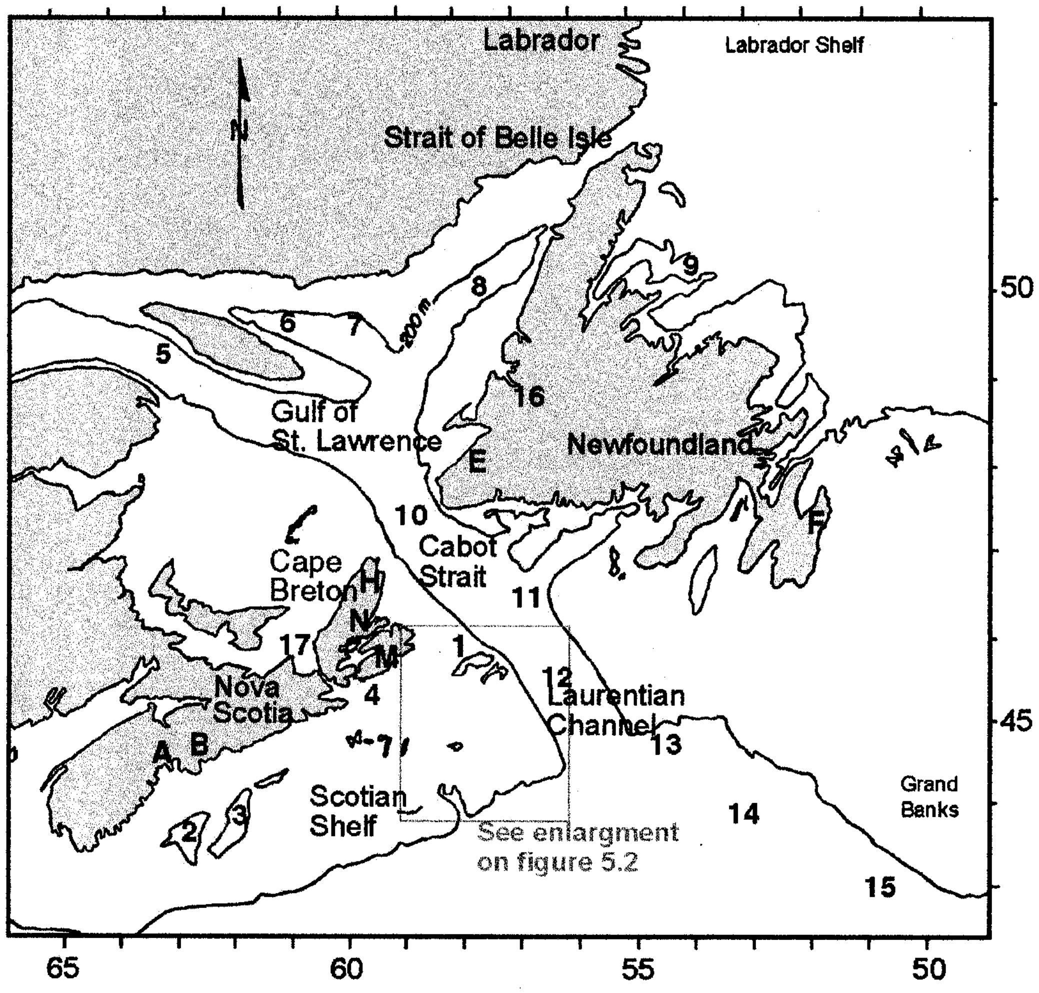

Figure 5.1: Location of St. Anne's Basin and bathymetry of the Scotian Shelf. Letters indicate sites mentioned in the discussion (see previous page).

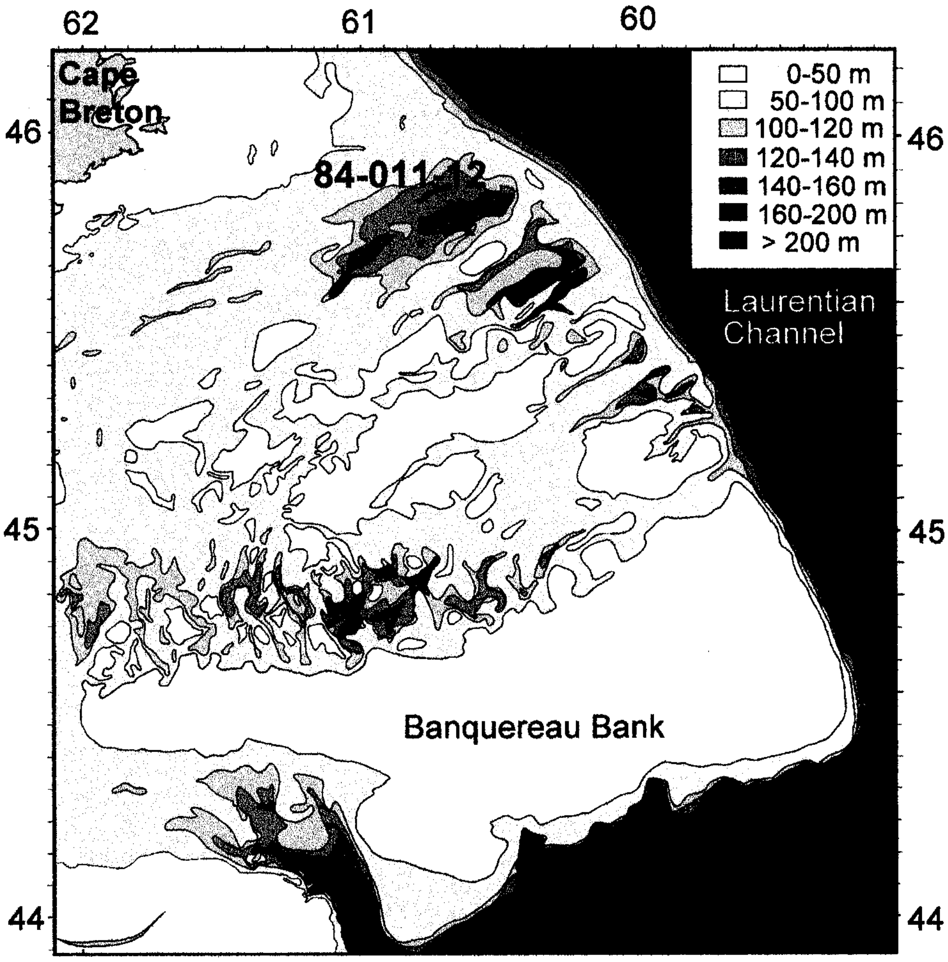

Figure 5.2: detailed bathymetry of the eastern Scotian Shelf and St. Anne's Basin (From Freeman 1986).

Core 84-011-12, as well as another core from the same basin (84-011-11), were previously studied for benthic foraminifera (Freeman 1986; Souchen 1986). Both cores contained a mid-Holocene interval characterized by *Brizalina subaenariensis*, suggesting warmer bottom water conditions at that time (Freeman 1986; Souchen 1986). The interval extended between 7000 and 8500 BP, based on radiocarbon ages obtained since these studies.

5.2 Environmental setting

St. Anne's Basin is located on the northeastern part of the Scotian Shelf, 50 km from the edge of the Laurentian Channel (fig. 5.1). The basin has a length of 7 km and a width of 3 km. It lies on the inner shelf, about 40 km south-south-east of Cape Breton Island. The core was taken near the center of the basin.

5.2.1 Sea surface circulation

The Laurentian Channel is a major exchange pathway between the Atlantic Ocean and the Gulf of St. Lawrence, and also a confluence zone for continental runoff from the St. Lawrence River, the Labrador Current, and offshore slope waters (Loder et al. 1997). The Labrador Current flows southward from the Labrador Shelf onto the northeast Newfoundland Shelf (fig. 5.3), the Grand Banks and the southern Newfoundland Shelf (Loder et al. 1997). The inner portion of the Labrador Current flows into the Gulf of St.

Lawrence through the eastern side of Cabot Strait while most of the outer Labrador Current flows southwestward, with a small portion meandering into the Laurentian Channel. There is an outflow from the Gulf of St. Lawrence on the western side of Cabot Strait. Part of it flows along the inner Scotian Shelf, while the rest flows toward the outer Scotian Shelf along the western edge of the Laurentian channel (Han et al. 1999).

5.2.2 Sea surface conditions

The sea surface conditions over the northeastern Scotian Shelf clearly reflect the inputs from the Gulf of St. Lawrence through Cabot Strait. Salinity is lower along the coast of Cape Breton and on the inner shelf (on average 31 psu), and gradually increases offshore (Loder et al. 1997; Petrie et al. 1996a). The peak of freshwater discharge into the Gulf from major rivers occurs in the spring. In summer, the freshwater plume extends along the western side of Cabot Strait, the inner Scotian Shelf and also along the edge of the Laurentian Channel (Loder et al. 1997). Surface salinity is therefore lower in summer, ranging from 29.5 along the northeast coast of Cape Breton to 31 on the edge of the Scotian Shelf. For these areas, surface salinity ranges from 31 to 32 in winter.

In winter, the water column is characterized by a 2 layer system: a cool fresh shelf water layer extending from the surface to a depth of 100 m (150 m on the inner shelf), and a slope derived water layer extending to the bottom (Petrie et al 1996a; Loder et al. 1997). The sea surface temperature is 0 °C over the inner shelf and 1 °C over the middle and outer shelf (Petrie et al. 1996a). The surface salinity is between 31 and 32 (see Petrie et al. 1996a). In terms of bottom water conditions, the Scotian Shelf can be divided into 2 distinct regions. On the northeastern half, bottom temperature is between 0 and 3 C and salinity between 31 and 32. On the southwestern half, bottom temperature is between 6 and 9 and salinity ranges between 32 and 34 (Loder et al. 1997).

In summer, water column stratification is stronger with the development of a warm surface layer in the upper 20 meters. Sea surface temperature displays a greater spatial variability and ranges from 12 to 18 °C (Petrie et al. 1996a; Loder et al. 1997). Temperature in the intermediate water mass ranges from 6 to 10 °C, salinity from 33.5 to 31.5. Winter bottom temperature and salinity (below 100 m water depth) are very similar to the summer ones, except for shallower areas like Sable Island (Loder et al. 1997).

For St. Anne's Basin, the mean sea surface temperature is 0 °C in February and 16 °C in August. Salinity is higher in February (30 psu) than in August (31.5 psu) (NOAA 1994). The duration of the sea ice cover is variable around Cape Breton. While the average duration is 80-100 days on the west side of the island, it is only 40 days along the southern coast and in St Anne Basin (Drinkwater et al. 1999).

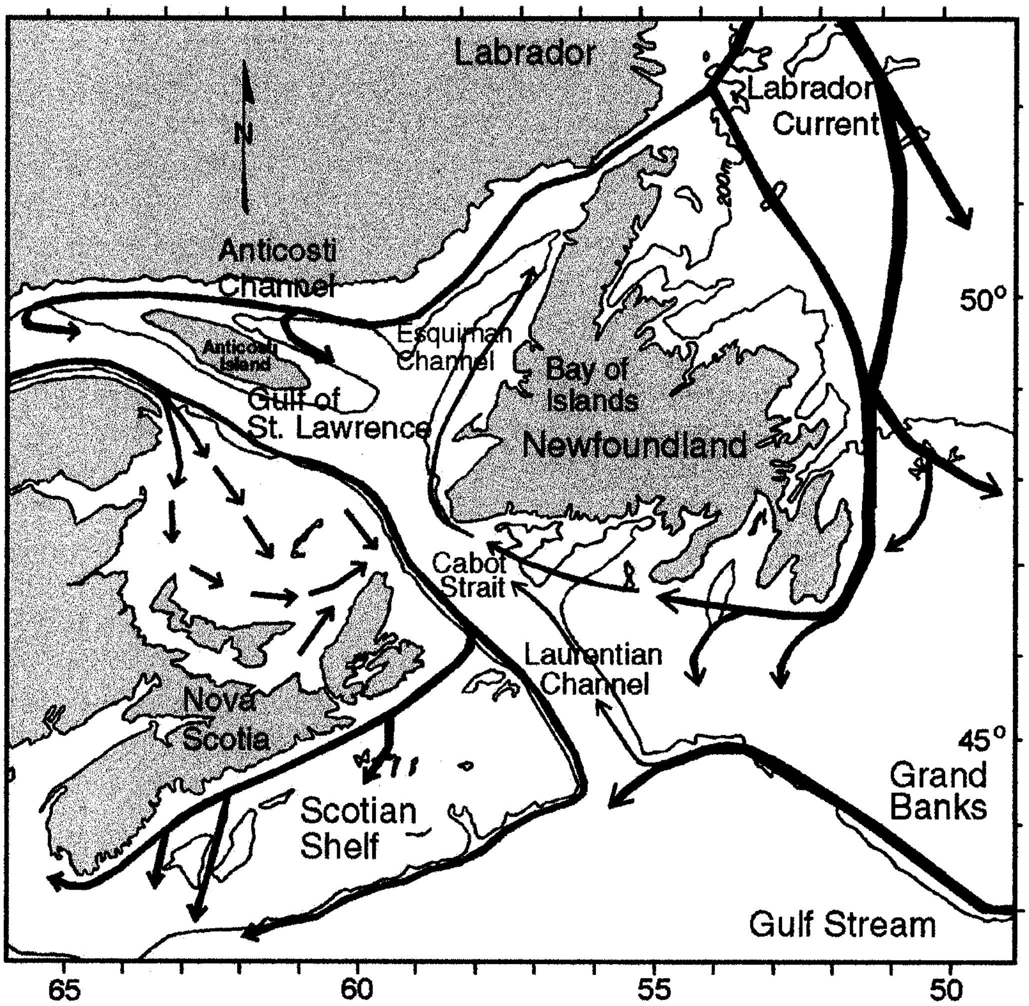

Figure 5.3: Surface circulation in the Gulf of St. Lawrence, around Newfoundland and on the Scotian Shelf (based on Greenberg and Petrie 1988; Han et al. 1999; Shore et al. 2000). bathymetric contour is 200 m.

5.2.3 Climate

Nova Scotia weather is affected by two large pressure systems, the subpolar Icelandic Low and the subtropical Bermuda-Azores High. Located near or along the favoured pathway of low pressure systems, Nova Scotia is the stormiest region of Canada. Storms become less frequent in summer, as the Bermuda-Azores High moves northward. The presence of cold water on the inner Scotian Shelf and in the southwestern Gulf of St. Lawrence also greatly affects the climate of Cape Breton. Fog is frequent, especially in spring and early summer, when warm, moist air moving onshore from the Gulf Stream mixes with air chilled by the Labrador Current (Phillips 1990).

In Cape Breton, the mean daily air temperature is -5°C in February and 17.5°C in August. Mean annual total precipitation ranges from 1400 mm/year in the south to 1600 mm/year on the Cape Breton Highlands. Snowfalls amount to 200 cm annually on the southern coast and increase towards the Cape Breton Highlands where they reach 400 cm/year (Environment Canada 1984). In summer, the dominant winds blow from the south and southwest at average speeds of 18 to 27 km/hr (Environment Canada 1984).

5.2.4 Cape Breton vegetation

Over most of Cape Breton, *Picea glauca* and *Abies balsamea* are the main forest trees, accompanied by *Populus balsamifera*, *Fraxinus americana*, and *Ulmus americana* (Rowe 1972). On hilly lands, *Acer rubrum*, *Betula papyrifera*, *B. alleghaniensis*, *Abies* *balsamea*, and *Picea glauca* can also be found. *Tsuga canadensis* and *Fagus grandifolia* are locally abundant on slopes and ravines. In areas with poor drainage, *Picea mariana* is common (Rowe 1972). The forest changes on the slopes of the highlands. It becomes predominantly deciduous, and the main tree species are *Acer saccharum*, *Fagus grandifolia*, *B. alleghaniensis*, *Acer rubrum*.

In the Cape Breton Plateau sub-region, above altitudes of 250 to 350 meters, conifers become more prominent. *Abies balsamea* is the dominant species, with *Picea glauca*, *P. mariana*, and *Betula papyrifera*, and minor elements like *B. alleghaniensis, Acer rubrum, Fagus* and *A. saccharum. Pinus* spp. is rare (Rowe 1972). On the high plateau, *Larix laricina* joins the other conifers (*Abies balsamea, Picea glauca* and *P. mariana*), and forest cover becomes discontinuous due to the presence of moss-covered or heath barrens. Tree are stunted on hills and ridges because of wind.

A very narrow band of dense low stands of *Abies balsamea*, *Picea mariana* and *P. glauca* is found along the Atlantic coast. This is the Eastern Atlantic Shore section. Most hardwoods are absent from this sub-region and the growth is slow due to exposure (Rowe 1972). *Sphagnum* bogs occupy areas with poor drainage (Rowe 1972; Environment Canada 1989).

5.3 Core stratigraphy

The core site is located in St. Anne Basin on the northern Scotian Shelf (45° 46.72'N; 58° 39.16'W) at a water depth of 270 meters (fig. 5.1). A piston core and a gravity core, respectively 750 cm and 120 cm in length were taken.

The gravity core is composed of dark yellowish brown mud in the upper 20 cm. The rest of the gravity core and the upper 448 cm of the piston core are composed of dark brown to dark olive gray mud.

In the piston core, olive grey silt is found in the 448-450 cm interval. Between 450 and 480 cm there is a dark olive grey muddy clay. At 480 cm, it is replaced by olive grey clay, stiffer and smoother in texture. From 518 cm to the base of the core, the clay has an emerald or bright green colour (close to 2.5Y 3/2). Both the piston and the gravity cores contain bands and lenses of slightly coarser sediment, frequent shell fragments and are bioturbated throughout (Freeman 1986).

Two radiocarbon ages were obtained on foraminifera from piston core 84-011-12 (table 5.1). An age of 3100 ± 60 years BP was measured at 65-67 cm and an age of 7930 ± 80 years BP at 640-650 cm. In addition to these dates, the increase in *Ambrosia* and *Rumex* at 20 cm probably corresponds to the beginning of the European settlement of Cape Breton and is assigned an age of 200 years (Schafer and Mudie 1980). We also assume that the surface represents the present day sediment deposition.

Between the radiocarbon dates, the ages were interpolated using sedimentation rates estimates. Sedimentation rates are estimated to 21 cm/1000 years for the last 3100 years. Between 3100 and 7930 years BP, the sedimentation rate is estimated to 120cm/1000 years. If we use this rate for the lowest part of the core (650-750 cm), the age at the base is estimated to ~8800 years. Radiocarbon ages are used throughout this paper and are included in the result diagrams (fig. 5.4, 5.5 and 5.6). For the calibrated ages, refer to table 5.1. The program CALIB 4.3 (Stuiver and Reimer 1993; Stuiver et al. 1998) was used to calibrate the ^{14}C ages.

The gravity core is correlated with the upper 60 cm of the piston core. This is based on the composition of the pollen assemblages and pollen percentage curves (fig. 5.5). The gravity and the piston cores were difficult to correlate precisely because the pollen percentage curves are not exactly identical. Dinoflagellate cysts assemblages also show differences between the two cores. According to Dave Scott (pers. comm. 2001), such differences are common, even between cores taken a short distance apart (as can be seen by looking on the seismic sections from Freeman 1986 and Souchen 1986). In St. Georges Bay, foraminifera and pollen assemblages from short cores taken a small distance apart show some differences (Schafer and Mudie 1980). The laboratory procedures might also have contributed to these differences, as the palynology samples were processed in two different laboratories (see method). Compression of sediments by the piston corer could explain why the 120 cm gravity core corresponds to a sedimentary section half as long (60 cm) in the piston core. There is also a possibility that the surface sediments are missing in the gravity core.

Table 5.1

Depth	Lab number	type of sample	^{14}C age	cal BP
65-67 cm	TO6232	foraminifera	3100 ± 60 BP	2758 (2830-2688)
640-650 cm	TO6233	foraminifera	7930 ± 80 BP	8317 (8413-8242)

5.4 Methods

5.4.1 Laboratory procedure

The sampling interval was 10 cm in the first two meters of the piston core, and 20 cm in the reminder of the core. This gives a resolution of 80 to 100 years.

For samples from the piston core, a tablet of *Lycopodium* spores was added to 5cc sediment samples. The samples were then washed through 120 micron and 10 micron sieves with distilled water. This sieving is used to remove the coarser fraction and part of the fine silt and clay. The sediment fraction between 10 and 120 microns was recovered and underwent chemical processing in an automated focused microwave digestion system (Micro-digest 3.6) following a procedure tested to ensure that the palynomorphs were not affected by the digestion (Loucheur 1999). The sediment was heated at 27% power, first with 10 % HCl for 15 minutes, then with concentrated HF for 20 minutes and finally, with $AlCl_3$ for 20 minutes. HCl and HF were used to remove carbonate and silicate. The $AlCl_3$ was used to neutralize HF.

The samples from the gravity core were processed differently. After the addition of *Lycopodium* spores tablet, they were disaggregated using a 0.02 % calgon solution in a hot water bath. The samples were then centrifuged, washed with water and decanted, before hot treatment with 10% HCl (~1 hour), and HF (~2-3 hours).

After the chemical processing the samples from both cores were washed again with distilled water in a 10 microns Nitex mesh sieve to remove the residues from the digestion. Slides were mounted with glycerin jelly.

5.4.2 Microscope analysis

Microscope studies were carried out on a Zeiss Ultraphot microscope, with transmitted light, at an average magnification of 250X or 400X. Counts were performed along latitudinal transects across the slide. When only a few transects were necessary, they were scattered throughout the slide.

Counts reached minima of 300 dinocysts and 300 pollen grains in the majority of samples. Lesser counts were reached in only a few samples, but were never below 200 pollen or dinocysts. Spores, organic lining of foraminifera, *Halodinium*, *Pediastrum* and reworked palynomorphs were also counted. All palynomorphs mentioned in the paper were counted simultaneously.

5.4.3 Reconstructions

The transfer functions used in this study are those adapted for dinocyst assemblages by Rochon et al. (1999) from the Best Analogue method of Guiot (1990).

August and February temperature and salinity, and the duration of sea ice cover were reconstructed. The reconstructions are based on the GEOTOP database of 540 reference sites (now published in de Vernal et al. 2001) and on 58 new sites from the Scotian Shelf and northwest Atlantic, added by the author (see appendix 2 to 9 in thesis).

The procedure starts with a logarithmic transformation of percentage abundance (see Rochon et al. 1999). The 10 closest modern analogues are then selected within the reference database, using an even weight for each taxa. The environmental data provided by this set of analogues, is used to calculate the most probable estimate for each sea surface parameter. Each estimate is a weighted average of these environmental data, the weight being determined by the degree of similarity (distance) between the fossil assemblage and each modern analogue selected. The minimum and maximum environmental values in the set of analogues are used to define the confidence interval.

The accuracy of the temperature reconstructions is ± 1.06 °C for February and ± 1.35 °C for August. For salinity, the accuracy of the reconstructions is ± 2.0 psu and ± 1.9 psu for February and August respectively. The reconstructed duration of the sea ice cover, is accurate to ± 1.36 month per year. The accuracy is the difference between the modern sea surface conditions (the instrumental values) and a reconstruction of these same sea surface conditions using the modern reference database.

5.5 Results

5.5.1 Concentrations of palynomorphs

Marine palynomorphs are abundant in core 84-011-12 (fig. 5.4). Dinoflagellate cyst concentrations are around 30,000 cysts/cm^3 throughout the piston core, except for a peak of 130,000 cysts/cm^3 at 90 cm (3300 BP). In the gravity core, concentrations are also around 30,000 cysts/cm^3.

Concentrations of organic linings of foraminifera are low at the base of the core (~2000 linings/cm^3), start to increase above 600 cm and reach a maximum of 19,000 at 170 cm (4000 BP). Between this peak and the top of the core, as well as in the gravity core, they remain between 5000 and 10,000 linings/cm^3.

Pollen concentrations are between 3000 and 5000 grains/cm^3 at the base (below 480 cm) and the top of the core (>50 cm), while they are higher (10,000 grains/cm^3) in between. In the gravity core, they are around 5000 grains/cm^3.

In most of the piston and in the gravity core, concentrations of 2000 to 4000 fern and moss spores/cm^3 are found. In the middle of the piston core (300-500 cm), they reach of peak of 24,000 spores/cm^3 (at 440 cm).

Reworked palynomorphs are not found in every sample and their concentrations remain low in both the piston and gravity cores, generally 100 palynomorphs/cm^3. In a few samples, they reach 1000 to 2000 individuals/cm^3.

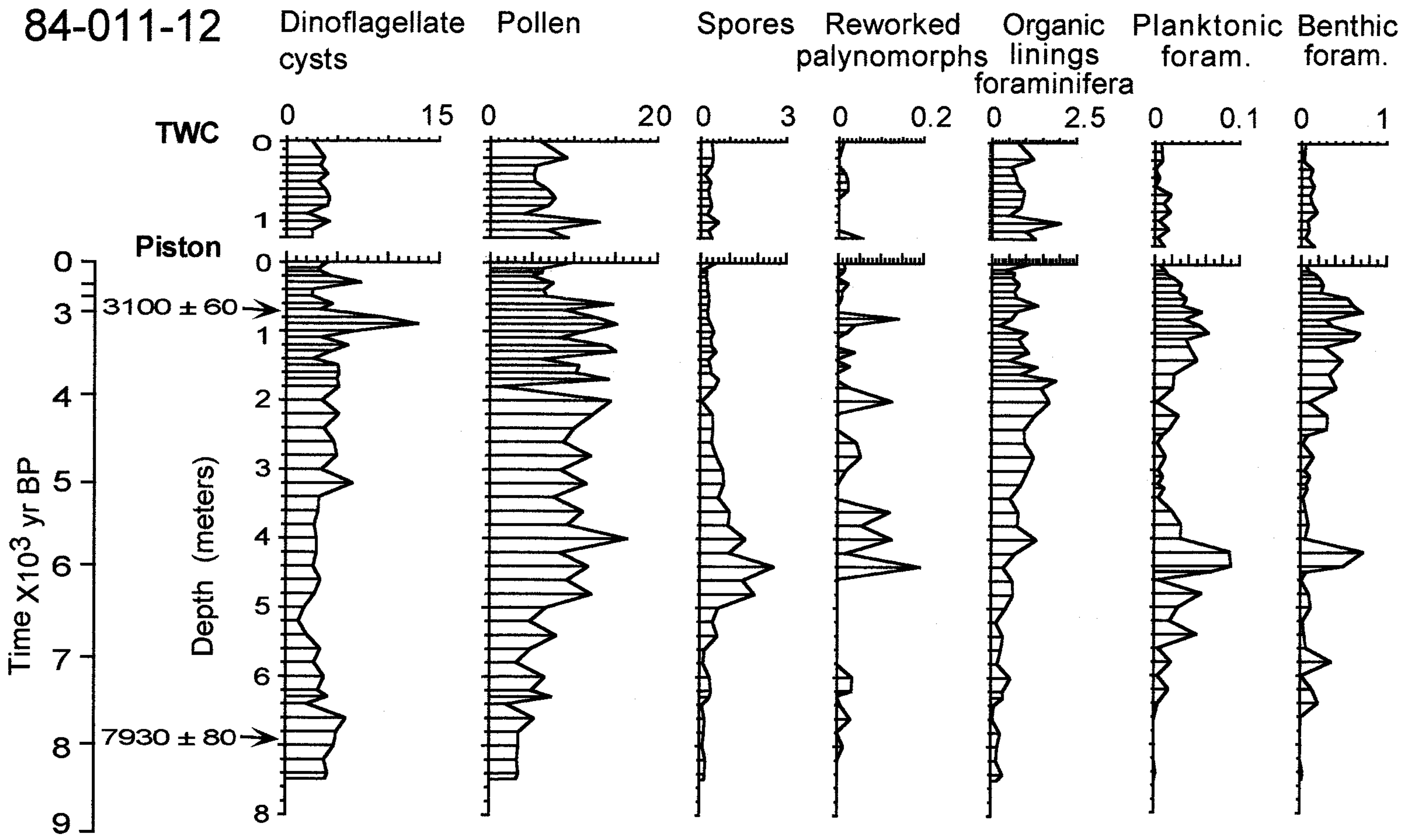

Figure 5.4: Concentrations of various palynomorphs per gram of sediments (x10^4). The spore category includes mainly spores of Filicales (Osmundaceae and Polypodiaceae), *Sphagnum* and *Lycopodium* (*L. annotinum, L. clavatum* and *L. lucidulum*). The vertical axis represents the downcore depth while the small scale to the left shows the radiocarbon ages. Total benthic and planktonic foraminiferal concentrations (per 10cc sediments) are from Freeman (1986).

5.5.2 Pollen assemblages

Pollen assemblages are dominated by pollen of conifers (mainly *Pinus*, *Picea*, *Abies*, *Tsuga*) and deciduous shrubs (*Betula*, *Alnus*) with some hardwood tree pollen (*Betula*, *Acer*, *Quercus*, *Fagus*, *Fraxinus* and *Ulmus*) and herbs (Cyperaceae; fig. 5.5).

Pollen assemblage zone A 745-680 cm (8800-8200 BP)

Pollen assemblage zone A is characterized by relatively low pollen concentrations, high percentages of *Pinus* pollen, and the maximum percentages of *Abies*, *Alnus*, and shrub *Betula*[1]. *Salix* and herbs (Cyperaceae, Polygonaceae) are also relatively important.

Pollen assemblage zone C1 540-440 cm (7000-6200 BP)

Pollen assemblage zone C1 is defined by the maximum percentages of *Pinus*, the appearance of *Tsuga* and by decreased proportion of shrub (*Betula*, *Alnus*) and *Abies* pollen. It is also the zone where the proportion of total *Betula* is the lowest.

---

[1] *Betula* pollen grain smaller than 20 microns are considered to represent shrub varieties (Dyer 1986).

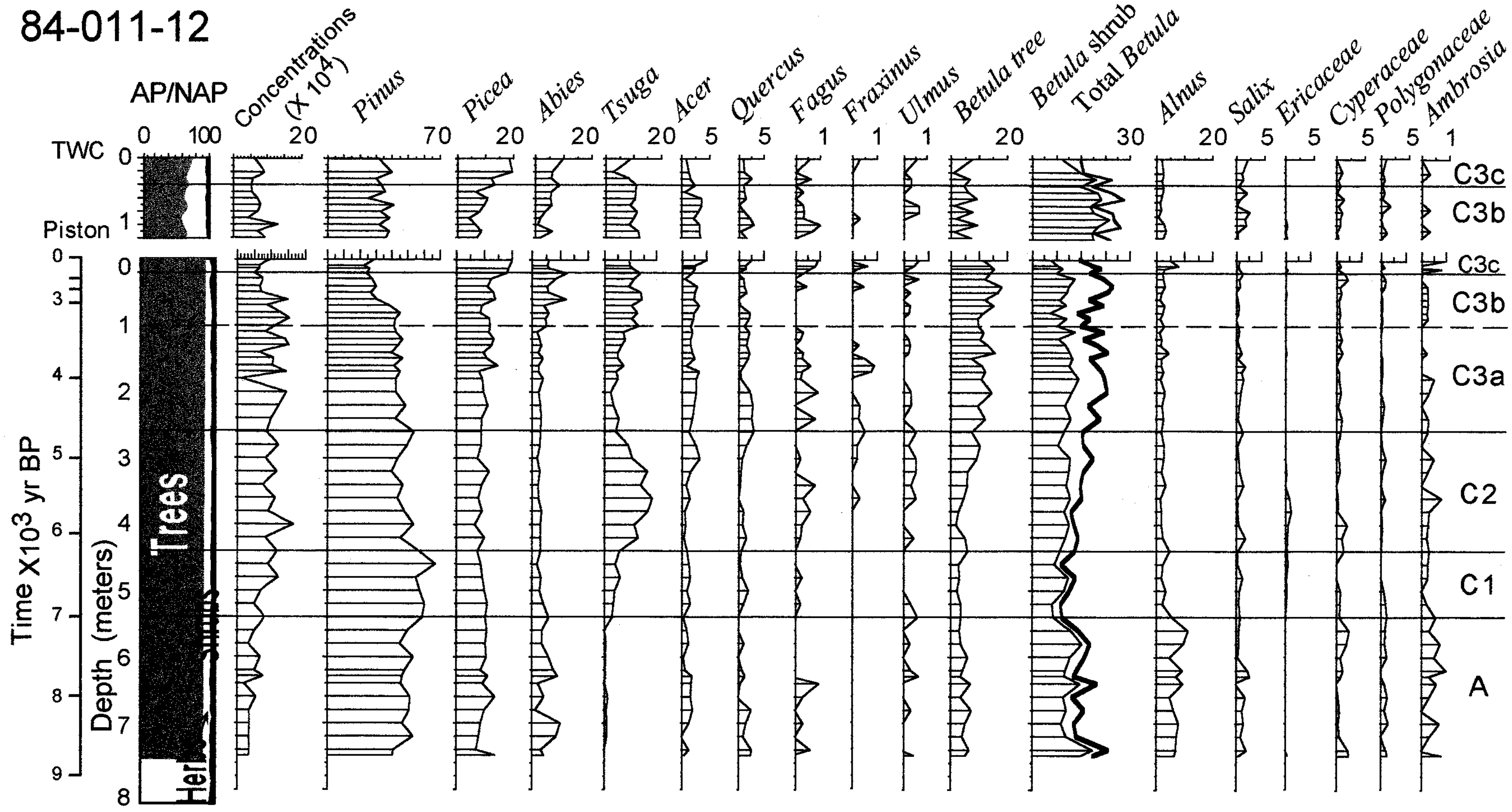

Figure 5.5: Pollen diagram of core 84-011-12. Percentages calculated on the pollen sum, which excludes spores. Proportions of tree, shrub and herb pollen are shown on the left. *Betula* pollen smaller than 20 microns are assumed to represent shrub variety. The solid line, right of the shrub-*Betula* curve is the total *Betula* pollen i.e. shrub and tree. The small scale to the left shows radiocarbon ages.

Pollen assemblage zone C2 440-260 cm (6200-4700 BP)

The peak of *Tsuga* pollen in zone C2 suggests a warmer climate and was traditionally used to define the hypsithermal in Nova Scotia. Percentages of tree *Betula* and hardwoods gradually increase in this zone, and *Fraxinus* first appears in the middle of the zone.

Pollen assemblage zone C3 upper 260 cm (4700 to 0 BP)

This zone starts with the decline of *Tsuga* and is characterized by the highest percentages of tree *Betula* (also total *Betula*) and hardwoods. In zone C3a, *Pinus* is still the main component of the assemblages, but its decline in zone C3b is accompanied by an increase of *Tsuga* and *Abies* percentages.

The upper 20 cm of the piston core reflect the beginning of land clearance (zone C3c) with a slight increase in *Ambrosia* and *Rumex* pollen. In addition, there are a slight decrease in *Betula* shrub, and an increase in *Picea.* These two changes also occur in the upper 40 cm of the gravity core and are used to locate zone C3c, because *Ambrosia* and *Rumex* do not increase at the top of that core.

In St. Georges Bay, Schafer and Mudie (1980) reported an increase in *Rumex* and *Ambrosia*, as well as decline in tree pollen, which is not seen in core 12. This probably corresponded to forest exploitation in Nova Scotia starting about 1760 AD. Their pollen records also show an increase in *Alnus* in zone C3c, which is present in the piston core.

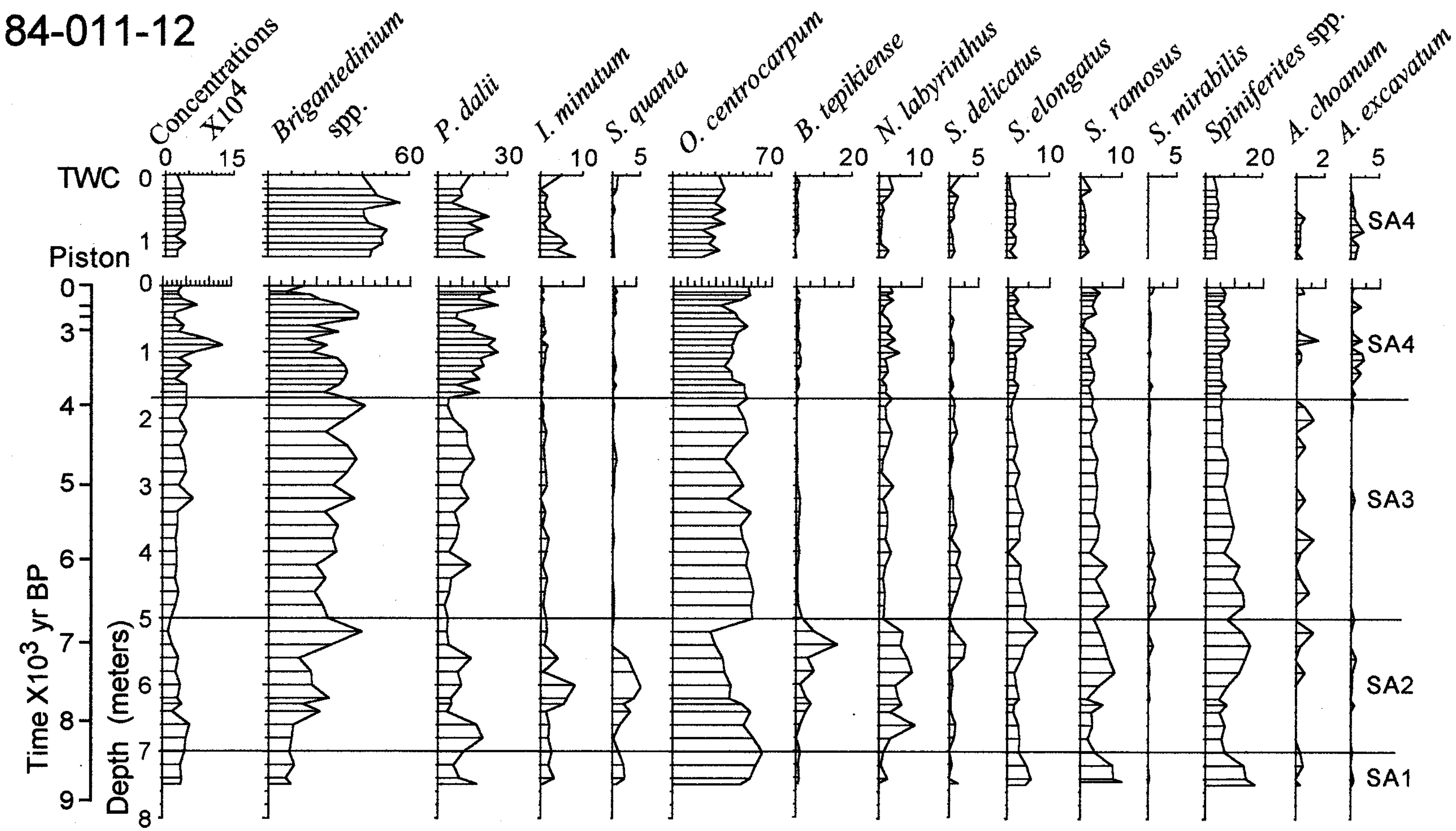

Figure 5.6: Dinoflagellate cyst diagram of core 84-011-12. *Brigantedinium* spp. includes *B. cariacoense* and *B. simplex*. *Spiniferites* total includes cysts belonging to the genus (*S. bulloides, S. delicatus, S. elongatus, S. frigidus, S. mirabilis, S. ramosus*). The vertical axis represents downcore depth. Scale on left shows the radiocarbon ages.

5.5.3 Dinoflagellate cyst assemblages

Assemblages throughout core 84-011-12 are dominated by *Brigantedinium* spp., *O. centrocarpum* and *Pentapharsodinium dalii.* Minor species are *Islandinium minutum, Selenopemphix quanta, Bitectatodinium tepikiense, Nematosphaeropsis labyrinthus, Spiniferites* spp., *Ataxiodinium choanum,* and cf. *Alexandrium tamarense*

Dinoflagellate cyst assemblage zone SA1 750-680 cm (8800 to 8200 BP)

In zone SA1 (fig. 5.6), assemblages are dominated by *O. centrocarpum* (50-60%), with *Spiniferites* spp. (mainly *S. ramosus* and *S. elongatus*), *P. dalii* and *Brigantedinium* spp. Proportions of other taxa (*I. minutum, S. quanta, B. tepikiense, N. labyrinthus A. choanum, cf. A. tamarense*) are low.

Dinoflagellate cyst assemblage zone SA2 680-500 cm (8200 to 6700 BP)

Zone SA2 is defined by the maximum relative abundance of *N. labyrinthus* and of other minor species, including *B. tepikiense, S. quanta.* Proportion of *O. centrocarpum* decreases throughout the zone and reaches a minimum of 30% at the top. *P. dalii* follows a similar trend. Percentages of *Brigantedinium* spp. and *B. tepikiense* show an inverse trend: they increase from 10% and 1 % at the base to 35% and 15% respectively at the top of zone SA2. *I. minutum* and *S. quanta* are more abundant in the middle of zone SA2. *A. choanum* and *S. mirabilis* are present in the upper part of the zone.

Dinoflagellate cyst assemblage zone SA3 500-170 cm (6700 to 4000 BP)

O. centrocarpum and *Brigantedinium* spp dominate the assemblages of zone SA3. Among the accompanying taxa, *Spiniferites* spp (mainly *S. ramosus* and *S. elongatus*) and *P. dalii* are the most abundant. There is a sharp decrease in the proportion of *B. tepikiense* and *N. labyrinthus* relative to zone SA2. Maximum percentages of *S. mirabilis* occur at the base of the zone. *A. choanum* is sporadically present.

Zone SA4 170-0 cm (last 4000 years) and all of the gravity core

Zone SA4 is dominated by *O. centrocarpum*, *Brigantedinium* spp. and *P. dalii*, which reaches its maximum relative abundance in this zone. A peak in total concentrations between 80 and 100 cm (3200-3400 BP) coincides with lower percentages of *Brigantedinium* spp., higher percentages of *P. dalii* and the occurrence of *A. choanum*. Maximum percentages (2%) of cf. *Alexandrium tamarense* cyst-type (Rochon et al. 1999) are found in this zone. This corresponds to influx of 1 to 200 cysts/cm^2 yr.

Differences in the percentages of *Brigantedinium* spp. and *O. centrocarpum* between the gravity and the upper part of the piston core are unexplained, considering that pollen assemblages in the gravity core are similar to those of the upper zone of the piston core. This is why a separate assemblage zone was not created for the gravity core dinoflagellate cyst assemblages. As previously stated, differences in processing could be responsible for these differences.

5.6 Relative sea level

The nearest site where the relative sea level (RSL) has been reconstructed is Sable Island (Scott et al. 1989b). According to these data, Sable Island was affected only by submergence during the Holocene. At 11,000 and 8100 BP, the RSL was respectively 49 m and 35 m lower than today. By 4000 BP, it was only about 10 m lower than the present day sea level.

There is no relative sea-level curve for St. Anne's Basin but we can assume that the sea level has been rising only throughout the Holocene. Stea et al. (1994) present evidence for a -65 m lowstand on the inner Scotian Shelf around 12,000 BP. By 10,000 BP, the sea level had already risen to 38 m below the present day level, and to –35m by 8000 BP.

Maps from Dyke and Prest (1987) show that banks were emergent at 11,000 BP but not at 10,000 BP. While not emergent, the banks would have been much shallower than today (about 10 m water depth instead of 50m). The water depth in the central part of the shelf around St. Anne’s Basin would have been 50 to 60 m and the water depth in St. Anne’s Basin itself would probably still have been about 200 m. The absence of banks immediately to the east of the Basin, where the shelf is 50-100 m deep, suggests that St.

Anne's Basin was still connected with the Laurentian Channel by at least shallow channels.

5.7 Reconstructions of sea surface conditions

Of all the parameters reconstructed for core 84-011-12, the sea surface temperatures (SST) for February and August values display the greatest changes (fig. 5.7). Variations in values of February salinity and in the sea ice cover duration, generally remain within the precision of the method for these parameters, except for a few intervals. August salinity is usually slightly higher than the modern average.

For the lowest part of the core (before 8600 BP), reconstructed temperatures and salinities are higher than today by 3-4 °C and by 1.5-2 psu. Following this, there is an interval from 8600 to 7000 BP characterized by cooler SST than today (1 °C cooler in February, 2 to 3 °C cooler in August), except for a possible spike in the February SST curve at 8000 BP. Sea ice cover also has a slightly longer duration than today (up to 1 month longer), while salinities are close to today's average.

Between 7000 and 6000 BP, SST is higher than the modern average, by up to 4 °C in August and up to 1.5 °C in February. Salinities are also higher than modern averages by 1 to 1.5 psu, while sea ice cover was probably less than 50% of the surface. After 6000, sea surface temperatures drop and remain 2 to 4 °C below today's average in August (1.5 °C lower in February) until 4000 BP.

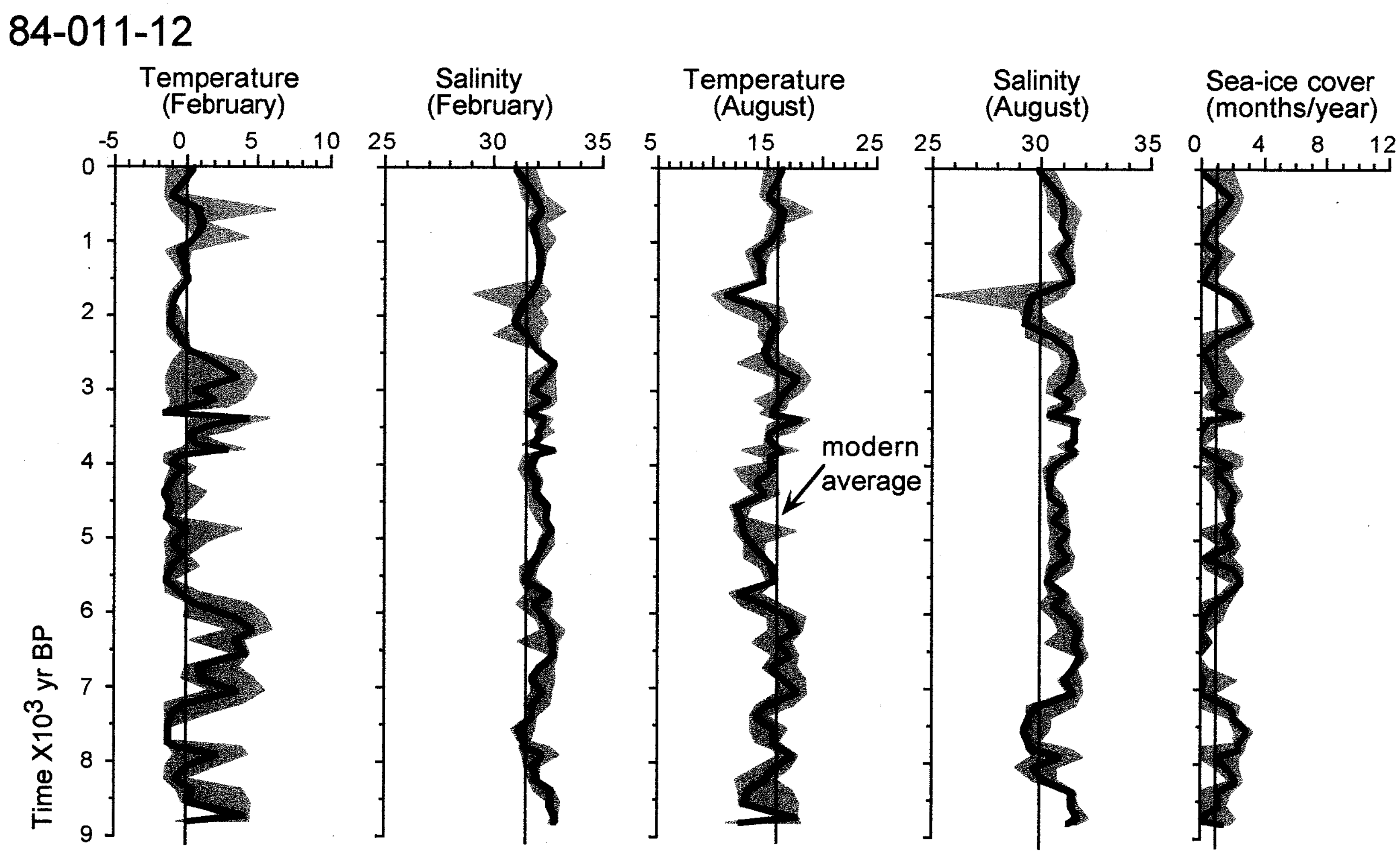

Figure 5.7: Reconstructions of sea surface conditions from core 84-011-12. The solid line represents the best estimate while the grey area shows the confidence interval. A vertical line across each curve indicates modern values. Ice cover duration is for a ice cover of at least 50% of the sea surface.

Another warm period, with intervals characterized by February SST 2 to 4 °C higher than the modern averages, is found between 4000 and 2500 BP. The August temperatures shows only a few excursions above the average. Again, the warm interval is followed by a drop in the SST, especially in August (as much as 5 °C lower than today) and an increase in the duration of the sea ice cover. In the last 1500 years, there is a gradual August SST increase and salinity decrease, while the other parameters are close to modern values.

5.8 Discussion

5.8.1 Palynomorph concentrations

Dinoflagellate cyst concentrations are comparable with those found in Canso and Emerald Basin (Scott et al. 1984), surface samples from the Scotian Shelf (Rochon et al. 1999; this study), Bay of Islands (Levac 2002a) and La Have Basin (Levac 2001). Unlike La Have Basin core 95-030-24, concentrations are constant throughout the core, without a concentration peak at the base of the core.

Organic lining concentrations are comparable to those found in Bay of Islands (Levac 2002a) and in the Gulf of St. Lawrence (Giroux 1990), but generally much higher than those in La Have Basin (2000-4000 linings/cm^3; Levac 2001). Interestingly, concentrations of linings are much higher that those of tests. In core 84-011-12, total concentrations of benthic foraminifera tests never reach more than 300 individuals per cubic cm of sediments and planktonics are even lower with the highest concentrations reaching 50 individuals/cm ^{3} (Freeman, 1986). In nearby core 84-011-11, concentrations of tests are comparable (Souchen, 1986). In other Scotian Shelf basins (Emerald and Canso Basins), concentrations of benthic foraminiferal tests are equally low (50-300 individuals/cm^{3}; Scott et al. 1984).

The fact that concentrations of linings are 10 to 20 times those of foraminifera can suggest that CaCO3 dissolution is important in St. Anne's Basin (and in all Scotian Shelf basins). Indeed, planktonic foraminifera are greatly affected by dissolution in the Scotian Shelf Basins (D.B. Scott, Dalhousie University, personal communication 2001). But we also have to take into account the size of the sieve. For the palynological analysis, the 10-120 micron size fraction of the sediment is used, whereas for the micropaleontological analysis, Scott et al. (1984; 1989a) Freeman (1986) and Souchen (1986) both studied the size fraction greater than 63 micron. However, as David B. Scott points out, foraminifera smaller than 63 micron are sometimes more abundant and this could account for the greater concentrations of organic linings in the palynological samples.

Pollen concentrations in St. Anne's Basin core are low in comparison to the pollen concentrations in Bay of Islands, which is expected from the more offshore location (Mudie 1982) but they are in the some order of magnitude as the pollen concentrations in La Have Basin core 24 (chapter 3).

5.8.2 General trends in the reconstructed sea surface conditions (fig. 5.8)

A few trends become apparent when comparing the reconstructions of sea surface conditions in La Have Basin, St. Anne's Basin and Bay of Islands cores (fig 5.8). In general, February SST is higher than today's average throughout the Holocene while August SST remained equal or lower than today's average. In intervals characterized by warmer SST (such as the early Holocene optimum), the difference between the reconstructed values and the present day average was greater for the February SST than for the August SST.

In the three cores, higher salinity values (both February and August) were reconstructed during the early Holocene optimum. During the cold interval following the optimum, salinity was generally lower, especially in La Have Basin, but given the precision of the method it is not significant. After this, reconstructed salinity values for La Have Basin generally remain close to the modern averages. In St. Anne's Basin and Bay of Islands, reconstructed August salinity is higher than today's average through most of these two cores. In Bay of Islands, February salinity was also slightly higher.

Overall, there is no evidence that various events are synchronous between the three basins.

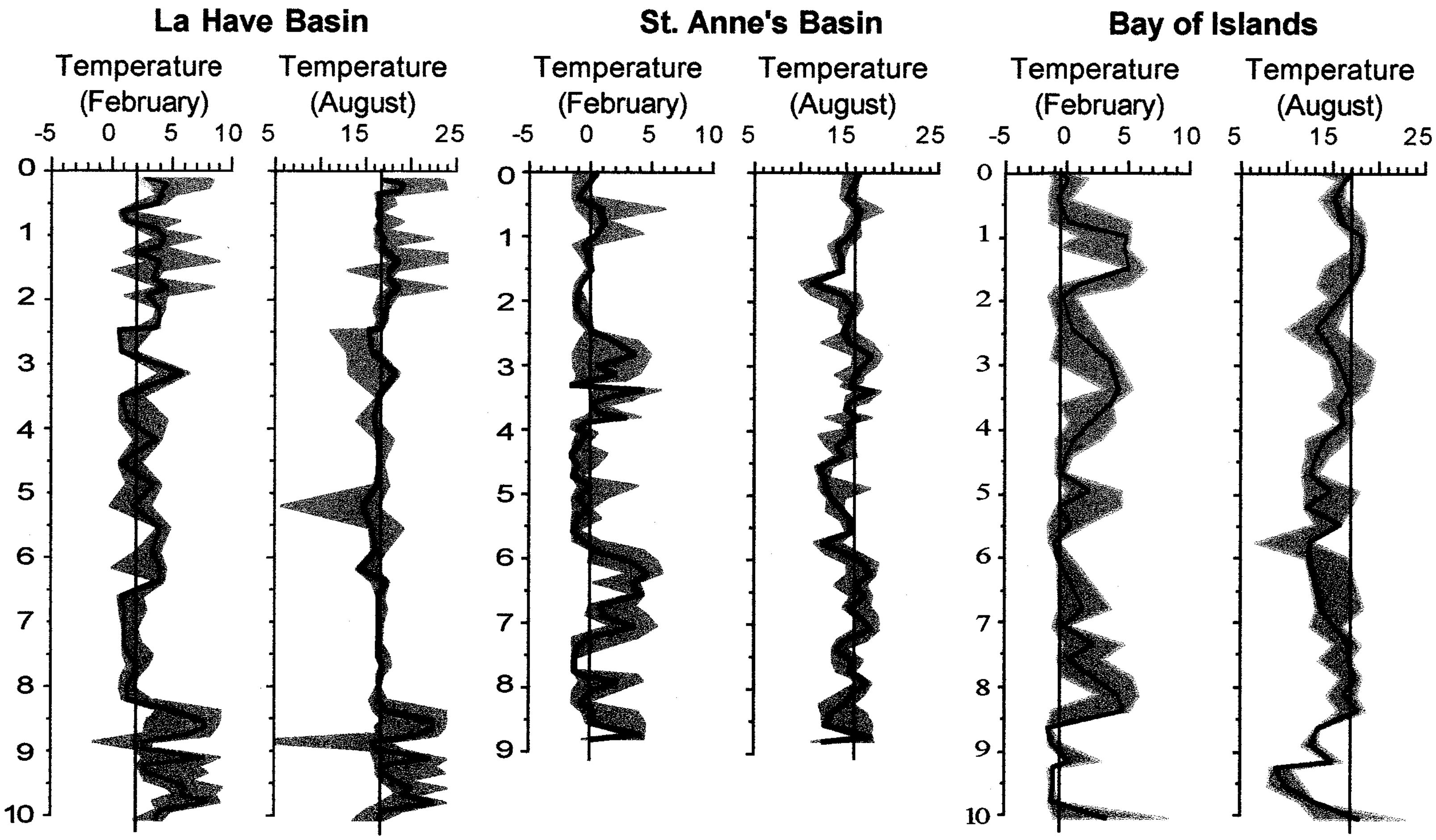

Figure 5.8: Comparison of SST reconstructions for cores 95-030-24, 84-011-12 and MD 99-2225 (La Have and St. Anne's Basin, and Bay of Islands). The vertical axis represents corrected radiocarbon ages. Setting is the same as figure 5.7.

5.8.3 Holocene sea surface conditions, Scotian Shelf Basin, the Gulf of St. Lawrence and Bay of Islands (Table 5.2)

For most of the cores, sea surface conditions were reconstructed using the best analogues method (Rochon et al. 1999) and the data are directly comparable. In Emerald and Canso Basins however, no transfer functions were initially performed by Scott et al. (1984) but transfer functions were done on the Emerald Basin core by Mudie et al. (2002; also Levac et al. 2000). For Canso Basin, the dinoflagellate cysts assemblages were compared with those of nearby cores on which transfer functions were performed. While this type of comparison cannot provide quantitative values for SST and salinity, it can at least be used to provide a time frame for the early Holocene warm interval, the subsequent cooling and the late Holocene cooling.

In St. Anne's Basin and Bay of Islands, the maximum reconstructed SST coincides with the maximum percentages of *B. tepikiense* and *Spiniferites* (and the presence of *S. mirabilis*), therefore the maximum representation of *B. tepikiense* and the abundance of *Spiniferites* spp. in nearby Canso Basin probably represent the early Holocene SST optimum. If we examine only the dinoflagellate cyst assemblages from zone B of Emerald Basin (Scott et al. 1984), the presence of *B. tepikiense* and *Spiniferites* spp., as well as the absence of *I. minutum* suggest that the SST optimum also occurred in the early Holocene in that Basin. However, transfer functions performed on combined data from core 77-002-20 (Scott et al. 1984) and core 87-003-004 (Mudie et al. 2002) are in contradiction with this interpretation. They indicate that August SST were 2 to 4 °C

Table 5.2: Summary of reconstructed SST in Scotian Shelf basins and the Gulf of St. Lawrence area. For Emerald and Canso Basins, the SST are inferred from dinoflagellate cyst assemblages.

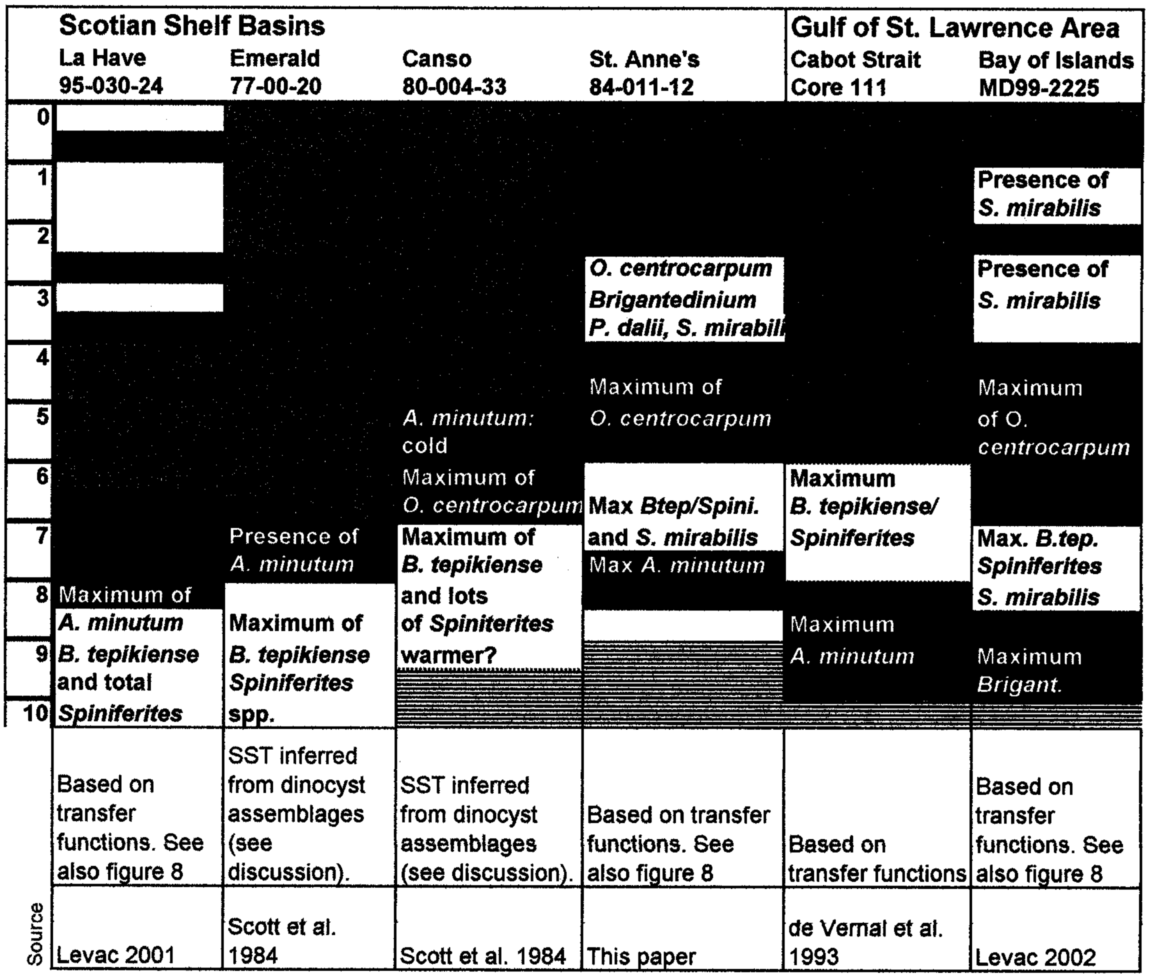

	Scotian Shelf Basins				Gulf of St. Lawrence Area	
	La Have 95-030-24	Emerald 77-00-20	Canso 80-004-33	St. Anne's 84-011-12	Cabot Strait Core 111	Bay of Islands MD99-2225
0–10	Maximum of **A. minutum** **B. tepikiense** **and total** ***Spiniferites***	Presence of *A. minutum* **Maximum of** ***B. tepikiense*** ***Spiniferites*** **spp.**	*A. minutum:* cold Maximum of *O. centrocarpum* **Maximum of** ***B. tepikiense*** **and lots** **of *Spiniferites*** **warmer?**	***O. centrocarpum*** ***Brigantedinium*** ***P. dalii, S. mirabil*** Maximum of *O. centrocarpum* **Max *Btep/Spini.*** **and *S. mirabilis*** Max *A. minutum*	**Maximum** ***B. tepikiense/*** ***Spiniferites*** Maximum *A. minutum*	**Presence of** ***S. mirabilis*** **Presence of** ***S. mirabilis*** Maximum of O. *centrocarpum* **Max. *B.tep.*** ***Spiniferites*** ***S. mirabilis*** Maximum *Brigant.*
	Based on transfer functions. See also figure 8	SST inferred from dinocyst assemblages (see discussion).	SST inferred from dinocyst assemblages (see discussion).	Based on transfer functions. See also figure 8	Based on transfer functions	Based on transfer functions. See also figure 8
Source	Levac 2001	Scott et al. 1984	Scott et al. 1984	This paper	de Vernal et al. 1993	Levac 2002

LEGEND

☐	■
SST markedly warmer than today (+2 to 5°C)	SST markedly cooler than today (-2 to -5°C)

below the present day average from 11,000 to ~ 3000 BP, equal to present from 3000 to 1500 BP and colder again from 1500 BP until the last few hundred years. The absence of *P. dalii* from Emerald Basin core 77-002-20 (Mudie 1980; Scott et al. 1984) is certainly disturbing as it is present in every surface sample from the Scotian Shelf (see appendices 2 to 9). Differences in processing could account for this.

An interval characterized by colder SST than today follows the SST optimum at all sites. The duration of this interval varies from 1000 to 4000 years. In La Have Basin, it coincides with maximum percentages of *I. minutum*. The presence of *I. minutum* is also recorded in Emerald and Canso Basins following the SST optimum, and it is therefore believed to represent similarly cooler conditions.

After 7000 BP, SST in winter were generally slightly higher than today in La Have Basin and gradually evolved towards the present days ones in the last few hundred years. Salinity and SST reconstructions show frequent oscillations around present day average values. Without quantitative reconstructions, it is difficult to tell what happened exactly in Canso Basin but we could assume that the sea surface conditions were similar to those in La Have Basin, based on similar increased proportions of *Brigantedinium* in the last 5000 years. As for the presence of frequent oscillations of SST and salinity, like those observed in the La Have Basin record, it is impossible to make that kind of assumption. The last 6500 years in Emerald Basin were also characterized by increased percentages of *Brigantedinium* and decreasing total dinocyst concentrations that Scott et al. (1984) interpreted as an indication of a progressive cooling of SST. Again, this suggest similar sea surface conditions as in La Have Basin. Reconstructions indicate colder SST in Emerald Basin for most of the Holocene until 3ka (Mudie et al. 2002) but do not show any of the oscillations recorded in other basins (La Have, St. Anne's, Bay of Islands).

In St. Anne's Basin, another interval characterized by generally warmer SST than today is recorded between 4000 and 2500 BP, followed by a cooling trend towards the present day conditions. Similar events are recorded in Bay of Islands. There, the warm event started at the same time but lasted longer (until 1000 BP).

5.8.4 Bottom water conditions in the Scotian Shelf Basins; comparison with sea surface conditions (table 5.3)[1]

In Scotian Shelf Basins, changes in qualitative bottom water conditions recorded by benthic foraminifera and stable isotope data (^{13}C, ^{18}O; Scott et al. 1984; 1989a) show some similarities with changes in the sea surface conditions. Apparently warmer bottom water conditions than today are recorded in the early Holocene, and in most cores, these warm intervals are synchronous with the early Holocene SST optimum. These warm conditions are generally followed by a gradual cooling of bottom water temperatures and a decrease in bottom salinities, toward the present day conditions.

Stable isotopes of carbon and oxygen were used to estimate the bottom water conditions in Canso Basin (Scott et al. 1989a). From 10,000 to 8000 BP, the bottom temperature increased from 4 to 10 °C and it remained around 10°C (8°C higher than

---

[1] See section 3.4.4 on page 45 about age problems in Emerald Basin core 77-002-20.

today) between 8000 and 7000 BP. The dinoflagellate cysts assemblages in this interval (10,000-7000 BP) also suggest warmer SST at that time. The bottom temperatures decreased in the last 7000 years. The decrease was more rapid since 2500 BP (see table 5.3).

In Emerald Basin, stable isotopes were also used on core 83-012-11 (Scott et al. 1989a). An age of 11,140 ^{14}C yr BP can be used to estimate the position of the Holocene in the core, unfortunately, no other dates are available within the Holocene section and the age of various events can only be estimated by comparing the foraminifera assemblages with those of core 77-002-20 (Scott et al. 1984). An interval of warmer bottom temperatures was recorded sometime during the Holocene (~8000 to ~ 2500 BP?) followed by a gradual cooling.

No isotope data is available for the two St. Anne's Basin cores, but we can assume that the *Brizalina subaenariensis* zone represents warmer bottom water temperature just as in Canso Basin. This interval starts a little later in St. Anne's Basin but it ends at the same time as in Canso Basin. In both St. Anne's Basin cores, the increase in *I. teretis* after 7000 BP suggests a gradual cooling of bottom waters (Freeman 1986; Souchen 1986).

Overall, changes in bottom water conditions appear to be more gradual than changes in the sea surface. Also, there are no indications for frequent late Holocene oscillations in bottom salinity and temperature (Scott et al. 1989a), these are restricted to the sea surface.

Table 5.3: Summary of palynological and micropaleontological data for the Scotian Shelf, Gulf of St. Lawrence and Bay of Islands.

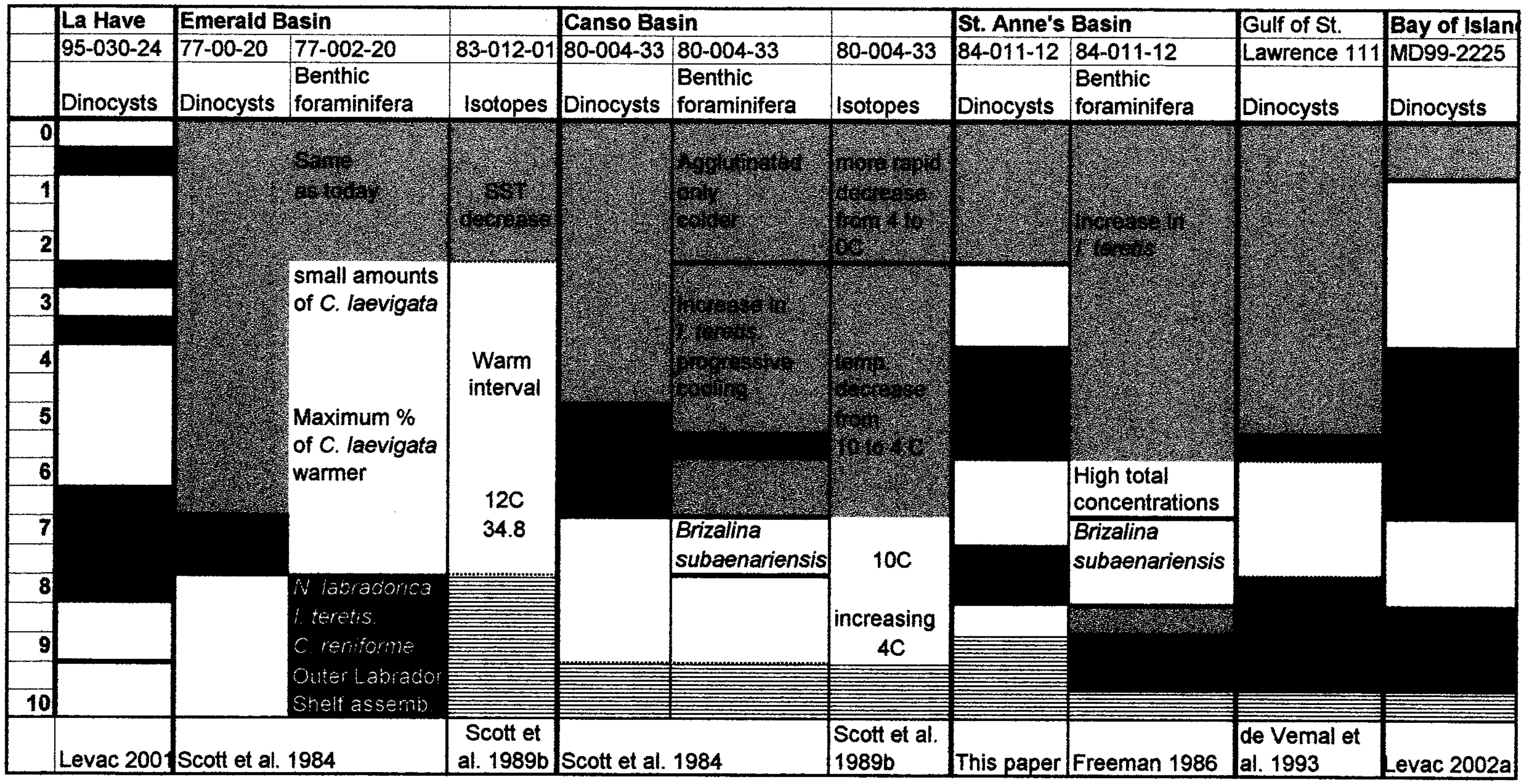

	La Have	Emerald Basin			Canso Basin			St. Anne's Basin		Gulf of St.	Bay of Islan
	95-030-24	77-00-20	77-002-20	83-012-01	80-004-33	80-004-33	80-004-33	84-011-12	84-011-12	Lawrence 111	MD99-2225
	Dinocysts	Dinocysts	Benthic foraminifera	Isotopes	Dinocysts	Benthic foraminifera	Isotopes	Dinocysts	Benthic foraminifera	Dinocysts	Dinocysts
0											
1			Same as today	SST decrease		Agglutinated only colder	more rapid decrease from 4 to 0C				
2									Increase in *I. teretis*		
3			small amounts of *C. laevigata*			Increase in *I. teretis*; progressive cooling					
4				Warm interval			temp. decrease from 10 to 4 C				
5			Maximum % of *C. laevigata* warmer								
6									High total concentrations		
7				12C 34.8		*Brizalina subaenariensis*			*Brizalina subaenariensis*		
8			*N. labradorica* *I. teretis.* *C. reniforme* Outer Labrador Shelf assemb				10C				
9							increasing 4C				
10											
	Levac 200	Scott et al. 1984		Scott et al. 1989b	Scott et al. 1984		Scott et al. 1989b	This paper	Freeman 1986	de Vernal et al. 1993	Levac 2002a

For detail about dinoflagellate cysts assemblages, refer to table 5.2

5.8.5 Regional paleoceanographic trends

One of the initial hypotheses of this paper was that the early Holocene SST optimum was progressively younger toward the northeast. This appears to be the case, at least on the Scotian Shelf. In La Have and Emerald Basins, the early Holocene SST optimum started before 10,000 BP and ended at 8500 BP in La Have (Levac 2001) and ~ 8000 BP in Emerald Basin (Scott et al. 1984). We cannot tell if it started earlier in Canso Basin as the record only begins around 9500 BP, but it ends later at ~ 7000 BP. In St. Anne's Basin, the SST optimum started and ended much later (from 7500 to 6000 BP). However, the record begins only at 8800 BP, therefore, it is possible that the optimum started earlier, especially since the SST are slightly higher than today at the very base of the record.

In Bay of Islands, there is evidence that the start of the SST optimum was delayed until 8600 BP by the Middle Stanley meltwater phase (Levac 2002a). The optimum ended ~ 6800 BP (Levac 2002a). The influx of meltwater must have been very large to affect sea surface conditions (both the salinity and temperature) inside the Bay of Islands; therefore it would be reasonable to assume that it affected the sea surface conditions throughout the Gulf of St. Lawrence as well. In fact, a slight cooling of SST is recorded in core 111 from Cabot Strait (de Vernal et al. 1993), just before an interval of warmer SST between ~7800 BP and 6000 BP. In St. Anne's Basin, benthic foraminifera indicate colder bottom water conditions (see table 5.3) coincident with the timing of the Middle Stanley phase. The occurrence of warmer temperatures than today at the sea surface of the same basin between 8800 and 8500 BP suggests that the cold, dense meltwater affected only the bottom conditions in that basin.

If we consider an earlier start for the SST optimum in St. Anne's Basin, then we could also propose that the Late Stanley meltwater phase (Moore et al. 2000) caused an interruption of the SST optimum in St. Anne's Basin between 8500 and 7500 BP. The meltwater event could have been weaker than the previous one (the Middle Stanley phase), transiting only along the southwestern side of the Gulf of St. Lawrence and Laurentian Channel, without affecting Bay of Islands, and then moving downstream along the inner Scotian Shelf.

Another objective of this study was to determine if the cool SST interval following the optimum was a regional phenomenon. The compilation of data from the Scotian Shelf (table 5.3) shows that the early Holocene SST optimum is followed in all basins by an interval of cooler SST. The duration of this interval appears to vary from 1000 to 3000 years. But while post-optimum cool SST intervals appears to be a standard feature of the Scotian Shelf (and Bay of Islands) records, differences in timing make their interpretation difficult and suggest that they could have different causes.

In La Have Basin (and in Emerald Basin), the timing of the post-optimum cool SST interval occurs just after the Late Stanley meltwater phase, therefore this cannot be the direct cause of this cooling. The timing would coincide with the collapse the Hudson Bay ice sheet around 8000 BP (which will be examined in the broader regional synthesis; Chapter 6). This event could also be time correlative with the cooler SST that precede the optimum in St. Anne’s Basin. This event would have put an end to the SST optimum in La Have Basin, while delaying (or interrupting) the optimum in St. Anne’s Basin.

The post-optimum cooling started 1000 years later (~7000 BP) in Canso Basin and Bay of Islands, and around 6000 BP in St. Anne's Basin and the Gulf of St. Lawrence. Therefore, the cooling must be caused by another event there. A short-lived cool interval in cores from the Laurentian Channel and Fan around 7100 is believed to represent the last meltwater pulse from the residual ice sheet (Keigwin and Jones 1995), but Moore et al. (2000) do not report any influx of meltwater at that time.

Over the Laurentian Fan, the SST optimum lasted from 10,000 to 6000 BP (Keigwin and Jones, 1995). Meltwater transiting through the Gulf of St. Lawrence and Laurentian Channel could be mixed before it reaches the Laurentian Fan and meltwater pulses may not be recorded in sediments from that area. This would account for such a long uninterrupted SST optimum over the Laurentian Fan. If so, it is possible that the early Holocene SST optimum would have lasted uninterrupted from ~ 10,000 until 6000 BP, in both La Have and St. Anne's Basin, if there had been no meltwater pulses or other cold spells.

The SST and salinity records from St. Anne's Basin indeed show oscillations around the present day average similar to those from La Have Basin and Bay of Islands records. At present, it is not possible to correlate the various oscillations between the three cores. Nevertheless, the short-duration cooling episodes around 500-700 years ago may correspond to the beginning of the Little Ice Age.

A late Holocene warm episode is reconstructed in St. Anne's Basin. It starts around 4000 BP, as in Bay of Islands, but it has a shorter duration, ending at 2500 BP. This event is difficult to explain because it started at the time of an intensification of the Labrador Current in the Labrador Sea (3500 BP; Fillon 1976) and a regional cooling trend. It is also not evident in the Gulf of St. Lawrence cores or in La Have, Emerald and Canso Basins.

At this point, the cause of this late Holocene warm event in St. Anne's Basin and Bay of Islands in uncertain. Because the climate of eastern Canada was dryer during the mid/late Holocene (Prentice et al. 1991; Gajewski et al. 2000) there may have been a reduction in freshwater runoff from the Gulf of St. Lawrence drainage basin. Another hypothesis would be a seasonal reduction of the Labrador Current.

A southward and offshore migration of the Gulf Stream after 4000 BP (Balsam and Heusser 1976) and a greater strength of the Labrador Current after 3500 BP (Fillon 1976) are believed to be responsible for a late Holocene cooling along the southeastern Canadian margin. The start of this late Holocene cooling varies throughout the region.

A bottom water cooling is suggested by benthic foraminifera in Emerald and Canso Basins (Scott et al. 1984) and St. Anne's Basin (Freeman 1986; Souchen 1986) starting at 4500 BP, 5000 BP and 6000 BP respectively.

At the sea surface, the cooling trend started around 7 ka in Emerald Basin (Scott et al. 1984), 5000 BP over the Laurentian Fan (Keigwin and Jones 1995) but much later further offshore, e.g. 2000 BP over the Fogo Seamount (Mudie 1992). The late Holocene cooling is apparently absent in records from the Gulf of St. Lawrence (de Vernal et al.

1993). In St. Anne's Basin, La Have Basin (Levac 2001) and Bay of Islands (Levac 2002a), a clear late Holocene cooling trend, as defined in other studies from the region, is difficult to see because of the SST oscillations. Levac (2001) suggested that the Late Holocene cooling was not a continuous trend but was instead a series of episodic sea surface cooling events, representing an increased influence of the cold Labrador Current, starting as early as 7000 years ago, i.e. during/after the post-optimum SST cooling episode. If so, the Late Holocene cooling trend would have started ~ 7000 BP in Bay of Islands and ~ 6000 BP in St. Anne's Basin.

5.8.6 Comparison with pollen diagrams from Cape Breton

The pollen diagram from St. Anne's Basin was correlated with pollen diagrams from lakes on the eastern side of Cape Breton: Wreck Cove (Livingstone and Estes 1967), Gillis Lake (Livingstone and Livingstone 1958), Salmon River Lake, Upper Gillis Lake, and McDougal Lake (Livingstone 1968) (see also summary in Anderson 1985).

While the St. Anne Basin pollen diagram shows similar trends as the onshore diagrams, a few differences can be noted. The first difference is the greater proportion of bisaccate pollen (mainly *Pinus* and *Picea*), which is due to preferential transport of this type of pollen toward the offshore (Mudie 1982). The greater proportion of *Pinus* may explain why the B zone (which is characterised by maximum representation of *Pinus* in the assemblages) does not stand out and cannot be delimited in the St. Anne Basin core. However, Livingstone (1968) also notes that the *Pinus* B zone is often absent in Nova

Scotia. In our diagram, the interval from 8800 to 7000 BP is assigned to zone A, despite the fact that zone B spans the interval from 8200 to 7000 BP in Cape Breton (Anderson 1985).

The absence of a clear *Quercus* maximum in zone C1 when compared to the C1 zones of other Nova Scotia records (Livingstone and Livingstone 1968) could reflect its much lower abundance in the Cape Breton vegetation relative to mainland Nova Scotia (Rowe 1972). Transport processes could also be involved (Mudie 1982).

Finally, changes in the proportions of conifer pollen made it possible to define subzones C3a and C3b in the St. Anne pollen diagram, just as in Gillis Lake (Livingstone and Livingstone 1958), while zone C3 was not subdivided in the other Cape Breton diagrams.

5.8.7 Interpretation of pollen assemblages and comparison with sea surface temperature

Pollen assemblages from zone A probably represent an open conifer forest where shrubs were still abundant. There is much evidence that most of the tree species represented in zone A were indeed growing in Cape Breton at that time. Green (1987) placed the arrival of *Pinus*, *Picea*, *Ulmus* and *Betula* around 9000 BP at Salmon River (southeast Cape Breton). However, a steep increase in the absolute pollen frequencies of *Picea* at Upper Gillies Lake (near Sydney, Cape Breton; Livingstone 1968) and absolute pollen frequencies from Wreck Cove (Livingstone and Estes 1967) on the Cape Breton Plateau strongly suggest that *Picea* could have been present there before 9000 BP. Also, the presence of *Betula papyrifera* (tree birch) macrofossils at McDougal Lake near Sydney (50 km north of Salmon River) indicates that this tree was growing in the area before 9000 BP (Livingstone 1968). The other tree species gradually followed, with *Tsuga* and *Ulmus* arriving in the area around 8200 BP, and *Abies* and *Acer* around 7900 BP. SST were higher than today at the base of the core (8800 BP) and again between 7500 and 6000 BP.

In the following zone C1 the decline of shrubs probably represents the development of a closed forest with more hardwoods, including *Fagus*, which arrived in the area around 6800 BP (Green 1987). The conifer forest was gradually transformed into a mixed conifer/hardwoods forest around 6200 BP (zone C2). The maximum abundance of *Tsuga* in zone C2 suggests climate conditions 1 to 2 °C warmer than today (Jetté and Mott 1995). The warm climatic conditions onshore at that time coincide with sea surface conditions that were colder than today.

The decline of *Tsuga* around 4700 BP is believed to be the result of a disease (Davis, 1981). In zone C3a, *Acer*, *Quercus*, *Fagus* and *Fraxinus* pollen actually reach their highest proportions. The onshore climate was probably still warm during this interval. This is also the time of the second warm SST interval in February(4000-2500 BP). The decline of *Pinus* and the increase of *Picea* around 3000 BP suggest cooler climatic conditions over Cape Breton. August SST were colder than today between 2500 and ~ 1500 BP.

5.9 Conclusions

1- On the Scotian Shelf, the early Holocene SST optimum appears to be progressively younger toward the northeast, beginning near 10,000 BP in La Have Basin and at 7500 BP in St. Anne's Basin.

2- Alternatively, the early Holocene SST optimum may have started earlier in St. Anne's Basin (8800 BP or before) and was interrupted between 8500 and 7500 BP, by the Late Stanley meltwater phase.

3- A cool SST interval followed the optimum in St. Anne's Basin. The causes for these cooler SST are unknown but may be related to similar events in Canso Basin, Gulf of St. Lawrence and Bay of Islands around that time. In the western part of the Scotian Shelf (La Have and Emerald Basins), the post-optimum cooling occurred earlier and appears to correspond with the collapse of the Hudson Bay ice sheet.

4- A late Holocene warm SST interval started at 4000 BP, as in Bay of Islands western Newfoundland, but with a shorter duration (ending ~2500 BP). This are still no explanations for this event but the pollen assemblage from Cape Breton suggests that climatic conditions were still relatively warm at that time.

5-Oscillations of SST and salinity, similar to those in La Have Basin and Bay of Islands, are recorded in St. Anne's Basin. Furthermore, the late Holocene cooling trend could have started as early as 6000 BP in St. Anne’s Basin, proceeding in a series of episodic sea surface cooling events.

6- Correlations with lake pollen records indicate that the start of the hypsithermal onshore was delayed relative to the SST optimum and occurred during the subsequent cold SST interval. They also indicate that climatic conditions were still warm onshore during the second warm SST interval. Finally, changes in vegetation indicate the start of a cooling trend onshore, just before the onset of a cooler August SST interval (from 2500 to 1500 BP).

CHAPTER 6 Synthesis and final discussion

6.1 Introduction

The initial objectives of this thesis were to provide quantitative data for paleoceanographic conditions/changes in the southeastern Canadian region, to improve the resolution and to obtain a more precise dating of various events (see Levac 2001).

The La Have Basin (fig. 6.1) record provided all this (see Levac 2001). Three main features stand out from the record and they differ from the conclusions of previous studies: 1) There is a difference in the timing of the hypsithermal and the Neoglacial events between the ocean and the land; for the hypsithermal, it is vegetation (and climate) which lag behind the SST optimum by about 2000 years. For the Neoglacial cooling, it appears to be the opposite scenario with an onset onshore 1500 years earlier than the ocean; 2) An interval characterized by colder SST than today occurs right after the marine SST optimum; 3) Recurrent intervals with lower SST and salinity than today are recorded during the last 6500 years.

These differences were further investigated using a record from Bay of Islands (fig. 6.1; Levac 2002a), and reconstruction showed the following trends which are similar to La Have Basin: the occurrence of an early Holocene SST optimum (even though it is delayed by a meltwater event from the Great Lakes) which is followed by a cool SST interval, a delay in the start of the hypsithermal on land relative to the occurrence of warm sea surface conditions, frequent oscillation of salinity and SST since 6000-7000 BP, and an earlier start for the Neoglacial cooling on land.

The reconstructions from Bay of Islands also show some differences with those from La Have Basin: the SST optimum is more important for February temperature than for August temperature, the subsequent cool SST interval starts later and a second warm SST interval occurs in the late Holocene.

The St. Anne's Basin (fig. 6.1) core was also used to examine the timing of the early Holocene SST optimum and of the subsequent cool interval (Levac 2002b). These two events appear to be progressively younger toward the northeast, at least on the Scotian Shelf. In addition, the same delay between the start of the hypsithermal onshore and the SST optimum is observed. Reconstructions from St. Anne's Basin showed the presence of a late Holocene warm interval similar to that reconstructed in Bay of Islands between 4 and 1 ka, but with a shorter duration (until 2500 BP).[1]

Explanation for some of the events that characterized the Holocene over the Scotian Shelf are not always found at a local/regional scale. Because the southeastern Canadian Margin is influenced by waters derived from the inner and outer branches of the Labrador Currents (see fig. 6.2), and therefore indirectly derived from the Canadian Arctic, unexplained paleoceanographic events could find their source further upstream. Among these are the recurrent oscillation in SST and salinity which characterizes the Holocene (Levac 2001; 2002a, 2002b), and the post-optimum SST cooling. While the start of the cool SST interval in La Have Basin coincides with the collapse of the Hudson

---

[1] The evolution of sea surface conditions on the southeastern Canadian Margin is summarized in detail in the previous chapter.

Strait ice (see Levac 2001 and Levac 2002b), the later occurrence of this cool interval in Bay of Islands and St. Anne's Basin indicates it has to have a different cause there.

6.1.1 Objectives

The main objective of this synthesis will be to try to answer questions about the inter-relationship between different regions along the eastern Canadian Margin. A detailed examination will be made of the individual signals along a south to north transect from La Have Basin to northern Baffin Bay. Special attention will be given to the comparison and timing of warm and cold intervals and to a more exact determination of the speed of changes and amplitude of signals throughout the Holocene. The goal is to exploit these exceptionally high resolution records, and make good use of these quantitative reconstructions.

Then the palynology literature for Labrador Shelf and Baffin Bay will be reviewed and compared with foraminiferal studies, and linked with the main paleoceanographic trends identified at the two northernmost sites of the transect (Labrador Shelf and North Water Polynya). We will see the importance of obtaining higher resolution records to understand the nature and the directions of paleoceanographic changes, especially when it comes to determining their rapidity.

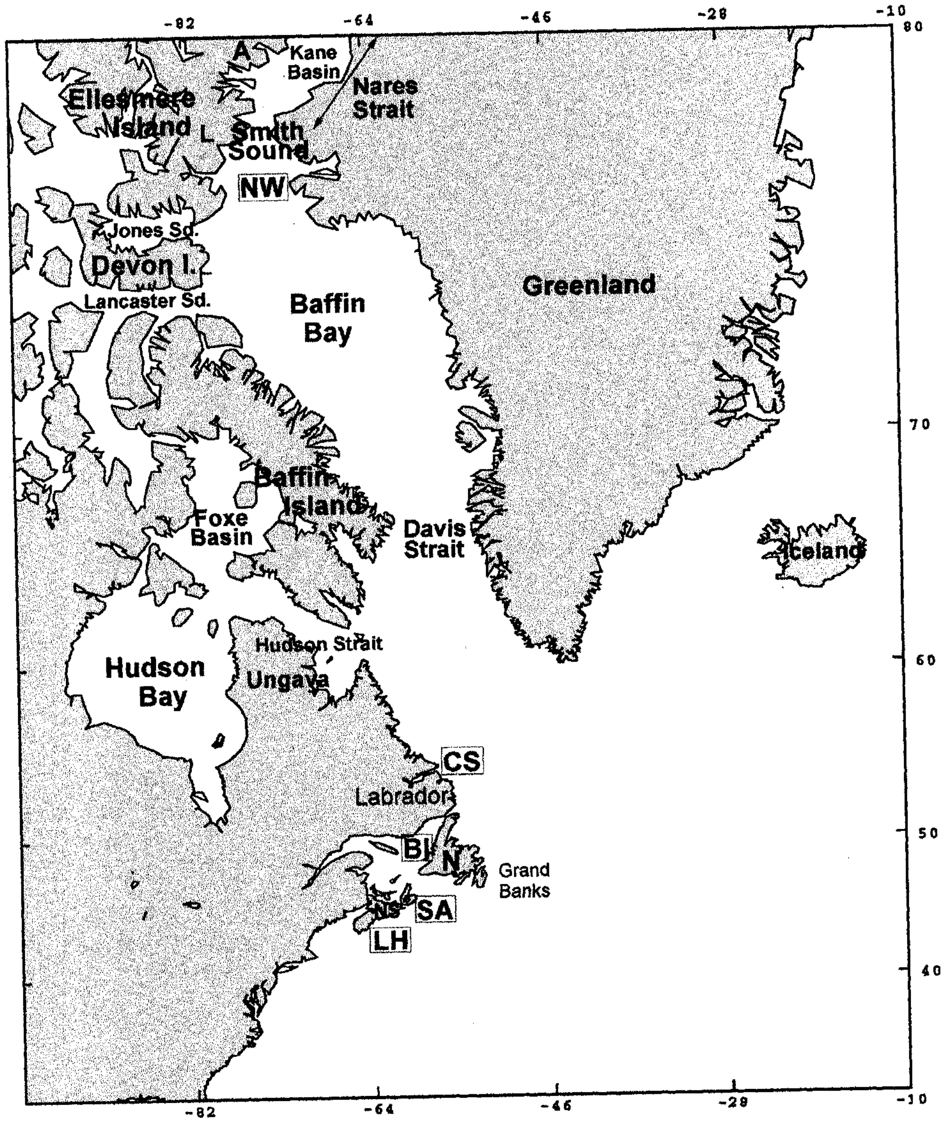

Figure 6.1: Regional geography and location of cores presented in the Scotian Shelf-Baffin Bay transect. LH: La Have Basin, SA: St. Anne's Basin, BI: Bay of Islands, CS: Cartwright Saddle, NW: North Water Polynya, N: Newfoundland, NS: Nova Scotia.

The third part will examine changes in sea surface conditions/circulation as inferred from various proxy/methods, based on deep-sea records from the Labrador Sea, Baffin Bay, Canadian Arctic, and the Greenland shelves. The potential impact of surface circulation changes in the North Atlantic on the sea surface conditions over the Scotian Shelf will be investigated.

In the fourth part, the impact of meltwater influx, which is an important variable/forcing, especially during the early Holocene, will be examined. Meltwater had many sources: the Great Lakes, the northern and eastern sector or the Laurentide ice sheet, and the Arctic. Important influx could have influenced the conditions on the Scotian Shelf and in Bay of Islands either through the St. Lawrence River or through the Labrador Current.

Evidence for the hypsithermal in terrestrial records from Labrador to the Arctic will be presented in part 5. Comparison of reconstructed sea surface conditions with pollen records from adjacent areas will address the question of the lead/lag between climate and sea surface conditions. Changes in atmospheric circulation in the Holocene, inferred both from long distance pollen influx to the Arctic and global circulation models will be examined in relation to changes in climate. The same will be done for the Neoglacial.

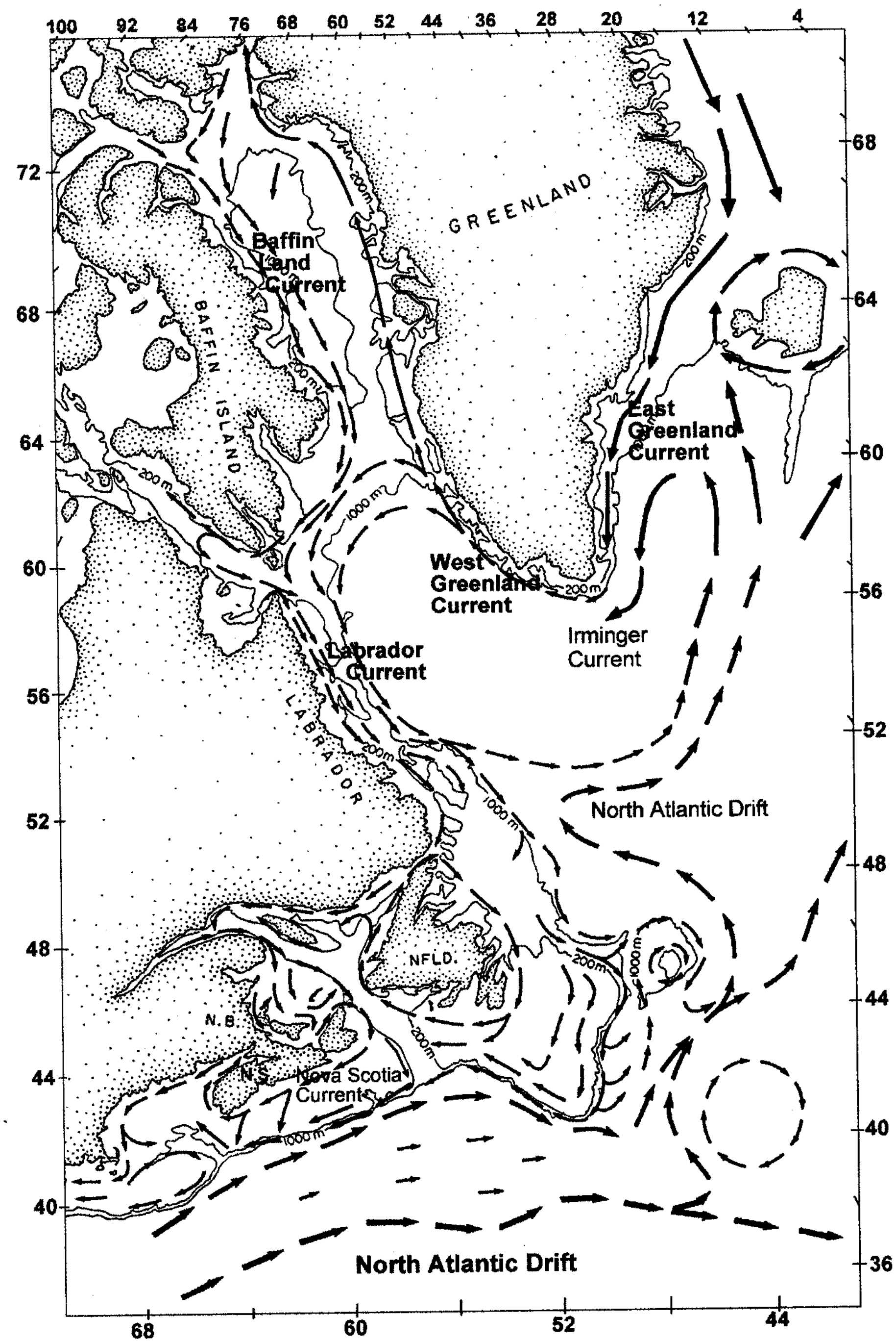

Figure 6.2: Surface circulation in the northwest North Atlantic, Labrador Sea and Baffin Bay (based on: Greenberg and Petrie 1988; Han et al. 1999; Shore et al. 2000).

6.2 Reconstructed sea surface conditions along a Scotian Shelf-northern Baffin Bay transect

6.2.1 Description of the sites

The south-north transect includes reconstructions from 5 cores from the southwest Scotian Shelf to the Labrador Shelf: La Have and St. Anne's Basins, Bay of Islands, Cartwright Saddle, and northern Baffin Bay (fig. 6.1 for locations; table 6.1 for details). Reconstructed sea surface temperature, salinity and the duration of seasonal sea ice cover (covering more than 50% of the sea surface), are presented in figures 6.3 to 6.5. Present average for August SST and salinity, and sea ice cover duration are shown in table 1.

The southernmost site, La Have Basin is located on the southwest part of the Scotian Shelf. Reconstructions are based on data from core 95-030-24, published in Levac (2001; see also chapter 3) and from. Surface conditions at that location are influenced by the Nova Scotia Current, derived in part from the Gulf of St. Lawrence and mixed with Labrador Current water from the Newfoundland Shelf (fig. 6.2).

St. Anne's Basin is located on the northeast part of the Scotian Shelf, near the Laurentian Channel and Cape Breton. This part of the Scotian Shelf is influenced by continental runoff from the St. Lawrence River, and waters derived from the Labrador Current (fig. 6.2). Reconstructions are based on data from core 84-011-12, published in Levac (2002b; see also chapter 5).

Bay of Islands is located along the western coast of Newfoundland and is influenced by the inner branch of the Labrador Current, which enters Cabot Strait and mixes with water masses in the Gulf of St. Lawrence (fig. 6.2). Reconstructions are based on core MD99-2225 (Levac 2002a; see chapter 4).

Cartwright Saddle is a basin on the Labrador Shelf, 75 km from the coasts. Surface conditions are cold and reflect primarily the presence of the Inner Labrador Current. Reconstruction from core 95-024-006, Cartwright Saddle, initially published in Levac and de Vernal (1997), relied on an older database of 371 reference sites (de Vernal et al. 1994). Reconstructions for the present paper were performed again using a larger reference database containing 598 sites (appendix 25).

When compared with Levac and de Vernal (1997), these new reconstructions show similar low salinity, low SST and long sea-ice cover duration before 6 ka, except that these new runs display more variability, especially for ice cover and salinity. In both runs, there are similar abrupt drops in sea-ice cover at 6ka and the disappearance of oscillations in surface salinity. Warmer SST than present are seen in the new run between 6-4 ka, while Levac and de Vernal (1997) initially reported the absence of warmer SST in this core. This is followed by a gradual decrease in SST and an increase in ice cover duration after 4 ka, probably the Neoglacial cooling trend, which appear to culminate between 1 and 2ka with the longest ice cover duration and the coldest SST.

The northernmost site of the transect is located in the North Water Polynya, in northernmost Baffin Bay. This is an arctic site that receives surface water from the West Greenland Current and the polar Nares Strait Current. For a detailed description of the site and the modern sea surface conditions refer to Levac et al. (2001) and to table 6.1. Reconstructions were initially published in Levac et al. (2001).

Table 6.1: Cores used for the south-north transect (see figure 6.1)

	Core number	**Location**	**Water depth**	**August SST**	**August salinity**	**Ice cover duration**	**Publication**
La Have Basin	95-030-24	43°46'N; 63°43'W	256	17	31.5	0	Levac, 2001
St. Anne's Basin	84-011-12	45°47'N; 58°39'W	270	16	30	40 days	Levac 2002b
Bay of Islands	MD99-2225	49°N; 58°05'W	104	17	30.7	60 days	Levac, 2002a
Cartwright Saddle	95-024-6	54°43'N, 56°27'W	530	6.5	31.3	6 months	Levac and de Vernal, 1997
North Water Polynya	91-039-7 and 8	77°16'N, 74°20'W	663	2.5	32	8 months	Levac et al. 2001
North Water Polynya	91-039-12	76°48'N, 71°51'W	823	2.5	32	8 months	Levac et al. 2001

6.2.2 Main trends in sea surface conditions along the transect, amplitude and rapidity of changes during the Holocene

Results from the reconstructions will not be described in detail here as this has already been done in previous chapters (chapters 3-5) and publications (Levac 2001; 2002a; 2002b; Levac et al. 2001). Rather, the main trends will be outlined here (fig. 6.3 to 6.5).

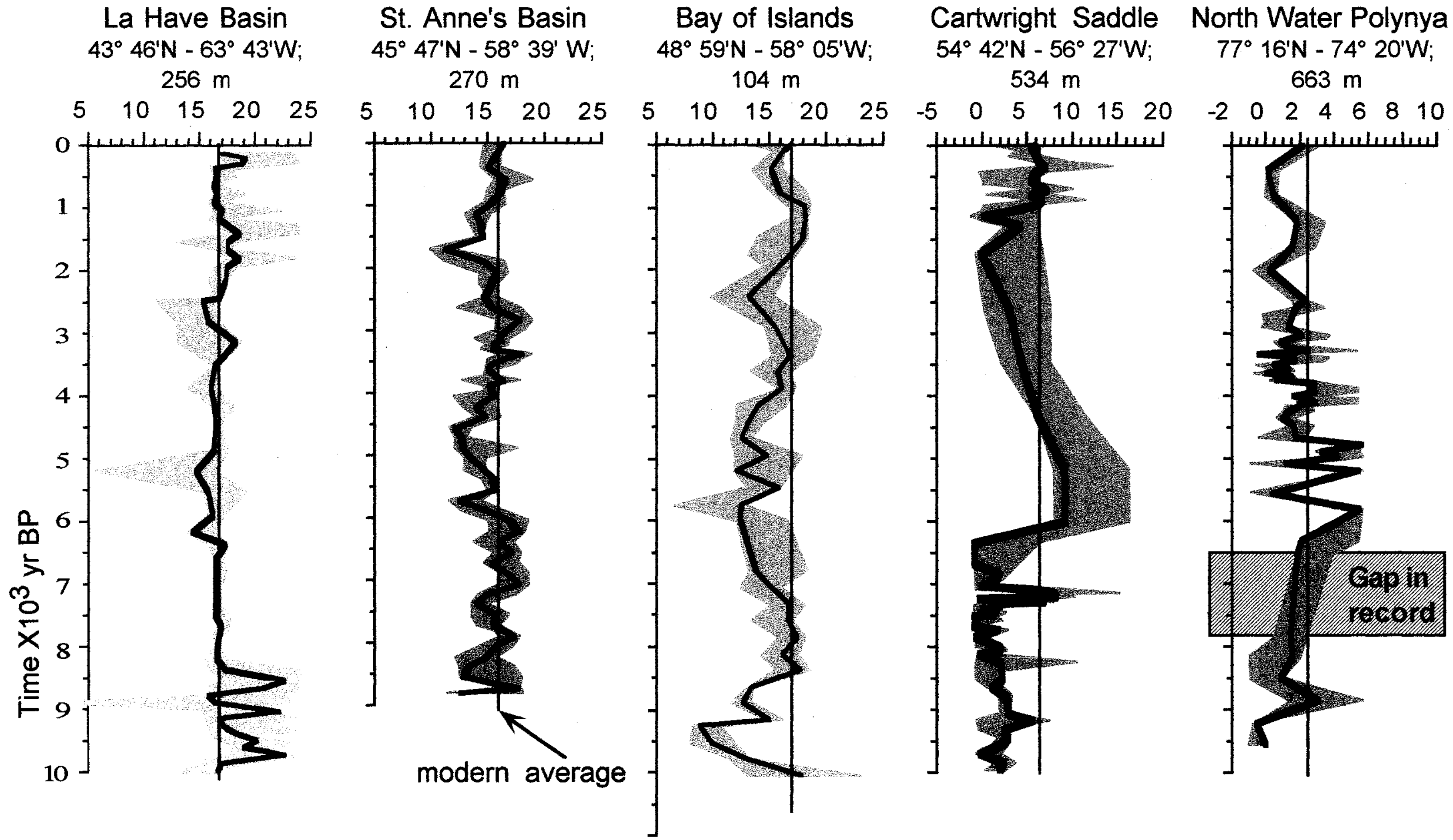

Figure 6.3: Reconstructed August sea surface temperature along the Scotian Shelf-northern Baffin Bay transect

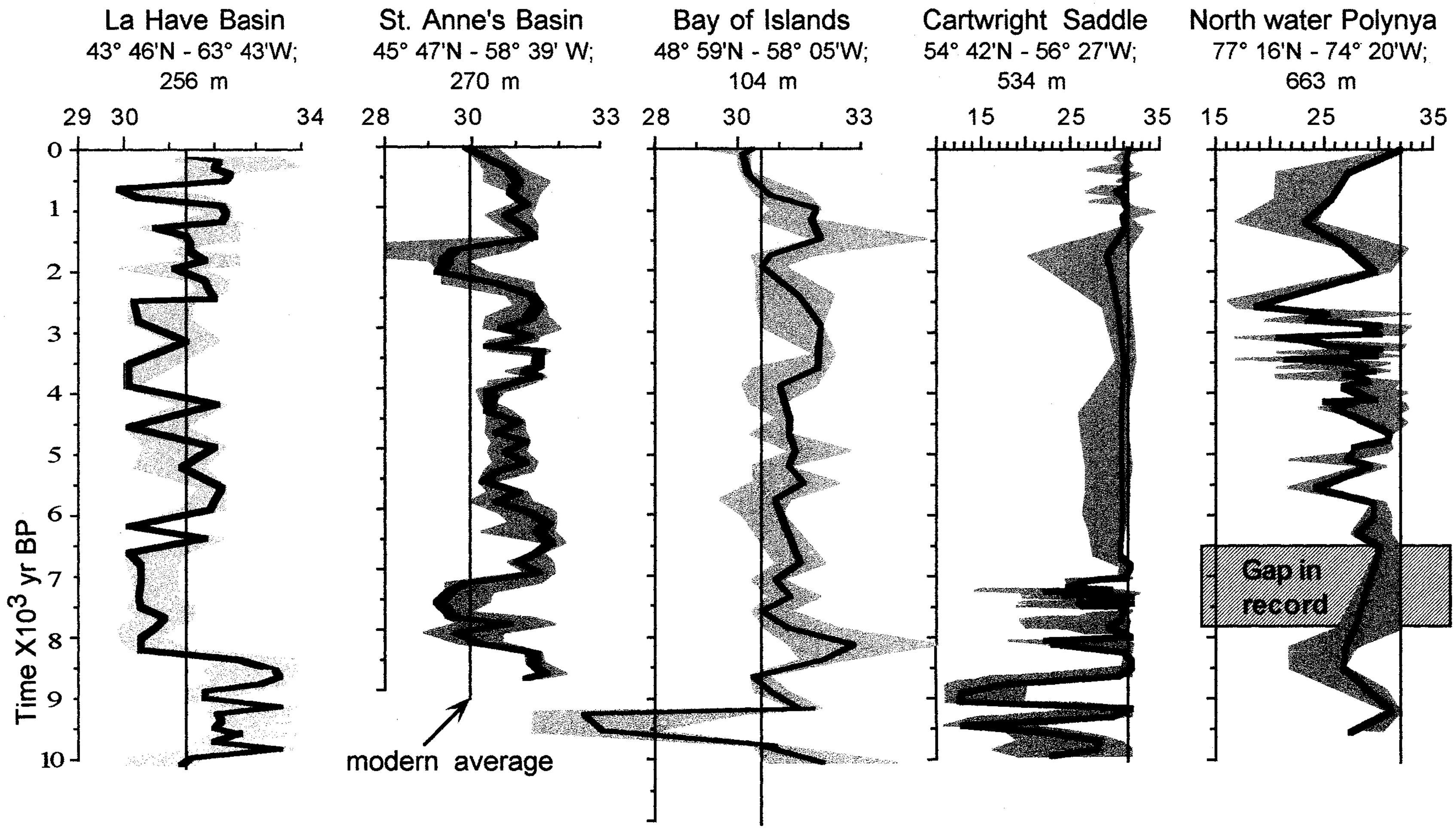

Figure 6.4: Reconstructed August sea surface salinity along the Scotian Shelf-northern Baffin Bay transect

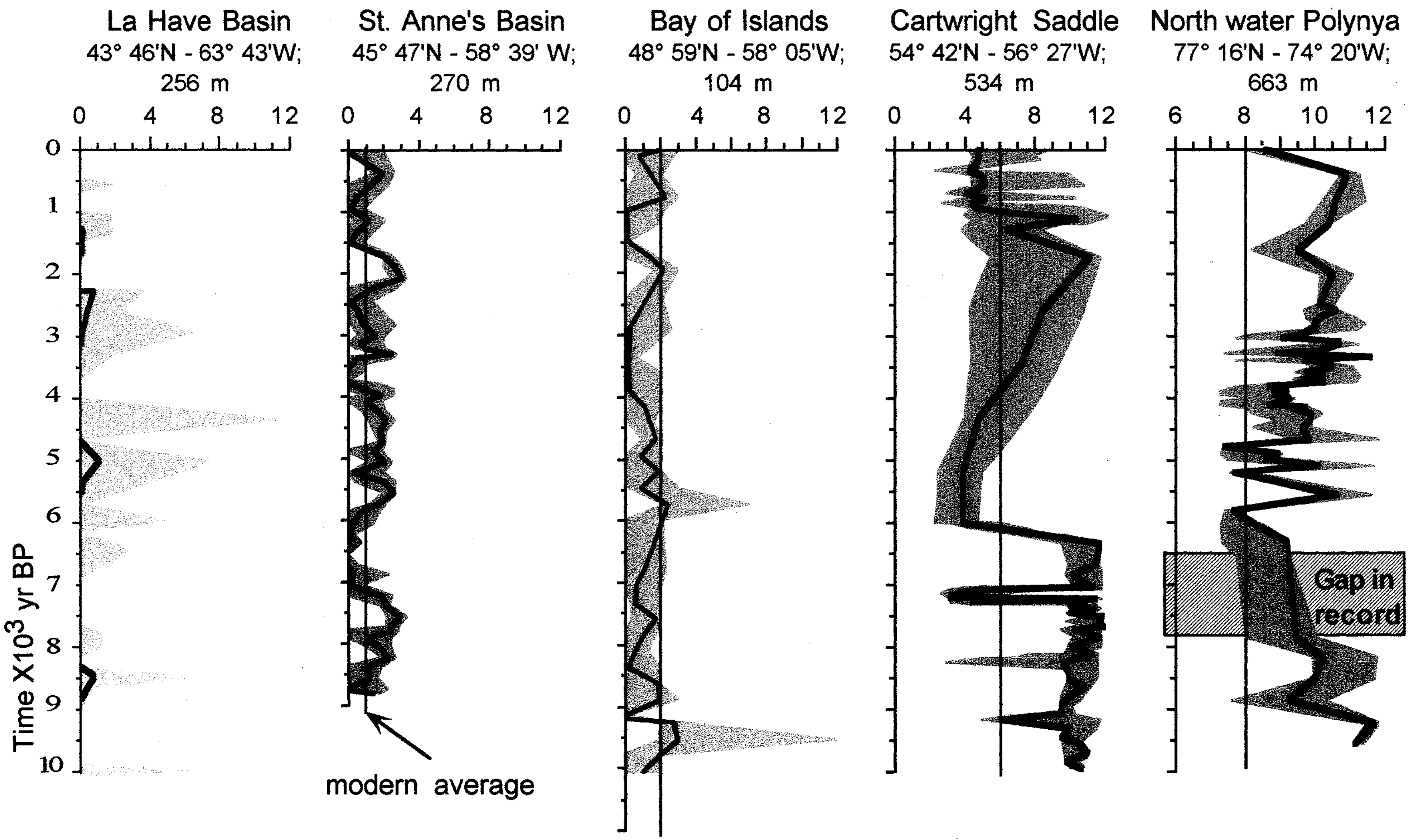

Figure 6.5: Reconstructed seasonal duration of the sea ice cover (greater than 50% of the sea surface) along the Scotian Shelf-northern Baffin Bay transect

Starting with August SST (fig. 6.3) , we see that before 8000 BP, SST values in La Have Basin are markedly higher than the modern average, which is in contrast with the other sites where SST were lower than the modern average. There is a 2000 years delay in sustained warming in Cartwright Saddle and NW Polynya (both at 6000 BP) relative to St. Anne's Basin at 7500 BP and Bay of Islands at 8500 BP.

In the mid-Holocene (6000-4000 BP), southern sites show opposite trends (lower SST than present) compared to Cartwright Saddle and NW Polynya (NWP) which both experienced the SST optimum later. After the start of the Neoglacial, ~4000 BP in NW Polynya and Cartwright Saddle, 3000 BP in Bay of Islands and St. Anne's Basin, all sites show a decrease in SST, while La Have remains warm.

The amplitude of changes varies throughout the Holocene and among sites. In the southernmost sites, changes in SST are rapid with amplitudes of ± 4-7°C in the early Holocene but with amplitudes of only ± 2°C after 8000 BP. These changes take place in less than 80 years in St. Anne's Basin or less than 200 years in La Have Basin and Bay of Islands. In Cartwright Saddle, the amplitude of changes is important (± 5 °C) throughout the Holocene. The amplitude of changes is also important in the NWP during the mid-Holocene. At this site, the apparently lower amplitude before 8000 and after 2000 BP probably reflects the lower sampling resolution. Changes in SST at these two sites take place in less then 60 years (where the resolution is best).

The most striking feature for the duration of the seasonal sea ice cover (fig. 6.4) is the important decrease in amplitude of signal changes from north to south. While it is ±

3-6 months in the north (NWP and Cartwright Saddle[2]), it is only ± 1-2 months for the other sites. The rapidity of these changes in salinity is comparable to that of SST changes, being less than 50 to 100 years in NW Polynya, Cartwright Saddle and St. Anne's Basin, and less than 200 years in La Have and Bay of Islands. The smaller amplitude of changes in NW Polynya (± 1-3 months), compared to CS (± 6 months), is probably due to its northern location: even during the interval of maximum SST, the ice cover duration never falls below the present day average duration of 8 months/year.

Before 8000 BP, August salinity (fig. 6.5) in La Have Basin displays some similarity with the August SST, being higher than the present average, while salinity at the other sites (except for St. Anne's Basin) is markedly lower than present. After 7000 BP, La Have Basin and Cartwright Saddle salinity stay close to present day average, while salinity in St. Anne's Basin and Bay of Islands generally remain above the present day average. NW Polynya differs from all the other sites with larger and rapid changes in salinity throughout the Holocene.

Changes in salinity are much greater and more rapid in the northern sites (NW Polynya and Cartwright Saddle), with amplitude of ± 10 to 20 psu, in less than 50 to 100 years. Salinity changes are also larger (3-5 psu) and generally more rapid (less than 200 years) in La Have Basin and Bay of Islands, before 8000 BP.

The apparent disappearance of oscillations after 7000 BP in the sea-ice cover and salinity curves of Cartwright Saddle is an artifact of a lower sampling resolution as we

---

[2] The increase in sea-ice cover duration in Cartwright Saddle after 4 ka could appear unreasonable if it was not for the consistent presence of arctic taxa *Impagidinium pallidum* and *Pyxidinopsis reticulata* after 6 ka.

will see in the next section. The same holds for the NW Polynya core after 2500 BP and below 8000 BP.

Overall, this south-north transect could be divided into three separate regions, based on differences in the amplitudes and direction of changes throughout the Holocene. The southernmost region would be the western Scotian Shelf with La Have Basin. St. Anne's Basin and Bay of Islands are generally very similar and could represent some sort of influence zone around the Gulf of St. Lawrence. Cartwright Saddle and NW Polynya are grouped together based on the large amplitude and frequency of changes (and the delayed occurrence of warm SST).

6.2.3 Resolution problems

Most scientists working on the Holocene are seeking to obtain records with the highest possible resolution. The nature of the geological record makes it sometimes difficult to find high resolution records that are also perfectly continuous (for example North Water site). Therefore, it appears that each scientist has their own definition of the term "high resolution".

Bioturbation is the main problem affecting the quality of stratigraphic signals in marine cores. It can cause a displacement and a reduction of the amplitude of stratigraphic signals (Bard et al. 1987). Many authors however, agree that when sediment accumulation rates are above 10 cm/kyr, the effects of bioturbation on the signal should be minimal at deepwater sites (Bard et al. 1987; Chapman and Shackleton 1998;

Anderson 2001; Bard 2001). Chapman and Shackleton (1998) even believe that meaningful century-scale climate records can be recovered with such sedimentation rates.

Anderson (2001) examined the attenuation of a signal by bioturbation for different sediment accumulation rates by convolving the GISP ice core oxygen isotope signal. He determined that sedimentation rates in excess of 50-70 cm/kyr are required to keep attenuation of millennial-scale event (2-4 kyr duration) under 5%. The importance of the attenuation increases with the depth of mixing and can be important for sedimentation rates of 10 cm/kyr, such as observed many deep-sea cores.

The size fraction of the signal carrier can also affect the quality of the signal, and fine fractions tend to be mixed more intensively. Bard (2001) determined that in deep sea sediments the potential shift in signal between different size fraction is negligible (<0.5-1kyr) when the sediment accumulation rates are above 10cm/kyr, whatever the event duration is. He also observed comparable signal amplitude in both the fine and coarse fractions when sedimentation rate is high (Bard 2001).

Bioturbation is primarily related to flux of organic carbon to the sea floor in addition to bottom oxygen and temperature. It can therefore vary significantly between locations (Trauth and Sarnthein 1997). These difference in bioturbation could make it more difficult to correlate cores from areas with different mixing depth.

In view of these studies (Bard et al. 1987; Chapman and Shackleton 1998; Anderson 2001; Bard 2001), it would appear that many deep-sea locations might have a resolution that is sufficient to detect millennial-scale paleoceanographic signals, but too low to give good estimates of their amplitude (Anderson 2001). Sufficient sediment accumulation rates are only found on the shelf locations (fig. 6.3 to 6.5).

The importance of obtaining comparable resolution to properly compare 2 paleoceanographic or paleoclimatic records is illustrated on figure 6.6. The cores from NW Polynya and Cartwright Saddle both contain intervals characterized by much lower resolution than the rest of the records. For CS it is between 6000 and 1500 BP, in NW Polynya, it is below 6000 BP and above 2500 BP. The record from NWP is also truncated by a gap of more than a thousand years at 6500-7900 BP.

Figure 6.6 shows the August SST and salinity as well as the ice cover duration after both cores were re-sampled to obtain more similar resolution. The number of samples was reduced below 6000 BP in CS to bring it closer to NWP. The CS samples retained were those that were the closest in time to those available in NWP. The NWP record was also re-sampled above 6000 BP to match the resolution of CS in that interval.

After this exercise, curves for SST and the duration of the ice cover show comparable trends, except for the last 1000 years. Salinity curves remain different, suggesting that there might have been more meltwater on the Labrador Shelf in the early Holocene but more meltwater in NW Polynya in the later half of the Holocene.

This shows that cores with comparable resolution, and samples with the same ages, records are easier to interpret and compare than those in figure 6.3 to 6.5. But it also shows how much information is lost when the resolution is not sufficiently high.

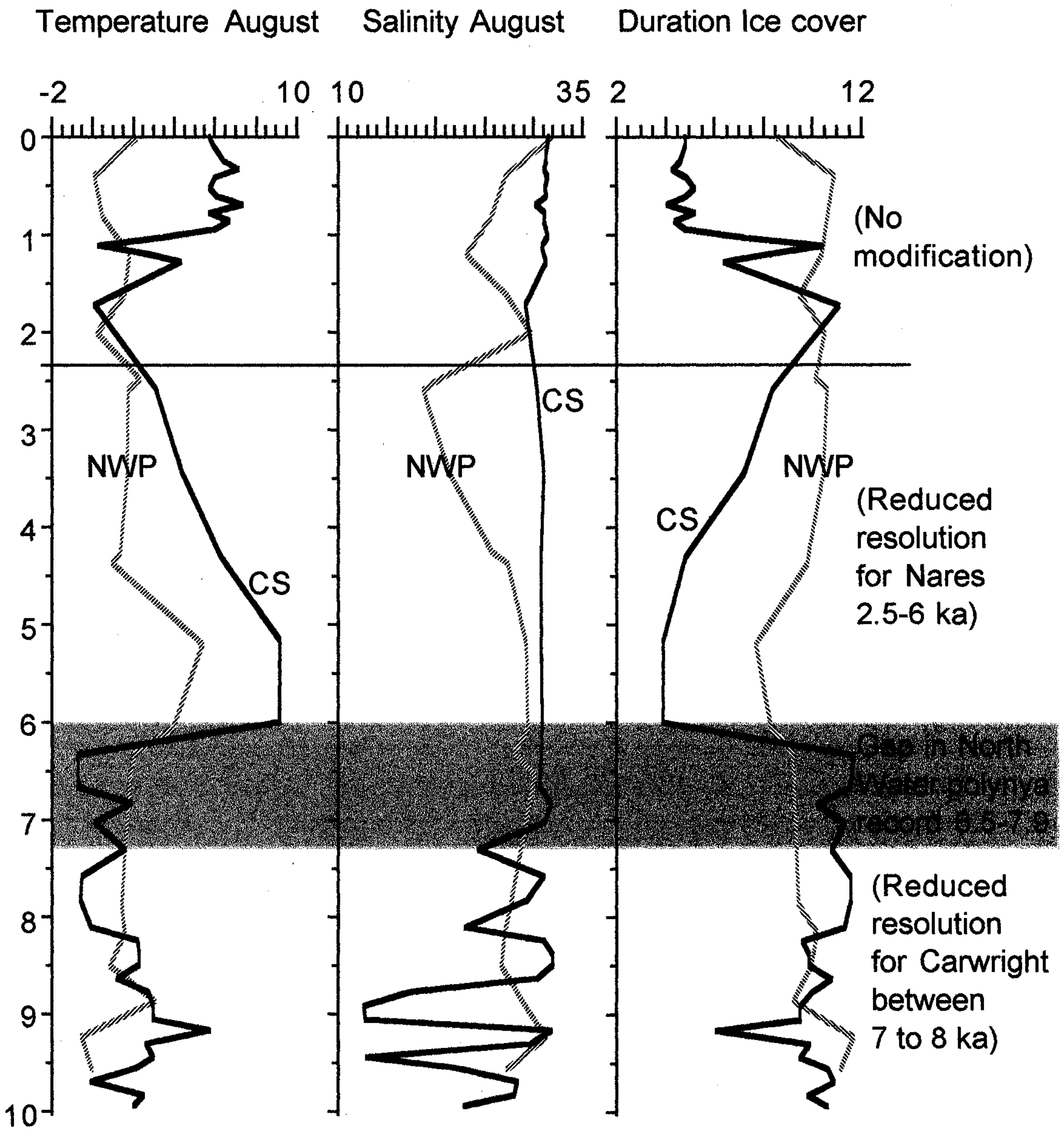

Figure 6.6: Comparison of Nares Strait and Cartwright Saddle records after re-sampling to reduce differences in resolution. The stippled curve represents the North Water Polynya while the black curve represents Cartwright Saddle. The vertical scale is the radiocarbon age.

6.3 Application of palynology to the paleoceanography of the Eastern Canadian Margin

The discussion in St. Anne's Basin paper (chapter 5) covered palynology/micropaleontological studies from Scotian Shelf, Gulf of St. Lawrence, and these will not be repeated here. Rather, we will examine paleoceanographic studies from Labrador Shelf, Baffin Bay, Labrador Sea and northwest North Atlantic, with emphasis mainly on palynological studies. The location of various sites mentioned in the text are shown on figure 6.7.

The numerous palynological studies undertaken along the eastern Canadian margin and in the Labrador Sea in the last 20 years stem from the pioneer work of Mudie (1980) who demonstrated the potential of pollen and dinoflagellate cysts as tools for paleoecological studies in the later Quaternary sediments of the region. She examined the distribution patterns of palynomorphs in coastal, shelf, and upper slope sediments from Nova Scotia to Baffin Bay: the preservation, the methods of transport and the taxonomy.

The usefulness of palynology is illustrated in an early study by Vilks and Mudie (1978) on the Labrador Shelf, where they challenged the CLIMAP (1976) maximum ice model. Vilks and Mudie (1978) combined foraminifera and pollen data to show that Cartwright Saddle probably remained seasonally open during the last glaciation. Foraminiferal assemblages indicate the presence of open water conditions in the summer, while pollen suggest the existence of tundra vegetation in the region.

The early use of dinoflagellate cyst assemblages to infer sea surface conditions was from cores in the Cartwright Saddle area on the Labrador Shelf and in Baffin Bay

(Mudie 1980; Vilks and Mudie 1983; Mudie and Short 1985; Aksu and Mudie 1985). Transfer functions for bethic foraminifera were used by Mudie et al. (1984) as a means to quantify paleoceanographic changes on the Labrador Shelf and in Melville lake.

Application of transfer functions on dinoflagellate cyst assemblages occurred later (Mudie et al. 1990; Aksu et al. 1992; Mudie 1992). These first studies were done on deep sea cores, using the Imbrie and Kipp method (see later section on deep sea), then the best analogue method was introduced (de Vernal et al. 1993; 1994; Rochon et al. 1999). These transfer functions were applied to the Labrador Shelf (Levac and de Vernal 1997; this study), NW Polynya (Levac et al. 2001), and the Scotian Shelf (Levac 2001; 2002a,b). Recently, Mudie et al. (2001) outlined the advantages of palynomorphs for paleoceanographic studies in the Arctic, and demonstrate that dinoflagellate cysts are the most suitable proxies for reconstructions of sea surface conditions.

Legend Figure 6.7

A: Agassiz Ice Cap
BI: Bay of Islands
L: Leffert Glacier
LH: La Have Basin
N: Newfoundland
NS: Nova Scotia
NW: North Water Polynya
SA: St. Anne's Basin

1- Core 76-029-40 (and numerous other cores; Aksu 1983); core 85-027-16 (Scott et al. 1989c); ODP Leg 105 (de Vernal et al. 1989);
2- Davis Strait Core 77-027-17 (Mudie and Aksu 1984; Mudie and Short 1985). Core 87-033-007 (de Vernal et al. 1994);
3- Core 77-5-1 and 77-1-2 (Aksu and Mudie 1985);
4- Core 84-031-21 (de Vernal and Hillaire-Marcel 1987)
5- Cartwright Saddle core 12 (Mudie et al. 1984; Vilks and Mudie 1978); core 91-045-006 (Levac and de Vernal 1997; this paper); cores 87-033-17 and 18 (Andrews et al. 1999);
6- Melville Lake core 79-018-111 (Mudie et al. 1984; Vilks and Mudie 1983);
7- Core 84-030-004 (Scott et al. 1989c); ODP site 646 (Aksu et al. 1992); core 90-013-013 (de Vernal et al. 2000);
8- Core 84-030-001 (Mudie 1992);
9- Orphan Knoll core 91-045-94 (Rahman and de Vernal 1994; de Vernal et al. 2000);
10- Fogo Seamount core 85001-11 and 75-009-114 (Mudie 1992);
11- Williams et al. 1995
12- Jennings et al. 2002
13- Short et al. 1994
14- Matthiessen and Baumann 1997
15- Core 77-21-159 (Mudie and Short 1985) (Osterman and Nelson 1989; Williams 1990);
16- Williams et al. 1995
17- Agassiz Ice Cap (Fisher et al. 1995; Koerner and Fisher 1990; Bourgeois 1990; Bourgeois et al. 2000);
18- Notre Dame Bay core 78-023-20 (Scott et al. 1984; 1989a);
19- Schafer et al. 1985; Alam et al. 1983;
20- Lamb 1980;
21- Axel Heiberg Island (Nichols 1972);
22- Cumberland Peninsula (Andrews et al. 1980; SHort et al. 1985; Boulton et al. 1976);
23- West Greenland (Fredskild 1985; Funder 1978);
24- Leffert Glacier (Blake 1989);
25- Labrador-Ungava (Short and Nichols 1977; Diaz et al. 1989).

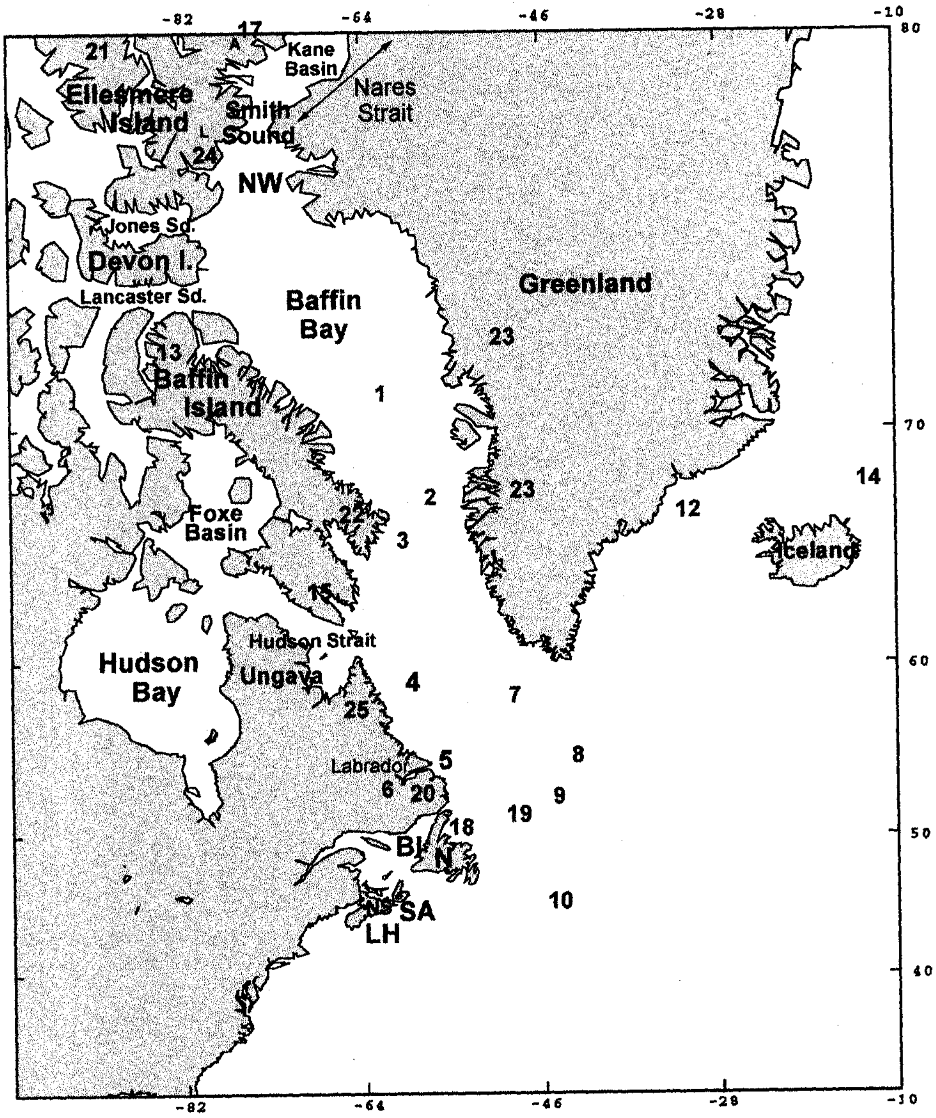

Figure 6.7: Location map indicating the various sites mentioned in this chapter. For the list of sites, see previous page.

6.3.1 Sea surface conditions on the Labrador Shelf

The early Holocene in Cartwright Saddle was characterized by low summer SST (fig. 6.3) and a long ice cover duration (10 months/year) until 6500 BP. Dinocyst assemblages in both core 6 (Levac and de Vernal 1997) and core 12 (Scott et al. 1984) are dominated by *A. minutum* and *Brigantedinium* spp., typical of Arctic environments. Vilks and Mudie (1978) had proposed that surface water above Cartwright Saddle remained seasonally open during the last glaciation based on foraminifera and pollen data from core 73-027-12. In view of the dinocyst assemblage composition and the sea surface reconstructions, it appears that sea surface conditions at Cartwright Saddle in the early Holocene were still typical of the late glacial or were under the influence of meltwater influx.

Transfer functions on benthic foraminifera in core 12 indicate cold bottom water conditions from 12,000 to 8000 BP (-0.5°C compared to 3°C today) and lower salinity (33.5 compared to 34.8 today) (Mudie et al. 1984). These bottom water temperatures are close to the reconstructed SST values for the early Holocene in core 6. However, reconstructed surface salinity in Cartwright Saddle shows a much greater difference with the present salinity, falling as low as 15 in some intervals. This is an indication that meltwater influx had a greater influence on sea surface conditions.

In nearby Lake Melville, dinoflagellate cyst assemblages between 7500-9000 BP had a low diversity and resembled modern assemblages now found below the West Greenland Current. More water from the shelf could enter Lake Melville because the sill was deeper at that time. A reduced number of foraminiferal species in Lake Melville in the early Holocene (~7800-8500 BP) was believed to correspond to reduced oxygen content during an early stage of deglaciation (Vilks and Mudie 1983).

Postglacial sea surface conditions appear to become established rapidly (fig. 6.3). SSTs were slightly higher than today between 6000 and 4000 BP. Dinocyst assemblages show an increase in the number of taxa and decrease in *A. minutum* (Levac and de Vernal 1997; Scott et al. 1984). Foraminifera assemblages appear to reflect outer Labrador Current conditions throughout the Holocene (Scott et al. 1984). Benthic species associated with non glacial shelf conditions, as well as the number of planktonics, increase after 7 ka in Cartwright Saddle core 87-033-17 (Andrews et al. 1999). Proportions of *E. excavatum* decline after ~ 8000 BP and reach a minimum in the mid-Holocene in core 12, which represents non-glacial conditions (Scott et al. 1984). In core 17, a similar decline of *E. excavatum* in the mid-Holocene is believed to represent warmer conditions (Andrews et al. 1999). Changes in bottom water were more gradual, with bottom temperature and salinity both increasing after ~ 12 ka reaching a maximum about 6000 BP. Reconstructions based on benthic foraminifera indicate a mid-Holocene interval of increased temperature between 8000 and 4000 BP (Mudie et al. 1984).

The dinocyst assemblages from core 84-030-21 (slope off northern Labrador) indicate that high interglacial conditions were probably re-established only after 4 ka in western Labrador Sea (de Vernal and Hillaire-Marcel 1987).

Dinoflagellate cyst assemblages in Lake Melville are dominated by *A. minutum* in the mid-Holocene (~ 4000 to 6500), and this was believed to indicate a strong influx of low salinity Arctic shelf water, but there are no indication from that core that surface water was warmer (Vilks and Mudie 1983). Transfer functions in that core indicate that bottom waters were slightly warmer between ~ 8000 to ~ 5500 BP and that salinity was also higher (Mudie et al. 1984) but this could be the result of a deeper sill depth.

SST in Cartwright Saddle decreases (by about 4-5°C) after 4000 BP but returns to present day values around 1 ka (fig. 6.3). Both core 12 (Cartwright Saddle) and core 111 (Lake Melville) show a very slight decrease in bottom water temperature after 3300 BP (Mudie et al. 1984).

Overall, sea surface conditions appear to have been cooler in the early Holocene, warmer in the mid-Holocene (~6000-4000 BP) and cooler since 4000 BP, at least in surface water.

6.3.2 Sea surface conditions in the Newfoundland Shelf/Grand Banks region

The shelves around Newfoundland have apparently also experienced warmer conditions than today at some time during the Holocene. Alam et al. (1983) report that planktonic foraminifera assemblages were displaced northward along the eastern Grand Banks slope during the early Holocene but there is no precise dating for that core. A cooling trend followed, which the authors believed resulted from the development of the cold inner core of the Labrador Current following the deglaciation of the Arctic islands.

The planktonic foraminifera record from the northeast Newfoundland rise and slope suggests the dominance of relatively warm northern component of the North

Atlantic Drift water during most of the Holocene. Foraminifera assemblages reflect colder Labrador Current water after 2500-1500 years BP (Schafer et al. 1985).

In Notre Dame Channel, dinoflagellate cyst assemblages generally reflect harsh Inner Labrador Current conditions with a dominance of *A. minutum* and *Brigantedinium*. However, low numbers of *Spiniferites* between 0.75 m and 1.5 m in piston core 78-023-20 suggest slightly warmer conditions than today (Scott et al. 1984). After correlation of the pollen record from core 20 with Newfoundland pollen record (see Macpherson 1988) an age of ca. 7000 to ~11.500 BP can be proposed for this interval.

Foraminifera assemblages in this core are typical of outer Labrador Current in the early and mid-Holocene. Around 4000 BP, calcareous species decline and agglutinated assemblages typical of inner Labrador Current take over (Scott et al. 1984).

6.3.3 Sea surface conditions in the northern Labrador Sea and Baffin Bay

A few multi-proxy studies were undertaken on cores from the northern Labrador Sea and Baffin Bay, to correlate marine and terrestrial data directly (Mudie and Aksu 1984; Aksu and Mudie 1985; Mudie and Short 1985; Aksu et al. 1992; de Vernal and Hillaire-Marcel 1987; de Vernal et al. 1994). Most of these studies however, have a resolution that is 1 or 2 orders of magnitude lower than that of the cores presented in the south to north transect (2 to 10 cm/kyr versus >100 cm/kyr; fig. 6.3) and only general comparison can be made. The interest in these cores lies in the fact that some of these studies were the first to propose paleoceanographic models for the region, based on multicore studies. They also showed the main differences between glacial and interglacial intervals in term of assemblages, dissolution, productivity and most importantly, the main changes in oceanic and atmospheric circulation.

Most of the cores from the region show a sharp increase in concentration of dinoflagellate cysts at the glacial-interglacial transition (Aksu and Mudie 1985; Mudie and Short 1985; de Vernal and Hillaire-Marcel 1987; Aksu et al. 1992; de Vernal et al. 1994). In NW Polynya, the concentration increases more gradually (Levac et al. 2001) and reaches a maximum between 7000 and 3000 BP, before decreasing in the late Holocene.

Mudie and Aksu's (1984) initial description of glacial versus interglacial dinoflagellate cyst assemblages in core 77-027-17 does not hold after the re-evaluation of the chronology by Andrews et al. (1998). Based on the $\delta^{18}O$ stratigraphy, the cores was believed to cover isotopic stages 1 to 10 (Mudie and Aksu 1984), but AMS ^{14}C dating indicate that it covers only the last 18,000 years (Andrews et al. 1998). This means a sedimentation rate of ~ 1m/1000 years for most of this core, which is comparable to that of NW Polynya core. However, the Holocene still only spans a 50 cm section. D.B. Scott (from Dalhousie University, personal communication 2002) also warns that Baffin Bay sedimentation is dominated by turbidity currents as shown by the study of core 85-027-16 (see Scott et al. 1989c).

With the new ages, core 77-027-17 now shows how the dinoflagellate cysts concentrations and assemblages evolved since 18,000 BP. Concentrations are low at 18,000 BP but show an increase sometime after 18,000 BP, and drop again, probably around the Younger Dryas. Total concentrations are highest during the Holocene. *Algidasphaeridium minutum* dominates the assemblages throughout the core, accompanied by *Brigantedinium simplex*, *P. faeroense* and the acritarch *Leiosphaera.* These species reflect cold conditions. The episodic increase in the proportion of "Atlantic" reflect inflow of Atlantic water through the West Greenland Current. These "Atlantic" species include *O. centrocarpum*, *N. labyrinthus*, *S. ramosus*, *S. elongatus*, *S. bulloideus* and *S. membranaceus* (Mudie and Aksu 1984). The percentage of Atlantic species generally follows the same trend as the total dinocyst concentrations, showing a slight increase after 18 ka, dropping during the Younger Dryas and reaching a maximum during the Holocene.

There is evidence for important foraminifera dissolution in core 77-027-17. Total planktonic concentrations are highest at 18,000 BP and immediately after, and reach their minimum during the Holocene. Benthic to planktonic ratios show an inverse relation with maxima during the Holocene (Aksu 1983; Mudie and Aksu 1984). This is another reason why dinoflagellate cysts are so useful for paleoceanographic studies in high latitudes (e.g. Mudie et al. 2001).

The ratio between warm indicator *O. centrocarpum* and cold indicator *A. minutum* was used in a few studies (Mudie and Aksu 1984; Mudie and Short 1985; Aksu and Mudie 1985) as a means to illustrate changes in water masses. Q-mode factor analysis of surface samples from Baffin Bay confirmed that assemblages dominated by *O. centrocarpum* correspond to areas dominated by the West Greenland Current, while assemblages dominated by *A. minutum* correspond to areas of mixing between Canadian Arctic water and west Greenland Current (Mudie and Short 1985).

In Davis Strait core 17, the *O. centrocarpum*/*A. minutum* ratio is maximum during the Holocene (Mudie and Aksu 1984; Mudie and Short 1985) but are also sometimes high before the Younger Dryas. In another core from Davis Strait (core 87-033-7; de Vernal et al. 1994) and in core 77-5-1 south of Davis Strait (Aksu and Mudie 1985), the records are not very detailed and the ratio simply shows an increase in the interglacial relative to the glacial interval.

In more detailed Holocene sections, the ratio is not constant during the Holocene. In the deep central Baffin Bay (core 76-029-34), the ratio is higher in the upper half of the Holocene, while in the west Baffin Bay (core 80-028-3), the peak in "Atlantic" dinos (mainly *O. centrocarpum*) occurs in the early Holocene (Mudie and Short 1985). This is more like NW Polynya, where the maximum percentages in *O. centrocarpum* are recorded between ~ 9000 and 4000 BP.

6.3.4 Quantitative reconstructions at deep sea sites

At ODP site 646, eastern Labrador Sea, reconstruction based on planktonic foraminifera gave SSTs of 0°C in winter and ~6°C in summer, and a salinity of ~ 34.7 psu for the last glacial. For the Holocene, SSTs of ~2°C in winter and 7 °C were reconstructed (Aksu et al. 1992). The author themselves believes these estimates (and estimates for other interglacials) are too low, probably due to preferential dissolution of warm water species (Aksu et al. 1992) as higher SST reconstructions were obtained from transfer functions based on dinocyst (Mudie et al. 1990; Mudie 1992). Also, planktonic foraminifera do not necessarily record the water conditions in the uppermost layer of the water column (Aksu et al. 1992) as shown by Wu and Hillaire-Marcel (1994) with *Neogloboquadrina pachiderma*.

Reconstructions of glacial sea surface conditions in Davis Strait (core 87-033-7; de Vernal et al. 1994) indicate a temperature between 1.5 and 4 °C and a salinity of 31-33 psu in August, with a seasonal ice-cover duration of 6-10 months/year. The curves increase abruptly at the glacial-interglacial transition and temperature reaches 6-7 °C, salinity 33.5 psu and ice cover duration drops to 1 month/year. Only slight changes in SST occur during the postglacial interval, but it should be noted that the Holocene in that core is represented by at most 6 samples (sediment section of ~50 cm).

These studies (Aksu et al. 1992; de Vernal et al. 1994) suggest that, in Davis Strait, the biggest changes between the last glacial and the present interglacial were an important reduction in the duration of the seasonal sea ice cover and an increase in SST of at most 5°C, but changes in salinity were at most 2 psu. In NW Polynya, variability in sea surface salinity *within* the Holocene showed a greater amplitude (7-17 psu) than these glacial/interglacial differences, while variability in SST showed comparable amplitude. Despite the difference in location, this suggests the possibility that the signal was "smoothed" due to the low resolution of these two cores.

de Vernal et al. (2001) underlined a series of potential problems with the use of foraminifera as proxies for sea surface conditions, either with the type of proxy itself (e.g.

dissolution, stratification) or with the method used (e.g. size of the sieve). They proposed a different picture of the Last Glacial maximum based on transfer functions using dinoflagellate cyst records throughout the North Atlantic. Winter SSTs were colder than present while summers were relatively mild, and this greater seasonality was probably due to the existence of a shallow mixed layer and low surface salinity. The discrepancies between reconstructions based on foraminifera versus those based on dinocysts are probably the result of a stronger stratification during glacial intervals.

Transfer functions (based on dinocysts) provide evidence for warmer SST than present during the mid-Holocene. Mudie (1992) reconstructed sea surface conditions (using Imbrie and Kipp method) in Fogo Seamount core 85001-11 (the early Holocene is unfortunately missing because of erosion). There was a mid-Holocene warm interval (with SST of 24°C), followed by a cooling toward the present day average of 19°C after 2000 BP.

At Orphan Knoll (east of Newfoundland, core 91-045-94), early Holocene August SST were between 2 and 5 °C warmer than today until 8500 BP. This timing is similar to La Have Basin, but surface salinities were lower. There was another warmer interval from 7000 to 6500 BP. After 6500 BP, sea surface conditions were 3 to 5 °C lower than present, with increased sea ice cover duration (de Vernal et al. 2000). On the southwest Greenland Rise (core 90-013-013), SSTs were warmer than the present average (by 2°C) from ~ 4000 to 6000 BP. It is possible that SSTs were also warmer during the early Holocene (Hillaire-Marcel et al. 2001).

Recently, much attention has been given to sea surface conditions at 6000 BP. Data gathered by Kerwin et al. (1999) for 6000 BP indicate warmer than present summer SST throughout the North Atlantic. This warming would have been more important around the Norwegian Sea (2 to 4°C) than in the Baffin Bay and the Labrador Sea (1 to 2°C). Recent simulations also show higher SST than the present from late August to November, as well as a reduction in sea ice thickness (Vettoretti et al. 1998). A compilation by Gajewski et al. (2000) for Labrador Sea and Baffin Bay show that the subarctic marine ecological assemblages replaced High and Low Arctic ones in Baffin Bay at 6 ka, and the mixed Low Arctic and Subarctic ones along the coast the Labrador.

Overall, sea surface conditions in that area show a similar pattern as those on the Labrador Shelf, with a cold early Holocene, warm mid-Holocene and late Holocene cooling. We also see that dinoflagellate cysts present advantages over foraminifera for the reconstruction of sea surface conditions at mid-high latitudes. High resolution is also important.

6.4 Surface circulation in the Labrador Sea, Baffin Bay and northwestern North Atlantic

6.4.1 Surface circulation before 8500 BP

Aksu (1983) and Mudie and Aksu (1984) proposed that during glacial intervals, the Baffin Land Current was weak or absent and the West Greenland Current dominated the circulation in the Labrador Sea and Baffin Bay. Mudie and Aksu (1984) also suggested that reduced Arctic water outflow to North Atlantic, due to Arctic Island channels blocked by ice, could explain the presence of subarctic planktonic foraminifera in early glacial stages. Aksu and Mudie (1985) later proposed that the West Greenland Current was shifted southward during glacials. New ^{14}C dates on core 76-029-40 (Andrews et al. 1998) brought important changes to the stratigraphy of some Baffin Bay cores on which these paleoceanographic models were based (Aksu 1983; Mudie and Aksu 1984). Andrews et al. (1998) believe that new cores are required to determine the paleoceanographic history of Baffin Bay. Scott et al. (1989c) had previously demonstrated the episodic nature of sedimentation in central Baffin Bay (with nearby core 85-027-16) which could lead to serious misinterpretations as in the case of core 76-029-40 (and other cores from central Baffin Bay) by Aksu (1983).

Keffer et al. (1988) showed that modifications in the wind patterns caused by the existence of an ice sheet during the last glacial resulted in a more southerly position of the subpolar-subtropical gyre boundary, which also corresponds to the position of the Gulf Stream.

More recent studies indicate that the Baffin Land Current was probably absent in the early Holocene too, and possibly the Labrador Current as well. Paleogeographic maps of the Canadian Arctic for 10,000 BP, based on molluscs and bowhead whales distribution, indicate the absence of surface flow from the Arctic into Baffin Bay and the absence of the Baffin Current (Dyke et al. 1996a, b). Also, the circulation in the Canadian Arctic Archipelago was dominated by abundant meltwater outflow before 8600 BP, which prevented the transport of driftwood into that region (Dyke et al. 1997). This is supported by the $\delta^{18}O$ values in marine molluscs which also indicate lower salinity at that time (Andrews et al. 1993).

Other studies point toward a more northward penetration of warm North Atlantic water in the early Holocene: Aksu and Piper (1979) believed, based on the presence of subarctic foraminifera, that subarctic water penetrated Baffin Bay between 9000-6000 BP and de Vernal and Hillaire-Marcel (1987) believed that contribution of the North Atlantic Drift to the West Greenland Current could have started as early as 10,000 BP. These authors point out however that the slope off northern Labrador was still affected by important influx of meltwater in the early Holocene (de Vernal and Hillaire-Marcel 1987). Rahman and de Vernal (1994) proposed that the absence of the Labrador Current allowed the penetration of warm surface water into southern Labrador Sea between 10,700 and 9000 BP.

6.4.2 Surface circulation, after 8500 BP

There are numerous indications for the establishment of the present day circulation in the Arctic, Baffin Bay and Labrador Sea around 8500 BP, when some of the main surface currents started to flow. After 8500 BP, the arrival of driftwood in the Canadian Arctic Archipelago (Dyke et al. 1997) is coincident with a restriction of the bowhead whale bone distribution (due to more sea ice; see Dyke et al. 1996b) and increased surface water salinity as recorded by molluscs, indicative of reduced meltwater (Andrews et al. 1993). Paleogeographic maps for that time indicate the opening of Lancaster Sound (between Baffin and Devon Islands), which allowed some surface flow into Baffin Bay (Dyke et al. 1997). Aksu (1983) had placed the onset of Arctic Ocean Surface Water flux through to Baffin Bay at ca. 8000 BP, based on the start of dissolution of foraminifera. Rahman and de Vernal (1994) believe that the Labrador Current started around 9000 BP and became stronger after 8400 BP, when the Irminger Current was established.

The northward flow of the West Greenland Current also starts by ~ 8400 BP. This would explain the expansion of the boreal-subarctic mollusc fauna into Baffin Bay as suggested by Funder and Weidick (1991; see also Dyke et al. 1996a).

6.4.3 Mid-Holocene

Funder and Weidick (1991) suggested a reduction of the inflow of polar water into Baffin Bay (or an increase in the inflow of warm Atlantic water) to explain the presence of boreal mollusc shells along the coasts of western Greenland between 8400 and 4900 BP. According to Dyke et al. (1996a) an expansion of the subarctic molluscs zone into eastern Baffin Bay from 8000 to 3000 BP suggest a warmer Baffin Land Current. Also, it was also suggested that changes in benthic foraminifera assemblages along the eastern Canadian Shelf during the mid-Holocene were associated with changes in inflow of polar water (Scott et al. 1984; Andrews et al. 1993).

However, Blake (1998) notes the existence of many different ecological classification schemes for mollusc species and that the interpretation of past water conditions depends on the classification used and can therefore be biased.

6.4.4 Changes in Arctic surface circulation and sea ice extent

Important changes in Arctic surface circulation did take place during the Holocene as shown by Dyke et al. (1997), based on the distribution of driftwood in the Canadian Arctic Archipelago. In addition to changes in the main Arctic currents, the ice extent in the Canadian Archipelago also varied greatly, affecting the distribution of bowhead whale (Dyke et al., 1996b). Changes in both of these two parameters no doubt influenced sea surface conditions downstream as the Labrador Current is derived, from Arctic waters.

Changes in position of the Trans Polar Drift and its effects downstream

Dyke et al. (1997) established that throughout the Holocene, the circulation in the Arctic operated according to three modes, depending on the position of the Trans-Polar Drift (TPD) (fig. 6.8), which influences the amount of icebergs and freshwater transiting through Fram Strait (along the eastern coast of Greenland) versus the Canadian Arctic Archipelago and affects the properties of the downstream currents (eg. Labrador Currents).

The circulation mode in operation today is characterized by a split of TPD water between the Canadian Arctic Archipelago and Fram Strait. At other times, the Arctic circulation was affected by a westward shift in the TPD, which would have then exited entirely through the Canadian Arctic Archipelago and joined the Baffin and Labrador Currents directly, without the warming effect of the North Atlantic Drift in the Irminger Basin. When the TPD shifted eastward, Arctic waters then exited through Fram Strait and in this case, the east Greenland Current would have been intensified, the Irminger Current as well and the Labrador Current would have been warmer (see Dyke et al. 1997).

The evidence is strong for changes in the mode of operation of the TPD, but establishing a link with sea surface conditions over the Scotian Shelf is difficult. The

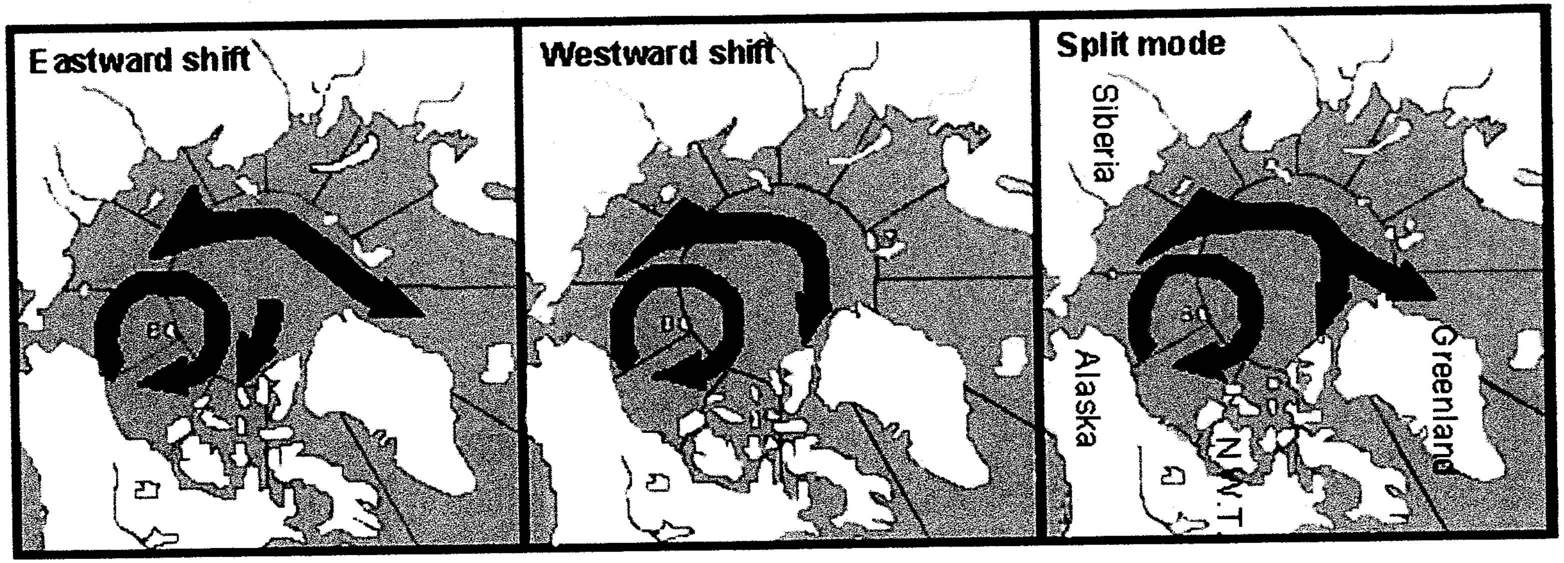

Figure 6.8: Circulation modes of the Transpolar Drift (from Dyke et al. 1997)

warm SST interval in St. Anne's Basin between 6000 and 7000 BP (fig. 6.3) seems to coincide with an eastward shift of the TPD, which Dyke et al. (1997) suggest would result in a warmer Labrador Current. On the Labrador shelf however, SST remained cold until 6000 BP.

Along the transect (fig. 6.3), August SSTs are generally cooler for most sites in the late Holocene. This coincides with a westward shift of the TPD, which in this case should mean a cooler Labrador Current. The warmer February SST in St. Anne's Basin (see Levac 2002b) and Bay of Islands (Levac 2002a) could be the result of increased ice cover over the Labrador Shelf at that time.

Changes in ice extent in the Canadian Arctic

Based on the distribution of bowhead whale bones in the Canadian Arctic Archipelago (CAA), Dyke et al. (1996b) concluded that the access of whales to the Arctic channels was more extensive during deglaciation (~10 to 8 ^{14}C ka) and during the mid-Holocene (ca. 6000 to ca. 3000 BP). This means less sea ice in the CAA. The duration of the seasonal sea ice cover in the North Water Polynya, in northern Baffin Bay, was also reduced between 6300 and 3600 BP (Levac et al. 2001).

The warm SST in St. Anne's Basin between 7000 and 6000 BP corresponds to an interval of reduced access for whales to the CAA and therefore, to more important ice conditions. The subsequent cool interval in St. Anne's Basin, between 6000 and 4000 BP coincides with an increased access to the CAA. It could be proposed that less open water conditions in the Arctic Channels correspond with warmer surface water conditions downstream, due to reduced inflow of Arctic water into Baffin Bay. Indeed, this was a time of slightly warmer SST in Cartwright Saddle.

Whale access to the CAA was reduced again in the last 3000 years (Dyke et al. 1996b) and the duration of the seasonal sea ice cover in the North Water Polynya was more important after 3600 BP. The Late Holocene warm interval in St. Anne's Basin and Bay of Islands started around 4000 BP, and cooler summer SST in Cartwright Saddle at that time would appear to be in contradiction if it was not for the fact that the warm interval in St. Anne's Basin and Bay of Islands was characterized by warmer winter SST rather than warmer summer SST.

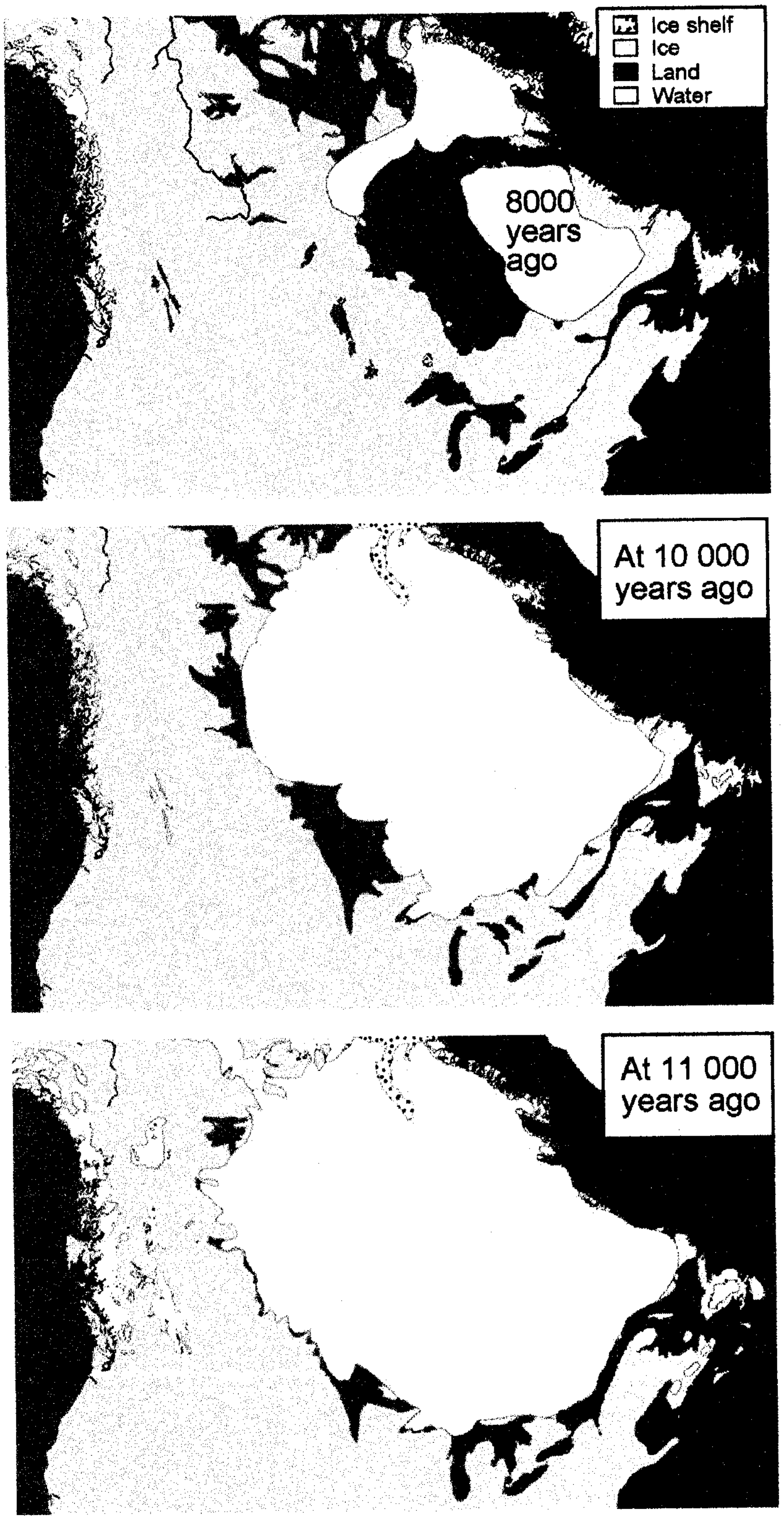

Figure 6.9: Ice Sheet boundaries at 8, 10 and 11 ka
(From Dyke and Prest 1987)

Isostatic rebound in Arctic

Andrews et al. (1993) suggest that, as isostatic uplift continued in the Canadian Arctic, the sills became shallower and the outflow through Fram Strait increased during the Holocene. An increase in freshwater outflow (probably as sea-ice from the Arctic Ocean) was detected in diatom records from the East Greenland Coast around 6000 BP (Williams, 1990). Williams et al. (1995) suggest that deeper Arctic channels during and after deglaciation allowed the inflow of Atlantic water into the Arctic but that around 6000 BP, the sills were high enough to cut this inflow. Similarly, Aksu (1983) had suggested that changes in the preservation of foraminifera in Baffin Bay during interglacials depends on the properties of bottom water, which are related to the inflow of Arctic water into Baffin Bay and controlled by the depth of NW Polynya.

6.5 Meltwater and freshwater influx

6.5.1 Influx from the Great Lakes

In chapter 5, we already established that meltwater influx probably had an impact on sea surface conditions of the eastern Canadian seaboard.

In Bay of Islands, salinity and SST are affected by the influx of meltwater of the Great Lakes' Middle Stanley Phase (~ 9600 to 9200 BP/10,300-10,500 cal BP) and remain low during the subsequent Main Mattawa cool climatic phase (9200-8500

BP/9200-10.200 cal BP; Anderson and Lewis 1992; Moore et al. 2000). Moore et al. (2000) also estimated the amounts of meltwater that flowed directly into the North Atlantic from the southern and eastern part of the Laurentide Ice Sheet. These were also important during the Middle Stanley Phase and possibly affected sea surface conditions on the Scotian Shelf through Labrador Current derived waters. Indeed, a drop in SST occurs around 9600 BP in La Have Basin, in the middle of the early Holocene SST optimum. The impact of this influx was probably small because salinity was not affected.

A subsequent interval, the Late Stanley phase, was characterized by important influx of meltwater, both from the Great Lakes and the eastern sector of the Laurentide Ice Sheet. Time wise, it could explain the lower SST than today in St. Anne's Basin around 8800-9000 BP but the fact that it had no effect on Bay of Islands and La Have Basin weaken this argument.

Sea surface salinities were consistently higher than today's average between 7000 and 1000 BP in St. Anne's Basin and Bay of Islands (fig. 6.4). The climate was drier in eastern Canada in the mid-Holocene (Gajewski et al. 2000) and reduced freshwater outflow through the Gulf of St. Lawrence could be proposed to explain the higher salinity at these two sites. Mean annual precipitations inferred from pollen data and from climatic models are lower than today for the 9 and 6 ka time slice, and similar to modern levels for 3000 BP (Webb et al. 1993). Reconstructions of mean annual precipitation from southwestern Newfoundland shows lower than modern values until ~4500 BP (McCarthy et al. 1995). Also, the discharge from the Great Lakes through the St. Lawrence did not reach the modern values until 4200 BP (McCarthy et al. 1995).

6.5.2 Hudson Strait 8.2 ka event

An important amount of meltwater was also released into the North Atlantic with the collapse of ice in Hudson Bay and the rapid drainage of lakes Agassiz and Ojibway through Hudson Strait (Teller 1987). Kerwin (1996) dated the collapse of the Hudson Bay ice sheet to 8000 BP.

The drop in SST (February and August) and in August salinity at La Have and St. Anne's Basins around 8000 BP could correspond to this event. They would suggest however, that the impact of this meltwater release was minimal, as changes in sea surface conditions were very small.

Lower salinity in Cartwright Saddle core 91-045-006 could correspond to this freshwater pulse (fig. 6.4) but a previous reconstruction showed no indication of that event (Levac and de Vernal 1997). A small reduction in $\delta^{18}O$ in planktonic foraminifera from another Cartwright Saddle core is recorded between 7.8-7.6 cal ka (Andrews et al. 1999).

There is much debate about the magnitude of this event on the sea surface conditions in Baffin Bay, on the Labrador Shelf and even further downstream. Barber et al. (1999) argue that this outflow of freshwater from Hudson Strait was responsible for the 8.2 ka cooling event recorded in the Greenland ice core (see Alley et al. 1997; Bond et al. 1997) but that the magnitude of this event on the regional climate was only a third that of the Younger Dryas.

Vilks et al. (1989) claim that tidal mixing was already taking place in Hudson Strait ca. 8000 BP, and that there was no surface plume of low salinity water flowing out of Hudson Strait. Also, while $\delta^{18}O$ in molluscs around the Ungava Peninsula indicate the influence of glacial meltwater between 8000 and 6000 BP, especially in estuaries, the drainage of Hudson Bay would have been very slow, with only very brief outburst of meltwater (Lauriol and Gray 1997).

6.5.3 Melting in the Arctic

Melt layers in the Agassiz ice cores indicate that melting was the greatest in the early Holocene (10,000 to 8000 BP) and that the interval between 8500 and 2500 BP was characterized by a fairly continuous decrease in the number of melt layers (Koerner and Fisher, 1990; Fisher et al. 1995). This homogeneous decreasing trend was interrupted by only two events: a sudden decrease at ca. 4000 BP and a small increase ~ 2500 BP.

The decrease ~ 4000 corresponds with the beginning of the second warm interval in St. Anne's Basin and Bay of Islands. Interestingly, Scott and Collins (1996) also suggested, based on sea-level curves, that melting in the Arctic continued until ~4000 BP, as a result of relatively warm conditions. In the northwest Labrador Sea (core 84-030-21), the dominance of *Brigantedinium* spp. until 4000 BP suggest that meltwater runoff through the Labrador Current was still significant (de Vernal and Hillaire-Marcel 1987).

The end of the Late Holocene warm interval in St. Anne's Basin at 2500 BP coincides with an increase in the number of melt layers of the Agassiz ice cores (Koerner and Fisher 1990; Fisher et al. 1995).

6.6 The terrestrial environment

6.6.1 Evidence for the Hypsithermal and the Neoglacial

Around Baffin Bay

Pollen records from the eastern Canadian Arctic indicate the occurrence of the hypsithermal during the mid-Holocene, generally between 6000 and 4000 BP, sometimes persisting as late as 3000 BP. The Neoglacial cooling started after 3000 BP. Some records also tend to indicate more complex scenarios with a deterioration around 5000 BP, in the middle of the warm interval.

In the northernmost sites, pollen suggest that the hypsithermal occurred relatively late. Pollen record from Axel Heiberg Island suggest relatively warm conditions between 4000 and 3000 BP, and a cooling after 3000 BP (Nichols 1972). Bourgeois (1986) interpreted the increase in regional pollen at 6000 BP in the Agassiz Ice cap as an indication that vegetation expanded near the ice cap. The late persistence of ice age conditions in that part of the Island probably prevented plant migration until that time. Most regional pollen types then peaked ~3000 BP, just before declining. In the central part of Ellesmere Island, the maximum plant density occurred earlier, from 7000 to 3500 BP (Hyvarinen 1985).

At Windy Lake on the Cumberland Peninsula (Baffin Island), the reconstruction of July air temperature indicates a warmer and wetter climate between 6000 and 4000 BP. A progressive decline in July temperature occurred in the last 3600 years. The temperature reconstruction shows much variability during the last 2500 years, with slightly warmer intervals of approximately 200 years duration, separated by slightly cooler intervals than today (Andrews et al. 1980). The time resolution for the Windy Lake core is ~ 50 years. This is consistent with a previous suggestion that climatic/paleoceanographic records are usually more complex when the resolution is higher. At Clyde River, Baffin Island, the local hypsithermal (6800-3100 BP) is interrupted by a climatic deterioration between 5600 and 4500 BP. and followed by a climatic deterioration in the last 3000 years (Short et al. 1985). Other pollen assemblages from short peat sections from Baffin Island indicate a climatic deterioration around 3000 to 2000 BP (Short and Andrews 1980).

Reconstructions of July temperatures on longer pollen records from the Cumberland Peninsula indicate warm and moist conditions also in the early Holocene (9200-8700 BP). The climate was then dry and cool until 6 ka, and July air temperatures were warmer again between 6000 and 4000 BP, or until 3000 BP at some sites. Most sites indicate a cooling after 2500 BP. There were also temperature oscillations superimposed on the main climatic changes (Short et al. 1985). Other similar reconstructions from Baffin Island show higher July air temperature than today from 6600 (base of record) to

2000 BP, with temperature starting to decline around 3ka and reaching a low between 1800 and 600 BP (Diaz et al. 1989).

Records from Northwest Territories suggest a warmer climate than today between 6000 and 5000 BP, a short-lived cooling 5000 to 4500 BP, followed by substantially warmer climate from 4500 to 3500 BP. Most records show a gradual cooling after 3300 BP, with temperature reaching a low ca. 2000 BP. Summer became warm again around 1000 BP (Nichols 1972). Reconstructions based on pollen from the region indicate significantly warmer July air temperatures between 6600 and 4500 BP, an interval with conditions similar to today at 5400-4800 BP, followed by another warm interval from 4800 to 2400 BP, after which temperature declined (Diaz et al. 1989).

Greenland

The Hypsithermal took place earlier in East Greenland (from 8500 to 5000 BP) than in West Greenland (7000 to 3000 or 2000 BP). The delay in West Greenland was probably caused by the proximity to the Laurentide Ice Sheet (Funder 1978). Other Holocene pollen records from West Greenland indicate the start of the Neoglacial cooling after 3300 BP (Fredskild 1985).

Evidence from glaciers

Evidence for a mid-Holocene Hypsithermal and a late Holocene climatic cooling are also provided by glaciers. A retreat of outlet glaciers on southeastern Ellesmere Island in the mid-Holocene allowed peat to grow between 5200 and 2600 BP. Peat growth stopped after 2500 BP as conditions deteriorated and a glacier advance is dated at 1000 BP (Blake 1981). The re-advance of Leffert glacier around 2000 years ago provides more evidence of climatic cooling. This is followed by an interval of retreat whose duration is unknown (Blake 1989).

On Cumberland Peninsula (Baffin Island), glacier readvance occurred earlier, around 4000 BP. Fluctuations of the cirque glacier margins also suggest rapid changes in climatic conditions around 1500 BP (Boulton et al. 1976).

In Labrador

Reconstructed July temperatures from pollen records in Quebec and Labrador increase above the present day average around 4800 and started to decline ~3000 BP and reached a minimum around 1500 BP (Diaz et al. 1989). Similar reconstructions in Labrador-Ungava indicate show warmer July temperature after 6500 or 6000 BP, and a decline since 3000 BP (Williams et al. 1995).

Closer to Cartwright Saddle core 6, the *Abies* acme between 7000 and 6000 BP is believed to represent the hypsithermal in southeast Labrador (Lamb 1980; King 1986).

Summer air temperature reconstructions indicate a maximum ~6000 BP (Webb et al. 1993). A decline in pollen flux after 3000 BP is interpreted as a climatic deterioration (Lamb 1980).

6.6.2 Timing of hypsithermal/Neoglacial relative to warm/cool SST

When the timing of the hypsithermal relative to the SST optimum is examined, the southern sites (La Have and St. Anne's Basins, Bay of Islands) appear to show a different story from the northern sites (Cartwright Saddle, NW Polynya): 1- in the south, there is evidence for a delayed hypsithermal relative to SST optimum (Levac 2001, 2002a,b); 2- in the north, hypsithermal and SST optimum occur at same time (this chapter).

I believe that the question about whether or not the hypsithermal is delayed relative to the warm SST probably cannot be answered now. The main problem is that climatic reconstructions are based on pollen assemblages, i.e. on a comparison of past tree distribution with the present day one, which means that: 1-if migration delays are involved, then even if climate was warmer than today, the composition of vegetation might not have shown it; 2-and if migration delays do not appear to be involved, potential delays in the establishment and expansion some taxa caused by interspecific competition remain a possibility.

In northern sites, given the distance and the relatively late deglaciation, it is reasonable to assume that migration delays are quite important (Nichols 1972; Bourgeois

1986). Much evidence for a mid-Holocene occurrence of the hypsithermal in Labrador and in the Arctic (Baffin and Ellesmere Islands, West Greenland) has been presented in the previous section. This coincides with warmer SST in both Cartwright Saddle and NW Polynya. It should be noted however that warm climatic conditions were also recorded in the Cumberland Peninsula (Baffin Island) in the early Holocene (Short et al. 1985) which again, raises the question of the migration delays.

In Nova Scotia, Green (1987) had suggested that competition from already established species and local environmental conditions could have played an important role in delaying the introduction or the expansion of later colonizers and that warmer climatic conditions made these species more competitive during the time interval defined as the hypsithermal. This does not mean however that the climate was not warmer before this time interval. It might have been warmer than today without being detrimental to the already established species, which declined only later, when conditions got much too warm for them, during what we call the hypsithermal.

This might be what we see in Nova Scotia and Newfoundland, where the arrival of taxa characterizing the hypsithermal is early relatively to their expansion. In Nova Scotia, this is the case for *Tsuga*, which arrived in central Nova Scotia as early as 9600 BP but did not peak until 7000 BP (Levac 2001). In Cape Breton, *Tsuga* arrived around 8200 BP but did not peak until 6200 BP (Levac 2002b). In Bay of Islands, percentages of *Fraxinus* pollen peaked more than a thousand years later than the arrival of this taxa in western Newfoundland.

As for the hypsithermal, the timing of the Neoglacial on land relative to cooler SST is different at the northern sites compared to the southern sites.

At the southern sites, the Neoglacial cooling on land started before the occurrence of cooler SST. The Neoglacial cooling around 2 ka in Nova Scotia and cooler SST are recorded only the last 500 years in La Have Basin (Levac 2001). In Cape Breton and Newfoundland, the Neoglacial started on land around 3000 BP (Levac 2002a,b) but in Bay of Islands, cooler SST are recorded only during the last 800 years, after the second SST optimum (Levac 2002a). In St. Anne's Basin, a thousand years long cool SST interval started at 2500 BP (Levac 2002b).

At the northern sites, SST become cooler at least a thousand years before the start of the Neoglacial n land. In Cartwright Saddle, SST declined after 4000, while the Neoglacial started around 3000 BP in Labrador (see previous section). NW Polynya SST are lower after 4500 BP but pollen records from the Arctic indicate that the Neoglacial started around 2000 to 3000 BP (previous section).

6.6.3 Atmospheric circulation

Many studies examined changes in atmospheric circulation during the late glacial and the Holocene. One approach was to observe changes in the amounts of exotic pollen in ice, lake or marine sediments. The other approach was through climate modeling.

Nichols et al. (1978) were among the first to suggest that exotic pollen could be used as indicators of paleowind. They examined the content from pollen traps laid throughout the Arctic (Labrador-Baffin Island) and determined that the source for the exotic pollen was the northeast Labrador-Ungava. They believe that the position of the 500 mb trough controls the influx of exotic pollen to the Arctic: when this pressure system shifts to the west, southerly airflow from Labrador-Ungava can reach the eastern Arctic, while a shift to the east results in lower exotic influxes. Important variations in exotic pollen during the Late Holocene in Cumberland Peninsula, which lies below this trough today, provide evidence for shift in the position of this pressure system and in the direction of dominant winds. Short and Andrews (1980) suggest that the difference in climate history between the northwest coast of Labrador-Ungava and the Cumberland Peninisula may also be associated with the low pressure centered over Baffin Island.

In Davis Strait and Northwest Labrador Sea, glacial and interglacial pollen assemblages show important differences in composition and diversity and depend on the position of the Arctic Front (Mudie and Aksu 1984; Aksu and Mudie 1985). In Baffin Bay, pollen assemblages from isotopic stage 1 are composed of conifer (*Picea*, *Pinus*) *Betula*, *Alnus*, Gramineae and minor amounts of *Salix*, Ericaceae, *Rumex*, Rosaceae and

Sphagnum, which is typical of the offshore sediments south of the present Arctic-Atlantic airfront. In contrast, *Picea* is absent in the pollen assemblages from stage 2 to 4 and herb pollen dominate. Such assemblages are found today in Baffin Bay sediments north of Arctic-Atlantic airfront, and they indicate the dominance of very cold dry Arctic Archipelago and westerly Arctic air masses during glacial intervals (Aksu and Mudie 1985). They suggest that the low pollen concentrations and diversity during glacial intervals are the result of a southward shift of the Arctic Front and that the relatively warm climate in southern Baffin Bay today is due to the penetration of warm cyclonic air at high latitude, which also carries the boreal tree and shrub pollen that are found in modern Baffin Bay sediments (Mudie and Aksu 1984; Aksu and Mudie 1985).

Seasonal differences in the relative proportions of exotic and regional pollen provide further support to the idea that wind direction (and pollen transport) is controlled by the position of the Arctic Front (Bourgeois et al. 1985; Bourgeois 1990). In snow samples from Devon Island ice cap, Bourgeois et al. (1985) found that exotic tree pollen dominate in winter, while pollen of Arctic plants dominate in summer. They suggest that the location of the Arctic front along the tree line in summer might prevent the northward transport of exotic (tree) pollen, but that this tree pollen is available for re-entrainment during the winter. Also, they suggest that precipitation during the summer might be responsible for the removal of pollen from the air, which would explain the lower pollen concentrations in the summer snow samples. Snow samples taken from the Agassiz Ice cap over a few years reveal that concentrations of exotic tree and shrub pollen (from the boreal forest) are much higher when a southerly flow into the Arctic Islands is coincident with the pollination season in the boreal forest (Bourgeois 1990). This demonstrates what Nichols et al. (1978) had previously suggested.

There are reports of higher concentrations of exotic pollen at the glacial/interglacial transition, or early Holocene, in Cumberland Peninsula (Short et al. 1985), in the eastern Labrador Sea (Aksu et al. 1992), along the eastern Canadian Margin (Mudie and McCarthy 1994), and in the Agassiz ice cap (Bourgeois et al. 2000).

Aksu et al. (1992) suggested that these are probably the result of stronger and more frequent cyclonic winds at the glacial/interglacial transition, since the existence of south to north gradients in pollen concentrations argues against a discharge from the melting ice. Mudie and McCarthy (1994) proposed a paleocirculation model for the eastern Canadian Margin, which uses the proportion of *Pinus* pollen in marine sediments to track the movement of air masses from mid-latitudes, where *Pinus* trees are abundant, into the Labrador Sea. *Pinus* and *Picea* dominated pollen assemblages in Labrador Sea sediments during the late Pleistocene, indicating increased long-distance transport. Since then, a decrease in *Pinus* relative to local pollen has been observed, first in the Fogo Seamount core (ca. 15,000 BP), then in Emerald Basin (ca. 10,000 BP), and finally around 10,000 BP in the Labrador Sea. This is probably related to the gradual weakening and disappearance of the high pressure ridge over the Laurentide Ice Sheet.

Based on a pollen record from the Agassiz ice cap, Bourgeois et al. (2000) suggested that anticyclonic circulation around the Laurentide Ice Sheet, as simulated by COHMAP (1988), could have transported *Picea* pollen from the Mackenzie Basin into the Arctic, and could explain the higher pollen concentrations in the early Holocene.

They also suggested that the atmospheric circulation was stronger because concentrations of *Pinus* were higher than today, despite that fact that *Pinus* traveled a longer distance at that time. With the melting of the Laurentide Ice Sheet and the northward migration of vegetation, sources of the exotic pollen were getting closer but the influx of pollen in the ice cap actually decreased (Bourgeois et al. 2000). With the establishment of westerly circulation pattern (COHMAP 1988), pollen was mainly carried south of Agassiz ice cap. Between 6000 and 3600 BP, ice core samples show parallel decreasing trends in tree pollen, $\delta^{18}O$ and summer melt layers, which suggest a gradual cooling. Increasing variability in the late Holocene (after 3600) might indicate frequent and relatively rapid changes in atmospheric conditions (Bourgeois et al. 2000). Frequent oscillations in reconstructed air temperature on Baffin Island during the last 2500 years suggest that changes in atmospheric circulation indeed have an impact on the local climate (Andrews et al. 1980).

In NW Polynya, total pollen concentrations are very low throughout the core and include approximately 70% exotic pollen. Total pollen concentrations are higher between 9000 and 4000 BP (both local and exotic contributions). This could indicate stronger southerly airflows and a greater penetration of warm air masses in the Arctic during the early and mid-Holocene. This penetration of warm air would have decreased gradually from the mid-Holocene.

6.6.4 Climatic models

Summer solar insolation was significantly greater than today between 12 and 6 ka, with a maximum at 9ka (Kutzbach and Webb 1993). Due to other forcings (residual Laurentide Ice Sheet) summer insolation became the predominant influence on climate only after 9 ka. Climatic changes throughout the Holocene also showed important regional variations (Webb et al. 1993). Emphasis here will be on the climatic changes in eastern North America.

The summer insolation maximum centered around 9 ka was due to the perihelion occurring in July (occurs today in January), to a greater tilt angle (24.23° instead of 23.45°) and to a greater eccentricity (Bradley 1999).

General circulation model (GCM) experiments prescribing the 9 ka solar insolation, and without ice caps, show warmer air temperature than today for the mid- and high northern latitudes (> 40° N), from May to September. When the models are run with the presence of the remaining ice caps however, they show that temperatures are lowered east of the ice sheet, i.e. over the North Atlantic and northwest Europe (Bradley 1999). This is consistent with the presence of an anticyclonic system over the Laurentide Ice Sheet, and surface wind circulation in a clockwise direction around the ice sheet. Winds would have been blowing from the northeast over eastern North America at 9 ka (COHMAP 1988; Kutzbach and Webb 1993) and climate remained cold due to the vicinity of the ice sheet (Vettoreti et al.1998).

The full thermal response to increased insolation was therefore manifested after 6 ka. Air temperature in eastern North America, inferred from pollen data and from GCMs indicate maximum warmth at 6 ka, when the influence of the Laurentide Ice Sheet had disappeared (Webb et al. 1993). This is after the summer insolation maximum, but at 6 ka, the summer insolation in the north hemisphere was still 4.7% higher than today (Kutzbach and Webb 1993; Vettoretti et al. 1998).

Models indicate enhanced monsoon activity at 6 ka because of intense heating of continental interior, resulting in increase southerly air flows (Kutzbach and Webb 1993). Warming over land areas is estimated to 1 to 2°C in mid- and high northern latitudes of North America, based on recent climatic simulations. These warmer conditions would have stretched from June to October (Vettoretti et al. 1998; Kerwin et al. 1999).

Simulation with the BIOME GCM (improved version of COHMAP 1988), indicate a warming of 1 to 2 °C in the Arctic at 6 ka, 1°C elsewhere in North America. At 9 ka, the climate was still colder than today for northeastern North America (Kutzbach et al. 1998).

6.6.5 Link between ocean and climate, between hypsithermal and warmer SST's

It appears that the ocean played a role in the warming on land at 6ka. Kerwin et al. (1999) showed, using climatic simulation, that warmer SST and reduced sea ice cover played an important role in the occurrence of warmer summer air temperature at high-latitude at 6ka. The ocean also contributed to maintaining warmer air temperature in the

Arctic during the winter months, despite the reduced insolation. Reasons include the large heat capacity of the ocean, the higher air temperature over high latitude oceans (Bradley 1999), the reduction in sea-ice thickness and the prolongation of the ice-free season (Vettoreti et al. 1998; Kerwin 1999).

6.7 Cyclicity/millenial cycles

Despite the fact that a short-term (1-2 kyr) rhythm has not been demonstrated in the three cores used for this study, it is important to mention a few recent hypotheses regarding global climatic mechanisms.

Bond et al. (1997) suggested the existence of such cycles based on changes in ice rafting debris in cores from the deep North Atlantic. Bond et al. (1999) proposed that short-term climatic/oceanic changes observed during the Holocene are comparable/related to Dansgaard/Oeschger oscillations because they are probably also the result of increased iceberg discharge in the North Atlantic, causing a freshening of surface waters. They differ by their lower amplitude. It is possible that the ocean is more stable during this interglacial and even relatively important fluxes of freshwater may be insufficient to trigger large changes in thermohaline circulation. The apparent absence of these short-term cycles in the Greenland ice core $\delta^{18}O$ record could be explained by an expansion of polar atmospheric circulation, which would prevent the air masses carrying the $\delta^{18}O$ signal (clouds, snow) from reaching interior Greenland.

Changes in the type of ice-rafted debris, this time in cores from the Arctic ocean and the Norwegian Sea, led Bischof (2000) to suggest that Holocene climate oscillated between two modes, i.e. the dominant warm and relatively ice free scenario of the present day, and short duration cold water incursions from the Arctic into the Norwegian Sea. He believes that these cold incursions are caused by re-organization of atmospheric pressure distribution in the Arctic.

Many papers attempt to establish a link or mention the possibility of a linkage between changes in paleocirculation and natural variability like the NAO (Keigwin and Pickart 1999; Jennings et al. 2002). In a variation on the same theme, Tremblay et al. (1997) attempted to establish a link between TransPolar Drift circulation modes and NAO index. Taylor and Stephens (1998) recently correlated the position of the Gulf Stream to the NAO. Periods of strong NAO index, which are characterized by stronger westerly winds, result in a more northerly path of the Gulf Stream.

While short-term (~10 years) variations in North Atlantic surface circulation might be associated with the NAO, it is not the case for the 1500 years drift-ice/cooling cycles. The basin wide distribution of these cooling events is contradictory to the NAO SST anomaly patterns (Bond et al. 2001). Rather, the cyclic drift-ice/cooling events correspond with higher concentrations of ^{14}C and ^{10}Be isotopes in the sediments and thus, are correlated with intervals of lower solar activity (Bond et al. 2001; Haigh 2001).

6.8 Conclusions

Overall, the Scotian Shelf-Baffin Bay transect can be divided into three regions, each exhibiting a different Holocene paleoceanographic story, affected to various degrees by the influx of meltwater and the proximity of the remaining Laurentide Ice Sheet, and presenting different characteristics in terms of the frequency and amplitude of changes. These three regions are: the southwestern Scotian Shelf (La Have Basin), the Gulf of St. Lawrence influence zone which includes St. Anne's Basin and Bay of Islands, and the Baffin Bay-Labrador Shelf zone, which includes Cartwright Saddle and NW Polynya.

The difference in the paleoceanographic story can be best illustrated by the SST optimum, whose occurrence is progressively younger as we move northward along the transect, with La Have Basin experiencing warmest SST first, followed by the Gulf Influence zone, then the Baffin Bay-Labrador Shelf region. The same can be said of the subsequent cool interval.

These different paleoceanographic stories are most likely due to the location of each region relative to the remaining ice sheet and to the meltwater influx. The SST optimum occurred earlier in La Have Basin, because it is more remote from the remaining ice sheet. The minimal changes in salinity during the Holocene suggest that meltwater influx had only a limited effect on the western Scotian Shelf. At sites under the influence of the Gulf of St. Lawrence, the SST optimum was delayed relative to La Have Basin, probably because of meltwater influx through the Gulf of St. Lawrence. It is possible that all 3 southernmost sites (La Have and St. Anne's Basins, Bay of Islands) could have experienced the SST optimum simultaneously, if there had been no meltwater influx through the Gulf of St. Lawrence. In Cartwright Saddle and NW Polynya, the SST optimum occurred after the influence from meltwater and the remaining ice sheet disappeared.

The amplitude and rapidity of changes, for all three parameters (SST, salinity and sea ice cover duration) is much greater at the Cartwright Saddle and NW Polynya sites throughout most of the Holocene, an indication of the proximity to important sources of meltwater. The amplitude of changes in sea surface conditions is also important in the early Holocene in the three southern sites but much smaller afterward.

Difficulties arise when trying to reconcile major changes in sea surface conditions with major changes in surface circulation, whether in the Arctic or the Labrador Sea. Nevertheless, some circumstantial evidence can be outlined. The end of the SST optimum in La Have Basin at 8500 BP coincides with the establishment of the present circulation, i.e. the re-establishment of the Baffin Land and Labrador Currents (Rahman and de Vernal 1994; Dyke et al. 1997; section 6.4.1) and the start of the surface water flux from the Arctic Ocean into Baffin Bay (Aksu 1983; Dyke et al. 1997; section 6.4.2). A reduction in the outflow of polar water from the Arctic Ocean from 8000 to about 3000 BP, as suggested by some authors (Scott et al. 1984; Funder and Weidick 1991; Andrews et al. 1993; section 6.4.3) could have contributed to the mid-Holocene warm SST at Cartwright Saddle, NW Polynya, and St. Anne's Basin.

Evidence for a link between changes in the Arctic (surface circulation, sea ice extent and melting) and sea surface conditions downstream (especially in St. Anne's Basin) are tenuous and difficult to prove since conditions at various sites along the transect are often in the opposite directions (section 6.4.4). An example of such (potential) connection is the coincidence of the SST optimum at St. Anne's Basin (7000-6000 BP) with an eastward shift in the TPD, which could result in a warmer Labrador Current. The absence of bowhead whale bones in the CAA suggests that channels were also blocked by ice during this interval, which could also have reduced inflow of Arctic water into Baffin Bay (Dyke et al. 1996b) (and possibly explain the reduced ice conditions in NW Polynya at that time). Another example is the coincidence of cooler conditions for most sites along the transect in the late Holocene, with a westward shift of the TPD, which would mean a cooler Labrador Current.

One of the leading themes of this study was also the timing of warm and cold intervals along the transect and unsuccessful attempts were made at connecting the various events. This suggests three things: 1- some events are localized and each region might have changed differently throughout the Holocene; 2- the resolution is not sufficient to allow "tracking" events downstream along the transect (for example meltwater events); 3- because of their lower resolution, paleoceanographic studies based on deep-sea cores present an simplified story of changes in surface circulation.

Other facts demonstrate the importance of obtaining high resolution records. Among these are the comparisons of our reconstructions with previous studies from Baffin Bay and Labrador Sea (see section 6.3), which show that changes in SST and salinity in Cartwright Saddle and NW Polynya *within* the Holocene have a greater amplitude than the glacial/interglacial differences estimated from cores with a lower resolution or from foraminiferal records. The amplitude and rapidity of SST oscillations during the Holocene is almost comparable to the SST drop which occurred during the Younger Dryas. Reconstructed August SST showed a drop of 6°C in less than 50 years in the Norwegian Sea during the Younger Dryas (Bradley 1999). Deep-sea corals from Orphan Knoll also showed a very rapid establishment of the Younger Dryas (Smith et al. 1997). In NW Polynya and St. Anne's Basin for example, SST changed by as much as 4-5°C in less than 100 years during the mid-Holocene and warm or cold intervals often lasted less than 500 years. In general, reconstructions for the 5 sites reveal a complex paleoceanographic history for the Holocene, a time period that is often considered eventless.

While sea surface conditions had a very complex history and display important regional differences, the Eastern Canadian Seaboard climate appears rather homogenous with the hypsithermal apparently centered around 6000 BP in most regions, (except Nova Scotia where is starts earlier). This is in contrast with the SST optimum which is progressively younger toward the north.

The atmosphere is a rapidly responding component of the climate system, and the fact that it does not respond to the summer insolation maximum of the early Holocene could indicate that another factor was controlling the climate. As demonstrated by climate models, the remaining Laurentide ice sheet maintained cold conditions over eastern North America until the mid-Holocene (Webb et al. 1993; Kutzbach and Webb 1993; Vettoretti et al. 1998). The warming in Labrador and in the Arctic could have proceeded rapidly as soon as the ice sheet was too reduced in size to have a strong influence on climate, and sea surface conditions on the Labrador Shelf and NW Polynya could also have warmed up after 6000 BP, probably due to a reduction in meltwater influx.

A disequilibrium between the vegetation and the climate could also account for the occurrence of the hypsithermal long after the summer insolation maximum. Holocene pollen assemblages record changes in vegetation, which involve northward migration, interspecific competition, climate (Delcourt and Delcourt 1987) and forest fire (Green 1981). Until paleoclimatic reconstructions independent from pollen are obtained, such as macrofossils, lake diatoms, fossil insect remains (Lowe and Walker 1997) or arcellaceans (McCarthy et al. 1995), the question of the lead/lag of the land versus the ocean cannot be answered with confidence. The present data indicates that the hypsithermal is delayed relative to the SST optimum in the south (La Have and St. Anne's Basins, Bay of Islands) but occurs at the same time in Cartwright Saddle and NW Polynya.

Understanding land-ocean interaction becomes even more difficult when the timing of the Neoglacial on land relative to the ocean is examined. The scenario is opposite to that of the hypsithermal, with the land leading the ocean at the southern locations (La Have and St. Anne's Basins, Bay of Islands), and the ocean leading the land at the northern locations (Cartwright Saddle and NW Polynya). While the ocean appears to exert an important control on the Arctic climate, as seen in section 6.6.5 (Vettoretti et al. 1998; Kerwin et al. 1999), it appears to be different in mid-latitude.

Comparison between sea surface conditions, as presented in this synthesis, and climate on the Eastern Canadian Seaboard, inferred empirically from pollen records, suggest that climate did not experience as many changes as the ocean, showing mainly the hypsithermal and the late Holocene cooling trend. On the other hand, some temperature reconstructions from Baffin Island (Andrews et al. 1980; Short et al. 1985; Diaz et al. 1989; section 6.6.1), as well as variations in exotic pollen influx to the Arctic (Nichols et al. 1978; Bourgeois et al. 2000; section 6.6.3), reveal shorter-term variations, especially in the late Holocene. This suggests that more detailed pollen records and/or quantitative reconstructions are necessary to detect these shorter-term climatic variations. Indeed, spectral analysis of pollen records from North America by Viau et al. (2002) demonstrated the presence of a 1500 yrs climatic variability during the last 14 000 years.

References

Aksu, A.E., 1983. Holocene and Pleistocene dissolution cycles in deep-sea cores of Baffin Bay and Davis Strait: Paleoceanographic implications. Marine Geology, **53**: 331-348.

Aksu, A.E., and Piper, D.J.W., 1979. Baffin Bay in the last 100,000 years. Geology, **7**: 245-248.

Aksu, A.E., and Mudie, P.J., 1985. Late Quaternary stratigraphy and paleoecology of northwest Labrador Sea. Marine Micropaleontology, **9**: 537-557.

Aksu, A.E., de Vernal, A., Mudie, P.J., 1989. High-resolution foraminiferal, palynological and stable isotopic records of upper Pleistocene sediment from Labrador Sea: paleoclimatic and paleoceanographic trends. *In*: S.P. Srivastava, M. Arthur, B. Clement et al. Proceedings of the Ocean Drilling Program, Scientific Results, **105**: 617-652.

Aksu, A.E., Mudie, P.J., de Vernal, A., and Gillespie, H., 1992. Ocean-atmosphere responses to climatic change in the Labrador Sea: Pleistocene plankton and pollen records. Palaeogeography, Palaeoclimatology, Palaeoecology, **92**: 121-137.

Alam, M., Piper, D.J.W., and Cooke, H.B.S., 1983. Late Quaternary stratigraphy and paleo-oceanography of the Grand Banks continental margin, eastern Canada. Boreas, **12**: 253-261.

Alley, R.B., Mayewski, P.A., Sowers, T., Stuiver, M., Taylor, K.C., Clark, P.U., 1997. Holocene climatic instability: a prominent, widespread event 8200 yr ago. Geology, **25**: 483-486.

Alley, R.B., Agutsdottir, A.M., and Fawcett, P.J., 1999. Ice-core evidence of Late-Holocene reduction in North Atlantic Ocean heat transport. *In*: P.U. Clark, R.S., Webb, and L.D. Keigwin (eds). Mechanisms of global climate change at millennial time scales. Geophysical monograph 112, p.301-312.

Amos, C.L. and Judge, J.T., 1991. Sediment transport on the eastern Canadian continental shelf. Continental Shelf Research, **11**: 1037-1068.

Anderson, C., 1987. The Canadian Atlantic Storms program (CASP). Science Review 1987, Research, Bedford Institute of Oceanography, Dartmouth, Nova Scotia, p. 25-29.

Anderson, D.M., 2001. Attenuation of millennial-scale events by bioturbation in marine sediments. Paleoceanography, **16**: 352-357.

Anderson, T.W. 1985. Late-Quaternary pollen records from Eastern Ontario, Quebec, and Atlantic Canada. *In*: V.M. Bryant, Jr. and Holloway, R.G. (eds.). Pollen records of Late-Quaternary North American sediments, American Association of Stratigraphic Palynologists Foundation, p. 281-326.

Anderson, T.W., and Lewis, C.F.M., 1992. Climatic influences of deglacial drainage changes in southern Canada at 10 to 8 ka suggested by pollen evidence. Géographie physique et Quaternaire, **46**: 255-272.

Anderson, T.W., and Macpherson, J.B., 1994. Wisconsinan Late-glacial environmental change in Newfoundland: a regional review. Journal of Quaternary Science, **9**: 171-178.

Andrews, J.H., Berti, A.A., and Norris, G., 1973. Key to the Quaternary pollen and spores of the Great Lakes Region. Life Sciences Miscellaneous Publication, Royal Ontario Museum, Toronto, 64 pages.

Andrews, J.T., Mode, W.N., and Davis, P.T. 1980. Holocene climate based on pollen transfer functions, eastern Canadian Arctic. Arctic and Alpine Research, **12**: 41-64.

Andrews, J.T., Dyke, A.S., Tedesco, K., White, J.W., 1993. Meltwater along the Arctic margin of the Laurentide Ice Sheet (8-12 ka): stable isotopic evidence and implications for past salinity anomalies. Geology, **21**: 881-884.

Andrews, J.T., Kirby, M.E., Aksu, A., Barber, D.C.; Meese, D., 1998. Late Quaternary detrital carbonate layers in Baffin Bay marine sediments (67 degrees -74 degrees N): correlation with Heinrich events in the North Atlantic. Quaternary Science Reviews, **17**: 1125-1137.

Andrews, J.T., Keigwin, L., Hall, F., Jennings, A.E., 1999. Abrupt deglaciation events and Holocene palaeoceanography from high-resolution cores, Cartwright Saddle, Labrador Shelf, Canada. Journal of Quaternary Science, **14**: 383-397.

Balsam, W., 1981. Late Quaternary sedimentation in the western North Atlantic: stratigraphy and paleoceanography. Palaeogeography, Palaeoclimatology, Palaeoecology, **35:** 215-240.

Balsam, W. L., Heusser, L. E., 1976. Direct correlation of sea surface paleotemperatures, deep circulation, and terrestrial paleoclimates: foraminiferal and palynological evidences from two cores off Chesapeake Bay. Marine Geology, **21**, 121-147.

Banfield, C.E., 1983. Climate. *In*: South, G.R. (ed.) Biogeography and ecology of the island of Newfoundland. Dr. W. Junk Publishers, Monographiae Biologicae, volume 48, p. 37-106.

Barber, D.C., Dyke, A. Hillaire-Marcel, C., Jennings, A.E., Andrews, J.T., Kerwin, M.W., Bilodeau, G., McNeely, R., Southon, J., Morehead, M.D., Gagnon, J.-M., 1999. Forcings of the cold event of 8,200 years ago by catastrophic drainage of Laurentide lakes. Nature, **400**: 344-348.

Bard, E., 2001. Paleoceanographic implications of the difference in deep-sea sediment mixing between large and fine particles. Paleoceanography, **16**: 235-239.

Bard, E., Arnold, M., Duprat, J., Moyes, J., and Duplessy, J.-C., 1987. Reconstruction of the last deglaciation: deconvolved records of $\delta^{18}O$ transects, micropaleontological variations and accelerator mass spectrometric ^{14}C dating. Climate Dynamics, **1**: 101-112.

Bassett, I.J., Crompton, C.W., and Parmelee, J.A., 1978. An atlas of airborne pollen grains and common fungus spores of Canada. Canada Department of Agriculture, Monograph no. 18, 321 pages.

Batten, D.J., 1996. Chapter 7c Colonial Chlorococcales. *In*: Jansonius, J. and D.C. McGregor (eds), Palynology: Principles and Applications. American Association of Stratigraphic Palynologists Foundation, vol. 1, p. 191-203.

Bischof, J., 2000. Ice drift, ocean circulation and climate change. Springer-Praxis books in environmental sciences, 215 pages.

Blake, W. Jr. 1981. Neoglacial fluctuations of glaciers, southeastern Ellesmere Island, Canadian Arctic Archipelago. Geografiska Annaler **63A**: 201-217.

Blake, W. Jr., 1989. Application of 14C AMS dating to the chronology of Holocene glacier fluctuations in the high Arctic, with special reference to Leffert Glacier, Ellesmere Island, Canada. Radiocarbon, **31**: 570-578.

Blake, W. Jr., 1998. The broad Yoldia, *Megayoldia thraciaeformis*, in northernmost Baffin Bay: radiocarbon ages and paleoceanographic implications. Bulletin of the Geological Society of Denmark, **44**: 129-138.

Bond, G., Showers, W., Cheseby, M., Lotti, R., et al., 1997. A pervasive millennial-scale cycle in North Atlantic Holocene and glacial climates. Science, **278**: 1257-1266.

Bond, G.C., Showers, W., Elliot, M., Evans, M., Lotti, R., Hajdas, I., Bonani, G. and Johnson, S., 1999. The North Atlantic's 1-2 kyr climate Rhythm: relation to Heinrich events, Dansgaard/Oeschger cycles and the little ice age. *In*: P.U. Clark, R.S., Webb, and L.D. Keigwin (eds). Mechanisms of global climate change at millennial time scales. Geophysical monograph 112, p. 35-58.

Bond, G., Kromer, B., Beer, J., Muscheler, R., Evans, M.N., Showers, W., Hoffman, S., Lotti-Bond, R., Hajdas, I., Bonani, G., 2001. Persistent solar influence on North Atlantic climate during the Holocene. Science, **294**: 2130-2136.

Boulton, G.S., Dickson, J.H., Nichols, H., Michols, M., and Short, S.K., 1976. Late Holocene glacier fluctuations and vegetation changes at Maktak Fiord, Baffin Islands, N.W.T., Canada. Arctic and Alpine Research, **8**: 343-356.

Bourgeois, J.C., 1986. A pollen record from the Agassiz ice cap, northern Ellesmere Island, Canada. Boreas, **15**: 345-354.

Bourgeois, J.C., 1990. Seasonal and annual variation of pollen content in the snow of a Canadian high Arctic ice cap. Boreas, **19**: 313-322.

Bourgeois, J.C., Koerner, R.M., and Alt, B.T., 1985. Airborne pollen: a unique air mass tracer, its influx to the Canadian high Arctic. Annals glaciology **7**: 109-116.

Bourgeois, J.C., Koerner, R.M., Gajemwski, K., and Fisher, D.A., 2000. A Holocene ice-core pollen record from Ellesmere Island, Nunavut, Canada. Quaternary research, **54**: 275-283.

Bradley, R.S., 1999. Chapter 12 Paleoclimatic modesl. *In*: Paleoclimatology: reconstructing climates of the Quaternary. 2nd edition. International Geophysics Series, vol. 68, p. 471-506.

Brookes, I.A., and Stevens, R.K., 1985. Radiocarbon age of rock-boring *Hiatella arctica* (Linné) and post-glacial sea-level change at Cow Head, Newfoundland. Canadian Journal of Earth Sciences, **22**: 136-140.

Brookes, I.A., Scott, D.B., and McAndrews, J.H., 1985. Postglacial relative sea-level change, Port au Port area, west Newfoundland. Canadian Journal of Earth Sciences, **22**: 1039-1047.

Buckley, D.E., 1991. Deposition and diagenetic alteration of sediment in Emerald Basin, the Scotian Shelf. Continental Shelf Research, **11**: 1099-1122.

Campbell, C., 1999. Holocene storminess on the Scotian Shelf: the last 7000 years, Master of Science Thesis, St. Mary's University, Halifax, Nova Scotia, 77 pages.

Carreto, J.I., Benavides, H.R., Negri, R.M., Glorioso, P.D., 1986. Toxic red-tide in the Argentine Sea. Phytoplankton distribution and survival of the toxic dinoflagellate *Gonyaulax excavata* in a frontal area. Journal of Plankton Research **8**: 15-28.

Chapman, M.R., Shackleton, N.J., 1998. What level of resolution is attainable in a deep-sea core? Results of a spectrophotometer study. Paleoceanography, **13**: 311-315.

CLIMAP Project Members, 1976. The surface of the ice-age Earth. Science, **191**: 1131-1137.

COHMAP, 1988. Climatic changes of the last 18,000 years: observation and model simulations. Science, **241**: 1043-1052.

Damman, A.W.H. 1983. An ecological subdivision of the island of Newfoundland. *In* G.R. South (ed.) Biogeography and ecology of the island of Newfoundland. Dr. W. Junk Publishers, Monographiae Biologicae, volume 48, p. 163-206.

Davis, M.B., 1981. Outbreaks of forest pathogens in Quaternary history. Proceedings IV International Palynology Conference, Lucknow, **3**: 216-227.

Davis, R.B., and Webb, T. III, 1975. The contemporary distribution of pollen in eastern North America: a comparison with the vegetation. Quaternary Research, **5**: 395-434.

Delcourt, P.A., and Delcourt, H.R., 1987. Chapter 6 Late Quaternary migrational strategies of trees species. *In*: Long-term forest dynamics of the temperate zone. Ecological Studies 63, Springer Verlag, p. 292-330.

de Vernal, A., and Hillaire-Marcel, C., 1987. Paleoenvironments along the eastern Laurentide ice sheet margin and timing of the last ice maximum and retreat. Géographie Physique et Quaternaire, **41**: 265-277.

de Vernal, A., and Mudie, P.J., 1989a. Late Pliocene to Holocene palynostratigraphy at ODP site 645, Baffin Bay. *In*: S.P. Srivastava, M. Arthur, B. Clement et al. Proceedings of the Ocean Drilling Program, Scientific Results, **105**: 387-399.

de Vernal, A., and Mudie, P.J., 1989b. Pliocene and Pleistocene palynostratigraphy at ODP sites 646 and 647, eastern and southern Labrador Sea. *In*: S.P. Srivastava, M. Arthur, B. Clement et al. Proceedings of the Ocean Drilling Program, Scientific Results, **105**: 401-422.

de Vernal, A., and Giroux, L., 1991. Distribution of organic walled microfossils in recent sediments from the Estuary and Gulf of St. Lawrence. *In* J.C. Therriault (ed.) The Gulf of St. Lawrence: small ocean of big estuary? Canadian Special Publication of Fisheries and aquatic sciences, **113**: 189-199.

de Vernal, A., and Mudie, P.J., 1992. Pliocene and Quaternary dinoflagellate cyst stratigraphy in the Labrador Sea: paleoenvironmental implications. *In*: M.J., Head, J.H., Wrenn, (eds). Neogene and Quaternary dinoflagellate cyst of the North Atlantic Ocean and adjacent seas: ecostratigraphy and biostratigraphy. American Association of Stratigraphic Palynologists Foundation, p. 329-346.

de Vernal, A., Guiot, J., Turon, J.-L., 1993. Late and postglacial paleoenvironments of the Gulf of St. Lawrence: marine and terrestrial palynological evidence. Géographie Physique et Quaternaire, **47**: 167-180.

de Vernal, A., Turon, J.-L., and Guiot, J., 1994. Dinoflagellate cyst distribution in high-latitude marine environments and quantitative reconstruction of sea-surface salinity, temperature, and seasonality. Canadian Journal of Earth Sciences, **31**: 48-62.

de Vernal, A., Bilodeau, G., Hillaire-Marcel, C., Kassou, N., 1992a. Quantitative assessment of carbonate dissolution in marine sediments from foraminifer linings vs. shell ratios: Davis Strait, northwest North Atlantic. Geology, **20**: 527-530.

de Vernal, A., Mudie, P.J., Harland, R., Morzadec-Kerfourn, M.T., Turon, J.-L., Wrenn, J.H., 1992b. Quaternary organic-walled dinoflagellate cysts of the North Atlantic ocean and adjacent seas: ecostratigraphy and biostratigraphy. *In*: M.J., Head, J.H., Wrenn, (eds) Neogene and Quaternary Dinoflagellate Cysts and Acritarchs. American Association of Stratigraphic Palynologists Foundation, p. 298-328.

de Vernal, A., Hillaire-Marcel, C., Turon, J.-L., Matthiessen, J., 2000. Reconstruction of sea surface temperature, salinity and sea-ice cover in the northern North Atlantic during the last glacial maximum based on dinocyst assemblages. Canadian Journal of Earth Sciences, **37**: 725-750.

de Vernal, A., Henry, M., Matthiessen, J., Mudie, P. J., Rochon, A., Boessenkool, K., Eynaud, F., Grøsfjeld, K., Guiot, J., Hamel, D., Harland, R., Head, M., Kunz-Pirrung, M., Levac, A., Loucheur, V., Peyron, O., Pospelova, V., Radi, T., Turon, J.-L., Voronina, E., 2001. Dinocyst assemblages as tracers of sea surface conditions in the northern North Atlantic, Arctic, sub-Arctic seas: the "n=677" database and derived transfer functions. Journal of Quaternary Science, **16**: 681-698.

Diaz, H.F., Andrews, J.T., and Short, S.K., 1989. Climate variations in northern North America (6000 BP to present) reconstructed from pollen and tree-ring data. Arctic and Alpine Research. **21**: 45-59.

Drinkwater, K.F., Pettipas, R.G., Bugden, G.L. Langille, P., 1999. Climatic data for the northwest Atlantic: a sea ice database for the Gulf of St. Lawrence and the Scotian Shelf. Canadian Technical Report of Hydrography and Ocean Sciences 199, 134 pages.

Dyer, A.K., 1986. A palynological investigation of the Late Quaternary vegetational history of the Baie Verte Peninsula, northcentral Newfoundland. Master's thesis, Department of Geography, Memorial University of Newfoundland, 182 pages.

Dyke, A., S., and Prest, V.K., 1987. Late Wisconsinan and Holocene history of the Laurentide Ice Sheet. Geographie Physique et Quaternaire, **41**: 237-263.

Dyke, A.S., and Savelle, J.M., 2001. Holocene history of the Bering Sea bowhead whale (*Balaena mysticetus*) in its Beaufort Sea summer grounds off southwestern Victoria Island, western Canadian Arctic. Quaternary Research **55**: 371-379.

Dyke, A.S., Dale, J.E., and McNeely, R.N., 1996a. Marine molluscs as indicators of environmental change in glaciated North america and Greenland during the last 18000 years. Géographie Physique et Quaternaire **50**: 125-184.

Dyke, A.S., Hooper, J., and Savelle, J.M., 1996b. A history of sea ice in the Canadian Arctic Archipelago on postglacial remains of the Bowhead Whale (*Balaena mysticetus*). Arctic, **49**: 235-255.

Dyke, A.S., England, J., Reimnitz, E., and Jetté, H., 1997. Changes in driftwood delivery to the Canadian Arctic Archipelago: the hypothesis of postglacial oscillations of the transpolar drift. Arctic, **50**: 1-16.

Edgecombe, R.B., Scott, D.B., Fader, G.B.J., 1999. New data from Halifax Harbour: paleoenvironment and a new Holocene sea-level curve for the inner Scotian Shelf. Canadian Journal of Earth Sciences, **36**: 805-817.

Edwards, L.E., Andrle, V.A.S., 1992. Distribution of selected dinoflagellate cysts in modern marine sediments. *In*: M.J., Head, J.H., Wrenn, (eds). Neogene and Quaternary dinoflagellate cyst of the North Atlantic Ocean and adjacent seas: ecostratigraphy and biostratigraphy, American Association of Stratigraphic Palynologists Foundation, p. 259-288.

El-Sabh, M.I., 1976. Surface circulation pattern in the Gulf of St. Lawrence. Journal of the fisheries research board, **33**: 124-138.`

Environment Canada, 1984. Climatic Atlas Canada: a series of maps portraying Canada's climate. Atmospheric Environment Service, Ottawa.

Environment Canada, 1989. Ecoclimatic regions of Canada. Ecological Land classification series no 23, 118 pp.

Fillon, R.H., 1976. Hamilton Bank, Labrador Shelf: postglacial sediment dynamics and paleo-oceanography. Marine Geology, **20**: 7-25.

Fisher, D.A., Koerner, R.M., and Reeh, N., 1995. Holocene climatic records from Agassiz Ice Cap, Ellesmere Island, NWT, Canada. The Holocene, **5**: 19-24.

Forbes, D.L., Shaw, J., and Eddy, B.G., 1993. Late Quaternary sedimentation and the postglacial sea-level minimum in Port au Port Bay and vicinity, west Newfoundland. Atlantic Geology, **29**: 1-26.

Fredskild, B. 1985. Holocene pollen records from West Greenland. *In*: J.T. Andrews (ed.). Quaternary Environments, Eastern Canadian Arctic, Baffin Bay and Western Greenland, p. 643-681.

Freeman, J.M. 1986. Paleoceanographic trends on the Northern Scotian Shelf. Unpublished honours thesis, Dalhousie University, 68 pages.

Funder, S., 1978. Holocene climates in Greenland, and North Atlantic atmospheric circulation. Danish meteorological institute, climatological papers no 4, p. 175-181.

Funder, S., and Weidick, A., 1991. Holocene boreal mooluscs in Greenland-paleoceanographic implications. Palaeogeography Palaeoclimatology Palaeoecology, **85**: 123-135.

Gajewski K., Vance, R., Sawada, M., Fung, I., Gignac, D., Halsey, L., John, J., Maisongrande, P. Mandell, P., Mudie, P.J., Richard, P.J.H., Sherin, A.G., Soroko, J., and Vitt, D.H., 2000. The climate of North America and adjacent ocean waters ca. 6 ka. Canadian Journal of Earth Sciences, **37:** 661-681.

Geological survey of Canada, 1958. Map 1057A, Bay of Island, Island of Newfoundland.

Giroux, L. 1990. Distribution moderne des palynomorphes dans l'estuaire et le golfe du Saint-Laurent. Master Thesis, Université du Québec à Montréal, 158 pages.

Green, D.G., 1981. Time series and postglacial forest ecology. Quaternary Research, **15**: 265-277.

Green, D.G., 1987. Pollen evidence for the postglacial origins of Nova Scotia's forest. Canadian Journal of Botany, **65**: 1163-1179.

Greenberg, D.A., and Petrie, B.D., 1988. The mean barotropic circulation on the Newfoundland Shelf and Slope. Journal of Geophysical Research, **93**: 15541-15550.

Guiot, J., 1990. Methods and programs of statistics for paleoclimatology and paleoecology. In, Guiot, J., Labeyrie, L., (Eds). Quantification des changements climatiques: méthode et programmes. Institut national des sciences de l'Univers (INSU-France), monographie no 1, 253 pages.

Haigh, J.D., 2001. Climate variability and the influence of the sun. Science, **294**: 2109-2111.

Han, G., Loder, J.H. and smith, P.C., 1999. Seasonal-mean hydrography and circulation in the Gulf of St. Lawrence and on the eastern Scotian and southern Newfoundland shelves. Journal of Physical Oceanography, **29**:1279-1301.

Hare, F.K., 1997. Canada's climate: an overall perspective. *In*: W.G., Bailey, T.R., Oke, W.R., Rouse (eds). The surface climates of Canada, McGill-Queen's University Press, p. 3-15.

Head, M.J., Harland, R., Matthiessen, J., 2001. Cold marine indicators of the late Quaternary: the new dinoflagellate cyst genus *Islandinium* and related morphotypes. Journal of Quaternary Science, **16**: 621-636.

Hillaire-Marcel, C., de Vernal, A., Bilodeau, G., Weaver, A.J., 2001. Absence of deep-water formation in the Labrador Sea during the last interglacial period. Nature, **410**: 1073-1077.

Hyvarinen, H. 1985. Holocene pollen stratigraphy of Baird Inlet, east-central Ellesmere Island, Arctic Canada. Boreas, **14**: 19-32.

Jennings, A.E., Knudsen, K.L., Hald, M., Hansen, C.V., and Andrews, J.T., 2002. A mid-Holocene shift in Arctic sea-ice variability on the East Greenland Shelf. The Holocene, **12**: 49-58.

Jetté, H., and Mott, R.J., 1995. Vegetation and climate of maritime Canada 6000 years BP: a synthesis. Géographie physique et Quaternaire, **49**: 141-162.

Keffer, T., Martinson, D.G., and Corliss, B.H., 1988. The position of the Gulf Stream during Quaternary glaciations. Science, **241**: 440- 442.

Keigwin, L.D., and Jones, G.A., 1995. The marine record of deglaciation from the continental margin off Nova Scotia. Paleoceanography, **10**: 973-985.

Keigwin, L.D., and Pickart, R.S., 1999. Slope water current over the Laurentian Fan on interannual to millenial time scales. Science, **286**: 520-523.

Kerwin, M.W., 1996. A regional stratigraphic isochron (ca. 8000 14C yr B.P.) from final deglaciation of Hudson Strait. Quaternary Research, **46**: 89-98.

Kerwin, M.W., Overpeck, J.T., Webb, R.S., de Vernal, A., Rind, D.H., and Healy, R.J., 1999. The role of oceanic forcing in mid-Holocene Northern Hemisphere climatic change. Paleoceanography, **14**: 200-210.

King, G.A., 1986. Deglaciation and vegetation history of western Labrador and adjacent Quebec, Ph.D. University of Minnesota, UMI, 266 pages.

King, L.H., Fader, G.B., 1986. Wisconsinan glaciation of the continental shelf, southeastern Canada, Geological Survey of Canada, Bulletin 363, 72 pages.

Koerner, R.M., and Fisher, D.A., 1990. A record of Holocene summer climate from a Canadian high-Arctic ice core. Nature, **343**: 630-631.

Koutitonsky, V.G. and Bugden, G.L., 1991. The physical oceanography of the Gulf of St. Lawrence: a review with emphasis on the synoptic variability of the motion. *In* J.C. Therriault (ed.) The Gulf of St. Lawrence: small ocean of big estuary? Canadian Special Publication of Fisheries and Aquatic Sciences, **113**: 57-90.

Kutzbach, J.E., Webb, T. III, 1993. Conceptual basis for understanding Late-Quaternary climates. *In*: H.E. Wright Jr., J.E. Kutzbach, T. Webb III, W.E. Ruddiman, F.A. Street-Perrott, P.J. Bartlein (eds). Global climates since the last glacial maximum. University of Minnesota Press, p. 5-23.

Kutzbach, J.E., Gallimore, R., Harrison, S., Behling, P., Selin, R., Laarif, F., 1998. Climate and biome simulations for the past 21,000 years. Quaternary Science Reviews, **17**: 473-506.

Lamb, H.F., 1980. Late Quaternary vegetational history of southeastern Labrador. Arctic and Alpine Research, **12**: 117-135.

Lapointe, M., 2000. Late Quaternary paleohydrology of the Gulf of St. Lawrence (Québec, Canada) based on diatom analysis. Palaeogeography, Palaeoclimatology, Palaeoecology, **156**: 261-276.

Lauriol, B., and Gray, J.T., 1997. La composition isotopique des mollusques marins et sa relation à la déglaciation de la Péninsule d'Ungava. Géographie Physique et Quaternaire, **51**: 185-199.

Levac, E. 2001. High resolution Holocene palynological record from the Scotian Shelf. Marine Micropaleontology, **43**: 179-197.

Levac, E., 2002a. Palynological records from Bay of Islands, Newfoundland: direct correlation of Holocene paleoceanographic and climatic changes. Submitted to Palynology, May 2002.

Levac, E., 2002b. Holocene paleoceanography of St. Anne's Basin, Scotian Shelf: palynological records. In preparation.

Levac, E., and de Vernal, A., 1997. Postglacial changes of terrestrial and marine environments along the Labrador coast: palynological evidences from cores 91-045-005 and 91-045-006, Cartwright Saddle. Canadian Journal of Earth Sciences, **34**: 1358-1365.

Levac, E., de Vernal, A., Blake, W. Jr. 2001. Holocene palynology of cores from the North Water Polynya, Baffin Bay. Journal of Quaternary Science, **16**: 353-363.

Levac, E., Mudie, P.J., Bertini, A., de Vernal, A. and Rochon, A. 2000. High resolution palynological records of late glacial and Holocene climate change, Atlantic Canada. CGU Annual Meeting, Banff.

Levac, E., Mudie, P.J., Rochon, A., 2002. Holocene evolution of sea surface conditions along the eastern Canadian Seaboard: a synthesis. In preparation.

Livingstone, D.A., 1968. Some interstadial and postglacial pollen diagrams from Eastern Canada. Ecological monographs, **38**: 87-125.

Livingstone, D.A., and Estes, A.H., 1967. A carbon-dated pollen diagram from the Cape Breton Plateau, Nova Scotia. Canadian Journal of Botany, **45**: 339-359.

Livingstone, D.A., and Livingstone, B.G.R., 1958. Late-glacial and postglacial vegetation from Gillis Lake in Richmond County, Cape Breton Island, Nova Scotia. American Journal of Science, **256**: 341-359.

Loder, J.W., Han, G., Hannah, C.G., Greenberg, D.A., Smith, P.C., 1997. Hydrography and baroclinic circulation in the Scotian Shelf region: winter versus summer. Canadian Journal of Fisheries and Aquatic Sciences, **54**: 40-56.

Loucheur, V., 1999. Nouveau protocole de préparation des sédiments pour l'analyse palynologique avec système micro-ondes: développement méthodologique et tests de reproductibilité. Master thesis, Université du Québec à Montréal, 52 pages.

Lowe, J.J., and Walker, M.J.C., 1997. Chapter 4 Biological evidence. *In*: Reconstructing Quaternary environments. Longman, New York, p. 162-236.

MacIntyre, H.L., Cullen, J.J., 1996. Primary production by suspended and benthic microalgae in a turbid estuary: time-scales of variability in San Antonio Bay, Texas. Marine Ecology Progress Series, **145**: 245-268.

MacIntyre, J.G., Cullen, J.J., Cembella, A.D., 1997. Vertical migration, nutrition and toxicity in the dinoflagellate *Alexandrium tamarense*. Marine Ecology Progress Series, **148**: 201-216.

Margalef, R., 1978. Life-forms of phytoplankton as survival alternatives in an unstable environment. Oceanologica Acta, **1**: 493-509.

Macpherson, J.B., 1981. Chapter 6 The development of the vegetation of Newfoundland and climatic change during the Holocene. *In*: A.G. Macpherson, and J.B., Macpherson, eds., The natural environment of Newfoundland, past and present. Department of Geography, Memorial University of Newfoundland, p. 189-217.

Macpherson, J.B., 1988. The late Pleistocene-Holocene pollen record from the Northeast Newfoundland shelf: comparison with the terrestrial record. Report submitted to the Atlantic Geoscience Centre, project 177-04-86.

Macpherson, J.B., 1995. A 6 ka BP reconstruction for the Island of Newfoundland from a synthesis of Holocene lake-sediment pollen records. Géographie physique et Quaternaire, **49**: 163-182.

Matthiessen, J., and Baumann, A., 1997. Dinoflagellate cyst records from the East Greenland continental margin during the last 15,000 years: implications for paleoceanographic reconstructions. *In*: H.C., Hass and M.A., Kaminski (eds). Contributions to the micropaleontology and paleoceanography of the north North Atlantic. Grzybowski Foundation Special Publication, no 5, p. 149-165.

McCarthy, F.M.G., Collins, E.S., McAndrews, J.H., Kerr, H.A., Scott, D.B., and Medioli, F.S., 1995. A comparison of postglacial arcellacean ("Thecamoebian") and pollen succession in Atlantic Canada, illustrating the potential of Arcellaceans for paleoclimatic reconstruction. Journal of Paleontology, **69**: 980-993.

Miller, A.A.L., Mudie, P.J., and Scott, D.B., 1982. Holocene history of Bedford Basin, Nova Scotia: foraminifera, dinoflagellate and pollen records. Canadian Journal of Earth Sciences, **19**: 2342-2367.

Moore, T.C. Jr., Walker, J.C.G., Rea, D.K., Lewis, C.F.M., Shane, L.C.K., and Smith, A.J., 2000. Younger Dryas interval and outflow from the Laurentide ice sheet. Paleoceanography, **15**: 4-18.

Mudie, P.J., 1980. Palynology of Later Quaternary marine sediments, Eastern Canada, Ph.D. Thesis, Dalhousie University, Halifax, Nova Scotia, 638 pages.

Mudie, P.J., 1982. Pollen distribution in recent marine sediments, eastern Canada. Canadian Journal of Earth Science, **19**: 729-747.

Mudie, P.J., 1992. Circum-Arctic Quaternary and Neogene marine palynofloras: paleoecology and statistical analysis. *In*: M.J. Head, J.H. Wrenn, (eds). Neogene and Quaternary dinoflagellate cyst of the North Atlantic Ocean and adjacent seas: ecostratigraphy and biostratigraphy, American Association of Stratigraphic Palynologists Foundation, p. 347-390.

Mudie, P.J., and Aksu, A.E., 1984. Palaeoclimate of Baffin Bay from 300,000-year record of foraminifera, dinoflagellates and pollen. Nature, **312**: 630-634.

Mudie, P.J., Keen, C.E., Hardy, I.A., and Vilks, G. 1984. Multivariate analysis and quantitative paleoecology of benthic foraminifera in surface and late Quaternary shelf sediments, northern Canada. Marine Micropaleontology, **8**: 283-313.

Mudie, P.J., and Short, S.K. 1985. Marine palynology of Baffin Bay. *In*: J.T. Andrews (ed). Studies of Baffin Island, West Greenland and Baffin Bay. Allen and Unwin, London, p. 263-308.

Mudie, P.J., Gilbault, J.-P., 1982. Ecostratigraphic and paleomagnetic studies of late Quaternary sediments on the Northweast Newfoundland Shelf, Current research, Part B, Geological Survey of Canada, paper 82-1B, p. 107-116.

Mudie, P.J. and Harland, R., 1996. Aquatic Quaternary. *In*: J. Jansonius, and D.C. McGregor, (eds). Palynology: principles and applications. American Association of Stratigraphic Palynologists Foundation, vol. 2, p. 843-877.

Mudie, P.J., McCarthy, F.M.G., 1994. Late Quaternary pollen transport processes, western North Atlantic: Data from box models, cross-margin and N-S transects. Marine Geology, **118**: 79-105.

Mudie, P.J., and Rochon, A., 2001. Distribution of dinoflagellate cysts in the Canadian Arctic marine region. Journal of Quaternary Science, **16**: 603-620.

Mudie, P.J., de Vernal, A., and Head, M., 1990. Neogene to Recent palynostratigraphy of circum-arctic basins: results of ODP Leg 104, Norwegian Sea, Leg 105 Baffin Bay and DSDP Site 611, Irminger Sea. *In*: U. Bleil, and J. Thiede, (eds). Geological history of the polar oceans: Arctic versus Antarctica. NATO ASI Series C, vol. 308. Kluwer Academics, Dordrecht, Netherlands, p. 609-628.

Mudie, P.J., Rochon, A., and Levac, E., 2002. Palynological records of red tides in Canada: past trends and implications for the future. In press in Palaeogeography, Palaeoclimatology, Palaeoecology.

Mudie, P.J., Harland, R., Matthiessen, J., and de Vernal, Anne, 2001. Marine dinoflagellate cysts and high latitude Quaternary paleoenvironmental reconstructions: an introduction. Journal of Quaternary Science, **16**: 595-602.

Nichols, H., 1972. Summary of the palynological evidence for late-Quaternary vegetational and climatic change in the central and eastern Canadian Arctic. *In*: Y. Vasari, H. Hyvarinen, and S. Hicks (eds.). Climatic changes in Arctic areas during the last ten-thousand years. Acta Universitatis Ouluensis, Oulu, p. 309-339.

Nichols, H., Kelly, P.M., and Andrews, J.T., 1978. Holocene palaeo-wind evidence from palynology in Baffin Island. Nature **273**: 140-142.

NOAA, 1994 (National Oceanic and Atmospheric Administration). World Ocean Atlas. U.S. Department of Commerce. 9 CD-Roms.

Parkhill, J.-P., Cembella, A.D., 1999. Effects of salinity, light and inorganic nitrogen on growth and toxigenicity of the marine dinoflagellate *Alexandrium tamarense* from northeastern Canada. Journal of Plankton Research, **21**: 939-955.

Petrie, B., and Drinkwater, K., 1993. Temperature and salinity variability on the Scotian Shelf and in the Gulf of Maine 1945-1990. Journal of Geophysical Research, **98**: 20079-20089.

Petrie, B., Topliss, B.J., Wright, D.G., 1987. Coastal upwelling and eddy development off Nova Scotia. Journal of Geophysical Research, **29**: 12979-12991.

Petrie, B., Toulany, B. and Garrett, C., 1988. The transport of water, heat and salt through the Strait of Belle Isle. Atmosphere-ocean **26**: 234-251.

Petrie, B., Drinkwater, K., Gregory, D., Pettipas, R., and Sandstrom, A., 1996a. Temperature and salinity Atlas for the Scotian Shelf and the Gulf of Maine. Canadian Technical Report of Hydrography and Ocean Sciences 171, 398 pages.

Petrie, B., Drinkwater, K., Sandstrom, A., Pettipas, R., Gregory, D., Gilbert, D., and Sekhon, P., 1996b. Temperature, salinity and sigma-t atlas for the Gulf of St. Lawrence. Canadian Technical Report of Hydrography and Ocean Sciences 178, 200 pages.

Phillips, D., 1990. The climate of Canada. Environment Canada, Ottawa, 176 pages.

Piper, D.J.W., 1991. Seabed geology of the Canadian eastern continental shelf. Continental Shelf Research, **11**: 1013-1035.

Piper, D.J.W., Mudie, P.J., Fader, G.B., Josenhans, H.W., MacLean, B., and Vilks, G., 1990. Chapter 10 Quaternary Geology. *In*: M.J. Keen, G.L. Williams, (eds). Geology of the continental margin of Eastern Canada, Geological survey of Canada, Geology of Canada, no 2, p. 475-607.

Pocklington, R., Leonard, J.D. Crewe, N.F., 1991. Sources of organic matter to surficial sediments from the Scotian Shelf and Slope, Canada. Continental Shelf Research, **11**: 8-10.

Prentice, I.C., Bartlein, P.J., and Webb III, T., 1991. Vegetation and climate change in eastern North America since the last glacial maximum. Ecology, **72**: 2038-2056.

Quinlan and Beaumont, 1981. A comparison of observed and theoretical post-glacial relative sea level in Atlantic Canada. Canadian Journal of Earth Sciences, **18**: 1146-1163.

Rahman, A., de Vernal, A., 1994. Surface oceanographic changes in the eastern Labrador Sea: nannofossil record of the last 31,000 years. Marine Geology, **121**: 247-263.

Reynolds, C.S., Smayda, T.J., 1998. Principles of species selection and community assembly in the phytoplankton: further exploration of the mandala. *In*: B. Reguera, J. Blanco, M.L. Fernandez, and T. Wyatt (eds). Harmful algae, Intergovernmental oceanographic commission of UNESCO, p. 7-9.

Rochon, A., and de Vernal, A., 1994. Palynomorph distribution in Recent sediments from the Labrador Sea. Canadian Journal of Earth Sciences, **31**: 115-127.

Rochon A., de Vernal, A., Turon, J.L., Matthiessen, J., and Head, M.J., 1999. Distribution of recent dinoflagellate cysts in surface sediments from the North Atlantic ocean and adjacent seas in relation to sea0surface parameters. American Association of Stratigraphic Palynologists Contribution Series 35, 152 pages.

Rowe, J.S., 1972. Forest regions of Canada, Environment Canada, Ottawa, 172 pp.

Ruddiman 2001. Earth's Climate: past and future. Freeman, New York, 465 p.

Sawada, M., Gajewski, K., de Vernal, A., and Richard, P., 1999. Comparison of marine and terrestrial Holocene climatic reconstructions from northeastern North America. The Holocene, **9**: 267-277.

Schafer, C.T. and Mudie, P.J., 1980. Spatial variability of foraminifera and pollen in two nearshore sediment sites, St. Georges Bay, Nova Scotia. Canadian Journal of Earth Sciences, **17**: 313-324.

Schafer, C.T., Tan, F.C., Williams, D.F., Smith, J.N., 1985. Late glacial to recent stratigraphy, paleontology, and sedimentary processes: Newfoundland continental slope and rise. Canadian Journal of Earth Sciences, **22**: 266-282.

Scott, D.B., Mudie, P.J., Vilks, G., and Younger, D.C., 1984. Latest PLeistocene-Holocene paleoceanographic trends on the continental margin of Eastern Canada: foraminiferal, dinoflagellate and pollen evidence. Marine Micropaleontology, **9**: 181-218.

Scott, D.B., Baki, V., Younger, C.D., 1989a. Late Pleistocene-Holocene paleoceanographic changes on the eastern Canadian margin: stable isotopic evidence. Palaeogeography, Palaeoclimatology, Palaeoecology, **74**: 279-295.

Scott, D.B., Boyd, R., Douma, M., Medioli, F.S., Yuill, S., Leavitt, E., Lewis, C.F.M., 1989b. Holocene relative sea-level change and Quaternary glacial events on a continental shelf edge: Sable Island Bank. *In*: D.B. Scott et al. (eds) Late Quaternary sea-level correlation and applications, p. 105-119.

Scott, D.B., Mudie, P.J., de Vernal, A., Hillaire-Marcel, C., Baki, V., MacKinnon, K.D., Medioli, F.S., and Mayer, L., 1989c. Lithostratigraphy, biostratigraphy and stable-isotope stratigraphy of cores from ODP leg 105 site surveys, Labrador Sea and Baffin Bay. In: S.P.

Srivastava, M. Arthur, B. Clement et al. Proceedings of ODP, Scientific Results, **105**: 561-582.

Scott, D.B., and Collins, E.S., 1996. Late mid-Holocene sea-level oscillation: a possible cause. Quaternary Science Reviews, **15**: 851-856.

Shaw, J., and Forbes, D.L., 1995. The postglacial relative sea-level lowstand in Newfoundland. Canadian Journal of Earth Science, **32**: 1308-1330.

Shaw, J., Forbes, D.L., Ceman, J.A., Asprey, K.A., Beaver, D.E., Wile, B., Frobel, D., and Jodrey, F., 1995. Cruise Report 94-138. Marine geological surveys in Chedabucto and St. George's Bay, Nova Scotia, and Bay of Islands, Newfoundland. Geological Survey of Canada Open File 3230.

Shaw, J., Grant, D.R., Guilbault, J.-P., Anderson, T.W., and Parrott, D.R., 2000. Submarine and onshore end moraines in southern Newfoundland: implications for the history of late Wisconsinan ice retreat. Boreas, **29**: 295-314.

Shore, J.A., Hannah, C.G., Loder, J.W., 2000. Drift pathways on the western Scotian Shelf and its environs. Canadian Journal of Fisheries and Aquatic Sciences, **57**: 2488-2505.

Short, S.K., Andrews, J.T., 1980. Palynology of six middle and late Holocene peat sections, Baffin island. Geographie physique et Quaternaire, **34**: 61-75.

Short, S.K., and Nichols, H., 1977. Holocene pollen diagrams from subarctic Labrador-Ungava: vegetational history and climatic change. Arctic and Alpine Research, **9**: 265-290.

Short, S.K., Mode, W.N., and Davis, P.T., 1985. The Holocene record from Baffin Island; modern and fossil pollen studies. *In*: Andrews, J.T. (ed). Quaternary environments; Eastern Canadian Arctic, Baffin Bay and West Greenland. p. 608-642.

Short, S.K., Andrews, J.T., Mode, W.N., 1989. Modern and late Quaternary pollen spectra of fiord sediments, eastern Baffin Island, Arctic Canada. Marine Micropaleontology, **15**: 181-202.

Short, S.K., Andrews, J.T., Williams, K.T., Weiner, N.J. and Elias, S.A., 1994. Late Quaternary marine and terrestrial environments, northwestern Baffin Island, Northwest Territories. Geographie Physique et Quaternaire, **48**: 85-95.

Simard, A., 1996. Distribution postglaciaire d'*Alexandrium excavatum* (Braarud 1945) Balech et Tangen 1985 le long des marges est-canadiennes: production et dispersion des kystes en relation avec les changements environnementaux. Unpublished master thesis, University of Quebec in Montreal, 144 pages.

Simard, A., and de Vernal, A., 1998. Distribution des kystes du type *Alexandrium excavatum* dans les sédiments récents et postglaciaires des marges est-canadiennes. Géographie Physique et Quaternaire, **52**: 361-371.

Smith, J., Risk, M.J., Schwarcz, H.P., McConnaughey, T.A., 1997. Rapid climate change in the North Atlantic during the Younger Dryas recorded by seep-sea corals. Nature, **386**: 818-820.

Smith, P.C., Schwing, F.B., 1991. Mean circulation and variability on the eastern Canadian continental shelf. Continental Shelf Research, **11**: 977-1012.

Souchen, D.B. 1986. Holocene benthonic foraminifera from the Northern Scotian Shelf. Unpublished honours thesis, Dalhousie University, 65 pages.

Therriault, J.-C., Levasseur, M., 1985. Control of phytoplankton production in the lower St. Lawrence estuary: light and freshwater runoff. Naturaliste Canadien, **112**: 77-96.

Stea, R.R., Boyd, R., Fader, G.B.J. Courtney, R.C., Scott D.B. and Pecore, S.S., 1994. Morphology and seismic stratigraphy of the inner continental shelf off Nova Scotia, Canada: evidence for a -65 metre lowstand between 11,650 and 11,250 ^{14}C yr B.P. Marine Geology, **117**: 135-154.

Stuiver, M., and Reimer, P.J., 1993. Extended 14C data base and revised CALIB 3.0 ^{14}C age calibration program. In: M. Stuiver, and R.S. Kra (eds) Calibration 1993. Radiocarbon, **35**: 215-230.

Stuiver, M., Reimer, P.J., Bard, E., Beck, J.W., Burr, G.S., Hughen, K.A., Kromer, B., McCormac, F.G., v.d. Plicht, J., and Spurk, M. (1998). INTCAL98 radiocarbon age calibration, 24,000-0 cal BP. Radiocarbon **40**:1041-1083.

Taylor, A.H., Stephens, J.A., 1998. The North Atlantic Oscillation and the latitude of the Gulf Stream. Tellus, **50A**; 134-142.

Teller, J.T., 1987. Proglacial lakes and the southern margins of the Laurentide ice sheet. *In*: W.F. Ruddiman, and H.E. Wright jr, (eds). North America and adjacent oceans during the last deglaciation. p. 39-69.

Trauth, M.H., and Sarnthein, M., 1997. Bioturbational mixing depth and carbon flux at the seafloor. Paleoceanography, **12**: 517-526.

Tremblay, L.-B., Mysak, L.A., and Dyke, A.S., 1997. Evidence from driftwood records for century-to-millenial scale variations of the high latitude atmospheric circulation during the Holocene. Geophysical Research Letters, **24**: 2027-2030.

Turon, J.-L. and other participants, 1999. Cruise report Images V Leg 2, Quebec-Reykjavik, June 30th to July 24th.

Ullah, W., 1992. Water resources atlas of Newfoundland. Water Resources Division, Government of Newfoundland and Labrador, 79 pages.

Vanderveer, D.G., and Sparkes, B.G., 1982. Regional Quaternary mapping an aid to mineral exploration in west-central Newfoundland. *In*: D.H., Davenport (ed.), Prospecting in areas of glaciated terrain. Canadian Institute of Mining and Metallurgy, p. 284-299

Vardy, S.R., 1991. The deglaciation and early postglacial environmental history of south-central Newfoundland: evidence from the palynostratigraphy and geochemical stratigraphy of lake sediments. Master's Thesis, Memorial University of Newfoundland, 208 pages.

Vettoretti, G., Peltier, W.R., and McFarlane, N.A., 1998. Simulations of mid-Holocene climate using an Atmospheric General Circulation Model. Journal of Climate, **11**: 2607-2627.

Viau, A.E., Gajewski, K., Fines, P., Akinson, D.E., and Sawada, M.C., 2002. Widespread evidence of 1500 yr climate variability in North America during the past 14 000 yr. Geology, **30**: 455-458.

Vilks, G., and Rashid, M.A., 1976. Post-glacial paleo-oceanography of Emerald Basin, Scotian Shelf. Canadian Journal of Earth Sciences, **13**: 1256-1267.

Vilks, G., and Mudie, P.J., 1978. Early deglaciation of the Labrador shelf. Science, **202**: 1181- 1183.

Vilks, G., and Mudie, P.J., 1983. Evidence for postglacial paleoceanographic and paleoclimatic changes in Lake Melville, Labrador, Canada. Arctic and Alpine research, **15**: 307-320.

Vilks, G., MacLean, B., Deonarine, B., Currie, C.G., and Moran, K., 1989. Late Quaternary paleoceanography and sedimentary environments in Hudson Strait. Géographie Physique et Quaternaire, **43**: 161-176.

Wall, D., Dale, B., Lohmann, G.P., and Smith, W.K., 1977. The environmental and climatic distribution of dinoflagellate cysts in modern sediments from regions in the North and South Atlantic oceans and adjacent seas. Marine Micropaleontology, **2**:121-200.

Webb, T. III, Bartlein, P.J., Harrison, S.P., and Anderson, K.H., 1993. Vegetation, lake levels, and climate in eastern North America for the past 18000 years. *In*: H.E. Wright, J.E. Kutzbach, T. Webb, III, W.E. Ruddiman, F.A. StreetPerrot, P.J. Bartlein, (eds). Global climates since the last glacial maximum. University of Minnesota Press, p. 415-460.

Williams, G.L., Lentin, J.K., and Fensome, R.A., 1998. The Lentin and Williams index of fossil dinoflagellates; 1998 edition. American Association of Stratigraphic Palynologists, Contribution Series number 34, 817 pages.

Williams, K.M., 1990. Late Quaternary paleoceanography of the western Baffin Bay region: evidence from fossil diatoms. Canadian Journal of Earth Sciences, **27**: 1487-1494.

Williams, K.M., Andrews, J.T., Weiner, N.J., and Mudie, P.J., 1995. Late Quaternary paleoceanography of the mid- to outer continental shelf, East Greenland, **27**: 352-363.

Wu, G.P., and Hillaire-Marcel, C., 1994. Oxygen isotope compositions of sinistral *Neogloboquadrina pachyderma* tests in surface sediments: North Atlantic Ocean. Geochimica Cosmochimica Acta, **58**: 1303-1312.

Zonneveld, K.A.F., Versteegh, G.J.M., and de Lange, G.J., 1997. Preservation of organic-walled dinoflagellate cysts in different oxygen regimes: a 10,000 year natural experiment. Marine Micropaleontology, **29**: 393-405.

LIST OF APPENDICES

Transfer functions

Appendix 1 Taxonomy (modified from Levac 2001)

The nomenclature is conform to the Lentin and Williams Index of Dinoflagellates (Williams et al., 1998). The family Protoperidiniaceae has been used instead of Contruentidiaceae (Fensome et al. 1998). The author referred to de Vernal et al. (1992a) and Rochon et al. (1999) for the identification of dinoflagellate cysts.

Division DINOFLAGELLATA (Bütschli, 1885) Fensome et al., 1993
Subdivision DINOKARYOTA Fensome et al., 1993
Class DINOPHYCEAE Pascher, 1914
Subclass PERIDINIPHYCIDAE

Order GONYAULACALES Taylor, 1980
Family GONYAULACACEAE Lindemann, 1928
- Subfamily CRIBROPERIDINIOIDEAE Fensome et al. 1993
  - Genus *Operculodinium* Wall, 1967
  - Species *Operculodinium centrocarpum* (Deflandre and Cookson, 1955) Wall, 1967

- Subfamily GONYAULACOIDEAE (Autonym)
  - Genus *Ataxiodinium* Reid 1974
  - Species *Ataxiodinium choanum* Reid 1974

  - Genus *Bitectatodinium* Wilson, 1973
  - Species *Bitectatodinium tepikiense* (Wilson, 1973)

  - Genus *Impagidinium* Stover and Evitt, 1978
  - Species *Impagidinium aculeatum* (Wall, 1967) Lentin and Williams, 1981

  - Genus *Nematosphaeropsis* Deflandre and Cookson, 1955 emend. Wrenn, 1988.
  - Species *Nematosphaeropsis labyrinthus* (Ostenfeld, 1903) Reid, 1974

  - Genus *Spiniferites* Mantell, 1850
  - Species *Spiniferites elongatus* Reid 1974
  - Species *Spiniferites ramosus* (Ehrenberg 1838) Loeblich and Leoblich 1966
  - Species *Spiniferites bulloideus* (Deflandre and Cookson, 1955) Sarjeant 1970

Suborder GONIODOMINEAE Fensome et al. 1993
Family GONIODOMACEAE Lindemann 1928
    Subfamily HELGOLANDINIOIDEAE Fensome et al. 1993
        Genus *Alexandrium Halim* 1960 emend. Balech 1990
        Species *Alexandrium excavatum* (Braarud 1945) Balech 1985

Order PERIDINIALES Haeckel, 1894
Suborder PERIDINIINEAE (Autonym)
Family PERIDINIACEAE Ehrenberd 1831
    Subfamily CALCIODINELLOIDEAE Fensome et al. 1993
        Genus *Pentapharsodinium* Indelicato and Loeblich III, 1986 emend. Montresor et al., 1993
        Species *Pentapharsodinium dalii* Indelicato and Loeblich III, 1986

Family PROTOPERIDINIACEAE Bujak and Davies 1998
    Subfamily PROTOPERIDINIOIDEAE (Autonym)
        Genus *Brigantedinium* Reid, 1977 ex Lentin and Williams, 1993
        Species *Brigantedinium cariacoense* (Wall, 1967) Lentin and Williams, 1993
        Species *Brigantedinium simplex* (Wall, 1965) ex Lentin and Williams, 1993

Note: Cysts of *Brigantedinium cariacoense* and *B. simplex* were grouped together because they are often difficult to distinguish. Bad orientation or folded cyst make it impossible to see the geometry of the archeopyle, on which diagnostic criterion are based.

        Genus *Selenopemphix* (Benedek, 1972) emend. Head, 1993
        Species *Selenopemphix quanta* (Bradford, 1975) Matsuoka, 1985
            (Synonym: *Multispinula quanta* Bradford 1975).

    Subfamily uncertain
        Genus *Islandinium* Head et al. 2001
        Species *minutum* (Harland and Reid in Harland et al. 1980) Matsuoka and Bujak, 1988
            (Synonym: *Algidasphaeridium? minutum* (Harland and Reid in Harland et al. 1980, Matsuoka and Bujak, 1988).

Appendix 2: identification and location of the new surface sediments samples

Location	**Core number**	**Core Type**	**Latitude**	**Longitude**	**Water depth**	**Database number**	**Number on map**
Scotian Shelf	80-004-38	G	**45.11 N**	**60.7933 W**	167	X639	1
Scotian Shelf	80-004-39	G	**45.1633 N**	**60.8266 W**	156	X640	1
Scotian Shelf	80-004-40	G	**45.18166 N**	**60.84 W**	135	X641	1
Scotian Shelf	80-004-41	G	**45.1966 N**	**60.855 W**		X642	1
Scotian Shelf	80-004-42	G	**45.2166 N**	**60.87 W**	103	X643	1
Scotian Shelf	80-004-43	G	**45.225 N**	**60.9 W**	60	X644	1
Scotian Shelf	80-004-44	G	**45.233 N**	**60.8916 W**	76	X645	1
West Scotian Shelf	81-006-7	G	**43.342 N**	**63.4995 W**	167	X646	2
West Scotian Shelf	92-003-36	G	**43.8835 N**	**62.798 W**	236	X647	3
West Scotian Slope	90015-16	Box	**42.63133 N**	**61.69483 W**	1976	X648	14
West Scotian Slope	90015-18	Box	**42.91867 N**	**61.82083 W**	536	X649	13
West Scotian Slope	90015-22	Box	**42.7105 N**	**63.542 W**	811	X650	7
West Scotian Slope	78-006-4	Box	**42.5366 N**	**61.636 W**	?	X651	14
West Scotian Slope	78-006-6	Box	**42.9166 N**	**61.8246 W**	700	X652	13
West Scotian Slope	78-006-8	Box	**42.887 N**	**61.747 W**	800	X653	13
St.Pierre Rise	HU99-36-007	Box	**44.501 N**	**55.874 W**	2340	X654	33
St.Pierre Rise	90015-8	Box	**44.81933 N**	**55.96717 W**	3847	X655	32
East Scotian Slope	HU99-36-008	Box	**43.302 N**	**57.639 W**	3847	X656	28
East Scotian Slope	HU99-36-009	Box	**43.315 N**	**57.3316 W**	3521	X657	29
Scotian Rise	HU99-36-011	Box	**42.462 N**	**59.611 W**	4115	X658	21
Scotian Slope	HU99-36-017	Box	**43.12 N**	**59.9962 W**	2202	X659	20
Scotian Slope	HU99-36-026	Box	**43.406 N**	**59.9978 W**	933	X660	22
East Newfoundland	77-034-60	Box	**48.995 N**	**49.92 W**	800	X661	38
East Newfoundland	83-033-3	Box	**49.9716 N**	**54.435 W**	330	X662	35
East Newfoundland	83-033-11	Box	**50.903 N**	**53.305 W**	442	X663	36
Hudson Canyon	MD99-2210	Box	**39.2245 N**	**72.276 W**	650	X664	41
Hudson Canyon	MD99-2211	Box	**39.233 N**	**72.258 W**	639	X665	41
Hudson Canyon	MD99-114.04	Box	**39.256 N**	**72.296 W**	417	X666	41
Bermuda Rise	89-038-16	Box	**36.006 N**	**66.09 W**	4654	X667	40
Hudson Canyon	MD99-1225	Box	**39.287 N**	**72.417 W**	150	X669	41

Appendix 2: identification and location of the new surface sediments samples

Scotian Rise	MC-13	Box	**43.06616 N**	**55.834 W**	3440	X670	30
Scotian Rise	MC-25	Box	**43.4833 N**	**54.867 W**	3890	X671	31
Scotian Rise	MC-21	Box	**44.6833 N**	**55.525 W**	1336	X672	34
Baltimore Canyon	89-038-20	Box	**37.5205 N**	**72.016 W**	3098	X673	43
Baltimore Canyon	89-038-21	Box	**38.404 N**	**73.2376 W**	1614	X674	42
Baltimore Canyon	89-038-25	Box	**38.8593 N**	**72.7108 W**	1256	X675	42
East Newfoundland	83-033-14	Box	**48.855 N**	**51.88 W**	330	A682	37
East Newfoundland	83-033-16	Box	**48.9135 N**	**51.8025 W**	335	A683	37
Tail of Grand Banks	91020-69	Box	**43.3095 N**	**49.14117 W**	1179	A685	39
West Scotian Slope	91020-6	Box	**42.17017 N**	**62.5925 W**	2680	X668?	9
Scotian Slope	HU2000-36-001	Box	**42.57 N**	**64.1399 W**	1075	X686	5
Scotian Slope	HU2000-36-004	Box	**42.57 N**	**64.133 W**	1068	X688	5
Scotian Slope	HU2000-36-009	Box	**42.708 N**	**63.5496 W**	907	X689	6
Scotian Slope	HU2000-36-020	Box	**42.896 N**	**62.25 W**	536	X690	10
Scotian Slope	HU2000-36-025	Box	**42.877 N**	**62.161 W**	650	X691	11
Scotian Slope	HU2000-36-026	Box	**42.7727 N**	**62.957 W**	1134	X692	8
Scotian Slope	HU2000-36-032	Box	**42.36 N**	**62.1316 W**	2414	X693	12
Scotian Slope	HU2000-36-036	Box	**42.76 N**	**61.565 W**	1582	X694	15
Scotian Slope	HU2000-36-041	Box	**43.108 N**	**60.64 W**	1664	X695	17
Scotian Slope	HU2000-36-043	Box	**43.0.2387 N**	**59.747 W**	2633	X696	23
Scotian Slope	HU2000-36-054	Box	**43.3716 N**	**59.8233 W**	2304	X697	24
Scotian Slope	HU2000-36-056	Box	**43.3478 N**	**59.86109 W**	2120	X698	24
Scotian Slope	HU2000-042-002	Box	**43.52557 N**	**59.2692 W**	1290	X699	27
Scotian Slope	HU2000-042-007	Box	**43.4224 N**	**59.6223 W**	2147	X700	26
Scotian Slope	HU2000-042-010	Box	**43.3803 N**	**59.8522 W**	1554	X701	25
Scotian Slope	HU2000-042-017	Box	**43.4109 N**	**59.8957 W**	1321	X702	25
Scotian Slope	HU2000-042-020	Box	**43.4563 N**	**59.8807 W**	790	X703	25
Scotian Slope	HU2000-042-030	Box	**43.289 N**	**60.1 W**	1372	X704	19
Scotian Slope	HU2000-042-037	Box	**43.065 N**	**60.39 W**	2614	X705	18
Scotian Slope	HU2000-042-042	Box	**43.0809 N**	**61.0091 W**	1390	X706	16
Scotian Slope	HU2000-042-057	Box	**42.9468 N**	**61.43247 W**	1159	X707	14
La Have Basin	HU2000-047-001	Box	**43.7667 N**	**63.7167 W**	260	X708	4

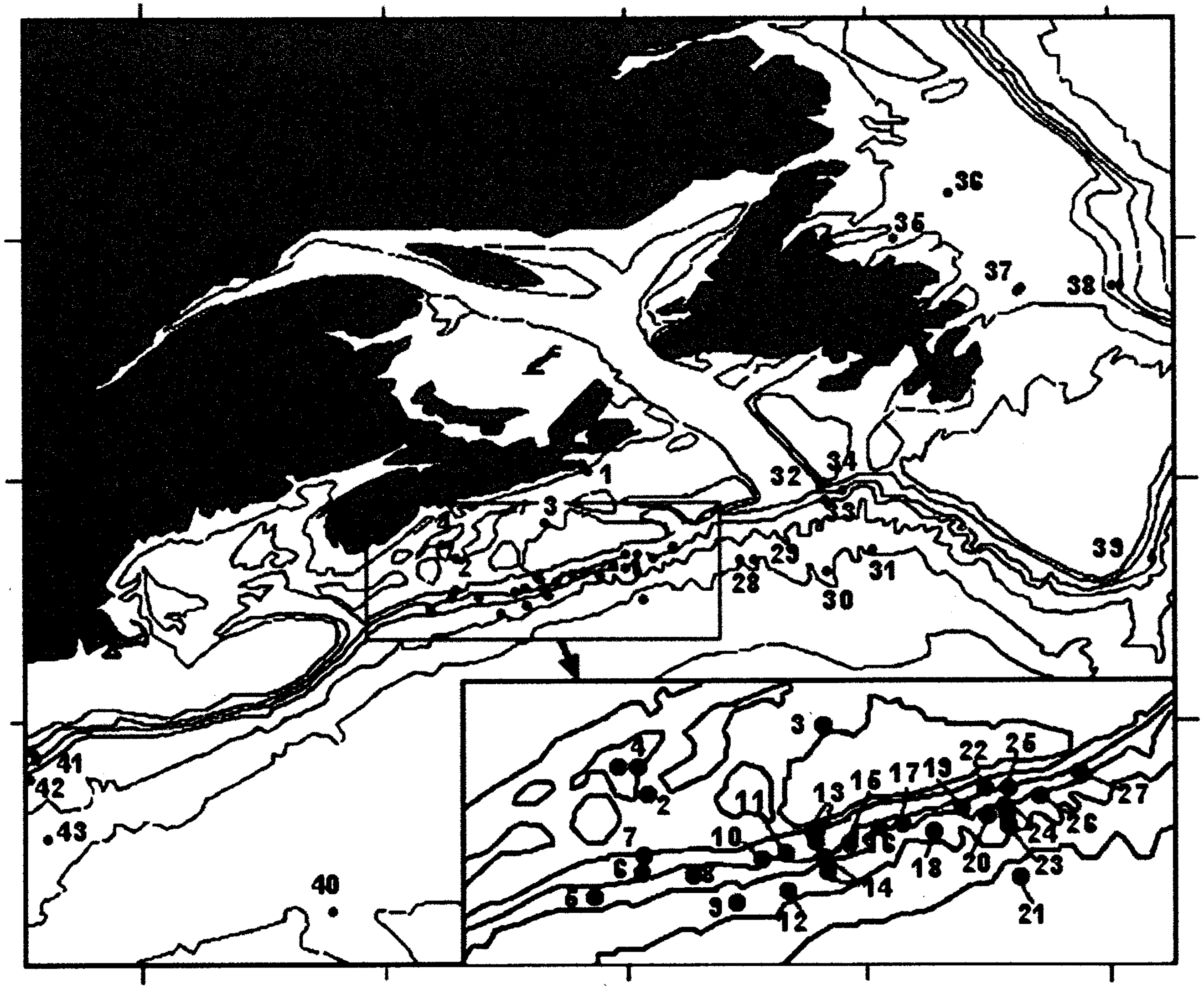

Appendix 3: Location map of new surface samples. Site numbers refer to appendix 2.

Appendix 4: Environmental parameters for the new sites

Core number	Databse Number	Temperature February	Deviation	Number of measurements	Temperature August	Deviation	Number of measurements	Salinity February	Deviation	Number of measurements	Salinity August	Deviation	Number of measurements	Duration of ice cover	Deviation	Median	Number of measurements
80-004-38	X639	0.80	1.16	176	16.21	1.68	575	31.07	0.31	37	29.89	0.83	85	0	0	0	0
80-004-39	X640	0.74	1.04	161	16.21	1.85	616	31.05	0.31	35	29.96	0.78	102	0	0	0	0
80-004-40	X641	0.74	1.05	159	16.32	1.9	633	31.06	0.31	35	29.96	0.78	102	0	0	0	0
80-004-41	X642	0.61	0.85	154	16.41	1.92	652	31.04	0.3	34	29.96	0.78	102	0	0	0	0
80-004-42	X643	0.60	0.85	151	16.4	1.92	648	31.03	0.29	33	29.96	0.78	102	0	0	0	0
80-004-43	X644	0.60	0.84	148	16.46	1.94	655	31.04	0.29	32	29.94	0.78	101	0	0	0	0
80-004-44	X645	0.60	0.84	148	16.46	1.94	656	31.04	0.29	32	29.94	0.78	101	0	0	0	0
81-006-7	X646	1.76	1.38	369	16.78	1.79	665	31.66	0.37	104	31.07	0.39	149	0	0	0	0
92-003-36	X647	1.47	1.59	1429	16.52	1.96	2134	32.01	0.55	88	31.04	0.38	189	0	0	0	0
90015-16	X648	5.26	2.89	339	18.6	2.22	434	32.57	0.34	24	31.95	0.41	48	0	0	0	0
90015-18	X649	4.21	2.11	409	18.17	1.85	590	32.46	0.32	54	31.82	0.36	112	0	0	0	0
90015-22	X650	3.27	3.44	285	17.51	1.86	572	31.8	0.32	47	31.46	0.6	93	0	0	0	0
78-006-4	X651	5.42	2.89	326	18.87	2.36	380	32.59	0.34	22	32.03	0.48	32	0	0	0	0
78-006-6	X652	4.21	2.11	409	18.17	1.85	590	32.46	0.32	54	31.82	0.36	112	0	0	0	0
78-006-8	X653	4.34	2.19	405	18.19	1.88	581	32.45	0.35	47	31.86	0.37	99	0	0	0	0
99-36-007	X654	2.34	1.09	55	16.19	1.15	62	32.49	0	1	32.03	0.29	11	0	0	0	0
90015-8	X655	1.32	1.39	103	16.08	1.43	99	32.44	0.77	2	32.05	2.93	15	0	0	0	0
HU99-36-008	X656	5.27	2.67	42	18.74	1.61	105	32.78	0.58	5	31.95	1.93	3	0	0	0	0
HU99-36-009	X657	5.21	2.65	44	18.78	1.74	89	32.71	0.65	4	31.93	0.2	6	0	0	0	0
HU99-36-011	X658	9.39	5.88	48	20.23	2.68	84	32.72	0.08	5	31.69	0	1	0	0	0	0
HU99-36-017	X659	3.09	1.36	156	17.31	1.87	346	32.18	0.43	3	31.5	0.34	29	0	0	0	0
HU99-36-026	X660	2.68	1.29	151	17.15	1.71	411	31.71	0.58	6	31.46	0.35	42	0	0	0	0
77-034-60	X661	0.18	1.98	91	10.66	1.95	194	33.85	0	1	32.3	0.78	36	0.39	0.79	0	38
83-033-3	X662	-0.30	1.96	4	12.17	1.25	59	32.92	0.45	4	31.27	0	1	0	0	0	0
83-033-11	X663	-1.74	0	1	10.22	1.41	88	32.96	0	1	31.5	0.57	23	0	0	0	0

Appendix 4: Environmental parameters for the new sites

Core number	Databse Number	Temperature February	Deviation	Number of measurements	Temperature August	Deviation	Number of measurements	Salinity February	Deviation	Number of measurements	Salinity August	Deviation	Number of measurements	Duration of ice cover	Deviation	Median	Number of measurements
MD99-2210	X664	9.11	2.9	414	24.06	156	672	34.16	0.89	34	33.95	1.1	44	0	0	0	0
MD99-2211	X665	9.12	2.95	407	24.07	1.57	674	33.14	0.89	33	33.98	1.09	43	0	0	0	0
MD99-114.04	X666	9.00	2.88	412	24.01	1.56	666	34.19	0.89	35	33.93	1.09	43	0	0	0	0
89-038-16	X667	19.60	0.55	4	27.03	0.83	148	36.59	0	1	36.17	0.06	44	0	0	0	0
MD99-1225	X669	8.75	2.77	436	23.96	1.54	665	34.16	0.87	39	33.84	1.11	43	0	0	0	0
MC-13	X670	4.23	2.02	19	19.2	1.76	57	34.3	0.78	7	32.94	0	1	0	0	0	0
MC-25	X671	4.37	2.58	24	18.68	1.91	63	32.81	0	1	32.77	0.23	2	0	0	0	0
MC-21	X672	1.77	1.21	92	16.66	1.84	126	32.43	0.77	2	32.05	0.29	15	0	0	0	0
89-038-20	X673	15.8	4.75	79	26.05	1.65	244	35.8	0.53	6	34	0.72	13	0	0	0	0
89-038-21	X674	9.36	2.79	226	24.9	1.1	441	34.63	0.89	40	33.56	1.54	33	0	0	0	0
89-038-25	X675	9.64	2.75	348	24.44	1.4	514	34.57	0.82	40	33.53	1.19	24	0	0	0	0
83-033-14	A682	-0.62	0.75	24	11.82	1.88	220	32.68	0	1	31.19	0.52	64	1.74	1.27	2	38
83-033-16	A683	-0.69	0.8	24	11.73	1.88	220	32.69	0	1	31.29	0.56	65	1.79	1.23	2	38
91020-69	A685	3.29	4.44	18	14.72	2.85	216	33.43	0.74	7	32.1	0.34	74	0	0	0	0
91020-6	X668?	6.37	3.07	127	18.9	1.91	233	32.95	0.03	2	31.25	0.96	9	0	0	0	0
HU2000-36-001	A686	3.42	3.359	262	17.975	2.083	857	31.849	0.573	50	31.639	0.501	57	0	0	0	0
HU2000-36-004	A688	3.42	3.359	262	17.975	2.083	857	31.849	0.573	50	31.639	0.501	57	0	0	0	0
HU2000-36-009	A689	3.26	3.433	286	17.47	1.822	562	31.799	0.326	47	31.464	0.611	89	0	0	0	0
HU2000-36-020	A690	4.37	2.097	356	18.082	1.83	560	32.433	0.347	51	31.737	0.33	130	0	0	0	0
HU2000-36-025	A691	4.37	2.097	356	18.082	1.83	560	32.433	0.347	51	31.737	0.33	130	0	0	0	0
HU2000-36-026	A692	4.39	3.472	167	17.97	1.66	483	32.165	0.352	27	31.502	0.569	117	0	0	0	0
HU2000-36-032	A693	6.28	2.823	239	19.059	1.801	225	32.704	0.354	12	31.868	0.393	19	0	0	0	0
HU2000-36-036	A694	4.64	2.422	383	18.494	2.181	532	32.5	0.357	35	31.946	0.382	71	0	0	0	0
HU2000-36-041	A695	3.52	1.458	136	17.698	2.059	406	32.142	0.34	6	31.855	0.408	29	0	0	0	0
HU2000-36-043	A696	3.20	1.627	73	17.436	2.013	272	32.43	0.006	2	31.631	0.276	15	0	0	0	0

Appendix 4: Environmental parameters for the new sites

Core number	Databse Number	Temperature February	Deviation	Number of measurements	Temperature August	Deviation	Number of measurements	Salinity February	Deviation	Number of measurements	Salinity August	Deviation	Number of measurements	Duration of ice cover	Deviation	Median	Number of measurements
HU2000-36-054	A697	2.71	1.289	151	17.014	1.787	391	31.724	0.534	7	31.462	0.35	43	0	0	0	0
HU2000-36-056	A698	2.71	1.289	151	17.014	1.787	391	31.724	0.534	7	31.462	0.35	43	0	0	0	0
HU2000-042-002	A699	2.46	0.838	133	17.16	1.913	281	31.8	0.628	3	31.433	0.332	52	0	0	0	0
HU2000-042-007	A700	2.46	0.838	133	17.16	1.913	281	31.8	0.628	3	31.433	0.332	52	0	0	0	0
HU2000-042-010	A701	2.69	1.295	152	17.023	1.786	395	31.724	0.534	7	31.452	0.35	43	0	0	0	0
HU2000-042-017	A702	2.69	1.295	152	17.023	1.786	395	31.724	0.534	7	31.452	0.35	43	0	0	0	0
HU2000-042-020	A703	2.65	1.245	154	17.029	1.732	401	31.724	0.534	7	31.46	0.339	46	0	0	0	0
HU2000-042-030	A704	2.73	1.318	163	17.356	1.829	377	31.711	0.584	6	31.485	0.372	37	0	0	0	0
HU2000-042-037	A705	3.16	1.303	184	17.634	2.166	353	32.056	0.535	2	31.754	0.407	29	0	0	0	0
HU2000-042-042	A706	3.60	1.595	177	17.917	1.92	443	32.276	0.348	9	31.899	0.359	48	0	0	0	0
HU2000-042-057	A707	4.18	2.139	339	18.189	2.123	540	32.514	0.332	33	31.947	0.388	75	0	0	0	0
HU-2000-047-001	A708	1.34	1.759	598	16.179	1.972	836	31.549	0.504	53	30.987	0.308	132	0	0	0	0

Appendix 5: Total dinoflagellate cyst counts and concentrations of various types of palynomorphs in new surface sediment samples

Core number	Database number	Number on map	Dinocyst count	Dinoflagellate cyst conc.	Pollen conc.	Spores conc.	Reworked palnomorphs conc.	Organic lining conc.	Halodinium conc.
80-004-38	X639	1	222	4297	11226	755	600	2322	329
80-004-39	X640	1	308	4415	9933	788	473	2021	502
80-004-40	X641	1	299	13021	29352	1176	1872	5835	1263
80-004-41	X642	1	268	10034	30571	2926	292	7758	1108
80-004-42	X643	1	304	3024	6765	430	149	1800	417
80-004-43	X644	1	295	17370	35859	2061	235	8773	1001
80-004-44	X645	1	322	13598	29032	211	253	4898	844
81-006-7	X646	2	193	1773	3715	309	96	1259	309
92-003-36	X647	3	314	8137	10002	1654	181	2280	311
90015-16	X648	14	418	28805	1309	551	206	5513	69
90015-18	X649	13	337	9519	2599	339	141	2457	0
90015-22	X650	7	302	18476	5812	795	428	5873	245
78-006-4	X651	14	498	23133	3159	882	372	1626	93
78-006-6	X652	13	325	31476	1453	872	194	8038	97
78-006-8	X653	13	309	39546	7039	1664	1407	12286	0
HU99-36-007	X654	33	346	48217	4599	697	697	7246	418
90015-8	X655	32	863	67648	6506	549	784	9093	1254
HU99-36-008	X656	28	531	29533	1947	389	389	2558	166
HU99-36-009	X657	29	626	17199	494	220	27	0	0
HU99-36-011	X658	21	300	9648	1447	193	161	1897	32
HU99-36-017	X659	20	498	19218	772	155	231	3705	0
HU99-36-026	X660	22	336	8872	1558	211	79	3380	53
77-034-60	X661	38	296	4107	5314	721	458	2802	971
83-033-3	X662	35	316	7864	8063	279	299	3758	871
83-033-11	X663	36	326	5775	13126	425	71	2569	443
MD99-2210	X664	41	431	18324	1573	85	978	1233	0
MD99-2211	X665	41	305	8407	13948	579	193	2563	55
MD99-114.04	X666	41	289	1660	3095	98	17	706	29
89-038-16	X667	40	296	4747	1299	144	16	367	80
MD99-1225	X669	41	302	1750	2856	116	0	1321	69
MC-13	X670	30	343	5298	710	216	62	803	0
MC-25	X671	31	373	13443	1117	288	0	36	0
MC-21	X672	34	860	103713	2653	121	0	3015	0
89-038-20	X673	43	304	2793	2802	165	37	119	0
89-038-21	X674	42	342	12884	11186	678	151	1167	0
89-038-25	X675	42	363	16495	10406	636	45	272	0
83-033-14	A682	37	339	4708	6000	236	28	472	278
83-033-16	A683	37	311	3429	17770	589	717	3191	2013
91020-69	A685	39	313	7652	5525	269	98	2543	318

Appendix 5: Total dinoflagellate cyst counts and concentrations of various types of palynomorphs in new surface sediment samples

Core number	Database number	Number on map	Dinocyst count	Dinoflagellate cyst conc.	Pollen conc.	Spores conc.	Reworked palnomorphs conc.	Organic lining conc.	Halodinium conc.
91020-6	X668?	9	397	15088	304	342	228	38	0
HU2000-36-001	X686	5	298	6402	752	193	107	3266	0
HU2000-36-004	X688	5	302	10743	960	213	0	3415	0
HU2000-36-009	X689	6	323	19470	2471	422	241	6510	0
HU2000-36-020	X690	10	301	8538	1957	113	0	2836	28
HU2000-36-025	X691	11	299	37076	7688	1240	124	8680	0
HU2000-36-026	X692	8	325	39180	3496	844	0	13623	0
HU2000-36-032	X693	12	303	7970	921	184	53	1184	0
HU2000-36-036	X694	15	301	17189	799	571	57	4511	0
HU2000-36-041	X695	17	329	41996	3446	766	128	10595	0
HU2000-36-043	X696	23	97	11378	234	0	117	234	0
HU2000-36-054	X697	24	322	31760	2269	493	0	5228	0
HU2000-36-056	X698	24	308	31086	3331	807	0	7671	0
HU2000-042-002	X699	27	301	21070	1820	350	0	4830	0
HU2000-042-007	X700	26	313	75468	1688	1205	0	11332	241
HU2000-042-010	X701	25	299	43255	3327	579	0	11139	0
HU2000-042-017	X702	25	308	27280	1683	443	0	3897	0
HU2000-042-020	X703	25	285	8589	1627	241	0	3526	90
HU2000-042-030	X704	19	307	27667	1718	814	0	5063	90
HU2000-042-037	X705	18	296	22862	852	697	0	1550	0
HU2000-042-042	X706	16	315	21225	1424	407	0	4747	0
HU2000-042-057	X707	14	288	9999	1250	417	0	3472	0
HU2000-047-001	X708	4	206	8054	11182	1681	0	1212	313

Appendix 6: Raw dinoflagellate cyst counts in the new surface samples

Number on map	Core number	No site	*cf. Alexandrium excavatum*	*Ataxiodinium choanum*	*Bitectatodinium tepikiense*	*Impagidinium aculeatum*	*Impagidinium pallidum*	*Impagidinium paradoxum*	*Impagidinium patulum*	*Impagidinium sphaericum*	*Impagidinium strialatum*	*Impagidinium spp.*	*Lingulodinium machaeophoru*	*Nematosphaeropsis labyrinthu*	*Operculodinium centrocarpum*	*O.centrocarpum short proces*	*O. centrocarpum arctic morphotype*	*Operculodinium israelianum*	*O. centrocarpum morphotype cezare*	*Pyxidinopsis reticulata*	*Spiniferites membranaceus*	*Spiniferites delicatus*	*Spiniferites elongatus*	*Spiniferites ramosus*	*Spiniferites belerius*	*Spiniferites bentorii*	*Spiniferites bulloideus*
1	80-004-38	x639	0	0	4	0	0	0	0	0	0	0	0	2	51	1	4	0	1	0	2	1	0	5	0	0	1
1	80-004-39	x640	0	1	10	0	0	0	0	0	0	0	1	3	89	0	0	0	0	0	1	0	1	8	0	0	6
1	80-004-40	x641	0	0	1	0	0	0	0	0	0	1	0	2	107	0	3	0	0	0	0	1	2	8	0	1	3
1	80-004-41	x642	0	1	3	0	0	0	0	0	0	0	0	2	124	2	0	0	0	0	0	6	2	6	0	0	1
1	80-004-42	x643	0	0	3	0	0	0	0	0	0	0	0	2	60	2	1	0	0	0	0	2	1	9	0	0	0
1	80-004-43	x644	0	0	3	0	0	0	0	0	0	0	0	3	83	2	1	0	0	0	0	2	0	4	0	0	1
1	80-004-44	x645	0	0	0	0	0	0	0	0	0	0	0	2	91	2	2	1	0	0	0	1	0	8	0	0	1
2	81-006-7	x646	0	0	2	0	0	1	0	0	0	0	0	5	45	1	0	0	1	0	0	0	2	4	0	0	0
3	92-036-36	x647	2	1	0	1	2	4	0	1	2	4	1	13	101	5	0	1	0	0	0	5	6	11	0	0	7
14	90-015-16	x648	0	1	38	1	0	0	0	0	0	2	0	10	214	1	1	2	0	0	0	1	9	21	0	0	0
13	90-015-18	x649	0	0	23	0	0	46	0	6	6	8	0	14	111	1	1	1	1	0	0	1	10	17	0	0	0
7	90-015-22	x650	0	0	18	1	0	4	0	0	0	2	0	14	97	4	2	0	1	0	0	0	1	10	0	0	0
14	78-006-4	x651	0	0	21	0	0	2	0	0	1	2	2	24	261	8	2	0	0	0	0	2	7	35	0	0	0
13	78-006-6	x652	0	2	19	1	0	0	0	0	0	1	0	12	183	2	1	1	0	0	0	0	11	14	0	0	0
13	78-006-8	x653	1	0	21	0	0	2	0	0	0	0	1	7	173	7	0	0	0	0	2	2	6	11	2	0	3
33	HU99036-7	x654	5	0	50	0	0	0	0	4	0	0	1	0	154	8	1	0	0	0	0	0	14	8	0	0	0
32	90-015-8	x655	5	0	137	0	5	0	0	0	1	2	1	5	407	6	0	3	0	0	0	2	43	8	1	0	0
28	HU99036-8	x656	11	6	53	0	1	1	1	0	0	2	0	8	282	6	8	0	1	0	0	0	21	11	0	0	0
29	HU99036-9	x657	1	2	45	0	0	1	0	1	0	0	1	11	415	8	7	0	13	0	0	3	28	11	0	0	0
21	HU99036-11	x658	3	2	35	1	1	0	2	6	1	5	0	10	149	4	0	2	2	0	0	1	17	6	0	0	1
20	HU99036-17	x659	1	1	41	0	0	3	0	2	0	2	1	8	301	6	2	0	2	0	0	1	20	9	0	0	0
22	HU99036-26	x660	0	0	28	0	0	3	0	0	0	8	3	2	142	3	3	0	1	0	1	0	4	22	0	0	1
38	77-034-60	x661	0	0	0	0	2	0	0	2	0	1	0	109	50	2	1	0	1	0	0	0	3	1	0	0	0
35	83-033-3	x662	0	0	0	0	1	0	0	0	0	1	0	16	34	0	1	0	0	0	0	0	0	1	0	0	0
36	83-033-11	x663	0	0	0	0	0	0	0	0	0	0	0	5	16	1	0	1	0	0	0	0	3	3	0	0	0

Appendix 6: Raw dinoflagellate cyst counts in the new surface samples

Number on map	Core number	No site	cf. *Alexandrium excavatum*	*Ataxiodinium choanum*	*Bitectatodinium tepikiense*	*Impagidinium aculeatum*	*Impagidinium pallidum*	*Impagidinium paradoxum*	*Impagidinium patulum*	*Impagidinium sphaericum*	*Impagidinium strialatum*	*Impagidinium* spp.	*Lingulodinium machaeophoru*	*Nematosphaeropsis labyrinthu*	*Operculodinium centrocarpum*	*O.centrocarpum* short proces	*O. centrocarpum* arctic morphotype	*Operculodinium israelianum*	*O. centrocarpum* morphotype cezare	*Pyxidinopsis reticulata*	*Spiniferites membranaceus*	*Spiniferites delicatus*	*Spiniferites elongatus*	*Spiniferites ramosus*	*Spiniferites belerius*	*Spiniferites bentorii*	*Spiniferites bulloideus*
41	MD99-2210	x664	11	1	30	0	1	1	0	0	0	0	2	1	149	5	0	0	0	0	1	1	19	10	1	0	1
41	MD99-2211	x665	1	1	2	0	0	15	0	0	4	5	2	32	100	1	0	2	0	0	0	4	2	16	0	0	1
41	MD99-114.04	x666	0	0	1	0	0	3	0	4	0	1	2	20	51	2	0	0	0	1	0	6	3	3	0	0	4
40	89-038-16	x667	0	0	13	3	0	9	1	2	1	5	5	9	140	1	0	5	0	0	1	1	11	19	1	2	11
41	MD99-1225	x669	1	0	1	0	0	0	1	0	0	2	0	11	70	1	0	0	1	0	1	3	1	15	4	0	5
30	MC-13	x670	2	0	37	3	0	0	10	5	0	7	0	9	207	2	0	0	0	0	0	0	19	8	0	0	0
31	MC-25	x671	1	0	23	0	2	0	1	1	0	2	0	17	234	1	2	2	0	1	0	1	20	3	1	0	1
34	MC-21	x672	2	3	126	0	4	0	1	0	0	2	4	2	501	9	0	2	0	0	0	0	48	2	0	0	0
43	89-038-20	x673	0	0	19	2	2	4	6	2	0	10	1	72	132	2	2	1	1	0	2	4	2	13	3	0	0
42	89-038-21	x674	0	0	5	1	0	7	3	0	2	10	2	45	127	5	0	3	1	1	0	8	4	10	0	2	6
42	89-038-25	x675	0	0	3	0	0	0	1	0	0	5	1	65	141	3	2	3	0	0	0	4	5	9	5	0	1
37	83-033-14	A682	0	0	1	0	1	0	0	1	0	2	2	3	206	2	1	0	0	0	0	5	18	6	0	0	0
37	83-033-16	A683	0	1	2	0	0	0	0	0	0	1	0	1	149	1	4	0	0	0	0	0	16	6	1	0	0
39	91020-69	A685	0	1	8	0	0	0	0	0	0	0	0	14	205	0	0	1	0	0	0	2	19	2	0	0	0
9	91020-6	A668	0	0	31	2	0	0	1	0	1	0	0	15	296	2	1	1	0	0	0	2	11	4	0	2	0
5	2000-36-001	X686	7	0	15	1	0	1	1	6	1	0	0	11	147	3	0	0	0	0	0	0	11	14	0	0	0
5	2000-36-004	X688	2	0	14	0	0	0	4	2	0	0	0	8	178	0	0	0	0	0	0	0	12	7	0	0	0
6	2000-36-009	X689	4	1	13	1	0	0	0	2	0	0	1	13	150	0	0	0	0	0	0	1	8	10	0	0	0
10	2000-36-020	X690	3	0	14	0	0	1	1	2	0	0	0	3	116	1	0	1	0	0	0	0	7	3	0	0	0
11	2000-36-025	X691	0	0	14	0	0	0	1	4	0	0	0	4	128	1	0	0	0	0	0	0	8	12	0	0	0
8	2000-36-026	X692	6	0	21	2	0	0	1	2	0	0	0	3	162	0	0	0	0	0	0	2	10	15	0	0	0
12	2000-36-032	X693	3	0	15	0	0	0	0	0	0	0	0	8	179	2	0	0	0	1	0	2	15	4	0	0	0
15	2000-36-036	X694	2	2	26	0	0	0	2	1	0	0	0	7	171	0	0	0	0	0	0	2	9	18	0	0	0
17	2000-36-041	X695	2	1	32	2	1	0	1	4	0	0	0	9	187	2	0	0	0	0	0	0	5	13	0	0	2
23	2000-36-043	X696	0	0	14	0	0	0	0	0	0	0	0	0	60	1	0	0	0	0	0	0	2	7	0	0	0

Appendix 6: Raw dinoflagellate cyst counts in the new surface samples

Number on map	Core number	No site	cf. *Alexandrium excavatum*	*Ataxiodinium choanum*	*Bitectatodinium tepikiense*	*Impagidinium aculeatum*	*Impagidinium pallidum*	*Impagidinium paradoxum*	*Impagidinium patulum*	*Impagidinium sphaericum*	*Impagidinium strialatum*	*Impagidinium* spp.	*Lingulodinium machaeophoru*	*Nematosphaeropsis labyrinthu*	*Operculodinium centrocarpum*	*O.centrocarpum* short proces	*O. centrocarpum* arctic morphotype	*Operculodinium israelianum*	*O. centrocarpum* morphotype *cezare*	*Pyxidinopsis reticulata*	*Spiniferites membranaceus*	*Spiniferites delicatus*	*Spiniferites elongatus*	*Spiniferites ramosus*	*Spiniferites belerius*	*Spiniferites bentorii*	*Spiniferites bulloideus*
24	2000-36-054	X697	3	1	28	1	1	0	3	22	0	0	0	7	169	3	0	0	0	0	0	0	9	8	0	0	0
24	2000-36-056	X698	2	0	21	0	0	0	1	1	0	0	0	9	149	1	0	0	0	0	0	1	8	18	0	0	0
27	2000-42-002	X699	5	1	29	2	0	0	0	0	0	0	0	6	157	2	0	0	0	0	0	1	6	5	0	0	0
26	2000-42-007	X700	1	0	26	2	0	0	0	0	0	1	0	4	197	3	0	0	0	0	0	0	4	14	0	0	0
25	2000-42-010	X701	1	0	30	0	1	1	1	0	0	0	0	3	157	4	0	1	0	0	0	0	11	8	0	0	0
25	2000-42-017	X702	3	0	25	0	0	0	2	0	0	0	0	3	173	1	0	0	0	1	0	0	4	19	0	0	0
25	2000-42-020	X703	2	1	22	0	2	0	0	5	0	0	0	1	90	0	0	1	0	0	0	1	1	19	0	0	0
19	2000-42-030	X704	1	0	29	0	0	0	0	2	0	1	0	5	153	0	0	1	0	0	0	0	10	16	0	0	0
18	2000-42-037	X705	2	0	23	1	0	0	1	0	0	1	0	10	168	1	0	0	0	0	0	0	9	11	0	0	0
42	2000-42-042	X706	1	0	25	0	0	0	2	0	0	0	0	7	158	1	0	0	0	0	0	0	8	18	0	0	0
14	2000-42-057	X707	0	0	19	2	0	0	2	3	0	1	0	4	125	0	0	2	0	0	0	2	3	16	0	0	0
4	2000-47-001	X708	3	0	2	0	0	0	0	0	0	0	0	0	36	2	0	0	0	0	0	1	1	6	0	0	0

Appendix 6: Raw dinoflagellate cyst counts in the new surface samples

Core number	No site	*Spiniferites mirabilis*	*Spiniferites spp*	*Pentapharsodinium dalei*	*Islandinium minutum*	*Islandinium cezare*	*Islandinium spp.*	*Brigatedinium spp*	*Brigatedinium cariacoense*	*Brigatedinium simplex*	*Selenopemphix spp.*	*Xandarodinium xanthum*	*Selenopemphix quanta*	*Trinovantedinium spp*	*Votadinium calvum*	*Polykrikos schwartzii*	Total
80-004-38	x639	0	3	7	57	2	0	79	2	0	0	0	0	0	0	0	222
80-004-39	x640	0	2	3	96	0	1	85	0	0	0	0	1	0	0	0	308
80-004-40	x641	3	4	6	75	2	0	79	0	0	0	0	1	0	0	0	299
80-004-41	x642	1	1	7	39	2	0	69	0	0	0	0	2	0	0	0	268
80-004-42	x643	1	2	2	66	1	0	151	1	0	0	0	0	0	0	0	304
80-004-43	x644	1	1	6	53	1	0	133	0	0	0	0	1	0	0	0	295
80-004-44	x645	0	2	8	63	7	0	134	0	0	0	0	0	0	0	0	322
81-006-7	x646	4	1	6	9	2	0	107	0	0	0	0	3	0	0	0	193
92-036-36	x647	4	2	39	27	0	0	72	0	1	0	0	2	0	0	0	314
90-015-16	x648	2	1	93	3	0	0	18	0	0	0	0	0	0	0	0	418
90-015-18	x649	3	0	32	6	0	0	44	1	0	0	0	5	0	0	0	337
90-015-22	x650	10	3	26	10	0	0	96	0	0	0	0	3	0	0	0	302
78-006-4	x651	11	7	104	1	0	0	7	0	0	0	0	0	1	0	0	498
78-006-6	x652	1	3	70	2	0	0	1	0	0	0	0	1	0	0	0	325
78-006-8	x653	2	5	51	4	0	0	8	1	0	0	0	0	0	0	0	309
HU99036-7	x654	1	1	68	7	0	0	24	0	0	0	0	0	0	0	0	346
90-015-8	x655	1	1	105	14	6	0	106	2	0	0	0	2	0	0	0	863
HU99036-8	x656	1	3	96	7	0	0	8	0	0	0	0	4	0	0	0	531
HU99036-9	x657	0	8	71	0	0	0	0	0	0	0	0	0	0	0	0	626
HU99036-11	x658	0	5	41	2	0	0	4	0	0	0	0	0	0	0	0	300
HU99036-17	x659	0	3	72	7	0	0	14	0	0	0	0	2	0	0	0	498
HU99036-26	x660	1	4	39	32	1	0	30	2	0	0	0	6	0	0	0	336
77-034-60	x661	0	0	26	43	22	0	32	0	0	0	0	1	0	0	0	296
83-033-3	x662	0	0	7	222	0	0	33	0	0	0	0	0	0	0	0	316
83-033-11	x663	0	0	30	211	0	0	53	0	0	0	0	3	0	0	0	326

Appendix 6: Raw dinoflagellate cyst counts in the new surface samples

Core number	No site	*Spiniferites mirabilis*	*Spiniferites spp*	*Pentapharsodinium dalei*	*Islandinium minutum*	*Islandinium cezare*	*Islandinium spp.*	*Brigatedinium spp*	*Brigatedinium cariacoense*	*Brigatedinium simplex*	*Selenopemphix spp.*	*Xandarodinium xanthum*	*Selenopemphix quanta*	*Trinovantedinium spp*	*Votadinium calvum*	*Polykrikos schwartzii*	Total
MD99-2210	x664	3	3	84	22	0	0	79	0	1	0	0	4	1	0	0	431
MD99-2211	x665	5	0	55	5	3	0	44	0	0	0	0	5	0	0	0	305
MD99-114.04	x666	6	4	64	20	0	0	86	0	0	0	0	7	1	0	0	289
89-038-16	x667	6	7	37	0	0	0	6	0	0	0	0	0	0	0	0	296
MD99-1225	x669	8	7	67	4	2	0	76	0	0	1	0	17	3	0	0	302
MC-13	x670	0	2	22	0	0	0	6	0	1	0	0	2	0	0	0	343
MC-25	x671	2	1	57	0	0	0	0	0	0	0	0	0	0	0	0	373
MC-21	x672	3	3	124	0	0	0	21	0	0	0	0	2	0	0	0	860
89-038-20	x673	9	2	12	0	0	0	2	0	0	0	0	0	0	0	0	304
89-038-21	x674	2	3	82	0	0	0	9	0	1	0	0	3	0	0	0	342
89-038-25	x675	3	6	94	0	0	0	10	0	0	0	0	2	0	0	0	363
83-033-14	A682	0	3	48	2	0	0	31	0	2	0	1	6	0	0	0	339
83-033-16	A683	0	3	29	13	0	0	66	1	11	0	0	2	0	0	0	311
91020-69	A685	2	1	14	0	0	0	43	0	0	0	0	0	0	0	0	313
91020-6	A668	5	0	20	0	0	0	0	0	0	0	0	0	0	0	0	397
2000-36-001	X686	2	0	24	2	0	0	48	0	0	0	0	4	0	0	0	298
2000-36-004	X688	4	1	22	9	0	0	36	0	0	0	0	3	0	0	0	302
2000-36-009	X689	9	0	29	3	0	0	75	0	0	0	0	2	1	0	0	323
2000-36-020	X690	9	1	9	12	0	0	117	0	0	0	0	1	0	0	0	301
2000-36-025	X691	9	2	16	9	0	0	91	0	0	0	0	0	0	0	0	299
2000-36-026	X692	6	1	35	4	0	0	54	0	0	0	0	1	0	0	0	325
2000-36-032	X693	3	2	18	4	0	0	47	0	0	0	0	0	0	0	0	303
2000-36-036	X694	2	3	35	4	0	0	17	0	0	0	0	0	0	0	0	301
2000-36-041	X695	2	1	27	4	0	0	33	0	0	0	0	0	0	0	1	329
2000-36-043	X696	0	0	7	0	0	0	6	0	0	0	0	0	0	0	0	97

Appendix 6: Raw dinoflagellate cyst counts in the new surface samples

Core number	No site	*Spiniferites mirabilis*	*Spiniferites spp*	*Pentapharsodinium dalei*	*Islandinium minutum*	*Islandinium cezare*	*Islandinium spp.*	*Brigatedinium spp*	*Brigatedinium cariacoense*	*Brigatedinium simplex*	*Selenopemphix spp.*	*Xandarodinium xanthum*	*Selenopemphix quanta*	*Trinovantedinium spp*	*Votadinium calvum*	*Polykrikos schwartzii*	Total
2000-36-054	X697	0	3	36	1	0	0	23	0	0	0	0	3	0	0	1	322
2000-36-056	X698	4	3	63	1	0	0	26	0	0	0	0	0	0	0	0	308
2000-42-002	X699	0	2	70	3	0	0	12	0	0	0	0	0	0	0	0	301
2000-42-007	X700	0	4	55	1	0	0	1	0	0	0	0	0	0	0	0	313
2000-42-010	X701	1	2	57	0	0	0	20	0	0	0	0	1	0	0	0	299
2000-42-017	X702	6	3	58	0	0	0	10	0	0	0	0	0	0	0	0	308
2000-42-020	X703	5	3	24	9	0	0	96	0	0	0	0	3	0	0	0	285
2000-42-030	X704	5	0	56	3	0	0	24	0	0	0	0	1	0	0	0	307
2000-42-037	X705	1	0	60	1	0	0	6	0	0	0	0	1	0	0	0	296
2000-42-042	X706	3	0	69	1	0	0	20	0	0	0	0	2	0	0	0	315
2000-42-057	X707	7	1	47	0	0	0	52	0	0	0	0	2	0	0	0	288
2000-47-001	X708	1	1	14	5	0	0	134	0	0	0	0	0	0	0	0	206

Appendix 7: Percentages of dinoflagellate cysts in the new surface samples

# on map	Carotte	TF Number	*cf. Alexandrium excavatum*	*Ataxiodinium choanum*	*Bitectatodinium tepikiense*	*Impagidinium aculeatum*	*Impagidinium pallidum*	*Impagidinium paradoxum*	*Impagidinium patulum*	*Impagidinium sphaericum*	*Impagidinium strialatum*	*Impagidinium spp.*	*Lingulodinium machaeoph*	*Nematosphaeropsis labyrir*	*Operculodinium centrocarp*	*O.centrocarpum short proc*	*O. centrocarpum arctic morphotype*	*Operculodinium israelianu*	*O. centrocarpum morphotype cezare*	*Pyxidinopsis reticulata*
1	80-004-38	x639	0	0	1.8	0	0	0	0	0	0	0	0	0.9	22.9	0.45	1.8	0	0.45	0
1	80-004-39	x640	0	0.3	3.2	0	0	0	0	0	0	0	0.3	1	28.9	0	0	0	0	0
1	80-004-40	x641	0	0	0.3	0	0	0	0	0	0	0.3	0	0.66	35.8	0	1	0	0	0
1	80-004-41	x642	0	0.37	1.1	0	0	0	0	0	0	0	0	0.7	46.3	0.7	0	0	0	0
1	80-004-42	x643	0	0	1	0	0	0	0	0	0	0	0	0.65	19.7	0.65	0.3	0	0	0
1	80-004-43	x644	0	0	1	0	0	0	0	0	0	0	0	1	28.1	0.7	0.3	0	0	0
1	80-004-44	x645	0	0	0	0	0	0	0	0	0	0	0	0.6	28.3	0.6	0.6	0.3	0	0
2	81-006-7	x646	0	0	1	0	0	0.5	0	0	0	0	0	2.5	23.3	0.5	0	0	0.5	0
3	92-036-36	x647	0.6	0.3	0	0.3	0.6	1.3	0	0.3	0.6	1.3	0.3	4.1	32.2	1.6	0	0.3	0	0
14	90-015-16	x648	0	0.2	9.1	0.2	0	0	0	0	0	0.5	0	2.4	51.2	0.2	0.2	0.5	0	0
13	90-015-18	x649	0	0	6.8	0	0	13.6	0	1.8	1.8	2.4	0	4.1	32.9	0.3	0.3	0.3	0.3	0
7	90-015-22	x650	0	0	5.9	0.3	0	1.3	0	0	0	0.7	0	4.6	32.1	1.3	0.7	0	0.3	0
14	78-006-4	x651	0	0	4.2	0	0	0.4	0	0	0.2	0.4	0.4	4.8	52.4	1.6	0.4	0	0	0
13	78-006-6	x652	0	0.6	5.8	0.3	0	0	0	0	0	0.3	0	3.7	56.3	0.6	0.3	0.3	0	0
13	78-006-8	x653	0.3	0	6.8	0	0	0.65	0	0	0	0	0.3	2.3	56	2.3	0	0	0	0
33	HU99036-7	x654	1.4	0	14.4	0	0	0	0	1.1	0	0	0.3	0	44.5	2.3	0.3	0	0	0
32	90-015-8	x655	0.6	0	15.4	0	0.6	0	0	0	0.1	0.2	0.1	0.6	47.2	0.7	0	0.3	0	0
28	HU99036-8	x656	2.1	1.1	10	0	0.2	0.2	0.2	0	0	0.4	0	1.5	53.1	1.1	1.5	0	0.2	0
29	HU99036-9	x657	0.15	0.3	7.2	0	0	0.15	0	0.15	0	0	0.15	1.8	66.3	1.3	1.1	0	2.1	0
21	HU99036-11	x658	1	0.66	11.6	0.3	0.3	0	0.6	2	0.3	1.6	0	3.3	49.7	1.3	0	0.6	0.6	0
20	HU99036-17	x659	0.2	0.2	8.2	0	0	0.6	0	0.4	0	0.4	0.2	1.6	60.4	1.2	0.4	0	0.4	0
22	HU99036-26	x660	0	0	8.3	0	0	0.9	2.4	0	0	0	0.9	0.6	42.3	0.9	0.9	0	0.3	0
38	77-034-60	x661	0	0	0	0	0.7	0	0.3	0.7	0	0	0	36.8	16.9	0.7	0.3	0	0.3	0
35	83-033-3	x662	0	0	0	0	0.3	0	0	0	0	0.3	0	5.1	10.7	0	0.3	0	0	0
36	83-033-11	x663	0	0	0	0	0	0	0	0	0	0	0	1.5	4.9	0.3	0	0.3	0	0
41	MD99-2210	x664	2.5	0.2	7	0	0.2	0.2	0	0	0	0	0.5	0.2	34.5	1.2	0	0	0	0

Appendix 7: Percentages of dinoflagellate cysts in the new surface samples

# on map	Carotte	TF Number	*cf. Alexandrium excavatum*	*Ataxiodinium choanum*	*Bitectatodinium tepikiense*	*Impagidinium aculeatum*	*Impagidinium pallidum*	*Impagidinium paradoxum*	*Impagidinium patulum*	*Impagidinium sphaericum*	*Impagidinium strialatum*	*Impagidinium spp.*	*Lingulodinium machaeopho*	*Nematosphaeropsis labyrin*	*Operculodinium centrocarp*	*O.centrocarpum short proc*	*O. centrocarpum arctic morphotype*	*Operculodinium israelianu*	*O. centrocarpum morphotype cezare*	*Pyxidinopsis reticulata*
41	MD99-2211	x665	0.3	0.3	0.65	0	0	4.9	0	0	1.3	1.6	0.65	10.5	32.8	0.3	0	0.65	0	0
41	MD99-114.04	x666	0	0	0.35	0	0	1	0.35	1.4	0	0	0.7	6.9	17.6	0.7	0	0	0	0.35
40	89-038-16	x667	0	0	4.4	1	0	3	0.33	0.7	0.33	1.7	1.7	3	47.3	0.33	0	1.7	0	0
41	MD99-1225	x669	0.3	0	0.3	0	0	0	0.3	0	0	0.66	0	3.6	23.2	0.3	0	0	0.3	0
30	MC-13	x670	0.6	0	10.8	0.9	2	0	2.9	1.4	0	0	0	2.6	60.3	0.6	0	0	0	0
31	MC-25	x671	0.26	0	6.2	0	0.54	0	0.26	0.26	0	0.54	0	4.6	62.7	0.26	0	0.54	0.54	0.26
34	MC-21	x672	0.23	0.35	14.6	0	0.46	0	0.1	0	0	0.23	0.46	0.35	58.2	1.05	0	0.23	0	0
43	89-038-20	x673	0	0	6.2	0.6	0.6	1.3	2	0.67	0	3.3	0.3	23.7	43.2	0.66	0.66	0.3	0.33	0
42	89-038-21	x674	0	0	1.5	0.3	0	2	0.9	0	0.6	2.9	0.6	13.1	37.1	1.5	0	0.9	0.3	0.3
42	89-038-25	x675	0	0	0.8	0	0.3	0	0.3	0	0	1.1	0.3	17.9	38.8	0.8	0	0.8	0.5	0
37	83-033-14	A682	0	0	0.3	0	0.3	0	0	0.3	0	0.6	0.6	0.9	60.6	0.6	0.3	0	0	0
37	83-033-16	A683	0	0.3	0.7	0	0	0	0	0	0	0.3	0	0.3	47.9	0.3	0	0	1.3	0
39	91020-69	A685	0	0	0.32	2.55	0	0	0	0	0	0	0	4.5	65.5	0	0	0.32	0	0
9	91020-6	A668	0	0	7.8	0.5	0	0	0.25	0	0.25	0	0	3.8	74.5	0.5	0.25	0.25	0	0
5	2000-36-001	X686	2.3	0	5	0.3	0	0.3	0.3	2	0.3	0	0	3.7	49.3	1	0	0	0	0
5	2000-36-004	X688	0.7	0	4.6	0	0	0	1.3	0.7	0	0	0	2.6	58.9	0	0	0	0	0
6	2000-36-009	X689	1.2	0.3	4	0.3	0	0	0	0.6	0	0	0.3	4	46.4	0	0	0	0	0
10	2000-36-020	X690	1	0	4.6	0	0	0.3	0.3	0.7	0	0	0	1	38.8	0	0	0.3	0	0
11	2000-36-025	X691	0	0	4.7	0	0	0	0.3	1.3	0	0	0	1.3	43.1	0	0	0	0	0
8	2000-36-026	X692	1.8	0	6.5	0.6	0	0	0.3	0.6	0	0	0	0.9	49.8	0	0	0	0	0
12	2000-36-032	X693	1	0	4.9	0	0	0	0	0	0	0	0	2.6	59.7	0	0	0	0	0.3
15	2000-36-036	X694	0.7	0.7	8.6	0	0	0	0.7	0.3	0	0	0	2.3	56.8	0	0	0	0	0
17	2000-36-041	X695	0.6	0.3	9.7	0.6	0.3	0	0.3	1.2	0	0	0	2.7	57.4	0	0	0	0	0
23	2000-36-043	X696	0	0	14.4	0	0	0	0	0	0	0	0	0	62.8	0	0	0	0	0
24	2000-36-054	X697	0.9	0.3	8.7	0.3	0.3	0	0.9	6.8	0	0	0	2.2	53.4	0	0	0	0	0
24	2000-36-056	X698	0.6	0	6.8	0	0	0	0.3	0.3	0	0	0	2.9	48.7	0	0	0	0	0

Appendix 7: Percentages of dinoflagellate cysts in the new surface samples

# on map	Carotte	TF Number	cf. *Alexandrium excavatum*	*Ataxiodinium choanum*	*Bitectatodinium tepikiense*	*Impagidinium aculeatum*	*Impagidinium pallidum*	*Impagidinium paradoxum*	*Impagidinium patulum*	*Impagidinium sphaericum*	*Impagidinium strialatum*	*Impagidinium* spp.	*Lingulodinium machaeoph*	*Nematosphaeropsis labyrin*	*Operculodinium centrocarp*	*O.centrocarpum* short proc	*O. centrocarpum* arctic morphotype	*Operculodinium israelianum*	*O. centrocarpum morphotype cezare*	*Pyxidinopsis reticulata*
27	2000-42-002	X699	1.7	0.3	9.6	0.7	0	0	0	0	0	0	0	2	52.7	0	0	0	0	0
26	2000-42-007	X700	0.3	0	8.3	0.6	0	0	0	0	0	0	0	1.3	63.9	0	0	0	0	0
25	2000-42-010	X701	0.3	0	10	0	0.3	0.3	0.3	0	0	0	0	1	53.8	0	0	0.3	0	0
25	2000-42-017	X702	1	0	8.1	0	0	0	0.8	0	0	0	0	1	56.5	0	0	0	0	0.3
25	2000-42-020	X703	0.7	0.3	7.7	0	0.7	0	0	1.7	0	0	0	0.3	31.6	0	0	0.3	0	0
19	2000-42-030	X704	0.3	0	9.5	0	0	0	0	0.6	0	0.3	0	1.6	50	0	0	0.3	0	0
18	2000-42-037	X705	0.7	0	7.8	0.3	0	0	0.3	0	0	0.3	0	3.4	57	0	0	0	0	0
16	2000-42-042	X706	0.3	0	8	0	0	0	0.6	0	0	0	0	2.2	50.8	0	0	0	0	0
14	2000-42-057	X707	0	0	6.6	0.7	0	0	0.7	1	0	0.3	0	1.4	43.4	0	0	0.7	0	0
4	2000-47-001	X708	1.4	0	1	0	0	0	0	0	0	0	0	0	18.5	0	0	0	0	0

Appendix 7: Percentages of dinoflagellate cysts in the new surface samples

TF Number	*Spiniferites membranaceus*	*Spiniferites delicatus*	*Spiniferites elongatus*	*Spiniferites ramosus*	*Spiniferites belerius*	*Spiniferites bentorii*	*Spiniferites bulloideus*	*Spiniferites frigidus*	*Spiniferites lazarus*	*Spiniferites mirabilis*	*Spiniferites spp*	*Pentapharsodinium dalei*	*Islandinium minutum*	*Islandinium cezare*	*Islandinium spp.*	*Brigatedinium spp*	Protoperidinoids	*Selenopemphix spp.*	*Selenopemphix quanta*	*Trinovantedinium applanat*	*Quinquecuspis concreta*	*Polykrikos schwartzii*	*Xandarodinium xanthum*
x639	0.9	0.45	0	2.25	0	0	0.45	0	0	0	1.35	3.1	25.7	0.9	0	36.5	0	0	0	0	0	0	0
x640	0.3	0	0.3	2.6	0	0	1.9	0	0	0	0.6	1	31.1	0	0.3	27.6	0	0	0.3	0	0	0	0
x641	0	0.3	0.66	2.7	0	0.3	1	0	0	1	1.3	2	25	0.66	0	26.4	0	0	0.3	0	0	0	0
x642	0	2.2	0.7	2.2	0	0	0.7	0	0	0.7	0.7	2.6	14.5	0.37	0	25.7	0	0	0.7	0	0	0	0
x643	0	0.65	0.3	3	0	0	0	0	0	0.3	0.65	0.65	21.7	0.3	0	50	0	0	0	0	0	0	0
x644	0	0.7	0	1.35	0	0	0.3	0	0	0.3	0.3	2	18	0.3	0	45.1	0	0	0.3	0	0	0	0
x645	0	0.3	0	2.5	0	0	0	0	0	0	0.6	2.5	19.6	2.2	0	41.6	0	0	0	0	0	0	0
x646	0	0	1	2.1	0	0	0	0	0	2.1	0.5	3.1	4.7	1	0	55.4	0	0	1.5	0	0	0	0
x647	0	1.6	1.9	3.5	0	0	2.2	0	0	1.2	0.6	12.4	8.6	0	0	23.2	0	0	0.6	0	0	0	0
x648	0	0.2	2.1	5	0	0	0	0	0	0.5	0.2	22.2	0.7	0	0	4.3	0	0	0	0	0	0	0
x649	0	0.3	3	5	0	0	0	0	0	0.9	0	9.5	1.8	0	0	13.3	0	0	1.5	0	0	0	0
x650	0	0	0.3	3.3	0	0	0	0	0	3.3	1	8.6	3.3	0	0	31.8	0	0	1	0	0	0	0
x651	0	0.4	1.4	7	0	0	0	0	0	2.2	1.4	20.9	0.2	0	0	1.4	0	0	0	0	0	0	0
x652	0	0	3.4	4.3	0	0	0	0	0	0.3	0.9	21.5	0.6	0	0	0.3	0	0	0.3	0	0	0	0
x653	0.65	0.65	1.9	3.5	0.65	0	1	0	0	0.65	1.6	16.5	1.3	0	0	2.9	0	0	0	0	0	0	0
x654	0	0	4	2.3	0	0	0	0	0	0.3	0.3	19.6	2	0	0	6.9	0	0	0	0	0	0	0
x655	0	0.2	5	0.9	0.1	0	0	0	0	0.1	0.1	12.2	1.6	0.7	0	12.5	0	0	0.2	0	0	0	0
x656	0	0	3.9	2.1	0	0	0	0	0	0.2	0.6	18.1	1.3	0	0	1.5	0	0	0.75	0	0	0	0
x657	0	0.5	4.5	1.8	0	0	0	0	0	0	1.3	11.3	0	0	0	0	0	0	0	0	0	0	0
x658	0	0.3	5.7	2	0	0	0.3	0	0	0	1.6	13.6	0.6	0	0	1.3	0	0	0	0	0	0	0
x659	0	0.2	4	1.8	0	0	0	0	0	0	0.6	14.5	1.4	0	0	2.8	0	0	0.4	0	0	0	0
x660	0.3	0	1.2	6.5	0	0	0.3	0	0	0.3	1.2	11.6	9.5	0.3	0	8.9	0.6	0	1.8	0	0	0	0
x661	0	0	1	0.3	0	0	0	0	0	0	0	8.8	14.5	7.4	0	10.8	0	0	0.3	0	0	0	0
x662	0	0	0	0.3	0	0	0	0	0	0	0	2.2	70.2	0	0	10.2	0	0	0	0	0	0	0
x663	0	0	0.9	0.9	0	0	0	0	0	0	0	9.2	64.7	0	0	16.2	0	0	0.9	0	0	0	0
x664	0.2	0.2	4.4	2.3	0.2	0	0.2	0	0	0.7	0.7	19.5	5.1	0	0	18.5	0	0	0.93	0.2	0	0	0

Appendix 7: Percentages of dinoflagellate cysts in the new surface samples

TF Number	*Spiniferites membranaceus*	*Spiniferites delicatus*	*Spiniferites elongatus*	*Spiniferites ramosus*	*Spiniferites belerius*	*Spiniferites bentorii*	*Spiniferites bulloideus*	*Spiniferites frigidus*	*Spiniferites lazarus*	*Spiniferites mirabilis*	*Spiniferites spp*	*Pentapharsodinium dalei*	*Islandinium minutum*	*Islandinium cezare*	*Islandinium spp.*	*Brigatedinium spp*	Protoperidinoids	*Selenopemphix spp.*	*Selenopemphix quanta*	*Trinovantedinium applanat*	*Quinquecuspis concreta*	*Polykrikos schwartzii*	*Xandarodinium xanthum*
x665	0	1.3	0.65	5.2	0	0	0.3	0	0	1.6	0	18	1.6	1	0	14.4	0	0	1.6	0	0	0	0
x666	0	2.1	1	1	0	0	1.4	0	0	2.1	1.4	22.1	6.9	0	0	29.7	0	0	2.4	0.35	0	0	0
x667	0.33	0.33	3.7	6.4	0.33	0.7	3.7	0	0	2	2.4	12.5	0	0	0	2	0	0	0	0	0	0	0
x669	0.3	1	0.3	4.97	1.3	0	1.6	0	0	2.6	2.3	22.2	1.3	0.66	0	25.2	0	0.3	5.6	1	0	0	0
x670	0	0	5.5	2.3	0	0	0	0	0	0	0.6	6.4	0	0	0	2	0	0	0.6	0	0	0	0
x671	0	0.26	5.4	0.8	0.26	0	0.26	0	0	0.54	0.26	15.3	0	0	0	0	0	0	0	0	0	0	0
x672	0	0	5.6	0.23	0	0	0	0	0	0.35	0.35	14.4	0	0	0	2.4	0	0	0.23	0	0	0	0
x673	0.66	1.3	0.66	4.3	1	0	0	0	0	3	0.66	3.9	0	0	0	0.66	0	0	0	0	0	0	0
x674	0	2.3	1.2	2.9	0	0.6	1.7	0	0	0.6	0.9	24	0	0	0	2.9	0	0	0.9	0	0	0	0
x675	0	1.1	1.4	2.5	1.4	0	0.3	0	0	0.8	1.6	25.9	0	0	0	2.8	0	0	0.5	0	0	0	0
A682	0	1.5	5.3	1.7	0	0	0	0	0	0	0.9	14	0.6	0	0	9.6	0	0	1.8	0	0	0	0.3
A683	0	0	5.1	1.9	0.3	0	0	0	0	0	1	9.3	4.2	0	0	25	0	0	0.7	0	0	0	0
A685	0	0.64	6	0.64	0	0	0	0.32	0	0.64	0.32	4.5	0	0	0	13.7	0	0	0	0	0	0	0
A668	0	0.5	2.8	1	0	0.5	0	0	0.75	1.25	0	5	0	0	0	0	0	0	0	0	0	0	0
X686	0	0	3.7	4.7	0	0	0	0	0	0.67	0	8	0.67	0	0	16.1	0	0	1.3	0	0	0	0
X688	0	0	4	2.3	0	0	0	0	0	1.3	0.3	7.3	3	0	0	11.9	0	0	1	0	0	0	0
X689	0	0.3	2.5	3.1	0	0	0	0	0	2.8	0	8.9	0.9	0	0	23.2	0	0	0.6	0	0	0	0
X690	0	0	2.3	1	0	0	0	0	0	3	0.3	3	4	0	0	38.9	0	0	0.3	0	0	0	0
X691	0	0	2.7	4	0	0	0	0	0	3	0.7	5.6	3	0	0	30.4	0	0	0	0	0	0	0
X692	0	0.6	3.1	4.6	0	0	0	0	0	1.8	0.3	10.8	1.2	0	0	16.6	0	0	0.3	0	0	0	0
X693	0	0.7	4.9	1.3	0	0	0	0	0	1	0.7	5.9	1.3	0	0	15.5	0	0	0	0	0	0	0
X694	0	0.7	3	6	0	0	0	0	0	0.7	1	11.6	1.3	0	0	5.6	0	0	0	0	0	0	0
X695	0	0	1.5	3.9	0	0	0.6	0	0	0.6	0.3	8.2	1.2	0	0	10	0	0	0	0	0	0.3	0
X696	0	0	2.1	7.2	0	0	0	0	0	0	0	7.2	0	0	0	6.2	0	0	0	0	0	0	0
X697	0	0	2.8	2.5	0	0	0	0	0	0	0.9	11.2	0.3	0	0	7.1	0	0	0.9	0	0	0.3	0
X698	0	0.3	2.6	5.8	0	0	0	0	0	1.3	1	20.4	0.3	0	0	8.4	0	0	0	0	0	0	0

Appendix 7: Percentages of dinoflagellate cysts in the new surface samples

TF Number	*Spiniferites membranaceus*	*Spiniferites delicatus*	*Spiniferites elongatus*	*Spiniferites ramosus*	*Spiniferites belerius*	*Spiniferites bentorii*	*Spiniferites bulloideus*	*Spiniferites frigidus*	*Spiniferites lazarus*	*Spiniferites mirabilis*	*Spiniferites* spp	*Pentapharsodinium dalei*	*Islandinium minutum*	*Islandinium cezare*	*Islandinium* spp.	*Brigatedinium* spp	Protoperidinoids	*Selenopemphix* spp.	*Selenopemphix quanta*	*Trinovantedinium applanat*	*Quinquecuspis concreta*	*Polykrikos schwartzii*	*Xandarodinium xanthum*
X699	0	0.3	2	1.6	0	0	0	0	0	0	0.7	23.2	1	0	0	4	0	0	0	0	0	0	0
X700	0	0	1.3	4.5	0	0	0	0	0	0	1.3	17.6	0.3	0	0	0.3	0	0	0	0	0	0	0
X701	0	0	3.7	2.7	0	0	0	0	0	0.3	0.7	19.1	0	0	0	6.7	0	0	0.3	0	0	0	0
X702	0	0	1.3	6.2	0	0	0	0	0	2	1	18.8	0	0	0	3.2	0	0	0	0	0	0	0
X703	0	0.3	0.3	6.7	0	0	0	0	0	1.7	1	8.4	3.1	0	0	33.7	0	0	1	0	0	0	0
X704	0	0	3.3	5.2	0	0	0	0	0	1.6	0	18.3	1	0	0	7.8	0	0	0.3	0	0	0	0
X705	0	0	3	3.7	0	0	0	0	0	0.3	0	20.3	0.3	0	0	2	0	0	0.3	0	0	0	0
X706	0	0	2.5	5.7	0	0	0	0	0	0.9	0	22	0.3	0	0	6.4	0	0	0.6	0	0	0	0
X707	0	0.7	1	5.5	0	0	0	0	0	2.4	0.3	16.3	0	0	0	18	0	0	0.7	0	0	0	0
X708	0	0.5	0.5	2.9	0	0	0	0	0	0.5	0.5	6.8	2.4	0	0	65	0	0	0	0	0	0	0

Appendix 8: Average percentages of the main taxa relative to water depth along the southeastern Canadian Margin

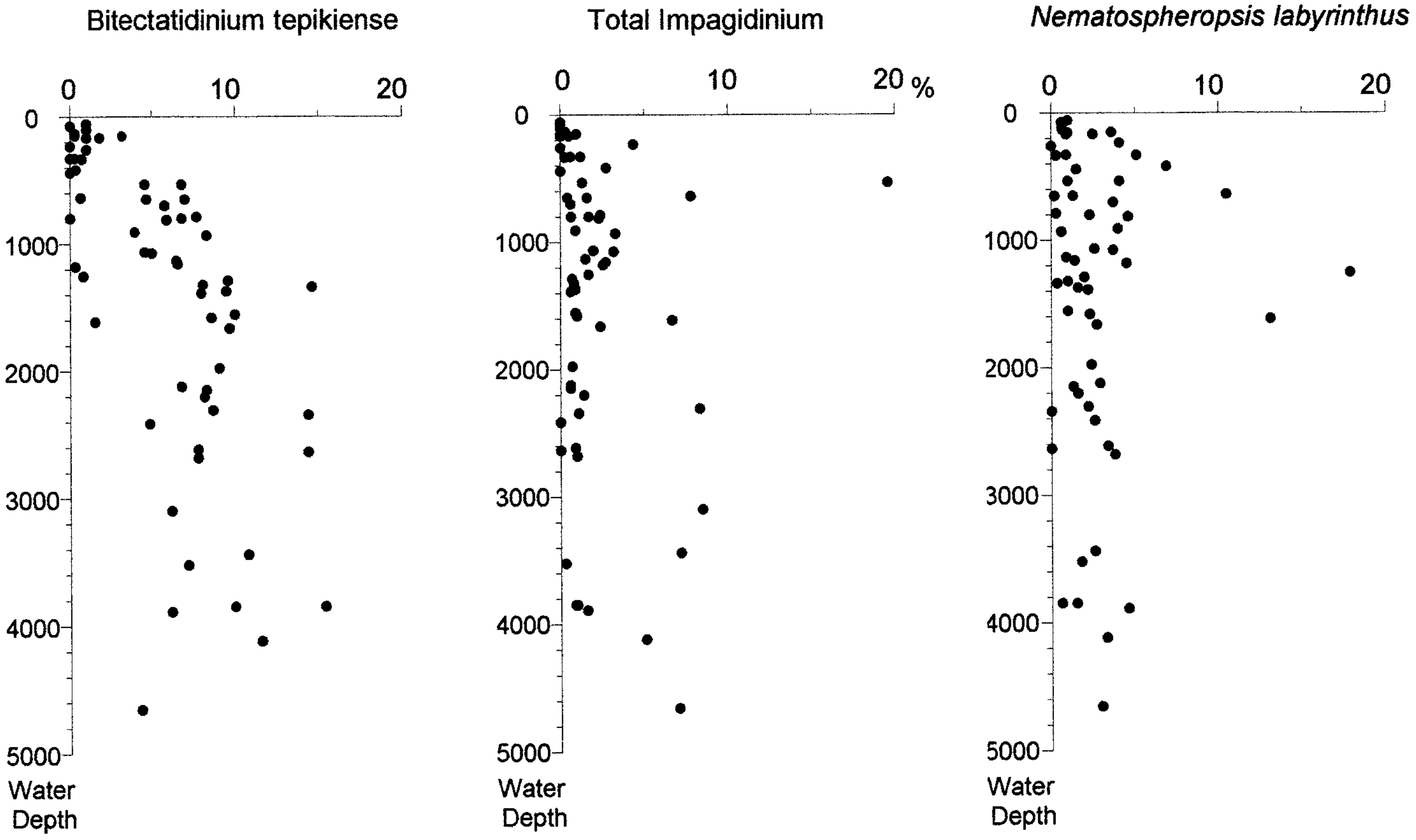

Appendix 8: Average percentages of the main taxa relative to water depth along the southeastern Canadian Margin

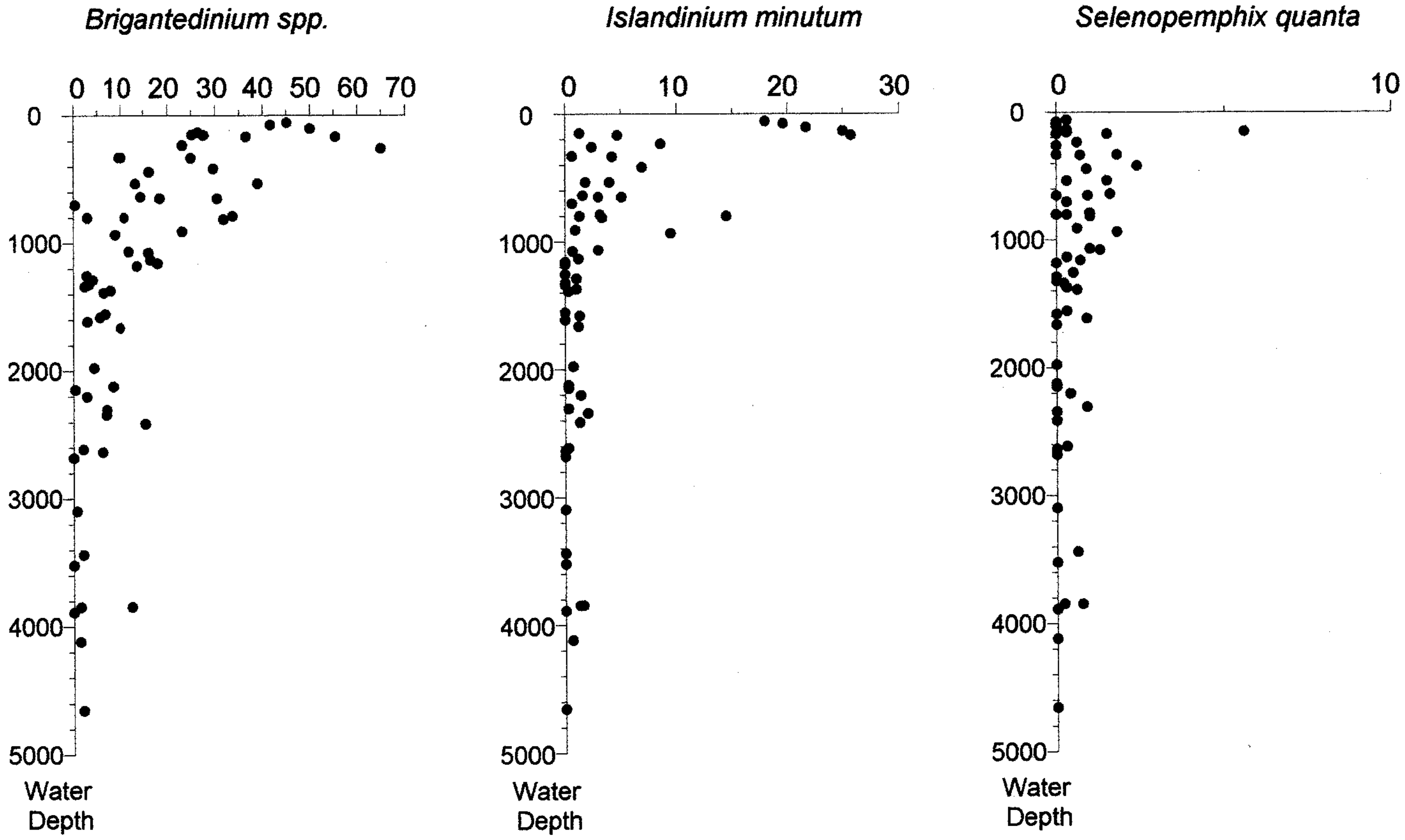

Appendix 8: Average percentages of the main taxa relative to water depth along the southeastern Canadian Margin

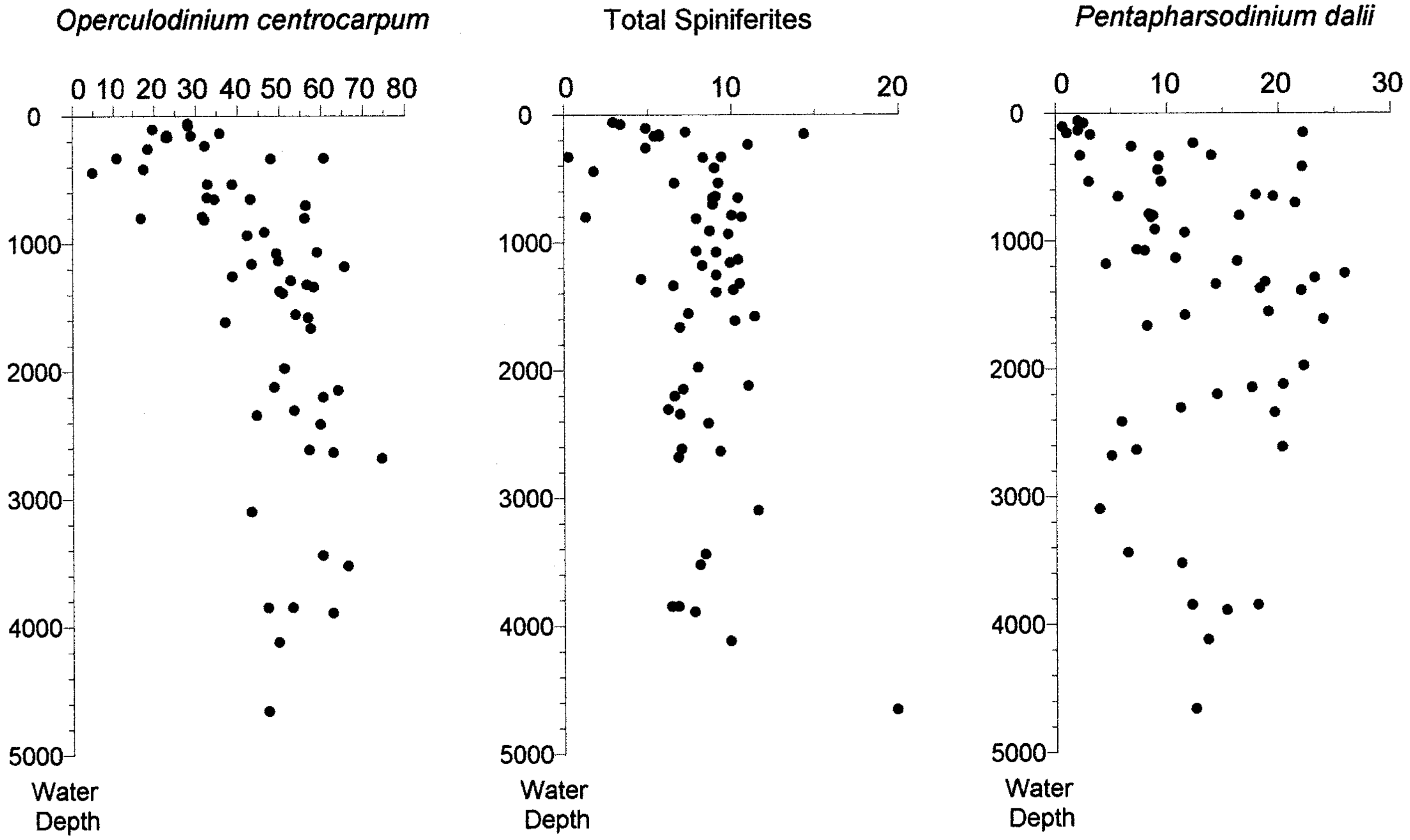
Operculodinium centrocarpum

Total Spiniferites

Pentapharsodinium dalii

Appendix 9: Average percentages of the main taxa in assemblages of the southeastern Canadian Margin

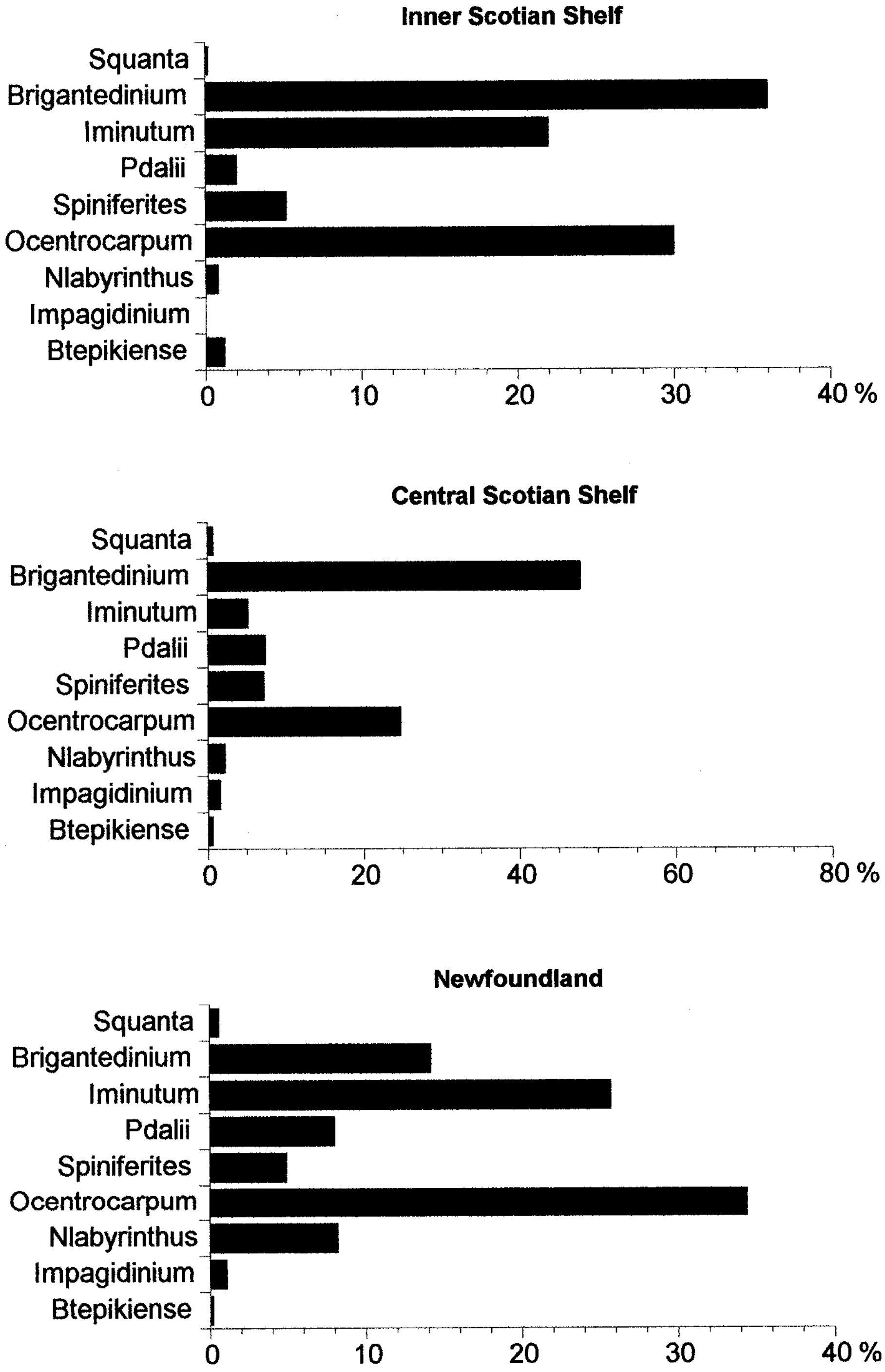

Appendix 9: Average percentages of the main taxa in assemblages of the southeastern Canadian Margin


Scotian Slope


Scotian Rise

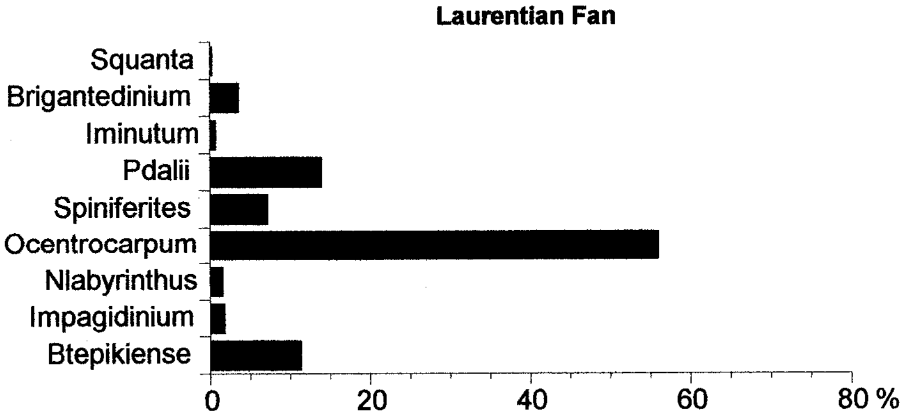
Laurentian Fan

Appendix 10: Concentrations of palynomorphs in core 95-030-24 La Have Basin

	Depth (cm)	Dinoflagellate cysts	Pollen	Spores	Reworked	Organic linings
TWC	0-1	10174	13912	1333	96	4095
	20-22	11714	15990	1634	174	5145
	10-12	8594	17425	1464	94	5903
	30-32	19788	25732	1799	313	8682
	40-42	12241	13788	1138	136	5506
	50-52	11905	10113	947	203	2942
	60-62	15476	2048	1890	51	4188
	70-72	24551	28842	2503	238	8700
	80-82	18336	21546	1360	218	4951
	90-92	10901	15795	1947	167	3170
	100-102	14033	16760	1251	45	3978
	110-112	16609	18771	1877	171	3583
	120-122	14229	15341	1298	93	5006
	130-132	15820	16906	2125	189	3825
	140-142	17520	13515	851	150	3103
	150-152	6919	12146	515	662	4785
	160-162	11991	14494	1195	112	2540
	170-172	18413	21214	1609	238	5006
	178-180	14525	18056	1609	134	5229
Piston	0-2	10360	11990	815	524	4365
	10-12	5130	9961	450	50	4155
	20-22	6382	11857	1064	188	3817
	30-32	7985	10567	1788	159	3178
	40-42	4693	8656	521	104	3285
	50-52	5799	9370	366	0	2991
	60-62	12286	28668	1365	227	7281
	70-72	0	0	0	0	0
	80-82	8371	9752	604	0	1726
	90-92	5887	8009	715	71	2932
	100-102	6760	9356	561	140	1263
	120-122	5865	9495	669	210	2063
	140-142	7999	19322	1251	400	3003
	160-162	6161	15632	1149	369	3241
	180-182	4154	11233	1106	87	1251
	200-202	5833	11578	506	126	2048
	220-222	5726	13367	967	171	2105
	240-242	5052	10133	427	122	989
	260-262	5263	9974	883	258	1987
	280-282	6382	14829	813	313	2800
	300-302	3052	11441	740	153	2196

Appendix 10: Concentrations of palynomorphs in core 95-030-24 La Have Basin

	Depth (cm)	Dinoflagellate cysts	Pollen	Spores	Reworked	Organic linings
Piston	320-322	4809	16587	1472	147	2405
	340-342	3091	16268	978	182	1888
	360-362	4511	21298	1997	241	1781
	380-382	4763	21383	1652	194	2090
	400-402	5030	21553	1725	146	2940
	420-422	6753	22775	1287	189	2217
	440-442	8591	29397	1315	127	3266
	460-462	15017	20265	1453	255	3780
	480-482	22625	29833	1602	501	6607
	500-502	14622	15412	1178	44	2239
	520-522	19240	17050	1721	235	2503
	540-542	9932	10528	834	79	1192
	560-562	11243	16010	95	159	1231
	580-582	15336	17200	1171	213	1810
	600-602	22212	17520	938	188	1564
	620-622	20891	14812	1277	102	1839
	640-642	14401	12475	847	115	1194
	660-662	1922	19942	1372	484	3552
	680-682	20022	13140	2138	313	1929
	700-702	21833	11822	2023	53	1757
	720-722	31772	15156	2781	278	1390
	740-742	45765	14087	3861	71	1501
	760-762	40545	9594	2252	167	1418
	780-782	57564	7126	730	174	2681
	800-802	43431	4581	169	64	4836
	820-822	31821	4981	245	172	2184

Appendix 11: Pollen and spores counts, and pollen percentages core 95-030-24, La Have Basin

Depth	0-2	TWC	10-12	TWC	20-22	TWC	30-32	TWC	40-42	TWC	50-52	TWC	60-62	TWC	70-72	TWC
	count	%	count	%	count	%	count	%	count	%	count	%	count	%	count	%
Total pollen	**427**		**457**		**369**		**329**		**303**		**295**		**401**		**242**	
Total tree pollen	**367**	85.7	**409**	88.9	**333**	90.2	**300**	91.2	**279**	92.1	**271**	91.9	**358**	89.3	**218**	90.1
Abies	22	5.14	17	3.7	7	1.9	10	3.04	7	2.31	10	3.39	6	1.5	9	3.72
Picea	71	16.6	65	14.1	44	11.9	47	14.3	42	13.9	42	14.2	49	12.2	24	9.92
Pinus	187	43.7	238	51.7	207	56.1	152	46.2	154	50.8	130	44.1	209	52.1	122	50.4
Tsuga	32	7.48	27	5.87	24	6.5	40	12.2	25	8.25	28	9.49	36	8.98	19	7.85
Acer	14	3.27	15	3.26	11	2.98	11	3.34	5	1.65	15	5.08	14	3.49	6	2.48
Betula >25µ	26	6.07	32	6.96	28	7.59	25	7.6	32	10.6	24	8.14	28	6.98	27	11.2
Carpinus	0	0	0	0	0	0	0	0	0	0	0	0	0	0	1	0.41
Carya	1	0.23	0	0	1	0.27	0	0	0	0	0	0	0	0	1	0.41
Corylus	1	0.23	0	0	0	0	0	0	0	0	0	0	0	0	0	0
Fagus	4	0.93	5	1.09	3	0.81	2	0.61	5	1.65	6	2.03	2	0.5	2	0.83
Fraxinus	0	0	0	0	0	0	0	0	0	0	0	0	0	0	0	0
Juglans	0	0	0	0	0	0	0	0	0	0	0	0	1	0.25	0	0
Quercus	9	2.1	8	1.74	8	2.17	12	3.65	8	2.64	10	3.39	10	2.49	6	2.48
Ulmus	0	0	2	0.43	0	0	1	0.3	0	0	5	1.69	2	0.5	0	0
Myrica gale	0	0	0	0	0	0	0	0	0	0	0	0	0	0	1	0.41
Ostrya	0	0	0	0	0	0	0	0	0	0	0	0	0	0	0	0
Tilia	0	0	0	0	0	0	0	0	1	0.33	1	0.34	1	0.25	0	0
Total shrub pollen	**31**	7.24	**21**	4.57	**21**	5.69	**19**	5.78	**13**	4.29	**12**	2.71	**30**	7.48	**14**	5.79
Betula <25 µ	18	4.21	13	2.83	5	1.36	9	2.74	7	2.31	3	1.02	17	4.24	8	3.31
Alnus spp	8	1.87	3	0.65	13	3.52	2	0.61	1	0.33	3	1.02	7	1.75	4	1.65
Ericaceae	0	0	0	0	0	0	1	0.3	1	0.33	3	1.02	0	0	0	0
Ilex /Nemopanthus	0	0	0	0	0	0	0	0	0	0	0	0	0	0	0	0
Myrica	0	0	0	0	0	0	0	0	0	0	0	0	0	0	0	0
Salix	5	1.17	5	1.09	3	0.81	7	2.13	4	1.32	3	1.02	6	1.5	2	0.83
Petalostemum	0	0	0	0	0	0	0	0	0	0	0	0	0	0	0	0
Total herb pollen	**29**	6.78	**27**	5.87	**15**	4.07	**10**	3.04	**11**	3.63	**12**	0.68	**13**	3.24	**10**	4.13
Ambrosia	2	0.47	3	0.65	1	0.27	1	0.3	0	0	0	0	1	0.25	1	0.41
Artemisia	9	2.1	1	0.22	0	0	1	0.3	0	0	0	0	0	0	0	0
Chenopodiaceae	4	0.93	0	0	1	0.27	0	0	1	0.33	0	0	0	0	1	0.41
Cyperaceae	4	0.93	16	3.48	5	1.36	1	0.3	3	0.99	3	1.02	4	1	1	0.41

Appendix 11: Pollen and spores counts, and pollen percentages core 95-030-24, La Have Basin

Depth	0-2	TWC	10-12	TWC	20-22	TWC	30-32	TWC	40-42	TWC	50-52	TWC	60-62	TWC	70-72	TWC
	count	%	count	%	count	%	count	%	count	%	count	%	count	%	count	%
Polygonaceae	2	0.47	6	1.3	2	0.54	0	0	1	0.33	0	0	2	0.5	3	1.24
Rosaceae	0	0	0	0	0	0	0	0	0	0	0	0	0	0	0	0
Typha	0	0	0	0	0	0	0	0	0	0	3	1.02	0	0	0	0
Gramineae	2	0.47	0	0	0	0	0	0	2	0.66	0	0	0	0	0	0
Rumex	0	0	0	0	0	0	0	0	0	0	0	0	0	0	0	0
Leguminoseae	0	0	0	0	0	0	0	0	0	0	0	0	0	0	0	0
Cornus	0	0	0	0	0	0	0	0	0	0	0	0	0	0	0	0
Sambucus	0	0	0	0	0	0	0	0	0	0	0	0	0	0	0	0
Unknown	6	1.4	1	0.22	6	1.63	7	2.13	4	1.32	6	2.03	6	1.5	4	1.65
Total spores	**41**		**47**		**31**		**23**		**25**		**27**		**46**		**21**	
L. annotinum	4		1		4		3		1		2		0		1	
L. clavatum	8		5		6		4		4		5		5		2	
L. lucidulum	2		7		2		3		7		5		5		5	
Osmunda spp.	1		4		0		0		1		3		0		0	
Monolete spores	2		13		9		3		4		3		7		7	
trilete spores	10		9		7		4		5		6		11		3	
Sphagnum	14		5		2		6		3		1		17		3	
Cystopteris	0		0		0		0		0		2		0		0	
L. obscurum	0		0		0		0		0		0		0		0	
Dryopteris	0		0		0		0		0		0		0		0	
Isoetes	0		3		1		0		0		0		1		0	

Appendix 11: Pollen and spores counts, and pollen percentages core 95-030-24, La Have Basin

Depth	80-82	TWC	90-92	TWC	100-102	TWC	110-112	TWC	120-122	TWC	130-132	TWC	140-142	TWC	150-152
	count	%	count	%	count	%	count	%	count	%	count	%	count	%	count
Total pollen	**396**		**284**		**341**		**330**		**331**		**325**		**270**		**167**
Total tree pollen	**353**	89.1	**261**	91.9	**325**	95.3	**309**	93.6	**295**	89.1	**311**	95.7	**237**	87.8	**155**
Abies	10	2.53	6	2.11	28	8.21	8	2.42	4	1.21	36	11.1	14	5.19	19
Picea	37	9.34	33	11.6	74	21.7	34	10.3	32	9.67	49	15.1	28	10.4	30
Pinus	206	52	138	48.6	129	37.8	191	57.9	163	49.2	138	42.5	126	46.7	61
Tsuga	29	7.32	24	8.45	28	8.21	22	6.67	21	6.34	40	12.3	14	5.19	18
Acer	12	3.03	14	4.93	8	2.35	9	2.73	13	3.93	8	2.46	6	2.22	2
Betula >25µ	42	10.6	29	10.2	38	11.1	34	10.3	47	14.2	20	6.15	24	8.89	16
Carpinus	0	0	0	0	0	0	0	0	0	0	0	0	0	0	0
Carya	0	0	0	0	0	0	0	0	0	0	0	0	0	0	0
Corylus	0	0	0	0	0	0	0	0	0	0	0	0	0	0	0
Fagus	5	1.26	4	1.41	2	0.59	0	0	3	0.91	10	3.08	7	2.59	4
Fraxinus	0	0	1	0.35	0	0	0	0	1	0.3	0	0	3	1.11	0
Juglans	0	0	0	0	0	0	1	0.3	0	0	0	0	1	0.37	0
Quercus	9	2.27	10	3.52	14	4.11	9	2.73	11	3.32	6	1.85	13	4.81	4
Ulmus	3	0.76	2	0.7	4	1.17	1	0.3	0	0	4	1.23	1	0.37	1
Myrica gale	0	0	0	0	0	0	0	0	0	0	0	0	0	0	0
Ostrya	0	0	0	0	0	0	0	0	0	0	0	0	0	0	0
Tilia	0	0	0	0	0	0	0	0	0	0	0	0	0	0	0
Total shrub pollen	**30**	7.58	**14**	4.93	**2**	0.59	**12**	3.64	**23**	6.95	**8**	2.46	**23**	8.52	**2**
Betula <25 µ	16	4.04	5	1.76	2	0.59	6	1.82	10	3.02	0	2.46	7	2.59	0
Alnus spp	7	1.77	4	1.41	0	0	4	1.21	8	2.42	4	1.23	7	2.59	0
Ericaceae	0	0	1	0.35	0	0	0	0	1	0.3	0	0	2	0.74	0
Ilex /Nemopanthus	0	0	0	0	0	0	0	0	0	0	0	0	0	0	0
Myrica	0	0	0	0	0	0	0	0	0	0	0	0	0	0	0
Salix	7	1.77	4	1.41	0	0	2	0.61	4	1.21	0	0	7	2.59	2
Petalostemum	0	0	0	0	0	0	0	0	0	0	4	1.23	0	0	0
Total herb pollen	**13**	3.28	**9**	3.17	**14**	4.11	**9**	2.73	**13**	3.93	**6**	1.85	**10**	3.7	**10**
Ambrosia	1	0.25	0	0	0	0	0	0	0	0	2	0.62	4	1.48	0
Artemisia	1	0.25	0	0	0	0	0	0	0	0	0	0	0	0	1
Chenopodiaceae	1	0.25	0	0	0	0	1	0.3	0	0	0	0	0	0	0
Cyperaceae	3	0.76	4	1.41	14	4.11	2	0.61	6	1.81	2	0.62	3	1.11	5

Appendix 11: Pollen and spores counts, and pollen percentages core 95-030-24, La Have Basin

Depth	80-82	TWC	90-92	TWC	100-102	TWC	110-112	TWC	120-122	TWC	130-132	TWC	140-142	TWC	150-152
	count	%	count	%	count	%	count	%	count	%	count	%	count	%	count
Polygonaceae	1	0.25	0	0	0	0	1	0.3	1	0.3	2	0.62	0	0	2
Rosaceae	0	0	0	0	0	0	0	0	0	0	0	0	0	0	0
Typha	0	0	0	0	0	0	0	0	0	0	0	0	0	0	0
Gramineae	1	0.25	1	0.35	0	0	1	0.3	1	0.3	0	0	0	0	2
Rumex	0	0	0	0	0	0	0	0	0	0	0	0	0	0	0
Leguminoseae	0	0	0	0	0	0	0	0	0	0	0	0	0	0	0
Cornus	0	0	0	0	0	0	0	0	0	0	0	0	0	0	0
Sambucus	0	0	0	0	0	0	0	0	0	0	0	0	0	0	0
Unknown	5	1.26	4	1.41	0	0	4	1.21	5	1.51	0	0	3	1.11	0
Total spores	**37**		**35**		**24**		**33**		**28**		**10**		**17**		**11**
L. annotinum	3		0		0		1		1		0		0		0
L. clavatum	2		4		6		6		0		0		2		1
L. lucidulum	2		3		2		4		3		0		3		0
Osmunda spp.	5		0		10		2		0		0		2		0
Monolete spores	7		6		2		6		7		0		3		4
trilete spores	7		9		2		10		6		4		2		2
Sphagnum	11		13		0		4		11		0		5		3
Cystopteris	0		0		0		0		0		0		0		0
L. obscurum	0		0		0		0		0		6		0		0
Dryopteris	0		0		0		0		0		0		0		0
Isoetes	0		0		2		0		0		0		0		1

Appendix 11: Pollen and spores counts, and pollen percentages core 95-030-24, La Have Basin

Depth	TWC	160-162	TWC	170-172	TWC	180-182	TWC	0-2	P	10-12	P	20-22	P	30-32	P	40-42
	%	count	%	count	%	count	%	count	%	count	%	count	%	count	%	count
Total pollen		**267**		**362**		**420**		**206**		**398**		**379**		**228**		**356**
Total tree pollen	92.81	**241**	90.26	**332**	91.21	**370**	88.1	**195**	94.7	**376**	94.5	**359**	94.7	**220**	96.5	**332**
Abies	11.38	14	5.243	15	4.121	12	2.857	39	18.9	55	13.8	54	14.2	15	6.58	25
Picea	17.96	34	12.73	44	12.09	36	8.571	34	16.5	57	14.3	50	13.2	27	11.8	52
Pinus	36.53	135	50.56	171	46.98	223	53.1	102	49.5	188	47.2	127	33.5	94	41.2	161
Tsuga	10.78	12	4.494	23	6.319	25	5.952	11	5.34	24	6.03	48	12.7	22	9.65	40
Acer	1.198	7	2.622	13	3.571	16	3.81	5	2.43	2	0.5		0	12	5.26	8
Betula >25µ	9.581	26	9.738	55	15.11	44	10.48	0	0	28	7.04	60	15.8	36	15.8	26
Carpinus	0	0	0	0	0	0	0	0	0	0	0	0	0	0	0	2
Carya	0	0	0	0	0	1	0.238	0	0	0	0	0	0	0	0	2
Corylus	0	0	0	0	0	0	0	0	0	6	1.51	0	0	0	0	2
Fagus	2.395	0	0	0	0	3	0.714	0	0	8	2.01	6	1.58	4	1.75	8
Fraxinus	0	1	0.375	3	0.824	1	0.238	2	0.97	0	0	0	0	0	0	0
Juglans	0	0	0	0	0	0	0	0	0	0	0	0	0	0	0	2
Quercus	2.395	12	4.494	7	1.923	9	2.143	0	0	8	2.01	10	2.64	10	4.39	4
Ulmus	0.599	0	0	0	0	0	0	1	0.49	0	0	4	1.06	0	0	0
Myrica gale	0	0	0	0	0	0	0	1	0.49	0	0	0	0	0	0	0
Ostrya	0	0	0	0	0	0	0	0	0	0	0	0	0	0	0	0
Tilia	0	0	0	1	0.275	0	0	0	0	0	0	0	0	0	0	0
Total shrub pollen	1.198	**18**	6.742	**20**	5.495	**37**	8.81	**3**	1.46	**6**	1.51	**2**	0.53	**2**	0.88	**6**
Betula <25 µ	0	5	1.873	11	3.022	20	4.762	3	1.46	4	1.01	0	0	2	0.88	4
Alnus spp	0	7	2.622	3	0.824	9	2.143	0	0	0	0	0	0	0	0	0
Ericaceae	0	1	0.375	1	0.275	0	0	0	0	2	0.5	2	0.53	0	0	0
Ilex /Nemopanthus	0	0	0	0	0	0	0	0	0	0	0	0	0	0	0	0
Myrica	0	0	0	0	0	0	0	0	0	0	0	0	0	0	0	2
Salix	1.198	5	1.873	5	1.374	8	1.905	0	0	0	0	0	0	0	0	0
Petalostemum	0	0	0	0	0	0	0	0	0	0	0	0	0	0	0	0
Total herb pollen	5.988	**8**	2.996	**10**	2.747	**13**	3.095	**8**	3.88	**16**	4.02	**18**	4.75	**6**	2.63	**18**
Ambrosia	0	0	0	1	0.275	3	0.714	1	0.49	2	0.5	6	1.58	0	0	2
Artemisia	0.599	0	0	0	0	0	0	2	0.97	2	0.5	0	0	0	0	0
Chenopodiaceae	0	0	0	0	0	1	0.238	1	0.49	0	0	0	0	0	0	0
Cyperaceae	2.994	5	1.873	1	0.275	3	0.714	0	0	0	0	6	1.58	4	1.75	4

Appendix 11: Pollen and spores counts, and pollen percentages core 95-030-24, La Have Basin

Depth	TWC	160-162	TWC	170-172	TWC	180-182	TWC	0-2	P	10-12	P	20-22	P	30-32	P	40-42
	%	count	%	count	%	count	%	count	%	count	%	count	%	count	%	count
Polygonaceae	1.198	0	0	0	0	1	0.238	0	0	4	1.01	2	0.53	2	0.88	10
Rosaceae	0	0	0	0	0	0	0	0	0	4	1.01	0	0	0	0	0
Typha	0	0	0	0	0	0	0	0	0	2	0.5	0	0	0	0	0
Gramineae	1.198	0	0	2	0.549	0	0	0	0	0	0	0	0	0	0	0
Rumex	0	0	0	1	0.275	0	0	0	0	0	0	2	0.53	0	0	0
Leguminoseae	0	0	0	0	0	0	0	0	0	2	0	2	0.53	0	0	2
Cornus	0	0	0	0	0	0	0	4	1.94	0	0	0	0	0	0	0
Sambucus	0	0	0	0	0	0	0	0	0	0	0	0	0	0	0	0
Unknown	0	3	1.124	5	1.374	5	1.19	0	0	0	0	0	0	0	0	0
Total spores		**20**		**17**		**36**		**14**		**18**		**34**		**20**		**20**
L. annotinum		2		1		0		0		2		4		2		2
L. clavatum		2		0		3		3		2		4		6		4
L. lucidulum		3		2		1		3		2		10		4		6
Osmunda spp.		1		1		2		0		2		0		2		0
Monolete spores		3		4		6		0		2		4		2		2
trilete spores		4		6		7		3		0		2		2		2
Sphagnum		5		3		17		3		6		10		2		4
Cystopteris		0		0		0		0		0		0		0		0
L. obscurum		0		0		0		0		2		0		0		0
Dryopteris		0		0		0		2		0		0		0		0
Isoetes		0		0		0		0		0		0		0		0

Appendix 11: Pollen and spores counts, and pollen percentages core 95-030-24, La Have Basin

Depth	P	50-52	P	60-62	P	80-82	P	90-92	P	100-102	P	120-122	P	140-142	P
	%	count	%	count	%	count	%	count	%	count	%	count	%	count	%
Total pollen		**307**		**288**		**115**		**336**		**400**		**497**		**386**	
Total tree pollen	92.7	**284**	92.5	**271**	93.77	**113**	100	**328**	97.6	**368**	92	**476**	95.77	**378**	97.93
Abies	6.98	46	15	20	6.92	5	4.425	38	11.3	10	2.5	39	7.847	63	16.32
Picea	14.5	24	7.82	41	14.19	29	25.66	25	7.44	63	15.8	67	13.48	61	15.8
Pinus	45	102	33.2	115	39.79	54	47.79	171	50.9	225	56.3	287	57.75	199	51.55
Tsuga	11.2	42	13.7	33	11.42	11	9.735	22	6.55	28	7	35	7.042	34	8.808
Acer	2.23	14	4.56	6	2.076	6	5.31	22	6.55	8	2	15	3.018	5	1.295
Betula >25µ	7.26	46	15	40	13.84	5	4.425	49	14.6	19	4.75	30	6.036	9	2.332
Carpinus	0.56	0	0	0	0	0	0	0	0	0	0	0	0	0	0
Carya	0.56	0	0	0	0	0	0	0	0	0	0	0	0	0	0
Corylus	0.56	0	0	0	0	0	0	0	0	0	0	0	0	0	0
Fagus	2.23	2	0.65	4	1.384	1	0.885	1	0.3	1	0.25	2	0.402	4	1.036
Fraxinus	0	2	0.65	0	0	1	0.885	0	0	0	0	0	0	0	0
Juglans	0.56	0	0	0	0	0	0	0	0	0	0	0	0	0	0
Quercus	1.12	6	1.95	6	2.076	1	0.885	0	0	14	3.5	1	0.201	3	0.777
Ulmus	0	0	0	2	0.692	0	0	0	0	0	0	0	0	0	0
Myrica gale	0	0	0	0	0	0	0	0	0	0	0	0	0	0	0
Ostrya	0	0	0	2	0.692	0	0	0	0	0	0	0	0	0	0
Tilia	0	0	0	2	0.692	0	0	0	0	0	0	0	0	0	0
Total shrub pollen	1.68	**4**	1.3	**2**	0.692	**0**	0	**2**	0.6	**21**	5.25	**16**	3.219	**2**	0.518
Betula <25 µ	1.12	0	0	1	0.346	0	0	2	0.6	17	4.25	15	3.018	1	0.259
Alnus spp	0	2	0.65	0	0	0	0	0	0	3	0.75	0	0	0	0
Ericaceae	0	1	0.33	1	0.346	0	0	0	0	1	0.25	0	0	1	0.259
Ilex /Nemopanthus	0	0	0	0	0	0	0	0	0	0	0	0	0	0	0
Myrica	0.56	0	0	0	0	0	0	0	0	0	0	0	0	0	0
Salix	0	1	0.33	0	0	0	0	0	0	0	0	1	0.201	0	0
Petalostemum	0	0	0	0	0	0	0	0	0	0	0	0	0	0	0
Total herb pollen	5.03	**19**	6.19	**15**	5.19	**2**	1.77	**6**	1.79	**11**	2.75	**5**	1.006	**6**	1.554
Ambrosia	0.56	0	0	4	1.384	1	0.885	0	0	1	0.25	1	0.201	0	0
Artemisia	0	2	0.65	2	0.692	0	0	0	0	1	0.25	0	0	0	0
Chenopodiaceae	0	0	0	0	0	0	0	0	0	0	0	0	0	0	0
Cyperaceae	1.12	10	3.26	1	0.346	1	0.885	5	1.49	5	1.25	3	0.604	6	1.554

Appendix 11: Pollen and spores counts, and pollen percentages core 95-030-24, La Have Basin

Depth	P	50-52	P	60-62	P	80-82	P	90-92	P	100-102	P	120-122	P	140-142	P
	%	count	%	count	%	count	%	count	%	count	%	count	%	count	%
Polygonaceae	2.79	7	2.28	4	1.384	0	0	0	0	2	0.5	0	0	0	0
Rosaceae	0	0	0	4	1.384	0	0	0	0	0	0	0	0	0	0
Typha	0	0	0	0	0	0	0	0	0	0	0	0	0	0	0
Gramineae	0	0	0	0	0	0	0	1	0.3	0	0	1	0.201	0	0
Rumex	0	0	0	0	0	0	0	0	0	0	0	0	0	0	0
Leguminoseae	0.56	0	0	0	0	0	0	0	0	0	0	0	0	0	0
Cornus	0	0	0	0	0	0	0	0	0	2	0.5	0	0	0	0
Sambucus	0	0	0	0	0	0	0	0	0	0	0	0	0	0	0
Unknown	0	0	0	0	0	0	0	0	0	0	0	0	0	0	0
Total spores		**12**		**12**		**7**		**30**		**24**		**38**		**25**	
L. annotinum		2		0		1		0		2		4		3	
L. clavatum		2		2		1		8		3		5		4	
L. lucidulum		4		2		1		6		6		7		6	
Osmunda spp.		0		0		1		3		1		1		4	
Monolete spores		0		0		0		3		1		3		4	
trilete spores		2		2		3		6		4		5		0	
Sphagnum		0		4		0		4		7		13		4	
Cystopteris		0		0		0		0		0		0		0	
L. obscurum		0		0		0		0		0		0		0	
Dryopteris		0		0		0		0		0		0		0	
Isoetes		2		2		0		0		0		0		0	

Appendix 11: Pollen and spores counts, and pollen percentages core 95-030-24, La Have Basin

Depth	160-162	P	180-182	P	200-202	P	220-222	P	240-242	P	260-262	P	280-282	P	300-302
	count	%	count	%	count	%	count	%	count	%	count	%	count	%	count
Total pollen	**381**		**384**		**458**		**470**		**332**		**539**		**474**		**448**
Total tree pollen	**372**	97.6	**365**	95.1	**447**	97.6	**463**	98.5	**329**	99.1	**514**	94.8	**464**	97.9	**441**
Abies	41	10.8	7	1.82	26	5.677	43	9.15	50	15.06	36	6.64	8	1.69	41
Picea	33	8.66	27	7.03	74	16.16	81	17.2	45	13.55	48	8.86	39	8.23	57
Pinus	216	56.7	267	69.5	277	60.48	272	57.9	147	44.28	313	57.7	360	75.9	243
Tsuga	36	9.45	26	6.77	30	6.55	37	7.87	72	21.69	81	14.9	49	10.3	88
Acer	11	2.89	10	2.6	10	2.183	4	0.85	10	3.012	14	2.58	3	0.63	4
Betula >25µ	29	7.61	20	5.21	20	4.367	18	3.83	4	1.205	16	2.95	2	0.42	8
Carpinus	0	0	0	0	0	0	0	0	0	0	0	0	0	0	0
Carya	0	0	0	0	0	0	0	0	0	0	0	0	0	0	0
Corylus	0	0	0	0	0	0	0	0	1	0.301	0	0	0	0	0
Fagus	3	0.79	0	0	1	0.218	0	0	0	0	0	0	0	0	0
Fraxinus	0	0	0	0	0	0	0	0	0	0	0	0	0	0	0
Juglans	0	0	0	0	0	0	0	0	0	0	0	0	0	0	0
Quercus	3	0.79	8	2.08	9	1.965	8	1.7	0	0	6	1.11	2	0.42	0
Ulmus	0	0	0	0	0	0	0	0	0	0	0	0	1	0.21	0
Myrica gale	0	0	0	0	0	0	0	0	0	0	0	0	0	0	0
Ostrya	0	0	0	0	0	0	0	0	0	0	0	0	0	0	0
Tilia	0	0	0	0	0	0	0	0	0	0	0	0	0	0	0
Total shrub pollen	**6**	1.57	**10**	2.6	**6**	1.31	**2**	0.43	**3**	0.904	**14**	2.58	**2**	0.42	**2**
Betula <25 µ	5	1.31	10	2.6	5	1.092	2	0.43	3	0.904	10	1.85	1	0.21	1
Alnus spp	0	0	0	0	0	0	0	0	0	0	3	0.55	0	0	0
Ericaceae	1	0.26	0	0	0	0	0	0	0	0	1	0.18	0	0	1
Ilex /Nemopanthus	0	0	0	0	0	0	0	0	0	0	0	0	0	0	0
Myrica	0	0	0	0	0	0	0	0	0	0	0	0	0	0	0
Salix	0	0	0	0	1	0.218	0	0	0	0	0	0	1	0.21	0
Petalostemum	0	0	0	0	0	0	0	0	0	0	0	0	0	0	0
Total herb pollen	**3**	0.79	**9**	2.34	**5**	1.092	**5**	1.06	**0**	0	**11**	2.03	**8**	1.69	**5**
Ambrosia	0	0	1	0.26	1	0.218	0	0	0	0	2	0.37	0	0	0
Artemisia	0	0	1	0.26	0	0	1	0.21	0	0	0	0	1	0.21	0
Chenopodiaceae	0	0	0	0	0	0	0	0	0	0	1	0.18	0	0	0
Cyperaceae	3	0.79	5	1.3	2	0.437	1	0.21	0	0	3	0.55	3	0.63	2

Appendix 11: Pollen and spores counts, and pollen percentages core 95-030-24, La Have Basin

Depth	160-162	P	180-182	P	200-202	P	220-222	P	240-242	P	260-262	P	280-282	P	300-302
	count	%	count	%	count	%	count	%	count	%	count	%	count	%	count
Polygonaceae	0	0	2	0.52	0	0	0	0	0	0	2	0.37	1	0.21	3
Rosaceae	0	0	0	0	0	0	0	0	0	0	0	0	0	0	0
Typha	0	0	0	0	0	0	0	0	0	0	0	0	0	0	0
Gramineae	0	0	0	0	0	0	0	0	0	0	0	0	0	0	0
Rumex	0	0	0	0	0	0	0	0	0	0	0	0	0	0	0
Leguminoseae	0	0	0	0	0	0	0	0	0	0	0	0	0	0	0
Cornus	0	0	0	0	1	0.218	0	0	0	0	0	0	1	0.21	0
Sambucus	0	0	0	0	1	0.218	3	0.64	0	0	2	0.37	0	0	0
Unknown	0	0	0	0	0	0	0	0	0	0	1	0.18	2	0.42	0
Total spores	**28**		**38**		**20**		**34**		**14**		**48**		**26**		**29**
L. annotinum	4		2		1		2		0		0		1		2
L. clavatum	4		12		5		10		1		6		3		4
L. lucidulum	5		5		6		8		3		2		1		4
Osmunda spp.	3		2		1		3		3		5		3		2
Monolete spores	4		2		3		1		1		9		9		5
trilete spores	1		2		0		2		1		6		3		2
Sphagnum	7		13		4		8		5		20		6		10
Cystopteris	0		0		0		0		0		0		0		0
L. obscurum	0		0		0		0		0		0		0		0
Dryopteris	0		0		0		0		0		0		0		0
Isoetes	0		0		0		0		0		0		0		0

Appendix 11: Pollen and spores counts, and pollen percentages core 95-030-24, La Have Basin

Depth	P	320-322	P	340-342	P	360-362	P	380-382	P	400-402	P	420-422	P	440-442	P
	%	count	%	count	%	count	%	count	%	count	%	count	%	count	%
Total pollen		**338**		**715**		**885**		**880**		**887**		**635**		**693**	
Total tree pollen	98.44	**327**	96.7	**703**	98.3	**867**	97.97	**863**	98.1	**867**	97.7	**605**	95	**684**	98.7
Abies	9.152	6	1.78	58	8.11	76	8.588	69	7.84	106	12	9	1.41	19	2.742
Picea	12.72	22	6.51	37	5.17	95	10.73	79	8.98	53	5.98	30	4.71	68	9.812
Pinus	54.24	260	76.9	502	70.2	547	61.81	586	66.6	592	66.7	486	76.3	550	79.37
Tsuga	19.64	30	8.88	83	11.6	124	14.01	107	12.2	88	9.92	56	8.79	33	4.762
Acer	0.893	1	0.3	7	0.98	6	0.678	1	0.11	10	1.13	5	0.78	4	0.577
Betula >25µ	1.786	2	0.59	6	0.84	10	1.13	12	1.36	12	1.35	2	0.31	2	0.289
Carpinus	0	0	0	0	0	0	0	0	0	0	0	0	0	0	0
Carya	0	0	0	0	0	0	0	0	0	0	0	0	0	0	0
Corylus	0	0	0	0	0	0	0	0	0	0	0	0	0	0	0
Fagus	0	0	0	0	0	0	0	0	0	1	0.11	0	0	0	0
Fraxinus	0	0	0	0	0	2	0.226	5	0.57	0	0	2	0.31	0	0
Juglans	0	0	0	0	0	1	0.113	0	0	0	0	0	0	0	0
Quercus	0	6	1.78	10	1.4	5	0.565	4	0.45	4	0.45	12	1.88	7	1.01
Ulmus	0	0	0	0	0	1	0.113	0	0	1	0.11	3	0.47	1	0.144
Myrica gale	0	0	0	0	0	0	0	0	0	0	0	0	0	0	0
Ostrya	0	0	0	0	0	0	0	0	0	0	0	0	0	0	0
Tilia	0	0	0	0	0	0	0	0	0	0	0	0	0	0	0
Total shrub pollen	0.446	**7**	2.07	**5**	0.7	**15**	1.695	**9**	1.02	**13**	1.47	**18**	2.83	**5**	0.722
Betula <25 µ	0.223	0	0	5	0.7	2	0.226	1	0.11	2	0.23	9	1.41	2	0.289
Alnus spp	0	0	0	0	0	0	0	0	0	1	0.11	2	0.31	0	0
Ericaceae	0.223	0	0	0	0	2	0.226	0	0	1	0.11	0	0	1	0.144
Ilex /Nemopanthus	0	0	0	0	0	0	0	0	0	0	0	0	0	0	0
Myrica	0	0	0	0	0	0	0	0	0	0	0	0	0	0	0
Salix	0	7	2.07	0	0	11	1.243	8	0.91	9	1.01	7	1.1	2	0.289
Petalostemum	0	0	0	0	0	0	0	0	0	0	0	0	0	0	0
Total herb pollen	1.116	**4**	1.18	**7**	0.98	**3**	0.339	**8**	0.91	**7**	0.79	**12**	1.88	**4**	0.577
Ambrosia	0	0	0	0	0	0	0	0	0	1	0.11	0	0	0	0
Artemisia	0	0	0	0	0	0	0	0	0	0	0	0	0	0	0
Chenopodiaceae	0	1	0.3	2	0.28	0	0	0	0	0	0	1	0.16	0	0
Cyperaceae	0.446	1	0.3	5	0.7	3	0.339	5	0.57	3	0.34	4	0.63	2	0.289

Appendix 11: Pollen and spores counts, and pollen percentages core 95-030-24, La Have Basin

Depth	P	320-322	P	340-342	P	360-362	P	380-382	P	400-402	P	420-422	P	440-442	P
	%	count	%	count	%	count	%	count	%	count	%	count	%	count	%
Polygonaceae	0.67	2	0.59	0	0	0	0	2	0.23	3	0.34	3	0.47	2	0.289
Rosaceae	0	0	0	0	0	0	0	0	0	0	0	0	0	0	0
Typha	0	0	0	0	0	0	0	0	0	0	0	0	0	0	0
Gramineae	0	0	0	0	0	0	0	0	0	0	0	0	0	0	0
Rumex	0	0	0	0	0	0	0	0	0	0	0	0	0	0	0
Leguminoseae	0	0	0	0	0	0	0	0	0	0	0	0	0	0	0
Cornus	0	0	0	0	0	0	0	0	0	0	0	0	0	0	0
Sambucus	0	0	0	0	0	0	0	0	0	0	0	0	0	0	0
Unknown	0	0	0	0	0	0	0	1	0.11	0	0	4	0.63	0	0
Total spores		**30**		**40**		**83**		**68**		**71**		**36**		**31**	
L. annotinum		0		2		5		7		9		4		3	
L. clavatum		12		6		8		19		10		9		9	
L. lucidulum		2		3		1		5		4		5		1	
Osmunda spp.		2		3		9		8		12		3		3	
Monolete spores		7		4		5		20		7		4		4	
trilete spores		2		3		1		2		4		1		5	
Sphagnum		5		19		53		7		25		10		6	
Cystopteris		0		0		1		0		0		0		0	
L. obscurum		0		0		0		0		0		0		0	
Dryopteris		0		0		0		0		0		0		0	
Isoetes		0		0		0		0		0		0		0	

Appendix 11: Pollen and spores counts, and pollen percentages core 95-030-24, La Have Basin

Depth	460-462	P	480-482	P	500-502	P	520-522	P	540-542	P	560-562 P		580-582 P		600-6
	count	%	count	%	count	%	count	%	count	%	count	%	count	%	count
Total pollen	**377**		**298**		**351**		**218**		**265**		**403**		**323**		**280**
Total tree pollen	**358**	95	**290**	97.3	**343**	97.7	**213**	97.7	**253**	95.5	**388**	96.3	**313**	96.9	**274**
Abies	5	1.33	2	0.67	23	6.55	26	11.9	9	3.4	12	2.98	7	2.167	36
Picea	18	4.77	9	3.02	18	5.13	7	3.21	10	3.77	63	15.6	8	2.477	9
Pinus	309	82	248	83.2	253	72.1	161	73.9	212	80	288	71.5	275	85.14	221
Tsuga	7	1.86	11	3.69	28	7.98	8	3.67	10	3.77	14	3.47	6	1.858	5
Acer	3	0.8	3	1.01	2	0.57	3	1.38	2	0.75	1	0.25	0	0	0
Betula >25µ	3	0.8	5	1.68	5	1.42	2	0.92	2	0.75	2	0.5	4	1.238	0
Carpinus	0	0	0	0	0	0	0	0	0	0	0	0	0	0	0
Carya	0	0	0	0	0	0	0	0	0	0	0	0	0	0	0
Corylus	0	0	0	0	0	0	0	0	0	0	0	0	0	0	0
Fagus	0	0	0	0	0	0	0	0	0	0	0	0	0	0	0
Fraxinus	0	0	0	0	0	0	0	0	0	0	0	0	0	0	0
Juglans	0	0	0	0	0	0	0	0	0	0	0	0	0	0	0
Quercus	13	3.45	11	3.69	14	3.99	6	2.75	8	3.02	8	1.99	13	4.025	3
Ulmus	0	0	1	0.34	0	0	0	0	0	0	0	0	0	0	0
Myrica gale	0	0	0	0	0	0	0	0	0	0	0	0	0	0	0
Ostrya	0	0	0	0	0	0	0	0	0	0	0	0	0	0	0
Tilia	0	0	0	0	0	0	0	0	0	0	0	0	0	0	0
Total shrub pollen	**12**	3.18	**8**	2.68	**6**	1.71	**3**	1.38	**9**	3.4	**14**	3.47	**7**	2.167	**6**
Betula <25 µ	6	1.59	2	0.67	1	0.28	2	0.92	5	1.89	2	0.5	2	0.619	2
Alnus spp	0	0	0	0	0	0	0	0	0	0	0	0	0	0	0
Ericaceae	0	0	0	0	0	0	0	0	0	0	0	0	0	0	0
Ilex /Nemopanthus	0	0	0	0	0	0	0	0	0	0	0	0	0	0	0
Myrica	0	0	0	0	0	0	0	0	0	0	0	0	0	0	0
Salix	6	1.59	6	2.01	5	1.42	1	0.46	4	1.51	12	2.98	5	1.548	4
Petalostemum	0	0	0	0	0	0	0	0	0	0	0	0	0	0	0
Total herb pollen	**7**	1.86	**0**	0	**2**	0.57	**2**	0.92	**3**	1.13	**1**	0.25	**3**	0.929	**0**
Ambrosia	0	0	0	0	1	0.28	0	0	0	0	0	0	0	0	0
Artemisia	1	0.27	0	0	0	0	0	0	1	0.38	0	0	0	0	0
Chenopodiaceae	1	0.27	0	0	0	0	0	0	0	0	0	0	0	0	0
Cyperaceae	4	1.06	0	0	1	0.28	1	0.46	2	0.75	1	0.25	2	0.619	0

Appendix 11: Pollen and spores counts, and pollen percentages core 95-030-24, La Have Basin

Depth	460-462	P	480-482	P	500-502	P	520-522	P	540-542	P	560-562 P		580-582 P		600-6
	count	%	count	%	count	%	count	%	count	%	count	%	count	%	count
Polygonaceae	1	0.27	0	0	0	0	0	0	0	0	0	0	0	0	0
Rosaceae	0	0	0	0	0	0	0	0	0	0	0	0	0	0	0
Typha	0	0	0	0	0	0	0	0	0	0	0	0	0	0	0
Gramineae	0	0	0	0	0	0	0	0	0	0	0	0	0	0	0
Rumex	0	0	0	0	0	0	0	0	0	0	0	0	0	0	0
Leguminoseae	0	0	0	0	0	0	0	0	0	0	0	0	0	0	0
Cornus	0	0	0	0	0	0	0	0	0	0	0	0	0	0	0
Sambucus	0	0	0	0	0	0	0	0	0	0	0	0	0	0	0
Unknown	0	0	0	0	0	0	1	0.46	0	0	0	0	1	0.31	0
Total spores	**29**		**16**		**24**		**22**		**21**		**24**		**22**		**15**
L. annotinum	5		3		3		3		2		5		2		0
L. clavatum	4		5		9		3		9		5		7		7
L. lucidulum	2		0		0		1		1		2		1		0
Osmunda spp.	3		2		1		4		2		3		1		3
Monolete spores	2		2		3		3		2		5		5		2
trilete spores	7		2		4		6		5		3		5		3
Sphagnum	6		2		4		2		0		1		1		0
Cystopteris	0		0		0		0		0		0		0		0
L. obscurum	0		0		0		0		0		0		0		0
Dryopteris	0		0		0		0		0		0		0		0
Isoetes	0		0		0		0		0		0		0		0

Appendix 11: Pollen and spores counts, and pollen percentages core 95-030-24, La Have Basin

Depth	2 P	620-622 P		640-642 P		660-662 P		680-682 P		700-702 P		720-722 P		740-742 P		760-762 P	
	%	count	%	count	%	count	%	count	%	count	%	count	%	count	%	count	%
Total pollen		**290**		**324**		**248**		**252**		**238**		**220**		**197**		**145**	
Total tree pollen	97.86	**285**	98.28	**311**	96	**229**	92.7	**241**	95.6	**222**	93.3	**195**	89.45	**160**	81.2	**101**	71.13
Abies	12.86	40	13.79	17	5.25	3	1.21	11	4.37	27	11.3	9	4.128	2	1.02	6	4.225
Picea	3.214	3	1.034	15	4.63	37	15	54	21.4	41	17.2	53	24.31	43	21.8	27	19.01
Pinus	78.93	224	77.24	247	76.2	176	71.3	163	64.7	141	59.2	127	58.26	108	54.8	60	42.25
Tsuga	1.786	9	3.103	11	3.4	7	2.83	3	1.19	2	0.84	2	0.917	0	0	2	1.408
Acer	0	1	0.345	3	0.93	3	1.21	0	0	0	0	0	0	3	1.52	2	1.408
Betula >25µ	0	4	1.379	5	1.54	0	0	1	0.4	2	0.84	3	1.376	1	0.51	3	2.113
Carpinus	0	0	0	0	0	0	0	0	0	0	0	0	0	0	0	0	0
Carya	0	0	0	0	0	0	0	0	0	0	0	0	0	0	0	0	0
Corylus	0	0	0	0	0	0	0	0	0	0	0	0	0	0	0	0	0
Fagus	0	0	0	0	0	0	0	0	0	0	0	0	0	0	0	0	0
Fraxinus	0	0	0	0	0	0	0	0	0	0	0	0	0	0	0	0	0
Juglans	0	0	0	0	0	0	0	0	0	0	0	0	0	0	0	0	0
Quercus	1.071	4	1.379	11	3.4	3	1.21	8	3.17	9	3.78	1	0.459	1	0.51	1	0.704
Ulmus	0	0	0	2	0.62	0	0	1	0.4	0	0	0	0	2	1.02	0	0
Myrica gale	0	0	0	0	0	0	0	0	0	0	0	0	0	0	0	0	0
Ostrya	0	0	0	0	0	0	0	0	0	0	0	0	0	0	0	0	0
Tilia	0	0	0	0	0	0	0	0	0	0	0	0	0	0	0	0	0
Total shrub pollen	2.143	**4**	1.379	**6**	1.85	**12**	4.86	**3**	1.19	**8**	3.36	**18**	8.257	**22**	11.2	**18**	12.68
Betula <25 µ	0.714	1	0.345	0	0	4	1.62	1	0.4	1	0.42	5	2.294	3	1.52	6	4.225
Alnus spp	0	1	0.345	1	0.31	2	0.81	0	0	0	0	4	1.835	3	1.52	1	0.704
Ericaceae	0	0	0	0	0	1	0.4	0	0	1	0.42	0	0	2	1.02	1	0.704
Ilex /Nemopanthus	0	0	0	0	0	0	0	0	0	0	0	0	0	0	0	0	0
Myrica	0	0	0	0	0	0	0	0	0	0	0	0	0	0	0	0	0
Salix	1.429	2	0.69	5	1.54	5	2.02	2	0.79	6	2.52	9	4.128	14	7.11	10	7.042
Petalostemum	0	0	0	0	0	0	0	0	0	0	0	0	0	0	0	0	0
Total herb pollen	0	**1**	0.345	**7**	2.16	**7**	2.83	**8**	3.17	**8**	3.36	**7**	3.211	**15**	7.61	**26**	18.31
Ambrosia	0	0	0	0	0	0	0	0	0	0	0	1	0.459	1	0.51	0	0
Artemisia	0	0	0	0	0	0	0	0	0	0	0	1	0.459	0	0	1	0.704
Chenopodiaceae	0	0	0	0	0	0	0	0	0	1	0.42	0	0	0	0	0	0
Cyperaceae	0	1	0.345	4	1.23	5	2.02	4	1.59	4	1.68	2	0.917	8	4.06	16	11.27

Appendix 11: Pollen and spores counts, and pollen percentages core 95-030-24, La Have Basin

Depth	2 P	620-622 P		640-642 P		660-662 P		680-682 P		700-702 P		720-722 P		740-742 P		760-762 P	
	%	count	%	count	%	count	%	count	%	count	%	count	%	count	%	count	%
Polygonaceae	0	0	0	0	0	0	0	0	0	0	0	0	0	0	0	3	2.113
Rosaceae	0	0	0	0	0	0	0	0	0	0	0	0	0	0	0	0	0
Typha	0	0	0	0	0	0	0	0	0	0	0	0	0	0	0	0	0
Gramineae	0	0	0	0	0	1	0.4	0	0	0	0	0	0	0	0	1	0.704
Rumex	0	0	0	0	0	0	0	0	0	0	0	0	0	0	0	0	0
Leguminoseae	0	0	0	0	0	0	0	0	0	0	0	0	0	0	0	0	0
Cornus	0	0	0	0	0	0	0	0	0	0	0	0	0	0	0	0	0
Sambucus	0	0	0	0	0	0	0	0	0	0	0	0	0	0	0	0	0
Unknown	0	0	0	3	0.93	1	0.4	4	1.59	3	1.26	3	1.376	6	3.05	5	3.521
Total spores		**25**		**22**		**17**		**41**		**38**		**40**		**54**		**27**	
L. annotinum		2		1		6		6		5		9		14		3	
L. clavatum		13		6		6		16		18		12		21		14	
L. lucidulum		0		1		0		0		0		0		0		0	
Osmunda spp.		6		4		0		5		8		5		5		3	
Monolete spores		1		3		1		9		3		8		8		4	
trilete spores		1		2		2		3		3		3		2		2	
Sphagnum		2		5		0		2		1		3		3		1	
Cystopteris		0		0		0		0		0		0		0		0	
L. obscurum		0		0		0		0		0		0		0		0	
Dryopteris		0		0		0		0		0		0		1		0	
Isoetes		0		0		2		0		0		0		0		0	

Appendix 11: Pollen and spores counts, and pollen percentages core 95-030-24, La Have Basin

Depth	780-782 P		800-802 P		820-822 P	
	count	%	count	%	count	%
Total pollen	**207**		**216**		**203**	
Total tree pollen	**156**	76.1	**187**	86.57	**169**	83.25
Abies	29	14.15	14	6.481	16	7.882
Picea	8	3.902	49	22.69	44	21.67
Pinus	101	49.27	102	47.22	86	42.36
Tsuga	4	1.951	3	1.389	4	1.97
Acer	8	3.902	1	0.463	0	0
Betula >25µ	5	2.439	16	7.407	13	6.404
Carpinus	0	0	0	0	0	0
Carya	1	0.488	1	0.463	2	0.985
Corylus	0	0	1	0.463	0	0
Fagus	0	0	0	0	0	0
Fraxinus	0	0	0	0	0	0
Juglans	0	0	0	0	0	0
Quercus	0	0	0	0	0	0
Ulmus	0	0	0	0	4	1.97
Myrica gale	0	0	0	0	0	0
Ostrya	0	0	0	0	0	0
Tilia	0	0	0	0	0	0
Total shrub pollen	**23**	11.22	**17**	7.87	**29**	14.29
Betula <25 µ	1	0.488	1	0.463	11	5.419
Alnus spp	2	0.976	1	0.463	3	1.478
Ericaceae	5	2.439	1	0.463	3	1.478
Ilex /Nemopanthus	0	0	0	0	0	0
Myrica	0	0	0	0	0	0
Salix	15	7.317	14	6.481	12	5.911
Petalostemum	0	0	0	0	0	0
Total herb pollen	**28**	13.66	**12**	5.556	**5**	2.463
Ambrosia	1	0.488	0	0	1	0.493
Artemisia	0	0	1	0.463	0	0
Chenopodiaceae	0	0	0	0	0	0
Cyperaceae	11	5.366	6	2.778	2	0.985

Appendix 11: Pollen and spores counts, and pollen percentages core 95-030-24, La Have Basin

Depth	780-782 P		800-802 P		820-822 P	
	count	%	count	%	count	%
Polygonaceae	11	5.366	0	0	0	0
Rosaceae	0	0	0	0	0	0
Typha	0	0	0	0	0	0
Gramineae	1	0.488	0	0	0	0
Rumex	0	0	0	0	0	0
Leguminoseae	0	0	0	0	0	0
Cornus	0	0	0	0	0	0
Sambucus	0	0	0	0	0	0
Unknown	4	1.951	5	2.315	2	0.985
Total spores	**21**		**8**		**10**	
L. annotinum	8		3		3	
L. clavatum	8		0		4	
L. lucidulum	0		1		0	
Osmunda spp.	0		1		2	
Monolete spores	4		0		0	
trilete spores	0		0		0	
Sphagnum	0		3		1	
Cystopteris	0		0		0	
L. obscurum	0		0		0	
Dryopteris	1		0		0	
Isoetes	0		0		0	

Appendix 12: Dinoflagellate cysts counts and percentages core 95-030-24, LaHave Basin

Depth (cm)	0-2 G		10-12 G		20-22 G		30-32 G		40-42 G	
Dinocyst species	count	%	cou	%	cou	%	coun	%	cou	%
Total cysts	**313**		**339**		**276**		**253**		**269**	
Achomosphaera		0		0		0	1	0.4		0
cf.Alexandrium excavatum	1	0.32		0		0	1	0.4	1	0.37
Ataxodinium choanum	1	0.32	2	0.59	3	1.09		0		0
Bitectatodinium tepikiense	2	0.64	2	0.59	3	1.09	1	0.4	1	0.37
Impagidinium aculeatum		0	1	0.29	1	0.36		0	1	0.37
Impagidinium pallidum		0		0		0		0		0
Impagidinium patulum		0		0		0		0		0
Impagidinium sphaericum		0		0		0		0		0
Impagidinium spp.		0		0	1	0.36		0		0
Impagidinium strialatum		0		0		0		0		0
Lingulodinium machaerophorum		0		0	1	0.36		0		0
Nematosphaerosis labyrinthus	5	1.6	13	3.83	8	2.9	2	0.79	3	1.12
Operculodinium centrocarpum	76	24.3	89	26.3	58	21	64	25.3	43	16
Operculodinium var. cezare	2	0.64	3	0.88	2	0.72		0	1	0.37
Operculodinium short process	2	0.64	3	0.88	3	1.09	1	0.4	2	0.74
Operculodinium var.arctique		0		0		0		0	1	0.37
Operculodinium israelianum	1	0.32		0		0		0		0
Operculodinium spp.	1	0.32		0		0		0		0
Pyxidiniopsis reticulata		0	2	0.59		0	1	0.4		0
Spiniferites delicatus		0	1	0.29		0		0		0
Spiniferites elongatus	4	1.28	1	0.29	4	1.45	3	1.19	1	0.37
Spiniferites ramosus	5	1.6	5	1.47	4	1.45	3	1.19	1	0.37
Spiniferites belerius		0	2	0.59		0		0		0
Spiniferites bentorii		0		0		0	2	0.79		0
Spiniferites bulloideus	3	0.96	2	0.59	2	0.72		0		0
Spiniferites frigidus		0		0		0		0		0
Spiniferites membranaceus		0	2	0.59		0		0		0
Spiniferites mirabilis	2	0.64	2	0.59	1	0.36		0		0
Spiniferites spp.	1	0.32	1	0.29	2	0.72	2	0.79	2	0.74
Pentapharsodinium dalei	47	15	60	17.7	33	12	27	10.7	37	13.8
Islandinium ? minutum	31	9.9	22	6.49	40	14.5	32	12.6	23	8.55
Islandinium var.cezare	1	0.32	6	1.77	3	1.09	1	0.4	1	0.37
Islandinium ? spp.		0		0	0	0		0		0
Brigantedinium spp.	122	39	111	32.7	102	37	109	43.1	149	55.4
Brigantedinium cariacoense		0	3	0.88		0		0		0
Brigantedinium simplex	6	1.92	4	1.18	5	1.81		0	1	0.37
Selenopemphix quanta		0	2	0.59		0	3	1.19		0
Polysphaeridium zohari		0		0		0		0		0
Trinovantedinium applanatum		0		0		0		0	1	0.37
Votadinium calvum		0		0		0		0		0
Polykrikos kofoidii		0		0		0		0		0

Appendix 12: Dinoflagellate cysts counts and percentages core 95-030-24, LaHave Basin

Depth (cm)	50-52 G		60-62 G		70-72 G		80-82 G		90-92 G	
Dinocyst species	cou	%	cou	%	coun	%	cou	%	cou	%
Total cysts	**352**		**303**		**206**		**337**		**195**	
Achomosphaera	2	0.57		0		0		0		0
cf.Alexandrium excavatum		0		0	2	0.97	1	0.3	1	0.51
Ataxodinium choanum	4	1.14	1	0.33		0	1	0.3	1	0.51
Bitectatodinium tepikiense	9	2.56	2	0.66	1	0.49	1	0.3	1	0.51
Impagidinium aculeatum	1	0.28	1	0.33		0	1	0.3		0
Impagidinium pallidum		0		0		0		0		0
Impagidinium patulum		0	1	0.33		0		0		0
Impagidinium sphaericum		0		0		0		0		0
Impagidinium spp.		0		0		0		0		0
Impagidinium strialatum		0		0		0		0		0
Lingulodinium machaerophorum		0		0		0		0		0
Nematosphaerosis labyrinthus	5	1.42	3	0.99	1	0.49	9	2.67	2	1.02
Operculodinium centrocarpum	85	24.1	69	22.8	38	18.4	61	18.1	44	22.4
Operculodinium var. cezare	3	0.85		0		0	1	0.3	2	1.02
Operculodinium short process	4	1.14	3	0.99		0	2	0.59	2	1.02
Operculodinium var.arctique		0		0		0		0		0
Operculodinium israelianum		0		0		0		0		0
Operculodinium spp.		0		0		0		0		0
Pyxidiniopsis reticulata		0		0		0		0		0
Spiniferites delicatus		0		0		0		0		0
Spiniferites elongatus	1	0.28	3	0.99	1	0.49	3	0.89	3	1.53
Spiniferites ramosus	3	0.85	2	0.66	7	3.4	4	1.19	4	2.04
Spiniferites belerius		0		0		0		0		0
Spiniferites bentorii		0		0		0		0		0
Spiniferites bulloideus		0		0		0		0		0
Spiniferites frigidus		0		0		0		0		0
Spiniferites membranaceus	2	0.57		0		0		0		0
Spiniferites mirabilis		0		0		0		0		0
Spiniferites spp.	8	2.27		0		0	1	0.3	2	1.02
Pentapharsodinium dalei	33	9.38	35	11.6	24	11.7	61	18.1	37	18.9
Islandinium ? minutum	50	14.2	16	5.28	19	9.22	20	5.93	0	0
Islandinium var.cezare	5	1.42		0		0	2	0.59	1	0.51
Islandinium ? spp.		0		0		0		0		0
Brigantedinium spp.	135	38.4	163	53.8	112	54.4	164	48.7	93	47.4
Brigantedinium cariacoense		0		0		0	2	0.59		0
Brigantedinium simplex	2	0.57	1	0.33	1	0.49	1	0.3	1	0.51
Selenopemphix quanta		0	3	0.99		0	2	0.59	1	0.51
Polysphaeridium zohari		0		0		0		0		0
Trinovantedinium applanatum		0		0		0		0		0
Votadinium calvum		0		0		0		0		0
Polykrikos kofoidii		0		0		0		0		0

Appendix 12: Dinoflagellate cysts counts and percentages core 95-030-24, LaHave Basin

Depth (cm)	100-102 G		110-112		120-122 G		130-132 G		140-142 G	
Dinocyst species	cou	%	cou	%	coun	%	cou	%	cou	%
Total cysts	**208**		**292**		**310**		**196**		**350**	
Achomosphaera		0		0	2	0.65	2	1.02		0
cf.Alexandrium excavatum		0		0		0		0		0
Ataxodinium choanum		0		0		0	2	1.02	2	0.57
Bitectatodinium tepikiense	2	0.96	2	0.68	2	0.65	4	2.04	3	0.86
Impagidinium aculeatum		0		0		0		0		0
Impagidinium pallidum		0	1	0.34		0		0		0
Impagidinium patulum		0		0		0		0		0
Impagidinium sphaericum		0		0		0		0		0
Impagidinium spp.				0		0				0
Impagidinium strialatum		0		0		0		0		0
Lingulodinium machaerophorum		0		0		0	2	1.02		0
Nematosphaerosis labyrinthus	2	0.96	3	1.03	2	0.65	4	2.04	5	1.43
Operculodinium centrocarpum	62	29.8	61	20.9	61	19.7	58	29.6	63	18
Operculodinium var. cezare		0		0	1	0.32		0		0
Operculodinium short process	4	1.92	1	0.34	2	0.65	2	1.02	3	0.86
Operculodinium var.arctique		0		0		0		0		0
Operculodinium israelianum		0		0		0		0		0
Operculodinium spp.		0		0		0		0		0
Pyxidiniopsis reticulata		0		0		0		0		0
Spiniferites delicatus		0		0	1	0.32		0		0
Spiniferites elongatus	4	1.92	2	0.68	6	1.94	2	1.02	3	0.86
Spiniferites ramosus		0	4	1.37	4	1.29	2	1.02	6	1.71
Spiniferites belerius		0		0		0		0		0
Spiniferites bentorii		0		0		0		0		0
Spiniferites bulloideus	2	0.96		0	1	0.32	4	2.04	2	0.57
Spiniferites frigidus		0		0		0		0		0
Spiniferites membranaceus		0		0		0		0		0
Spiniferites mirabilis		0		0		0		0		0
Spiniferites spp.		0		0	1	0.32	6	3.06		0
Pentapharsodinium dalei	22	10.6	71	24.3	83	26.8	26	13.3	103	29.4
Islandinium ? minutum	42	20.2	19	6.51	18	5.81	20	10.2	21	6
Islandinium var.cezare	6	2.88		0	2	0.65	4	2.04		0
Islandinium ? spp.		0		0		0		0		0
Brigantedinium spp.	60	28.8	126	43.2	120	38.7	54	27.6	138	39.4
Brigantedinium cariacoense	1	0.48	1	0.34	3	0.97		0		0
Brigantedinium simplex	1	0.48		0		0	2	1.02		0
Selenopemphix quanta		0	1	0.34	1	0.32	2	1.02	1	0.29
Polysphaeridium zohari				0		0				0
Trinovantedinium applanatum		0		0		0		0		0
Votadinium calvum		0		0		0		0		0
Polykrikos kofoidii		0		0		0		0		0

Appendix 12: Dinoflagellate cysts counts and percentages core 95-030-24, LaHave Basin

Depth (cm)	150-152		160-162 G		170-172 G		180-182 G		0-2 P	
Dinocyst species	cou	%	coun	%	cou	%	coun	%	cou	%
Total cysts	**284**		**320**		**309**		**325**		**179**	
Achomosphaera		0		0		0		0		0
cf.Alexandrium excavatum		0	3	0.93	1	0.32	1	0.31		0
Ataxodinium choanum		0		0		0	1	0.31		0
Bitectatodinium tepikiense	4	1.41		0	2	0.65	2	0.62	4	2.23
Impagidinium aculeatum		0	2	0.62	1	0.32		0	2	1.12
Impagidinium pallidum		0		0		0		0		0
Impagidinium patulum		0		0		0		0		0
Impagidinium sphaericum		0		0		0		0		0
Impagidinium spp.		0		0	1	0.32		0		
Impagidinium strialatum		0		0		0		0		0
Lingulodinium machaerophorum		0		0		0		0	1	0.56
Nematosphaerosis labyrinthus	4	1.41	1	0.31	2	0.65	4	1.23	2	1.12
Operculodinium centrocarpum	64	22.5	44	13.7	42	13.6	78	24	41	22.9
Operculodinium var. cezare	2	0.7		0		0		0		0
Operculodinium short process	2	0.7	3	0.93	2	0.65	1	0.31	4	2.23
Operculodinium var.arctique	3	1.06		0		0	1	0.31		0
Operculodinium israelianum		0		0		0		0		0
Operculodinium spp.		0		0		0		0		0
Pyxidiniopsis reticulata		0		0		0		0		0
Spiniferites delicatus		0		0	1	0.32		0		0
Spiniferites elongatus	1	0.35	3	0.93	7	2.27	5	1.54		0
Spiniferites ramosus	1	0.35	6	1.87	3	0.97	4	1.23	2	1.12
Spiniferites belerius		0	1	0.31		0		0		0
Spiniferites bentorii		0		0		0		0		0
Spiniferites bulloideus		0	5	1.56	1	0.32	3	0.92		0
Spiniferites frigidus	2	0.7		0		0		0	2	1.12
Spiniferites membranaceus		0		0		0		0		0
Spiniferites mirabilis		0		0	1	0.32		0		0
Spiniferites spp.	4	1.41		0		0	1	0.31	3	1.68
Pentapharsodinium dalei	58	20.4	112	34.9	72	23.3	47	14.5	4	2.23
Islandinium ? minutum	23	8.1	26	8.1	27	8.74	29	8.92	32	17.9
Islandinium var.cezare	8	2.82	1	0.31	1	0.32	3	0.92		0
Islandinium ? spp.		0		0		0		0		0
Brigantedinium spp.	106	37.3	112	34.9	141	45.6	144	44.3	80	44.7
Brigantedinium cariacoense		0	1	0.31	1	0.32		0		0
Brigantedinium simplex		0		0		0		0		0
Selenopemphix quanta	2	0.7		0	3	0.97	1	0.31	2	1.12
Polysphaeridium zohari		0		0		0		0		0
Trinovantedinium applanatum		0		0		0		0		0
Votadinium calvum		0		0		0		0		0
Polykrikos kofoidii		0		0		0		0		0

Appendix 12: Dinoflagellate cysts counts and percentages core 95-030-24, LaHave Basin

Depth (cm)	10-12 P		20-22 P		30-32 P		40-42 P		50-52 P	
Dinocyst species	coun	%	cou	%	cou	%	cou	%	coun	%
Total cysts	**208**		**204**		**140**		**180**		**220**	
Achomosphaera		0	2	0.98		0		0		0
cf.Alexandrium excavatum	0	0	4	1.96		0		0		0
Ataxodinium choanum	8	3.85	2	0.98		0	0	0		0
Bitectatodinium tepikiense	12	5.77	8	3.92	4	2.86	4	2.22	8	3.64
Impagidinium aculeatum	5	2.4		0		0		0		0
Impagidinium pallidum		0		0		0		0		0
Impagidinium patulum		0		0		0		0		0
Impagidinium sphaericum		0		0		0		0		0
Impagidinium spp.		0								0
Impagidinium strialatum		0		0		0		0		0
Lingulodinium machaerophorum	2	0.96		0		0		0		0
Nematosphaerosis labyrinthus	4	1.92	4	1.96	4	2.86	2	1.11		0
Operculodinium centrocarpum	50	24	64	31.4	34	24.3	38	21.1	46	20.9
Operculodinium var. cezare		0		0		0	2	1.11	4	1.82
Operculodinium short process	2	0.96		0		0		0		0
Operculodinium var.arctique		0		0		0		0		0
Operculodinium israelianum		0		0		0		0		0
Operculodinium spp.		0		0		0		0		0
Pyxidiniopsis reticulata		0		0		0		0		0
Spiniferites delicatus		0		0		0		0		0
Spiniferites elongatus	2	0.96	4	1.96	6	4.29	2	1.11		0
Spiniferites ramosus		0	2	0.98		0		0		0
Spiniferites belerius		0		0		0		0		0
Spiniferites bentorii		0		0		0		0		0
Spiniferites bulloideus		0	2	0.98		0		0		0
Spiniferites frigidus		0		0		0		0		0
Spiniferites membranaceus		0		0		0		0		0
Spiniferites mirabilis		0		0		0		0		0
Spiniferites spp.	8	3.85	10	4.9	4	2.86		0	2	0.91
Pentapharsodinium dalei	4	1.92	16	7.84	8	5.71	14	7.78	12	5.45
Islandinium ? minutum	66	31.7	30	14.7	20	14.3	60	33.3	20	9.09
Islandinium var.cezare	2	0.96		0		0		0	10	4.55
Islandinium ? spp.		0		0		0		0		0
Brigantedinium spp.	38	18.3	52	25.5	52	37.1	54	30	114	51.8
Brigantedinium cariacoense		0	2	0.98	4	2.86		0	2	0.91
Brigantedinium simplex	2	0.96	2	0.98	2	1.43	2	1.11		0
Selenopemphix quanta	2	0.96		0	2	1.43	2	1.11	2	0.91
Polysphaeridium zohari		0		0		0		0		0
Trinovantedinium applanatum		0		0		0		0		0
Votadinium calvum		0		0		0		0		0
Polykrikos kofoidii	1	0.48		0		0		0		0

Appendix 12: Dinoflagellate cysts counts and percentages core 95-030-24, LaHave Basin

Depth (cm)	60-62 P		70-72 P		80-82 P		90-92 P		100-102 P	
Dinocyst species	coun	%	cou	%	coun	%	coun	%	coun	%
Total cysts	**109**		**103**		**97**		**247**		**289**	
Achomosphaera		0		0		0		0		0
cf.Alexandrium excavatum	1	0.92		0		0		0		0
Ataxodinium choanum	2	1.83	1	0.96	1	1.03		0	3	1.04
Bitectatodinium tepikiense	2	1.83	3	2.88	2	2.06	2	0.81	2	0.69
Impagidinium aculeatum		0		0		0	1	0.4		0
Impagidinium pallidum		0		0		0		0		0
Impagidinium patulum		0		0		0		0		0
Impagidinium sphaericum		0		0		0		0		0
Impagidinium spp.		0		0		0		0		0
Impagidinium strialatum		0		0		0		0		0
Lingulodinium machaerophorum		0		0		0		0		0
Nematosphaerosis labyrinthus		0	4	3.85	3	3.09	1	0.4	2	0.69
Operculodinium centrocarpum	16	14.7	25	24	19	19.6	53	21.5	30	10.4
Operculodinium var. cezare		0	2	1.92		0		0	3	1.04
Operculodinium short process		0		0	2	2.06	1	0.4		0
Operculodinium var.arctique		0		0		0		0		0
Operculodinium israelianum		0	2	1.92	3	3.09	2	0.81	1	0.35
Operculodinium spp.		0		0		0		0		0
Pyxidiniopsis reticulata		0		0		0		0		0
Spiniferites delicatus		0		0		0		0		0
Spiniferites elongatus		0	1	0.96	2	2.06		0	1	0.35
Spiniferites ramosus		0	2	1.92		0		0	2	0.69
Spiniferites belerius		0		0		0		0		0
Spiniferites bentorii		0		0		0		0		0
Spiniferites bulloideus		0		0		0		0		0
Spiniferites frigidus		0		0		0		0		0
Spiniferites membranaceus		0		0		0		0		0
Spiniferites mirabilis		0		0		0		0		0
Spiniferites spp.		0	1	0.96	2	2.06	4	1.62	3	1.04
Pentapharsodinium dalei	6	5.5	9	8.65	14	14.4	23	9.31	33	11.4
Islandinium ? minutum	10	9.17	12	11.5	11	11.3	15	6.07	38	13.1
Islandinium var.cezare	4	3.67	3	2.88	1	1.03	3	1.21	5	1.73
Islandinium ? spp.		0		0		0		0		0
Brigantedinium spp.	68	62.4	36	34.6	33	34	140	56.7	160	55.4
Brigantedinium cariacoense		0	1	0.96		0	1	0.4	2	0.69
Brigantedinium simplex		0	1	0.96		0		0	1	0.35
Selenopemphix quanta		0		0	3	3.09	1	0.4	3	1.04
Polysphaeridium zohari		0		0	1	1.03		0		0
Trinovantedinium applanatum		0		0		0		0		0
Votadinium calvum		0		0		0		0		0
Polykrikos kofoidii		0		0		0		0		0

Appendix 12: Dinoflagellate cysts counts and percentages core 95-030-24, LaHave Basin

Depth (cm)	120-122 P		140-142 P		160-162 P		180-182 P		200-202 P	
Dinocyst species	cou	%	cou	%	coun	%	cou	%	coun	%
Total cysts	**307**		**330**		**289**		**318**		**296**	
Achomosphaera		0	1	0.3		0		0		0
cf.Alexandrium excavatum		0	1	0.3		0		0	1	0.34
Ataxodinium choanum		0		0		0		0	1	0.34
Bitectatodinium tepikiense	1	0.33	0	0	2	0.69	5	1.58	2	0.68
Impagidinium aculeatum		0	2	0.61		0	1	0.32	2	0.68
Impagidinium pallidum	1	0.33		0		0		0		0
Impagidinium patulum		0		0		0		0		0
Impagidinium sphaericum		0		0		0		0	3	1.01
Impagidinium spp.		0		0		0		0		0
Impagidinium strialatum		0		0		0		0		0
Lingulodinium machaerophorum		0	1	0.3		0		0		0
Nematosphaerosis labyrinthus	4	1.3	4	1.21	1	0.35		0	3	1.01
Operculodinium centrocarpum	72	23.5	78	23.6	67	23.3	58	18.3	55	18.6
Operculodinium var. cezare	4	1.3		0	2	0.69	1	0.32	5	1.69
Operculodinium short process	2	0.65	5	1.52	5	1.74	5	1.58	6	2.03
Operculodinium var.arctique		0		0	1	0.35		0		0
Operculodinium israelianum	2	0.65	3	0.91	2	0.69		0	1	0.34
Operculodinium spp.		0		0		0		0		0
Pyxidiniopsis reticulata		0		0		0		0		0
Spiniferites delicatus		0		0		0	1	0.32		0
Spiniferites elongatus	4	1.3	4	1.21	4	1.39	4	1.26	3	1.01
Spiniferites ramosus	1	0.33	4	1.21	4	1.39	2	0.63	3	1.01
Spiniferites belerius		0		0		0		0		0
Spiniferites bentorii		0		0		0		0		0
Spiniferites bulloideus		0		0	1	0.35	1	0.32	3	1.01
Spiniferites frigidus		0		0		0		0		0
Spiniferites membranaceus		0		0		0		0		0
Spiniferites mirabilis		0		0		0		0		0
Spiniferites spp.	3	0.98	2	0.61	5	1.74	2	0.63	2	0.68
Pentapharsodinium dalei	16	5.21	39	11.8	29	10.1	28	8.83	34	11.5
Islandinium ? minutum	27	8.79	33	10	21	7.29	26	8.2	27	9.12
Islandinium var.cezare	6	1.95	4	1.21	4	1.39	5	1.58	5	1.69
Islandinium ? spp.		0		0		0		0		0
Brigantedinium spp.	158	51.5	140	42.4	134	46.5	177	55.8	136	45.9
Brigantedinium cariacoense		0	4	1.21	3	1.04		0	2	0.68
Brigantedinium simplex	4	1.3		0		0		0		0
Selenopemphix quanta	2	0.65	1	0.3	3	1.04	2	0.63	2	0.68
Polysphaeridium zohari		0	4	1.21	1	0.35		0		0
Trinovantedinium applanatum		0		0		0		0		0
Votadinium calvum		0		0		0		0		0
Polykrikos kofoidii		0		0		0		0		0

Appendix 12: Dinoflagellate cysts counts and percentages core 95-030-24, LaHave Basin

Depth (cm)	220-222 P		240-242 P		260-262 P		280-282 P		300-302 P	
Dinocyst species	coun	%	cou	%	coun	%	coun	%	cou	%
Total cysts	**302**		**324**		**286**		**204**		**289**	
Achomosphaera		0	0	0		0		0		0
cf.Alexandrium excavatum		0	1	0.31		0	2	0.98	3	1.04
Ataxodinium choanum		0		0		0	1	0.49		0
Bitectatodinium tepikiense	3	0.99	2	0.62	1	0.35	2	0.98	3	1.04
Impagidinium aculeatum		0		0	1	0.35		0	5	1.73
Impagidinium pallidum		0		0		0		0		0
Impagidinium patulum		0		0		0		0		0
Impagidinium sphaericum		0		0		0		0		0
Impagidinium spp.		0		0		0	1	0.49	1	0.35
Impagidinium strialatum		0		0		0		0	0	0
Lingulodinium machaerophorum		0		0		0		0		0
Nematosphaerosis labyrinthus	1	0.33	2	0.62	1	0.35		0	5	1.73
Operculodinium centrocarpum	51	16.9	44	13.6	33	11.5	57	27.9	68	23.5
Operculodinium var. cezare		0		0	2	0.7	6	2.94	13	4.5
Operculodinium short process	6	1.99		0	1	0.35	2	0.98	3	1.04
Operculodinium var.arctique		0	1	0.31		0		0		0
Operculodinium israelianum	1	0.33	2	0.62		0	1	0.49	1	0.35
Operculodinium spp.		0		0		0		0		0
Pyxidiniopsis reticulata		0		0		0		0		0
Spiniferites delicatus		0		0		0		0		0
Spiniferites elongatus	4	1.32	6	1.85	6	2.1	7	3.43	9	3.11
Spiniferites ramosus		0	2	0.62	4	1.4	3	1.47	7	2.42
Spiniferites belerius		0		0		0		0		0
Spiniferites bentorii		0		0		0		0		0
Spiniferites bulloideus	3	0.99	1	0.31	1	0.35	5	2.45	4	1.38
Spiniferites frigidus		0		0		0		0		0
Spiniferites membranaceus		0		0		0		0		0
Spiniferites mirabilis		0		0		0		0		0
Spiniferites spp.	5	1.66	4	1.23		0	5	2.45	1	0.35
Pentapharsodinium dalei	9	2.98	36	11.1	18	6.29	26	12.7	21	7.27
Islandinium ? minutum	19	6.29	10	3.09	22	7.69	7	3.43	20	6.92
Islandinium var.cezare	2	0.66	3	0.93	2	0.7		0		0
Islandinium ? spp.		0		0	0	0		0		0
Brigantedinium spp.	189	62.6	207	63.9	190	66.4	76	37.3	125	43.3
Brigantedinium cariacoense		0	1	0.31	4	1.4	1	0.49		0
Brigantedinium simplex	2	0.66		0		0		0		0
Selenopemphix quanta	7	2.32	2	0.62		0		0		0
Polysphaeridium zohari		0		0		0	2	0.98		0
Trinovantedinium applanatum		0		0		0		0		0
Votadinium calvum		0		0		0		0		0
Polykrikos kofoidii		0		0		0		0		0

Appendix 12: Dinoflagellate cysts counts and percentages core 95-030-24, LaHave Basin

Depth (cm)	320-322 P		340-342 P		360-362 P		380-382 P		400-402 P	
Dinocyst species	count	%	coun	%	cou	%	cou	%	cou	%
Total cysts	**98**		**247**		**301**		**197**		**207**	
Achomosphaera		0		0		0		0		0
cf.Alexandrium excavatum		0	2	0.81		0		0		0
Ataxodinium choanum		0		0		0		0		0
Bitectatodinium tepikiense	1	1.02	4	1.62	3	1	1	0.51	4	1.93
Impagidinium aculeatum		0	2	0.81	1	0.33	2	1.02		0
Impagidinium pallidum		0		0		0	4	2.03		0
Impagidinium patulum		0		0		0	1	0.51		0
Impagidinium sphaericum		0		0		0		0	1	0.48
Impagidinium spp.				0		0				
Impagidinium strialatum		0		0		0		0	1	0.48
Lingulodinium machaerophorum		0		0		0		0		0
Nematosphaerosis labyrinthus		0	1	0.4	1	0.33	4	2.03	1	0.48
Operculodinium centrocarpum	26	26.5	71	28.7	75	24.9	30	15.2	39	18.8
Operculodinium var. cezare		0		0	3	1	13	6.6	14	6.76
Operculodinium short process	1	1.02	2	0.81	2	0.66	2	1.02		0
Operculodinium var.arctique		0		0	1	0.33		0		0
Operculodinium israelianum	1	1.02		0		0		0		0
Operculodinium spp.				0		0				
Pyxidiniopsis reticulata		0		0		0		0		0
Spiniferites delicatus		0		0		0		0		0
Spiniferites elongatus	1	1.02	7	2.83	8	2.66	8	4.06	9	4.35
Spiniferites ramosus		0	5	2.02	4	1.33	1	0.51	3	1.45
Spiniferites belerius		0		0		0		0		0
Spiniferites bentorii		0		0		0		0		0
Spiniferites bulloideus	4	4.08	2	0.81	6	1.99	4	2.03	5	2.42
Spiniferites frigidus		0		0		0	1	0.51		0
Spiniferites membranaceus		0		0		0		0		0
Spiniferites mirabilis		0		0		0		0		0
Spiniferites spp.		0	5	2.02	5	1.66	2	1.02	6	2.9
Pentapharsodinium dalei	4	4.08	28	11.3	29	9.63	31	15.7	19	9.18
Islandinium ? minutum	12	12.2	13	5.26	32	10.6	18	9.14	13	6.28
Islandinium var.cezare	6	6.12	1	0.4		0	6	3.05	1	0.48
Islandinium ? spp.		0		0		0		0		0
Brigantedinium spp.		0	102	41.3	128	42.5	68	34.5	89	43
Brigantedinium cariacoense	41	41.8	1	0.4	1	0.33		0		0
Brigantedinium simplex		0		0		0		0	1	0.48
Selenopemphix quanta	1	1.02	1	0.4	2	0.66		0	1	0.48
Polysphaeridium zohari		0		0		0		0		0
Trinovantedinium applanatum		0		0		0		0		0
Votadinium calvum		0		0		0	1	0.51		0
Polykrikos kofoidii		0		0		0		0		0

Appendix 12: Dinoflagellate cysts counts and percentages core 95-030-24, LaHave Basin

Depth (cm)	420-422 P		440-442 P		460-462 P		480-482 P		500-502 P	
Dinocyst species	cou	%	cou	%	cou	%	cou	%	cou	%
Total cysts	**286**		**211**		**294**		**226**		**333**	
Achomosphaera		0		0		0		0		0
cf.Alexandrium excavatum		0		0		0		0		0
Ataxodinium choanum		0		0		0	2	0.88	1	0.3
Bitectatodinium tepikiense	6	2.1	8	3.79	12	4.08	5	2.21	3	0.9
Impagidinium aculeatum	4	1.4	2	0.95		0		0	1	0.3
Impagidinium pallidum		0		0		0		0		0
Impagidinium patulum	1	0.35		0		0		0		0
Impagidinium sphaericum		0		0		0		0		0
Impagidinium spp.	4	1.4			1	0.34		0		0
Impagidinium strialatum		0		0		0		0		0
Lingulodinium machaerophorum		0		0		0		0		0
Nematosphaerosis labyrinthus	1	0.35	5	2.37	4	1.36	3	1.33	3	0.9
Operculodinium centrocarpum	35	12.2	32	15.2	40	13.6	27	11.9	28	8.41
Operculodinium var. cezare	5	1.75	7	3.32	7	2.38	4	1.77	4	1.2
Operculodinium short process	2	0.7	1	0.47	3	1.02	1	0.44	2	0.6
Operculodinium var.arctique		0		0		0		0		0
Operculodinium israelianum		0		0		0		0		0
Operculodinium spp.		0				0		0		0
Pyxidiniopsis reticulata		0		0		0		0		0
Spiniferites delicatus		0		0		0		0		0
Spiniferites elongatus	6	2.1	3	1.42	4	1.36	4	1.77	3	0.9
Spiniferites ramosus	5	1.75	4	1.9	3	1.02		0		0
Spiniferites belerius		0		0		0		0		0
Spiniferites bentorii		0		0		0		0		0
Spiniferites bulloideus	9	3.15	8	3.79	1	0.34	6	2.65	2	0.6
Spiniferites frigidus		0		0		0		0		0
Spiniferites membranaceus		0		0		0		0		0
Spiniferites mirabilis		0		0		0		0		0
Spiniferites spp.	2	0.7	3	1.42	2	0.68	4	1.77	2	0.6
Pentapharsodinium dalei	36	12.6	24	11.4	47	16	43	19	30	9.01
Islandinium ? minutum	13	4.55	33	15.6	98	33.3	71	31.4	153	45.9
Islandinium var.cezare	1	0.35	1	0.47	9	3.06	4	1.77	2	0.6
Islandinium ? spp.		0		0		0		0		0
Brigantedinium spp.	153	53.5	78	37	59	20.1	52	23	99	29.7
Brigantedinium cariacoense		0		0		0		0		0
Brigantedinium simplex	2	0.7	1	0.47		0		0		0
Selenopemphix quanta	1	0.35		0	4	1.36		0		0
Polysphaeridium zohari		0	1	0.47		0		0		0
Trinovantedinium applanatum		0		0		0		0		0
Votadinium calvum		0		0		0		0		0
Polykrikos kofoidii		0		0		0		0		0

Appendix 12: Dinoflagellate cysts counts and percentages core 95-030-24, LaHave Basin

Depth (cm)	520-522 P		540-	P	560-562 P		580-582 P		600-602 P	
Dinocyst species	coun	%	coun	%	coun	%	cou	%	coun	%
Total cysts	**245**		**250**		**283**		**287**		**354**	
Achomosphaera		0	1	0.4		0		0		0
cf.Alexandrium excavatum		0	2	0.8	4	1.41	4	1.39	3	0.85
Ataxodinium choanum		0	1	0.4	2	0.71	1	0.35		0
Bitectatodinium tepikiense	3	1.22	7	2.8	10	3.53	9	3.13	12	3.38
Impagidinium aculeatum		0		0		0		0	1	0.28
Impagidinium pallidum		0		0		0		0		0
Impagidinium patulum		0		0		0		0		0
Impagidinium sphaericum		0		0		0		0		0
Impagidinium spp.		0	1	0.4		0				
Impagidinium strialatum		0		0		0		0		0
Lingulodinium machaerophorum		0		0		0		0		0
Nematosphaerosis labyrinthus	2	0.81		0	2	0.71		0		0
Operculodinium centrocarpum	35	14.2	43	17.2	56	19.8	60	20.8	57	16.1
Operculodinium var. cezare	10	4.07	12	4.8		0	9	3.13	9	2.54
Operculodinium short process	1	0.41	1	0.4	4	1.41	2	0.69	4	1.13
Operculodinium var.arctique		0		0		0		0		0
Operculodinium israelianum		0		0		0		0		0
Operculodinium spp.		0		0		0				
Pyxidiniopsis reticulata		0		0		0		0		0
Spiniferites delicatus		0		0		0		0		0
Spiniferites elongatus	2	0.81	4	1.6	4	1.41	5	1.74	1	0.28
Spiniferites ramosus	7	2.85	8	3.2	11	3.89	4	1.39	8	2.25
Spiniferites belerius		0		0		0		0		0
Spiniferites bentorii		0		0		0		0		0
Spiniferites bulloideus		0		0	1	0.35	6	2.08	7	1.97
Spiniferites frigidus		0		0		0	1	0.35		0
Spiniferites membranaceus		0		0		0		0		0
Spiniferites mirabilis		0		0		0	1?	0.35		0
Spiniferites spp.	4	1.63	2	0.8	4	1.41	2	0.69	1	0.28
Pentapharsodinium dalei	66	26.8	63	25.2	35	12.4	73	25.3	122	34.4
Islandinium ? minutum	67	27.2	51	20.4	57	20.1	65	22.6	87	24.5
Islandinium var.cezare	3	1.22	1	0.4	5	1.77	2	0.69	3	0.85
Islandinium ? spp.		0		0	5	1.77		0		0
Brigantedinium spp.	44	17.9	53	21.2	81	28.6	42	14.6	37	10.4
Brigantedinium cariacoense		0		0		0		0	1	0.28
Brigantedinium simplex		0		0		0	1	0.35		0
Selenopemphix quanta	1	0.41		0	2	0.71	1	0.35	1	0.28
Polysphaeridium zohari		0		0		0		0		0
Trinovantedinium applanatum		0		0		0		0		0
Votadinium calvum		0		0		0		0		0
Polykrikos kofoidii		0		0		0		0		0

Appendix 12: Dinoflagellate cysts counts and percentages core 95-030-24, LaHave Basin

Depth (cm)	620-622 P		640-642 P		660-662 P		680-682 P		700-702 P	
Dinocyst species	coun	%	coun	%	cou	%	coun	%	coun	%
Total cysts	**409**		**374**		**215**		**384**		**410**	
Achomosphaera		0		0	1	0.47		0		0
cf.Alexandrium excavatum		0	1	0.27	4	1.86	2	0.52	3	0.73
Ataxodinium choanum		0	2	0.53		0		0	1	0.24
Bitectatodinium tepikiense	20	4.89	20	5.35	9	4.19	27	7.03	33	8.05
Impagidinium aculeatum	1	0.24		0	1	0.47	1	0.26		0
Impagidinium pallidum		0		0		0		0		0
Impagidinium patulum		0		0		0		0		0
Impagidinium sphaericum		0		0		0		0		0
Impagidinium spp.				0		0		0		0
Impagidinium strialatum		0		0		0		0		0
Lingulodinium machaerophorum		0		0		0		0		0
Nematosphaerosis labyrinthus		0		0		0	1	0.26		0
Operculodinium centrocarpum	84	20.5	67	17.9	60	27.9	116	30.2	125	30.5
Operculodinium var. cezare	6	1.47	12	3.21		0	11	2.86	10	2.44
Operculodinium short process	4	0.98	2	0.53	6	2.79	4	1.04	8	1.95
Operculodinium var.arctique		0		0		0		0	1	0.24
Operculodinium israelianum		0		0	1	0.47		0		0
Operculodinium spp.				0		0				
Pyxidiniopsis reticulata		0		0		0		0		0
Spiniferites delicatus		0		0		0		0		0
Spiniferites elongatus	8	1.96	5	1.34	6	2.79	17	4.43	16	3.9
Spiniferites ramosus	12	2.93	9	2.41	14	6.51	9	2.34	9	2.2
Spiniferites belerius		0		0		0	1	0.26	1	0.24
Spiniferites bentorii		0		0	2	0.93	3	0.78	1	0.24
Spiniferites bulloideus	7	1.71	9	2.41		0	7	1.82	2	0.49
Spiniferites frigidus		0		0		0		0		0
Spiniferites membranaceus		0		0		0		0	1	0.24
Spiniferites mirabilis		0	1	0.27		0	2	0.52	2	0.49
Spiniferites spp.	5	1.22	3	0.8	5	2.33	2	0.52	1	0.24
Pentapharsodinium dalei	141	34.5	119	31.8	51	23.7	127	33.1	142	34.6
Islandinium ? minutum	68	16.6	78	20.9	24	11.2	7	1.82	9	2.2
Islandinium var.cezare		0	1	0.27	2	0.93	1	0.26		0
Islandinium ? spp.		0		0		0		0		0
Brigantedinium spp.	50	12.2	43	11.5	29	13.5	46	12	44	10.7
Brigantedinium cariacoense		0		0		0		0		0
Brigantedinium simplex		0		0		0		0		0
Selenopemphix quanta	3	0.73	2	0.53		0		0	1	0.24
Polysphaeridium zohari		0		0		0		0		0
Trinovantedinium applanatum		0		0		0		0		0
Votadinium calvum		0		0		0		0		0
Polykrikos kofoidii		0		0		0		0		0

Appendix 12: Dinoflagellate cysts counts and percentages core 95-030-24, LaHave Basin

Depth (cm)	720-722 P		740-742 P		760-762 P		780-782 P		800-802 P	
Dinocyst species	coun	%	coun	%	coun	%	cou	%	coun	%
Total cysts	**457**		**384**		**486**		**322**		**295**	
Achomosphaera	2	0.44	1	0.26		0		0		0
cf.Alexandrium excavatum	9	1.97	35	9.11	68	14	65	20.2	1	0.34
Ataxodinium choanum		0	1	0.26	6	1.23	1	0.31	1	0.34
Bitectatodinium tepikiense	27	5.91	13	3.39	21	4.32	11	3.42	8	2.71
Impagidinium aculeatum		0		0		0		0		0
Impagidinium pallidum		0		0		0		0		0
Impagidinium patulum		0		0		0		0		0
Impagidinium sphaericum		0		0		0		0		0
Impagidinium spp.		0	2	0.52		0		0		0
Impagidinium strialatum		0		0		0		0		0
Lingulodinium machaerophorum		0		0		0		0		0
Nematosphaerosis labyrinthus	3	0.66	2	0.52		0	1	0.31		0
Operculodinium centrocarpum	166	36.3	122	31.8	125	25.7	81	25.2	58	19.7
Operculodinium var. cezare	8	1.75	9	2.34	5	1.03	4	1.24	1	0.34
Operculodinium short process	11	2.41	2	0.52	5	1.03	4	1.24	2	0.68
Operculodinium var.arctique	6	1.31	4	1.04		0	1	0.31	2	0.68
Operculodinium israelianum		0		0		0		0		0
Operculodinium spp.		0		0		0		0		0
Pyxidiniopsis reticulata		0		0		0		0		0
Spiniferites delicatus		0		0		0		0		0
Spiniferites elongatus	15	3.28	5	1.3	8	1.65	3	0.93	4	1.36
Spiniferites ramosus	9	1.97	6	1.56	5	1.03		0		0
Spiniferites belerius	1	0.22		0		0		0		0
Spiniferites bentorii		0		0		0		0		0
Spiniferites bulloideus		0	1	0.26	1	0.21		0		0
Spiniferites frigidus		0	2	0.52		0		0		0
Spiniferites membranaceus	1	0.22		0		0		0		0
Spiniferites mirabilis		0		0	1	0.21		0		0
Spiniferites spp.	1	0.22	2	0.52	2	0.41	1	0.31		0
Pentapharsodinium dalei	164	35.9	130	33.9	171	35.2	79	24.5	97	32.9
Islandinium ? minutum	3	0.66	5	1.3	11	2.26	5	1.55	6	2.03
Islandinium var.cezare	1	0.22		0		0	2	0.62	2	0.68
Islandinium ? spp.		0	1	0.26		0		0		0
Brigantedinium spp.	28	6.13	40	10.4	55	11.3	59	18.3	101	34.2
Brigantedinium cariacoense	2	0.44		0		0	1	0.31	4	1.36
Brigantedinium simplex		0		0		0		0	7	2.37
Selenopemphix quanta		0	1	0.26	2	0.41	4	1.24	1	0.34
Polysphaeridium zohari		0		0		0		0		0
Trinovantedinium applanatum		0		0		0		0		0
Votadinium calvum		0		0		0		0		0
Polykrikos kofoidii		0		0		0		0		0

Appendix 12: Dinoflagellate cysts counts and percentages core 95-030-24, LaHave Basin

Depth (cm)	820-822 P	
Dinocyst species	cou	%
Total cysts	**445**	
Achomosphaera		0
cf.Alexandrium excavatum		0
Ataxodinium choanum	1	0.22
Bitectatodinium tepikiense	45	10.1
Impagidinium aculeatum		0
Impagidinium pallidum		0
Impagidinium patulum		0
Impagidinium sphaericum		0
Impagidinium spp.		0
Impagidinium strialatum		0
Lingulodinium machaerophorum		0
Nematosphaerosis labyrinthus		0
Operculodinium centrocarpum	74	16.6
Operculodinium var. cezare	1	0.22
Operculodinium short process	10	2.25
Operculodinium var.arctique	3	0.67
Operculodinium israelianum		0
Operculodinium spp.		0
Pyxidiniopsis reticulata		0
Spiniferites delicatus		0
Spiniferites elongatus	12	2.7
Spiniferites ramosus	1	0.22
Spiniferites belerius		0
Spiniferites bentorii		0
Spiniferites bulloideus		0
Spiniferites frigidus		0
Spiniferites membranaceus		0
Spiniferites mirabilis		0
Spiniferites spp.	1	0.22
Pentapharsodinium dalei	175	39.3
Islandinium ? minutum	13	2.92
Islandinium var.cezare	6	1.35
Islandinium ? spp.		0
Brigantedinium spp.	101	22.7
Brigantedinium cariacoense	2	0.45
Brigantedinium simplex		0
Selenopemphix quanta		0
Polysphaeridium zohari		0
Trinovantedinium applanatum		0
Votadinium calvum		0
Polykrikos kofoidii		0

Appendix 13: Concentrations of palynomorphs in core MD99-22-25, Bay of Islands

Depth	Dinocysts	Pollen	Spores	Reworked	Organic linings	Pediastrum	Halodinium
0	7251	33047	5176	24	2929	0	1653
10	10099	35476	985	0	3127	32	2378
40	10339	48957	1816	0	1224	30	2076
80	14664	36511	1254	77	1929	38	1544
100	20820	45653	2090	188	3846	0	1170
120	26650	53485	1861	324	5340	0	1699
150	25990	47203	2280	139	4561	0	2052
180	18060	56166	2072	0	7743	218	2945
200	8192	25778	1227	107	2935	0	1548
250	13068	39465	2508	80	1087	0	1254
300	15334	37487	2160	0	1184	0	1045
350	9720	35536	1505	0	251	0	418
400	15370	47359	1806	0	2554	0	602
450	20646	58136	2066	64	6492	0	885
500	21999	97828	3192	67	23032	456	2736
550	23143	65275	4561	0	6841	0	1425
600	20542	49436	1463	0	8988	0	941
650	24552	81105	3010	0	10201	167	1839
700	21252	78339	4052	0	12928	193	1929
750	19617	54482	2408	257	5920	100	702
800	16545	69901	4013	53	8863	373	334
850	5229	58251	2137	35	3902	512	1208
1000	7983	63890	2656	120	4679	169	699
1050	9650	43562	1505	0	5853	200	752
1100	10525	51930	1347	35	4701	175	666
1150	25168	90146	2822	0	16305	2174	1170
1200	25600	45778	1971	0	9048	2329	269
1250	8886	40433	1792	27	3344	0	418
1300	31165	70922	2389	95	11497	0	1045
1350	22436	22924	836	0	5156	0	139
1400	19978	35297	1612	0	5554	0	1344
1460	3517	1149	274	51	2607	0	34
1500	1278	199	13	6	395	0	0
1600	1724	92	15	200	123	0	15
1700	27296	32778	2513	114	11879	114	800
1800	21912	17677	1164	317	11220	0	0

Appendix 14: Raw pollen and spores counts in core MD99-22-25, Bay of Islands

Depth (cm)	*Abies*	*Picea*	*Pinus*	*Tsuga*	*Acer*	*Betula*	*Carya*	*Fagus*	*Juglans*	*Tilia*	*Ulmus*	**total trees**	*Betula shrub*	*Alnus*	*Ericaceae*	*Myrica*	*Salix*	*Fraxinus*	**Total shrubs**	*Ambrosia*	*Artemisia*	*Liguliflore*	*Chenopodiaceae*	*Caryophyllaceae*	*Cyperaceae*	*Gramineae*	*Rumex*	*Other Polygonaceae*	*Leguminoseae*
0	35	107	63	4	7	81	0	0	0	1	1	**299**	47	38	1	1	0	0	**87**	5	1	0	0	0	6	5	1	3	0
10	37	124	66	1	2	70	0	0	1	0	1	**302**	50	19	1	0	2	0	**72**	8	1	0	1	0	6	2	3	0	0
40	53	137	63	6	10	123	0	0	0	0	1	**393**	116	30	0	0	1	0	**147**	4	1	0	1	0	11	1	0	3	0
80	47	129	67	5	3	141	0	0	0	0	1	**393**	83	21	1	0	1	0	**106**	1	0	0	1	0	13	0	0	6	0
100	48	139	89	4	9	129	0	0	0	0	1	**419**	82	25	1	0	2	0	**110**	0	1	0	1	0	6	1	0	3	0
120	62	179	93	8	4	118	0	0	0	0	0	**464**	118	45	2	0	3	0	**168**	2	0	0	0	0	10	0	1	9	0
150	40	104	44	6	2	82	0	0	0	0	0	**278**	87	22	0	0	4	0	**113**	2	2	0	1	0	6	0	0	6	0
180	97	154	65	7	3	91	0	0	0	0	1	**418**	51	19	0	0	2	0	**72**	1	1	0	0	0	8	0	0	7	0
200	38	148	58	5	1	91	1	1	1	1	1	**345**	74	35	0	0	2	0	**111**	2	2	0	0	0	13	0	0	3	0
250	44	151	49	9	2	85	0	0	0	0	2	**342**	59	44	1	0	0	0	**104**	1	0	0	1	0	16	0	0	0	0
300	51	166	69	6	0	89	0	0	0	0	1	**382**	94	40	0	0	4	0	**138**	3	0	1	1	0	6	1	0	1	0
350	25	88	71	3	4	85	0	0	0	0	0	**276**	93	36	0	0	5	0	**134**	0	2	0	0	0	7	0	0	0	0
400	32	115	90	2	1	77	0	0	0	0	0	**317**	110	27	1	0	1	0	**139**	1	0	0	1	0	4	0	0	1	3
450	24	62	95	5	2	126	0	0	0	0	0	**314**	31	30	1	0	6	2	**70**	1	0	0	0	0	3	1	0	0	0
500	38	82	92	4	2	115	0	0	1	0	0	**334**	46	28	1	0	5	0	**80**	2	1	0	1	0	3	0	1	1	0
550	27	68	87	3	6	150	0	0	0	0	1	**342**	71	22	0	0	10	0	**103**	0	3	0	1	0	4	0	0	1	0
600	40	101	78	6	1	111	0	2	0	0	0	**339**	87	25	1	0	11	0	**124**	1	0	0	1	0	5	0	0	0	0
650	43	99	98	14	3	97	0	0	0	0	0	**354**	68	40	0	0	9	2	**119**	1	1	0	0	0	4	0	0	1	0
700	21	92	111	11	5	73	0	0	0	0	0	**313**	54	17	2	0	6	3	**82**	1	1	0	1	1	4	0	0	0	0
750	30	79	129	5	3	132	0	0	0	0	1	**379**	100	37	0	0	10	0	**147**	1	1	0	2	0	4	0	0	3	0
800	17	43	117	5	4	80	0	0	0	0	1	**267**	115	15	0	0	8	0	**138**	1	1	1	0	0	5	0	0	2	0
850	32	73	156	6	1	105	0	0	0	0	2	**375**	155	69	2	0	10	0	**236**	2	1	0	2	0	3	1	0	2	0
1000	20	75	119	4	2	61	0	0	0	0	0	**281**	84	40	2	0	10	0	**136**	1	1	0	1	0	3	0	0	4	0
1050	28	88	118	5	2	78	0	0	0	0	0	**319**	111	53	1	0	14	1	**180**	1	1	0	1	0	6	0	1	1	1
1100	15	49	93	1	4	84	0	0	0	0	4	**250**	152	73	0	0	12	0	**237**	1	1	0	1	0	4	0	0	3	0
1150	40	93	130	1	6	59	0	0	0	0	2	**333**	143	64	0	0	10	1	**218**	3	0	0	0	0	10	2	0	1	0
1200	22	54	100	0	2	79	0	0	0	0	0	**257**	108	112	1	0	12	0	**233**	2	0	0	1	0	8	0	0	2	0

Appendix 14: Raw pollen and spores counts in core MD99-22-25, Bay of Islands

Depth (cm)	*Abies*	*Picea*	*Pinus*	*Tsuga*	*Acer*	*Betula*	*Carya*	*Fagus*	*Juglans*	*Tilia*	*Ulmus*	**total trees**	*Betula shrub*	*Alnus*	*Ericaceae*	*Myrica*	*Salix*	*Fraxinus*	**Total shrubs**	*Ambrosia*	*Artemisia*	*Liguliflore*	*Chenopodiaceae*	*Caryophyllaceae*	*Cyperaceae*	*Gramineae*	*Rumex*	*Other Polygonaceae*	*Leguminoseae*
1250	36	73	97	2	2	138	0	0	0	0	1	**349**	194	94	1	0	19	0	**308**	2	0	0	3	0	8	0	0	2	0
1300	30	51	106	0	1	60	0	0	0	0	1	**249**	142	56	0	0	13	0	**211**	0	2	0	0	0	4	0	0	2	0
1350	29	38	111	1	1	32	0	1	0	0	2	**215**	68	33	0	0	0	0	**101**	1	0	0	0	0	6	0	0	2	0
1400	29	16	116	0	2	41	0	0	0	0	0	**204**	136	32	0	0	9	0	**177**	1	2	0	0	0	6	0	0	0	0
1460	2	5	24	0	1	1	0	1	0	0	0	**34**	17	5	0	0	1	0	**23**	0	2	0	0	0	7	0	0	1	0
1500	2	27	28	0	0	1	0	0	0	0	0	**58**	11	5	0	0	1	0	**17**	2	6	0	0	0	8	1	0	4	0
1600	0	1	1	0	0	1	0	0	0	0	0	**3**	1	1	0	0	0	0	**2**	0	0	0	0	0	0	0	0	1	0
1700	10	10	46	0	0	61	1	0	0	0	1	**129**	97	36	0	0	6	0	**139**	1	0	0	0	0	12	0	0	0	0
1800	10	14	36	0	0	17	0	0	0	0	0	**77**	66	9	0	0	5	0	**80**	1	2	0	0	0	7	0	0	0	0

Appendix 14: Raw pollen and spores counts in core MD99-22-25, Bay of Islands

Depth (cm)	*Nyssa*	*Plantago*	*Morus*	*Rosaceae*	*Cornus*	*tricolporate*	Unknown	**Total herbs**	**Total pollen**	*L. annotinum*	*L.clavatum*	*L. lucidulum*	monolete spore	trilete spore	*Sphagnum*	*Osmunda*	*Dryopteris*	*Athyrium*	Isoetes	**Total spores**
0	2	1	2	0	0	0	3	**29**	**415**	3	4	0	10	9	35	3	0	1	0	**65**
10	1	0	0	0	0	0	0	**22**	**396**	0	1	0	6	3	0	0	0	0	1	**11**
40	0	0	0	1	0	2	2	**26**	**566**	0	2	4	8	0	6	1	0	0	0	**21**
80	0	0	0	0	0	1	3	**25**	**524**	0	1	2	10	2	3	0	0	0	0	**18**
100	0	0	0	1	0	1	3	**17**	**546**	1	1	3	10	2	8	0	0	0	0	**25**
120	0	0	0	0	0	1	6	**29**	**661**	1	1	0	19	3	7	2	0	0	0	**23**
150	0	0	0	0	0	0	6	**23**	**414**	2	4	0	7	2	3	1	1	0	0	**20**
180	0	0	0	0	0	0	7	**24**	**515**	0	3	1	7	1	6	1	0	0	0	**19**
200	0	0	0	0	0	0	7	**27**	**483**	1	0	2	12	3	5	0	0	0	0	**23**
250	0	0	0	0	0	2	8	**28**	**472**	0	1	5	9	1	12	1	0	0	0	**29**
300	0	0	0	0	0	0	5	**18**	**538**	0	1	4	16	2	3	3	0	0	0	**31**
350	0	0	0	0	0	0	6	**15**	**425**	0	1	2	8	0	7	0	0	0	0	**18**
400	0	0	0	0	0	1	5	**16**	**472**	2	1	1	6	2	2	4	0	0	0	**18**
450	0	0	0	0	0	0	2	**7**	**394**	0	0	0	7	1	4	1	1	0	0	**14**
500	0	0	0	0	0	2	3	**14**	**429**	1	2	1	5	2	1	2	0	0	0	**14**
550	0	0	0	0	0	0	4	**13**	**458**	3	2	1	13	3	9	1	0	0	0	**32**
600	0	0	0	0	0	0	3	**10**	**473**	0	2	2	7	1	1	1	0	0	0	**14**
650	0	0	0	0	0	1	2	**10**	**485**	1	1	2	8	3	2	1	0	0	0	**18**
700	0	0	0	0	1	0	2	**11**	**406**	1	1	1	8	2	6	2	0	0	0	**21**
750	0	0	0	0	0	1	4	**16**	**546**	5	3	2	7	1	5	1	0	0	0	**24**
800	0	0	0	0	0	0	3	**13**	**418**	1	1	1	9	3	9	0	0	0	0	**24**
850	0	0	0	0	0	0	5	**16**	**627**	6	1	2	9	1	4	0	0	0	0	**23**
1000	0	0	0	0	0	0	6	**16**	**433**	3	3	0	7	4	0	1	0	0	0	**18**
1050	0	0	0	0	0	1	9	**22**	**521**	3	1	0	9	1	4	0	0	0	0	**18**
1100	0	0	0	0	0	1	3	**14**	**501**	3	1	0	7	0	2	0	0	0	0	**13**
1150	0	0	0	0	0	0	8	**24**	**575**	3	3	2	9	1	2	0	0	0	0	**18**
1200	0	0	0	0	0	1	7	**21**	**511**	2	3	1	7	3	6	0	0	0	0	**22**

Appendix 14: Raw pollen and spores counts in core MD99-22-25, Bay of Islands

Depth (cm)	*Nyssa*	*Plantago*	*Morus*	*Rosaceae*	*Cornus*	*tricolporate*	Unknown	**Total herbs**	**Total pollen**	*L. annotinum*	*L.clavatum*	*L. lucidulum*	monolete spore	trilete spore	*Sphagnum*	*Osmunda*	*Dryopteris*	*Athyrium*	Isoetes	**Total spores**
1250	0	0	0	0	0	0	4	**19**	**677**	9	6	0	5	6	4	0	0	0	0	**30**
1300	0	0	0	0	0	0	7	**15**	**475**	1	3	1	7	3	1	0	0	0	0	**16**
1350	0	0	0	1	0	0	0	**10**	**329**	1	1	2	4	0	4	0	0	0	0	**12**
1400	0	0	0	0	0	0	4	**13**	**394**	5	3	3	3	3	1	0	0	0	0	**18**
1460	0	0	0	0	0	0	0	**10**	**67**	0	10	2	0	1	3	0	0	0	0	**16**
1500	0	0	0	0	0	0	7	**28**	**103**	1	1	0	3	0	2	0	0	0	0	**7**
1600	0	0	0	0	0	0	0	**1**	**6**	0	0	0	1	0	0	0	0	0	0	**1**
1700	0	0	0	2	0	2	2	**19**	**287**	5	1	2	9	3	2	0	0	0	0	**22**
1800	0	0	0	0	0	0	0	**10**	**167**	4	2	0	4	1	0	0	0	0	0	**11**

Appendix 15: Pollen percentages in core MD99-22-25, Bay of Islands

Depth (cm)	*Abies*	*Picea*	*Pinus*	*Tsuga*	*Acer*	*Betula*	*Carya*	*Fagus*	*Juglans*	*Tilia*	*Ulmus*	**total trees**	*Betula shrub*	*Alnus*	*Ericaceae*	*Myrica*	*Salix*	*Fraxinus*	**Total shrubs**
0	8.43	25.78	15.18	0.96	1.68	19.52	0	0	0	0.24	0.24	**72**	11.32	9.16	0.24	0.24	0	0	**21**
10	9.3	31.2	16.6	0.25	0.5	17.6	0	0	0.25	0	0.25	**76**	12.6	4.8	0.25	0	0.5	0	**18.2**
40	9.4	24.2	11.1	1.1	1.8	21.73	0	0	0	0	0.2	**69.5**	20.5	5.3	0	0	0.2	0	**26**
80	8.96	24.62	12.8	0.95	0.6	26.9	0	0	0	0	0.2	**75**	15.8	4	0.2	0	0.2	0	**20.2**
100	8.8	25.5	16.3	0.73	1.6	23.6	0	0	0	0	0.2	**76.7**	15	4.6	0.2	0	0.4	0	**20.2**
120	9.4	27	14	1.2	0.6	17.8	0	0	0	0	0	**70**	17.9	6.8	0.3	0	0.5	0	**25.5**
150	9.7	25.1	10.63	1.4	0.5	19.8	0	0	0	0	0	**67.1**	21	5.3	0	0	1	0	**27.3**
180	18.8	29.9	12.6	1.36	0.6	17.7	0	0	0	0	0.2	**81.2**	9.9	3.7	0	0	0.4	0	**14**
200	7.9	30.6	12	1	0.2	18.8	0.2	0.2	0.2	0.2	0.2	**71.5**	15.3	7.2	0	0	0.4	0	**22.9**
250	9.3	32	10.4	1.9	0.4	18	0	0	0	0	0.4	**72.4**	12.5	9.3	0.2	0	0	0	**22**
300	9.5	30.8	12.8	1.1	0	16.5	0	0	0	0	0.2	**70.9**	17.5	7.4	0	0	0.7	0	**25.6**
350	5.9	21	16.7	0.7	0.9	20	0	0	0	0	0	**65.2**	21.9	8.5	0	0	1.2	0	**31.6**
400	6.8	24.4	19.1	0.4	0.2	16.3	0	0	0	0	0	**67.2**	23.3	5.7	0.2	0	0.2	0	**29.4**
450	6.4	15.7	24.1	1.26	0.5	31.9	0	0	0	0	0	**79.9**	7.9	7.6	0.25	0	1.5	0.5	**17.8**
500	8.85	19.1	21.4	0.92	0.5	26.8	0	0	0.2	0	0	**77.8**	10.7	6.5	0.2	0	1.2	0	**18.6**
550	5.9	14.8	18.9	0.65	1.3	32.7	0	0	0	0	0.2	**74.5**	15.5	4.8	0	0	2.2	0	**22.5**
600	8.5	21.3	16.5	1.2	0.2	23.5	0	0.4	0	0	0	**71.6**	18.4	5.3	0.2	0	2.3	0	**26.2**
650	8.9	20.4	20.2	2.9	0.62	20	0	0	0	0	0	**73**	14	8.2	0	0	1.8	0.4	**24.4**
700	5.2	22.7	27.3	2.7	1.23	18	0	0	0	0	0	**77.1**	13.3	4.2	0.5	0	1.5	0.74	**20.2**
750	5.5	14.5	23.7	0.92	0.55	24.3	0	0	0	0	0.2	**69.7**	18.4	6.8	0	0	1.8	0	**27**
800	4	10.3	28	1.2	0.95	19.1	0	0	0	0	0.24	**63.8**	27.5	3.6	0	0	1.9	0	**33**
850	5.1	11.6	24.4	0.95	0.16	16.7	0	0	0	0	0.32	**59.2**	24.7	11	0.32	0	1.6	0	**37.6**
1000	4.6	17.3	27.5	0.92	0.5	14.1	0	0	0	0	0	**64.9**	19.4	9.2	0.46	0	2.3	0	**31.4**
1050	5.4	16.9	22.6	0.96	0.4	15	0	0	0	0	0	**61.3**	21.3	10.2	0.2	0	2.7	0.2	**34.6**
1100	3	9.8	18.6	0.2	0.8	16.8	0	0	0	0	0.8	**50**	30.3	14.6	0	0	2.4	0	**47.3**

Appendix 15: Pollen percentages in core MD99-22-25, Bay of Islands

Depth (cm)	*Abies*	*Picea*	*Pinus*	*Tsuga*	*Acer*	*Betula*	*Carya*	*Fagus*	*Juglans*	*Tilia*	*Ulmus*	**total trees**	*Betula shrub*	*Alnus*	*Ericaceae*	*Myrica*	*Salix*	*Fraxinus*	**Total shrubs**
1150	7	16	22.6	0.18	1	10.3	0	0	0	0	0.35	**57.4**	24.9	11.1	0	0	1.7	0.2	**37.9**
1200	4.3	10.6	19.6	0	0.4	15.5	0	0	0	0	0	**50.4**	21.1	21.9	0.2	0	2.3	0	**45.5**
1250	5.3	10.8	14.3	0.3	0.3	20.4	0	0	0	0	0.15	**51.6**	28.6	13.9	0.15	0	2.8	0	**45.5**
1300	6.3	10.7	22.3	0	0.2	12.6	0	0	0	0	0.2	**52.3**	29.9	11.8	0	0	2.7	0	**44.4**
1350	8.8	11.5	33.7	0.3	0.3	9.7	0	0.3	0	0	0	**64.6**	20.7	10	0	0	0	0	**30.7**
1400	7.4	4.1	29.4	0	0.5	10.4	0	0	0	0	0	**51.8**	34.5	8.1	0	0	2.3	0	**44.9**
1460	3	7.4	35.8	0	1.5	1.5	0	1.5	0	0	0	**50.7**	25.4	7.5	0	0	1.5	0	**34.4**
1500	1.9	26.2	27.2	0	0	1	0	0	0	0	0	**56.3**	10.7	4.8	0	0	1	0	**16.5**
1600																			
1700	3.5	3.5	16	0	0	21.2	0.4	0	0	0	0.35	**44.9**	33.8	12.5	0	0	2.1	0	**48.4**
1800	6	8.4	21.5	0	0	10.2	0	0	0	0	0	**46.1**	39.5	5.4	0	0	3	0	**47.9**

Appendix 15: Pollen percentages in core MD99-22-25, Bay of Islands

Depth (cm)	*Ambrosia*	*Artemisia*	*Liguliflore*	*Chenopodiaceae*	*Caryophyllaceae*	*Cyperaceae*	*Gramineae*	*Rumex*	*Other Polyg.*	*Leguminoseae*	*Polygonaceae total*	*Nyssa*	*Plantago*	*Morus*	*Rosaceae*	*Cornus*	*Tricolpate*	Unknown	**Total herbs**
0	1.2	0.24	0	0	0	1.44	1.2	0.24	0.72	0	0.72	0.5	0.24	0.5	0	0	0	0.72	**7.72**
10	2	0.25	0	0.25	0	1.51	0.25	0.75	0	0	0	0.25	0	0	0	0	0	0	**5.26**
40	0.7	0.2	0	0.2	0	1.9	0.2	0	0.5	0	0.5	0	0	0	0.2	0	0.4	0.4	**5.2**
80	0.2	0	0	0.2	0	2.5	0	0	1.1	0	1.1	0	0	0	0	0	0.2	0.6	**5.9**
100	0	0.2	0	0.2	0	1.1	0.2	0	0.55	0	0.55	0	0	0	0.2	0	0.2	0.5	**3.7**
120	0.3	0	0	0	0	1.5	0	0.15	1.36	0	1.36	0	0	0	0	0	0.2	0.9	**5.72**
150	0.5	0.5	0	0.24	0	1.4	0	0	1.4	0	1.4	0	0	0	0	0	0	1.4	**6.84**
180	0.2	0.2	0	0	0	1.6	0	0	1.36	0	1.36	0	0	0	0	0	0	1.4	**6.12**
200	0.4	0.4	0	0	0	2.7	0	0	0.62	0	0.62	0	0	0	0	0	0	1.4	**6.14**
250	0.2	0	0	0.2	0	3.4	0	0	0	0	0	0	0	0	0	0	0.4	1.3	**5.5**
300	0.6	0	0.2	0.2	0	1.1	0.2	0	0.2	0	0.2	0	0	0	0	0	0	0.9	**3.6**
350	0	0.4	0	0	0	1.6	0	0	0	0	0	0	0	0	0	0	0	1.4	**3.4**
400	0.2	0	0	0.2	0	0.8	0	0	0.2	0.6	0.8	0	0	0	0	0	0.2	1.1	**4.1**
450	0.3	0	0	0	0	0.76	0.25	0	0	0	0	0	0	0	0	0	0	0.5	**1.76**
500	0.5	0.2	0	0.2	0	0.7	0	0.2	0.2	0	0.2	0	0	0	0	0	0.5	0.7	**3.4**
550	0	0.65	0	0.22	0	0.87	0	0	0.2	0	0.2	0	0	0	0	0	0	0.87	**3.01**
600	0.2	0	0	0.2	0	1.05	0	0	0	0	0	0	0	0	0	0	0	0.63	**2.08**
650	0.2	0.2	0	0	0	0.8	0	0	0.2	0	0.2	0	0	0	0	0	0.4	0.2	**2.2**
700	0.3	0.25	0	0.25	0.25	1	0	0	0	0	0	0	0	0	0	0.3	0	0.5	**2.75**
750	0.2	0.2	0	0.2	0	0.74	0	0	0.55	0	0.55	0	0	0	0	0	0.2	0.74	**3.38**
800	0.2	0.24	0.24	0	0	1.2	0	0	0.5	0	0.5	0	0	0	0	0	0	0.74	**3.66**
850	0.3	0.16	0	0.32	0	0.48	0.16	0	0.32	0	0.32	0	0	0	0	0	0	0.8	**2.88**
1000	0.2	0.23	0	0.23	0	0.7	0	0	0.92	0	0.92	0	0	0	0	0	0	1.38	**4.61**
1050	0.2	0.2	0	0	0	1.15	0	0.2	0.2	0.2	0.4	0	0	0	0	0	0.2	1.7	**4.45**
1100	0.2	0.2	0	0.2	0	0.8	0	0	0.6	0	0.6	0	0	0	0	0	0.2	0.6	**3.4**

Appendix 15: Pollen percentages in core MD99-22-25, Bay of Islands

Depth (cm)	*Ambrosia*	*Artemisia*	*Liguliflore*	*Chenopodiaceae*	*Caryophyllaceae*	*Cyperaceae*	*Gramineae*	*Rumex*	*Other Polyg.*	*Leguminoseae*	*Polygonaceae total*	*Nyssa*	*Plantago*	*Morus*	*Rosaceae*	*Cornus*	*Tricolpate*	Unknown	**Total herbs**
1150	0.5	0	0	0	0	1.7	0.35	0	0.2	0	0.2	0	0	0	0	0	0	1.4	**4.35**
1200	0.4	0	0	0.2	0	1.6	0	0	0.4	0	0.4	0	0	0	0	0	0.2	1.4	**4.6**
1250	0.3	0	0	0.45	0	1.2	0	0	0.3	0	0.3	0	0	0	0	0	0	0.6	**3.15**
1300	0	0.4	0	0	0	0.84	0	0	0.4	0	0.4	0	0	0	0	0	0	1.5	**3.54**
1350	0.3	0	0	0	0	1.2	0	0	0.6	0	0.6	0	0	0	0.3	0	0	0	**3**
1400	0.3	0.5	0	0	0	1.5	0	0	0	0	0	0	0	0	0	0	0	1	**3.25**
1460	0	3	0	0	0	10.4	0	0	1.5	0	0	0	0	0	0	0	0	0	**14.9**
1500	1.9	5.8	0	0	0	7.8	1	0	3.9	0	0	0	0	0	0	0	0	6	**26.4**
1600																			
1700	0.4	0	0	0	0	4.2	0	0	0	0	0	0	0	0	0.7	0	0.7	0.7	**6.65**
1800	0.6	1.2	0	0	0	4.2	0	0	0	0	0	0	0	0	0	0	0	0	**6**

Appendix 16: Raw dinoflagellate cyst counts in core MD99-22-25, Bay of Islands

Depth (cm)	*cf. Alexandrium tamarense*	*Ataxodinium choanum*	*Bitectatodinium tepikiense*	*Impagidinium aculeatum*	*Impagidinium pallidum*	*Lingulodinium machaerophorum*	*Nematosphaeropsis labyrinthus*	*Operculodinium centrocarpum*	*O. centrocarpum short processes*	*O. centrocarpum var. arctic*	*Operculodinium israelianum*	*O. centrocarpum cezare*	*Pyxidiniopsis reticulata*	*Spiniferites membranaceus*	*Spiniferites delicatus*	*Spiniferites elongatus*	*Spiniferites ramosus*	*Spiniferites bentorii*	*Spiniferites bulloideus*	*Spiniferites frigidus*	*Spiniferites lazus*	*Spiniferites mirabilis*	*Spiniferites spp.*	*Pentapharsodinium dalei*	*Islandinium minutum*	*Algidasphaeridium var. cezare*	*Brigantedinium spp.*	*Brigantedinium cariacoense*	*Brigantedinium simplex*	*Selenopemphix quanta*	*Votadinium calvum*	Total
0	1	5	3	0	0	1	16	99	0	1	0	2	0	0	1	3	32	0	0	2	0	0	1	24	4	0	104	0	6	1	1	**307**
10	0	1	4	0	0	0	13	81	1	1	0	0	0	1	7	7	17	0	9	1	1	0	6	21	4	0	130	1	2	0	0	**308**
40	0	4	3	0	1	0	13	126	4	2	1	0	0	0	10	3	32	0	1	0	0	0	2	36	0	0	96	1	2	1	0	**338**
80	0	2	4	0	0	0	12	155	1	1	0	0	0	0	0	2	31	0	10	0	0	2	1	65	1	0	90	0	1	0	0	**378**
100	0	2	6	0	0	0	7	115	6	0	0	0	0	0	2	14	30	0	4	0	0	5	0	38	7	0	96	0	0	0	0	**332**
120	0	2	5	0	0	0	8	116	4	1	0	0	0	0	2	2	46	0	1	0	1	3	0	48	2	0	75	0	0	1	0	**317**
150	0	2	8	0	0	0	2	130	3	1	0	0	0	0	5	2	42	0	2	0	0	6	3	112	0	0	55	0	0	0	0	**373**
180	0	1	1	0	0	0	4	97	3	3	0	0	1	0	6	4	29	0	1	0	0	0	4	40	0	5	124	0	1	0	0	**324**
200	0	2	2	0	0	0	7	78	1	1	0	0	0	0	2	1	20	0	0	0	0	0	2	15	0	2	174	0	0	0	0	**307**
250	0	2	0	0	0	0	4	126	1	1	1	0	0	1	6	4	36	0	0	2	0	0	4	88	0	0	47	0	0	0	0	**323**
300	0	1	5	1	0	0	4	182	4	1	0	0	0	0	3	7	34	0	0	0	0	2	4	44	0	0	31	0	0	1	0	**324**
350	0	5	6	0	0	0	10	170	9	0	0	0	0	1	4	5	20	1	0	0	0	2	1	39	0	0	37	0	0	0	0	**310**
400	1	2	3	0	0	0	5	170	3	12	0	0	0	0	3	7	14	0	0	0	0	2	2	22	0	0	90	0	0	1	0	**337**
450	0	6	12	0	1	0	2	116	2	3	0	0	0	0	5	5	33	0	0	0	0	1	2	12	7	0	114	0	0	0	0	**321**
500	0	4	1	0	0	0	2	141	5	0	0	0	0	0	1	4	22	0	0	0	0	1	3	27	3	0	114	0	0	0	0	**328**
550	0	2	5	0	0	0	0	158	2	1	2	1	0	1	0	5	11	0	0	0	0	0	1	31	6	0	84	0	0	0	0	**310**
600	0	1	3	0	0	0	1	180	2	0	0	1	0	0	0	3	14	0	0	0	0	0	2	25	5	0	66	0	0	0	0	**303**
650	0	2	1	0	0	0	0	168	6	5	1	1	0	0	1	6	13	0	0	0	0	0	3	40	0	0	75	0	0	1	0	**323**
700	0	3	4	0	0	0	0	173	1	0	1	0	0	0	0	10	13	0	0	0	0	0	1	25	8	1	63	0	0	2	0	**305**
750	0	0	8	0	0	0	1	140	1	2	0	1	0	1	0	3	12	0	0	0	0	0	2	48	4	1	79	0	0	0	0	**303**

Appendix 16: Raw dinoflagellate cyst counts in core MD99-22-25, Bay of Islands

Depth (cm)	*cf. Alexandrium tamarense*	*Ataxodinium choanum*	*Bitectatodinium tepikiense*	*Impagidinium aculeatum*	*Impagidinium pallidum*	*Lingulodinium machaerophorum*	*Nematosphaeropsis labyrinthus*	*Operculodinium centrocarpum*	*O. centrocarpum short processes*	*O. centrocarpum var. arctic*	*Operculodinium israelianum*	*O. centrocarpum cezare*	*Pyxidiniopsis reticulata*	*Spiniferites membranaceus*	*Spiniferites delicatus*	*Spiniferites elongatus*	*Spiniferites ramosus*	*Spiniferites bentorii*	*Spiniferites bulloideus*	*Spiniferites frigidus*	*Spiniferites lazus*	*Spiniferites mirabilis*	*Spiniferites spp.*	*Pentapharsodinium dalei*	*Islandinium minutum*	*Algidasphaeridium var. cezare*	*Brigantedinium spp.*	*Brigantedinium cariacoense*	*Brigantedinium simplex*	*Selenopemphix quanta*	*Votadinium calvum*	Total
800	0	6	1	0	1	0	0	151	1	0	0	0	0	0	0	9	8	0	0	0	0	0	1	17	20	2	82	0	0	1	0	**300**
850	0	3	3	0	0	0	0	132	3	5	2	0	0	0	1	7	15	0	0	0	0	0	3	14	5	1	101	0	0	1	0	**296**
1000	0	1	5	0	0	0	1	175	3	1	1	2	1	0	2	13	16	0	0	0	0	1	4	14	0	1	90	0	0	0	0	**331**
1050	0	4	28	0	3	0	2	89	3	1	0	0	0	0	0	15	27	0	0	0	0	0	4	25	4	0	131	0	0	1	0	**337**
1100	0	15	17	0	4	0	5	75	3	1	3	0	1	0	4	21	36	0	0	0	0	1	1	32	3	0	78	0	0	0	0	**300**
1150	0	5	29	0	0	1	6	69	6	2	2	0	0	0	3	12	35	0	1	0	0	0	3	23	5	0	97	0	0	2	0	**301**
1200	0	9	29	1	0	0	12	74	6	2	0	0	1	0	14	2	29	0	0	0	0	1	6	94	3	0	61	0	0	3	0	**347**
1250	0	2	14	0	0	0	1	111	1	3	0	1	0	0	13	6	44	0	0	0	0	0	6	33	0	0	95	0	0	3	0	**333**
1300	0	5	23	0	0	0	14	83	1	3	1	0	0	0	8	11	22	0	0	0	0	2	6	104	4	0	40	0	0	1	0	**328**
1350	1	4	11	0	1	0	4	57	5	0	0	0	0	0	3	12	21	0	0	0	0	0	0	100	14	0	88	0	0	1	0	**322**
1400	0	1	6	0	0	0	0	62	0	0	0	0	0	0	4	13	22	0	0	0	0	0	2	22	16	0	74	0	0	0	0	**222**
1460	13	0	29	0	1	0	0	48	0	0	0	0	0	0	0	2	6	0	0	0	0	0	1	15	5	0	85	0	0	0	0	**205**
1500	0	0	3	0	0	0	0	40	0	0	0	0	0	0	0	10	1	0	0	0	0	0	2	3	6	0	286	0	0	24	0	**375**
1600	0	0	0	0	0	0	0	3	0	0	0	0	0	0	0	0	0	0	0	0	0	0	0	4	0	0	104	0	0	1	0	**112**
1700	1	2	8	0	0	0	0	38	0	0	0	0	0	0	0	7	24	0	1	1	0	0	4	32	25	0	90	0	0	0	0	**233**
1800	3	1	18	0	0	0	0	59	2	0	0	0	0	0	4	8	44	0	0	0	0	0	5	12	13	0	36	0	0	2	0	**207**

Appendix 17: Dinoflagellates cyst percentages in core MD99-22-25, Bay of Islands

Depth (cm)	*cf. Alexandrium excavatum*	*Ataxodinium choanum*	*Bitectatodinium tepikiense*	*Impagidinium aculeatum*	*Impagidinium pallidum*	*Lingulodinium machaerophorum*	*Nematosphaeropsis labyrinthus*	*Operculodinium centrocarpum*	*O. centrocarpum short processes*	*O. centrocarpum var. arctic*	*Operculodinium israelianum*	*O. centrocarpum cezare*	*Pyxidiniopsis reticulata*	*Spiniferites membranaceus*	*Spiniferites delicatus*	*Spiniferites elongatus*	*Spiniferites ramosus*	*Spiniferites bentorii*	*Spiniferites bulloideus*
0	0.32	1.63	0.97	0	0	0.32	5.21	32.25	0	0.32	0	0.65	0	0	0.32	0.98	10.42	0	0
10	0	0.32	1.29	0	0	0	4.19	26.13	0.32	0.32	0	0	0	0.32	2.25	2.25	5.48	0	2.9
40	0	1.2	0.9	0	0.3	0	3.8	37.3	1.2	0.6	0.3	0	0	0	2.95	0.9	9.5	0	0.3
80	0	0.53	1.05	0	0	0	3.16	40.8	0.26	0.26	0	0	0	0	0	0.53	8.16	0	2.63
100	0	0.6	1.8	0	0	0	2.1	34.6	1.8	0	0	0	0	0	0.6	4.2	9	0	1.2
120	0	0.63	1.6	0	0	0	2.5	36.6	1.3	0.3	0	0	0	0	0.6	0.6	14.5	0	0.3
150	0	0.53	2.15	0	0	0	0.53	34.8	0.8	0.26	0	0	0	0	1.3	0.53	11.2	0	0.53
180	0	0.3	0.3	0	0	0	1.2	29.9	0.9	0.9	0	0	0.3	0	1.85	1.23	8.95	0	0.3
200	0	0.65	0.65	0	0	0	2.3	25.4	0.32	0.32	0	0	0	0	0.65	0.32	6.5	0	0
250	0	0.62	0	0	0	0	1.2	39	0.31	0.31	0.31	0	0	0.31	1.86	1.2	11.1	0	0
300	0	1.6	1.9	0	0	0	3.2	54.8	2.9	0	0	0	0	0.3	1.3	1.6	6.5	0.3	0
350	0	0.3	1.5	0.3	0	0	1.2	56	1.2	0.3	0	0	0	0	0.9	2.2	10.5	0.3	0
400	0.3	0.6	0.9	0	0	0	1.5	50.5	0.9	3.6	0	0	0	0	0.9	2.1	4.15	0	0
450	0	1.9	3.7	0	0.3	0	0.6	36.1	0.6	0.9	0	0	0	0	1.6	1.6	10.3	0	0
500	0	1.2	0.3	0	0	0	0.6	43	1.5	0	0	0	0	0	0.3	1.2	6.7	0	0
550	0	0.65	1.6	0	0	0	0	51	0.65	0.32	0.65	0.32	0	0.32	0	1.6	3.5	0	0
600	0	0.3	1	0	0	0	0.3	59.4	0.7	0	0	0.3	0	0	0	1	4.6	0	0
650	0	0.62	0.3	0	0	0	0	52	1.9	1.6	0.3	0.3	0	0	0.3	1.9	4	0	0
700	0	1	1.3	0	0	0	0	56.7	0.33	0	0.33	0	0	0	0	3.3	4.3	0	0
750	0	0	2.6	0	0.65	0	0.3	46	0.3	0.65	0	0.3	0	0.3	0	1	3.9	0	0
800	0	1.9	0.3	0	0.3	0	0	48.7	0.3	0	0	0	0	0	0	2.9	2.6	0	0

Appendix 17: Dinoflagellates cyst percentages in core MD99-22-25, Bay of Islands

Depth (cm)	*cf. Alexandrium excavatum*	*Ataxodinium choanum*	*Bitectatodinium tepikiense*	*Impagidinium aculeatum*	*Impagidinium pallidum*	*Lingulodinium machaerophorum*	*Nematosphaeropsis labyrinthus*	*Operculodinium centrocarpum*	*O. centrocarpum short processes*	*O. centrocarpum var. arctic*	*Operculodinium israelianum*	*O. centrocarpum cezare*	*Pyxidiniopsis reticulata*	*Spiniferites membranaceus*	*Spiniferites delicatus*	*Spiniferites elongatus*	*Spiniferites ramosus*	*Spiniferites bentorii*	*Spiniferites bulloideus*
850	0	1	1	0	0	0	0	44.6	1	1.7	0.7	0	0	0	0.3	2.4	5.1	0	0
1000	0	0.3	1.5	0	0	0	0.3	52.9	0.91	0.3	0.3	0.6	0.3	0	0.6	3.9	4.8	0	0
1050	0	1.2	8.3	0	0.9	0	0.6	26.4	0.9	0.3	0	0	0	0	0	4.5	8	0	0
1100	0	5	5.7	0	1.3	0	1.7	25	1	0.3	1	0	0.3	0	1.3	7	12	0	0
1150	0	1.7	9.6	0	0	0.3	2	22.9	2	0.7	0.7	0	0	0	1	4	11.6	0	0.3
1200	0	2.6	8.4	0.3	0	0	3.5	21.3	1.7	0.6	0	0	0.3	0	4	0.6	8.4	0	0
1250	0	0.6	4.2	0	0	0	0.3	33.3	0.3	0.9	0	0.3	0	0	3.9	1.8	13.2	0	0
1300	0	1.5	7	0	0	0	4.3	25.3	0.3	0.9	0.3	0	0	0	2.4	3.3	6.7	0	0
1350	0.3	1.2	3.4	0	0.3	0	1.2	17.8	1.6	0	0	0	0	0	0.93	3.7	6.5	0	0
1400	0	0.4	2.7	0	0	0	0	27.8	0	0	0.4	0	0	0	1.8	5.8	9.9	0	0
1460	6.3	0	14.1	0	0.5	0	0	23.4	0	0	0	0	0	0	0	1	2.9	0	0
1500	0	0	0.8	0	0	0	0	10.7	0	0	0	0	0	0	0	2.7	0.26	0	0
1600	0	0	0	0	0	0	0	2.7	0	0	0	0	0	0	0	0	0	0	0
1700	0.4	0.8	3.3	0	0	0	0	16	0.8	0	0.8	0	0	0	0	3.4	10	0	0.4
1800	1.4	0.5	8.7	0	0	0	0	28.5	1	0	0	0	0	0	2	3.9	21	0	0

Appendix 17: Dinoflagellates cyst percentages in core MD99-22-25, Bay of Islands

Depth (cm)	*Spiniferites frigidus*	*Spiniferites lazus*	*Spiniferites mirabilis*	*Spiniferites spp.*	*Pentapharsodinium dalei*	*Algidasphaeridium minutum*	*Algidasphaeridium var. cezare*	*Brigantedinium spp.*	*Brigantedinium cariacoense*	*Brigantedinium simplex*	*Selenopemphix quanta*	*Votadinium calvum*
0	0.65	0	0	0.32	7.82	1.3	0	33.87	0	1.95	0.32	0.32
10	0.32	0.32	0	1.92	6.77	1.29	0.65	41.93	0.32	0.65	0	0
40	0	0	0	0.6	10.65	0	0	28.4	0.3	0.6	0.3	0
80	0	0	0.53	0.26	17.1	0.26	0.53	23.7	0	0.26	0	0
100	0	0	1.5	0	11.4	2.1	0	28.9	0	0	0	0
120	0	0.3	0.95	0	15.14	0.6	0	23.7	0	0	0.3	0
150	0	0	1.6	0.8	30	0	0	14.7	0	0	0	0
180	0	0	0	1.23	12.3	1.54	0	38.7	0	0.3	0	0
200	0	0	0	0.65	4.9	0	0.65	56.7	0	0	0	0
250	0.62	0	0	1.2	27.2	0	0	14.6	0	0	0	0
300	0	0	0.65	0.3	12.6	0	0	11.9	0	0	0.3	0
350	0	0	0.6	1.2	13.6	0	0	9.6	0	0	0	0
400	0	0	0.6	0.6	6.5	0	0	26.7	0	0	0.3	0
450	0	0	0.3	0.6	3.7	2.2	0	35.5	0	0	0	0
500	0	0	0.3	0.9	8.2	0.9	0	34.7	0	0	0	0
550	0	0	0	0.32	10	1.9	0	27	0	0	0	0
600	0	0	0	0.7	8.2	1.6	0	21.8	0	0	0	0
650	0	0	0	0.9	12.4	0	0	23.2	0	0	0.3	0
700	0	0	0	0.33	8.2	2.6	0.33	20.7	0	0	0.65	0
750	0	0	0	0.65	15.7	1.3	0.3	25.9	0	0	0	0
800	0	0	0	0.3	5.5	6.5	0.65	29.7	0	0	0.3	0

Appendix 17: Dinoflagellates cyst percentages in core MD99-22-25, Bay of Islands

Depth (cm)	*Spiniferites frigidus*	*Spiniferites lazus*	*Spiniferites mirabilis*	*Spiniferites spp.*	*Pentapharsodinium dalei*	*Algidasphaeridium minutum*	*Algidasphaeridium var. cezare*	*Brigantedinium spp.*	*Brigantedinium cariacoense*	*Brigantedinium simplex*	*Selenopemphix quanta*	*Votadinium calvum*
850	0	0	0	1	4.7	1.7	0.3	34.1	0	0	0.3	0
1000	0	0	0.3	1.2	4.2	0	0.3	27.2	0	0	0	0
1050	0	0	0	1.2	7.4	1.2	0	38.9	0	0	0.3	0
1100	0	0	0.3	0.3	10.7	1	0	26	0	0	0	0
1150	0	0	0	1	7.6	1.7	0	32.2	0	0	0.7	0
1200	0	0	0.3	1.7	27.1	0.9	0	17.6	0	0	0.9	0
1250	0	0	0	1.8	9.9	0	0	28.5	0	0	0.9	0
1300	0	0	0.6	1.8	31.7	1.2	0	12.2	0	0	0.3	0
1350	0	0	0	0	31	4.3	0	27.4	0	0	0.3	0
1400	0	0	0	0.9	9.9	7.2	0	33.2	0	0	0	0
1460	0	0	0	0.5	7.3	2.4	0	41.5	0	0	0	0
1500	0	0	0	0.5	0.8	1.6	0	76.3	0	0	6.4	0
1600	0	0	0	0	3.6	0	0	92.8	0	0	0.9	0
1700	0	0	0	1.7	13.5	10.4	0	37.7	0	0	0.8	0
1800	0	0	0	2.4	5.8	6.3	0	17.5	0	0	1	0

Appendix 18: Concentrations of palynomorphs in core 84-011-12 St. Anne's Basin

	Depth (cm)	Dinoflagellate cysts	Pollen	Spores	Reworked	Organic linings
TWC	1-3	25317	60934	3646	120	7812
	20-22	37820	91760	4340	0	12400
	30-32	33668	55552	3472	0	5729
	40-42	40823	52401	1286	161	7072
	50-52	31048	53642	3298	222	7638
	60-62	38717	68755	2513	228	9594
	70-72	42140	77354	3063	0	9190
	80-82	40975	69440	3655	0	8680
	90-92	20460	40770	2236	0	5129
	100-102	42722	130634	6076	0	20398
	110-112	25614	69440	2741	0	10050
	120-122	24747	93165	3761	579	13020
Piston	0-2	41033	95968	5126	129	11106
	10-12	31873	62521	1294	164	4272
	14-16	34621	62930	2288	86	6611
	20-22	44094	50152	1740	0	6170
	30-32	73092	75228	2373	237	8068
	40-42	26077	64359	2420	83	6692
	50-52	25794	68524	2848	82	7475
	60-62	45136	147953	2718	0	13591
	70-72	34173	89254	2473	0	7644
	80-82	95684	128717	2563	1424	5695
	90-92	129313	152613	3495	388	2330
	100-102	68773	112343	4699	213	10465
	110-112	35409	84427	3518	0	8041
	120-122	60917	140963	3661	0	9458
	130-132	45279	151448	5436	388	10873
	140-142	26808	62979	2738	0	5148
	150-152	50806	106242	3286	274	13417
	160-162	51892	103129	3661	0	8543
	170-172	49997	142387	6407	0	18866
	179-181	52143	11745	5072	267	14684
	200-202	35859	144807	516	1281	17086
	220-222	52284	123488	4272	0	12815
	240-242	37224	100116	4538	0	9611
	260-262	47376	88579	3822	450	9892
	280-282	50120	121207	5606	534	12548
	300-302	34949	84655	7766	194	10679
	320-322	65498	115618	8258	0	8828
	340-342	32402	77102	6407	0	5553

Appendix 18: Concentrations of palynomorphs in core 84-011-12
St. Anne's Basin

	Depth (cm)	**Dinoflagellate cysts**	**Pollen**	**Spores**	**Reworked**	**Organic linings**
	360-362	31888	111672	10374	1220	7933
	380-382	28022	92266	9682	569	7689
	400-402	30186	165311	15805	1281	13242
	420-422	30356	83760	10029	186	6872
Piston	440-442	27426	118440	25888	1942	3560
	460-462	34076	92401	15063	0	6295
	480-482	28447	122046	19222	0	6407
	500-502	18629	67074	6407	0	4094
	520-522	13194	48298	4530	0	1294
	540-542	21612	79425	6007	0	3560
	560-562	34600	48723	1602	0	2803
	580-582	27587	32037	1052	0	1861
	600-602	38711	66032	3382	356	5695
	620-622	32037	49891	3838	334	3337
	630-632	41648	74975	3337	0	3560
	640-642	21358	20150	763	63	763
	660-662	58734	52767	1570	314	471
	680-682	50169	35597	1446	0	2669
	700-702	48056	35088	1017	127	1907
	720-722	38139	33276	1907	0	1430
	740-742	41699	34986	1729	0	3356
	750-752	39411	32291	1398	0	1780

Appendix 19: Raw pollen and spores counts, 84-011-12P St Anne's Basin

Depth	*Abies*	*Picea*	*Pinus*	*Tsuga*	*Acer*	*Betula*	*Carya*	*Fagus*	*Fraxinus*	*Juglans*	*Quercus*	*Tillia*	*Ulmus*	**total trees**	*Betula shrub*	*Alnus*	Ericaceae	*Myrica*	*Salix*	**Total shrubs**	*Ambrosia*	*Artemisia*	Chenopodiaceae	Cyperaceae	Gramineae	*Rumex*
1-3 TWC	34	65	113	32	3	26	0	2	1	0	3	0	2	281	44	6	0	0	7	57	5	0	0	0	0	0
20-22 TWC	17	58	118	8	4	3	0	0	0	0	3	0	0	211	59	7	0	0	3	69	0	0	0	3	1	6
30-32 TWC	18	39	96	27	5	21	0	2	0	0	8	1	1	218	83	6	0	0	4	93	1	1	1	1	0	0
40-42 TWC	27	43	109	36	8	15	0	0	0	0	3	0	1	242	65	8	0	0	1	74	1	0	0	2	0	0
50-52TWC	17	20	111	33	2	19	0	1	0	0	3	1	0	207	83	6	0	0	6	95	1	0	1	0	0	0
60-62 TWC	16	32	76	32	11	27	0	0	0	0	4	0	0	198	85	4	0	0	2	91	1	0	2	4	0	0
70-72TWC	17	29	124	27	11	4	0	1	0	0	0	0	2	215	72	5	0	0	0	77	0	0	0	1	1	0
80-82 TWC	10	24	100	34	9	23	0	1	0	0	3	0	2	206	77	2	0	0	7	86	2	0	0	3	0	0
90-92TWC	5	13	119	31	7	6	0	1	1	0	7	0	0	190	98	8	0	0	5	111	1	1	0	0	0	0
101-103 TWC	2	19	96	26	10	28	0	3	0	0	9	0	0	193	80	10	1	0	5	96	1	2	0	2	1	0
110-112TWC	18	26	116	36	10	4	0	2	0	0	1	0	0	213	74	7	0	0	1	82	1	1	1	0	0	0
120-122 TWC	5	22	115	39	11	23	0	1	0	0	5	0	0	221	81	11	1	0	1	94	1	1	0	1	0	0
0-2 Piston	20	69	97	32	18	39	0	3	0	0	8	0	2	288	26	17	0	0	0	35	3	0	1	1	2	0
10-12	26	101	110	47	12	68	1	4	3	3	6	0	2	388	51	37	0	0	2	90	0	2	0	4	1	0
14-16	31	92	129	54	13	76	0	3	1	0	7	0	1	407	62	14	2	0	3	81	4	0	1	1	1	0
20-22	39	57	77	43	6	44	1	1	0	0	0	0	0	268	31	7	0	0	4	42	0	0	0	5	1	0
30-32	26	39	88	36	2	38	0	0	0	0	3	0	2	234	55	8	0	0	2	65	0	0	0	7	1	0
40-42	24	50	136	42	14	81	1	2	2	0	5	2	0	359	68	13	0	0	3	84	1	0	0	3	1	0
50-52	22	51	104	53	10	63	0	0	0	0	6	1	1	311	55	7	1	0	0	63	1	1	1	4	0	0
60-62	46	53	116	55	9	46	0	0	0	0	0	0	0	325	43	5	0	0	1	49	1	1	0	2	1	0
70-72	17	36	153	41	14	60	0	0	0	1	1	0	1	324	53	11	0	0	2	66	1	0	0	2	0	1
80-82	27	39	203	57	11	51	0	0	0	0	10	1	1	400	33	9	0	0	2	44	1	1	2	3	0	0
90-92	19	46	166	41	9	37	0	0	0	0	8	0	0	326	55	5	0	0	0	60	1	2	1	2	0	0
100-102	27	63	217	69	9	51	0	0	0	0	6	0	0	442	54	14	0	0	2	70	0	0	2	3	0	0
110-112	6	39	143	24	7	39	0	1	0	0	7	0	0	266	59	4	0	0	2	65	0	1	1	2	0	1
120-122	13	62	216	36	8	47	0	1	0	0	8	0	1	392	50	8	0	0	1	59	0	3	1	5	1	0
130-132	13	49	172	25	7	51	0	0	1	0	6	0	1	325	53	6	0	0	2	61	0	1	1	2	0	0

Appendix 19: Raw pollen and spores counts, 84-011-12P St Anne's Basin

Depth	*Abies*	*Picea*	*Pinus*	*Tsuga*	*Acer*	*Betula*	*Carya*	*Fagus*	*Fraxinus*	*Juglans*	*Quercus*	*Tillia*	*Ulmus*	**total trees**	*Betula shrub*	*Alnus*	Ericaceae	*Myrica*	*Salix*	**Total shrubs**	*Ambrosia*	*Artemisia*	Chenopodiaceae	Cyperaceae	Gramineae	*Rumex*
140-142	12	56	229	29	12	90	1	2	0	0	12	0	1	444	88	25	1	0	6	120	1	0	1	7	2	0
150-152	15	42	181	19	10	28	0	1	2	0	7	0	0	305	64	7	0	0	1	72	0	1	0	2	2	0
160-162	8	50	140	24	3	38	1	2	3	0	3	0	0	272	51	6	0	0	6	63	0	1	0	0	0	1
170-172	10	33	181	18	14	48	0	1	3	0	1	0	0	309	66	10	0	0	4	80	0	1	0	2	0	0
179-181	17	41	187	22	13	47	2	1	0	0	2	0	0	332	83	6	0	0	6	95	2	0	1	2	0	0
200-202	8	33	144	8	10	49	0	3	0	0	8	0	1	264	55	10	0	0	3	68	1	0	2	3	0	0
220-222	10	36	155	11	8	30	0	0	1	0	9	0	1	261	43	6	0	0	2	51	0	1	0	1	2	0
240-242	12	34	158	20	8	45	0	3	1	0	10	1	0	292	59	9	1	0	1	70	1	0	2	4	1	0
260-262	12	35	211	17	6	29	0	0	2	0	12	1	2	327	51	7	0	0	5	63	1	0	0	3	0	0
280-282	13	40	225	41	13	47	0	0	1	0	7	1	1	389	48	12	0	0	1	61	0	1	0	1	0	0
300-302	8	33	190	47	16	40	0	1	1	0	3	0	2	341	68	12	0	0	2	82	2	0	0	2	1	0
320-322	12	48	162	67	7	24	0	0	0	0	2	0	2	324	61	7	0	1	3	72	1	0	1	3	0	0
340-342	8	33	169	50	3	21	0	3	0	0	1	0	1	289	51	12	1	0	5	69	0	0	0	0	0	0
360-362	9	29	159	67	6	17	0	1	1	0	0	0	2	291	57	5	3	0	1	66	3	1	1	1	0	0
380-382	11	30	154	54	2	7	9	2	0	0	3	0	0	272	43	6	4	0	1	54	1	1	1	1	0	0
400-402	12	25	208	44	3	7	0	1	0	0	3	0	0	303	59	7	2	0	2	70	1	1	0	8	1	0
420-422	14	45	205	58	2	23	0	1	0	0	7	0	2	357	62	10	2	0	8	82	1	1	1	5	0	0
440-442	11	28	208	21	4	22	0	0	0	0	2	2	0	298	41	17	1	0	1	60	1	1	1	1	0	0
460-462	8	36	275	17	6	12	0	0	0	0	2	0	0	356	37	9	2	1	0	49	1	1	1	0	2	0
480-482	13	38	220	24	7	13	0	1	0	0	3	0	0	319	59	7	1	0	5	72	1	1	3	0	1	0
500-502	10	36	206	14	4	8	0	0	0	0	7	1	0	286	47	12	1	0	2	62	0	0	1	3	0	0
520-522	24	64	348	19	10	21	0	1	0	0	5	0	2	494	47	12	1	0	3	63	1	1	1	4	0	0
540-542	21	37	210	10	1	13	0	0	0	0	0	0	2	294	31	20	0	0	3	54	2	0	0	2	0	0
560-562	13	40	183	0	4	11	0	0	0	0	0	0	0	251	59	42	0	0	2	103	1	0	0	9	0	0
580-582	14	41	179	2	5	14	0	0	0	0	4	0	1	260	80	38	0	0	2	120	3	0	0	8	0	0
600-602	22	40	197	1	1	22	0	0	0	0	0	0	0	283	58	17	0	0	1	76	2	0	0	3	0	0
620-622	23	26	144	1	2	13	0	0	0	0	2	0	1	212	41	28	0	0	7	76	3	1	0	4	0	0

Appendix 19: Raw pollen and spores counts, 84-011-12P St Anne's Basin

Depth	*Abies*	*Picea*	*Pinus*	*Tsuga*	*Acer*	*Betula*	*Carya*	*Fagus*	*Fraxinus*	*Juglans*	*Quercus*	*Tillia*	*Ulmus*	**total trees**	*Betula shrub*	*Alnus*	Ericaceae	*Myrica*	*Salix*	**Total shrubs**	*Ambrosia*	*Artemisia*	Chenopodiaceae	Cyperaceae	Gramineae	*Rumex*
630-632	31	38	157	1	7	12	1	0	0	0	4	0	2	253	45	24	0	0	9	78	1	1	1	3	0	0
640-642	7	30	146	0	6	22	0	3	0	0	1	0	0	215	62	30	0	0	0	92	2	0	0	0	0	0
660-662	14	46	173	4	6	12	0	1	0	0	0	1	0	257	43	16	0	0	6	65	1	0	0	1	1	0
680-682	4	32	163	2	7	23	0	0	0	0	8	0	1	240	45	20	0	0	4	69	0	0	0	2	0	0
700-702	28	24	129	2	4	14	0	1	0	0	4	0	0	206	33	22	0	0	4	59	2	0	0	1	0	0
720-722	30	28	186	3	0	14	0	0	0	0	3	0	0	264	49	25	0	0	3	77	1	1	0	2	1	0
740-742	11	24	141	0	5	22	0	2	0	0	9	0	0	214	85	24	0	0	7	116	0	1	0	8	0	0
750-752	11	35	103	0	1	13	0	0	0	1	6	0	1	171	50	16	1	0	1	68	2	0	1	6	0	0

Appendix 19: Raw pollen and spores counts, 84-011-12P St Anne's Basin

Depth	Other Polygonaceae	Unknown	*Typha*	**Total herbs**	**Total Pollen**	*L. annotinum*	*L.clavatum*	*L. lucidulum*	monolete spore	trilete spore	*Sphagnum*	*Osmunda*	*Typha*	Isoetes	**Total spores**
1-3 TWC	3	5	0	13	351	0	3	1	3	9	5	0	0	0	21
20-22 TWC	1	5	0	16	296	0	1	0	4	2	7	0	0	0	14
30-32 TWC	2	3	0	9	320	1	1	1	5	7	3	0	0	2	20
40-42 TWC	1	6	0	10	326	0	1	0	3	1	1	0	0	2	8
50-52TWC	2	3	0	7	309	1	1	0	4	4	7	0	0	2	19
60-62 TWC	1	4	0	12	301	0	2	1	2	1	4	0	0	1	11
70-72TWC	5	4	0	11	303	1	3	1	4	2	1	0	0	0	12
80-82 TWC	1	6	0	12	304	1	3	3	2	5	2	0	0	0	16
90-92TWC	2	5	0	9	310	0	4	2	4	1	6	0	0	0	17
101-103 TWC	1	5	0	12	301	1	1	1	4	1	4	0	0	2	14
110-112TWC	3	3	0	9	304	0	1	2	5	1	2	0	0	1	12
120-122 TWC	0	4	0	7	322	1	2	3	3	1	3	0	0	0	13
0-2 Piston	0	5	0	14	337	0	1	1	3	2	8	2	1	0	18
10-12	3	2	0	10	483	0	1	2	5	2	0	0	0	0	10
14-16	0	9	0	7	495	1	5	0	3	1	7	1	0	0	18
20-22	1	7	0	7	268	1	4	0	5	0	5	0	0	0	15
30-32	3	0	0	18	317	0	2	0	2	3	2	0	0	1	10
40-42	3	0	1	9	452	1	2	1	5	3	4	0	0	1	17
50-52	0	4	0	11	385	1	1	1	3	2	7	0	0	1	16
60-62	1	1	0	7	381	1	1	0	1	0	3	0	0	1	7
70-72	0	3	0	7	397	2	1	1	2	1	1	0	0	1	9
80-82	1	0	0	8	452	1	2	0	4	0	1	0	0	1	9
90-92	1	0	0	7	393	0	2	2	2	0	2	0	0	1	9
100-102	1	0	0	6	526	1	3	0	10	1	7	0	0	0	22
110-112	0	0	0	5	336	1	1	3	5	0	3	0	0	1	14
120-122	0	1	0	11	462	0	1	0	5	1	4	0	0	1	12
130-132	0	0	0	4	390	0	2	2	6	2	1	0	0	1	14

Appendix 19: Raw pollen and spores counts, 84-011-12P St Anne's Basin

Depth	Other Polygonaceae	Unknown	*Typha*	**Total herbs**	**Total Pollen**	*L. annotinum*	*L.clavatum*	*L. lucidulum*	monolete spore	trilete spore	*Sphagnum*	*Osmunda*	*Typha*	Isoetes	**Total spores**
140-142	0	0	0	11	575	1	6	1	8	1	6	0	0	2	25
150-152	1	5	0	11	388	1	1	1	5	1	1	0	0	0	12
160-162	1	0	0	3	338	0	2	1	4	1	1	0	0	3	12
170-172	1	7	0	11	400	0	2	1	9	4	1	0	0	1	18
179-181	1	7	0	13	440	1	3	2	5	0	8	0	0	0	19
200-202	0	1	0	7	339	1	1	2	1	0	4	0	0	3	12
220-222	2	0	0	6	318	2	1	2	2	1	3	0	0	0	11
240-242	1	4	0	13	375	1	0	1	8	1	6	0	0	0	17
260-262	0	0	0	4	394	0	0	0	6	3	7	0	0	1	17
280-282	1	1	0	4	454	2	2	1	6	0	10	0	0	0	21
300-302	4	4	0	13	436	0	6	1	8	3	16	0	0	6	40
320-322	1	4	0	10	406	0	1	3	6	1	17	0	0	1	29
340-342	0	3	0	3	361	1	4	0	4	1	19	0	0	1	30
360-362	3	0	0	9	366	0	2	1	10	2	18	0	0	1	34
380-382	0	1	0	5	324	0	5	6	6	1	14	0	0	2	34
400-402	1	2	0	14	387	1	6	0	5	0	21	0	0	4	37
420-422	1	3	0	12	451	0	4	0	7	2	35	0	0	6	54
440-442	0	0	0	8	366	2	1	1	8	6	60	0	0	2	80
460-462	0	0	0	5	411	1	3	0	8	10	39	0	0	6	67
480-482	0	3	0	9	400	4	7	0	7	8	36	0	0	1	63
500-502	2	0	0	11	360	4	4	0	8	6	14	0	0	0	36
520-522	5	0	1	20	577	3	12		13	7	19	0	0	2	56
540-542	4	1	0	9	357	3	3	0	10	3	7	1	0	1	28
560-562	3	5	0	13	365	1	2	0	4	4	1	0	0	0	12
580-582	3	2	0	14	396	1	4	1	5	1	1	0	0	0	13
600-602	4	3	0	12	371	1	6	1	3	3	4	0	0	1	19
620-622	2	1	0	11	299	2	3	1	2	7	7	0	0	0	22

Appendix 19: Raw pollen and spores counts, 84-011-12P St Anne's Basin

Depth	Other Polygonaceae	Unknown	*Typha*	**Total herbs**	**Total Pollen**	*L. annotinum*	*L.clavatum*	*L. lucidulum*	monolete spore	trilete spore	*Sphagnum*	*Osmunda*	*Typha*	Isoetes	**Total spores**
630-632	0	0	0	6	337	2	2	0	4	2	4	0	0	1	15
640-642	2	6	0	10	317	1	1	0	3	6	0	0	0	1	12
660-662	4	7	0	14	336	1	5	0	0	3	1	0	0	0	10
680-682	2	6	1	11	320	2	1	0	5	2	3	0	0	0	13
700-702	4	4	0	11	276	0	0	0	4	3	1	0	0	0	8
720-722	0	3	0	8	349	8	2	1	5	2	1	0	0	1	20
740-742	3	2	0	14	344	1	7	0	2	3	2	0	0	2	17
750-752	3	0	0	15	254	0	1	0	2	4	4	0	0	0	11

Appendix 20: Pollen percentages core 84-011-12 St Anne's Basin

Depth (cm)	***Abies***	***Picea***	***Pinus***	***Tsuga***	***Acer***	***Betula***	***Carya***	***Fagus***	***Fraxinus***	***Juglans***	***Quercus***	***Tilia***	***Ulmus***	**total trees**	***Betula shrub***	***Alnus***	***Ericaceae***	***Myrica***	***Salix***
1-3 TWC	9.7	18.5	32.2	9.1	0.8	7.4	0	0.56	0.3	0	0.85	0	0.56	79.97	12.5	1.7	0	0	2
20-22TWC	5.7	19.6	39.9	2.7	1.3	1	0	0	0	0	1	0	0	71.2	19.9	2.4	0	0	1
30-32TWC	5.6	12.2	30	8.4	1.6	6.5	0	0.6	0	0	2.5	0.3	0.3	68	25.9	1.9	0	0	1.2
40-42 TWC	8.3	13.2	33.4	11	2.4	4.6	0	0	0	0	0.9	0	0.3	74.1	19.9	2.5	0	0	0.3
50-52TWC	5.5	6.5	35.9	10.7	0.6	6.1	0	0.3	0	0	1	0.3	0	66.9	26.9	1.9	0	0	1.9
60-62 TWC	5.3	10.6	25.5	10.6	3.6	9	0	0	0	0	1.3	0	0	65.9	28.2	1.3	0	0	0.6
70-72TWC	5.6	9.6	40.9	8.9	3.6	1.3	0	0.3	0	0	0	0	0.66	70.86	23.7	1.6	0	0	0
80-82 TWC	3.3	7.9	32.9	11.2	3	7.6	0	0.33	0	0	1	0	0.66	67.89	25.3	0.65	0	0	2.3
90-92TWC	1.6	4.2	38.4	10	2.2	1.9	0	0.3	0.3	0	2.2	0	0	61.1	31.6	2.6	0	0	1.6
100-102 TWC	0.7	6.3	31.9	8.6	3.3	9.3	0	1	0	0	3	0	0	64.1	26.6	3.3	0.33	0	1.7
110-112 TWC	5.9	8.5	38.1	11.8	3.3	1.3	0	0.66	0	0	0.33	0	0	69.89	24.3	2.3	0	0	0.33
120-122 TWC	1.5	6.8	35.7	12.1	3.4	7.1	0	0	0	0	1.5	0	0	68.1	25.1	3.4	0.3	0	0.3
0-2 Piston	5.9	20.5	28.8	9.5	5.3	11.6	0	0.9	0	0	2.4	0	0.6	85.5	7.7	5	0	0	0.6
10-12	5.4	20.9	22.8	9.7	2.5	14	0.2	0.8	0.6	0.6	1.2	0	0.4	79.1	10.5	7.8	0	0	0.4
14-16	6.3	18.6	26	10.9	2.6	15.3	0	0.6	0.2	0	1.4	0	0.2	82.1	12.5	2.8	0.4	0	0.6
20-22	12.3	18	24.3	13.6	1.9	13.8	0.3	0.3	0	0	0	0	0	84.5	9.8	2.2	0	0	1.26
30-32	8.2	12.3	27.7	11.3	0.6	12	0	0	0	0	0.95	0	0.6	73.65	17.3	2.5	0	0	0.6
40-42	5.3	11.1	30.1	9.3	3.1	17.9	0.22	0.44	0.44	0	1.1	0.44	0	79.44	15	2.9	0	0	0.67
50-52	5.7	13.2	27	13.7	2.6	16.4	0	0	0	0	1.5	0.25	0.25	80.6	14.3	1.82	0.25	0	0
60-62	12.1	13.9	30.4	14.4	2.4	12.1	0	0	0	0	0	0	0	85.3	11.3	1.3	0	0	0.26
70-72	4.28	9.1	38.5	10.3	3.5	15.1	0	0	0	0.25	0.25	0	0.25	81.53	13.8	2.8	0	0	0.5
80-82	6	8.6	44.9	12.6	2.4	11.3	0	0	0	0	2.2	0.2	0.2	88.4	7.3	2	0	0	0.4
90-92	4.8	11.7	42.2	10.4	2.3	9.4	0	0	0	0	2	0	0	82.8	14	1.25	0	0	0
100-102	5.1	12	41.2	13.1	1.7	9.7	0	0	0	0	1.1	0	0	83.9	10.3	2.7	0	0	0.4
110-112	1.8	11.6	42.5	7.1	2.1	11.6	0	0.3	0	0	2.1	0	0	79.1	17.5	1.2	0	0	0.6
120-122	2.8	13.4	46.7	7.8	1.7	10.2	0	0.2	0	0	1.7	0	0.2	84.7	10.8	1.7	0	0	0.2
130-132	3.3	12.6	44.1	6.4	1.7	13.1	0	0	0.25	0	1.5	0	0.25	83.2	13.6	1.5	0	0	0.5
140-142	2.1	9.7	39.8	5	2.1	15.6	0.2	0.3	0	0	2.1	0	0.2	77.1	15.3	4.3	0.2	0	1

Appendix 20: Pollen percentages core 84-011-12 St Anne's Basin

Depth (cm)	***Abies***	***Picea***	***Pinus***	***Tsuga***	***Acer***	***Betula***	***Carya***	***Fagus***	***Fraxinus***	***Juglans***	***Quercus***	***Tilia***	***Ulmus***	**total trees**	***Betula* shrub**	***Alnus***	***Ericaceae***	***Myrica***	***Salix***
150-152	3.9	10.8	46.6	4.9	2.6	7.2	0	0.26	0.5	0	1.8	0	0	78.56	16.4	1.8	0	0	0.26
160-162	2.3	14.8	41.4	7.1	0.9	11.2	0.3	0.6	0.9	0	0.9	0	0	80.4	15.1	1.8	0	0	1.8
170-172	2.5	8.2	45.2	4.5	3.5	12	0	0.25	0.75	0	0.25	0	0	77.15	16.5	2.5	0	0	1
179-181	3.9	9.3	42.5	5	2.9	10.7	0.5	0.2	0	0	0.5	0	0	75.5	18.9	1.4	0	0	1.4
200-202	2.3	9.7	42.4	2.3	2.9	14.5	0	0.9	0	0	2.3	0	0.3	77.6	16.2	2.9	0	0	0.9
220-222	3.1	11.3	48.7	3.4	2.5	9.4	0	0	0.3	0	2.8	0	0.3	81.8	13.5	1.9	0	0	0.6
240-242	3.2	9.1	42.1	5.3	2.1	12	0	0.8	0.26	0	2.6	0.25	0	77.71	15.7	2.4	0	0	0.26
260-262	3	8.9	53.5	4.3	1.5	7.4	0	0	0.5	0	3	0.25	0.5	82.85	12.94	1.8	0	0	1.3
280-282	2.9	8.8	49.5	9	2.9	10.3	0	0	0.2	0	1.5	0.2	0.2	85.5	10.6	2.6	0	0	0.2
300-302	1.8	7.6	43.6	10.8	3.7	9.2	0	0.2	0.2	0	0.7	0	0.5	78.3	15.6	2.7	0	0	0.5
320-322	2.9	11.8	40	16.5	1.7	5.9	0	0	0	0	0.5	0	0.5	79.8	15	1.7	0.25	0	0.7
340-342	2.2	9.1	46.8	13.8	0.8	5.8	0	0.8	0	0	0.3	0	0.3	79.9	14.1	3.3	0	0.3	1.4
360-362	2.5	7.9	43.4	18.3	1.6	4.6	0	0.3	0.3	0	0	0	0.5	79.4	15.6	1.4	0.8	0	0.3
380-382	3.4	9.2	47.5	16.7	0.6	2.7	0	0.6	0	0	0.9	0	0	81.6	13.3	1.8	1.2	0	0.3
400-402	3.1	6.5	53.7	11.4	0.8	1.8	0	0.26	0	0	0.8	0	0	78.36	15.2	1.8	0.5	0	0.5
420-422	3.1	10	45.5	12.9	0.4	5.1	0	0.2	0	0	1.5	0	0.4	79.1	13.7	2.2	0.4	0	1.8
440-442	3	7.6	56.8	5.7	1.1	6	0	0	0	0	0.5	0.5	0	81.2	11.2	4.6	0.3	0	0.3
460-462	1.9	8.7	66.9	4.1	1.4	2.9	0	0	0	0.24	0.24	0	0	86.38	9	2.2	0.5	0	0.24
480-482	3.2	9.5	55	6	1.7	3	0	0.25	0	0	0.75	0	0	79.4	14.7	1.75	0.25	0	1.25
500-502	2.8	10	57.2	3.9	1.1	2.2	0	0	0	0	1.9	0.3	0	79.4	13	3.3	0.3	0	0.55
520-522	4.1	11.1	60.3	3.3	1.7	3.6	0	0.2	0	0	0.9	0	0.3	85.5	8.1	2.1	0.2	0	0.5
540-542	5.9	10.4	58.8	2.8	0.3	3.6	0	0	0	0	0	0	0.56	82.36	8.7	5.6	0	0	0.8
560-562	3.5	10.9	49.9	0	1.1	2.99	0	0	0	0	0	0	0	68.39	16	11.4	0	0	0.5
580-582	3.5	10.3	45.2	0.5	1.3	3.5	0	0	0	0	1	0	0.25	65.55	20.2	9.6	0	0	0.5
600-602	5.9	10.8	53.1	0.26	0.26	5.9	0	0	0	0	0	0	0	76.22	15.6	4.6	0	0	0.26
620-622	7.7	8.7	48.2	0.3	0.7	4.3	0	0	0	0	0.7	0	0.3	70.9	13.7	9.4	0	0	2.3
630-632	9.2	11.3	46.6	0.3	2.1	3.6	0.3	0	0	0	1.2	0	0.6	75.2	13.3	7.1	0	0	2.7
640-642	2.2	9.5	46	0	1.9	6.9	0	0.95	0	0	0.3	0	0	67.75	19.5	9.5	0	0	0

Appendix 20: Pollen percentages core 84-011-12 St Anne's Basin

Depth (cm)	***Abies***	***Picea***	***Pinus***	***Tsuga***	***Acer***	***Betula***	***Carya***	***Fagus***	***Fraxinus***	***Juglans***	***Quercus***	***Tilia***	***Ulmus***	**total trees**	***Betula* shrub**	***Alnus***	***Ericaceae***	***Myrica***	***Salix***
660-662	4.2	13.7	51.5	1.2	1.8	3.6	0	0.3	0	0	0	0.3	0	76.6	12.8	4.76	0	0	1.8
680-682	1.2	10	50.9	0.6	2.2	7.2	0	0	0	0	2.5	0	0.3	74.9	14	6.2	0	0	1.2
700-702	10.1	8.7	46.7	0.7	1.4	5.1	0	0.3	0	0	1.4	0	0	74.4	11.95	8	0	0	1.4
720-722	8.6	8	53.3	0.85	0	4	0	0	0	0	0.85	0	0	75.6	14	7.1	0	0	0.85
740-742	3.2	7	41	0	1.45	6.4	0	0.6	0	0	2.6	0	0	62.25	24.7	7	0	0	2
750-752	4.3	13.8	40.5	0	0.4	5.1	0	0	0	0.4	2.4	0	0.4	67.3	19.7	6.3	0.4	0	0.4

Appendix 20: Pollen percentages core 84-011-12 St Anne's Basin

Depth (cm)	**Total shrubs**	***Ambrosia***	***Artemisia***	***Chenopodiaceae***	***Caryophyllaceae***	***Cyperaceae***	***Gramineae***	***Rumex***	***Other Polygonaceae***	***Typha***	**Unknown**		**Total herbs**
1-3 TWC	16.2	1.4	0	0	0	0	0	0	0.85	0	1.1	0.3	3.7
20-22TWC	23.3	0	0	0	0	1	0.3	2	0.3	0	1.7	0	5.4
30-32TWC	29	0.3	0.3	0.3	0	0.3	0	0	0.6	0	0.9	0	3
40-42 TWC	22.7	0.3	0	0	0	0.6	0	0	0.3	0	1.8	0	3.1
50-52TWC	30.7	0.3	0	0.3	0	0	0	0	0.6	0	1	0	2.3
60-62 TWC	30.1	0.33	0	0.66	0	1.3	0	0	0.33	0	1.3	0	4
70-72TWC	25.3	0	0	0	0	0.3	0.3	0	1.6	0	1.3	0	3.6
80-82 TWC	28.25	0.65	0	0	0	1	0	0	0.33	0	2	0	3.9
90-92TWC	35.8	0.3	0.3	0	0	0.65	0	0	0	0	1.6	0	2.9
100-102 TWC	31.93	0.33	0.66	0	0	0.66	0.3	0	0.3	0	1.7	0	3.9
110-112 TWC	26.93	0.33	0.33	0.33	0	0	0	0	1	0	1	0	3
120-122 TWC	29.1	0.3	0.3	0	0	0.3	0	0	0	0	1.2	0	2.2
0-2 Piston	10.4	0.9	0	0.3	0	0.3	0.6	0	0	0	1.5	0	4.1
10-12	18.6	0	0.4	0	0	0.8	0.2	0	0.6	0	0	0	2.1
14-16	16.4	0.8	0	0.2	0	0.2	0.2	0	0	0	0	0	7
20-22	13.25	0	0	0	0	1.6	0.3	0	0.3	0	0	0	7
30-32	20.4	0	0	0	0	2.2	0.3	0	0.95	0	2.2	0	5.7
40-42	18.6	0.22	0	0	0	0.67	0.22	0	0.67	0.22	0	0	2
50-52	16.4	0.25	0.25	0.25	0	1	0	0	0	0	1	0	2.8
60-62	12.86	0.25	0.25	0	0	0.5	0.25	0	0.25	0	0.25	0	1.75
70-72	17.1	0.25	0	0	0	0.5	0	0.25	0.25	0.25	0.75	0	1.8
80-82	9.7	0.2	0.2	0.4	0	0.66	0	0	0.2	0	0	0	1.66
90-92	15.25	0.25	0.5	0.25	0	0.5	0	0	0.25	0	0	0	1.8
100-102	13.4	0	0	0.4	0	0.6	0	0	0.2	0	0	0	1.2
110-112	19.3	0	0.3	0.3	0	0.6	0	0.3	0	0	0	0	1.5
120-122	12.7	0	0.6	0.2	0	1.1	0.2	0	0	0	0.2	0	2.3
130-132	15.6	0	0.25	0.25	0	0.5	0	0	0	0	0	0	4
140-142	20.8	0.2	0	0.2	0	1.2	0.3	0	0	0	0	0	1.9

Appendix 20: Pollen percentages core 84-011-12 St Anne's Basin

Depth (cm)	**Total shrubs**	***Ambrosia***	***Artemisia***	***Chenopodiaceae***	***Caryophyllaceae***	***Cyperaceae***	***Gramineae***	***Rumex***	***Other Polygonaceae***	***Typha***	**Unknown**		**Total herbs**
150-152	18.46	0	0.26	0	0	0.5	0.5	0	0.26	0	1.26	0	2.8
160-162	18.7	0	0.3	0	0	0	0	0.3	0.3	0	0	0	0.9
170-172	20	0	0.25	0	0	0.5	0	0	0.25	0	1.75	0	2.75
179-181	21.7	0.5	0	0.2	0	0.5	0	0	0.2	0	1.6	0	3
200-202	20	0.3	0	0.6	0	0.9	0	0	0	0	0.3	0	2.1
220-222	16	0	0.3	0	0	0.3	0.6	0	0.6	0	0	0	1.8
240-242	18.36	0.26	0	0.5	0	1.1	0.26	0	0.26	0	1.1	0	3.5
260-262	16.04	0.25	0	0	0	0.76	0	0	0	0	0	0	1
280-282	13.4	0	0.2	0	0	0.2	0	0	0.2	0	0.2	0	0.8
300-302	18.8	0.5	0	0	0	0.5	0.2	0	0.9	0	0.9	0	13
320-322	17.65	0.25	0	0.25	0	0.7	0	0	0.25	0	1	0	2.5
340-342	19.1	0	0	0	0	0	0	0	0	0	0.8	0	0.8
360-362	18.1	0.8	0.3	0.3	0	0.3	0	0	0.8	0	0	0	2.5
380-382	16.6	0.3	0.3	0.3	0	0.3	0	0	0	0	0.3	0	1.5
400-402	18	0.26	0.26	0	0	2.1	0.26	0	0.26	0	0.5	0	3.6
420-422	18.1	0.2	0.2	0.2	0	1.1	0	0	0.2	0	0.7	0	2.7
440-442	16.4	0.3	0.3	0.3	0	1.4	0	0	0	0	0	0	2.2
460-462	11.94	0.24	0.24	0.24	0	0	0.5	0	0	0	0	0	1.2
480-482	17.95	0.25	0.25	0.75	0	0	0.25	0	0	0	0.75	0	2.2
500-502	17.15	0	0	0.3	0	0.8	0	0	0.55	0	1.4	0	3.1
520-522	10.9	0.2	0.2	0.2	0	0.7	0	0	0.9	0	1.2	0	3.5
540-542	15.1	0.56	0	0	0	0.56	0	0	1.1	0	0.3	0	2.5
560-562	27.9	0.3	0	0	0	2.5	0	0	0.8	0	0	0	3.5
580-582	30.3	0.75	0	0	0	2	0	0	0.75	0	0.5	0	4
600-602	20.46	0.5	0	0	0	0.8	0	0	1.1	0	0.8	0	3.2
620-622	25.4	1	0.3	0	0	1.3	0.7	0	0	0	0.3	0	11
630-632	23.1	0.3	0.3	0.3	0	0.9	0	0	0	0	0	0	1.8
640-642	29	0.6	0	0	0	0	0	0	0.6	0	1.9	0	3.1

Appendix 20: Pollen percentages core 84-011-12 St Anne's Basin

Depth (cm)	**Total shrubs**	***Ambrosia***	***Artemisia***	***Chenopodiaceae***	***Caryophyllaceae***	***Cyperaceae***	***Gramineae***	***Rumex***	***Other Polygonaceae***	***Typha***	**Unknown**		**Total herbs**
660-662	19.3	0.3	0	0	0	0.3	0.3	0	1.2	0	2.1	0	4.2
680-682	21.4	0	0	0	0	0.6	0	0	0.6	0.3	1.6	0.3	3.4
700-702	21.35	0.7	0	0	0	0.3	0	0	1.4	0	1.4	0	4
720-722	21.95	0.3	0.3	0	0	0.57	0.3	0	0	0	0.85	0	2.3
740-742	33.7	0	0.3	0	0	2.3	0	0	0.9	0	0.6	0	4.1
750-752	26.8	0.8	0	0.4	0	2.4	0	0	1.2	0	1.2	0	5.9

Appendix 21: Raw dinoflagellate cysts counts core 84-011-12, St. Anne's basin

Depth (cm)	*cf. Alexandrium excavatum*	*Ataxodinium choanum*	*Bitectatodinium tepikiense*	*Impagidinium aculeatum*	*Impagidinium pallidum*	*Nematosphaeropsis labyrinthus*	*Operculodinium centrocarpum*	*O. centrocarpum short processes*	*O. centrocarpum var. arctic*	*Operculodinium israelianum*	*Spiniferites membranaceus*	*Spiniferites delicatus*	*Spiniferites elongatus*	*Spiniferites ramosus*	*Spiniferites bulloideus*	*Spiniferites mirabilis*	*Spiniferites hyperacanthus*	*Spiniferites spp.*	*Pentapharsodinium dalei*	*Algidasphaeridium minutum*	*Algidasphaeridium spp.*	*Brigantedinium spp.*	*Brigantedinium simplex*	*Selenopemphix quanta*	*Polykrikos schwartzii*	Total
1-3 TWC	0	0	3	0	0	5	69	2	0	0	0	4	1	1	0	0	0	0	29	10	0	84	0	2	0	210
20-22TWC	0	0	1	0	0	4	45	0	0	0	0	0	1	3	0	0	0	1	12	0	0	54	0	1	0	122
30-32 TWC	1	0	1	0	0	6	86	3	0	0	0	4	3	0	0	0	0	3	27	4	0	118	0	0	0	256
40-42 TWC	1	0	3	0	0	2	90	2	0	0	0	3	6	2	0	0	0	3	18	3	0	168	0	0	0	301
50-52TWC	2	0	2	0	0	3	104	0	0	0	0	2	5	3	0	0	0	2	38	4	0	113	0	1	0	279
60-62 TWC	2	2	3	0	0	2	92	2	0	0	0	3	6	4	0	0	0	2	74	8	0	139	0	0	0	339
70-72TWC	4	1	2	0	0	2	111	2	0	0	0	0	6	3	0	0	0	0	39	2	0	129	0	0	0	301
80-82 TWC	7	1	4	0	0	2	69	1	0	0	0	1	3	4	0	0	0	0	62	5	0	162	0	0	0	321
90-92TWC	0	0	1	0	0	1	99	1	0	1	0	2	7	2	0	0	0	1	39	16	0	159	0	1	0	330
100-102 TWC	4	1	0	0	0	2	81	1	0	1	0	2	6	3	3	0	0	1	35	20	0	154	0	1	0	315
110-112 TWC	3	0	0	0	0	7	100	1	0	0	0	3	2	6	0	0	0	0	35	11	0	132	0	1	0	301
120-122 TWC	2	1	1	0	0	3	56	2	0	0	0	1	6	0	0	0	0	3	54	22	0	116	0	1	0	268
0-2 Piston	1	1	0	0	0	8	169	5	0	1	0	0	7	8	0	2	0	0	65	1	0	47	0	1	0	316
10-12	0	2	4	0	1	12	210	6	0	0	1	0	4	17	2	1	0	1	94	2	0	29	1	3	0	390
14-16	0	0	0	0	1	6	219	7	0	0	0	0	7	15	0	0	0	4	71	0	0	71	0	1	0	402
20-22	1	0	4	0	0	10	154	5	0	0	0	0	8	10	0	0	0	2	54	2	0	68	0	2	0	320
30-32	5	0	3	0	0	4	104	3	0	0	0	0	4	8	0	0	0	1	79	0	0	96	0	1	0	308
40-42	0	0	2	0	0	1	138	5	0	0	0	0	7	11	0	0	1	2	26	0	0	120	0	4	0	317
50-52	0	0	2	0	0	6	145	2	0	0	0	2	11	3	0	0	1	0	23	2	0	117	0	0	0	314
60-62	0	0	3	0	1	9	166	2	0	0	0	1	19	1	0	0	1	3	50	2	0	60	0	0	0	318

Appendix 21: Raw dinoflagellate cysts counts core 84-011-12, St. Anne's basin

Depth (cm)	*cf. Alexandrium excavatum*	*Ataxodinium choanum*	*Bitectatodinium tepikiense*	*Impagidinium aculeatum*	*Impagidinium pallidum*	*Nematosphaeropsis labyrinthus*	*Operculodinium centrocarpum*	*O. centrocarpum short processes*	*O. centrocarpum var. arctic*	*Operculodinium israelianum*	*Spiniferites membranaceus*	*Spiniferites delicatus*	*Spiniferites elongatus*	*Spiniferites ramosus*	*Spiniferites bulloideus*	*Spiniferites mirabilis*	*Spiniferites hyperacanthus*	*Spiniferites spp.*	*Pentapharsodinium dalei*	*Algidasphaeridium minutum*	*Algidasphaeridium spp.*	*Brigantedinium spp.*	*Brigantedinium simplex*	*Selenopemphix quanta*	*Polykrikos schwartzii*	Total
70-72	1	1	2	0	1	5	134	0	0	0	0	0	9	7	0	0	1	2	42	3	0	87	0	1	0	296
80-82	6	0	5	0	2	12	147	4	0	0	0	1	14	11	0	0	0	1	82	0	0	51	0	0	0	336
90-92	0	0	5	0	0	5	138	2	0	0	0	2	12	11	0	0	0	0	71	5	0	82	0	0	0	333
100-102	6	1	3	0	0	15	137	0	0	0	0	2	5	5	0	0	1	3	82	3	0	59	0	0	0	322
110-112	7	1	5	0	0	4	127	0	0	0	0	2	6	7	0	0	0	3	57	3	0	91	0	1	0	314
120-122	2	0	5	0	0	6	120	3	0	0	0	0	6	8	0	0	0	3	64	2	0	106	0	2	1	328
130-132	5	0	0	0	0	6	131	5	0	0	0	0	5	10	0	0	0	3	45	1	0	106	0	0	0	317
140-142	2	0	3	0	1	2	152	3	0	0	1	1	5	11	0	0	0	1	64	2	0	116	0	0	0	364
150-152	0	0	3	1	0	5	159	2	2	0	0	2	8	6	0	0	2	4	25	0	0	93	0	2	0	314
160-162	2	0	0	0	0	5	166	2	0	0	0	0	6	8	0	0	0	3	57	1	0	77	0	0	1	328
170-172	0	0	2	0	0	9	162	2	1	1	0	2	4	9	0	0	0	2	14	0	0	101	0	0	0	309
179-181	1	2	1	0	1	5	161	2	0	0	0	3	3	9	0	0	1	2	14	2	0	145	0	1	1	354
200-202	0	4	1	0	0	5	161	3	0	0	1	2	3	12	1	0	0	0	20	1	0	105	0	0	0	319
220-222	0	0	1	0	0	9	162	2	0	0	0	4	5	7	0	1	0	0	37	4	0	74	0	0	0	306
240-242	0	2	1	0	0	6	133	2	0	0	0	1	7	8	0	0	0	2	38	2	0	102	0	1	0	305
260-262	0	0	2	0	0	3	134	0	0	0	2	2	5	15	1	0	0	4	56	3	0	136	0	3	0	366
280-282	0	0	1	0	0	2	156	6	0	0	0	0	10	12	0	0	1	4	38	4	0	117	0	1	0	352
300-302	0	0	2	0	0	12	180	4	0	0	0	0	6	14	0	0	1	2	34	5	0	99	0	1	0	360
320-322	2	2	5	0	1	3	123	1	0	0	0	2	8	12	0	0	0	3	42	0	0	117	0	0	1	322
340-342	0	0	4	0	1	6	172	1	0	0	0	2	12	10	0	0	0	3	22	3	0	75	0	0	0	311
360-362	0	0	3	0	1	6	153	2	0	0	0	4	9	14	0	0	0	5	29	1	0	94	0	0	0	321

Appendix 21: Raw dinoflagellate cysts counts core 84-011-12, St. Anne's basin

Depth (cm)	*cf. Alexandrium excavatum*	*Ataxodinium choanum*	*Bitectatodinium tepikiense*	*Impagidinium aculeatum*	*Impagidinium pallidum*	*Nematosphaeropsis labyrinthus*	*Operculodinium centrocarpum*	*O. centrocarpum short processes*	*O. centrocarpum var. arctic*	*Operculodinium israelianum*	*Spiniferites membranaceus*	*Spiniferites delicatus*	*Spiniferites elongatus*	*Spiniferites ramosus*	*Spiniferites bulloideus*	*Spiniferites mirabilis*	*Spiniferites hyperacanthus*	*Spiniferites spp.*	*Pentapharsodinium dalei*	*Algidasphaeridium minutum*	*Algidasphaeridium spp.*	*Brigantedinium spp.*	*Brigantedinium simplex*	*Selenopemphix quanta*	*Polykrikos schwartzii*	Total
380-382	0	4	2	0	0	5	163	3	0	0	0	1	10	13	1	0	1	3	26	6	0	89	0	1	0	328
400-402	0	1	4	0	0	9	170	3	0	0	0	6	1	7	0	0	3	4	15	4	0	91	0	0	0	318
420-422	0	0	2	0	0	5	173	0	0	0	0	4	11	21	0	0	1	3	46	1	0	67	0	0	0	334
440-442	0	1	2	0	2	3	187	4	0	0	0	7	10	12	0	0	4	1	19	5	0	82	0	0	0	339
460-462	0	3	2	0	1	5	202	3	0	0	0	5	13	19	0	0	2	7	17	3	0	68	0	1	0	351
480-482	0	0	3	0	0	4	174	4	0	0	0	2	14	21	0	0	4	2	9	2	0	72	0	1	1	313
500-502	2	0	7	0	1	3	177	2	0	0	0	0	13	10	0	0	0	2	13	4	0	79	0	1	0	314
520-522	0	4	22	0	1	19	92	4	0	1	0	3	25	16	0	0	0	1	13	5	0	135	0	0	0	341
540-542	0	1	50	0	0	17	102	7	0	0	0	10	15	20	0	0	3	6	16	3	0	90	0	0	0	340
560-562	3	0	14	0	1	22	115	11	0	1	0	8	11	22	0	0	0	4	46	13	0	42	0	11	0	324
580-582	1	2	22	0	0	27	126	8	0	5	0	1	6	28	0	1	0	5	29	2	0	62	0	16	0	341
600-602	1	0	5	0	0	12	130	2	0	8	0	2	7	14	0	0	0	2	32	26	0	59	0	19	0	319
620-622	0	0	12	0	1	15	130	1	0	14	0	1	9	5	0	0	1	0	18	20	0	82	0	15	0	324
630-632	2	0	17	0	0	17	154	6	0	3	0	1	5	17	0	0	0	1	18	17	0	46	0	8	0	312
640-642	0	0	12	0	0	9	185	6	0	4	0	1	5	9	0	0	0	2	13	4	0	73	0	13	0	336
660-662	0	0	6	0	0	32	188	4	0	2	0	4	10	11	0	0	0	1	62	8	0	40	0	6	0	374
680-682	0	0	1	0	0	12	260	11	0	2	0	4	14	8	0	0	0	0	87	8	0	45	0	1	0	453
700-702	1	1	6	0	0	4	241	6	0	4	0	0	11	13	0	0	0	2	41	10	0	33	0	5	0	378
720-722	0	2	4	0	0	2	236	8	0	6	0	2	19	31	0	0	0	3	26	7	0	44	0	10	0	400
740-742	2	0	5	0	1	8	224	7	0	11	0	0	24	32	1	0	1	1	38	13	0	31	0	11	0	410
750-752	1	1	3	0	1	0	150	10	3	2	1	5	14	34	0	0	0	1	51	2	0	30	0	3	0	312

Appendix 22: Dinoflagellate cyst percentages core 84-011-12 St. Anne's Basin

Depth (cm)	*cf. Alexandrium excavatum*	*Ataxiodinium choanum*	*Bitectatodinium tepikiense*	*Impagidinium aculeatum*	*Impagidinium pallidum*	*Nematosphaeropsis labyrinthus*	*Operculodinium centrocarpum*	*O. centrocarpum short processes*	*O. centrocarpum var. arctic*	*Operculodinium israelianum*	*Spiniferites membranaceus*	*Spiniferites delicatus*	*Spiniferites elongatus*	*Spiniferites ramosus*	*Spiniferites bulloideus*	*Spiniferites mirabilis*	*Spiniferites hyperacanthus*	*Spiniferites spp.*	*Pentapharsodinium dalei*	*Algidasphaeridium minutum*	*Brigantedinium spp.*	*Brigantedinium simplex*	*Selenopemphix quanta*
1-3 TWC	0	0	1.4	0	0	2.4	32.8	0.95	0	0	0	1.9	0.5	0.5	0	0	0	0	13.8	4.8	40	0	0.95
20-22	0	0	0.8	0	0	3.3	36.9	0	0	0	0	0	0.8	2.5	0	0	0	0.8	9.8	0	44.3	0	0.8
30-32	0.4	0	0.4	0	0	2.3	33.6	1.1	0	0	0	1.6	1.1	0	0	0	0	1.1	10.5	1.6	46.2	0	0
40-42	0.33	0	1	0	0	0.66	29.9	0.66	0	0	0	1	2	0.7	0	0	0	1	5.9	1	55.8	0	0
50-52	0.7	0	0.7	0	0	1.1	37.3	0	0	0	0	0.7	1.8	1.1	0	0	0	0.7	13.6	1.4	40.5	0	0.4
60-62	0.6	0.6	0.9	0	0	0.6	27.1	0.6	0	0	0	0.9	1.8	1.2	0	0	0	0.6	21.8	2.3	41	0	0
70-72	1.3	0.3	0.7	0	0	0.7	36.9	0.7	0	0	0	0	2	1	0	0	0	0	13	0.7	42.7	0	0
80-82	2.2	0.3	1.2	0	0	0.6	21.5	0.3	0	0	0	0.3	0.9	1.2	0	0	0	0	19.3	1.6	50.5	0	0
90-92	0	0.3	0	0	0	0.3	30	0.3	0	0.3	0	0.6	2.1	0.6	0	0	0	0.3	11.8	4.8	48.2	0	0.3
100-102	1.3	0.3	0	0	0	0.6	25.7	0.3	0	0.3	0	0.6	1.9	1	1	0	0	0.3	11.1	6.3	48.9	0	0.3
110-112	1	0	0	0	0	2.3	33.2	0.3	0	0	0	1	0.7	2	0	0	0	0	11.6	3.6	43.9	0	0.3
120-122	0.7	0.4	0.4	0	0	1.2	20.9	0.7	0	0	0	0.4	2.2	0	0	0	0	1.2	20.1	8.2	43.2	0	0.4
Piston																							
0-2	0.3	0.3	0	0	0	2.5	53.4	1.6	0	0.3	0	0	2.2	2.5	0	0.9		0	20.5	0.3	14.8	0	0.3
10-12	0	0.5	1	0	0.2	3	54	1.5	0	0	0.2	0	1	4.4	0.5	0.5		0.2	24	0.5	7.5	0.2	0.8
14-16	0	0	0	0	0.3	1.5	54.5	1.7	0	0	0	0	1.7	3.7	0	0	0	1	17.7	0	17.7	0	0.25
20-22	0.3	0	1.3	0	0	3.1	48.2	0	1.5	0	0	0	2.5	3.1	0	0	0	0.6	16.9	0.6	21.3	0	0.6
30-32	1.6	0	1	0	0	1.3	33.8	1	0	0	0	0	1.3	2.6	0	0	0	0.3	25.6	0	31.2	0	0.3
40-42	0	0	0.65	0	0	0.3	43.8	1.6	0	0	0	0	2.2	3.5	0	0	0.3	0.7	8.2	0	38.1	0	0.65
50-52	0	0	0.64	0	0	1.9	46.2	0.64	0	0	0	0.64	3.5	1	0	0	0.3	0	7.3	0.6	37.3	0	0
60-62	0	0	0.9	0	0.3	2.8	52.4	0.6	0	0	0	0.3	6	0.3	0	0	0.3	0.9	15.8	0.6	18.8	0	0
70-72	0.3	0.3	0.67	0	0.3	1.7	45.3	0	0	0	0	0	3	2.3	0	0	0.3	0.7	14.2	1	29.4	0	0.33
80-82	1.8	1.5	0.6	0	0	3.6	43.7	1.2	0	0	0	0.3	4.2	3.3	0	0	0	0.3	24.3	0	15.2	0	0

Appendix 22: Dinoflagellate cyst percentages core 84-011-12 St. Anne's Basin

Depth (cm)	*cf. Alexandrium excavatum*	*Ataxiodinium choanum*	*Bitectatodinium tepikiense*	*Impagidinium aculeatum*	*Impagidinium pallidum*	*Nematosphaeropsis labyrinthus*	*Operculodinium centrocarpum*	*O. centrocarpum short processes*	*O. centrocarpum var. arctic*	*Operculodinium israelianum*	*Spiniferites membranaceus*	*Spiniferites delicatus*	*Spiniferites elongatus*	*Spiniferites ramosus*	*Spiniferites bulloideus*	*Spiniferites mirabilis*	*Spiniferites hyperacanthus*	*Spiniferites spp.*	*Pentapharsodinium dalei*	*Algidasphaeridium minutum*	*Brigantedinium spp.*	*Brigantedinium simplex*	*Selenopemphix quanta*
90-92	0	0	1.5	0	0	1.5	41.4	0.6	0	0	0	0.6	3.6	3.3	0	0	0	0	21.3	1.5	24.6	0	0
100-102	1.9	0.3	0.9	0	0	4.6	42.5	0	0	0	0	0.6	1.5	1.5	0	0	0.3	0.9	25.5	0.9	18.3	0	0
110-112	2.2	0.3	1.6	0	0	1.3	40.3	0.3	0	0	0	0.6	1.9	2.2	0	0	0	1	18.1	0.95	28.9	0	0.3
120-122	0.6	0	1.4	0	0	1.8	36.5	0.9	0	0	0	0	1.8	2.4	0	0	0	0.9	19.4	0.6	32.1	0	0.6
130-132	1.6	0	0	0	0	1.9	41.2	1.6	0	0	0	0	1.6	3.1	0	0	0	0.9	14.1	0.3	33.3	0	0.3
140-142	0.5	0	0.8	0	0.3	0.5	41.8	0.8	0	0	0.3	0.3	1.4	3	0	0	0	0.3	17.6	0.5	31.9	0	0
150-152	0	0	1	0.3	0	1.6	50.6	0.65	0.6	0	0	0.65	2.5	1.9	0	0	0.7	1.3	8	0	29.6	0	0.65
160-162	0.6	0	0	0	0	1.5	50.6	0.6	0	0	0	0	1.8	2.4	0	0	0	0.9	17.4	0.3	23.5	0	0
170-172	0	0	0.65	0	0	2.9	52.4	0.65	0.3	0.3	0	0.65	1.3	2.9	0	0	0	0.7	4.5	0	32.7	0	0
179-181	0.3	0.56	0.3	0	0.3	1.4	45.5	0.56	0	0	0	0.85	0.9	2.5	0	0	0.3	0.6	3.95	0.56	40.9	0	0.3
200-202	0	1.2	0.3	0	0	1.6	50.5	0.94	0	0	0.3	0.6	0.9	3.8	0.3	0	0	0	6.3	0.3	32.9	0	0
220-222	0	0	0.3	0	0	2.9	53	0.6	0	0	0	1.3	1.6	2.3	0	0.3	0	0	12.1	1.3	24.2	0	0
240-242	0	0.6	0.3	0	0	2	43.7	0.6	0	0	0	0.3	2.3	2.6	0	0	0	0.6	12.5	0.6	33.5	0	0.3
260-262	0	0	0.5	0	0	0.8	36.6	0	0	0	0.5	0.5	1.4	4	0.3	0	0	1.1	15.3	0.8	37.2	0	0.8
280-282	0	0	0.3	0	0	0.6	44.3	1.7	0	0	0	0	2.8	3.4	0	0	0.3	1.1	10.8	1.1	33.2	0	0.3
300-302	0	0	0.5	0	0	3.3	50	1.1	0	0	0	0	1.7	3.9	0	0	0.3	0.5	9.4	1.4	27.5	0	0.3
320-322	0.6	0.6	1.5	0	0.3	0.9	38.3	0.3	0	0	0	0.6	2.5	3.7	0	0	0	0.9	13	0	36.4	0	0
340-342	0	0	1.3	0	0.3	1.9	55.3	0.3	0	0	0	0.6	3.8	3.2	0	0	0	1	7.1	1	24.1	0	0
360-362	0	0	0.9	0	0.3	1.9	47.7	0.6	0	0	0	1.2	2.8	4.4	0	0	0	1.6	9	0.3	29.3	0	0
380-382	0	1.2	0.6	0	0	1.5	49.7	0.9	0	0	0	0.3	3	4	0.3	0	0.3	0.9	7.9	1.8	27.2	0	0.3
400-402	0	0.3	1.2	0	0	2.8	53.5	1	0	0	0	1.9	0.3	2.2	0	0	1	1.3	4.7	1.25	28.6	0	0
420-422	0	0	0.6	0	0	1.5	51.8	0	0	0	0	1.2	3.3	6.3	0	0	0.3	0.9	13.8	0.3	20	0	0
440-442	0	0.3	0.6	0	0.6	0.9	55.1	1.2	0	0	0	2.1	2.9	3.5	0	0	1.2	0.3	5.6	1.5	24.2	0	0

Appendix 22: Dinoflagellate cyst percentages core 84-011-12 St. Anne's Basin

Depth (cm)	*cf. Alexandrium excavatum*	*Ataxiodinium choanum*	*Bitectatodinium tepikiense*	*Impagidinium aculeatum*	*Impagidinium pallidum*	*Nematosphaeropsis labyrinthus*	*Operculodinium centrocarpum*	*O. centrocarpum short processes*	*O. centrocarpum var. arctic*	*Operculodinium israelianum*	*Spiniferites membranaceus*	*Spiniferites delicatus*	*Spiniferites elongatus*	*Spiniferites ramosus*	*Spiniferites bulloideus*	*Spiniferites mirabilis*	*Spiniferites hyperacanthus*	*Spiniferites spp.*	*Pentapharsodinium dalei*	*Algidasphaeridium minutum*	*Brigantedinium spp.*	*Brigantedinium simplex*	*Selenopemphix quanta*
460-462	0	0.9	0.6	0	0.3	1.4	57.4	0.9	0	0	0	1.4	3.7	5.4	0	0	0.6	2	4.8	0.9	19.4	0	0.3
480-482	0	0	1	0	0	1.3	55.6	1.3	0	0	0	0.6	4.5	6.7	0	0	1.3	0.6	2.9	0.6	23	0	0.3
500-502	0.6	0	2.2	0	0.3	1	56.5	0.6	0	0	0	0	4.1	3.2	0	0	0	0.6	4.1	1.3	25.2	0	0.3
520-522	0	1.2	6.5	0	0.3	5.6	27	1.2	0	0.3	0	0.9	7.2	4.7	0	0	0	0.3	3.8	1.5	39.5	0	0
540-542	0	0.3	14.7	0	0	5	30	2	0	0	0	2.9	4.4	5.9	0	0	0.9	1.8	4.7	0.9	26.5	0	0
560-562	0.9	0	4.3	0	0.3	6.8	35.5	3.4	0	0.3	0	2.5	3.4	6.8	0	0	0	1.2	14.2	4	13	0	3.4
580-582	0.3	0.6	6.5	0	0	7.9	36.9	2.3	0	1.5	0	0.3	1.7	8.2	0	0.3	0	1.5	8.5	0.6	18.2	0	4.7
600-602	0.3	0	1.6	0	0	3.8	40.8	0.6	0	2.5	0	0.6	2.2	4.4	0	0	0	0.6	10	8.1	18.5	0	6
620-622	0	0	3.7	0	0.3	4.6	40.2	0.3	0	4.3	0	0.3	2.8	1.5	0	0	0.3	0	5.5	6.2	25.4	0	4.6
630-632	0.6	0	5.4	0	0	5.4	49.5	1.9	0	1	0	0.3	1.6	5.4	0	0	0	0.3	5.8	5.4	14.8	0	2.5
640-642	0	0	3.6	0	0	2.7	55	1.8	0	1.2	0	0.3	1.5	2.7	0	0	0	0.6	3.9	1.2	21.6	0	3.9
660-662	0	0	1.6	0	0	8.5	50.3	1.1	0	0.5	0	1.1	2.7	2.9	0	0	0	0.3	16.6	2.1	10.7	0	1.6
680-682	0	0	0.2	0	0	2.7	57.6	2.4	0	0.4	0	0.9	3	1.8	0	0	0	0	19.2	1.8	10	0	0.2
700-702	0.3	0.3	1.6	0	0	1	63.8	1.6	0	1	0	0	2.9	3.5	0	0	0	0.5	10.8	2.6	8.8	0	1.3
720-722	0	0.5	1	0	0	0.5	59	2	0	1.5	0	0.5	4.8	7.8	0	0	0	0.8	6.5	1.75	11	0	2.5
740-742	0.5	0	1.2	0	0	2	54.7	1.7	0	2.7	0	0	5.8	7.8	0.3	0	0.3	0.3	9.3	3.2	7.5	0	2.7
750-752	0.3	0.3	0.9	0	0.3	0	48.3	3.2	0.9	0.6	0.3	1.6	4.5	11	0	0	0	0.3	16.5	0.6	9.6	0	0.9

Appendix 23: List of taxa included in the surface sample database and the 4-letter code used to identify each taxon.

Species	Code	Notes
Polykrikos schwartzii	Polk	
Lingulodinium machaerophorum	Lmac	
Operculodinium centrocarpum	Ocen	
Operculodinium centrocarpum short processed form	Ocss	grouped with Ocen
Operculodinium cf. *janduchenei*	Ojan	
Ataxiodinium choanum	Atax	
Bitectatodinium tepikiense	Btep	
Indeterminate *Impagidinium*	Ispp	
Impagidinium aculatum	Iacu	
Impagidinium pallidum	Ipal	
Impagidinium paradoxum	Ipar	
Impagidinium patulum	Ipat	
Impagidinium sphaericum	Isph	
Impagidinium strialatum	Istr	
Nematosphaeropsis labyrinthus	Nlab	
Indeterminate *Spiniferites*	Sssp	
Spiniferites bentorii	Sben	
Spiniferites belerius	Sbel	Grouped with Smem
Spiniferites bulloides	Sbul	
Spiniferites delicatus	Sdel	
Spiniferites elongatus	Selo	
Spiniferites frigidus	Sfri	
Spiniferites lazus	Slaz	
Spiniferites membranaceus	Smem	
Spiniferites mirabilis	Smir	
Spiniferites ramosus	Sram	
Pyxidinopsis reticulata	Pret	
cf *Alexandrium tamarense*-type cyst	Alex	
Pentapharsodinium dalei	Pdal	
Brigantedinium spp.	Bspp	
Brigantedinium cariacoense	Bcar	Grouped with Bspp
Brigantedinium simplex	Bsim	Grouped with Bspp
Protoperidinium americanum	Pame	
Miscellaneous congruentidiacean cysts	Peri	Includes *Lejeunecysta* spp., *Protoperidinium stellatum, Votadinium calvum,* and *Quincecuspis concreta*

Protoperidinium nudum	Pnud	Grouped with Squa
Selenopemphix nephroides	Sele	Grouped with Peri
Selenopemphix quanta	Squa	
Trinovantedinium applanatum	Tapp	
Xandarodinium xanthum	Xand	
Islandinium minutum	Amin	
Islandinium cezare	Amic	

Appendix 23: DIN598 surface sample reference database.

Site number	Alex	Atax	Btep	Iacu	Ipal	Ipar	Ipat	Isph	Istr	Lmac	Nlab	Ocen	Oarc
E003	0	0	0	0	0	0	0	0	0	0	0	34	0
E004	0	0	11	0	0	0	0	0	0	0	22	22	0
E005	0	0	0	0	0	0	0	0	0	0	6	53	0
E006	0	0	0	0	0	0	0	0	0	0	0	7	0
E007	0	5	0	0	0	0	0	0	0	0	0	30	0
E008	0	0	0	0	0	0	0	0	0	0	0	52	0
E010	0	0	0	0	0	0	0	0	0	0	22	33	0
E012	0	0	0	0	0	0	0	0	0	0	6	70	0
E013	0	0	0	0	0	0	0	0	0	0	26	22	0
E014	0	0	0	0	0	0	0	0	0	0	7	7	0
E015	0	0	0	0	0	0	0	0	0	0	0	20	0
E016	0	0	0	0	0	0	0	0	0	0	34	10	0
E017	0	0	0	0	0	0	0	0	0	0	4	21	0
E018	0	0	0	0	0	0	0	0	0	0	0	56	0
E019	0	3	0	0	0	0	0	0	0	0	44	31	0
E020	0	0	0	0	0	0	0	0	0	0	4	18	0
E021	0	0	0	0	0	0	0	0	0	0	63	56	0
E022	0	0	0	0	0	0	0	0	0	0	3	13	0
G023	0	0	3	0	0	0	0	0	0	0	90	69	0
G024	0	7	14	0	0	0	0	0	0	0	223	264	0
G025	0	3	7	0	0	0	0	0	0	0	316	104	0
G026	0	7	4	0	0	0	0	0	0	0	86	108	0
G027	0	0	23	0	0	0	0	0	0	0	346	215	0
G028	0	7	3	0	0	0	0	0	0	0	298	234	0
G029	0	0	3	0	0	0	0	0	0	0	289	253	0
G030	0	7	10	0	0	0	0	0	0	0	244	231	0
G031	0	3	23	0	0	0	0	0	0	0	337	164	0
G032	0	7	0	0	0	0	0	0	0	0	217	197	0
G033	0	3	50	0	0	0	0	0	0	0	47	332	0
G034	0	3	36	0	0	0	0	0	0	0	54	333	0
G035	0	5	27	0	0	0	0	0	0	0	41	315	0
G037	0	4	4	0	0	0	0	0	0	0	14	65	0
G038	0	6	0	0	0	0	0	0	0	0	6	63	0
G039	0	0	0	0	0	0	0	0	0	0	0	23	0
G040	0	0	3	0	0	0	0	0	0	0	20	115	0
G041	0	0	15	0	0	0	0	0	0	0	8	123	0
G042	0	9	12	0	0	0	0	0	0	0	30	119	0
G043	0	4	11	0	0	0	0	0	0	0	11	74	0
G044	0	12	8	0	0	0	0	0	0	0	24	88	0
G045	0	0	2	0	0	0	0	0	0	0	17	157	0
G046	0	4	12	0	0	0	0	0	0	0	4	91	0
G047	0	3	14	0	0	0	0	0	0	0	17	126	0
G048	0	3	24	0	0	0	0	0	0	0	15	90	0

Appendix 23: DIN598 surface sample reference database.

Site number	Alex	Atax	Btep	Iacu	Ipal	Ipar	Ipat	Isph	Istr	Lmac	Nlab	Ocen	Oarc
G049	0	7	10	0	0	0	0	0	0	0	43	151	0
G050	0	3	0	0	0	0	0	0	0	0	30	82	0
G051	0	0	0	0	0	0	0	0	0	0	102	482	0
G052	0	0	23	0	0	0	0	0	0	0	36	468	0
G053	0	0	131	0	0	0	3	0	0	0	68	387	0
G054	0	0	4	0	0	0	0	0	0	0	199	420	0
G055	0	3	10	0	0	0	0	0	0	0	176	281	0
G056	0	0	6	0	0	0	0	0	0	0	261	331	0
G057	0	2	11	0	2	0	0	2	0	0	170	395	0
G058	0	0	45	0	0	0	0	0	0	0	6	218	0
G059	0	0	0	0	0	0	0	0	0	0	145	315	0
G060	0	6	24	0	0	0	0	0	0	0	114	395	0
G061	0	0	5	0	0	0	0	0	0	0	220	390	0
G062	0	0	9	0	0	0	0	0	0	0	180	162	0
G063	3	2	11	0	0	0	0	0	0	0	111	356	0
G064	0	3	13	0	0	0	0	0	0	0	130	212	0
G065	0	0	45	0	0	0	0	0	0	0	117	337	0
G066	5	0	81	0	0	0	0	2	0	0	72	357	0
G067	3	0	14	0	0	0	0	0	0	0	52	14	0
G068	3	3	9	0	0	0	0	0	0	0	136	186	0
G069	0	0	0	0	0	0	0	0	0	0	10	58	0
G070	16	0	0	0	0	0	0	0	0	0	20	68	0
G071	4	0	4	0	0	0	0	0	0	0	36	133	0
G072	0	7	0	0	0	0	0	0	0	0	7	208	0
G073	0	0	72	0	3	0	0	3	0	0	66	309	0
A074	6	3	269	0	0	0	0	3	0	0	25	455	0
G075	3	6	103	0	0	0	0	0	0	0	6	318	0
G076	0	8	124	0	0	0	0	0	0	0	8	451	0
G077	12	0	32	0	0	0	0	0	0	0	8	341	0
G078	10	3	94	0	0	0	0	0	0	0	7	428	0
G079	6	6	6	0	0	0	0	0	0	0	39	286	0
B080	0	0	0	0	10	0	0	0	0	0	10	731	0
B081	0	0	0	0	0	0	0	0	0	0	2	783	0
B082	0	0	0	0	0	0	0	0	0	0	0	870	0
L087	0	2	0	2	6	2	0	20	0	0	516	275	0
L088	0	0	0	7	0	0	0	14	0	0	715	132	0
L089	0	0	0	0	0	0	0	43	0	0	422	177	0
L090	2	0	3	0	4	0	0	12	0	0	652	101	0
L091	0	2	6	3	2	0	0	13	0	0	283	449	0
L092	0	0	9	0	2	4	0	0	0	0	170	486	0
L093	0	0	6	2	8	6	0	0	0	0	498	260	0
L094	2	0	2	0	4	0	0	26	0	0	400	256	0
A099	0	0	2	2	0	0	0	9	0	0	301	363	0

Appendix 23: DIN598 surface sample reference database.

Site number	Alex	Atax	Btep	Iacu	Ipal	Ipar	Ipat	Isph	Istr	Lmac	Nlab	Ocen	Oarc
A100	0	0	3	0	0	0	0	19	0	0	397	411	0
A103	0	0	5	1	0	0	0	5	0	0	129	749	0
A104	0	0	14	0	0	0	0	5	0	0	264	495	0
A105	0	0	0	0	0	0	0	14	0	0	474	120	0
A106	0	0	3	0	0	0	0	18	0	0	247	508	0
A107	0	0	0	0	0	3	0	12	0	0	445	422	0
A108	0	0	0	0	0	4	0	20	0	0	460	240	0
A109	0	0	3	0	0	0	0	11	0	0	269	439	0
A110	0	0	7	0	0	0	0	7	0	0	217	362	0
A111	0	0	0	3	0	3	0	20	0	0	425	252	0
A112	0	0	0	0	0	0	0	0	0	0	241	259	0
A113	0	0	12	6	0	12	0	6	0	0	90	561	0
A114	0	0	13	15	0	40	0	3	3	0	28	386	0
A115	0	0	2	2	0	11	0	11	0	0	71	535	0
A116	0	0	0	0	0	29	0	16	0	0	54	390	0
A118	0	1	12	4	0	16	0	8	0	0	93	574	0
A119	0	0	0	57	0	46	11	11	0	0	80	414	0
A120	0	0	13	0	0	19	0	22	3	0	57	121	0
A121	0	0	2	0	0	3	0	0	0	0	52	733	0
A122	0	4	4	4	0	0	0	13	0	0	101	332	0
A123	0	0	3	0	0	0	0	3	0	0	45	607	0
A124	0	0	0	0	0	0	1	1	0	0	45	905	0
A125	0	1	0	0	0	0	0	1	0	0	33	917	0
A126	0	2	0	0	0	0	0	1	0	2	63	821	0
A127	0	0	0	18	0	21	3	30	0	0	596	289	0
A128	0	0	0	2	0	4	0	3	0	0	53	589	0
A129	0	8	0	0	0	8	0	11	0	0	123	265	0
H130	0	0	0	0	0	0	0	0	0	0	0	146	0
H131	0	0	0	0	0	0	0	0	0	0	0	122	0
H132	0	0	0	0	0	0	0	0	0	0	0	60	0
H133	0	0	0	0	9	0	0	0	0	0	0	181	0
H134	0	0	0	0	0	0	0	0	0	0	0	318	0
H135	0	0	0	0	2	0	0	0	0	0	0	134	0
H136	0	0	0	0	52	0	0	0	0	0	0	399	0
H137	0	0	0	0	56	0	0	0	0	0	0	557	0
H138	0	0	0	0	75	0	0	0	0	0	0	456	0
H139	0	0	0	0	26	0	0	0	0	0	0	521	0
H140	0	0	0	0	6	0	0	0	0	0	0	121	0
H141	0	0	0	0	0	0	0	0	0	0	0	23	0
H142	0	0	0	0	0	0	0	0	0	0	0	15	0
H143	0	0	0	0	0	0	0	0	0	0	0	39	0
H144	0	0	0	0	0	0	0	0	0	0	0	19	0
H145	0	0	0	0	2	0	0	0	0	0	0	34	0

Appendix 23: DIN598 surface sample reference database.

Site number	Alex	Atax	Btep	Iacu	Ipal	Ipar	Ipat	Isph	Istr	Lmac	Nlab	Ocen	Oarc
A149	0	0	4	0	4	1	0	1	0	0	53	568	0
A150	0	4	24	0	0	0	0	2	0	0	103	543	0
L151	0	0	7	21	66	7	0	62	0	0	524	145	0
L152	0	0	3	1	6	2	0	8	0	0	475	333	0
L153	0	0	6	1	2	1	0	1	0	0	232	479	0
A154	0	2	0	14	0	2	0	0	2	0	83	728	0
A155	0	0	6	16	0	16	0	25	0	0	73	174	0
A156	0	0	12	0	0	0	0	8	0	0	386	273	0
S158	0	2	0	0	10	0	0	2	0	0	157	47	0
S159	0	0	0	0	4	0	0	0	0	0	84	8	0
S160	0	0	0	0	0	0	0	0	0	0	10	29	0
L162	0	0	0	0	22	0	0	0	0	0	619	7	0
L163	0	0	0	0	0	0	0	21	0	0	579	62	0
L164	0	0	0	0	14	0	0	5	0	0	591	63	0
A168	0	0	6	0	0	0	0	2	0	0	175	721	0
A170	0	0	0	0	0	17	0	0	0	0	414	259	0
A171	0	0	10	0	0	7	0	27	0	0	409	140	0
A173	0	0	28	6	6	0	0	9	0	0	266	259	0
A174	0	3	3	0	3	10	0	30	0	0	209	588	0
A175	0	0	7	7	7	88	0	22	0	0	691	88	0
L178	0	0	29	0	19	5	0	52	0	0	552	138	0
A179	0	0	2	27	0	8	27	0	6	707	0	82	0
A180	0	3	96	116	0	17	3	23	0	53	43	272	0
A181	0	3	17	0	0	0	0	0	0	0	14	834	0
A182	0	0	20	5	0	0	0	0	0	0	11	808	0
A183	0	0	88	9	0	0	0	0	0	176	9	313	0
A184	0	0	0	22	0	20	5	4	4	673	2	63	0
N185	0	4	35	0	1	0	0	0	0	0	53	599	0
N186	0	0	19	0	0	0	0	0	0	2	73	689	0
N189	0	0	7	0	235	0	0	4	0	0	221	427	0
N190	0	0	0	0	117	0	0	2	0	0	189	309	0
N191	0	0	0	0	128	0	0	0	0	0	256	480	0
N192	0	0	0	0	27	0	0	0	0	0	46	245	0
N193	0	0	0	0	21	0	0	0	0	0	51	222	0
N194	0	0	0	0	39	0	0	0	0	0	106	776	0
N195	0	0	0	0	9	0	0	0	0	0	90	874	0
N196	0	0	9	0	21	0	0	5	0	0	80	739	0
N197	0	0	9	0	16	0	0	2	0	0	108	780	0
N198	2	7	16	0	2	0	0	2	0	0	106	413	0
N200	0	0	0	0	46	0	0	4	0	0	89	846	0
N206	0	0	41	0	0	0	0	0	0	0	177	415	0
N207	0	0	18	0	17	0	0	7	0	0	129	526	0
N208	0	0	22	1	13	0	0	1	0	0	133	476	0

Appendix 23: DIN598 surface sample reference database.

Site number	Alex	Atax	Btep	Iacu	Ipal	Ipar	Ipat	Isph	Istr	Lmac	Nlab	Ocen	Oarc
N209	0	0	3	0	4	0	0	1	0	0	87	436	0
N210	0	0	5	0	9	0	0	0	0	0	144	749	0
N211	0	4	9	0	4	0	0	0	0	0	20	461	0
N212	0	0	15	0	0	0	0	6	0	0	122	765	0
N213	0	0	6	0	1	0	0	0	0	0	64	733	0
N214	0	0	4	0	3	0	0	0	0	0	75	772	0
N215	0	1	4	0	6	0	0	3	0	0	105	774	0
N216	0	0	5	0	1	0	0	1	0	0	84	809	0
N217	0	0	18	0	1	0	0	1	0	0	81	430	0
N218	0	0	19	0	2	0	0	0	0	0	121	456	0
N219	0	2	19	0	1	0	0	4	0	0	115	471	0
N220	0	1	6	0	0	0	0	0	0	0	118	444	0
N221	0	0	15	0	1	0	0	1	0	2	86	408	0
N222	0	0	17	0	0	0	0	3	0	0	141	467	0
N223	0	0	8	0	0	0	0	0	0	0	57	309	0
N224	0	1	3	0	14	0	0	3	0	0	84	863	0
N225	3	0	13	0	3	0	0	3	0	0	124	544	0
N226	0	2	12	0	0	0	0	2	0	0	99	663	0
N227	0	0	0	0	5	0	0	0	0	0	109	153	0
N228	0	0	1	0	0	0	0	1	0	0	44	102	0
N229	0	0	0	0	1	0	0	0	0	0	23	19	0
N230	0	0	1	0	1	0	0	1	0	0	34	64	0
N231	0	0	1	0	10	0	0	0	0	0	60	157	0
N232	0	0	1	0	2	0	0	0	0	0	38	83	0
N233	0	0	0	0	1	0	0	0	0	0	45	159	0
N234	0	0	3	0	9	0	0	0	0	0	94	560	0
N235	0	0	3	0	11	0	0	0	0	0	140	787	0
N236	0	0	13	0	17	0	0	0	0	0	178	717	0
N237	0	3	18	0	55	0	0	18	0	0	140	561	0
N238	1	0	30	0	0	0	0	0	0	0	31	510	0
N239	3	2	40	0	2	0	0	1	0	0	24	533	0
N240	4	2	31	0	2	0	0	0	0	0	20	562	0
N241	1	3	24	0	3	0	0	0	0	0	12	659	0
N242	0	0	182	0	0	0	0	0	0	0	51	324	0
N245	0	3	42	0	5	0	0	0	0	0	5	730	0
N246	0	2	82	0	2	0	0	0	0	0	38	469	0
N248	0	0	30	0	2	0	0	0	0	2	22	710	0
N249	4	0	20	0	2	0	0	0	0	2	14	451	0
Z253	0	0	0	0	0	0	0	0	0	0	0	0	0
Z254	0	0	0	0	0	0	0	0	0	0	0	0	0
Z255	0	0	0	0	0	0	0	0	0	0	0	0	0
B256	0	0	0	0	15	0	0	0	0	0	0	34	0
B257	0	0	0	0	35	0	0	0	0	0	0	250	0

Appendix 23: DIN598 surface sample reference database.

Site number	Alex	Atax	Btep	Iacu	Ipal	Ipar	Ipat	Isph	Istr	Lmac	Nlab	Ocen	Oarc
A258	8	0	25	2	0	0	2	11	0	0	42	215	0
A259	5	0	10	8	0	0	5	35	0	0	38	352	0
A260	5	0	12	0	0	0	5	24	0	0	24	337	0
A261	0	0	0	0	0	0	12	6	0	0	18	64	0
A262	6	0	46	2	0	0	30	10	0	0	36	533	0
A263	5	0	42	0	0	0	5	14	2	2	25	538	0
A264	0	0	0	15	0	15	31	0	0	656	0	99	0
A265	0	0	0	5	0	8	5	0	5	707	10	79	0
A266	0	0	0	9	0	9	9	9	9	687	9	118	0
N268	0	0	66	0	0	0	0	0	0	0	21	458	0
N269	0	0	67	0	0	0	0	0	0	0	5	245	0
K271	0	16	42	0	0	0	0	0	0	94	0	440	0
K275	0	6	37	0	0	0	0	0	0	6	11	361	0
K277	11	0	24	0	0	0	0	0	0	11	0	340	0
M280	0	2	12	0	7	0	0	0	0	0	168	654	0
M281	0	2	2	0	6	0	0	0	0	0	67	860	0
M282	0	0	0	0	46	0	0	0	0	0	189	744	0
M283	0	0	0	0	193	0	0	0	0	0	413	326	0
M284	0	0	0	0	10	0	0	0	0	0	52	45	0
M285	0	0	4	0	14	0	0	0	0	0	103	698	0
M286	0	1	2	0	15	0	0	0	0	0	89	729	0
M287	0	2	2	0	105	0	0	0	0	0	164	528	0
M288	0	0	1	0	101	0	0	0	0	0	170	544	0
M289	0	0	0	0	3	0	0	0	0	0	3	11	0
M290	0	0	7	0	0	0	0	0	0	0	0	13	0
M291	0	0	0	0	0	0	0	0	0	0	0	5	0
M292	0	0	0	0	0	0	0	0	0	0	5	5	0
M293	0	0	0	0	2	0	0	0	0	0	2	4	0
M297	0	0	0	0	14	0	0	0	0	0	142	528	0
M298	0	0	3	0	3	0	0	0	0	0	68	877	0
M299	0	3	3	0	12	0	0	0	0	0	86	723	0
M300	0	0	0	0	10	0	0	0	0	0	131	789	0
M301	0	2	3	0	5	0	0	0	0	0	104	791	0
M303	0	1	4	0	9	0	0	0	0	0	85	719	0
M304	0	0	6	0	32	0	0	0	0	0	159	635	0
M305	0	0	2	0	6	0	0	0	0	0	80	780	0
M306	0	1	9	0	6	0	0	1	0	0	110	653	0
M307	0	1	6	0	6	0	0	0	0	0	91	735	0
M308	0	1	9	0	10	0	0	1	0	0	151	627	0
M309	0	4	15	0	8	0	0	0	0	0	206	583	0
M310	0	1	5	0	5	0	0	1	0	0	137	573	0
M311	0	0	5	0	7	0	0	0	0	0	119	706	0
M312	0	0	6	0	9	0	0	0	0	0	100	752	0

Appendix 23: DIN598 surface sample reference database.

Site number	Alex	Atax	Btep	Iacu	Ipal	Ipar	Ipat	Isph	Istr	Lmac	Nlab	Ocen	Oarc
M313	0	4	5	0	14	0	0	0	0	0	109	728	0
M314	0	0	4	0	297	0	0	4	0	0	230	323	0
M315	0	0	2	0	110	0	0	0	0	0	144	634	0
M316	0	0	1	0	98	0	0	0	0	0	169	670	0
M317	0	0	2	0	64	0	0	2	0	0	185	592	0
M318	0	0	1	0	88	0	0	0	0	0	168	609	0
M319	0	0	0	0	328	0	0	1	0	0	278	337	0
M320	0	2	0	0	214	0	0	0	0	0	317	399	0
M321	0	0	1	0	62	0	0	0	0	0	132	696	0
M322	0	0	6	0	10	0	0	0	0	1	129	722	0
M323	0	0	9	0	9	0	0	1	0	0	106	703	0
M324	0	1	7	0	4	0	0	1	0	1	146	522	0
M325	0	0	0	0	5	0	0	1	0	0	212	386	0
M326	0	1	6	0	4	0	0	1	0	0	86	842	0
M327	0	0	0	0	50	0	0	0	0	0	101	749	0
M328	0	0	3	0	265	0	0	3	0	0	198	278	0
M329	0	0	6	0	234	0	0	0	0	0	260	220	0
M330	0	0	3	0	260	0	0	0	0	0	249	183	0
M331	0	0	0	0	255	0	0	0	0	0	247	220	0
M332	0	0	0	0	360	0	0	3	0	0	270	201	0
M333	0	0	0	0	64	0	0	0	0	0	84	77	0
M334	0	0	0	0	17	0	0	0	0	0	34	46	0
M335	0	0	3	0	61	0	0	0	0	0	64	47	0
M336	0	0	2	0	204	0	0	0	0	0	206	362	0
M337	0	0	0	0	287	0	0	0	0	0	323	306	0
M338	0	0	0	0	204	0	0	0	0	0	229	477	0
M339	0	0	0	0	97	0	0	0	0	0	212	651	0
M340	0	0	0	0	16	0	0	0	0	0	172	655	0
M341	0	0	0	0	403	0	0	0	0	0	323	188	0
M342	0	0	0	0	179	0	0	0	0	0	147	510	0
M343	0	0	0	0	146	0	0	0	0	0	204	515	0
M344	0	0	0	0	29	0	0	10	0	0	184	141	0
M345	0	0	0	0	20	0	0	0	0	0	34	44	0
M346	0	0	4	0	17	0	0	0	0	0	4	17	0
M347	0	0	0	0	231	0	0	0	0	0	128	487	0
M348	0	0	0	0	0	0	0	0	0	0	0	0	0
M349	0	0	3	0	75	0	0	0	0	0	160	345	0
M350	0	2	2	0	153	0	0	4	0	0	207	397	0
M351	0	0	0	0	129	0	0	8	0	0	174	525	0
M352	0	0	7	0	148	0	0	0	0	0	221	458	0
M353	0	0	0	0	1	0	0	0	0	0	29	19	0
M354	0	0	2	0	125	0	0	0	0	0	179	139	0
M355	0	0	0	0	211	0	0	0	0	0	207	251	0

Appendix 23: DIN598 surface sample reference database.

Site number	Alex	Atax	Btep	Iacu	Ipal	Ipar	Ipat	Isph	Istr	Lmac	Nlab	Ocen	Oarc
M356	0	0	0	0	246	0	0	0	0	0	271	167	0
M357	0	0	0	0	83	0	0	0	0	0	199	26	0
M358	0	0	0	0	65	0	0	0	0	0	109	120	0
M359	0	4	0	0	78	0	0	0	0	0	202	149	0
M360	0	0	0	0	2	0	0	0	0	0	36	34	0
M361	0	0	0	0	230	0	0	0	0	0	260	277	0
M362	0	0	1	0	46	0	0	0	0	0	121	399	0
M363	0	0	0	0	26	0	0	0	0	0	97	319	0
M365	0	0	0	0	37	0	0	0	0	0	100	284	0
M366	0	0	1	0	17	0	0	0	0	1	68	270	0
M367	0	0	0	0	170	0	0	0	0	0	180	430	0
M368	0	0	0	0	25	0	0	2	0	0	96	314	0
M369	0	0	0	0	136	0	0	0	0	0	246	449	0
P370	0	0	0	0	34	0	0	0	0	0	201	144	0
P371	0	0	0	0	11	0	0	0	0	0	34	79	0
P372	0	0	0	0	0	0	0	0	0	0	9	35	0
P373	0	0	0	0	8	0	0	0	0	0	0	17	0
P374	0	0	0	0	9	0	0	0	0	0	9	0	0
P375	0	0	0	0	0	0	0	0	0	0	0	33	0
P376	0	0	0	0	7	0	0	0	0	0	7	7	0
P377	0	0	0	0	0	0	0	0	0	0	0	8	0
P378	0	0	0	0	19	0	0	0	0	0	0	19	0
Z379	2	0	0	0	4	0	0	0	0	0	0	126	0
Z380	0	0	4	0	0	0	0	0	0	0	0	314	0
Z381	3	0	3	0	0	0	0	3	0	0	0	302	0
Z382	0	0	11	0	3	0	0	0	0	0	3	415	0
Z383	0	0	3	0	3	0	0	0	0	0	0	158	0
Z384	0	0	3	0	0	0	0	0	0	0	0	295	0
Z385	0	0	4	0	2	0	0	0	0	0	0	150	0
Z386	0	0	5	0	10	0	0	0	0	0	3	174	0
Z387	0	0	10	0	7	0	0	0	0	0	5	192	0
Z388	0	0	3	0	6	0	0	0	0	0	3	327	0
Z389	0	0	0	0	5	0	0	0	0	0	0	122	0
Z390	0	0	0	0	0	0	0	2	0	0	5	102	0
Z391	0	0	4	0	4	0	0	0	0	0	0	90	0
Z392	0	2	0	0	0	0	0	0	0	0	2	66	0
Z393	0	0	3	0	3	0	0	0	0	0	3	68	0
Z394	0	0	10	0	3	0	0	0	0	0	0	58	0
Z395	0	0	1	0	2	0	0	0	0	0	1	40	0
Z396	0	0	2	0	2	0	0	0	0	0	2	48	0
Z397	0	0	2	0	2	0	0	0	0	0	0	66	0
N398	0	0	53	0	0	0	0	4	0	4	126	575	0
N399	0	0	19	0	0	0	0	0	0	0	80	554	0

Appendix 23: DIN598 surface sample reference database.

Site number	Alex	Atax	Btep	Iacu	Ipal	Ipar	Ipat	Isph	Istr	Lmac	Nlab	Ocen	Oarc
N400	0	0	22	0	0	0	0	0	0	0	156	478	0
N401	0	0	31	0	0	0	0	16	0	0	87	575	0
N402	0	2	42	0	6	0	0	0	0	0	90	522	0
A405	0	0	0	18	0	6	22	12	4	813	2	14	0
A406	0	0	8	42	0	38	34	17	13	373	0	89	0
A407	0	0	38	9	0	38	19	0	28	28	0	75	0
A408	0	0	6	70	0	29	6	0	0	116	0	186	0
A409	0	0	0	45	0	22	7	45	15	75	0	134	0
A410	0	0	0	53	0	9	0	0	9	27	0	150	0
A411	0	0	16	149	0	20	0	4	0	36	0	402	0
A412	0	0	66	530	0	71	5	61	5	0	5	45	0
A413	0	0	0	662	0	35	0	56	0	0	21	14	0
A414	0	0	25	911	0	0	0	0	0	0	0	13	0
A415	0	5	16	0	5	11	0	5	0	0	196	296	0
A416	0	0	0	0	0	0	0	0	0	0	15	215	0
A417	0	8	19	3	0	5	0	5	0	0	94	256	0
A418	0	0	15	0	0	0	0	30	0	0	231	284	0
A419	0	0	17	0	0	0	0	0	0	0	8	682	0
A420	2	2	29	0	0	0	0	2	0	2	13	709	0
A421	0	5	5	0	0	0	0	2	0	0	10	362	0
A422	5	0	0	0	0	0	0	0	0	0	3	310	0
A423	4	0	14	0	0	0	0	0	0	0	8	458	0
A424	8	0	28	0	0	0	85	18	2	3	23	583	0
A425	2	0	10	0	0	0	5	0	0	5	12	464	0
A426	6	0	0	0	0	0	2	0	0	4	0	688	0
A427	10	0	14	2	0	0	4	0	0	4	0	430	0
A428	7	0	2	2	0	0	5	0	0	0	10	459	0
Z432	0	0	0	0	0	0	0	0	0	0	0	15	178
Z434	0	0	0	0	0	0	0	0	0	0	28	139	444
Z435	0	3	0	0	3	0	0	0	0	0	0	8	98
Z436	0	0	0	0	0	0	0	0	0	0	0	80	159
Z437	0	0	0	0	0	0	0	0	0	0	0	0	553
Z438	0	0	0	0	6	0	0	0	0	0	0	111	228
Z439	0	0	0	0	11	0	0	0	0	0	0	220	214
Z445	0	0	0	0	0	0	0	0	0	0	0	0	0
Z446	0	0	0	0	0	0	0	0	0	0	0	0	0
Z448	0	0	0	0	0	0	0	0	0	0	0	0	0
Z449	0	0	0	0	0	0	0	0	0	0	0	25	0
Z450	0	0	0	0	0	0	0	0	0	0	0	0	0
Z452	0	0	0	0	0	0	0	0	0	0	0	0	0
Z453	0	0	0	0	0	0	0	0	0	0	0	0	0
Z454	0	0	0	0	0	0	0	0	0	0	0	0	0
Z455	0	0	0	0	0	0	0	0	0	0	0	0	0

Appendix 23: DIN598 surface sample reference database.

Site number	Alex	Atax	Btep	Iacu	Ipal	Ipar	Ipat	Isph	Istr	Lmac	Nlab	Ocen	Oarc
Z457	0	0	0	0	0	0	0	0	0	0	0	0	0
Z458	0	0	0	0	9	0	0	0	0	0	0	0	0
Z459	0	0	0	0	0	0	0	0	0	0	0	0	0
Z460	0	0	0	0	0	0	0	0	0	0	0	0	0
Z461	0	0	0	0	0	0	0	0	0	0	0	0	0
Z462	0	0	0	0	0	0	0	0	0	0	0	0	0
Z463	0	0	0	0	0	0	0	0	0	0	0	0	0
Z464	0	0	0	0	9	0	0	0	0	0	0	0	0
Z466	0	0	19	0	0	0	0	0	0	0	0	0	0
Z467	0	0	0	0	0	0	0	0	0	0	0	9	0
Z468	0	0	0	0	0	0	0	0	0	0	0	0	0
Z469	0	0	0	0	0	0	0	0	0	0	0	9	0
Z470	0	0	0	0	0	0	0	0	0	0	0	0	0
Z471	0	0	0	0	0	0	0	0	0	0	0	0	0
Z472	0	0	0	0	0	0	0	0	0	0	0	0	0
Z473	0	0	0	0	0	0	0	0	0	0	0	0	0
Z474	0	0	0	0	8	0	0	0	0	0	0	0	0
Z475	0	0	0	0	5	0	0	0	0	0	0	3	0
Z476	0	0	0	0	0	0	0	0	0	0	0	0	0
Z477	0	0	0	0	0	0	0	0	0	0	0	0	0
Z478	0	0	0	0	16	0	0	0	0	0	0	0	0
Z479	0	0	0	0	0	0	0	0	0	0	0	0	0
Z480	0	0	0	0	39	0	0	0	0	0	0	0	0
Z481	0	0	0	0	31	0	0	0	0	0	0	0	0
Z482	0	0	0	0	0	0	0	0	0	0	0	0	0
Z483	0	0	0	0	0	0	0	0	0	0	0	0	0
Z484	0	0	0	0	0	0	0	0	0	0	0	0	0
Z485	0	0	0	0	0	0	0	0	0	0	0	0	0
Z486	0	0	0	0	33	0	0	0	0	0	0	0	0
Z487	0	0	0	0	0	0	0	0	0	0	0	29	0
Z488	0	0	0	0	0	0	0	0	0	0	0	0	0
Z489	0	0	0	0	0	0	0	0	0	0	0	0	0
Z491	0	0	0	0	0	0	0	0	0	0	0	0	0
Z492	0	0	0	0	0	0	0	0	0	0	0	0	0
Z493	0	0	0	0	0	0	0	0	0	0	0	0	0
Z494	0	0	0	0	0	0	0	0	0	0	0	0	0
Z495	0	0	0	0	0	0	0	0	0	0	0	7	0
Z496	0	0	0	0	0	0	0	0	0	0	0	6	0
Z497	0	0	0	0	0	0	0	0	0	0	8	47	0
Z498	0	0	0	0	5	0	0	0	0	0	0	13	0
Z499	0	0	0	0	87	0	0	0	0	0	158	273	0
Z500	0	0	0	0	58	0	0	0	0	0	48	131	0
Z501	0	0	0	0	20	0	0	0	0	0	4	16	0

Appendix 23: DIN598 surface sample reference database.

Site number	Alex	Atax	Btep	Iacu	Ipal	Ipar	Ipat	Isph	Istr	Lmac	Nlab	Ocen	Oarc
Z502	0	0	0	0	26	0	0	0	0	0	0	164	0
Z503	0	0	0	0	31	0	0	0	0	0	0	233	0
Z504	0	0	0	0	0	0	0	0	0	0	0	80	0
Z505	0	0	0	0	264	0	0	0	0	0	176	108	0
Z506	0	0	0	0	116	0	0	0	0	0	22	22	0
Z507	0	0	0	0	0	0	0	0	0	0	0	14	0
Z508	0	0	0	0	0	0	0	0	0	0	0	37	0
Z509	0	0	0	0	260	0	0	0	0	0	71	18	0
Z510	0	0	0	0	116	0	0	0	0	0	116	17	0
Z511	0	0	0	0	256	0	0	0	0	0	286	15	0
Z512	0	0	0	0	316	0	0	0	0	0	194	36	0
Z513	0	0	0	0	263	0	0	0	0	0	243	39	0
Z514	0	0	0	0	164	0	0	0	0	0	317	26	0
Z515	0	0	0	0	307	0	0	0	0	0	248	134	0
Z516	0	0	0	0	60	0	0	0	0	0	91	44	0
Z517	0	0	0	0	0	0	0	0	0	0	7	0	0
Z518	0	0	0	0	0	0	0	0	0	0	0	26	0
Z519	0	0	0	0	0	0	0	0	0	0	0	9	0
Z520	0	0	0	0	27	0	0	0	0	0	18	0	0
Z521	0	0	0	0	45	0	0	0	0	0	55	118	0
Z522	0	0	0	0	0	0	0	0	0	0	0	10	0
Z523	0	0	0	0	0	0	0	0	0	0	0	13	0
Z524	0	0	0	0	0	0	0	0	0	0	0	28	0
Z526	0	0	0	0	7	0	0	0	0	0	0	0	0
Z527	0	0	0	0	18	0	0	0	0	0	0	9	0
Z528	0	0	0	0	0	0	0	0	0	0	0	0	0
Z529	0	0	17	0	0	0	0	0	0	0	0	0	0
Z530	0	0	0	0	0	0	0	0	0	0	0	7	0
Z531	0	0	0	0	0	0	0	0	0	0	0	27	0
A532	0	0	2	0	0	0	0	0	0	0	231	189	0
A533	0	0	5	0	8	0	0	0	0	0	238	302	0
A534	0	0	0	0	3	0	0	0	0	0	251	74	0
Z535	0	7	0	0	3	0	0	0	0	0	3	207	0
Z536	0	3	0	0	0	0	0	0	0	0	3	142	0
Z537	0	0	0	0	0	2	0	0	0	0	4	73	0
Z538	0	0	3	0	2	0	0	2	0	0	3	236	0
Z539	0	0	2	0	0	0	0	0	0	0	8	280	0
Z540	0	0	2	0	5	0	0	0	0	0	2	321	0
Z541	0	0	0	0	2	0	0	0	0	0	3	268	0
Z542	0	0	0	0	5	0	0	0	0	0	12	165	0
Z543	0	0	0	0	0	0	0	0	0	0	0	4	0
Z544	0	0	0	0	0	0	0	0	0	0	0	0	0
Z545	0	0	0	0	0	0	0	0	0	0	0	0	0

Appendix 23: DIN598 surface sample reference database.

Site number	Alex	Atax	Btep	Iacu	Ipal	Ipar	Ipat	Isph	Istr	Lmac	Nlab	Ocen	Oarc
Z546	0	0	0	0	0	0	0	0	0	0	0	3	0
Z547	0	0	0	0	0	0	0	0	0	0	0	568	0
Z548	0	0	0	0	0	0	0	0	0	0	14	27	0
Z549	0	0	0	0	0	0	0	0	0	0	0	17	4
Z550	0	0	4	0	4	0	0	0	0	0	44	718	23
Z551	0	0	0	0	2	0	0	0	0	0	39	829	9
Z552	0	0	0	0	1	0	0	0	0	0	15	654	0
Z553	0	0	0	0	0	0	0	0	0	0	16	656	12
Z554	0	0	0	0	0	0	0	0	0	0	10	510	7
Z555	0	0	0	0	11	0	0	11	0	0	21	383	0
Z556	0	0	0	0	0	0	0	0	0	0	0	202	0
Z557	0	0	9	0	9	0	0	0	0	0	0	175	0
Z558	0	0	0	0	3	0	0	0	0	0	29	353	0
Z559	0	0	8	0	15	0	0	4	0	0	15	509	0
Z560	0	0	3	0	0	0	0	0	0	0	13	426	0
Z561	0	0	14	0	0	0	0	4	0	0	0	230	0
Z562	0	0	0	0	3	0	0	6	0	0	6	239	0
Z563	0	0	0	0	0	0	0	0	0	0	0	63	175
Z564	0	0	0	0	0	0	0	0	0	0	0	170	40
Z565	0	0	0	0	48	0	0	0	0	0	0	714	0
P566	0	0	0	0	0	0	0	0	0	0	0	0	18
P567	0	0	0	0	5	0	0	0	0	0	0	0	0
P568	0	0	0	0	0	0	0	0	0	0	0	0	13
P569	0	0	0	0	0	0	0	0	0	0	0	0	0
P570	0	0	0	0	0	0	0	0	0	0	0	13	13
P571	0	0	0	0	0	0	0	0	0	0	0	6	0
P572	0	0	0	0	0	0	0	0	0	0	0	0	0
P573	0	0	0	0	0	0	0	0	0	0	0	6	0
P574	0	0	0	0	0	0	0	0	0	0	0	0	0
P575	0	0	0	0	0	0	0	0	0	0	0	13	13
P576	0	0	0	0	0	0	0	0	0	0	0	13	0
P577	0	0	0	0	0	0	0	0	0	0	0	18	0
P578	0	0	0	0	0	0	0	0	0	0	0	26	0
P579	0	0	0	0	0	0	0	0	0	0	0	247	7
P580	0	0	0	0	7	0	0	0	0	0	0	7	0
Z602	0	0	0	0	0	0	0	0	0	0	0	99	0
Z603	0	0	0	0	0	0	0	0	0	0	0	359	0
Z604	0	0	0	0	0	0	0	0	0	0	0	159	0
Z605	0	0	0	0	11	0	0	0	0	0	5	220	0
Z606	0	0	0	0	98	0	0	0	0	0	293	260	0
N607	0	0	0	0	0	0	0	0	0	26	0	500	0
N608	0	0	0	0	0	0	0	0	0	156	0	589	0
N609	0	0	4	0	0	0	0	0	0	27	0	777	0

Appendix 23: DIN598 surface sample reference database.

Site number	Alex	Atax	Btep	Iacu	Ipal	Ipar	Ipat	Isph	Istr	Lmac	Nlab	Ocen	Oarc
N610	0	0	0	0	0	0	0	0	0	41	0	863	0
N611	0	0	0	0	0	0	0	0	0	224	0	318	0
N612	0	0	0	0	0	0	0	0	0	51	0	707	0
N613	0	0	0	0	0	0	0	0	0	10	0	857	0
N614	0	0	7	0	0	0	0	0	0	53	0	776	0
N615	0	7	13	0	0	0	0	0	0	39	0	684	0
N616	0	0	17	0	0	0	0	0	0	22	0	624	0
N617	0	0	0	0	0	0	0	0	0	136	0	477	0
N620	0	0	0	0	0	0	0	0	0	0	0	717	0
N622	0	0	3	0	0	0	0	0	0	3	0	611	0
N623	0	4	4	0	0	0	0	0	0	30	0	342	0
N626	0	0	0	0	0	0	0	0	0	20	0	656	0
N627	0	0	0	0	0	0	0	0	0	0	0	385	0
N628	0	11	0	0	0	0	0	0	0	0	0	484	0
N629	0	0	0	0	0	0	0	0	0	10	0	730	0
N630	0	0	3	0	0	0	0	0	0	0	5	499	0
N631	0	3	0	0	0	0	0	0	0	0	0	345	0
N632	0	0	0	0	0	0	0	0	0	4	0	405	0
N633	0	0	24	0	0	0	0	0	0	12	0	353	0
N634	0	0	22	0	0	0	0	0	0	0	0	656	0
N635	0	0	0	0	0	0	0	0	0	9	0	673	0
N636	0	0	3	0	0	0	0	0	0	0	0	752	0
N637	0	0	7	0	0	0	0	0	0	0	0	578	0
N638	0	0	3	0	0	0	0	0	0	0	0	761	0
X639	0	0	18	0	0	0	0	0	0	0	9	260	0
X640	0	3	33	0	0	0	0	0	0	3	10	292	0
X641	0	0	3	0	0	0	0	0	0	0	7	374	0
X642	0	4	11	0	0	0	0	0	0	0	7	472	0
X643	0	0	10	0	0	0	0	0	0	0	7	208	0
X644	0	0	10	0	0	0	0	0	0	0	10	293	0
X645	0	0	0	0	0	0	0	0	0	0	6	298	0
X646	0	0	10	0	0	5	0	0	5	0	25	240	0
X647	7	3	0	3	7	13	0	3	7	3	42	345	0
X648	0	2	92	2	0	0	0	0	0	0	24	523	0
X649	0	0	70	0	0	140	0	18	18	0	43	347	0
X650	0	0	61	3	0	13	0	0	0	0	47	350	0
X651	0	0	43	0	0	4	0	0	2	4	49	554	0
X652	0	6	59	3	0	0	0	0	0	0	38	581	0
X653	3	0	69	0	0	7	0	0	0	3	23	592	0
X654	14	0	145	0	0	0	0	12	0	3	0	473	0
X655	6	0	160	0	6	0	0	0	1	1	6	482	0
X656	21	11	101	0	2	2	2	0	0	0	15	565	0
X657	2	3	73	0	0	2	0	2	0	2	18	716	0

Appendix 23: DIN598 surface sample reference database.

Site number	Alex	Atax	Btep	Iacu	Ipal	Ipar	Ipat	Isph	Istr	Lmac	Nlab	Ocen	Oarc
X658	10	7	122	3	3	0	7	21	3	0	35	538	0
X659	2	2	83	0	0	6	0	4	0	2	16	631	0
X660	0	0	86	0	0	9	0	0	0	9	6	460	0
X661	0	0	0	0	7	0	0	7	0	0	369	183	0
X664	26	2	70	0	2	2	0	0	0	5	2	360	0
X666	0	0	4	0	0	11	0	14	0	7	70	187	0
X668	0	0	79	5	0	0	3	0	3	0	38	761	0
X669	3	0	3	0	0	0	3	0	0	0	38	245	0
X670	6	0	109	9	21	0	29	15	0	0	26	615	0
X671	3	0	63	0	5	0	3	3	0	0	46	644	0
X672	2	4	148	0	5	0	1	0	0	5	2	599	0
X673	0	0	65	7	7	14	21	7	0	3	247	469	0
X674	0	0	15	3	0	21	9	0	6	6	138	408	0
X675	0	0	9	0	0	0	3	0	0	3	186	419	0
A682	0	0	3	0	3	0	0	3	0	6	9	622	0
A683	0	3	7	0	0	0	0	0	0	0	3	502	0
A685	0	3	26	0	0	0	0	0	0	0	45	659	0
X686	23	0	50	3	0	3	3	20	3	0	37	503	0
X688	7	0	46	0	0	0	13	7	0	0	26	589	0
X689	12	3	40	3	0	0	0	6	0	3	40	464	0
X690	10	0	46	0	0	3	3	7	0	0	10	388	0
X691	0	0	47	0	0	0	3	13	0	0	13	431	0
X692	18	0	65	6	0	0	3	6	0	0	9	498	0
X693	10	0	49	0	0	0	0	0	0	0	26	597	0
X694	7	7	86	0	0	0	7	3	0	0	23	568	0
X695	6	3	97	6	3	0	3	12	0	0	27	574	0
X696	0	0	144	0	0	0	0	0	0	0	0	628	0
X697	9	3	87	3	3	0	9	68	0	0	22	534	0
X698	6	0	68	0	0	0	3	3	0	0	29	487	0
X699	17	3	96	7	0	0	0	0	0	0	20	527	0
X700	3	0	83	6	0	0	0	0	0	0	13	639	0
X701	3	0	100	0	3	3	3	0	0	0	10	538	0
X702	10	0	81	0	0	0	8	0	0	0	10	565	0
X703	7	3	77	0	7	0	0	17	0	0	3	316	0
X704	3	0	95	0	0	0	0	6	0	0	16	500	0
X705	7	0	78	3	0	0	3	0	0	0	34	570	0
X706	3	0	80	0	0	0	6	0	0	0	22	508	0
X707	0	0	66	7	0	0	7	10	0	0	14	434	0
X708	14	0	10	0	0	0	0	0	0	0	0	185	0

Appendix 23: DIN598 surface sample reference database.

Site number	Pret	Smem	Selo	Sram	Sben	Smir	Pdal	Amin	Amic	Bspp	Peri	Sele	Squa
E003	0	0	17	6	0	0	331	90	0	472	0	0	51
E004	0	0	11	0	0	0	211	78	0	600	0	0	44
E005	0	0	6	0	0	0	129	241	0	518	0	0	47
E006	0	0	0	0	0	0	279	125	0	500	0	0	88
E007	0	0	5	0	0	0	303	76	5	561	0	0	15
E008	0	0	6	0	0	0	116	93	0	628	0	0	105
E010	0	0	22	11	0	0	144	78	0	644	0	0	44
E012	0	0	19	6	0	0	217	25	0	631	0	0	25
E013	0	0	4	0	0	0	383	62	0	423	0	0	80
E014	0	0	18	7	0	0	465	35	0	277	0	0	184
E015	0	0	4	0	0	0	277	76	0	542	0	0	80
E016	0	0	17	14	0	0	352	85	0	440	0	0	48
E017	0	0	13	13	0	0	191	98	0	451	0	0	209
E018	0	0	20	0	0	0	385	103	0	341	0	0	95
E019	0	0	31	20	0	0	262	48	0	483	0	0	78
E020	0	0	22	9	0	0	268	103	0	491	0	0	85
E021	0	0	30	23	0	0	381	73	0	315	0	0	60
E022	0	0	7	16	0	0	459	108	0	331	0	0	62
G023	0	0	14	10	0	0	538	66	0	174	0	0	35
G024	0	0	47	64	0	0	230	51	0	57	0	0	44
G025	0	0	10	0	0	0	306	10	0	195	0	0	47
G026	0	0	11	37	0	0	313	78	0	216	0	0	138
G027	0	0	23	10	0	0	245	10	0	77	0	0	50
G028	0	0	31	37	0	0	247	34	0	85	0	0	24
G029	0	0	45	26	0	0	237	39	0	78	0	0	29
G030	0	0	43	3	0	0	261	54	0	117	0	0	30
G031	0	0	42	8	0	0	241	54	0	99	0	0	28
G032	0	0	40	20	0	0	357	23	0	123	0	0	17
G033	0	0	12	6	0	0	382	22	0	146	0	0	0
G034	0	0	23	3	0	0	416	18	0	111	0	0	3
G035	0	0	19	11	0	0	416	14	0	149	0	0	3
G037	0	0	36	39	0	0	79	79	0	652	0	0	29
G038	0	0	31	44	0	0	131	131	0	569	0	0	19
G039	0	0	13	23	0	0	61	100	0	765	0	0	16
G040	0	0	22	50	0	0	266	95	0	420	0	0	8
G041	0	0	27	88	0	0	330	73	0	314	0	0	23
G042	0	0	42	53	0	0	264	92	0	365	0	0	15
G043	0	0	7	19	0	0	181	93	0	600	0	0	0
G044	0	0	20	40	0	0	175	124	0	506	0	0	4
G045	0	0	27	32	0	0	127	177	0	430	0	0	30
G046	0	0	41	37	0	0	211	231	0	351	0	0	17
G047	0	0	55	60	0	0	282	106	0	316	0	0	20
G048	0	0	27	75	0	0	457	33	0	263	0	0	15

Appendix 23: DIN598 surface sample reference database.

Site number	Pret	Smem	Selo	Sram	Sben	Smir	Pdal	Amin	Amic	Bspp	Peri	Sele	Squa
G049	0	0	20	66	0	0	354	82	0	243	0	0	26
G050	0	0	25	27	0	0	290	167	0	366	0	0	11
G051	0	0	11	11	0	0	380	0	0	15	0	0	0
G052	0	0	9	14	0	0	368	9	0	73	0	0	0
G053	0	0	9	18	0	0	199	0	0	185	0	0	0
G054	0	0	33	31	0	0	285	2	0	26	0	0	0
G055	0	0	48	45	0	0	288	0	0	147	0	0	3
G056	0	0	34	23	0	0	306	6	0	34	0	0	0
G057	0	0	46	26	0	0	301	3	0	41	0	0	2
G058	0	0	11	23	0	0	85	158	11	441	0	0	3
G059	0	0	17	26	0	0	153	157	0	166	0	0	21
G060	0	0	21	21	0	0	322	0	0	96	0	0	0
G061	0	0	30	52	0	0	212	11	0	80	0	0	0
G062	0	0	27	14	0	2	486	43	0	59	0	0	18
G063	0	0	32	13	0	0	262	167	5	32	0	0	5
G064	0	0	20	7	0	0	573	0	0	33	0	0	10
G065	0	0	17	24	0	0	265	10	0	186	0	0	0
G066	0	0	33	11	0	0	373	11	0	56	0	0	0
G067	0	0	10	7	0	0	359	77	0	401	0	0	63
G068	0	0	44	18	0	0	260	44	0	240	0	0	56
G069	0	0	0	3	0	0	281	119	0	461	0	0	68
G070	0	0	13	7	0	0	345	117	0	319	0	0	94
G071	0	0	14	47	0	0	165	154	0	419	0	0	25
G072	0	0	7	30	0	0	53	224	0	449	0	0	17
G073	0	0	20	17	0	0	198	26	0	281	0	0	6
A074	0	0	6	9	0	0	96	6	0	115	0	0	6
G075	0	0	8	3	0	0	253	6	0	295	0	0	0
G076	0	0	19	4	0	0	75	11	0	301	0	0	0
G077	0	0	14	14	0	0	233	14	0	325	0	0	6
G078	0	0	7	13	0	0	167	17	0	251	0	0	3
G079	0	0	0	0	0	0	39	19	0	578	0	0	19
B080	0	0	248	0	0	0	0	0	0	0	0	0	0
B081	0	0	208	1	0	0	0	0	0	5	0	0	0
B082	0	0	114	0	0	0	0	9	0	6	0	0	0
L087	0	0	4	22	0	0	130	2	0	12	0	0	6
L088	0	0	10	0	0	0	58	7	0	51	0	0	7
L089	0	0	3	3	0	0	22	65	0	248	0	0	16
L090	0	0	2	0	0	0	114	0	0	29	2	0	50
L091	0	0	11	26	0	0	159	0	0	30	0	0	10
L092	0	0	12	39	0	0	258	0	0	9	0	0	0
L093	0	0	4	12	0	0	182	0	0	21	0	0	0
L094	0	0	0	20	0	0	144	7	0	96	9	0	18
A099	0	0	4	13	0	0	213	0	0	62	0	0	18

Appendix 23: DIN598 surface sample reference database.

Site number	Pret	Smem	Selo	Sram	Sben	Smir	Pdal	Amin	Amic	Bspp	Peri	Sele	Squa
A100	0	0	13	3	0	0	67	0	0	56	0	0	29
A103	0	0	15	36	0	0	37	0	0	14	0	0	5
A104	0	0	9	9	0	0	18	0	0	127	0	0	55
A105	0	0	0	0	0	0	100	131	0	103	0	0	45
A106	0	0	15	20	0	0	31	0	0	82	0	0	56
A107	3	0	15	18	0	0	21	0	0	41	0	0	6
A108	0	4	8	0	0	0	0	4	0	180	0	0	16
A109	0	0	42	3	0	0	0	0	0	178	0	0	6
A110	0	0	38	0	0	0	0	0	0	259	0	0	41
A111	0	0	23	6	0	0	3	0	0	207	0	0	25
A112	0	0	0	0	0	0	0	0	0	276	0	0	103
A113	3	0	152	0	0	15	3	0	0	72	3	3	0
A114	0	0	35	0	0	170	3	0	0	271	3	0	5
A115	0	0	234	10	0	48	0	0	0	55	2	0	5
A116	0	0	144	0	3	73	0	0	0	211	0	0	3
A118	4	0	162	2	0	13	2	0	0	53	1	2	10
A119	0	0	184	11	0	115	0	0	0	69	0	0	0
A120	0	0	35	3	0	0	0	0	0	497	0	0	3
A121	0	0	136	1	0	16	0	0	0	41	0	0	3
A122	4	0	122	17	0	88	0	0	0	235	0	0	8
A123	3	3	189	14	0	58	3	0	0	56	0	0	8
A124	0	0	25	4	0	7	4	0	0	1	0	0	3
A125	0	3	31	1	0	4	0	0	0	3	3	0	3
A126	0	0	35	5	0	6	2	0	0	39	4	0	16
A127	9	0	12	0	0	6	0	0	0	6	0	0	0
A128	0	1	227	0	0	7	0	0	0	86	0	0	3
A129	0	0	46	3	0	0	118	0	0	252	11	0	121
H130	0	0	71	3	0	0	161	104	28	486	0	0	2
H131	0	0	66	2	0	0	185	93	44	488	0	0	0
H132	0	0	22	2	0	0	56	201	104	554	0	0	0
H133	0	0	96	7	0	0	232	94	28	350	0	0	2
H134	0	0	98	11	0	0	426	37	14	96	0	0	0
H135	0	0	98	2	0	0	259	217	42	246	0	0	0
H136	0	0	155	18	0	0	224	18	10	124	0	0	0
H137	0	0	92	31	0	0	215	0	0	48	0	0	0
H138	0	0	72	9	0	0	349	0	0	38	0	0	0
H139	0	0	64	13	0	0	195	67	22	93	0	0	0
H140	0	0	17	4	0	0	766	34	11	41	0	0	0
H141	0	0	6	48	0	0	889	11	4	19	0	0	0
H142	0	0	9	29	0	0	904	20	6	17	0	0	0
H143	0	0	10	2	0	0	885	31	8	25	0	0	0
H144	0	0	10	0	0	0	952	11	2	6	0	0	0
H145	0	0	26	2	0	0	883	6	6	42	0	0	0

Appendix 23: DIN598 surface sample reference database.

Site number	Pret	Smem	Selo	Sram	Sben	Smir	Pdal	Amin	Amic	Bspp	Peri	Sele	Squa
A149	0	0	5	1	0	0	266	0	0	88	0	0	7
A150	0	0	85	2	0	0	109	0	0	42	4	0	50
L151	0	0	0	10	0	0	21	14	3	117	0	0	0
L152	0	0	5	26	0	0	101	1	0	31	0	0	3
L153	0	0	1	36	0	0	199	1	0	33	1	0	4
A154	0	0	114	8	0	0	5	0	0	8	0	0	10
A155	0	0	44	0	0	495	0	0	0	142	0	0	0
A156	0	0	92	8	0	0	20	12	0	90	0	0	24
S158	0	0	8	3	0	0	86	44	2	633	0	0	7
S159	4	0	4	0	0	0	324	220	0	348	0	0	4
S160	0	0	0	20	0	0	20	225	10	676	0	0	10
L162	0	0	7	0	0	0	149	0	7	172	0	0	7
L163	0	0	0	0	0	0	113	26	0	159	0	0	36
L164	0	0	10	0	0	0	96	24	0	173	0	0	24
A168	0	0	5	56	0	0	30	0	0	3	0	0	2
A170	0	0	0	0	0	0	0	0	0	224	0	0	0
A171	0	0	37	3	0	3	80	0	0	239	0	0	7
A173	0	0	79	13	0	0	209	0	0	82	0	0	13
A174	0	0	27	0	0	3	40	0	0	73	0	0	0
A175	0	0	15	15	0	0	0	0	0	0	0	0	0
L178	0	0	0	0	0	0	33	48	0	110	0	0	10
A179	6	49	0	47	0	39	0	0	0	0	0	0	0
A180	3	30	0	86	7	203	0	0	0	17	0	10	17
A181	0	7	27	3	0	3	0	0	0	24	10	0	24
A182	0	4	37	7	0	7	0	0	0	42	0	0	27
A183	0	31	4	97	4	137	0	0	0	18	22	4	44
A184	0	31	0	41	5	72	0	0	0	36	18	0	0
N185	0	0	10	43	0	11	241	0	0	4	0	0	0
N186	0	0	10	19	0	16	156	0	0	14	0	0	2
N189	0	0	7	0	0	0	25	0	0	75	0	0	0
N190	0	0	3	2	0	0	3	3	0	369	2	0	2
N191	0	0	0	0	0	0	32	8	0	96	0	0	0
N192	0	0	23	13	0	0	628	0	0	17	0	0	1
N193	0	0	6	21	0	0	649	3	0	26	0	0	0
N194	0	0	0	0	0	0	43	0	0	34	0	0	2
N195	0	0	3	3	0	0	1	0	0	19	0	0	1
N196	0	0	7	0	0	0	26	2	0	111	0	0	0
N197	0	0	2	2	0	0	55	0	0	26	0	0	0
N198	0	0	5	16	0	2	248	2	0	120	0	0	41
N200	0	0	7	0	0	0	4	0	0	4	0	0	0
N206	0	0	6	8	0	0	246	0	0	64	0	0	18
N207	0	0	13	17	0	0	235	0	0	19	0	0	7
N208	0	0	7	3	0	1	312	0	0	17	0	0	1

Appendix 23: DIN598 surface sample reference database.

Site number	Pret	Smem	Selo	Sram	Sben	Smir	Pdal	Amin	Amic	Bspp	Peri	Sele	Squa
N209	0	0	2	7	0	2	437	0	0	14	0	0	3
N210	0	0	5	5	0	0	79	0	0	5	0	0	0
N211	0	0	38	122	0	2	339	0	0	0	0	0	0
N212	0	0	6	3	0	12	71	0	0	0	0	0	0
N213	0	0	1	6	0	3	169	0	0	10	0	0	5
N214	0	0	3	6	0	4	109	0	0	17	0	0	6
N215	0	0	6	3	0	0	59	0	0	30	0	0	4
N216	0	0	3	6	0	5	50	1	0	33	0	0	2
N217	0	0	10	7	0	0	394	0	0	40	0	0	14
N218	0	0	9	9	0	0	313	0	0	47	0	0	15
N219	0	0	7	11	0	3	293	1	0	37	0	0	18
N220	0	0	10	16	0	1	330	0	0	23	0	0	19
N221	0	0	14	13	0	2	404	0	1	12	1	0	22
N222	0	0	6	33	0	3	301	0	0	17	0	0	3
N223	0	0	0	12	0	8	520	0	0	45	0	0	33
N224	0	0	1	0	0	0	29	0	0	3	0	0	1
N225	0	0	30	14	0	1	53	27	0	77	0	0	39
N226	0	0	45	5	0	1	47	2	0	36	0	0	33
N227	0	0	38	8	0	0	447	0	0	177	0	0	63
N228	0	0	3	6	0	0	811	2	0	20	2	0	10
N229	0	0	2	4	0	0	914	0	0	24	3	0	10
N230	0	0	3	6	0	0	861	0	0	23	0	0	4
N231	0	0	3	22	0	0	728	0	0	19	0	0	0
N232	0	0	2	7	0	0	862	0	0	4	0	0	0
N233	0	0	2	9	0	0	770	0	0	13	0	0	0
N234	0	0	0	22	0	0	264	0	0	44	0	0	3
N235	0	0	3	0	0	0	16	0	0	40	0	0	0
N236	0	0	0	0	0	0	0	0	0	74	0	0	0
N237	0	0	21	37	0	9	134	0	0	0	0	0	3
N238	0	0	10	99	0	7	179	6	0	72	0	0	31
N239	0	0	5	128	0	13	197	0	0	17	1	0	28
N240	0	0	4	115	0	16	209	0	0	7	1	0	24
N241	0	0	13	83	0	24	157	0	0	4	0	0	16
N242	0	0	6	91	0	0	335	0	0	0	0	0	6
N245	0	0	4	51	0	22	126	0	0	8	0	0	3
N246	0	7	16	64	0	11	249	0	0	20	0	0	18
N248	0	0	4	21	0	12	165	0	0	27	0	0	4
N249	2	0	4	31	0	4	426	0	0	29	0	2	4
Z253	0	0	0	0	0	0	0	667	0	333	0	0	0
Z254	0	0	28	0	0	0	0	611	0	333	0	0	28
Z255	0	0	0	0	0	0	0	613	65	323	0	0	0
B256	0	0	19	0	0	0	5	223	34	670	0	0	0
B257	0	0	50	0	0	0	35	275	15	340	0	0	0

Appendix 23: DIN598 surface sample reference database.

Site number	Pret	Smem	Selo	Sram	Sben	Smir	Pdal	Amin	Amic	Bspp	Peri	Sele	Squa
A258	0	0	17	36	0	21	198	6	0	408	0	0	8
A259	0	8	13	48	0	10	129	10	3	324	0	0	3
A260	0	0	10	41	0	34	140	5	0	359	0	0	5
A261	0	0	6	47	0	23	35	18	6	713	0	0	53
A262	0	0	10	63	0	53	101	4	0	95	0	0	11
A263	0	0	14	51	0	18	224	0	0	49	0	0	12
A264	23	23	0	53	0	53	0	0	0	8	15	8	0
A265	3	13	3	69	0	28	0	0	0	51	5	5	5
A266	9	14	0	33	5	33	5	0	0	24	14	0	0
N268	0	0	11	158	0	13	209	0	0	26	0	0	34
N269	0	13	8	184	0	0	400	0	0	29	0	0	27
K271	0	31	21	63	10	199	10	0	0	26	31	0	16
K275	0	0	26	37	0	32	364	0	0	80	9	9	17
K277	0	0	19	78	0	30	383	0	0	89	5	0	11
M280	0	0	9	0	0	0	58	4	0	56	0	0	11
M281	0	0	5	0	0	2	27	2	0	24	0	0	0
M282	0	0	2	0	0	0	4	0	0	15	0	0	0
M283	0	0	3	0	0	0	11	3	0	52	0	0	0
M284	0	0	10	0	0	0	21	608	7	247	0	0	0
M285	0	0	29	0	0	0	82	51	0	19	0	0	1
M286	0	0	15	0	0	1	27	87	1	30	0	0	1
M287	0	0	2	0	0	0	7	108	0	81	0	0	0
M288	0	0	15	0	0	0	39	78	0	49	0	0	0
M289	0	0	0	0	0	0	3	584	5	392	0	0	0
M290	0	0	0	0	0	0	0	283	26	671	0	0	0
M291	0	0	0	0	0	0	0	608	57	330	0	0	0
M292	0	0	0	0	0	0	3	487	42	458	0	0	0
M293	0	0	0	0	0	0	2	644	86	261	0	0	0
M297	0	0	12	0	0	0	71	123	7	95	0	0	5
M298	0	0	0	0	0	0	36	0	0	6	0	0	0
M299	0	0	0	0	0	0	83	0	0	63	0	0	27
M300	0	0	6	0	0	0	13	10	0	38	0	0	3
M301	0	0	4	0	0	2	65	1	0	19	0	0	3
M303	0	0	15	0	0	1	113	0	0	43	0	0	4
M304	0	0	11	0	0	0	66	4	0	85	0	0	1
M305	0	1	22	0	0	1	98	0	0	7	0	0	1
M306	0	0	12	2	0	0	155	1	0	41	0	0	2
M307	0	0	9	1	0	2	121	0	0	19	0	0	2
M308	0	0	19	2	0	1	118	0	0	54	0	0	3
M309	0	1	32	3	0	0	79	0	0	58	0	0	4
M310	0	0	16	1	0	0	214	1	0	36	0	0	4
M311	0	0	16	2	0	1	109	0	0	25	0	0	3
M312	0	0	13	0	0	1	100	0	0	19	0	0	0

Appendix 23: DIN598 surface sample reference database.

Site number	Pret	Smem	Selo	Sram	Sben	Smir	Pdal	Amin	Amic	Bspp	Peri	Sele	Squa
M313	0	0	2	0	0	0	44	4	0	89	0	0	0
M314	0	0	0	0	0	0	15	7	0	119	0	0	0
M315	0	0	2	0	0	0	4	2	2	97	0	0	0
M316	0	0	5	0	0	0	13	8	1	29	0	0	4
M317	0	0	4	0	0	0	31	12	11	90	1	0	1
M318	0	0	9	0	0	0	41	1	0	76	0	0	3
M319	0	0	12	0	0	0	30	0	0	11	0	0	0
M320	0	0	8	0	0	0	31	1	0	26	0	0	2
M321	0	0	1	0	0	0	0	12	2	94	0	0	0
M322	0	0	6	0	0	0	27	0	0	91	0	0	5
M323	0	0	4	0	0	1	58	1	1	86	2	0	12
M324	0	1	11	1	0	2	226	0	8	38	0	0	13
M325	0	0	12	1	0	0	241	0	10	111	0	0	11
M326	0	0	4	0	0	1	17	2	1	34	0	0	1
M327	0	0	1	0	0	0	9	2	11	75	1	0	1
M328	0	0	0	0	0	0	11	11	5	225	0	0	3
M329	0	0	10	0	0	0	102	0	0	163	0	0	6
M330	0	0	6	0	0	0	24	78	93	96	0	0	3
M331	0	0	0	0	0	0	12	100	0	158	0	0	8
M332	0	0	3	0	0	0	24	10	0	128	0	0	0
M333	0	0	7	0	0	0	10	276	128	350	0	0	3
M334	0	0	6	0	0	0	17	240	131	509	0	0	0
M335	0	0	3	0	0	0	6	356	87	370	0	0	3
M336	0	0	5	0	0	0	22	17	12	170	0	0	0
M337	0	0	0	0	0	0	63	2	2	10	0	0	2
M338	0	0	2	0	0	0	5	23	19	42	0	0	0
M339	0	0	5	0	0	0	30	0	0	5	0	0	0
M340	0	0	5	0	0	0	65	1	0	75	0	0	10
M341	0	0	9	0	0	0	9	3	0	65	0	0	0
M342	0	0	16	0	0	0	56	0	0	92	0	0	0
M343	0	0	17	0	0	0	42	3	0	73	0	0	0
M344	0	0	10	0	0	0	5	97	87	432	0	0	5
M345	0	0	0	0	0	0	10	275	103	515	0	0	0
M346	0	0	0	0	0	0	21	123	76	733	0	0	4
M347	0	0	21	0	0	0	30	0	0	103	0	0	0
M348	0	0	0	0	0	0	0	134	8	858	0	0	0
M349	0	0	10	0	0	0	24	78	10	294	0	0	0
M350	0	0	19	0	0	0	15	11	6	179	0	0	2
M351	0	0	8	0	0	0	28	5	0	124	0	0	0
M352	0	0	15	0	0	0	18	7	0	125	0	0	0
M353	0	0	3	0	0	0	935	3	0	7	0	0	3
M354	0	0	7	0	0	0	60	362	0	125	0	0	0
M355	0	0	0	4	0	0	13	137	9	167	0	0	0

Appendix 23: DIN598 surface sample reference database.

Site number	Pret	Smem	Selo	Sram	Sben	Smir	Pdal	Amin	Amic	Bspp	Peri	Sele	Squa
M356	0	0	0	0	0	0	20	99	20	177	0	0	0
M357	0	0	0	0	0	0	490	98	16	85	0	0	3
M358	0	0	2	0	0	0	542	83	12	60	0	0	7
M359	0	0	4	0	0	0	82	344	25	113	0	0	0
M360	0	0	2	0	0	0	914	3	0	6	0	0	2
M361	0	0	4	0	0	0	9	94	9	119	0	0	0
M362	0	0	15	1	0	0	21	285	25	81	0	0	3
M363	0	0	12	0	0	0	16	458	6	63	0	0	2
M365	0	0	12	0	0	0	20	427	41	76	0	0	4
M366	0	0	4	0	0	0	12	584	7	34	0	0	2
M367	0	0	9	0	0	0	7	123	0	80	0	0	0
M368	0	0	4	0	0	0	27	462	2	67	0	0	2
M369	0	0	13	0	0	0	21	64	0	72	0	0	0
P370	11	0	0	0	0	0	92	34	0	483	0	0	0
P371	0	0	0	0	0	0	11	45	11	809	0	0	0
P372	0	0	0	4	0	0	4	70	9	868	0	0	0
P373	0	0	0	8	0	0	8	76	0	882	0	0	0
P374	0	0	0	0	0	0	0	9	0	972	0	0	0
P375	0	0	8	0	0	0	0	114	0	846	0	0	0
P376	0	0	0	0	0	0	7	221	7	745	0	0	0
P377	0	0	0	0	0	0	0	262	8	721	0	0	0
P378	0	0	0	0	0	0	0	407	0	556	0	0	0
Z379	0	0	172	0	0	0	678	6	0	13	0	0	0
Z380	0	0	468	0	0	0	214	0	0	0	0	0	0
Z381	0	0	485	7	0	0	81	7	0	105	0	0	0
Z382	0	0	375	6	0	0	73	11	0	95	0	0	0
Z383	0	0	210	3	0	0	486	40	0	92	0	0	3
Z384	0	0	482	3	0	0	120	6	0	84	3	0	0
Z385	0	0	141	0	0	0	688	0	0	12	0	0	1
Z386	0	0	257	1	0	0	509	8	0	33	0	0	1
Z387	0	0	207	0	0	0	544	7	0	27	0	0	0
Z388	0	0	235	0	0	0	354	15	0	51	0	0	3
Z389	0	0	152	0	0	0	702	2	0	16	0	0	0
Z390	0	0	118	0	0	0	753	5	0	16	0	0	0
Z391	0	0	106	1	0	0	764	10	0	19	0	0	1
Z392	0	0	63	2	0	0	824	19	0	21	0	0	0
Z393	0	0	110	0	0	0	775	14	0	23	0	0	0
Z394	0	0	82	3	0	0	795	24	0	24	0	0	0
Z395	0	0	40	1	0	0	896	9	0	10	0	0	0
Z396	0	0	40	0	0	0	873	15	3	13	0	0	2
Z397	0	0	71	0	0	0	827	9	0	21	0	0	0
N398	0	0	8	24	0	0	36	0	0	126	8	0	16
N399	0	0	19	9	0	0	99	0	0	174	0	0	38

Appendix 23: DIN598 surface sample reference database.

Site number	Pret	Smem	Selo	Sram	Sben	Smir	Pdal	Amin	Amic	Bspp	Peri	Sele	Squa
N400	0	0	22	11	0	0	133	0	0	133	0	0	44
N401	0	0	0	0	0	0	63	0	0	205	8	0	0
N402	0	2	17	19	0	2	161	0	0	90	0	0	25
A405	0	6	0	26	4	14	0	0	0	26	4	24	0
A406	0	81	4	47	4	199	0	0	0	13	8	17	0
A407	0	245	0	132	0	330	0	0	0	19	0	0	0
A408	0	145	6	12	6	372	0	0	0	17	0	0	0
A409	0	269	0	0	15	351	0	0	0	15	0	0	0
A410	0	0	0	9	0	743	0	0	0	0	0	0	0
A411	0	12	0	60	0	245	0	0	0	0	24	4	16
A412	0	0	0	0	0	167	0	0	0	40	0	0	0
A413	0	0	0	0	0	211	0	0	0	0	0	0	0
A414	0	0	0	0	0	51	0	0	0	0	0	0	0
A415	0	0	122	5	0	0	317	0	0	0	0	0	0
A416	0	0	24	5	0	0	737	0	0	5	0	0	0
A417	0	0	75	5	0	0	385	0	0	32	3	0	19
A418	0	0	52	45	0	0	254	0	0	7	0	0	7
A419	0	0	48	72	0	2	32	4	0	103	0	0	32
A420	0	0	46	90	0	7	29	13	0	51	0	0	4
A421	0	0	37	45	0	0	390	5	0	122	0	0	17
A422	0	0	8	24	0	3	484	5	0	136	0	0	21
A423	0	0	27	41	2	2	224	12	0	183	0	0	25
A424	0	0	33	27	0	2	52	5	0	107	0	0	23
A425	0	0	24	33	0	12	43	19	0	340	0	0	24
A426	0	0	24	20	0	2	71	6	0	170	0	0	4
A427	0	0	24	22	0	10	77	16	0	383	0	0	2
A428	0	0	19	92	0	2	101	17	0	237	0	0	41
Z432	0	0	10	0	0	0	604	114	45	15	0	0	5
Z434	0	0	0	0	0	0	361	28	0	0	0	0	0
Z435	0	0	28	0	0	0	30	513	35	275	5	0	3
Z436	0	0	27	0	0	0	301	257	0	142	18	0	9
Z437	0	0	39	0	0	0	350	0	0	58	0	0	0
Z438	0	0	35	0	0	0	281	152	0	164	0	0	12
Z439	0	0	55	0	0	0	374	5	0	121	0	0	0
Z445	0	0	0	0	0	0	0	250	0	750	0	0	0
Z446	0	0	0	0	0	0	0	247	637	97	0	0	0
Z448	0	0	0	0	0	0	0	657	190	105	0	0	0
Z449	0	0	0	0	0	0	0	600	275	67	0	0	0
Z450	0	0	0	0	0	0	0	300	433	167	0	0	0
Z452	0	0	0	0	0	0	0	687	26	243	0	0	0
Z453	0	0	0	0	0	0	0	480	80	360	0	0	0
Z454	0	0	0	0	0	0	9	664	236	82	0	0	0
Z455	0	0	0	0	0	0	0	519	222	111	0	0	0

Appendix 23: DIN598 surface sample reference database.

Site number	Pret	Smem	Selo	Sram	Sben	Smir	Pdal	Amin	Amic	Bspp	Peri	Sele	Squa
Z457	0	0	0	0	0	0	0	538	202	227	0	0	0
Z458	0	0	0	0	0	0	9	627	73	200	0	0	0
Z459	0	0	0	0	0	0	0	581	295	124	0	0	0
Z460	0	0	0	0	0	0	0	676	235	88	0	0	0
Z461	0	0	0	0	0	0	0	591	250	159	0	0	0
Z462	0	0	0	0	0	0	0	538	114	303	0	0	0
Z463	0	0	0	0	0	0	0	696	182	99	0	0	0
Z464	0	0	0	0	0	0	9	423	153	306	0	0	0
Z466	0	0	0	0	0	0	9	642	151	142	0	0	0
Z467	0	0	0	0	0	0	17	534	207	190	0	0	0
Z468	0	0	0	0	0	0	16	656	56	216	0	0	0
Z469	0	0	0	0	0	0	0	514	121	346	0	0	0
Z470	0	0	0	0	0	0	0	454	263	268	0	0	0
Z471	0	0	0	0	0	0	0	624	140	204	0	0	0
Z472	0	0	0	0	0	0	0	348	323	206	0	0	0
Z473	0	0	0	0	0	0	0	693	0	307	0	0	0
Z474	0	0	0	0	0	0	0	496	176	224	0	0	16
Z475	0	0	3	0	0	0	0	706	128	110	0	0	0
Z476	0	0	0	0	0	0	0	394	312	239	0	0	0
Z477	0	0	0	0	0	0	0	859	0	133	0	0	0
Z478	0	0	0	0	0	0	0	475	213	221	0	0	0
Z479	0	0	0	0	0	0	0	394	152	394	0	0	0
Z480	0	0	0	0	0	0	0	245	137	480	0	0	0
Z481	0	0	0	0	0	0	0	594	156	188	0	0	31
Z482	0	0	0	0	0	0	0	362	172	431	0	0	9
Z483	0	0	0	0	0	0	0	538	190	203	0	0	0
Z484	0	0	0	0	0	0	0	519	222	259	0	0	0
Z485	0	0	0	0	0	0	0	604	307	59	0	0	0
Z486	0	0	0	0	0	0	0	667	137	163	0	0	0
Z487	0	0	0	0	0	0	49	539	88	265	0	0	0
Z488	0	0	0	0	0	0	0	718	19	146	0	0	0
Z489	0	0	0	0	0	0	0	584	356	40	0	0	0
Z491	0	0	0	0	0	0	0	873	0	127	0	0	0
Z492	0	0	0	0	0	0	0	907	57	24	0	0	0
Z493	0	0	0	0	0	0	0	739	0	261	0	0	0
Z494	0	0	0	0	0	0	0	721	0	279	0	0	0
Z495	0	0	7	0	0	0	0	647	22	287	0	0	0
Z496	0	0	0	0	0	0	0	582	47	288	0	0	0
Z497	0	0	0	0	0	0	8	481	85	364	0	0	0
Z498	0	0	3	0	0	0	0	783	68	117	0	0	0
Z499	0	0	22	0	0	0	0	131	131	169	0	0	0
Z500	0	0	17	0	0	0	0	234	165	292	0	0	0
Z501	0	0	0	0	0	0	0	343	97	500	0	0	0

Appendix 23: DIN598 surface sample reference database.

Site number	Pret	Smem	Selo	Sram	Sben	Smir	Pdal	Amin	Amic	Bspp	Peri	Sele	Squa
Z502	0	0	22	0	0	0	0	168	47	569	0	0	0
Z503	0	0	19	0	0	0	0	321	69	314	0	0	0
Z504	0	0	0	0	0	0	0	432	88	336	0	0	0
Z505	0	0	14	0	0	0	0	142	162	122	0	0	0
Z506	0	0	15	0	0	0	0	474	93	231	0	0	0
Z507	0	0	5	0	0	0	0	477	54	450	0	0	0
Z508	0	0	0	0	0	0	0	439	159	308	0	0	0
Z509	0	0	30	0	0	0	0	225	101	290	0	0	0
Z510	0	0	0	0	0	0	0	314	223	207	0	0	0
Z511	0	0	0	0	0	0	0	211	75	150	0	0	0
Z512	0	0	10	0	0	0	0	199	66	163	0	0	0
Z513	0	0	4	0	0	0	0	208	66	151	0	0	0
Z514	0	0	32	0	0	0	0	175	95	190	0	0	0
Z515	0	0	10	0	0	0	0	114	17	155	0	0	0
Z516	0	0	20	0	0	0	0	433	99	187	0	0	0
Z517	0	0	0	0	0	0	0	437	99	437	0	0	0
Z518	0	0	0	0	0	0	0	612	164	164	0	0	0
Z519	0	0	0	0	0	0	0	383	252	327	0	0	0
Z520	0	0	0	0	0	0	0	611	62	212	0	0	35
Z521	0	0	0	0	0	0	0	464	55	227	0	0	0
Z522	0	0	0	0	0	0	0	452	159	293	0	0	0
Z523	0	0	13	0	0	0	0	572	69	322	0	0	0
Z524	0	0	0	0	0	0	9	594	170	142	0	0	0
Z526	0	0	0	0	0	0	0	716	67	164	0	0	45
Z527	0	0	0	0	0	0	9	696	54	161	0	0	0
Z528	0	0	0	0	0	0	0	752	137	68	0	0	0
Z529	0	0	0	0	0	0	0	626	122	217	0	0	0
Z530	0	0	0	0	0	0	0	428	178	368	0	0	0
Z531	0	0	9	0	0	0	0	427	218	291	0	0	0
A532	0	0	2	34	0	0	451	4	0	42	0	0	40
A533	0	0	3	13	0	0	432	0	0	0	0	0	0
A534	0	0	0	0	0	0	204	311	0	147	0	0	7
Z535	0	0	20	13	0	0	682	7	0	50	0	0	7
Z536	0	0	10	6	0	0	790	3	0	42	0	0	0
Z537	0	0	10	0	0	0	874	12	10	14	0	0	2
Z538	0	0	32	0	0	0	693	14	2	12	0	0	2
Z539	0	0	50	10	0	0	629	3	0	17	0	0	0
Z540	0	0	101	8	0	0	548	3	0	11	0	0	2
Z541	0	0	30	2	0	2	655	0	0	40	0	0	0
Z542	0	0	94	0	0	0	713	0	0	11	0	0	0
Z543	0	0	0	0	0	0	0	579	31	385	0	0	0
Z544	0	0	0	0	0	0	0	740	0	231	0	0	0
Z545	0	0	0	0	0	0	0	506	11	461	0	0	0

Appendix 23: DIN598 surface sample reference database.

Site number	Pret	Smem	Selo	Sram	Sben	Smir	Pdal	Amin	Amic	Bspp	Peri	Sele	Squa
Z546	0	0	0	0	0	0	0	508	47	425	0	0	0
Z547	0	0	31	0	0	0	154	116	14	116	0	0	0
Z548	0	0	36	0	0	0	919	0	0	5	0	0	0
Z549	0	0	8	0	0	0	971	0	0	0	0	0	0
Z550	0	0	67	27	0	0	80	2	0	29	0	0	0
Z551	0	0	42	11	0	0	57	0	0	6	4	0	2
Z552	0	1	87	0	0	0	209	0	0	34	0	0	0
Z553	0	4	86	0	0	0	148	0	0	53	25	0	0
Z554	0	0	68	0	0	0	315	21	0	68	0	0	0
Z555	0	0	46	0	0	0	262	206	0	60	0	0	0
Z556	0	0	119	0	0	0	385	147	0	147	0	0	0
Z557	0	0	349	4	0	0	153	231	0	70	0	0	0
Z558	0	0	13	0	0	0	237	324	0	42	0	0	0
Z559	0	0	30	4	0	0	166	219	0	30	0	0	0
Z560	0	0	71	3	0	0	426	42	0	16	0	0	0
Z561	0	0	288	7	0	0	363	61	0	32	0	0	0
Z562	0	0	48	0	0	0	439	227	0	33	0	0	0
Z563	0	0	0	0	0	0	762	0	0	0	0	0	0
Z564	0	0	30	0	0	0	760	0	0	0	0	0	0
Z565	0	0	0	95	0	0	143	0	0	0	0	0	0
P566	0	0	0	0	0	0	0	707	60	216	0	0	0
P567	0	0	0	0	0	0	0	699	86	210	0	0	0
P568	0	0	0	0	0	0	0	669	58	260	0	0	0
P569	0	0	0	0	0	0	0	712	51	232	0	0	0
P570	0	0	7	0	0	0	0	664	53	250	0	0	0
P571	0	0	0	0	0	0	6	675	92	221	0	0	0
P572	0	0	0	0	0	0	0	773	61	167	0	0	0
P573	0	0	0	0	0	0	0	547	75	358	0	0	0
P574	0	0	0	0	0	0	0	789	18	187	0	0	0
P575	0	0	0	0	0	0	0	784	72	118	0	0	0
P576	0	0	0	0	0	0	0	738	63	188	0	0	0
P577	0	0	0	0	0	0	0	656	61	264	0	0	0
P578	0	0	6	0	0	0	0	813	39	116	0	0	0
P579	0	0	73	0	0	0	20	513	47	93	0	0	0
P580	0	0	7	0	0	0	0	871	95	14	0	0	0
Z602	0	0	8	12	0	0	4	24	0	345	369	20	75
Z603	9	0	16	16	0	2	33	0	0	368	121	9	54
Z604	0	0	8	61	0	0	0	53	0	348	341	0	30
Z605	0	0	11	5	0	0	33	0	0	412	225	60	11
Z606	187	0	81	16	0	0	65	0	0	0	0	0	0
N607	0	0	0	13	0	0	13	0	0	346	0	0	51
N608	0	6	0	28	0	0	50	0	0	122	6	0	44
N609	0	0	0	0	0	0	53	0	0	102	0	0	38

Appendix 23: DIN598 surface sample reference database.

Site number	Pret	Smem	Selo	Sram	Sben	Smir	Pdal	Amin	Amic	Bspp	Peri	Sele	Squa
N610	0	4	0	0	4	0	11	0	0	44	0	0	33
N611	0	12	0	0	12	0	47	0	0	282	0	0	94
N612	0	0	0	30	0	0	61	0	0	40	20	0	91
N613	0	0	13	31	3	3	13	0	0	49	0	0	23
N614	0	0	20	53	0	0	23	0	0	53	0	0	0
N615	0	0	0	39	0	0	66	0	0	66	0	0	86
N616	0	0	13	48	0	0	122	0	0	92	0	0	57
N617	0	0	0	0	0	0	45	0	0	136	0	0	205
N620	0	0	0	0	0	0	0	0	0	170	38	0	75
N622	0	0	13	67	0	0	180	0	0	18	0	0	95
N623	0	0	11	15	0	15	63	0	0	268	4	0	242
N626	0	0	0	7	0	20	0	0	0	53	0	0	146
N627	0	0	0	0	0	0	0	0	0	462	0	0	154
N628	0	0	5	37	0	0	64	0	0	181	0	0	191
N629	0	0	20	49	0	7	78	0	0	33	0	0	65
N630	0	0	16	54	0	3	156	0	0	70	0	0	81
N631	0	20	7	43	0	0	191	0	0	43	0	0	128
N632	0	4	4	48	0	0	159	0	0	132	0	0	225
N633	0	0	12	71	0	0	106	0	0	318	0	0	106
N634	0	0	43	11	0	0	97	0	0	65	11	0	97
N635	0	0	44	18	0	0	88	0	0	80	0	0	58
N636	0	0	42	24	0	3	59	0	0	24	0	0	73
N637	0	0	48	54	0	7	61	0	0	116	0	0	116
N638	0	0	27	36	0	0	48	0	0	57	0	0	45
X639	0	14	0	27	0	0	32	260	9	370	0	0	0
X640	0	3	3	46	0	0	10	315	0	279	0	0	3
X641	0	3	7	37	3	10	20	255	7	269	0	0	3
X642	0	22	7	26	0	4	26	146	7	258	0	0	7
X643	0	7	3	30	0	3	7	219	3	503	0	0	0
X644	0	7	0	14	0	3	20	181	3	454	0	0	3
X645	0	3	0	28	0	0	25	197	22	420	0	0	0
X646	0	0	10	20	0	20	30	50	10	560	0	0	15
X647	0	16	20	59	0	13	127	88	0	238	0	0	7
X648	0	2	22	51	0	5	225	7	0	44	0	0	0
X649	0	3	30	52	0	9	98	18	0	137	0	0	15
X650	0	0	3	34	0	34	88	34	0	323	0	0	10
X651	0	4	14	72	0	22	213	2	0	14	0	0	0
X652	0	0	34	44	0	3	219	6	0	3	0	0	3
X653	0	13	20	53	0	7	168	13	0	30	0	0	0
X654	0	0	41	23	0	3	197	20	0	70	0	0	0
X655	0	2	50	11	0	1	123	16	7	126	0	0	2
X656	0	0	40	21	0	2	183	13	0	15	0	0	8
X657	0	5	45	18	0	0	115	0	0	0	0	0	0

Appendix 23: DIN598 surface sample reference database.

Site number	Pret	Smem	Selo	Sram	Sben	Smir	Pdal	Amin	Amic	Bspp	Peri	Sele	Squa
X658	0	3	59	24	0	0	142	7	0	14	0	0	0
X659	0	2	41	18	0	0	146	14	0	28	0	0	4
X660	0	3	12	71	0	3	120	99	3	99	0	0	19
X661	0	0	10	3	0	0	88	146	75	108	0	0	3
X664	0	5	44	28	0	7	196	51	0	187	0	0	9
X666	4	21	11	25	0	21	225	70	0	303	0	0	25
X668	0	5	28	10	5	13	51	0	0	0	0	0	0
X669	0	14	3	82	0	27	229	14	7	259	0	3	58
X670	0	0	56	24	0	0	65	0	0	21	0	0	6
X671	3	3	54	14	0	5	155	0	0	0	0	0	0
X672	0	0	56	2	0	4	146	0	0	25	0	0	2
X673	0	21	7	55	0	31	41	0	0	7	0	0	0
X674	3	25	12	49	6	6	252	0	0	31	0	0	9
X675	0	11	14	43	0	9	269	0	0	29	0	0	6
A682	0	15	54	18	0	0	143	6	0	98	3	0	18
A683	0	0	65	23	0	0	94	42	0	254	0	0	7
A685	0	6	64	6	0	6	45	0	0	138	0	0	0
X686	0	0	37	47	0	7	80	7	0	161	0	0	13
X688	0	0	40	23	0	13	73	30	0	119	0	0	10
X689	0	3	25	31	0	28	89	9	0	232	0	0	6
X690	0	0	23	10	0	30	30	40	0	389	0	0	3
X691	0	0	27	40	0	30	53	30	0	304	0	0	0
X692	0	6	31	46	0	18	108	12	0	166	0	0	3
X693	3	7	49	13	0	10	59	13	0	155	0	0	0
X694	0	7	30	60	0	7	116	13	0	56	0	0	0
X695	0	0	15	39	0	6	82	12	0	100	0	0	0
X696	0	0	21	72	0	0	72	0	0	62	0	0	0
X697	0	0	28	25	0	0	112	3	0	71	0	0	9
X698	0	3	26	58	0	13	204	3	0	84	0	0	0
X699	0	3	20	16	0	0	232	10	0	40	0	0	0
X700	0	0	13	45	0	0	176	3	0	3	0	0	0
X701	0	0	37	27	0	3	191	0	0	67	0	0	3
X702	3	0	13	62	0	20	188	0	0	32	0	0	0
X703	0	3	3	67	0	17	84	31	0	337	0	0	10
X704	0	0	33	52	0	16	183	10	0	78	0	0	3
X705	0	0	30	37	0	3	203	3	0	20	0	0	3
X706	0	0	25	57	0	9	220	3	0	64	0	0	6
X707	0	7	10	55	0	24	163	0	0	180	0	0	7
X708	0	5	5	29	0	5	68	24	0	650	0	0	0

Appendix 23: DIN598 surface sample reference database.

Site number	Tapp	Qcon	Psch	Parc
E003	0	0	0	0
E004	0	0	0	0
E005	0	0	0	0
E006	0	0	0	0
E007	0	0	0	0
E008	0	0	0	0
E010	0	0	0	0
E012	0	0	0	0
E013	0	0	0	0
E014	0	0	0	0
E015	0	0	0	0
E016	0	0	0	0
E017	0	0	0	0
E018	0	0	0	0
E019	0	0	0	0
E020	0	0	0	0
E021	0	0	0	0
E022	0	0	0	0
G023	0	0	0	0
G024	0	0	0	0
G025	0	0	0	0
G026	0	0	0	0
G027	0	0	0	0
G028	0	0	0	0
G029	0	0	0	0
G030	0	0	0	0
G031	0	0	0	0
G032	0	0	0	0
G033	0	0	0	0
G034	0	0	0	0
G035	0	0	0	0
G037	0	0	0	0
G038	0	0	0	0
G039	0	0	0	0
G040	0	0	0	0
G041	0	0	0	0
G042	0	0	0	0
G043	0	0	0	0
G044	0	0	0	0
G045	0	0	0	0
G046	0	0	0	0
G047	0	0	0	0
G048	0	0	0	0

Appendix 23: DIN598 surface sample reference database.

Site number	Tapp	Qcon	Psch	Parc
G049	0	0	0	0
G050	0	0	0	0
G051	0	0	0	0
G052	0	0	0	0
G053	0	0	0	0
G054	0	0	0	0
G055	0	0	0	0
G056	0	0	0	0
G057	0	0	0	0
G058	0	0	0	0
G059	0	0	0	0
G060	0	0	0	0
G061	0	0	0	0
G062	0	0	0	0
G063	0	0	0	0
G064	0	0	0	0
G065	0	0	0	0
G066	0	0	0	0
G067	0	0	0	0
G068	0	0	0	0
G069	0	0	0	0
G070	0	0	0	0
G071	0	0	0	0
G072	0	0	0	0
G073	0	0	0	0
A074	0	0	0	0
G075	0	0	0	0
G076	0	0	0	0
G077	0	0	0	0
G078	0	0	0	0
G079	0	0	0	0
B080	0	0	0	0
B081	0	0	0	0
B082	0	0	0	0
L087	0	0	0	0
L088	0	0	0	0
L089	0	0	0	0
L090	19	0	9	0
L091	3	0	3	0
L092	5	0	7	0
L093	2	0	0	0
L094	11	0	4	0
A099	7	0	7	0

Appendix 23: DIN598 surface sample reference database.

Site number	Tapp	Qcon	Psch	Parc
A100	3	0	0	0
A103	2	0	3	0
A104	5	0	0	0
A105	3	0	10	0
A106	10	0	10	0
A107	15	0	0	0
A108	52	0	12	0
A109	23	0	25	0
A110	31	0	38	0
A111	20	0	14	0
A112	34	0	86	0
A113	63	0	0	0
A114	8	0	20	0
A115	6	0	8	0
A116	32	0	45	0
A118	43	0	0	0
A119	0	0	0	0
A120	83	0	143	0
A121	12	0	1	0
A122	46	0	21	0
A123	6	0	3	0
A124	4	0	0	0
A125	2	0	1	0
A126	2	0	2	0
A127	9	0	0	0
A128	23	0	2	0
A129	5	0	29	0
H130	0	0	0	0
H131	0	0	0	0
H132	0	0	0	0
H133	0	0	0	0
H134	0	0	0	0
H135	0	0	0	0
H136	0	0	0	0
H137	0	0	0	0
H138	0	0	0	0
H139	0	0	0	0
H140	0	0	0	0
H141	0	0	0	0
H142	0	0	0	0
H143	0	0	0	0
H144	0	0	0	0
H145	0	0	0	0

Appendix 23: DIN598 surface sample reference database.

Site number	Tapp	Qcon	Psch	Parc
A149	1	0	0	0
A150	18	0	13	0
L151	0	0	3	0
L152	1	0	3	0
L153	1	0	1	0
A154	25	0	0	0
A155	0	0	9	0
A156	35	0	39	0
S158	0	0	0	0
S159	0	0	0	0
S160	0	0	0	0
L162	0	0	7	0
L163	0	0	5	0
L164	0	0	0	0
A168	0	0	0	0
A170	52	0	34	0
A171	0	0	40	0
A173	0	0	28	0
A174	0	0	10	0
A175	51	0	7	0
L178	5	0	0	0
A179	0	0	0	0
A180	0	0	0	0
A181	34	0	0	0
A182	20	0	11	0
A183	44	0	0	0
A184	5	0	0	0
N185	0	0	0	0
N186	0	0	0	0
N189	0	0	0	0
N190	0	0	0	0
N191	0	0	0	0
N192	0	0	0	0
N193	0	0	0	0
N194	0	0	0	0
N195	0	0	0	0
N196	0	0	0	0
N197	0	0	0	0
N198	16	0	2	0
N200	0	0	0	0
N206	25	0	0	0
N207	11	0	0	0
N208	13	0	0	0

Appendix 23: DIN598 surface sample reference database.

Site number	Tapp	Qcon	Psch	Parc
N209	2	0	0	0
N210	0	0	0	0
N211	0	0	0	0
N212	0	0	0	0
N213	3	0	0	0
N214	1	0	0	0
N215	2	0	3	0
N216	1	0	0	0
N217	4	0	0	0
N218	6	0	2	0
N219	20	0	1	0
N220	32	0	0	0
N221	19	0	0	0
N222	11	0	0	0
N223	8	0	0	0
N224	0	0	0	0
N225	67	0	4	0
N226	53	0	0	0
N227	0	0	0	0
N228	0	0	0	0
N229	0	0	0	0
N230	0	0	0	0
N231	0	0	0	0
N232	0	0	0	0
N233	0	0	0	0
N234	0	0	0	0
N235	0	0	0	0
N236	0	0	0	0
N237	0	0	0	0
N238	6	0	16	0
N239	1	0	5	0
N240	0	0	4	0
N241	0	0	2	0
N242	0	0	6	0
N245	0	0	0	0
N246	0	0	22	0
N248	0	0	0	0
N249	0	0	4	0
Z253	0	0	0	0
Z254	0	0	0	0
Z255	0	0	0	0
B256	0	0	0	0
B257	0	0	0	0

Appendix 23: DIN598 surface sample reference database.

Site number	Tapp	Qcon	Psch	Parc
A258	0	0	0	0
A259	0	0	0	0
A260	0	0	0	0
A261	0	0	0	0
A262	0	0	0	0
A263	0	0	0	0
A264	0	0	0	0
A265	0	0	0	0
A266	0	0	0	0
N268	0	0	4	0
N269	0	0	21	0
K271	0	0	0	0
K275	0	0	6	0
K277	0	0	0	0
M280	12	0	7	0
M281	3	0	2	0
M282	0	0	0	0
M283	0	0	0	0
M284	0	0	0	0
M285	0	0	0	0
M286	1	0	0	0
M287	0	0	0	0
M288	1	0	1	0
M289	0	0	0	0
M290	0	0	0	0
M291	0	0	0	0
M292	0	0	0	0
M293	0	0	0	0
M297	2	0	0	0
M298	3	0	3	0
M299	0	0	0	0
M300	0	0	0	0
M301	2	0	2	0
M303	2	0	2	0
M304	0	0	1	0
M305	2	0	0	0
M306	2	0	3	0
M307	4	0	1	0
M308	3	0	2	0
M309	4	0	2	0
M310	2	0	3	0
M311	3	0	2	0
M312	1	0	0	0

Appendix 23: DIN598 surface sample reference database.

Site number	Tapp	Qcon	Psch	Parc
M313	1	0	1	0
M314	0	0	0	0
M315	2	0	0	0
M316	3	0	0	0
M317	1	0	2	0
M318	3	0	1	0
M319	2	0	0	0
M320	0	0	0	0
M321	0	0	0	0
M322	2	0	1	0
M323	2	0	6	0
M324	13	0	6	0
M325	11	0	0	0
M326	1	0	0	0
M327	0	0	0	0
M328	0	0	0	0
M329	0	0	0	0
M330	6	0	0	0
M331	0	0	0	0
M332	0	0	0	0
M333	0	0	0	0
M334	0	0	0	0
M335	0	0	0	0
M336	0	0	0	0
M337	4	0	0	0
M338	0	0	0	0
M339	0	0	0	0
M340	1	0	0	0
M341	0	0	0	0
M342	0	0	0	0
M343	0	0	0	0
M344	0	0	0	0
M345	0	0	0	0
M346	0	0	0	0
M347	0	0	0	0
M348	0	0	0	0
M349	0	0	0	0
M350	0	0	0	0
M351	0	0	0	0
M352	0	0	0	0
M353	0	0	0	0
M354	0	0	0	0
M355	0	0	0	0

Appendix 23: DIN598 surface sample reference database.

Site number	Tapp	Qcon	Psch	Parc
M356	0	0	0	0
M357	0	0	0	0
M358	0	0	0	0
M359	0	0	0	0
M360	0	0	0	0
M361	0	0	0	0
M362	0	0	0	0
M363	0	0	0	0
M365	0	0	0	0
M366	0	0	0	0
M367	0	0	0	0
M368	0	0	0	0
M369	0	0	0	0
P370	0	0	0	0
P371	0	0	0	0
P372	0	0	0	0
P373	0	0	0	0
P374	0	0	0	0
P375	0	0	0	0
P376	0	0	0	0
P377	0	0	0	0
P378	0	0	0	0
Z379	0	0	0	0
Z380	0	0	0	0
Z381	0	0	3	0
Z382	0	0	8	0
Z383	0	0	3	0
Z384	0	0	3	0
Z385	0	0	2	0
Z386	0	0	0	0
Z387	0	0	0	0
Z388	0	0	3	0
Z389	0	0	0	0
Z390	0	0	0	0
Z391	0	0	1	0
Z392	0	0	0	0
Z393	0	0	3	0
Z394	0	0	0	0
Z395	0	0	0	0
Z396	0	0	2	0
Z397	0	0	0	0
N398	0	0	20	0
N399	0	0	9	0

Appendix 23: DIN598 surface sample reference database.

Site number	Tapp	Qcon	Psch	Parc
N400	0	0	0	0
N401	0	0	16	0
N402	0	0	21	0
A405	6	0	0	0
A406	13	0	0	0
A407	38	0	0	0
A408	29	0	0	0
A409	7	0	0	0
A410	0	0	0	0
A411	12	0	0	0
A412	5	0	0	0
A413	0	0	0	0
A414	0	0	0	0
A415	16	0	5	0
A416	0	0	0	0
A417	19	0	70	0
A418	0	0	75	0
A419	0	0	0	0
A420	0	0	0	0
A421	0	0	0	0
A422	0	0	0	0
A423	0	0	0	0
A424	0	0	0	0
A425	0	0	7	0
A426	0	0	2	0
A427	0	0	0	0
A428	0	0	5	0
Z432	0	0	0	15
Z434	0	0	0	0
Z435	0	0	0	0
Z436	0	0	9	0
Z437	0	0	0	0
Z438	0	0	0	12
Z439	0	0	0	0
Z445	0	0	0	0
Z446	0	0	0	19
Z448	0	0	0	48
Z449	0	0	0	33
Z450	0	0	0	100
Z452	0	0	0	43
Z453	0	0	0	80
Z454	0	0	0	9
Z455	0	0	0	148

Appendix 23: DIN598 surface sample reference database.

Site number	Tapp	Qcon	Psch	Parc
Z457	0	0	0	34
Z458	0	0	0	82
Z459	0	0	0	0
Z460	0	0	0	0
Z461	0	0	0	0
Z462	0	0	0	45
Z463	0	0	0	22
Z464	0	0	0	99
Z466	0	0	0	38
Z467	0	0	0	43
Z468	0	0	0	56
Z469	0	0	0	9
Z470	0	0	0	15
Z471	0	0	0	32
Z472	0	0	0	123
Z473	0	0	0	0
Z474	0	0	0	80
Z475	0	0	0	46
Z476	0	0	0	55
Z477	0	0	0	7
Z478	0	0	0	74
Z479	0	0	0	61
Z480	0	0	0	98
Z481	0	0	0	0
Z482	0	0	0	26
Z483	0	0	0	70
Z484	0	0	0	0
Z485	0	0	0	30
Z486	0	0	0	0
Z487	0	0	0	29
Z488	0	0	0	117
Z489	0	0	0	20
Z491	0	0	0	0
Z492	0	0	0	12
Z493	0	0	0	0
Z494	0	0	0	0
Z495	0	0	0	29
Z496	0	0	0	76
Z497	0	0	0	8
Z498	0	0	0	10
Z499	0	0	0	27
Z500	0	0	0	55
Z501	0	0	0	20

Appendix 23: DIN598 surface sample reference database.

Site number	Tapp	Qcon	Psch	Parc
Z502	0	0	0	4
Z503	0	0	0	13
Z504	0	0	0	64
Z505	0	0	0	14
Z506	0	0	0	26
Z507	0	0	0	0
Z508	0	0	0	56
Z509	0	0	0	6
Z510	0	0	0	8
Z511	0	0	0	8
Z512	0	0	0	15
Z513	0	0	0	27
Z514	0	0	0	0
Z515	0	0	0	14
Z516	0	0	0	67
Z517	0	0	0	20
Z518	0	0	0	34
Z519	0	0	0	28
Z520	0	0	0	35
Z521	0	0	0	36
Z522	0	0	0	87
Z523	0	0	0	13
Z524	0	0	0	57
Z526	0	0	0	0
Z527	0	0	0	54
Z528	0	0	0	43
Z529	0	0	0	17
Z530	0	0	0	20
Z531	0	0	0	27
A532	0	0	4	0
A533	0	0	0	0
A534	0	0	3	0
Z535	0	0	0	0
Z536	0	0	0	0
Z537	0	0	0	0
Z538	0	0	0	0
Z539	0	0	2	0
Z540	0	0	0	0
Z541	0	0	0	0
Z542	0	0	0	0
Z543	0	0	0	0
Z544	0	0	0	29
Z545	0	0	0	22

Appendix 23: DIN598 surface sample reference database.

Site number	Tapp	Qcon	Psch	Parc
Z546	0	0	0	17
Z547	0	0	0	0
Z548	0	0	0	0
Z549	0	0	0	0
Z550	0	0	0	0
Z551	0	0	0	0
Z552	0	0	0	0
Z553	0	0	0	0
Z554	0	0	0	0
Z555	0	0	0	0
Z556	0	0	0	0
Z557	0	0	0	0
Z558	0	0	0	0
Z559	0	0	0	0
Z560	0	0	0	0
Z561	0	0	0	0
Z562	0	0	0	0
Z563	0	0	0	0
Z564	0	0	0	0
Z565	0	0	0	0
P566	0	0	0	0
P567	0	0	0	0
P568	0	0	0	0
P569	0	0	0	6
P570	0	0	0	0
P571	0	0	0	0
P572	0	0	0	0
P573	0	0	0	13
P574	0	0	0	6
P575	0	0	0	0
P576	0	0	0	0
P577	0	0	0	0
P578	0	0	0	0
P579	0	0	0	0
P580	0	0	0	0
Z602	0	36	8	0
Z603	0	13	0	0
Z604	0	0	0	0
Z605	0	5	0	0
Z606	0	0	0	0
N607	0	0	51	0
N608	0	0	0	0
N609	0	0	0	0

Appendix 23: DIN598 surface sample reference database.

Site number	Tapp	Qcon	Psch	Parc
N610	0	0	0	0
N611	0	0	12	0
N612	0	0	0	0
N613	0	0	0	0
N614	13	0	3	0
N615	0	0	0	0
N616	4	0	0	0
N617	0	0	0	0
N620	0	0	0	0
N622	10	0	0	0
N623	0	0	4	0
N626	99	0	0	0
N627	0	0	0	0
N628	27	0	0	0
N629	10	0	0	0
N630	113	0	0	0
N631	220	0	0	0
N632	18	0	0	0
N633	0	0	0	0
N634	0	0	0	0
N635	31	0	0	0
N636	17	0	0	0
N637	14	0	0	0
N638	24	0	0	0
X639	0	0	0	0
X640	0	0	0	0
X641	0	0	0	0
X642	0	0	0	0
X643	0	0	0	0
X644	0	0	0	0
X645	0	0	0	0
X646	0	0	0	0
X647	0	0	0	0
X648	0	0	0	0
X649	0	0	0	0
X650	0	0	0	0
X651	2	0	0	0
X652	0	0	0	0
X653	0	0	0	0
X654	0	0	0	0
X655	0	0	0	0
X656	0	0	0	0
X657	0	0	0	0

Appendix 23: DIN598 surface sample reference database.

Site number	Tapp	Qcon	Psch	Parc
X658	0	0	0	0
X659	0	0	0	0
X660	0	0	0	0
X661	0	0	0	0
X664	2	0	0	0
X666	4	0	0	0
X668	0	0	0	0
X669	10	0	0	0
X670	0	0	0	0
X671	0	0	0	0
X672	0	0	0	0
X673	0	0	0	0
X674	0	0	0	0
X675	0	0	0	0
A682	0	0	0	0
A683	0	0	0	0
A685	0	0	0	0
X686	0	0	0	0
X688	0	0	0	0
X689	0	0	0	0
X690	0	0	0	0
X691	0	0	0	0
X692	0	0	0	0
X693	0	0	0	0
X694	0	0	0	0
X695	0	0	3	0
X696	0	0	0	0
X697	0	0	3	0
X698	0	0	0	0
X699	0	0	0	0
X700	0	0	0	0
X701	0	0	0	0
X702	0	0	0	0
X703	0	0	0	0
X704	0	0	0	0
X705	0	0	0	0
X706	0	0	0	0
X707	0	0	0	0
X708	0	0	0	0

Appendix 24 Notes about the modern surface sediment database

Each modern reference site is identified by its own number, preceded by a letter which refers to one of the following geographical regions:

A= North Atlantic
B= Baffin Bay
E= St. Lawrence Estuary
G= Gulf of St. Lawrence
H= Hudson Bay
L= Labrador Sea
N= Norwegian Sea
M= Arctic
Z= Arctic
P= Polynya
X= New surface samples added (this study, appendices 2 to 9)

Note about appendices 28, 30 and 32, modern analogues files

Each modern analogue file contains 2 lines for each fossil spectra (each sample in the core). The first number of the first line indicates the depth downcore (or the composite depth when piston and trigger weight cores were combined). The reminder of the first line is the list of the 10 closest analogues. These modern sites are identified by one letter and three numbers. The letters refer to the geographic location (see above).

The second line shows the distance between the fossil spectra and each modern analogues. A distance below 100 is considered good. 999 would indicate a no-analogue situation.

Appendix 25: Environmental data for DIN598

Site number	February SST	February salinity	August SST	August salinity	Average ice duration	Median ice duration
E003	-1.1	27	8.4	24.3	3	3
E004	-1.1	27	8.4	24.4	3	3
E005	-1	27	8	24.5	3	3
E006	-1	27	8.1	24.6	3	3
E007	-1	27	8.2	24.6	3	3
E008	-1	27	8.1	24.6	3	3
E010	-1.1	28.1	8.7	25.2	3	3
E012	-1.1	29.1	10.1	25.2	2.5	3
E013	-1.1	29.1	10	26	3	3
E014	-1.1	29.1	10.3	25.6	3	3
E015	-1.2	28.2	10.7	27.3	3	3
E016	-1.1	28.4	10.6	27.2	3	3
E017	-1.1	29.1	10.9	27.1	3	3
E018	-1.1	29	12.4	27.9	3	3
E019	-1.2	30.2	11.9	27.9	2.5	3
E020	-1.2	30.1	11.5	27.9	2.5	3
E021	-1.2	30.2	12.3	27.9	2.5	3
E022	-1.5	31.6	14.3	28.9	2.1	2
G023	-1.4	31.3	13.1	28	2.5	3
G024	-1.5	31.9	14.6	29.4	2.1	2
G025	-1.4	31.6	13.2	28.4	2.1	2
G026	-1.4	31.3	12.9	27.9	2.5	3
G027	-1.5	32	13.2	28.5	2.6	3
G028	-1.5	31.9	13.6	29.1	2.6	3
G029	-1.3	31.3	14.6	28.9	2.3	2
G030	-1.3	31.3	14.9	29	2.3	2
G031	-1.3	31.8	15.1	29.2	2.3	2
G032	-1.4	31.8	15.3	29.9	2.5	3
G033	-1.4	31.9	15.7	30.4	2.5	3
G034	-1.4	31.6	15.9	30.2	2	2
G035	-1.4	31.6	14.7	31	2	2
G037	-1.4	32.4	10.2	29.7	2.1	2
G038	-1.4	32.4	10.5	29.8	2.1	2
G039	-1.4	32.4	10.5	29.8	2.1	2
G040	-1.4	32.3	13.2	30.3	2.1	2
G041	-1.4	32.4	13.2	30.3	2.1	2
G042	-1.4	32.3	13.5	30.4	2.1	2
G043	-1.4	32.3	13.2	30.3	2.1	2
G044	-1.4	32.3	13.2	30.4	2.1	2
G045	-1.3	32.4	13.2	30.4	2.1	2
G046	-1.4	32.3	13.2	30.4	2.1	2
G047	-1.4	32.4	13.1	30.5	2.1	2
G048	-1.5	32.5	13.4	30.4	2.1	2

Appendix 25: Environmental data for the DIN598

Site number	February SST	February salinity	August SST	August salinity	Average ice duration	Median ice duration
G049	-1.4	32.5	13.4	30.4	2.1	2
G050	-1.5	32.5	13.4	30.4	2.1	2
G051	-1.5	31.9	15.7	30.4	2.5	2
G052	-1.5	31.9	15.7	30.4	2.5	3
G053	-1.5	31.9	15.8	30.5	2.5	3
G054	-1.5	32.2	15.7	30.3	2	2
G055	-1.5	32.3	13.5	30.3	2.3	2
G056	-1.5	32.4	14.2	30.5	2	2
G057	-1.5	32.2	15.4	30.4	1.8	2
G058	-1.5	32.4	15	30.5	2.6	3
G059	-1.5	32.4	15	30.5	2.6	3
G060	-1.5	32.4	15	30.5	2.6	3
G061	-1.4	32	14.4	30.5	2.6	3
G062	-1.4	31.8	15.1	29.1	2.6	3
G063	-1.5	31.8	15.2	29.3	1.8	2
G064	-1.5	31.8	15.2	29.3	1.8	2
G065	-1.4	31.3	15.9	30.2	2.9	3
G066	-1.5	31.5	15.5	30.5	1.8	2
G067	-1.2	30.2	12.3	27.9	2.5	3
G068	-1.4	31.7	13.6	29.4	2.3	2
G069	-1.4	30.2	16.3	27.3	2	2
G070	-1.3	32	15.2	30.1	2.3	2
G071	-1.3	30.9	16.8	29.3	3.3	3
G072	-1.3	30.9	17.2	29.2	3	3
G073	-1.3	31.4	16.4	29.7	2.1	2
A074	1.8	32.4	16.5	32.1	0	0
G075	0	31.8	15	30.9	0	0
G076	0.2	31.8	16.5	30.9	0	0
G077	0.1	32	14.9	31.5	0	0
G078	0.1	32	14.9	31.5	0.1	0
G079	-0.2	31.6	16.3	30.7	0.1	0
B080	-1.3	33	3.3	31	9.4	9
B081	-1.3	33	2.2	31	9.3	9
B082	-1.3	33	3.7	31	9.6	9
L087	1.3	34.4	6.7	34.2	0.5	0
L088	-1.3	34.9	6.6	33.8	2.9	3
L089	-1.3	34.5	5.3	33.3	2.6	2.5
L090	3.6	34.8	7.1	34.2	2.6	2.5
L091	3.5	34.7	8.2	34.6	0	0
L092	3.4	34.7	7.6	34.5	0	0
L093	3.4	34.8	6.8	34.5	0.5	0
L094	3.6	34.8	7.7	34.5	0.5	0
A099	4	34.9	8	34.6	0	0

Appendix 25: Environmental data for the DIN598

Site number	February SST	February salinity	August SST	August salinity	Average ice duration	Median ice duration
A100	2.1	34.2	7	34.4	0	0
A103	3.4	34.5	9	34.5	0	0
A104	4.6	34.6	8.8	34.6	0	0
A105	4	34.6	7	33.9	0.1	0
A106	5.1	35	10	34.9	0	0
A107	6.3	35	10.2	35	0	0
A108	6.4	35.1	10	35.1	0	0
A109	6.4	35.1	10	35.1	0	0
A110	6.4	35.1	10	35.1	0	0
A111	6.4	35.1	10	35.1	0	0
A112	6.4	35.2	9.9	35.2	0	0
A113	8.6	35.3	11.9	35.2	0	0
A114	9.1	35.3	13.5	35.3	0	0
A115	9.3	35.4	13.6	35.3	0	0
A116	9.2	35.4	13.9	35.4	0	0
A118	10	35.2	14	35.2	0	0
A119	10.5	35.4	15.3	35.4	0	0
A120	10.5	35.4	15.3	35.4	0	0
A121	9.5	35.4	15	35.4	0	0
A122	10.6	35.4	15.7	35.4	0	0
A123	11.5	35.4	16.6	35.6	0	0
A124	9.7	35.5	15	35.4	0	0
A125	10.8	35.5	16.9	35.4	0	0
A126	9.4	35.3	12.8	35.3	0	0
A127	6	34.7	12.3	34.6	0	0
A128	8.9	35.3	12.4	35.3	0	0
A129	8.1	35.4	11.8	35.2	0	0
H130	-1.6	30	5.7	30.6	7.6	7
H131	-1.6	30	5.7	30.6	7.6	7
H132	-1.6	30	5.5	31.2	7.3	7
H133	-1.6	30	5.4	31	7.5	7
H134	-1.6	30	6	28.8	7.5	8
H135	-1.6	30	5.4	31	6.8	7
H136	-1.6	30	6.3	28	7.1	7
H137	-1.6	30	5.4	27.9	7.6	7.5
H138	-1.6	30	5.5	27.9	7.7	8
H139	-1.6	30	6.8	28.1	7.5	7
H140	-1.6	30	6	27	7.3	7
H141	-1.6	30	6.6	20	6.4	6
H142	-1.6	30	5.6	20.9	6.4	6
H143	-1.6	30	4	25.8	7.2	7
H144	-1.6	30	3.4	22.6	7.4	7
H145	-1.6	30	4.6	26.8	7.7	8

Appendix 25: Environmental data for the DIN598

Site number	February SST	February salinity	August SST	August salinity	Average ice duration	Median ice duration
A149	5.5	35.2	10	35.2	0	0
A150	6.9	35.3	11.9	35.2	0	0
L151	6	34.8	11.4	34.6	0	0
L152	3.5	34.8	6.8	34.5	0.5	0
L153	3.5	34.8	6.9	34.4	0	0
A154	7.4	35.2	11.5	35.1	0	0
A155	10.8	35.5	16.7	35.6	0	0
A156	6.4	34.9	11.2	35.1	0	0
S158	-1.5	32.8	5.8	32.1	4.4	4
S159	-1.5	34.6	6.5	31.3	4.4	4
S160	-1.4	33.2	7.6	32	4.4	4
L162	-0.5	34.2	6.3	32.6	0.2	0
L163	2.9	34.7	7.4	33.4	0.2	0
L164	-0.1	34.3	6.4	32.7	0.2	0
A168	3.6	34.8	9.2	34.7	0	0
A170	6.5	35.1	10.5	35	0	0
A171	6.1	35.1	10.5	35.1	0	0
A173	6.3	35	11.3	35	0	0
A174	6	35	11.9	34.9	0	0
A175	5.7	34.8	13.8	34.7	0	0
L178	6	34.4	13.4	34.1	0	0
A179	15.2	35.7	20.2	36.1	0	0
A180	11.8	35.3	20.7	34.7	0	0
A181	9.4	35.4	13.9	35.4	0	0
A182	9.8	35.5	14.7	35.4	0	0
A183	11.6	35.3	20.6	34.5	0	0
A184	16.2	36.3	22.7	36.4	0	0
N185	6.3	34.1	14.1	33.3	0	0
N186	6.3	34.1	14.1	33.3	0	0
N189	-0.3	34.9	4.7	34.2	0.9	0
N190	-0.4	34.7	6.1	34.6	0.9	0
N191	-0.6	34.7	6.7	34.7	0.2	0
N192	-0.3	34.7	7	34.7	0.2	0
N193	-0.1	34.7	7.6	34.7	0	0
N194	0.9	34.9	7.5	34.8	0	0
N195	1.5	35	7.7	34.8	0	0
N196	1.9	35.1	7.9	34.9	0	0
N197	2.1	35.1	8	34.9	0	0
N198	5.9	35.1	11.2	35.1	0	0
N200	-1	34.8	4.5	33.9	3.2	3
N206	7.5	35.2	12.3	35.2	0	0
N207	7.2	35.2	12.2	35.2	0	0
N208	7	35.1	12.1	35.2	0	0

Appendix 25: Environmental data for the DIN598

Site number	February SST	February salinity	August SST	August salinity	Average ice duration	Median ice duration
N209	6.9	35.1	11.7	35.1	0	0
N210	3.4	34.9	10.6	35	0	0
N211	3.6	34.9	10.4	35	0	0
N212	6.1	35.2	11.3	35	0	0
N213	6.5	35.2	11.3	35	0	0
N214	6.5	35.2	11.3	35	0	0
N215	6.6	35.2	11.3	35	0	0
N216	6.6	35.2	11.2	35	0	0
N217	7.4	35.2	12.4	35	0	0
N218	7.4	35.2	12.4	35	0	0
N219	7.6	35	12.4	35	0	0
N220	6.9	34.6	12.7	34.2	0	0
N221	6.6	34.5	12.8	33.8	0	0
N222	6.5	34.5	12.9	33.8	0	0
N223	5.3	33.4	13.1	33	0	0
N224	6.6	35.2	11.4	35.1	0	0
N225	8.8	35.3	12.1	35.3	0	0
N226	8.9	35.3	12	35.3	0	0
N227	3.2	34.8	7.4	34.6	0	0
N228	2.9	34.8	7.6	34.6	0	0
N229	2.9	34.8	7.7	34.7	0	0
N230	2.8	34.8	8.1	34.8	0	0
N231	2.2	34.7	8	34.8	0	0
N232	2	34.7	8.4	34.9	0	0
N233	2	34.7	8.3	34.8	0	0
N234	2.3	35	8.5	34.9	0	0
N235	1.7	35	8.4	34.9	0	0
N236	1.8	35	8.6	34.9	0	0
N237	3.1	34.9	10.5	35	0	0
N238	6.8	35.1	13.3	35.1	0	0
N239	6.8	35.1	13.4	35.1	0	0
N240	6.8	35.1	13.4	35.1	0	0
N241	6.7	35.1	13.5	35.1	0	0
N242	6.4	35.1	14.6	34.9	0	0
N245	6.8	35.2	13.7	35	0	0
N246	6.4	35.1	14	34.9	0	0
N248	5.1	33.4	14.5	32.6	0	0
N249	4.1	32.5	14.6	31.5	0	0
Z253	-1.5	32.5	0.5	32	11	11
Z254	-1.5	32.5	0.5	32	9.2	9
Z255	-1.5	32.5	1	32	7.1	7
B256	-1.5	32.5	2.6	32	8.1	8
B257	-1.5	32.5	2.5	32	8	8

Appendix 25: Environmental data for the DIN598

Site number	February SST	February salinity	August SST	August salinity	Average ice duration	Median ice duration
A258	2.1	32.1	16.9	31.1	0	0
A259	2.1	32.1	16.9	31.1	0	0
A260	2.1	32.1	16.9	31.1	0	0
A261	4.4	32.5	18.2	31.9	0	0
A262	4.4	32.5	18.2	31.9	0	0
A263	2.7	32.2	17.1	31.2	0	0
A264	15.2	35.8	20.1	36.1	0	0
A265	14.6	35.8	18.4	36.1	0	0
A266	14.9	35.8	19.8	36	0	0
N268	6.7	35.1	13.8	35	0	0
N269	6.5	35.1	14.6	34.9	0	0
K271	4.6	33.8	16	31.1	0	0
K275	3.6	32.5	16.1	30	0	0
K277	4.5	33.5	15.7	31.5	0	0
M280	1.2	34.8	8	34.8	0	0
M281	3.4	35.1	9.1	35	0	0
M282	0.6	34.9	7	34.8	0.1	0
M283	-0.2	34.8	5.4	34.6	0.3	0
M284	-1.7	34.3	0.9	31.3	8.8	9
M285	-1.5	34.9	4.9	33.8	0.8	0
M286	-1.5	35	5	34.2	1.8	2
M287	-0.3	34.8	4	34.1	0.7	0
M288	-1.5	34.7	2.5	33.3	4.2	4
M289	-1.8	33.1	-0.7	30.8	11.9	12
M290	-1.8	33.3	-1.2	30.3	11.9	12
M291	-1.7	33	-0.7	30.6	11.1	11
M292	-1.7	33	-0.7	30.8	11.8	12
M293	-1.7	33	-0.8	31.2	11.6	12
M297	-1.5	34.5	3.9	33.7	5.3	5
M298	3.6	34.9	10.6	35	0	0
M299	6.3	35.2	11.3	35.1	0	0
M300	5.1	35.1	9.8	35.1	0	0
M301	6.6	35.2	11.1	35.1	0	0
M303	3.2	35.2	8.2	35.1	0	0
M304	3.6	35.1	7.1	35	0	0
M305	3.8	34.9	6.5	34.8	0.7	0
M306	5.3	35.1	9	35.1	0	0
M307	5.5	35.1	9.6	35	0	0
M308	5.9	35.1	9.9	34.9	0	0
M309	6	35.1	9.9	34.9	0	0
M310	5.7	35	10.2	34.6	0	0
M311	4.5	35.1	8.7	35.1	0	0
M312	3.1	35.1	7.6	35.1	0	0

Appendix 25: Environmental data for the DIN598

Site number	February SST	February salinity	August SST	August salinity	Average ice duration	Median ice duration
M313	2.9	35	7.1	34.7	0.5	0
M314	-1.5	34.7	5.7	34	0.5	0
M315	0.3	34.9	6	34.4	0.5	0
M316	0.5	34.9	6	34.5	0.5	0
M317	0.3	34.9	6.2	35.1	0	0
M318	-0.5	34.7	6	34.1	0.8	0
M319	-1.5	34.7	4.5	34.2	3.5	4
M320	-1.5	34.6	3.1	31.6	4	4
M321	0.1	34.7	5.8	34.6	0.1	0
M322	4.4	35.1	9	35.2	0	0
M323	5.8	35.1	10.2	35.1	0	0
M324	6.9	35.1	11.5	35	0	0
M325	6.9	35.2	11.7	34.8	0	0
M326	6.8	35.2	11.2	35.1	0	0
M327	1.3	34.7	6.5	34.7	0.1	0
M328	-0.1	34.7	4.7	34.3	2.3	2
M329	-1.5	34.6	2.7	31.4	6.8	7
M330	-1.5	33.7	1.1	31.8	8.3	9
M331	-1.5	33	3.3	32.2	3.5	3
M332	-1.5	34.6	3	32.2	6.6	6.5
M333	-1.8	34.2	1.3	31.5	8.8	9
M334	-1.8	34.2	0.8	31	8.8	9
M335	-1.8	34.2	1.1	31.2	8.8	9
M336	-1.5	34.2	1.7	31.5	4.4	4
M337	0.1	34.9	5.1	34.1	0.6	0
M338	-1.5	34.9	4.4	33.6	3.5	3
M339	0.4	34.9	5.4	34.4	2.2	2
M340	3.5	34.9	10.4	35	0	0
M341	-1.5	34.8	2.9	31.9	4.6	4.5
M342	-1.9	34.7	1.6	31.9	4.6	4.5
M343	-1.9	34.7	-0.1	31.8	7.8	8
M344	-1.9	34.3	-0.3	32.7	11.6	12
M345	-1.7	33.8	-0.3	33	10	10
M346	-1.9	33	-0.3	33	11.2	11.5
M347	-1.9	34.9	1.7	33.7	5.7	5
M348	-1.9	33	-0.8	30.3	11.1	11
M349	-1.5	34.7	2.2	33.3	6.4	6.5
M350	-1.9	34.8	1.7	33.3	4.6	4.5
M351	-1.9	34.3	1.8	31.5	6.8	7
M352	-1.9	34.7	3.5	32.8	5.5	5.5
M353	-0.4	34.7	6	33.9	0.8	0
M354	-1	34.7	3.8	33.5	2.2	1
M355	-0.8	34.8	4.1	33.7	2.2	1

Appendix 25: Environmental data for the DIN598

Site number	February SST	February salinity	August SST	August salinity	Average ice duration	Median ice duration
M356	-0.8	34.8	4.3	33.7	2.2	1
M357	-1	34.7	4.9	33.9	2.2	1
M358	-1	34.7	4.8	33.9	2.2	1
M359	-1	34.7	4.4	33.7	2.2	1
M360	-1.1	34.7	4	33.5	2.2	1
M361	-1.5	34.8	4.1	34	3.1	3
M362	-1.7	34.4	0.2	31.8	11.2	11.5
M363	-1.9	33.5	1	31.9	10.7	11
M365	-1.8	33.5	0.4	32.3	10.7	11
M366	-1.8	33.4	0.1	32.2	10.8	11
M367	-1.3	34.7	3.8	33.9	0.5	0
M368	-1.9	33.9	0	32.6	11.6	12
M369	-1.7	34.7	4.3	34.2	0.9	0
P370	-1.8	33.7	-1.1	30.7	11.9	12
P371	-1.8	33.3	-0.5	31	11.8	12
P372	-1.7	33	-0.7	30.9	11.8	12
P373	-1.7	33	-0.7	30.5	11.9	12
P374	-1.7	33	-1.1	30.5	11.1	11
P375	-1.7	33	-0.6	30.7	11.9	12
P376	-1.7	33	-0.7	30.4	11.1	11
P377	-1.7	33	-0.8	30.4	11.9	12
P378	-1.7	33	-1	30	11.1	11
Z379	-1.5	34.5	4.9	34	3.5	4
Z380	-1.5	34.5	5	33.6	4.2	4.5
Z381	-1.5	34.5	5.6	33.2	4.2	4.5
Z382	-1.5	34.5	3.8	33.4	4.2	4.5
Z383	-1.5	34.5	3.8	32.6	4.8	5
Z384	-1.5	33	6.2	32.7	4.8	5
Z385	-1.5	33	5	33.6	4.2	4.5
Z386	-1.5	33	6.6	32.9	4.8	5
Z387	-1.5	33	5.3	32.5	5.8	6
Z388	-1.5	33	5.1	32.5	5.8	6
Z389	-1.5	33	5.7	31.7	5.8	6
Z390	-1.5	33	4.5	31.8	5.8	6
Z391	-1.5	33	4.6	30.7	5.8	6
Z392	-1.5	33	4.7	33.8	5.8	6
Z393	-1.5	33	5	32.6	7.4	7
Z394	-1.5	33	5.2	32.6	7.4	7
Z395	-1.5	33	5	31.9	6.2	6
Z396	-1.5	33	5.2	32.1	7.4	7
Z397	-1.5	33	5.1	31.4	5.8	6
N398	7.2	34.5	12.4	34.2	0	0
N399	7	34.5	12.5	34.2	0	0

Appendix 25: Environmental data for the DIN598

Site number	February SST	February salinity	August SST	August salinity	Average ice duration	Median ice duration
N400	7	34.5	12.5	34.2	0	0
N401	7	34.5	12.5	34.2	0	0
N402	7	34.5	12.5	34.2	0	0
A405	15.4	36	20.4	36.3	0	0
A406	14.6	36	20.6	36	0	0
A407	13.8	35.9	19.3	36.3	0	0
A408	13.5	35.7	18.4	35.7	0	0
A409	13.4	35.7	17.9	35.7	0	0
A410	13	35.7	18.6	35.7	0	0
A411	11.6	34.6	21.3	34.4	0	0
A412	11.5	35.6	17.6	35.6	0	0
A413	12.4	35.6	18.2	35.5	0	0
A414	12.4	35.5	17.9	35.5	0	0
A415	6.5	35.2	10.9	35.2	0	0
A416	0.7	34.7	7.2	34.6	0	0
A417	7	35.2	11.7	34.9	0	0
A418	7	35.2	11.5	34.9	0	0
A419	4.4	33	18.1	31.8	0	0
A420	4.6	32.9	17.2	32.2	0	0
A421	4.6	33.1	18.2	31.6	0	0
A422	4.8	33	18.5	31.8	0	0
A423	3.9	32.9	17.8	31.6	0	0
A424	4.2	32.8	16.3	32.2	0	0
A425	4.7	33.1	18	32.1	0	0
A426	4.9	33	17.1	32.2	0	0
A427	4.1	32.6	15.6	32.3	0	0
A428	3.9	32.6	16	32.4	0	0
Z432	-1.7	29.7	1.2	26.8	11.5	12
Z434	-1.8	29.1	-0.5	24.9	11.9	12
Z435	-2	31.5	1.3	27.6	10.9	11
Z436	-0.9	31.1	4.7	21.6	9.1	9
Z437	-1.2	30	3.1	20	8.9	9
Z438	-0.8	30.9	4.6	21.3	10.5	11
Z439	-1	30.2	3.5	20.3	8.9	9
Z445	-1.5	12.2	1.7	11.4	9.1	9
Z446	-1.5	14.7	0.9	11	9.8	9
Z448	-1.5	12.2	1.7	11.4	9.4	9
Z449	-1.5	13.3	2.4	12.3	9.6	10
Z450	-1.5	18.2	0.4	16.3	10.3	10
Z452	-1.5	13.2	2	12.8	9.6	10
Z453	-1.5	21.3	0	17.8	9.8	10
Z454	-1.5	15.1	4.4	16.1	9.6	10
Z455	-1.5	20	2.5	19	9.7	10

Appendix 25: Environmental data for the DIN598

Site number	February SST	February salinity	August SST	August salinity	Average ice duration	Median ice duration
Z457	-1.5	17	4.3	17	9.9	10
Z458	-1.5	12	3.4	12	9.1	9
Z459	-1.5	18.2	0.4	16.3	10.3	10
Z460	-1.5	17.2	2.4	19.2	10	10
Z461	-1.5	16.9	2.8	19	10.2	10
Z462	-1.5	16.8	3.3	18.5	9.9	10
Z463	-1.5	13.5	2.7	14	9.1	9
Z464	-1.5	14.3	1.6	14.5	9.9	10
Z466	-1.5	21.1	0	17.4	10.5	9
Z467	-1.5	22.7	0.1	18.9	10.5	10
Z468	-1.5	13.4	2.2	13.7	10.6	10
Z469	-1.5	15.7	3.5	16.9	9.7	10
Z470	-1.5	18.1	2.5	19.9	9.9	10
Z471	-1.5	17.3	2.1	19.2	10	10
Z472	-1.5	18.1	2.5	19.9	10.3	11
Z473	-1.5	17.1	2.7	18.7	10.9	11
Z474	-1.5	16.3	2.5	17.7	10.1	10.5
Z475	-1.5	15.3	1.6	16.2	10.6	11
Z476	-1.5	15.8	1.1	16.5	10	10
Z477	-1.5	19.3	0.2	18	10	10
Z478	-1.5	17.5	0.4	17.4	10	10
Z479	-1.5	23.9	-0.4	20.3	10.7	11
Z480	-1.5	22.3	-0.8	20.2	10.7	11
Z481	-1.5	22.7	0.1	18.9	10.5	10
Z482	-1.5	23.9	-0.4	20.3	10.7	11
Z483	-1.5	19.2	1.8	20.8	10.6	10
Z484	-1.5	15.3	1.6	16.2	10.6	11
Z485	-1.5	13.7	3.9	13.9	9.2	9
Z486	-1.5	14.9	3.2	15.8	9.2	9
Z487	-1.5	17.5	0.6	16.4	10.5	10
Z488	-1.5	14.4	2.9	15.1	10.5	10.5
Z489	-1.5	12.2	1.7	11.4	9.4	9
Z491	-1.5	11	3.1	10.7	9.3	9
Z492	-1.5	16.8	3.3	18.8	9.9	10
Z493	-1.5	16.8	3.3	18.8	9.9	10
Z494	-1.5	19.2	1.8	20.8	10.6	10
Z495	-1.5	20.5	0	20.5	11.5	12
Z496	-1.5	20.5	0	20.5	11.5	12
Z497	-1.5	20.5	0	20.5	11.5	12
Z498	-1.5	18	0.2	18.7	10.6	11
Z499	-1.5	22.3	-1.4	22.2	12	12
Z500	-1.5	20.8	-0.9	21.8	11.7	12
Z501	-1.5	20.8	-1	21.8	11.7	12

Appendix 25: Environmental data for the DIN598

Site number	February SST	February salinity	August SST	August salinity	Average ice duration	Median ice duration
Z546	-0.7	31	1	30.6	9.1	9
Z547	-0.9	31.1	4.7	21.6	9.1	9
Z548	-0.2	30.4	4.3	28.2	9	9
Z549	-0.2	30.4	3.9	30	8.4	8
Z550	3.9	34.5	9.1	34.3	0	0
Z551	3.2	34.7	8.9	34.5	0	0
Z552	2.4	34.9	8.2	34.6	0	0
Z553	1.3	34.9	8.1	34.6	0	0
Z554	1.1	34.9	8.2	34.7	0	0
Z555	-1.7	35.2	1.1	31.7	7.9	7
Z556	-1.7	35.2	1.1	31.7	8.2	8
Z557	-1.7	32.4	2.2	31.6	7.1	7
Z558	-1.7	35.7	1.4	25.2	9.4	9
Z559	-1.7	37.1	-0.1	30.1	10.1	10
Z560	-0.6	34	4.8	33.8	4.3	4
Z561	-1.4	33	3.6	32.7	6.4	6
Z562	-1.4	33	3.6	32.7	4.3	4
Z563	-1.6	30	1	27.3	11.7	12
Z564	-1.6	29.7	0	27.7	11.8	12
Z565	-1.7	29.4	-0.7	27.9	12	12
P566	-1.7	32.4	2.5	31.9	8.2	8
P567	-1.7	32.1	0.8	31.6	8.4	8
P568	-1.7	32.5	2.3	32	8.4	8
P569	-1.7	32.3	1.4	31.8	8.4	8
P570	-1.7	33.2	2.9	32.7	8.2	8
P571	-1.7	32.5	2.5	32	9.8	9
P572	-1.7	32.4	0.8	31.9	11.1	11
P573	-1.7	32.1	1.8	31.6	9.8	9
P574	-1.7	32.5	2.3	32	8.4	8
P575	-1.7	32.6	2.8	32.1	8.2	8
P576	-1.7	32.5	2.5	32	9.8	9
P577	-1.7	32.1	0.8	31.6	8.4	8
P578	-1.7	30.7	0.7	30.2	9.9	9
P579	-1.7	32.8	3.4	32.3	8.4	8
P580	-1.7	33.1	2.9	32.6	8.2	8
Z602	8.1	31.7	15.1	31.7	0	0
Z603	8.1	31.9	15.2	31.9	0	0
Z604	8.1	31.9	15.2	31.9	0	0
Z605	7.8	31.9	14.9	31.8	0	0
Z606	4.1	32.9	12.1	32.7	0	0
N607	1.7	31	16.3	28.2	0	0
N608	2.2	31	16.5	29.4	0	0
N609	2.7	31.4	16.4	28.8	0	0

Appendix 25: Environmental data for the DIN598

Site number	February SST	February salinity	August SST	August salinity	Average ice duration	Median ice duration
N610	2.7	31.3	16.4	28.8	0	0
N611	2.9	31.4	16.4	28.5	0	0
N612	4	32.4	16	30.8	0	0
N613	2.9	28.6	14.7	25.7	0	0
N614	1.6	32.3	16.2	30.9	0	0
N615	2.6	31.5	14.7	25.5	0	0
N616	3.7	31.8	15.8	30.3	0	0
N617	4	32.3	15.3	30.7	0	0
N620	4.1	32.5	14.7	29.4	0	0
N622	4.2	32.5	14.3	24.8	0	0
N623	4.2	32.5	14.8	30.2	0	0
N626	4.7	32.8	14	26	0	0
N627	4.9	33.2	13.7	27.5	0	0
N628	5.1	33.2	14.2	26.6	0	0
N629	4.9	33	14.6	29.5	0	0
N630	4.7	32.9	14.3	28	0	0
N631	4.8	33	14.1	30.2	0	0
N632	4.8	33	14.1	30.2	0	0
N633	4.6	32.8	13.9	30.1	0	0
N634	4.6	32.9	13.8	30.1	0	0
N635	4.5	32.9	13.6	31	0	0
N636	4.5	32.8	13.4	31.2	0	0
N637	5.2	33.8	12.9	30.9	0	0
N638	4.7	33.4	12.8	31.7	0	0
X639	0.8	31.1	16.2	29.9	0	0
X640	0.7	31.1	16.2	30	0	0
X641	0.6	31.1	16.3	30	0	0
X642	0.6	31.1	16.4	30	0	0
X643	0.6	31	16.4	30	0	0
X644	0.6	31	16.5	29.9	0	0
X645	0.6	31	16.5	29.9	0	0
X646	1.8	31.8	16.8	31.1	0	0
X647	6.4	33	18.9	31.2	0	0
X648	5.3	32.6	18.6	31.9	0	0
X649	4.2	32.5	18.2	31.8	0	0
X650	3.3	31.8	17.5	31.5	0	0
X651	6	32.5	18.2	31.9	0	0
X652	4.2	32.5	18.2	31.8	0	0
X653	5.4	32.6	18.9	32.5	0	0
X654	2.3	32.5	16.2	32	0	0
X655	1.3	32.4	16.1	32.1	0	0
X656	5.3	32.9	18.7	32	0	0
X657	5.2	32.9	18.8	32.2	0	0

Appendix 25: Environmental data for the DIN598

Site number	February SST	February salinity	August SST	August salinity	Average ice duration	Median ice duration
X658	9.4	33.3	20.2	31.7	0	0
X659	3.1	32.2	17.3	31.5	0	0
X660	2.7	31.7	17.1	31.5	0	0
X661	0.2	33.9	10.7	32.2	0.4	0
X664	9.1	34.2	24.1	33.9	0	0
X666	9	34.2	24	33.9	0	0
C668	6.4	33	18.9	31.2	0	0
X669	7	33.3	22.5	32.4	0	0
X670	4.2	33.3	19.2	32.9	0	0
X671	4.4	33.3	18.7	32.8	0	0
X672	1.8	32.4	16.7	32.1	0	0
X673	15.8	35.8	26.1	34	0	0
X674	9.4	34.6	24.9	33.6	0	0
X675	9.6	34.6	22.7	33.5	0	0
A682	-0.6	32.7	11.8	31.2	1.8	2
A683	-0.7	32.7	11.7	31.3	1.8	2
A685	3.3	33.4	14.7	32.1	0	0
X686	3.4	31.8	17.9	31.6	0	0
X688	3.4	31.8	17.9	31.6	0	0
X689	3.3	31.8	17.5	31.5	0	0
X690	4.4	32.4	18.1	31.7	0	0
X691	4.4	32.4	18.1	31.7	0	0
X692	4.4	32.2	18	31.5	0	0
X693	6.2	32.7	19	31.9	0	0
X694	4.6	32.5	18.5	31.9	0	0
X695	3.5	32.1	17.7	31.8	0	0
X696	3.2	32.4	17.4	31.6	0	0
X697	2.7	31.7	17	31.5	0	0
X698	2.7	31.7	17	31.5	0	0
X699	2.4	31.8	17.2	31.4	0	0
X700	2.4	31.8	17.2	31.4	0	0
X701	2.7	31.7	17	31.4	0	0
X702	2.7	31.7	17	31.4	0	0
X703	2.6	31.7	17	31.4	0	0
X704	2.7	31.7	17.3	31.5	0	0
X705	3.2	32	17.6	31.7	0	0
X706	3.6	32.3	17.9	31.9	0	0
X707	4.2	32.5	18.2	31.9	0	0
X708	1.3	31.5	16.2	30.9	0	0

Appendix 26: Validation test of the DIN576 and DIN598 surface reference database

Average differences between instrumental values and reconstructed values

DIN576	Temperature February	Salinity February	Temperature August	Salinity August	Average ice duration	Median ice duration
Minimum	0	0	0	0	0	0
Maximum	7.9	17.8	10.8	18.5	11	11.3
Sum	387	580	738.9	725.1	389.3	414.3
Points	576	576	576	576	576	576
Mean	0.6717	1.0069	1.2828	1.2589	0.67587	0.71927
Median	0.2	0.3	0.8	0.4	0.1	0.2
RMS	1.3303	2.4644	1.9271	2.5075	1.5324	1.5767
Std deviation	**1.1493**	**2.0712**	**1.4393**	**1.9805**	**1.3765**	**1.4044**
Variance	1.3209	5.068	2.0717	4.7112	1.8948	1.9722
Std error	0.047887	0.093801	0.059972	0.090438	0.057356	0.058515
Skewness	2.879	4.6479	2.3199	3.9984	3.8176	3.7149
Kurtosis	9.9697	25.199	7.4667	20.256	18.515	17.786
DIN598						
Minimum	0	0	0	0	0	0
Maximum	7.3	16.8	10.7	16.3	1039	11.6
Sum	397.5	590.4	725.6	426.7	384.4	405.1
Points	598	598	598	598	598	598
Mean	0.66472	0.98729	1.2134	1.2152	0.64281	0.67742
Median	0.2	0.3	0.8	0.5	0.2	0
RMS	1.2568	2.2809	1.8199	2.3251	1.4356	1.5209
Std deviation	**1.0675**	**2.0578**	**1.3575**	**1.984**	**1.2848**	**1.3628**
Variance	1.1395	4.2347	1.8429	3.9361	1.6506	1.8572
Std error	0.043652	0.084151	0.055513	0.081131	0.052538	0.055729
Skewness	2.8493	4.3757	2.4741	3.685	4.0228	3.8683
Kurtosis	10.272	22.814	8.8579	17.553	20.977	19.762

Appendix 27: Correlation between measured and reconstructed parameters using the DIN576 surface sample reference database

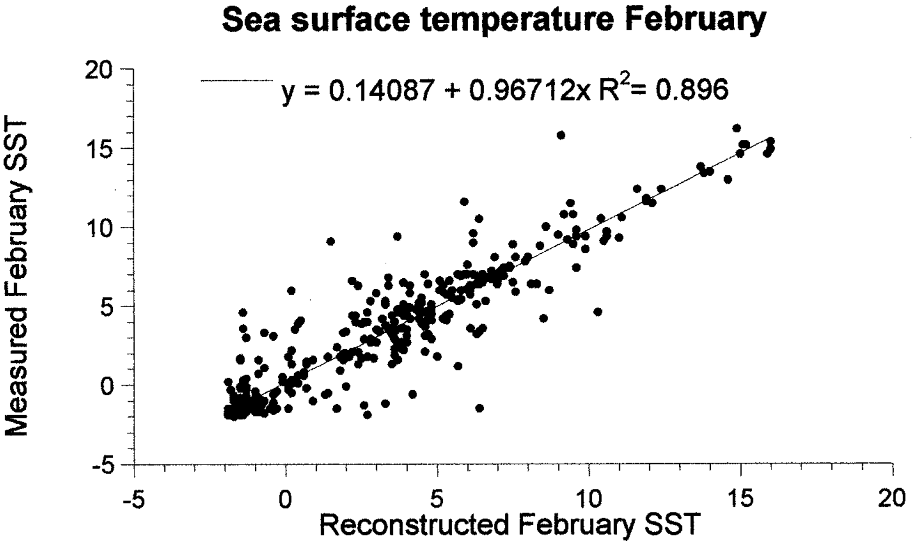

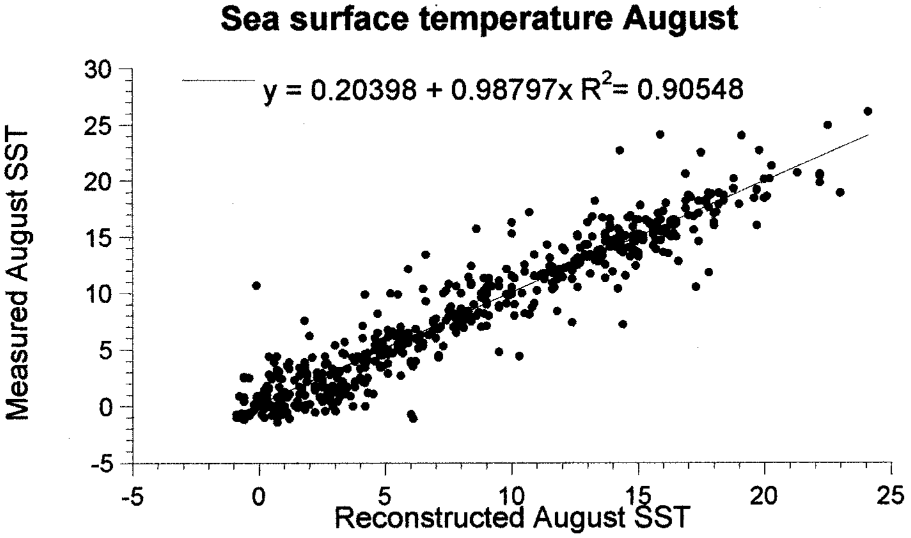

Appendix 27: Correlation between measured and reconstructed parameters using the DIN576 surface sample reference database

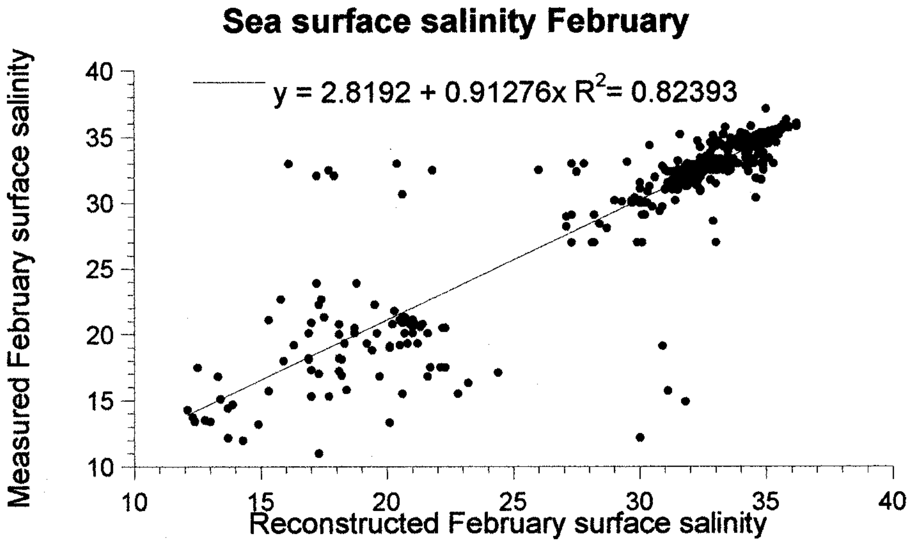

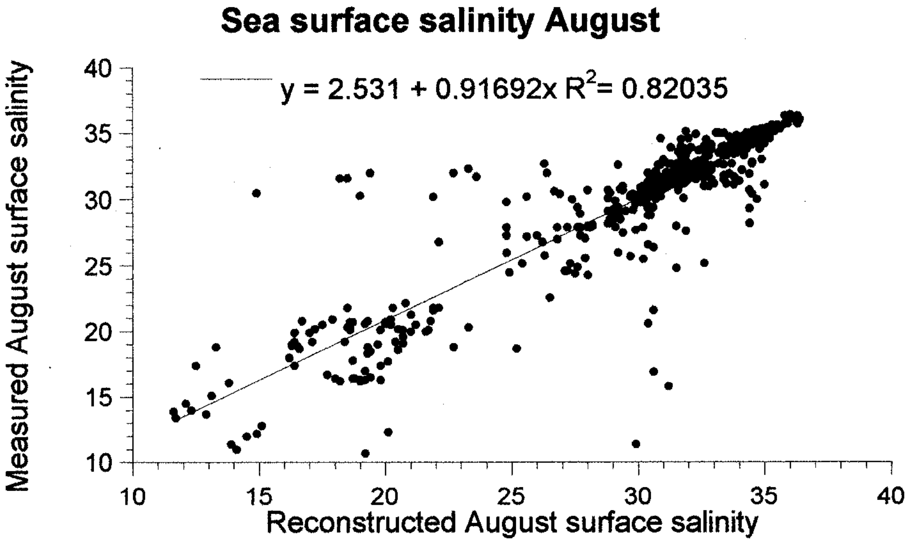

Appendix 27: Correlation between measured and reconstructed parameters using the DIN576 surface sample reference database

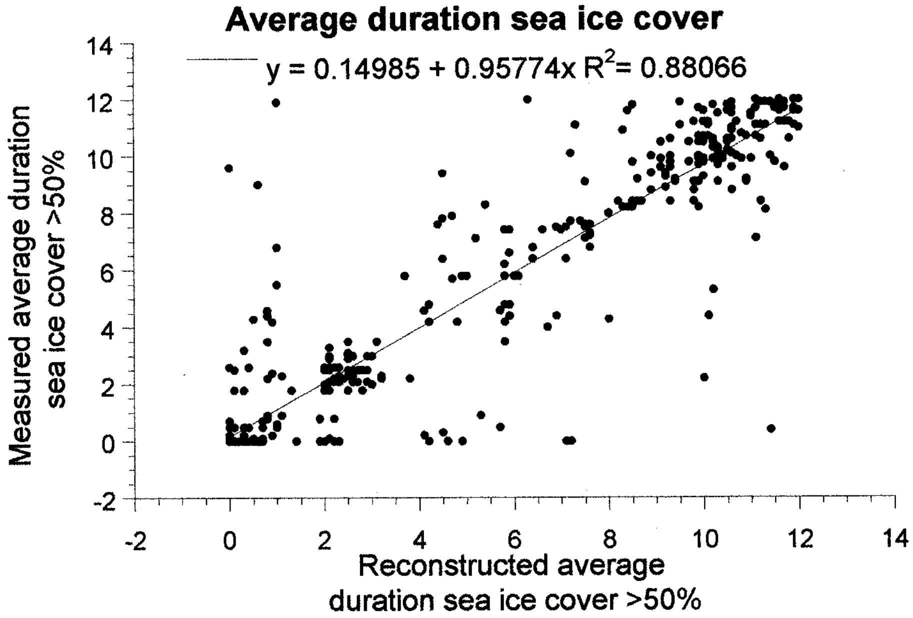
Average duration sea ice cover

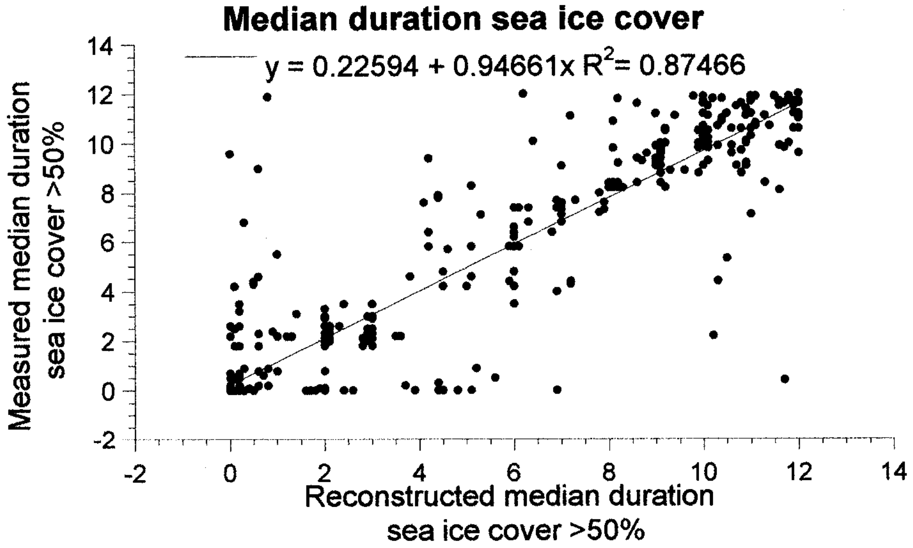
Median duration sea ice cover

Appendix 27: Correlation between measured and reconstructed parameters using the DIN598 surface sample reference database

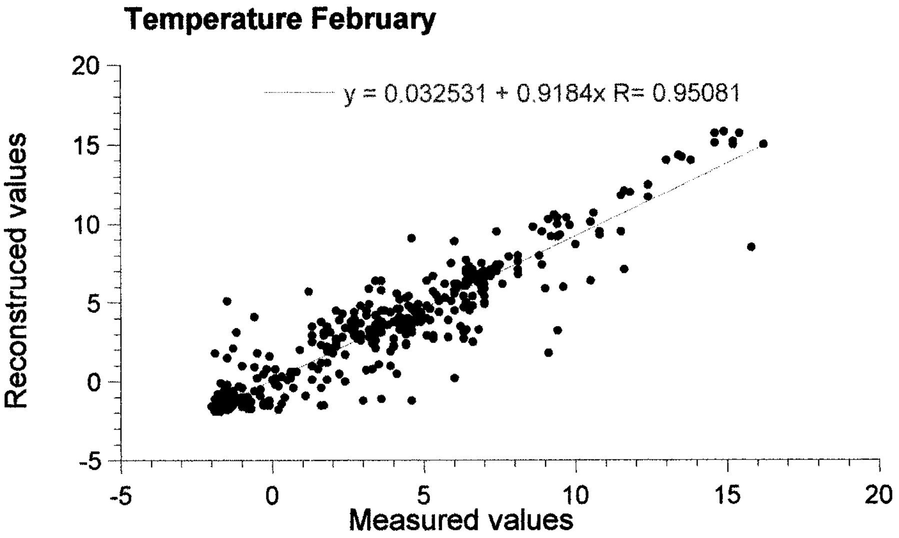

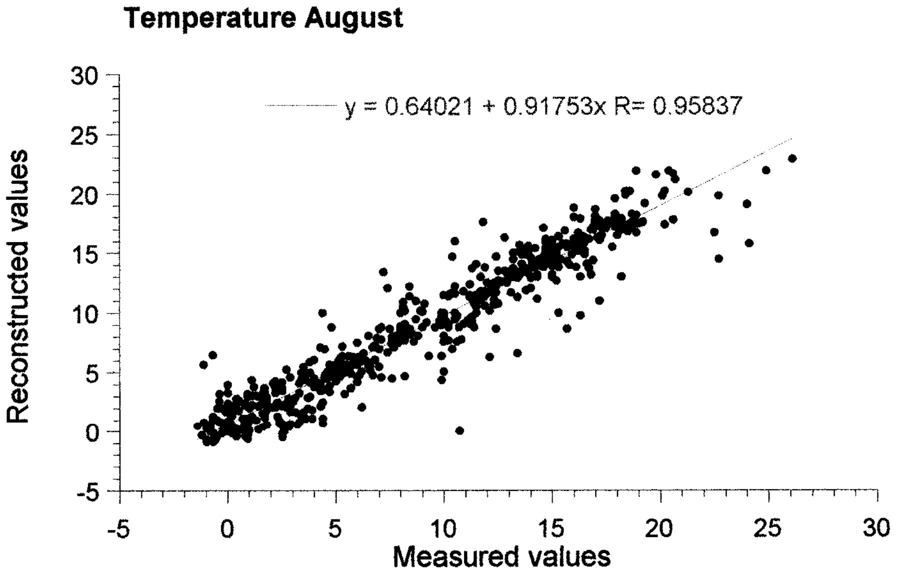

Appendix 27: Correlation between measured and reconstructed parameters using the DIN598 surface sample reference database

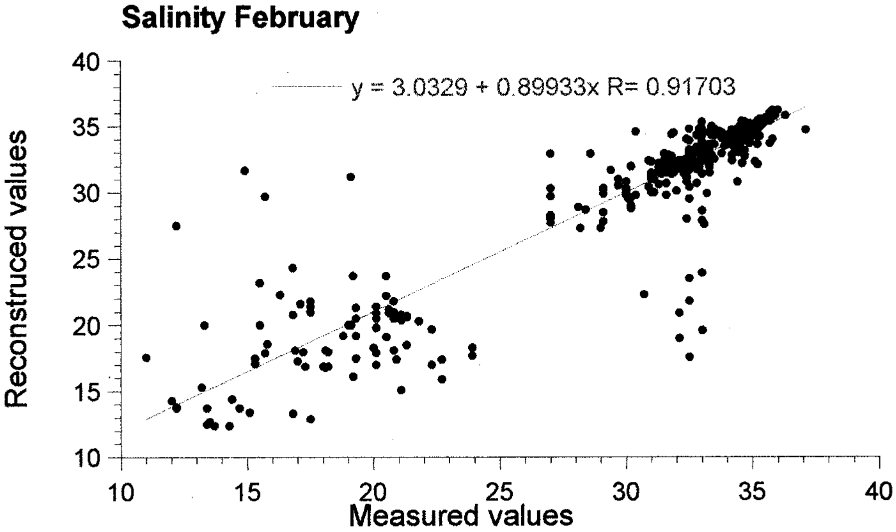

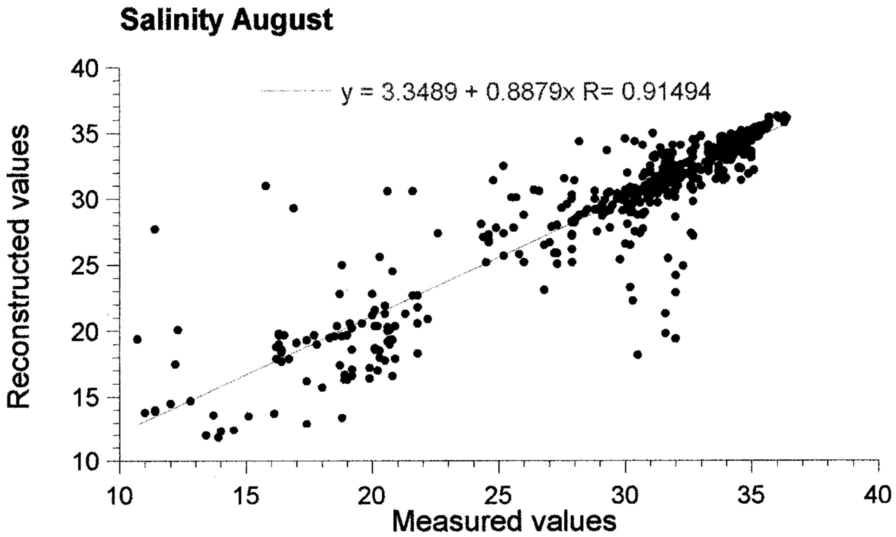

Appendix 27: Correlation between measured and reconstructed parameters using the DIN598 surface sample reference database

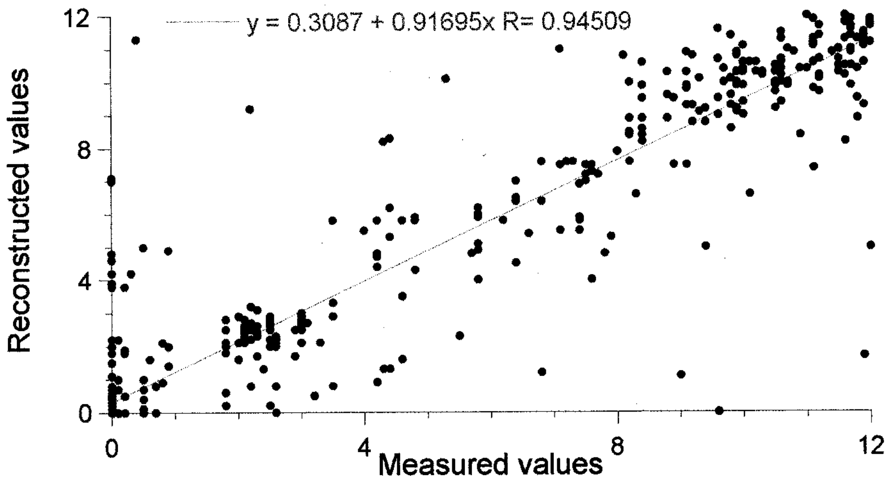

Average duration ice cover

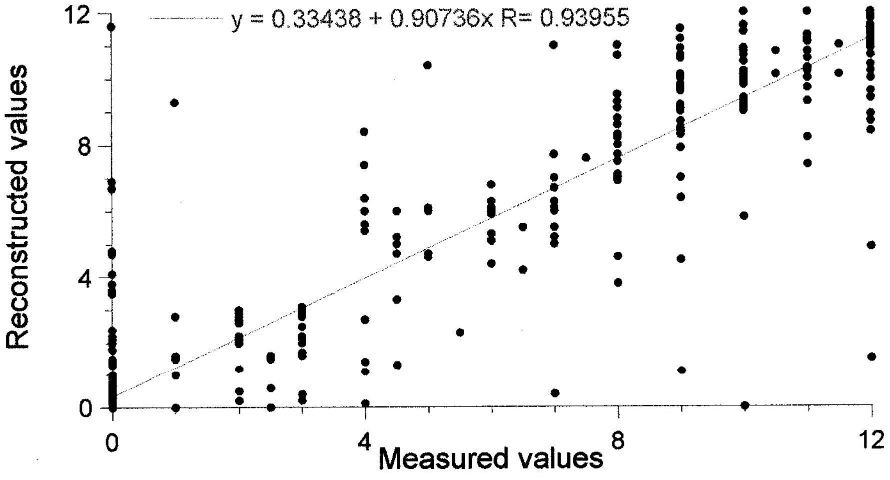

Median duration ice cover

Appendix 28

Modern analogues for La Have Basin core 95-030-24

```
    1   10    1
   0 A259A428A425A423A260X669X646X666A258X642
       44  58  58  62  63  68  94  98 102 112
  10    0X666X646X669A259X644X639X642X641A425
       53  60  73  82 102 105 106 110 112 114
  20   10X646X666X642A425X639X644A259X641X650
       24  49  74  75  79  83  91  99 101 101
  30 A428A423A425A259A427X642X669  20X641A260
       55  87  96 106 119 119 123 131 131 132
  40   30A428A259X669A425A423A260X644X646X639
       49  71  83  88 100 102 108 133 135 135
  50 X639X644X642X646X650X660X640X649  40A425
       35  70  73  77  78  90  99 105 115 122
  60 X642  50A425X646X666X644A421A682A423A259
       65  71  77  78  84  88  89 102 106 113
  70 A428A259A423A427A425A260  60A258X669X647
       49  85  86  87  98 100 116 135 139 153
  80 A428  70X669A259X666A423A260A425X647A421
       57  58  59  70  95 100 103 103 105 122
  90   80A428A259A423A260X669A425A421A258A682
       67  78  86  91  97 102 127 135 138 141
 100 X642A421X666X646A425A423A682X644X641A259
       66  74  88  94  94  98  99 107 118 120
 110  100A421X666A423X642A425A682A259X646A149
       15  64  78  94  98 103 104 115 116 122
 120  110A421A682A423X666X646X642A425X639X669
       25  66  86 100 102 111 112 119 125 127
 130  120A423A259A428A260A425X669A258N198X666
       53  55  61  81  84  86  87 102 109 117
 140  130A421X666A423A425A259X642A682N399N198
       55  56  71  84 106 107 107 112 118 119
 150  140X639X646X642A421X650A423X644X660X666
       46  85  90 107 115 120 121 121 122 123
 160 A423A428A427A259A260A422A258X669A425A421
       64  68  97  98 113 125 136 139 139 152
 170  160A428A423A259A425A260A421X669A427X666
       30  58  60  80  92 102 102 105 119 122
 180  170A428A259A423A425X669A260X646X642A421
       17  54  59  64  71  84  88 106 106 114
```

```
290 X644X642M346X639 180X646X643A425X641X640
      57  69  73  77  83 101 119 121 122 143
300  290X639X646X644X642M346X641X643X666A425
      38  66  75  75  86  93  95 126 126 131
320  300X641X646X644X642X645X639X643M346A682
      33  54  62  81  82  91  98 106 107 108
340 X647A428A422H130H131 320A261X645S158A426
      62  86 106 107 110 110 111 116 117 119
360 X642X646X639X641X644A682A425A421X643M346
      72  79  83  84  89 102 108 122 126 132
380  360X642N633X639X644X646A425X643N623N616
      33  88  89 103 117 133 136 139 139 141
400 A428A259A425A423X669X646 380X639A260X642
      83  84  93  95  97  99 101 105 113 114
420 X642X644X646X643X640A425X641X639M346 400
      33  56  58  62  82  83  89  91  94  97
440 A428 420A425A259A423A260X669X646A427X642
      63  73  74  77  79  98 105 106 111 116
460  440X641H132H130X646X642H131X644X645M346
      55  73  84  92  96  97  98 103 103 107
480 A427A423A428Z381X664A425 460A259K277A260
      71 118 119 147 163 165 173 185 186 186
500  480A259A428A423A425A260A258A424A427N225
      80  99 103 111 112 122 125 126 139 162
520 N633X642N623N616N637Z382A425A423Z557A421
      76  90 108 110 112 122 124 125 126 128
540 A423A427A428A259A425A260A258A424X664 520
      45  51  68  72  76  87  93  94 103 114
560 X642X639X646A425X641X644A682Z382 540A421
      77  85  89  97  97  99 105 108 115 119
580  560X646X639A682A421X641X666X642A425A423
      56 111 118 133 139 148 149 149 155 160
600  580X639X646X660X642X649X650X644A425Z382
      39  90  99 112 118 128 137 137 138 143
620  600X639X646X642N633X660A425X644X650A423
      12  85  97 107 112 113 122 122 125 127
640  620X639X650X649X660X646X642X644X640N399
      39  74  75  81  85 111 134 137 143 153
660  640X660X649X639X650X642X646X648X659N238
      23  53  84  96  97 136 140 147 156 161
```

```
680   660X639X660X649X650X642X646A423A421Z559
       16  88  90 113 122 123 127 134 143 146
700   680X639X642X644X641X646M346X643A425X640
       30  55  78  79  87  87 104 110 123 138
720   700X639X660A421A682X642Z559A423X646X666
       33  99 120 125 129 139 139 144 145 153
740  A427X654X664A423 720K277X655X660X659A424
      124 133 133 139 143 187 187 187 225 226
760  X664A423X655 740A424A258A427A259A260A428
       63  96 102 104 105 107 109 121 141 149
780  X664 760X654A427A423K277X655X660X656A424
      113 118 126 140 156 175 197 226 236 237
800   780X654X664A423A427K277X660X655X659X656
       46 123 137 161 166 179 183 189 207 225
820  X660 800Z561Z557N634N616N633X648X659N269
       71 113 114 139 147 150 153 162 163 169
840   820X660X654X664X655A423X659A427K277Z561
       44  97 104 142 149 155 156 172 177 181
860  X664X654A427 840A423X655K277A424A258X653
       64  84 111 115 125 127 138 180 218 219
880  X654X655 860X659A423X664X660X653N238A263
       79  91 103 103 107 111 117 123 127 134
900   880X654X664X655K277X659X660A423X672X656
       24  42  92 108 113 140 148 149 154 157
920  X656 900X654X658X664X659X655A263X653A424
       65  74  84  99 104 108 114 125 131 132
940   920X664X656X654K277A424A423A258X658A427
       55 116 144 162 201 205 222 227 234 236
960  X656X658X657 940X671N240X654N241K277N239
      302 417 422 422 425 439 461 519 542 542
980  X664X654X656A427K277A424A258X655A423A428
      144 229 248 263 269 279 286 306 309 328
1000 A423A427N633N616K277X664X660N634X654X655
       96 101 109 146 148 154 160 162 165 170
1020 1000X660N633N634X655N616N269X648Z561X649
       77  95 128 155 158 161 162 164 181 184
```

Appendix 29: Reconstructed sea surface conditions for core 95-030-24 La Have Basin

	February SST			February salinity			August SST			August
Depth (cm)	Lower limit	Most probable estimate	Upper limit	Lower limit	Most probable estimate	Upper limit	Lower limit	Most probable estimate	Upper limit	Lower limit
0	2.1	2.7	4.4	32.1	32.3	32.9	16.8	17	18.1	31.2
10	2.5	4.6	8.4	32.2	32.9	34	17	19.3	23.6	31.3
20	3.2	4.1	8	31.6	32.6	33.1	18.2	18.9	24	31.6
30	3.7	4	5.1	32.5	32.7	33	16.1	16.4	18	31.4
40	2	3.8	4.3	32	32.6	32.7	16.3	16.5	18.4	31.2
50	0.6	0.8	1	31	31.1	31.1	16.2	16.3	16.5	29.9
60	0.8	1.2	5.6	31.1	31.4	32.8	16.4	16.6	19.3	30
70	2.1	3.7	3.9	32.1	32.6	32.7	16	16.3	17.2	31.3
80	3.6	4.3	7.3	32.5	32.7	33.4	16.2	17	22.5	31.9
90	2.1	3.9	4.2	32.1	32.6	32.7	16	16.7	17	31.2
100	1	2.3	5.9	31.2	31.8	33.4	16.8	17.6	24	30.4
110	3.1	3.9	9	32	32.5	33.4	17.8	18.6	24	31.1
120	0	3.6	4.2	32.5	32.7	33.1	13	17.6	18.5	31.4
130	2.1	3.5	3.7	32.1	32.7	32.8	16.7	17.6	17.7	31.1
140	3.9	4.5	8.6	32.9	33	34.3	17.8	18.6	24	31.5
150	1.1	2.9	4.5	31.3	32.2	33	16.4	17.5	18.4	29.9
160	3.7	3.9	4.3	32.6	32.8	32.9	15.9	17.3	17.6	31.5
170	3.5	3.9	3.9	32.5	32.7	32.8	16.3	17	17.4	31.7
180	2.1	3.6	3.9	32.1	32.6	32.7	16.1	16.7	17	31.2
290	-1.9	0.3	0.7	31	31.3	32.8	-0.3	14.4	16.5	29.9
300	0.5	0.6	3.2	31.2	31.2	32.1	11.1	15.3	16.3	30.1
320	0.6	0.8	1.8	31.2	31.3	32	13	15.8	16.5	30.1
340	4	5.8	6.4	31.8	32.9	33	13.1	18.3	18.8	31.1
360	0.6	0.8	2.6	31.1	31.2	32.1	16.3	16.4	16.8	30
380	0.7	1.3	4.6	31.2	31.4	32.6	14.1	16	16.4	30
400	1.9	3.7	4.1	32	32.6	32.7	16.2	16.4	18.2	31.3
420	0.6	0.7	2.4	31.1	31.2	32.1	16.4	16.4	17	30
440	1.2	3.5	4.1	31.5	32.5	32.7	16	16.3	17.7	30.5
460	-0.1	1.8	3.2	30.7	31.7	32.3	5.6	14.7	16.4	30.2
480	3.8	4	4.8	32.6	32.7	33.4	15.4	15.7	19.3	31.7
500	2.1	3.4	4	32.1	32.5	32.7	15.8	16.2	17.2	31.3
520	0	4	4.5	31.3	32.5	32.8	14.1	14.4	16.3	30
540	3.8	3.9	4.3	32.6	32.8	32.9	15.7	17.3	17.7	31.5
560	0.6	0.8	2.6	31.1	31.2	32.2	16.3	16.4	17.1	30
580	0.7	1.1	2.9	31.2	31.4	32.1	16.2	16.4	17.5	30.1
600	0.9	1.1	2.1	31.3	31.4	31.8	16.3	16.4	16.9	30.2
620	0.9	1.1	2.5	31.2	31.3	32	16.3	16.4	16.9	30.2
640	1	1.4	3.5	31.2	31.4	32	16.3	16.5	17.7	30.1

Appendix 29: Reconstructed sea surface conditions for core 95-030-24 La Have Basin

	February SST			February salinity			August SST			August
Depth (cm)	Lower limit	Most probable estimate	Upper limit	Lower limit	Most probable estimate	Upper limit	Lower limit	Most probable estimate	Upper limit	Lower limit
660	1.3	2.1	3.1	31.4	31.6	32.3	16.7	16.9	18	30.3
680	0.8	1.8	2.3	31.1	31.5	31.7	16.3	16.7	17	29.9
700	0.7	1.3	1.9	31.1	31.3	31.6	16.3	16.5	16.7	29.9
720	0.9	1.4	3.2	31.2	31.3	32.1	15.5	16.5	17.4	30.2
740	3.8	4.9	9.1	32.6	32.9	34.1	16	17.3	24.1	32.1
760	3.1	7.6	9.1	32.7	33.8	34.2	17.2	22.4	24.1	31.8
780	2.8	7.8	8.8	32.5	33.9	34.1	16.1	22.6	23.8	32.1
800	2.8	6.2	8.2	32.6	33.5	34	16.6	20.7	23	31.9
820	-1.5	2.6	3.3	31.8	32	33.3	3.7	15.8	17.4	31.4
840	2.1	2.7	3.3	31.9	32	32.9	15.9	16.4	18.9	31.5
860	2.8	7.6	9.1	32.5	33.8	34.1	16.1	22.1	24.1	32.1
880	2.3	2.6	6.9	32.4	32.6	33.7	16.4	16.7	22.6	31.9
900	2.4	3	8	32.5	32.7	34	16.5	17.1	24.1	32.1
920	2.8	4.7	6.2	32.6	32.8	33	16.8	18.2	19.2	32
940	4.7	6.1	9.2	32.8	33.3	34	18.2	20.1	24.1	32
960	5.4	5.8	8.5	32.9	33	33.3	18.7	19	20.2	31.6
980	3.3	7.9	9.1	32.6	33.9	34.1	17	22.6	24.1	32
1000	3.9	4	4.8	32.4	32.8	32.9	15.1	16.9	19	30.1
1020	2.2	3.7	4.2	31.9	32.5	32.8	14	16.6	17.1	30.1

Appendix 29: Reconstructed sea surface conditions for core 95-030-24 La Have Basin

	alinity		Average ice duration			Median ice duration		
Depth (cm)	Most probable estimate	Upper limit	Lower limit	Most probable estimate	Upper limit	Lower limit	Most probable estimate	Upper limit
0	31.4	32.2	0	0	0	0	0	0
10	32.1	33.5	0	0	0	0	0	0
20	32	33.9	0	0	0	0	0	0
30	32.3	32.3	0	0	0	0	0	0
40	32.2	32.3	0	0	0	0	0	0
50	29.9	30.4	0	0	0	0	0	0
60	30.3	31.9	0	0	1.8	0	0	2
70	32.2	32.4	0	0	0	0	0	0
80	32.3	32.4	0	0	0	0	0	0
90	32.2	32.4	0	0	0	0	0	0
100	30.7	33.5	0	0	1.8	0	0	2
110	31.4	33.5	0	0	1.8	0	0	2
120	31.5	31.7	0	0.2	1.8	0	0.2	2
130	31.5	31.6	0	0.1	0.2	0	0.1	0.2
140	31.8	34	0	0.1	0.4	0	0.1	0.4
150	31.1	31.6	0	0	0.1	0	0	0.1
160	31.8	32.4	0	0	0	0	0	0
170	31.9	32.3	0	0	0	0	0	0
180	32	32.1	0	0	0	0	0	0
290	30.3	32.7	0	1.4	11.2	0	1.4	11.5
300	30.2	31.6	0	0.8	3.6	0	0.8	3.7
320	30.3	31.5	0	0.4	2.3	0	0.4	2.3
340	31.4	32.2	0.2	0.1	6.4	0.2	0.1	5.9
360	30.1	31.2	0	0	1.8	0	0	2
380	30.1	30.2	0	0	0	0	0	0
400	32.1	32.3	0	0	0	0	0	0
420	30.1	31.4	0	0	11.2	0	0	11.5
440	32	32.3	0	0	0	0	0	0
460	31.3	31.8	0	1.1	7.4	0	1.1	7
480	32.2	32.3	0.1	0.1	3.8	0.1	0.1	4.1
500	31.9	32.3	0	0	0.1	0	0	0.1
520	30.1	30.1	0	0	4.8	0	0	5
540	31.8	32.3	0	0	0	0	0	0
560	30.1	31.4	0	0	2.8	0	0	3.1
580	30.4	31.2	0	0	1.8	0.1	0	2
600	30.4	31.2	0	0	0	0	0	0
620	30.3	31.3	0	0	0	0	0	0
640	30.4	31.6	0	0	0	0	0	0

Appendix 29: Reconstructed sea surface conditions for core 95-030-24 La Have Basin

	alinity		Average ice duration			Median ice duration		
Depth (cm)	Most probable estimate	Upper limit	Lower limit	Most probable estimate	Upper limit	Lower limit	Most probable estimate	Upper limit
660	30.9	31.6	0	0	0	0	0	0
680	30.7	31.1	0	0	0	0	0	0
700	30.4	30.8	0	0	1.4	0	0	1.4
720	30.4	31.5	0	0	1	0	0	1
740	32.6	33.9	0	0	0	0	0	0
760	33.4	33.9	0	0	0	0	0	0
780	33.5	33.8	0	0	0	0	0	0
800	33.1	33.6	0	0	0	0	0	0
820	31.8	32.9	0	0.8	6.6	0	0.7	6.3
840	31.8	31.9	0	0.4	0.8	0	0.4	0.7
860	33.5	33.9	0	0	0.4	0	0	0.4
880	32.1	33.6	0	0	0	0	0	0
900	32.2	33.9	0	0	0	0	0	0
920	32	32.6	0	0	0	0	0	0
940	32.6	33.9	0	0	0	0	0	0
960	32	32.1	0	0	0	0	0	0
980	33.5	33.9	0	0	0	0	0	0
1000	31.5	31.7	0	0	0	0	0	0
1020	31.3	31.6	0	0	6.4	0	0	6

Appendix 30
Modern analogues for Bay of Islands core MD99-2225

```
    1   10    1
   0 B686G044G042G035G049G048A421G028A420G047
        0  74  77  79  80  85  89  91  93  94
  10 X642G065B686   0G061X648X643G035X639A685
       80  93  95  95  97  98 101 101 103 103
  40   10G055G060B686A685A421X675G057N402G035
       66  95 100 100 104 116 118 119 123 125
  80 G060X648G052G065B686G035G055G061G033N248
       66  67  70  73  73  74  77  79  84  90
 100 X648A420  80A685X653G035G044A683G065G043
       44  63  64  75  78  79  81  84  85  85
 120  100X648B686A420G035G048A421A423A419X675
       32  56  72  76  78  82  83  88  91  92
 150  120X648N245A685N248X651N185X653X675G060
       34  72  90  93  94  98 102 108 111 112
 180 B686 150G043G044A683G040X642G052G035G061
       87  92  93 103 104 105 108 110 111 111
 200  180G060G055B686A685G053G052G065G035G061
       69  90 101 101 102 113 118 120 121 128
 250  200Z536G055A421G060G051Z535G054Z539A685
       62 100 105 108 110 111 112 117 117 120
 300 A685X648G060X675 250G055N246N185N248A421
       55  71  75  76  79  79  92  95  96  98
 350  300X648A685G060N185X651N248X675N186G055
       34  54  65  87  92  93  94  95  96  97
 400  350A685B686Z550G055A420X648G060A419A421
       58  90  93 106 125 127 128 128 129 131
 450  400X642B686X648X640G076G043A420X643G044
       84  94  96  99 108 109 115 117 117 118
 500  450A683G043G044A421G035X648A420B686G076
       59  60  63  70  72  74  77  81  83  85
 550  500A683G076G043G075G078G035G044A421G077
       48  57  70  74  82  84  95  98  99  99
 600  550A683G043G052G076G035G078G033G075G044
       18  40  47  53  55  58  62  63  67  69
 650  600A421Z535A683Z536A426Z550A422A419N638
       67  95 106 111 112 116 119 122 124 126
 700 A683G046A421G048G058G047G041G044G042G037
       23  56  59  68  68  69  74  74  74  75
```

```
 750 X655G052G058Z550 700G077G043A683G065X648
       76  80  83  90  94  95  96  96  96  97
 800 A683G072H133G046G038H139G044H130H134G058
       45  71  73  75  78  80  82  83  86  87
 850  800A683X642B686A421G046G058G076G044G043
       59  68  98 100 107 109 110 114 115 115
1000  850A685X648Z550A419A420G076G060B686A683
       67  75 105 108 117 118 121 122 130 130
1050 G076G048A683G035G073G042B686G078G044G047
       67  68  68  75  78  78  79  80  82  82
1100 1050X648B686A685G076G035G044A420G042G048
       60 108 125 131 133 136 141 143 146 148
1150 B6861100G048G042G047G035G049G044X648A683
       61  73  80  83  91  92  93  93 100 101
1200 1150X648G035B686G048X642G049G042N246X653
       57 101 122 125 126 133 134 139 144 146
1250 1200N269A421A419B686A685X648A682N633G048
       78 112 126 128 136 137 138 140 144 147
1300 X6481250G035X653B686G048A685G033G034G042
       67  78  91 100 101 104 105 111 112 112
1350 G048G042G044G047G035G049G0781300G046A683
       50  51  53  56  60  61  64  66  67  67
1400 1350A683G046X642G043X640G044G058G047X643
       58  71  90  91  91 100 103 106 106 107
1460 G078G077X654A427G075X655X664A074G076A423
       50  58  70  84  84  97 102 106 117 123
1500 E008G039E012A683E003G037E018E017A419E020
       70  72  75  82  84  87  94  96  97  98
1600 E015E008E006E007E005P373G069G039E003E012
       45  46  48  57  62  67  68  71  79  80
1700 G046A683G047G048G041G042G044G078G037G077
       34  45  52  54  55  62  62  65  66  73
1800 1700X664G078A683G077X642G046A423X640G041
       51  75 103 112 114 115 115 118 122 122
```

Appendix 31: Reconstructed sea surface conditions for core MD99-2225 Bay of Islands

		February SST			February salinity		
Depth (cm)	Lower limit	Most probable estimate	Upper limit	Lower limit	Most probable estimate	Upper limit	Lower limit
0	-1.4	-0.4	-0.4	32	32	32.3	13.4
10	-1.1	0.1	1.8	31.1	31.2	32	15.6
40	-1.5	-0.7	0.3	31.2	31.7	32.3	13.6
80	-1.5	0.2	5.3	31.8	32.4	32.5	15.2
100	1	4.9	5.2	32.6	32.6	33	16.8
120	-0.7	4.7	5	31.9	32.6	32.6	17
150	4.9	5.1	6.6	32.6	32.8	34.6	14
180	-0.7	0.9	5.1	32.1	32.2	32.7	13.2
200	-1.5	-0.3	0.7	32.2	32.3	32.6	14.7
250	-0.7	0.4	2.3	32.3	33.1	34	9.9
300	-1.3	3.4	4.1	32.5	33.2	33.7	14.7
350	3.2	4.2	5.5	32.6	32.9	33.3	15.3
400	-0.7	3.5	3.8	32.1	33.1	33.2	13.4
450	0.3	2	4	31.3	32.2	32.9	16.1
500	-0.9	0.6	2.8	32.2	32.4	32.7	12.1
550	-0.8	0	0.5	31.9	32.5	32.6	12
600	-0.9	-0.4	0	32.4	32.6	32.7	11.7
650	0.1	1.9	4.6	32.8	32.9	34.3	11.9
700	-0.8	-0.6	4.6	32.3	32.7	32.8	11.9
750	-1.5	0.4	1.7	31.9	32.3	32.5	13.2
800	-1.4	-0.9	-0.7	30.6	32.2	32.6	6.6
850	-0.8	-0.7	0.4	31.4	32.4	32.5	12.1
1000	-0.6	1.4	3.7	32.4	32.8	33.6	13.2
1050	-1.1	-0.2	0.1	31.8	32.1	32.6	12.6
1100	-0.2	2.2	4.8	32	32.3	32.8	15.1
1150	-0.7	0.1	2.9	31.9	32.1	32.3	13.4
1200	-0.3	2.2	5.5	32	32.3	32.6	16
1250	2.6	4.2	6	32.5	33.5	35.1	14.4
1300	-1.2	4.7	5.1	32.4	32.8	33.5	15.8
1350	-1.5	-1.5	-1.4	32.3	32.4	32.5	13.2
1400	-1.4	-1.1	-0.4	32.4	32.5	32.7	11.7
1460	0.1	0.2	2.9	32	32	32.6	14.9
1500	-1.4	-1.1	-1	27.6	28.5	32.5	8.2
1600	-1.3	-1.1	-1	27	27.8	29.3	8.1
1700	-1.4	-1.3	-0.6	32.3	32.4	32.7	11.4
1800	-0.9	3.3	8.4	32.3	33.2	34.2	13.3

Appendix 31: Reconstructed sea surface conditions for core MD99-2225 Bay of Islands

	August SST			August salinity			Average ic
Depth (cm)	Most probable estimate	Upper limit	Lower limit	Most probable estimate	Upper limit	Lower limit	Most probable estimate
0	16.9	16.9	29.1	30.4	30.4	2	2
10	16.3	16.5	30	30.1	30.3	0	0.8
40	15.1	16.2	30.1	30.2	30.3	0.6	1.5
80	15.9	18.3	30.5	30.8	31.7	0	1.9
100	18.2	18.6	30.9	31.9	32	0	0.1
120	18.3	18.4	30.5	31.8	31.9	0.1	0.2
150	18.1	18.4	31.9	32	34.6	0	0.1
180	16.9	17.2	30.4	30.8	31.8	0.1	1.5
200	16	16.8	30.5	30.6	31.1	1.6	2
250	13.2	15.4	30.5	31.5	32.4	0	1.2
300	15.5	19.6	30.6	32	32.1	0	0.2
350	16.8	18.7	31.9	31.9	32.4	0	0.1
400	15.9	16.8	30.4	31.9	32.2	0	0.2
450	16.2	17.4	30.1	31	31.8	0.1	0.2
500	14.1	16.5	30.3	31.1	31.1	0.2	1
550	13.2	14.7	31	31.2	31.3	0	1.3
600	12.6	13.3	30.3	31.2	31.2	1	1.6
650	14.8	18	31.4	31.4	32.7	0	0.8
700	12.1	17	30.4	31.2	31.3	0	1.8
750	15.9	16	30.4	31.6	32.5	0	0.8
800	12.4	12.8	29.5	30.9	31.2	2	2.3
850	12.3	16.6	30.1	31	31.1	0	2
1000	13.7	18.3	31	31.5	32.2	0	1
1050	15.2	16.1	30.3	30.9	31	0	0.6
1100	16.8	18.2	30.8	31.3	32	0.3	0.4
1150	16.7	17	30.4	30.6	31.3	0.3	1.7
1200	17.4	18.2	30.7	31.2	32.5	0	1
1250	16.2	17.6	31.3	32.8	34.9	0	0.5
1300	17.8	18.6	31.6	32.1	32.7	0.1	0.2
1350	13.4	13.5	30.4	30.4	30.7	2.1	2.1
1400	12.7	13.4	30.4	30.8	31.3	1.4	2
1460	15	16.2	31.5	31.5	32.1	0	0.1
1500	8.8	10.5	24.7	25.9	30.1	2.2	2.7
1600	9.9	11.8	24.6	26.4	28	2	3
1700	12.9	13.2	30.4	30.6	31.3	1.5	2
1800	17.9	23.2	30.8	32.1	33.9	0	1

Appendix 31: Reconstructed sea surface conditions for core MD99-2225 Bay of Islands

	e duration		Median ice duration	
Depth (cm)	Upper limit	Lower limit	Most probable estimate	Upper limit
0	2.1	0	2	3
10	2.6	0	0.8	2.7
40	2.3	0.6	1.5	2.1
80	2.6	0	2.3	3
100	2	0	0.1	2.2
120	2	0.1	0.2	2
150	0.2	0	0.1	0.2
180	2	0.1	1.5	2
200	2.5	1.7	2.2	3
250	2.1	0	1.2	2.2
300	2.4	0	0.2	2.6
350	0.6	0	0.1	0.7
400	2.1	0	0.2	2.1
450	2	0.1	0.2	2
500	1.9	0.2	1.1	2
550	1.4	0	1.4	1.6
600	1.9	1.1	1.7	2.1
650	1.6	0	0.9	1.8
700	1.9	0	1.9	2
750	2.5	0.1	0.9	3
800	7.5	2.2	2.4	7
850	2.1	0	2.1	2.2
1000	2.1	0	1.1	2.3
1050	1.9	0	0.6	2
1100	2	0.3	0.5	2
1150	2	0.4	1.7	2
1200	1.8	0	1	1.8
1250	1.2	0	0.5	1.3
1300	2	0.1	0.2	2
1350	2.1	0.1	2	2
1400	2.1	0	2	3
1460	0.1	0	0	0
1500	3	2	2.8	3
1600	11.9	2	3	12
1700	2.1	0	2	2
1800	2	0	1	2

Appendix 32
Modern analogues for St. Anne's Basin core 84-011-12

```
    1    10     1
0001 X644X642G034G040G035G073G023G045G077G071
       107 118 129 130 131 134 136 137 141 142
0020 G035G052G065A423N400G040A421G077G073A419
        71  77  78  79  81  82  83  83  85  86
0030 X693G033G034G077G052Z554G0750020G035G079
       168 170 171 172 175 176 179 187 193 195
0040 0030X708G077X693G075G078G052G076A683G043
        49  94 100 106 125 125 129 130 135 135
0050 0040G077A423G078A683X708X693G040G071G035
        30  48  86  93 105 109 116 116 117 117
0060 0050G043G078G075G077X708G035A683G033G076
        49  95  96 100 102 104 115 119 119 125
0070 0060G077G078G075G035G076A683G052G033G043
        53  59  68  73 110 111 115 117 118 118
0080 0070G078G077X708G075G043X699G033G035X693
        27  63  64  78  83 111 119 135 137 139
0090 A683E012G040G045G043G0460080G041G037G077
        68  84  89 100 104 119 123 123 124 125
0101 0090G072G038G050G071A683G040X708E012G045
        83 113 115 119 121 124 128 132 137 139
0110 0101G071G040A422G050G077G059E012G045G070
        33 113 126 142 143 143 145 146 147 151
0120 0110G077G034G079E004E012G043A683E005G078
       121 134 139 143 147 150 150 150 154 155
1000 X693G035X648A423X694X689X653G077A420X698
        82  97  98 102 107 108 114 115 115 116
1010 1000G035G049A421G048G042G028G062X648G024
        50  75  82  89  92  99 101 104 105 106
1014 G052G073A6831010G040G035G065G041A423G048
        56  61  62  63  64  64  74  74  76  79
1020 1014G077A423G040G035G071G041G073A683G048
        33  36  44  56  57  58  65  66  68  68
1030 G0771020G078A423G071G040G052G035G066A422
        15  27  54  60  81  95 100 101 106 109
1040 A683A423A419G041G077G048G040G047G045A421
        45  45  49  60  83  83  85  89  93  95
```

```
1050 X693G065G052G0331040A685X648G035A683G076
       77   95   95   98 101 107 108 110 111 114
1060 1050G034G052G033Z560G065G035X693M285Z559
       33   93   95   95   98 107 107 111 113 115
1070 A423G035A683G077A4211060G078A420G034G048
       69   73   75   76   83   87   96   97 103 104
1080 1070G066G077X693X699X655G065G052G078G061
       86   95   99 113 113 120 123 125 131 132
1090 G052G065G035G033G061X6481080A683G034G043
       61   66   84   85   89   91   93   98 106 109
1100 X693X6991090G077G078X694G066G033G035X698
       82 107 107 113 117 121 121 125 127 130
1110 1100G077G078X699A423X693G075G035X708A074
       48   51   61   94 101 113 116 117 127 128
1120 G077A423G078G0711110G040G041G035G048A683
       27   54   65   69   70   76   81   83   85   88
1130 1120G077G078G052G065G066G061A423G040G043
       51   57   94 103 113 114 115 116 117 118
1140 1130X708G077G078G052G043X693A683X655G040
       53   84   85 112 119 122 128 128 135 136
1150 A423A683A419X6481140X693X642G040G035A420
       98 101 105 115 117 117 119 119 125 126
1160 G077G052G065G061G078G040G043G035A683G033
       69   79 100 102 103 107 109 109 110 110
1170 1160G052G065G061G043X643G033G035G040A683
       84   89   90   95 113 115 117 121 122 123
1180 1170X642A683X708G044X644G072X643G043X641
       99 110 140 146 151 153 154 159 160 162
1200 1180G043G044A683X642G035G033X640G072G042
       71 103 110 123 129 130 147 148 152 156
1220 1200G052G061X693G065A685X648G056G035G054
       72 104 106 119 119 122 129 133 138 142
1240 A683G044G035G0421220G040A421G049G043G037
       50   55   64   67   71   76   76   77   81   82
1260 1240G040G041A683G045G048A423G047G071G037
       52   71   76   81   91   97   99 101 107 109
1280 A683A4231260G040A419A421A422G041E012G077
       51   68   72   75   77   83   91   96 102 103
1300 1280G061G040G052G065A423G035A419A683G073
       22   67   68   70   71   74   76   81   82   93
1320 G078G077G043G075A683G035X699G076X708G033
      106 120 127 131 131 131 133 138 138 141
```

```
1340  1320G065G052G061G073X648G035A683G033A685
        76  88  88 101 113 113 116 116 119 119
1360  1340G052G065G061A683G073G040G043X648G035
        10 115 115 121 130 134 134 138 139 139
1380  A683G044G035A421G0421360A420G049G048G047
        62  80  85  85  87  96 101 102 104 105
1400  1380X642A685X644X648X693X643X653X694G052
        87 118 126 126 126 129 133 155 162 163
1420  1400X648X693G061G052X653G065A683G040X698
        75 105 112 115 115 123 125 126 129 138
1440  1420X693A685X642X648A420X708X694X653X643
        60 140 142 143 153 175 176 176 177 181
1460  1440A685X642A420A683X648A421A419A682X693
        29 124 128 131 137 142 151 152 153 161
1480  1460A419A420A425X693A685X648A423X704X698
        74  93 100 119 121 122 135 140 142 142
1500  G077A423G078A683A419X655A420G073G052G035
        52  76  79  84  95  95  98  99 122 123
1520  G076G035X648A685G065G0331500G073G044X694
       127 141 141 144 144 148 153 157 162 164
1540  1520X648X693A685X694X653X698G065A420X689
        76  95 108 110 119 130 131 174 178 178
1560  G068A423G071G073G077G024G041G047G048X664
       144 155 158 160 167 176 179 180 182 184
1580  1560G068G024A423A419X706G048G049X689A420
       110 110 111 112 116 124 126 128 129 129
1600  G071G068G045G041G047A423G049G0401580G029
        59  72  82  84  88  90  92 102 103 103
1620  1600G073G068G062G031G047G045G041G027A423
        57  84 107 109 110 112 114 116 117 117
1630  1620G071A423G077G068G073G041G078G047G049
        69  88  93  94  95 104 113 114 119 121
1640  1630A419A423G073N400G027G041G048G077A683
        50  58  86  93  96 100 106 113 113 113
1660  1640G029G027G062G031G035G073G068G024G028
        47  77  81  81  96  98  98 100 101 104
1680  1660G061G052Z560G056G040G035A683A682G054
        51  86  90  99 101 103 104 105 106 110
1700  A683A423G077A421G035G047G048G078G049A419
        41  44  58  60  66  67  67  68  74  74
1720  1700A683A419A421G047G048A423G041G042G037
        52  55  70  70  91  95  97 102 102 104
```

```
1740 A423A419A420G041G071A4281720G068G047G077
       50  74  86 100 102 105 106 107 108 112
1750 A682A683A421A423A4191740X664Z535G077X708
      144 148 151 156 170 177 178 185 190 196
```

Appendix 33: Reconstructed sea surface conditions for core 84-011-12 St. Anne's Basin

	February SST			February salinity			August SST		
Depth (cm)	Lower limit	Most probable estimate	Upper limit	Lower limit	Most probable estimate	Upper limit	Lower limit	Most probable estimate	Upper limit
1	-1.4	0.3	0.5	31	31.1	31.8	15.2	16.4	16.5
20	-1.5	-1.4	-0.9	31.5	31.6	32.3	14	15.1	15.9
30	-1.3	3.4	6.2	31.8	32.4	33.3	15.7	17.8	19
40	0.9	2	4.3	31.6	31.9	32.3	15.8	16.7	18.1
50	0.1	1.2	2.4	32	32	32.8	14.8	15.9	16.9
60	-1.4	-0.1	0.8	32	32.2	32.4	12.9	14.5	15.5
70	-0.1	0	0.1	32	32.1	32.3	14.5	14.8	14.9
80	-0.1	0.1	0.2	32	32	32.1	14.5	14.8	15
90	-1.2	-0.9	-0.6	29.1	31.9	32.6	10.1	11.6	12.2
101	-1.3	-1.1	-0.6	30.9	31.5	32.1	11.2	14	16.3
110	-1.3	-1.2	0.6	31	31.4	32.5	13.7	15.2	17
120	-1.3	-0.7	0	31.4	31.7	32.1	14.1	15.1	16
1000	-0.1	4.5	5.8	31.7	32.5	32.7	15.5	18.1	18.8
1010	-1.4	1	4.6	31.7	32.1	32.5	14.3	15.9	18.1
1014	-1.4	-1.3	-0.2	31.7	31.9	32.5	12.1	15.3	15.9
1020	-0.7	0	3.9	31.9	32.1	32.8	14.9	15.4	17.6
1030	-0.2	0.1	0.2	32	32	32.2	14.9	15	15.8
1040	-0.9	2.1	4	32.6	32.8	32.9	12.2	15.4	17.9
1050	-1.4	3.7	5	31.6	32.4	32.8	15.8	17.9	18.9
1060	-1.4	0.6	4.4	31.7	31.9	32.9	15.8	16.7	18.2
1070	-1.1	2.1	4.1	31.7	32.6	32.9	13.9	16.3	16.9
1080	-1.1	0.2	2.9	31.6	32	32.6	15.3	15.7	16.9
1090	-1.5	-1.5	-1.4	31.4	31.7	31.9	14.5	15.6	15.7
1100	0.5	4.3	5.9	31.8	32.4	32.7	16.3	18.1	18.9
1110	0.1	1.8	3.9	32	32.2	32.5	14.9	16.2	17.9
1120	0	0.6	3.3	31.9	32.1	32.8	14.9	15.3	17.5
1130	0	0.3	1.3	32	32.1	32.3	14.9	15.1	15.4
1140	0.2	0.7	2.5	31.5	31.8	32	15	15.6	16.1
1150	-0.3	2.9	4.2	32.6	32.9	32.9	12.8	16.5	18
1160	-1.5	-0.4	0.1	31.4	31.9	32	14.7	15.2	15.7
1170	-1.5	-1	-0.2	31.3	31.8	31.9	14.9	15.5	15.8
1180	-1	-0.2	0.7	31.2	31.6	32.1	12	15.5	16
1200	-1.4	-0.9	-0.3	31.5	32	32.3	13.1	14.1	15.7
1220	-1.5	-1.3	1.4	31.7	32	32.1	14.2	14.9	16.2
1240	-1.4	-0.9	0.5	31.7	32.5	32.6	11.7	12.4	13.6
1260	-1.4	-1.2	-0.7	32	32.4	32.5	12.2	12.9	13.2
1280	-0.9	0.1	4	32.4	32.7	32.8	12.1	13	17.9
1300	-1.4	-0.8	1.4	32.1	32.3	32.8	13	13.7	14.8
1320	-1.3	-0.1	0.1	32	32	32.4	12.9	14.7	14.9
1340	-1.4	-1.1	0.9	31.3	31.7	32	14.6	15.5	15.9

Appendix 33: Reconstructed sea surface conditions for core 84-011-12 St. Anne's Basin

	February SST			February salinity			August SST		
Depth (cm)	Lower limit	Most probable estimate	Upper limit	Lower limit	Most probable estimate	Upper limit	Lower limit	Most probable estimate	Upper limit
1360	-1.4	-1.4	-1	31.3	31.6	31.9	15.4	15.7	16.1
1380	-1.4	-0.4	0.9	31.6	32.6	32.7	11.7	12.6	14.3
1400	0.2	0.6	4.4	31.1	31.9	32.7	12.6	15	16.6
1420	-0.1	3.5	5.5	31.9	32.3	32.6	15	17.2	18.7
1440	3.2	4.7	5.9	32.3	32.7	33.3	15.2	17.6	18.2
1460	0.3	3.5	4	31.1	32.8	33	13.8	16.1	17.3
1480	3.5	4.1	4.5	32.7	32.9	33	15.8	17.2	17.9
1500	0	0.8	3.7	32	32.2	32.8	14.7	15.4	17.7
1520	-0.4	1	4.8	31.7	31.9	32.8	16	16.7	18.6
1540	1.8	3.7	5.5	31.8	32.3	32.7	16.1	17.9	18.7
1560	-1.4	-0.2	3.9	31.5	31.8	32.6	14	15	17.5
1580	-1.4	-1	1.3	31.7	31.8	32	13.5	14.3	15.1
1600	-1.4	-1.3	-1.2	30.9	31.2	31.9	13.5	15.7	17
1620	-1.4	-1.3	-1.3	31.3	31.4	31.7	14	15.8	16.1
1630	-1.1	-0.6	3.9	31.2	31.4	32.7	15.5	16.5	17.1
1640	-0.8	2.3	4.4	31.4	32.3	33.1	16.4	17.4	18
1660	-1.3	0.1	2.3	31.5	31.8	32.2	14.5	15.7	17.1
1680	-1.4	-0.8	-0.1	31.7	31.9	32.1	12.2	15.1	15.7
1700	-0.6	0.4	4	31.9	32.7	32.8	12.4	13.4	17.2
1720	-0.3	0.4	4.5	32.7	32.7	33.1	12.6	13.2	18.1
1740	2.8	4.1	4.4	32.9	32.9	33	16.3	17.8	17.9
1750	-0.6	0.1	4.4	32.6	32.8	33	11.6	12.7	18.1

Appendix 33: Reconstructed sea surface conditions for core 84-011-12 St. Anne's Basin

	August salinity			Average ice duration			Median ice duration		
Depth (cm)	Lower limit	Most probable estimate	Upper limit	Lower limit	Most probable estimate	Upper limit	Lower limit	Most probable estimate	Upper limit
1	29.8	30	30.2	0	0.3	2	0	0.3	2
20	30.3	30.8	31.3	1.3	2.2	2.6	1.3	2.4	3
30	30.4	31.3	31.8	0	0.9	2.4	0	1	2.8
40	30.9	31.2	31.4	0	0.3	1.3	0	0.4	1.5
50	31.2	31.4	31.5	0	0.1	0.7	0	0.2	0.7
60	30.5	30.9	31.4	0.1	1	2.1	0.1	1	2
70	30.9	31.3	31.5	0	0.4	1.3	0	0.4	1.2
80	31.1	31.4	31.5	0.1	0.2	0.9	0	0.2	0.9
90	25.2	30	31	1.9	2	2.5	2	2.2	3
101	29.2	29.6	30	2	2.5	3.1	2.1	2.5	3
110	29.1	29.6	30.6	2.2	2.8	3.3	1.5	2.7	2.8
120	29.3	30.5	31.3	0	1.4	2.6	0	1.4	2.5
1000	31.2	31.7	31.9	0	0.4	2	0	0.4	2
1010	30.8	31.2	31.7	0.3	1.4	2	0.3	1.4	2
1014	30.2	30.4	31.3	2	2.3	2.6	2	2.6	3
1020	30.4	31.1	31.5	0	1	2.3	0	1.1	2.5
1030	30.8	31.4	31.5	0	0.2	1.3	0	0.2	1.4
1040	31	31.5	31.7	0	0.7	1.9	0	0.8	2
1050	30.3	31.4	31.8	0.2	0.9	2.7	0.2	1	3
1060	30.3	30.7	32.1	0.6	1.6	2.2	0.7	1.7	2.3
1070	31.1	31.4	31.6	0	0.7	1.9	0	0.7	2
1080	30.4	31	31.5	0.4	1.1	2.1	0.5	1.2	2.3
1090	30.4	30.4	30.9	2.4	2.5	2.8	1.6	2.9	3
1100	30.4	31.6	31.8	0	0.5	2.4	0	0.5	2.7
1110	31.5	31.5	31.6	0	0.2	0.7	0	0.2	0.8
1120	31.4	31.5	31.6	0	0	0.9	0	0	2.4
1130	31.4	31.5	31.5	0	0	0.7	0	0	3
1140	30.8	31.2	31.5	0	0	0.1	0	0	2.8
1150	31.3	31.6	31.7	0	0.4	1.9	0	0.4	2
1160	30.4	31.1	31.5	0	0.9	2.6	0	1	3
1170	30.4	30.7	31.1	0.8	1.9	2.6	1.2	2.2	3
1180	30.1	30.4	30.8	0	1	1.9	0	1.1	2.1
1200	30.2	30.4	30.5	0.7	1.7	2.1	0.8	1.7	2
1220	30.4	30.4	30.9	1.1	2.2	2.6	1.1	2.5	3
1240	30.4	31.1	31.2	1.4	1.9	2.1	0	2	2.5
1260	30.3	30.6	31.2	1.8	2	2.1	0	2	3
1280	30.5	31.3	31.4	0	1.5	1.9	0	1.6	2
1300	30.4	30.8	31.3	1.2	2.1	2.5	1.6	2.3	3
1320	30.5	31.3	31.5	0.1	0.3	2	0	0.3	2
1340	30.3	30.6	31.4	0.4	2.1	2.7	0.5	2.3	3

Appendix 33: Reconstructed sea surface conditions for core 84-011-12 St. Anne's Basin

	August salinity			Average ice duration			Median ice duration		
Depth (cm)	Lower limit	Most probable estimate	Upper limit	Lower limit	Most probable estimate	Upper limit	Lower limit	Most probable estimate	Upper limit
1360	30.2	30.4	30.5	2	2.6	2.7	2.2	2.8	3
1380	30.4	31.1	31.3	1.3	1.7	2.1	0	1.8	2.8
1400	30	30.6	31.4	0	0.7	1.7	0	0.7	1.8
1420	30.6	31.4	31.9	0	0.3	1.4	0	0.3	1.5
1440	30.9	31.7	31.9	0	0.1	0.3	0	0.1	0.3
1460	30.2	31.6	31.9	0	0	0.7	0	0	0.7
1480	31.7	31.8	32.2	0	0	0	0	0	0
1500	31.5	31.5	31.7	0	0	0.5	0	0	2
1520	30.8	31.1	31.9	0	0.3	2.3	0	0.3	2.3
1540	31.2	31.6	31.9	0	0.1	0.8	0	0.1	0.8
1560	29.4	29.9	31.6	0	1.9	2.5	0	1.7	2.3
1580	29.4	29.6	30.5	1.8	2.1	2.3	1.1	1.9	2
1600	29.3	29.4	30.4	2.2	3	3.3	2	2.7	3
1620	29.4	29.6	29.9	2.2	2.5	2.9	2	2.3	2.8
1630	29.4	29.7	31.5	0	2.5	2.8	0	2.3	2.6
1640	29.7	30.9	31.9	0	1	2.4	0	1	2.2
1660	28.9	29.7	30.7	1	1.8	2.4	1	1.7	2.3
1680	29.7	30.2	30.7	1.9	2.3	2.7	1.8	2.5	3.1
1700	31.2	31.4	31.6	0	1.2	1.9	0	1.3	2
1720	31.3	31.4	31.7	0	1.3	1.6	0	1.5	1.7
1740	31.5	31.7	32.2	0	0	2.3	0	0	2.2
1750	31.2	31.3	31.6	0	1.5	1.8	0	1.7	2